EFFECTIVE ESTIMATION OF MARGINAL QUANTILES IN STEADY-STATE SIMULATIONS

A Dissertation
Presented to
The Academic Faculty

By

Athanasios Lolos

In Partial Fulfillment
of the Requirements for the Degree
Doctor of Philosophy in the
H. Milton Stewart School of Industrial and Systems Engineering
College of Engineering

Georgia Institute of Technology

May 2023

EFFECTIVE ESTIMATION OF MARGINAL QUANTILES IN STEADY-STATE SIMULATIONS

Thesis committee:

Dr. Christos Alexopoulos, Advisor
H. Milton Stewart School of Industrial and Systems Engineering
Georgia Institute of Technology

Dr. David Goldsman
H. Milton Stewart School of Industrial and Systems Engineering
Georgia Institute of Technology

Dr. Seong-Hee Kim
H. Milton Stewart School of Industrial and Systems Engineering
Georgia Institute of Technology

Dr. Enlu Zhou
H. Milton Stewart School of Industrial and Systems Engineering
Georgia Institute of Technology

Dr. Kemal Dinçer Dingeç
Department of Industrial Engineering
Gebze Technical University

Dr. James R. Wilson
Edward P. Fitts Department of Industrial and Systems Engineering
North Carolina State University

Date approved: April 20, 2023

Know thyself.

Socrates

To my wife Alexandra Manta and our family.

ACKNOWLEDGMENTS

This dissertation is a requirement for the completion of my doctoral studies in Operations Research at Georgia Institute of Technology. Working on this dissertation has been a fascinating journey and I would like to thank the people who has a major impact on the successful completion of this journey.

First, I would like to express my deepest gratitude to my advisor, Professor Christos Alexopoulos for his supervision and unequivocal support and guidance. I started working with Professor Alexopoulos at the beginning of my Ph.D. studies and from the first moment our collaboration has been exceptional. During these five years, Professor Alexopoulos has guided me through my every step of my Ph.D. studies, always having in his mind my best interest. Under his supervision I gained valuable experiences and skills while working on several interesting research topics. Our work has already led to numerous publications and more research papers are being prepared for submission. Furthermore, I would like to thank Professor Alexopoulos for his full support on crucial steps during my Ph.D. studies that have become the milestones for achieving my future career goals. Having him as my mentor has not only helped me on a professional level, but on a personal level as well, which has been of great importance for me considering the additional challenges that I had to face as an international student. I feel truly blessed for having Professor Alexopoulos as my advisor during the challenging task of earning a Ph.D. degree in Operations Research and I will be forever grateful to him for that.

I would like to also thank the members of my thesis committee and my collaborators for their help in the preparation of this work. Specifically, I would like to thank Professor David Goldsman for his valuable insight and comments as well as his always-positive attitude. It has been a great experience working with him in several papers while preparing this work and I am always looking forward towards our research meetings. I would also like to thank Professor Kemal Dinçer Dingeç for his sharp suggestions and constructive feedback as they have helped me significantly with my research. I had a great time working with Professor Dingeç on several papers. Next, I would like to thank Professor James R. Wilson for his remarkable guidance and support. Professor Wilson has been always available for consultation and discussion even at very late hours. I will always remember our 3:00 a.m. phone calls and his detailed, lengthy and valuable feedback on the new research topics that we were working on, and for those I will be always grateful to him. I would also like to thank Professor Seong-Hee Kim for her valuable feedback and beneficial and constructive comments. Further, I would like to thank Professor Enlu Zhou for her useful feedback and remarkable suggestions.

I would also like to thank Joseph Haden Boone, who is currently a Ph.D. student in Operations Research at Georgia Institute of Technology. I started collaborating with Haden during the first year of my Ph.D. studies while he was still an undergraduate student. I worked closely with him during the first three years of my Ph.D. studies and we have co-authored several papers. He has been a great collaborator and I had an amazing time working with him. Haden is a very sharp individual and his exceptional programming skills have been very useful throughout our collaboration. For all these reasons, I am grateful to Haden and I am looking also forward to seeing him achieving his career goals.

Besides the crucial and useful contributions and support at a professional level, during all these years I have received valuable support at a personal level from a great number of people without whom this journey towards my Ph.D. would be less fascinating and unique.

I would like to begin with the most important person in my life, my wife Alexandra Manta. Her love and support have been the pillars of my efforts towards my Ph.D. degree. Alexandra and I were together in Greece and we came to the United States in 2018 to pursue our Ph.D. studies, as she was also accepted in a Ph.D. program, and studied Economics at Emory University. She has always been there for me and we have experienced all the good and the bad things together during these five years. We actually got married in 2022 (at the beginning of the fifth year of our Ph.D. studies). She always motivates me, cheers me up and knows what I truly need. I feel so blessed to have her by my side during all these years and I know for sure that she has played a pivotal role in my success and making these five years unique. Alexandra is also graduating from her Ph.D. program in May 2023, as she has already held her thesis defense and we will move together to Virginia. I have a feeling that our next experiences are going to be uniquely remarkable and I am looking forward to our next journey and challenges. I will be forever grateful to Alexandra for her crucial role during my Ph.D. studies.

I would also like to thank my parents Ioannis Lolos and Athina Papadima and my siblings Nikos Lolos and Lemonia-Roxani Lolou as I would not be at Georgia Institute of Technology pursuing my Ph.D. studies without them. They have supported me through every step of my life and I know that I can always depend on them if needed, which is of great importance when undertaking difficult challenges. I will be forever grateful to them for what they have done for me all these years. I would also like to thank my relatives in Greece for their love and support and I would like to specifically mention my grandfather Nikos, my grandmother Roula, and my grandmother Lemonia for their love and blessings. I would also like to express my gratitude to people who are no longer with us but they have played an important role in my life and becoming who I am today.

Next, I would like to thank my friends in Greece and in the United States for their help and support. During my Ph.D. studies in the United States, I had the opportunity to make friends from all over the world from my Ph.D. and MBA programs, who made this whole experience even more fascinating. I also made new Greek friends to whom I am grateful. Specifically, I would like to thank Konstantinos Milios, Eva Kallou and Thaleia Doudali for the great experiences that we have shared together.

Last but not least, I would like to thank Professor Spiridon Reveliotis and Mrs. Aleka Delistrati, Professor Alexopoulos' wife, for the great times that we had together and their tremendous support. The experiences that we have shared will be forever in my memory and thus I am deeply grateful to them.

TABLE OF CONTENTS

LIST OF TABLES

LIST OF FIGURES

SUMMARY

Simulation is perhaps the most widely used systems-engineering tool in a variety of engineering and scientific domains. Large-scale applications of simulation provide critical support for planning and analysis in the governmental and military sectors as well as in numerous industries, including aerospace, electronics, finance, healthcare, manufacturing, supply chains, and telecommunications.

Steady-state simulations play a crucial role in the design and performance evaluation of complex production and service systems (Conway [1], Fishman [2], Hopp and Spearman [3], Law [4]).

While the steady-state mean of a simulation response characterizes central tendency, a (marginal) steady-state quantile characterizes the long-run risk associated with the individual realizations (Nelson [5]). The estimation of a steady-state quantile is typically a substantially harder problem than the estimation of the mean: while both problems are subject to effects from the potential presence of an initial transient, substantial serial correlation in the simulation output process, and departures from normality, quantile estimation is adversely affected by additional issues ranging from the inherent bias of point estimators and the nature of the marginal distribution such as nonexistence of a probability density function (p.d.f.), or a p.d.f. with discontinuities and multimodalities with sharp peaks (Alexopoulos *et al.* [6]). These theoretical and computational challenges associated with steady-state quantile estimation have hindered the growth in this area over the last few decades.

This thesis has two main goals: (1) the formulation of the theoretical foundations for procedures based on Standardized Time Series (STS) for estimating steady-state quantiles with confidence intervals (CIs) having given coverage probability and, potentially precision; and (2) the development and experimental evaluation of three automated methods for effective estimation of marginal quantiles in steady-state simulations: (i) the first fully automated sequential procedure for estimating steady-state quantiles based on STSs computed from

nonoverlapping batches; (ii) a fully automated fixed-sample-size procedure for steady-state quantile estimation based on a single time series; and (iii) the first fully automated fixed-sample-size procedure for steady-state quantile estimation based on sample paths generated by independent replications.

Chapter 1 presents a detailed literature review of the current methods for steady-state quantile estimation and introduces the main topics of this dissertation. Chapter 2 contains the theoretical results that constitute the basis of the proposed methods in Chapters 4–6 and provides results from an empirical evaluation of a variety of estimators for the variance parameter of the empirical-quantile process. Chapter 3 contains exact (or nearly exact) calculations for the expected values of the variance-parameter estimators in Chapter 2 for the special case of i.i.d. data. Chapter 4 presents and evaluates SQSTS, the first fully automated sequential procedure for estimating steady-state *quantiles* based on STSs that are computed from nonoverlapping batches of observations. Chapter 5 presents and evaluates FQUEST, a fully automated, fixed-sample-size method for estimating steady-state quantiles based on a single run. Chapter 6 presents and evaluates FIRQUEST, the first fully automated, fixed-sample-size method for estimating steady-state quantiles based on a user-specified number of independent replications. Finally, Chapter 7 contains overall conclusions, final remarks, and potential future directions.

Some of the contents of this thesis will have been published or submitted for publication by the time of the submission of this dissertation.

CHAPTER 1

INTRODUCTION

Simulation is perhaps the most widely used systems-engineering tool in the fields of industrial engineering, operations research, and the management sciences. Large-scale applications of simulation provide critical support for planning and analysis in the governmental and military sectors as well as in numerous industries, including aerospace, electronics, finance, healthcare, manufacturing, supply chains, and telecommunications.

Steady-state simulations play a crucial role in the design and performance evaluation of complex production and service systems (Conway [1], Fishman [2], Hopp and Spearman [3], Law [4]).

While the steady-state mean of a simulation response characterizes central tendency, a (marginal) steady-state quantile characterizes the long-run risk associated with the individual realizations (Nelson [5]). For example, let Y_k $(k \geq 1)$ denote the loss in the value of a financial portfolio over the kth time period of a fixed length (e.g., a single trading day). Thus, $Y_k > 0$ represents the magnitude of the loss and $Y_k \leq 0$ indicates a gain of magnitude $-Y_k$ over the kth time period. For each value y, let $F(y) \equiv P(Y_k \leq y)$ denote the cumulative distribution function (c.d.f.) of the steady-state distribution of Y_k that is achieved as $k \to \infty$. Given $p \in (0, 1)$, the $100p\%$ value at risk for the portfolio is the p-quantile $y_p \equiv F^{-1}(p) \equiv \inf\{x : F(y) \geq p\}$ of the steady-state loss distribution. Thus, for $p = 0.95$, the long-run probability that the loss in one period will not exceed $y_{0.95}$ is equal to 95% (Alexopoulos *et al.* [7]). Another application of steady-state quantile estimation can be found in contracts between manufacturers and clients, which typically include stipulations related to quantiles for cycle times, e.g., a guarantee that 95% of items are delivered within one month.

To set the tone for the literature review below as well as the content of the remaining chapters, let $\{Y_k : k \geq 1\}$ be a stationary process with marginal c.d.f. $F(y)$ and marginal probability density function (p.d.f.) $f(y)$. For each $k \geq 1$, define the indicator function $I_k(y) \equiv 1$ if $Y_k \leq y$ or $I_k(y) \equiv 0$ otherwise. If $\{Y_1, \ldots, Y_n\}$ is a finite sample from this process, we let $Y_{(1)} \leq \cdots \leq Y_{(n)}$ be the respective order statistics and define the empirical c.d.f. $F_n(y) \equiv n^{-1} \sum_{k=1}^{n} I_k(y)$, $x \in \mathbb{R}$. The point estimator of y_p is $\widetilde{y}_p(n) \equiv Y_{(\lceil np \rceil)}$, where $\lceil \cdot \rceil$ is the ceiling function. Let $\overline{I}(y_p; n) \equiv n^{-1} \sum_{k=1}^{n} I_k(y_p)$ and assume that the limit $\sigma^2_{I(y_p)} \equiv \lim_{n\to\infty} n\text{Var}\big[\overline{I}(y_p; n)\big]$ exists and is finite. We shall refer to $\sigma^2_{I(y)}$ as the variance parameter of the indicator process $\{I_k(y) : k \geq 1\}$. Under appropriate conditions detailed in Chapter 2, one can show that the variance parameter $\sigma^2_p = \lim_{n\to\infty} n\text{Var}\big[\widetilde{y}_p(n)\big]$ exists and can be written as $\sigma^2_p = \sigma^2_{I(y_p)}/f^2(y_p) < \infty$. To compute a CI for y_p, one needs to estimate the variance of $\widetilde{y}_p(n)$ or the variance parameter σ^2_p.

Unfortunately, theoretical and computational challenges associated with steady-state quantile estimation have hindered the growth in this area over the last few decades. These challenges include dealing with: (i) start-up/initialization problems in simulation experiments (Law [4]); (ii) substantial serial correlation in the underlying stochastic process $\{Y_k : k \geq 1\}$; (iii) the bias of the quantile point estimator $\widetilde{y}_p(n)$ (Wu [8]); and (iv) a variety of issues associated with the marginal distribution $F(y)$, including nonexistence of the p.d.f. $f(y)$, or a p.d.f. with discontinuities and multimodalities with sharp peaks (Alexopoulos *et al.* [6]), and departures from global smoothness, e.g., nondifferentiability of $f(y)$ or $F(y)$. In fact, the startup problem in item (i) above may have a more-pronounced effect in quantile estimation compared to the estimation of the steady-state mean. As a result, the literature on procedures for steady-state quantile estimation is substantially thinner than that of procedures related to the estimation of the steady-state mean.

The nonsequential methods of Iglehart [9], Moore [10], and Seila [11, 12] assume that the output process $\{Y_k : k \geq 1\}$ is regenerative, and use quantile estimates from a fixed number of regenerative cycles as basic observations. The method of Iglehart [9] delivers an approximate CI for y_p based on a suitably adapted central limit theorem (CLT); however, this method can be hard to apply reliably without making a pilot run to gather substantial preliminary information about the c.d.f. $F(y)$. The method of Seila [11, 12] uses batches containing a fixed number of regenerative cycles and applies jackknifing within each batch so as to reduce the bias of: (i) the quantile estimator computed from each batch; and (ii) the final quantile estimator obtained by averaging the within-batch point estimates. The method of Moore [10] differs from the previous two in that it computes the variance estimate for the sample quantile through a sequence of subsample assignments. For each assignment the entire sample of n cycles (assumed to be power of 2) is divided into two subsamples, A and B, each consisting of $n/2$ cycles. The kth assignment of cycle i goes into subsample A if the logical product (bit-by-bit) of the binary representations of k and i has an even number of 1's or into subsample B otherwise. Seila [12] compares the three aforementioned methods in [9]–[12] and elaborates on their advantages and disadvantages. The main drawback of all three methods is that in a complex or congested system with infrequent regeneration epochs, a large sampling effort may be needed to simulate a sufficient number of regenerative cycles so as to ensure good performance of the point estimators and CIs for the quantile of interest. These challenges escalate for extreme quantiles (Seila [12]).

The indirect method of Bekki *et al.* [13] delivers point estimators and CIs for a set of selected quantiles of job cycle times in a manufacturing system. This fixed-sample-size (nonsequential) method estimates a given quantile y_p by a four-term Cornish-Fisher expansion (Fisher and Cornish [14]) based on the standard normal quantile z_p and the first four sample moments of the job cycle times $\{Y_1, \ldots, Y_n\}$. The method has the advantage of estimating multiple quantiles simultaneously without storing or sorting data. However, a sample moment computed from strongly correlated data often requires a large sample for accurate estimation of the associated true moment, and this problem worsens for higher-order moments. The impact of this problem can be clearly seen in the authors' use of sample sizes of 30 and 60 million to analyze job cycle times in simple queueing systems with server utilizations below and above 90%, respectively. In addition, this method may yield unreliable point estimators of y_p if the marginal density $f(y)$ exhibits highly nonnormal behavior since the Cornish-Fisher expansion does not produce approximations at the same level of accuracy for different non-normal distributions. Such a pathology occurs in job cycle times from an M/M/1/LIFO queueing system [i.e., a single-server system with a last in, first out (LIFO) queue discipline] because the steady-state distribution of a cycle time typically has such larger values of its absolute skewness and its kurtosis that a four-term Cornish-Fisher expansion cannot adequately "adjust" z_p so as to estimate y_p accurately. This problem was partially rectified in Bekki *et al.* [15] by combining the four-term Cornish-Fisher expansion with a Box-Cox transformation; nevertheless, the revised procedure still requires relatively large sample sizes. Furthermore, the Cornish-Fisher expansion is known to produce less reliable approximations as the probability p approaches zero or one (extreme quantile estimation), cf. Bekki *et al.* [13].

Raatikainen [16, 17] introduced the first sequential quantile-estimation procedures in the simulation literature. In Raatikainen [16] estimates of several selected quantiles are computed by the extended P^2 algorithm (Jain and Chlamtac [18]). The P^2 method approximates the inverse empirical c.d.f. $F_n^{-1}(u) \equiv Y_{(\lceil nu \rceil)}$ for $u \in (0,1)$ using a piecewise-quadratic function $Q_n(u)$ to obtain the point estimate $\mathring{y}_p(n) \equiv Q_n(p)$ of y_p for a selected value of p. In Raatikainen [17] the CI for y_p is based on the following: a heuristic approximation to the large-sample behavior of $n^{1/2}[\mathring{y}_p(n) - y_p]$, spectral estimation of the variance parameter $\sigma^2_{I(y_p)}$ of the indicator process $\{I_k(y_p) : k \geq 1\}$, and estimation of the unknown value $f(y_p)$ expressed as an approximation to the reciprocal of the derivative $Q_n'(y_p)$. The procedure in Raatikainen [17] stops when the CI for each selected quantile satisfies its relative precision requirement. Simultaneous CIs were computed using Bonferroni's inequality, hence they are conservative. Four main issues limit the applicability of this methodology: (i) although it avoids sorting and has low storage requirements, the method lacks a rigorous basis ensuring that $\mathring{y}_p(n) \underset{n \to \infty}{\Longrightarrow} y_p$, where $\underset{n \to \infty}{\Longrightarrow}$ denotes weak convergence as $n \to \infty$ (Billingsley [19]); (ii) the CI for y_p requires estimating the unknown value $f(y_p)$, but the author's approximation to $1/Q'_n(y_p)$ is not guaranteed to converge in distribution to $f(y_p)$ as $n \to \infty$ because of problem (i) and because $Q'_n(u)$ is not guaranteed to converge in distribution to the derivative $\frac{\mathrm{d}}{\mathrm{d}u}F^{-1}(u) = 1/f(y_u)$ for each $u \in (0,1)$ as $n \to \infty$; (iii) the conservative nature of the CIs due to Bonferroni's inequality; and (iv) recent numerical experiments (Alexopoulos *et al.* [7] and Chapters 4–6 of this dissertation) indicate that the advantages of efficient sorting techniques and inexpensive storage have now surpassed those of the extended P^2 algorithm.

McNeil and Frey [20] developed a fixed-sample-size method for estimating extreme quantiles of the negative log-return on a financial asset price. The method fits a GARCH-type model (Bollerslev *et al.* [21]) to a return dataset of size n using a pseudo-maximum-likelihood approach. Then y_p is estimated from the $k+1$ largest order statistics of the estimated residuals using a generalized Pareto approximation to the extreme upper tail of the c.d.f. of the residuals. This method requires that n is sufficiently large, $k \ll n$, and $p > 1 - k/n$; but no general guidelines are provided for setting the values of n and k. Further, the method does not return a CI for y_p.

The fixed-sample-size procedure of Drees [22] fits an extreme-value distribution to a negative log-return dataset to deliver point estimators and CIs for certain extreme quantiles. However, this procedure is not designed to deliver a consistent point estimator for an arbitrary, user-specified y_p or a CI that satisfies user-specified requirements on its coverage probability and precision as $n \to \infty$. Instead, Drees's method requires the user to select a sequence of positive probabilities $\{p_n : n \geq 1\}$ and a positive integer sequence $\{k_n : n \geq 1\}$ with the following asymptotic properties as $n \to \infty$: (i) $p_n = O(1/n)$; (ii) $k_n \to \infty$ with $k_n = o(n)$; (iii) $\ln^2\{n \ln^4[\ln(n)]\} = o(k_n)$; (iv) $\ln(np_n) = o(k_n^{1/2})$; and (v) $np_n = o(k_n)$. Unfortunately, no guidance is offered on how to select these sequences in practice. Given n, p_n and k_n, point and CIs of y_{p_n} are computed from the $k_n + 1$ largest order statistics of the observed returns. If properties (i)–(v) hold (along with some technical assumptions detailed in Drees [22]) and if $\alpha \in (0,1)$, then as $n \to \infty$ this procedure delivers a CI of y_{p_n}

with asymptotic coverage probability $1 - \alpha$. However, in its current formulation, it is clear that Drees's nonsequential procedure cannot be extended to the estimation of an arbitrary extreme quantile (Alexopoulos *et al.* [23]).

The sequential algorithms of Chen and Kelton [24, 25] are based on a few (typically 3) approximately i.i.d. simulation runs. On each run of the authors' zoom-in (ZI) algorithm, each iteration recomputes the required size of a data buffer as well as lower and upper bounds on the order statistics used to estimate y_p so that the ZI algorithm progressively "zooms in" toward y_p. The end of the first run is based on six stopping rules. The subsequent runs use the ending buffer size from the first run and stop when the buffer is full. The results from all runs are not i.i.d. due to their joint dependence on the random buffer size realized on the first run. On each run of the quasi-independent (QI) algorithm of Chen and Kelton [24], every iteration attempts to collect approximately i.i.d. observations by applying progressively larger spacing between the observations used to compute a quantile estimator. The run ends after 15 iterations. Although the authors find that the ZI algorithm outperforms the QI algorithm in highly correlated processes, the ZI algorithm's reliance on several user-specified parameters makes it difficult to implement as a robust procedure requiring minimal user intervention. The two-phase QI algorithm of Chen and Kelton [25] outperforms the authors' original QI algorithm and it provides an estimate of the steady-state p.d.f. (the two-phase QI algorithm's steps are further discussed in Alexopoulos *et al.* [7]). Unfortunately, the two-phase QI algorithm can require relatively large sample sizes and was outperformed by the recent Sequest method of Alexopoulos *et al.* [7] with respect to sampling efficiency.

Dong and Nakayama [26] developed quantile-estimation methods based on Latin hypercube sampling (LHS) for a finite-horizon simulation given a fixed number of independent random inputs and a single response Y with c.d.f. $F(y)$. The goal is to generate s dependent runs yielding dependent and identically distributed responses $\{Y_1, \ldots, Y_s\}$ that are used to build an asymptotically valid CI for the quantile $y_p \equiv F^{-1}(p)$ as $s \to \infty$. The resulting CI has reduced half-length (HL) compared with the usual CI based on s i.i.d. runs. However, these LHS-based methods do not apply to an infinite-horizon simulation, where we seek to estimate the steady-state quantile y_p of the dependent responses $\{Y_k : k \geq 1\}$ generated within a single prolonged run. The latter remark also applies to the LHS-based method of Jin *et al.* [27].

Recently, Alexopoulos *et al.* [23, 7] developed two state-of-the-art automated sequential procedures for steady-state quantile estimation. The Sequest method of Alexopoulos *et al.* [7] is an automated sequential procedure that delivers CIs for nonextreme quantiles ($0.05 \leq p \leq 0.95$) with user-specified absolute or relative precision. The algorithm takes advantage of ideas from recent batch-means-based methods (Tafazzoli and Wilson [28]) and sectioning (Asmussen and Glynn [29], Section III.5a) and incorporates techniques to (i) reduce the bias in the point estimator due to the initial transient or inadequate run length; and (ii) adjust the CI HL to compensate for distorting effects due to autocorrelation or skewness in the quantile estimators computed from the nonoverlapping batches. The Sequem procedure of Alexopoulos *et al.* [23] is an extension of Sequest in the sense that it uses the maximum-transformation technique of Heidelberger and Lewis [30] to overcome problems related to the CI coverage probability for extreme quantiles ($p \geq 0.95$ or $p \leq 0.05$) in the absence of CI precision requirements. The maximum-transformation technique converts the estimation of extreme quantiles to nonextreme quantiles. For example, let $p \geq 0.95$ and let $\{Y_1^*, \ldots, Y_c^*\}$ be an independent and identically distributed (i.i.d.) sample from the c.d.f. $F(y)$. Also, let $c = \lfloor \ln(0.9)/\ln(p) \rfloor$, where $\lfloor \cdot \rfloor$ is the floor function, and define the r.v. $V = \max\{Y_1^*, \ldots, Y_c^*\}$. Since the c.d.f. of V is $F_V(v) = F(v)^c$, we have $F_V(y_p) = F(y_p)^c = p^c \equiv q$; so, estimating y_p reduces to estimating the q-quantile of the distribution of V. (To estimate lower extreme quantiles, one uses an analogous minimum transformation.)

The Sequem method arranges the dataset $\{Y_1, \ldots, Y_n\}$ into L contiguous groups, each consisting of cm consecutive observations, so that $n = cmL$. Each group is arranged in a $c \times m$ matrix whose rows are formed from consecutive nonoverlapping batches of size m within the group—that is, the first batch of m observations in the group forms the first row of the associated matrix, the second batch of m observations in the group forms the second row of the matrix, and so on. The basic observations are the maxima down each column (Alexopoulos *et al.* [23]). Sequem also uses a sectioning mechanism to obtain a point estimator of y_p: the technique applies the maximum transformation to the entire simulation-generated time series of length n by conceptually arranging that time series into a $c \times (mL)$ matrix so that the first subseries of mL consecutive observations form the first row of the matrix, the second subseries of mL consecutive observations form the second row of the matrix, and so on. For more details and an illustration, see Figures 1–2 of Alexopoulos *et al.* [23]. When applied to a suite of difficult test processes, Sequest and Sequem exhibited ease of use, close conformance to user-specified requirements on the coverage probability and precision of the CI, and outperformed previously established methods with regard to sample size requirements.

The methodology of standardized time series (STS) was proposed by Schruben [31], Goldsman and Schruben [32], and Goldsman *et al.* [33] for the estimation of the steady-state mean; see Alexopoulos *et al.* [34] for a detailed review of the related literature. With regard to this problem, Dong and Glynn [35] laid theoretical foundations for sequential, asymptotically valid CI procedures based on the STS method. The sufficient conditions for their work include the strong approximation assumption of Damerdji [36]; certain regularity conditions involving the behavior of the sequential procedure as a function of the simulation clock and sample path; and weak convergence of the denominator of the final CI pivot quantity to a random variable (r.v.) that is positive almost surely (a.s.) when the precision requirement of the CI approaches zero.

Although STS-based estimation methods for the steady-state mean date back to the early 1980s, the use of STSs for quantile estimation is only a recent development. In fact, the first application of this methodology for the very special case of i.i.d. data was proposed by Calvin and Nakayama [37]. Alexopoulos *et al.* [38, 39] have raised the stakes substantially by laying out a theoretical framework for STS-based steady-state quantile estimation in dependent processes, established asymptotic properties for a variety of variance-parameter estimators based on nonoverlapping batches, and closed various theoretical gaps related to STS-based variance-parameter estimation dating back to the 1980s. In particular, Alexopoulos *et al.* [39] formulate an estimator for the variance parameter σ_p^2 of the quantile process, which is a linear combination of (i) the average of the STS "area" estimators for σ_p^2 computed from each nonoverlapping batch (see Equations (2.14)–(2.16) in Chapter 2) and (ii) a sectioning-based variance-parameter estimator of σ_p^2 that involves the associated batched quantile estimators (BQEs) as well as the full-sample quantile estimator. Alexopoulos *et al.* [39] show that this combined estimator of σ_p^2 converges weakly to a scaled chi-squared r.v. with nearly twice the degrees of freedom (d.f.) compared to each of its constituents as the batch size tends to infinity while the batch count is held constant.

This thesis has two main goals: (1) the formulation of the theoretical foundations for STS-based procedures for estimating steady-state quantiles with CIs having given coverage probability and, potentially precision; and (2) the development and experimental evaluation of three automated methods for effective estimation of marginal quantiles in steady-state simulations: (i) the first fully automated sequential procedure for estimating steady-state *quantiles* based on STSs computed from nonoverlapping batches; (ii) a fully automated fixed-sample-size procedure for steady-state quantile estimation based on a single run; and (iii) the first fully automated fixed-sample-size procedure for steady-state quantile estimation based on independent replications.

Chapter 2 of this thesis lays out and builds on the theoretical findings of Alexopoulos *et al.* [38, 39] by presenting the asymptotic properties for a variety of variance-parameter estimators for the sample quantile computed from nonoverlapping batches. In particular, Chapter 2 contains the proof of a CLT (Theorem 2.3.4) for the vector of signed weighted areas of the STSs computed from nonoverlapping batches of the simulation output as the batch size increases while the batch count remains fixed. This result is the basis for the key steps of the sequential and fixed-sample-size procedures in Chapters 4–6 of this dissertation. Chapter 2 ends with (i) an empirical performance evaluation of several estimators of the variance parameter σ_p^2; (ii) derivation of STS-based area estimators of σ_p^2 using alternative weight functions (not in the current literature), and (iii) an empirical evaluation of the estimators for σ_p^2 in item (ii).

In Chapter 3, we perform a comparison of the variance-parameter estimators of σ_p^2 in Chapter 2 based on exact (or nearly exact) calculations of their expected values for the special case of i.i.d. samples from a set of distributions with tractable joint moments of order statistics.

Chapter 4 of this thesis formulates and evaluates the first fully automated sequential procedure for estimating steady-state *quantiles* based on STSs that are computed from nonoverlapping batches of observations. Our so called "SQSTS" procedure incorporates elements from two existing sequential methods having different objectives: the SPSTS method of Alexopoulos *et al.* [40] for estimation of the steady-state mean and the Sequest method of Alexopoulos *et al.* [7] for estimation of steady-state quantiles.

In comparison with the SPSTS and Sequest procedures, the proposed SQSTS method has the following key differences and advantages: (i) SQSTS is substantially simpler than Sequest in that the former only relies on statistical tests for independence and normality and manages to avoid CI adjustments for skewness and autocorrelation; (ii) SQSTS modifies the approach of SPSTS with adjustments targeting issues associated with the small-sample bias of the STS-based variance estimator (for instance, SQSTS adds a rebatching step); (iii) it overcomes an ad hoc compensation for the variance estimator used in SPSTS to resolve small-sample bias issues; and (iv) most importantly, it uses a combined estimator of σ_p^2 from Chapter 2 with smaller asymptotic variability (as the batch size tends to infinity) than the respective estimator of σ_p^2 employed in Sequest.

While sequential estimation methods are important, users are often constrained by simulation models that are not integrated with the underlying sequential method or by datasets that are limited due to budget constraints. For example, when the implementation of the Sequest method (Alexopoulos *et al.* [7]) in the Sequest app [41] encounters a failed statistical test or an insufficient sample size to compute a CI with a given precision, it reports an estimate of the additional observations that should be generated and halts. If the data are generated by a simulation model, the user may have to restart the model and rerun Sequest from scratch; and this cycle may need to be repeated multiple times until the method can terminate successfully. The literature contains a few fixed-sample-size procedures for estimating the steady-state mean; see Law [4]. The most efficient is the N-Skart procedure of Tafazzoli *et al.* [42] which applies the randomness test of von Neumann [43] to batch means computed from dynamically reconstructed batches with intervening "spacers." If the method determines that additional data are required, it seeks permission from the user to proceed with the computation of a CI that employs adjustments for the residual lag-1 autocorrelation and skewness between the batch means. The latter CI is delivered by default when the sample size is sufficient to pass the randomness test with an appropriate set of spaced batch means.

To the best of our knowledge, no commercial simulation software contains a fixed-sample-size procedure for computing CIs for steady-state quantiles. Both Arena [44] and Simio [45] incorporate a rudimentary fixed-sample-size procedure for estimating the steady-state *mean* based on a single replication. The procedure uses the method of nonoverlapping batch means (NBMs) (Fishman [2]) and a simple rebatching scheme that ends up with a batch count between 20 and 39. The respective batch means are subjected to the one-sided randomness test of von Neumann [43] with type-I error 0.10 (to guard against positive autocorrelation among the batch means). If the batch means pass the test, the method delivers a CI based on Student's t ratio; otherwise, it delivers an exorbitant CI HL indicating that the batch means failed the randomness test. Unfortunately, neither software package incorporates a method for computing CIs for steady-state quantiles based on a sufficiently long run. Simio computes nonparametric CIs from replicate statistics, such as the average cycle time or average waiting time in a buffer, but does not even have a function that computes a sample quantile from a tally statistic collected during a replication. (It should be clear that the distribution of the average cycle time collected during a replication is different from the marginal distribution of the cycle time in steady state.)

In Chapter 5 of this thesis, we develop and evaluate FQUEST, a fully automated fixed-sample-size procedure for computing CIs for steady-state quantiles based on a single run. Although there are a few fixed-sample-size procedures for quantile estimation (e.g., Heidelberger and Lewis [30] and Bekki *et al.* [13]), to the best of our knowledge, FQUEST is the first such method that (i) uses the STS methodology; (ii) addresses the simulation initialization problem; and (iii) warns the user when the dataset is insufficient and, subject to user's approval, delivers a heuristic CI. Although FQUEST is applicable to i.i.d.samples, one can use simpler nonparametric methods (Conover [46], pp. 143–148) or apply more advanced variance reduction methods; cf. Dong and Nakayama [26] and references therein. Our FQUEST method draws elements from three procedures: (i) the SQSTS method presented in Chapter 4; (ii) the Sequest method of Alexopoulos *et al.* [7], and (iii) the N-Skart method of Tafazzoli *et al.* [42]. Since the aforementioned methods have different objectives, as explained above, FQUEST delineates from all three with regard to its scope, structure, and the computation of the final CI. Specifically, FQUEST is designed to provide a CI for a selected steady-state quantile, with a user-specified error probability, based on a single time series of an arbitrary fixed length. If the sample size is insufficient, FQUEST issues a warning and the user has the option to terminate the procedure early without getting a CI. In any case, the user can utilize the output of FQUEST as the first step for obtaining a conservative estimate of the sample size required to compute a CI with a certain absolute or relative precision.

FQUEST incorporates the combined variance-parameter estimator presented in Chapter 2 and also employed in the sequential SQSTS method in Chapter 4. The theoretical basis for its statistical tests is outlined in Theorem 2.3.4. The method employs this result to remove a subset of data that are potentially contaminated by the initial transient as well as to obtain a sufficiently large batch size (subject to the sample size limitation). If all statistical tests are passed, FQUEST constructs a CI based on the empirical quantile computed from the entire (truncated) sample and the combined estimator of the variance parameter. However, when some of the statistical tests fail due to an insufficient sample size, the algorithm notifies the user asking for permission to proceed with the construction of a CI. If the user approves, FQUEST delivers the full-sample point estimator and an asymmetric CI for y_p formed from a set of CIs obtained from the full-sample point estimator, the BQEs, and the batched (average) STS area estimator for the variance parameter of the quantile process; otherwise, the process is terminated.

Steady-state analysis methods based on a single simulation replication are convenient in the sense that data from the onset of the run may have to be eliminated to diminish the effects of initialization bias. Unfortunately, the potential of pronounced autocorrelation in the underlying output process may require excessively large sample sizes to attenuate this correlation effect and yield reliable CIs for the performance measure of interest. On the other hand, steady-state estimation methods based on independent replications are convenient and reduce the correlation problems. For practical purposes the need for such tools is further enhanced by the fact that multiple replications can be made simultaneously on different cores/threads within a single computer or on different computers on a network, provided that the software being used for simulation supports this (Law [4]). On the negative side, independent replications can induce systematic bias if insufficient truncation is applied at the onset of each replication (Alexopoulos and Goldsman [47], Fishman [48]). Further, for fixed-sample-size procedures, one has to decide on the number of replications and the run length within each replication.

In Chapter 6 of this thesis, we develop and evaluate FIRQUEST, the first fully automated, fixed-sample-size method for estimating steady-state quantiles based on independent replications. FIRQUEST is essentially an extension of the FQUEST procedure in Chapter 5 with adjustments to handle the user-specified number of independent replications and more aggressive steps to remove any potential warm-up effects that can induce a systematic bias across replicate estimates (Alexopoulos and Goldsman [47]).

The remainder of this thesis is organized as follows. Chapter 2 contains the theoretical results that constitute the basis of the proposed methods in Chapters 4–6 and provides results from the empirical evaluation of a variety of variance-parameter estimators. Chapter 3 contains exact (or nearly exact) calculations for the expected values of the variance-parameter estimators in Chapter 2 for the special case of i.i.d. data. Chapter 4 presents and evaluates SQSTS, the first fully automated sequential procedure for estimating steady-state *quantiles* based on STSs that are computed from nonoverlapping batches of observations. Chapter 5 presents and evaluates FQUEST, a fully automated, fixed-sample-size method for estimating steady-state quantiles based on a single run. Chapter 6 presents and evaluates FIRQUEST, the first fully automated, fixed-sample-size method for estimating steady-state quantiles based on a user-specified number of independent replications. Finally, Chapter 7 contains overall conclusions, final remarks, and potential future directions.

CHAPTER 2

THEORETICAL FOUNDATIONS AND EMPIRICAL EVALUATION OF VARIANCE-PARAMETER ESTIMATORS AND CONFIDENCE INTERVALS FOR STEADY-STATE QUANTILES

This chapter contains the basic notation, assumptions, and core results that form the foundation for designing the procedures in Chapters 4–6 to estimating marginal quantiles in steady-state simulations.

Specifically, in Section 2.1 we introduce the notation that will be used throughout this thesis. Section 2.2 states the main assumptions needed to establish the core theoretical results for quantile estimation. Section 2.3 presents the asymptotic properties for quantiles based on nonoverlapping batches that form the foundation of the theory needed for the design of effective procedures for quantile estimation. In Section 2.4 we discuss the computational effort required to efficiently compute the estimates of the variance parameter of the quantile estimation process based on the STS methodology. Section 2.5 introduces the main test processes that will be used for the empirical performance evaluation of the quantile estimation methods of this thesis. Section 2.6 contains an initial empirical evaluation of the performance of the main variance-parameter estimators, while Section 2.7 contains an extended empirical evaluation of the performance of a larger set of variance-parameter estimators. In Section 2.8 we assess weight functions from the literature for STS based variance parameter estimation. In Section 2.9 we develop new alternative weight functions, while in Section 2.10 we evaluate their performance.

2.1 Notation

For $p \in (0, 1)$, the p-quantile of a r.v. X with c.d.f. $F(y)$ is defined as

$$y_p \equiv F^{-1}(p) \equiv \inf\{y : F(y) \geq p\}.$$

Our goal is the computation of a point estimate and a CI for y_p based on a stationary sample path $\{Y_k : k \geq 1\}$, which is a warmed-up (i.e., truncated and reindexed) version of the original sequence of simulation outputs. Let $\{Y_k : k = 1, \ldots, n\}$ denote a time series of length n consisting of the first n successive outputs, and let $Y_{(1)} \leq \cdots \leq Y_{(n)}$ be the respective order statistics. The classical point estimator of y_p is the empirical p-quantile $\widetilde{y}_p(n) \equiv Y_{(\lceil np \rceil)}$, where $\lceil \cdot \rceil$ denotes the ceiling function.

For each $y \in \mathbb{R}$ and $k \geq 1$, we define the indicator r.v. $I_k(y) \equiv 1$ if $Y_k \leq x$, and $I_k(y) \equiv 0$ otherwise; hence $\mathrm{E}[I_k(y_p)] = p$. For $n \geq 1$, we let $\overline{I}(y_p; n) \equiv n^{-1} \sum_{k=1}^{n} I_k(y_p)$; and for each $\ell \in \mathbb{Z}$, we let $\rho_I(\ell; y_p) \equiv \mathrm{Corr}[I_k(y_p), I_{k+\ell}(y_p)]$ denote the autocorrelation function of the indicator process $\{I_k(y_p) : k \geq 1\}$ at lag ℓ. Below we also adopt the following notation: Z denotes an r.v. from $N(0, 1)$, the standard normal distribution; $\mathbf{Z}_\nu \equiv \left[Z_1, \ldots, Z_\nu\right]^{\mathsf{T}}$ denotes a $\nu \times 1$ vector whose components are i.i.d. $N(0, 1)$; χ^2_ν denotes a chi-squared r.v. with ν degrees d.f.; t_ν denotes an r.v. having Student's t distribution with ν d.f.; and $t_{\delta,\nu}$ denotes the δ-quantile of t_ν.

The assumptions and the core results that are outlined in the following sections are the key elements for variance cancellation methods (Asmussen and Glynn [29], Chapters III–IV) to develop $100(1 - \alpha)\%$ CIs for y_p with form

$$\widetilde{y}_p(n) \pm t_{1-\alpha/2,\nu} \widehat{\sigma}_p / \sqrt{n}, \tag{2.1}$$

where $\widehat{\sigma}^2_p$ is an estimator of the (quantile) variance parameter $\sigma^2_p \equiv \lim_{n\to\infty} n\mathrm{Var}\left[\widetilde{y}_p(n)\right]$ and the d.f. ν depend on the underlying quantile-estimation method. The CIs in Equation

(2.1) will be asymptotically valid in the sense that their coverage probability will tend to the nominal value $1-\alpha$ as $n \to \infty$.

2.2 Assumptions

In this section we list the key assumptions for the processes $\{Y_k : k \geq 1\}$ and $\{I_k(y_p) : k \geq 1\}$. Let $D \equiv D[0,1]$ be the space of real-valued functions on $[0,1]$ that are right continuous with left-hand limits, and let $C \equiv C[0,1]$ be the subspace of continuous functions on the same interval. We use the following notation and key properties of the space D. Each $\zeta \in D$ is bounded on $[0,1]$ with at most countably many discontinuities; thus ζ is continuous almost everywhere (a.e.) on $[0,1]$ (Billingsley [19], p. 122; Kolmogorov and Fomin [49], §§28.3–28.4). Let $\|\zeta\| \equiv \sup\{|\zeta(t)| : t \in [0,1]\}$ be the sup norm, and let Λ denote the class of strictly increasing, continuous mappings of $[0,1]$ onto itself, where $\mathbb{I} \in \Lambda$ denotes the identity map. Thus each $\lambda \in \Lambda$ must have $\lambda(0) = 0$ and $\lambda(1) = 1$. For $\zeta, \omega \in D$, let $d(\zeta, \omega) \equiv \inf_{\lambda \in \Lambda} \max\{\|\lambda - \mathbb{I}\|, \|\zeta - \omega \circ \lambda\|\}$ denote the distance between ζ and ω in the Skorohod J_1 metric on D, where $\omega \circ \lambda(t) \equiv \omega[\lambda(t)]$ for each $t \in [0,1]$ (Billingsley [19], pp. 121–129; Whitt [50], §3.3). Hence with the metric $d(\zeta, \omega)$, the space D is separable—i.e., it contains a countable dense subset (Billingsley [19], Theorem 12.2). Since the definition of $d(\zeta, \omega)$ includes the case where $\lambda(t) = \mathbb{I}(t) \equiv t$ for $t \in [0,1]$, we have $d(\zeta, \omega) \leq \|\zeta - \omega\|$ for $\zeta, \omega \in D$.

Geometric-Moment Contraction (GMC) Condition (Wu [8]). The process $\{Y_k : k \geq 1\}$ is defined by a function $\xi(\cdot)$ of a sequence of i.i.d. r.v.'s $\{\varepsilon_k : k \in \mathbb{Z}\}$ such that $Y_k = \xi(\ldots, \varepsilon_{k-1}, \varepsilon_k)$ for $k \geq 0$. Moreover, there exist constants $\psi > 0$, $C^* > 0$, and $r \in (0,1)$ such that for two independent sequences $\{\varepsilon_k : k \in \mathbb{Z}\}$ and $\{\varepsilon'_k : k \in \mathbb{Z}\}$ each consisting of i.i.d. variables distributed like ε_0, we have

$$\mathrm{E}[|\xi(\ldots, \varepsilon_{-1}, \varepsilon_0, \varepsilon_1, \ldots, \varepsilon_k) - \xi(\ldots, \varepsilon'_{-1}, \varepsilon'_0, \varepsilon_1, \ldots, \varepsilon_k)|^{\psi}] \leq C^* r^k, \quad \text{for } k \geq 0.$$

The GMC condition holds for a large collection of processes, including autoregressive–moving average time series (Shao and Wu [51]), a rich collection of linear and nonlinear processes with short-range dependence, and a broad class of Markov chains; see Alexopoulos *et al.* [7, 39] for an extended list of citations and empirical methods for verifying the GMC assumption. Recently, Dingeç *et al.* [52] have established the validity of the GMC condition for the waiting-time process (prior to service) in an M/M/1 queueing system and a G/G/1 system with non-heavy-tailed service-time distributions.

Density-Regularity (DR) Condition. The p.d.f. $f(\cdot)$ is bounded on $\mathbb{R}$ and continuous a.e. on $\mathbb{R}$; moreover, $f(y_p) > 0$, and the derivative $f'(y_p)$ exists.

Short-Range Dependence (SRD) of the Indicator Process. The indicator process $\{I_k(y_p) : k \geq 1\}$ has the SRD property so that

$$0 < \sum_{\ell \in \mathbb{Z}} \rho_I(\ell; y_p) \leq \sum_{\ell \in \mathbb{Z}} |\rho_I(\ell; y_p)| < \infty. \tag{2.2}$$

Thus the variance parameters for the r.v.'s $\overline{I}(y_p; n)$ and $\widetilde{y}_p(n)$ satisfy the relations

$$\left.\begin{aligned} \sigma^2_{I(y_p)} \equiv \lim_{n\to\infty} n\mathrm{Var}\big[\overline{I}(y_p; n)\big] = p(1-p) \sum_{\ell \in \mathbb{Z}} \rho_I(\ell; y_p) \in (0, \infty), \\ \sigma^2_p = \lim_{n\to\infty} n\mathrm{Var}\big[\widetilde{y}_p(n)\big] = \frac{\sigma^2_{I(y_p)}}{f^2(y_p)} \in (0, \infty). \end{aligned}\right\} \tag{2.3}$$

Functional Central Limit Theorem (FCLT) for the Indicator Process. We define the following sequence of random functions $\{\mathscr{I}_n : n \geq 1\}$ in D,

$$\mathscr{I}_n(t; y_p) \equiv \frac{\lfloor nt \rfloor}{\sigma_{I(y_p)} n^{1/2}} [\overline{I}(y_p; \lfloor nt \rfloor) - p], \quad \text{for } t \in [0,1] \text{ and } n \geq 1, \tag{2.4}$$

where $\lfloor \cdot \rfloor$ denotes the floor function. We assume that this random-function sequence satisfies the FCLT

$$\mathscr{I}_n \underset{n \to \infty}{\Longrightarrow} \mathscr{W} \tag{2.5}$$

in D with the appropriate metric, where $\mathscr{W}$ denotes a standard Brownian motion on $[0,1]$; and $\underset{n\to\infty}{\Longrightarrow}$ denotes weak convergence as $n \to \infty$ (Billingsley [19], pp. 1–6 and Theorem 2.1). Hereafter, the argument y_p is omitted from the notation for random functions unless it is needed to avoid ambiguity.

Remark 2.2.1. If the SRD condition defined by Equations (2.2) and (2.3) holds, then for all practical purposes it is generally reasonable to assume the validity of the FCLT defined by Equations (2.4) and (2.5) (Whitt [50], p. 107, last paragraph).

Remark 2.2.2. Recently, Dingeç *et al.* [53] proved that if $\{Y_k : k \geq 1\}$ is stationary and satisfies the GMC and DR conditions, then the associated indicator process $\{I_k(y_p) : k \geq 1\}$ satisfies the SRD properties in Equation (2.3). This result and Remark 2.2.1 provide good theoretical and practical evidence of the mutual compatibility of the GMC, SRD, and FCLT conditions.

2.3 Asymptotic Properties Based on Nonoverlapping Batches

We focus now on the asymptotic properties that are based on nonoverlapping batches. Given a fixed batch count $b \geq 2$, for $j = 1, \ldots, b$, the jth nonoverlapping batch of size $m \geq 1$ consists of the subsequence $\{Y_{(j-1)m+1}, \ldots, Y_{jm}\}$, where we assume $n = bm$. The batch mean of the associated indicator r.v.'s for the jth batch is $\overline{I}(y_p; j, m) \equiv m^{-1} \sum_{\ell=1}^{m} I_{(j-1)m+\ell}(y_p)$. Similarly to the full-sample case, we define the order statistics $Y_{j,(1)} \leq \cdots \leq Y_{j,(m)}$ corresponding to the jth batch and denote the jth BQE of y_p as $\widehat{y}_p(j,m) \equiv Y_{j,(\lceil mp \rceil)}$.

Theorem 2.3.1. *(Alexopoulos* et al. *[7]) If the output process $\{Y_k : k \geq 1\}$ satisfies the GMC and DR conditions, and the indicator process $\{I_k(y_p) : k \geq 1\}$ satisfies the SRD and the respective FCLT conditions, then we obtain the Bahadur representation*

$$\widehat{y}_p(j,m) = y_p - \frac{\overline{I}(y_p; j, m) - p}{f(y_p)} + O_{\text{a.s.}}\left[\frac{(\log m)^{3/2}}{m^{3/4}}\right], \quad \textit{as } m \to \infty \tag{2.6}$$

for $j = 1, \ldots, b$, where the big-$O_{\text{a.s.}}$ notation for the remainder

$$Q_{j,m} \equiv \widehat{y}_p(j,m) - y_p + \frac{\overline{I}(y_p; j, m) - p}{f(y_p)} = O_{\text{a.s.}}\left[\frac{(\log m)^{3/2}}{m^{3/4}}\right] \tag{2.7}$$

means there exist associated r.v.'s $\mathscr{U}_j$ and $\mathscr{R}_j$ that are bounded a.s. and satisfy

$$|Q_{j,m}| \le \mathscr{U}_j \frac{(\log m)^{3/2}}{m^{3/4}}, \quad \textit{for } m \ge \mathscr{R}_j \textit{ and } j = 1, \ldots, b \textit{ a.s.} \tag{2.8}$$

Further,

$$m^{1/2}\big[\widehat{y}_p(1,m) - y_p, \ldots, \widehat{y}_p(b,m) - y_p\big]^{\mathsf{T}} \underset{m \to \infty}{\Longrightarrow} \sigma_p \mathbf{Z}_b \tag{2.9}$$

in $\mathbb{R}^b$ with the standard Euclidean metric.

2.3.1 Standardized Time Series for Quantile Estimation

The full-sample STS process for quantile estimation is defined as

$$T_n(t) \equiv \frac{\lfloor nt \rfloor}{n^{1/2}}[\widetilde{y}_p(n) - \widetilde{y}_p(\lfloor nt \rfloor)], \quad \text{for } n \ge 1 \text{ and } t \in [0,1], \tag{2.10}$$

where $\widetilde{y}_p(\lfloor nt \rfloor)$ is the empirical p-quantile (i.e., the $\lceil p\lfloor nt \rfloor \rceil$-th order statistic) computed from the partial sample $\{Y_k : k = 1, \ldots, \lfloor nt \rfloor\}$. We have the following key result.

Theorem 2.3.2. *(Alexopoulos* et al. *[39]) If $\{Y_k : k \ge 1\}$ satisfies the assumptions of Theorem 2.3.1, then in $\mathbb{R} \times D$,*

$$\big[n^{1/2}(\widetilde{y}_p(n) - y_p), T_n\big] \underset{n \to \infty}{\Longrightarrow} \sigma_p\big[\mathscr{W}(1), \mathscr{B}\big],$$

where $\mathscr{B}(t) \equiv \mathscr{W}(t) - t\mathscr{W}(1)$ for $t \in [0,1]$ is a standard Brownian bridge process that is independent of $\mathscr{W}(1)$.

The full-sample STS area estimator of the variance parameter σ_p^2 is $A_p^2(w;n)$, where:

$$A_p(w;n) \equiv n^{-1} \sum_{k=1}^{n} w(k/n) T_n(k/n), \quad \text{for } n \geq 1 \tag{2.11}$$

and $w(\cdot)$ is a deterministic weight function that is bounded and continuous almost everywhere in $[0,1]$ (so that $w(t)\mathscr{B}(t)$ is Riemann integrable on $[0,1]$); and the r.v.

$$Z(w) \equiv \int_0^1 w(t)\mathscr{B}(t)\,dt \sim N(0,1). \tag{2.12}$$

Remark 2.3.1. The r.v. $Z(w)$ is the signed, weighted area enclosed by the random function $w(t)\mathscr{B}(t)$ for $t \in [0,1]$ and the t-axis so that $Z(w)$ is normally distributed. The r.v.'s $\{A_p(w;n) : n \geq 1\}$ are designed to yield the following weak-convergence results that parallel Equation (2.9):

$$A_p(w;n) \underset{n \to \infty}{\Longrightarrow} \sigma_p Z(w) \quad \text{and} \quad A_p^2(w;n) \underset{n \to \infty}{\Longrightarrow} \sigma_p^2 \chi_1^2. \tag{2.13}$$

Weight functions that satisfy condition (2.12) include the constant $w_0(t) \equiv \sqrt{12}$ (Schruben [31]), the quadratic $w_2(t) \equiv \sqrt{840}(3t^2 - 3t + 1/2)$ (Goldsman *et al.* [33]), and the orthonormal family $\{w_{\cos,\ell}(t) \equiv \sqrt{8}\pi\ell\cos(2\pi\ell t) : \ell = 1, 2, \ldots\}$ (Foley and Goldsman [54]). A brief discussion on the effectiveness of these weights functions for the quantile estimation problem at hand will be given in Remark 2.3.2 below.

Theorem 2.3.3. *(Alexopoulos* et al. *[39]) If $\{Y_k : k \geq 1\}$ satisfies the assumptions of Theorem 2.3.1, then Equation (2.13) holds.*

The aforementioned results can be extended for the case of nonoverlapping batches of size m (so that $n = bm$). For $j = 1, \ldots, b$, we define $\widehat{y}_p(j, \lfloor mt \rfloor)$ as the empirical p-quantile computed from the partial sample $\{Y_{(j-1)m+k} : k = 1, \ldots, \lfloor mt \rfloor\}$, and the STS-based quantile-estimation process formed from the batch j as

$$T_{j,m}(t) \equiv \frac{\lfloor mt \rfloor}{m^{1/2}} \left[\widehat{y}_p(j,m) - \widehat{y}_p(j, \lfloor mt \rfloor) \right], \quad \text{for } t \in [0,1] \text{ and } m \geq 1. \tag{2.14}$$

Further, we define the signed (weighted) area computed from batch j as

$$A_p(w; j, m) \equiv m^{-1} \sum_{k=1}^{m} w(k/m) T_{j,m}(k/m). \tag{2.15}$$

The batched STS area estimator is the average of the squared signed areas, namely,

$$\mathscr{A}_p(w; b, m) \equiv b^{-1} \sum_{j=1}^{b} A_p^2(w; j, m). \tag{2.16}$$

Since the underlying process $\{Y_k : k \geq 1\}$ is stationary, as $m \to \infty$ each $T_{j,m}(\cdot)$ has the same asymptotic distribution as the full-sample STS $T_n(\cdot)$ in Theorem 2.3.2, namely $T_{j,m} \underset{m \to \infty}{\Longrightarrow} \sigma_p \mathscr{B}(\cdot)$. Similarly, because $\mathscr{A}_p^2(w; 1, m) = A_p^2(w; m)$ for $m \geq 1$, Theorem 2.3.3 and the stationarity of the underlying process $\{Y_k : k \geq 1\}$ ensure that as $m \to \infty$, each of the signed areas weakly converges to $\sigma_p Z$, that is $A_p(w; j, m) \underset{m \to \infty}{\Longrightarrow} \sigma_p Z$ for $j = 1, \ldots, b$.

Theorems 2.3.4 and 2.3.5 below establish the asymptotic validity of the main CIs used in the Sequest method of Alexopoulos *et al.* [7], the SQSTS sequential method in Chapter 4, and the fixed-sample-size methods in Chapters 5 and 6. In particular, Theorem 2.3.4 establishes the asymptotic independence of the quantile-based STS processes $\{T_{j,m}(\cdot) : j = 1, \ldots, b\}$ as well as the asymptotic independence of the respective signed areas $\{A_p(w; j, m) : j = 1, \ldots, b\}$ as the batch size $m \to \infty$. The convergence of $\{A_p(w; j, m) : j = 1, \ldots, b\}$ to i.i.d. $\sigma_p Z$ r.v.'s constitutes the basis for the statistical tests of our newly developed procedures in Chapters 4–6.

Theorem 2.3.4. *If $\{Y_k : k \geq 1\}$ satisfies the assumptions of Theorem 2.3.1, then as $m \to \infty$, the $b \times 1$ vector of the signed areas $\left[A_p(w; 1, m), \ldots, A_p(w; b, m)\right]^{\mathsf{T}}$ converges weakly to* *the same distributional limit as the (scaled) vector of BQEs in Theorem 2.3.1:*

$$\left[A_p(w;1,m),\ldots,A_p(w;b,m)\right]^{\mathsf{T}} \underset{m\to\infty}{\Longrightarrow} \sigma_p \boldsymbol{Z}_b. \tag{2.17}$$

Further,

$$\mathscr{A}_p(w;b,m) \underset{m\to\infty}{\Longrightarrow} \sigma_p^2\chi_b^2/b. \tag{2.18}$$

Proof. Most of the proof is devoted to establishing Equation (2.17). Then Equation (2.18) follows immediately by a straightforward application of the continuous mapping theorem (Whitt [50]). We define the following notation:

$$\left.\begin{array}{rcl} \mathscr{I}_{j,m}(t) & \equiv & \frac{\lfloor mt\rfloor}{\sigma^2_{I(y_p)}m^{1/2}}\big(\bar{I}(y_p;j,\lfloor mt\rfloor)-p\big), \\ \mathscr{T}_{j,m}(t) & \equiv & \sigma_p[\mathscr{I}_{j,m}(t)-t\,\mathscr{I}_{j,m}(1)], \\ \Delta_n(\zeta,w) & \equiv & n^{-1}\sum_{k=1}^n w(k/n)\zeta(k/n), \quad \text{and} \\ \Delta(\zeta,w) & \equiv & \int_0^1 w(t)\zeta(t)\,dt, \end{array}\right\} \text{ for } t\in[0,1] \text{ and } j=1,\ldots,b, \tag{2.19}$$

and $\zeta \in D$. From the aforementioned it follows that

$$A_p(w;j,m) \equiv \Delta_m(T_{j,m},w), \quad \text{for } j=1,\ldots,b \text{ and } m\geq 1.$$

For $j=1,\ldots,b$ and for each probabilistic or deterministic element $\zeta\in D$, we define the functionals $\mathfrak{X}_j\{\zeta\}\in D$, and $\mathfrak{B}_j\{\zeta\}\in D$ as:

$$\left.\begin{array}{rcl} \mathfrak{X}_j\{\zeta\}(t) & \equiv & b^{1/2}\big[\zeta\big(\tfrac{j+t-1}{b}\big)-\zeta\big(\tfrac{j-1}{b}\big)\big], \quad \text{and} \\ \mathfrak{B}_j\{\zeta\}(t) & \equiv & \mathfrak{X}_j\{\zeta\}(t)-t\mathfrak{X}_j\{\zeta\}(1), \end{array}\right\} \text{ for } t\in[0,1]. \tag{2.20}$$

To prove the desired conclusions (2.17) and (2.18), we will need to apply the generalized continuous mapping theorem (GCMT) (Whitt [50], Theorem 3.4.4). In this situation, we must first prove the following intermediate result:

$$\left.\begin{array}{l}\text{For every } \eta \in C \text{ and every sequence } \{\eta_n : n \geq 1\} \subset D \text{ with } \lim\limits_{n\to\infty} d(\eta_n, \eta) = 0, \\ \text{we have for } j = 1, \ldots, b, \ \lim\limits_{n\to\infty} d(\mathfrak{X}_j\{\eta_n\}, \mathfrak{X}_j\{\eta\}) = 0, \\ \lim\limits_{n\to\infty} d(\mathfrak{B}_j\{\eta_n\}, \mathfrak{B}_j\{\eta\}) = 0, \quad \text{and} \quad \lim\limits_{m\to\infty} \Delta_m(\mathfrak{B}_j\{\eta_n\}, w) = \Delta(\mathfrak{B}_j\{\eta\}, w).\end{array}\right\} \tag{2.21}$$

We define the sequence $\{\delta_n : n \geq 1\}$ as

$$\delta_n \equiv d(\eta_n, \eta) + n^{-1}, \quad \text{for } n \geq 1 \text{ so that } \lim_{n\to\infty} \delta_n = 0. \tag{2.22}$$

The definition of $d(\eta_n, \eta)$ and the inequality $d(\eta_n, \eta) < \delta_n$ imply that for every $n \geq 1$, there exists $\lambda_n \in \Lambda$, such that the following equations hold

$$\left.\begin{array}{rl}\|\lambda_n - \mathbb{I}\| = & \sup_{t\in[0,1]} |\lambda_n(t) - t| < \delta_n, \quad \text{and} \\ \|\eta_n - \eta\circ\lambda_n\| = & \sup_{t\in[0,1]} |\eta_n(t) - \eta\circ\lambda_n(t)| < \delta_n.\end{array}\right\} \tag{2.23}$$

Indeed, if such λ_n did not exist, then by the definition of $d(\eta_n, \eta)$, we would have that $d(\eta_n, \eta) > \delta_n$, a contradiction.

Since $\delta_n \to 0$ as $n \to \infty$, the second equation in (2.23) implies $\lim_{n\to\infty} \|\eta_n - \eta\circ\lambda_n\| = 0$. The first part of Equation (2.23) implies that $\lambda_n \xrightarrow[n\to\infty]{} \mathbb{I}$ uniformly. Further, notice that η is also uniformly continuous on the compact set $[0, 1]$ (Rudin [55],Theorem 4.19). In the next paragraph we will establish the uniform convergence of $\eta\circ\lambda_n$ to η as $n \to \infty$. Recall that λ_n and $\mathbb{I}$ are bounded on the compact set $[0, 1]$.

Since η is uniformly continuous, for every $\epsilon > 0$ there is a $\delta > 0$ such that for every $y_1, y_2 \in [0, 1]$ with $|y_1 - y_2| < \delta$, we have $|\eta(y_1) - \eta(y_2)| < \epsilon$. Moreover, since λ_n converges uniformly to $\mathbb{I}$, there exists an n' such that $|\lambda_n(y) - \mathbb{I}(y)| < \delta$ for all $n > n'$ and $y \in [0, 1]$. By considering $y_1 = \lambda_n(y)$ and $y_2 = \mathbb{I}(y)$, for every $\epsilon > 0$, it follows that $|\eta(\lambda_n(y)) - \eta(\mathbb{I}(y))| < \epsilon$ for all $n > n'$ and all $y \in [0, 1]$. This proves that $\eta\circ\lambda_n \xrightarrow[n\to\infty]{} \eta\circ\mathbb{I} = \eta$

uniformly; hence

$$\lim_{n\to\infty} \|\eta - \eta\circ\lambda_n\| = 0 \tag{2.24}$$

(Rudin [55],Theorem 7.9).

Next we show that $d(\mathfrak{X}_j\{\eta_n\}, \mathfrak{X}_j\{\eta\}) \to 0$; and $d(\mathfrak{B}_j\{\eta_n\}, \mathfrak{B}_j\{\eta\}) \to 0$ for $j = 1, \ldots, b$ as $n \to \infty$. For each $t \in [0,1]$ and $n \geq 1$, by the triangle inequality and the definition of $\|\cdot\|$, we have

$$\begin{aligned}
\left|b^{1/2}\left[\eta_n(t) - \eta(t)\right]\right| &\leq \left|b^{1/2}\left[\eta_n(t) - \eta\circ\lambda_n(t)\right]\right| + \left|b^{1/2}\left[\eta(t) - \eta\circ\lambda_n(t)\right]\right| \\
&\leq b^{1/2}\left[\,\|\eta_n - \eta\circ\lambda_n\| + \|\eta - \eta\circ\lambda_n\|\,\right], && (2.25)\\
|\mathfrak{X}_j\{\eta_n\}(t) - \mathfrak{X}_j\{\eta\}(t)| &= \left|b^{1/2}\left[\eta_n\left(\tfrac{j+t-1}{b}\right) - \eta\left(\tfrac{j+t-1}{b}\right)\right] - b^{1/2}\left[\eta_n\left(\tfrac{j-1}{b}\right) - \eta\left(\tfrac{j-1}{b}\right)\right]\right| \\
&\leq 2b^{1/2}\left[\,\|\eta_n - \eta\circ\lambda_n\| + \|\eta - \eta\circ\lambda_n\|\,\right] && (2.26)\\
|\mathfrak{B}_j\{\eta_n\}(t) - \mathfrak{B}_j\{\eta\}(t)| &\leq |\mathfrak{X}_j\{\eta_n\}(t) - \mathfrak{X}_j\{\eta\}(t)| + t|\mathfrak{X}_j\{\eta_n\}(1) - \mathfrak{X}_j\{\eta\}(1)| \\
&\leq 4b^{1/2}\left[\,\|\eta_n - \eta\circ\lambda_n\| + \|\eta - \eta\circ\lambda_n\|\,\right]. && (2.27)
\end{aligned}$$

Equations (2.26) and (2.27) are obtained by using Equations (2.25) and (2.26), respectively. Equations (2.26)–(2.27) and the definition of $\|\cdot\|$ imply that

$$\left.\begin{aligned}
\|\mathfrak{X}_j\{\eta_n\} - \mathfrak{X}_j\{\eta\}\| &\leq 2b^{1/2}\left[\,\|\eta_n - \eta\circ\lambda_n\| + \|\eta - \eta\circ\lambda_n\|\,\right] \quad \text{and} \\
\|\mathfrak{B}_j\{\eta_n\} - \mathfrak{B}_j\{\eta\}\| &\leq 4b^{1/2}\left[\,\|\eta_n - \eta\circ\lambda_n\| + \|\eta - \eta\circ\lambda_n\|\,\right],
\end{aligned}\right\} \tag{2.28}$$

for $j = 1, \ldots, b$.

Results similar to Equation (2.28) are needed for $|\Delta_m(\mathfrak{B}_j\{\eta_n\}, w) - \Delta(\mathfrak{B}_j\{\eta\}, w)|$, for $j = 1, \ldots, b$. By the triangle inequality, we have

$$\begin{aligned}
|\Delta_m(\mathfrak{B}_j\{\eta_n\}, w) - \Delta(\mathfrak{B}_j\{\eta\}, w)| \leq\ & |\Delta_m(\mathfrak{B}_j\{\eta_n\}, w) - \Delta_m(\mathfrak{B}_j\{\eta\}, w)| \\
& + |\Delta_m(\mathfrak{B}_j\{\eta\}, w) - \Delta(\mathfrak{B}_j\{\eta\}, w)|,
\end{aligned} \tag{2.29}$$

for $m \geq 1$. Since $w(\cdot)\mathfrak{B}_j\{\eta\}(\cdot)$ is Riemann integrable on $[0, 1]$, we have

$$\lim_{m\to\infty} \Delta_m(\mathfrak{B}_j\{\eta\}, w) = \Delta(\mathfrak{B}_j\{\eta\}, w). \tag{2.30}$$

By the triangle inequality, the definition of $\|\cdot\|$, and Equation (2.27), we also have

$$\begin{aligned}|\Delta_m(\mathfrak{B}_j\{\eta_n\}, w) - \Delta_m(\mathfrak{B}_j\{\eta\}, w)| &\leq m^{-1} \sum_{k=1}^{m} |w(k/m)[\mathfrak{B}_j\{\eta_n\}(k/m) - \mathfrak{B}_j\{\eta\}(k/m)]| \\ &\leq 4\|w\|b^{1/2}\big[\,\|\eta_n - \eta\circ\lambda_n\| + \|\eta - \eta\circ\lambda_n\|\big]. \end{aligned}\tag{2.31}$$

Equations (2.22)–(2.24) and (2.28)–(2.31) imply that the intermediate result (2.21) holds.

Next we must verify that assumptions of the GCMT are satisfied, before it is applied to the weak convergence results in Equation (2.21). This verification requires some care. Let

$$\begin{aligned}\mathfrak{F} \equiv \Big\{\gamma \in D : &\text{ There exists } \{\gamma_k : k \geq 1\} \subset D \text{ with} \\ &\lim_{k\to\infty} d(\gamma_k, \gamma) = 0, \text{ but } \Delta_k(\gamma_k, w) \nrightarrow \Delta(\gamma, w)\Big\}\end{aligned}\tag{2.32}$$

be the set of every deterministic element γ in D to which some deterministic sequence of elements $\{\gamma_k : k \geq 1\}$ in D converges with respect to d, but the associated real sequence $\big\{\Delta_k(\gamma_k, w) : k \geq 1\big\}$ does not converge to $\Delta(\gamma, w)$. If in Equation (2.32) we take

$$\left.\begin{aligned}\gamma_k &\equiv \mathfrak{B}_j\{\eta_{kb}\}, \qquad \text{for } k \geq 1 \quad \text{and} \\ \gamma &\equiv \mathfrak{B}_j\{\eta\},\end{aligned}\right\}$$

then we observe that since $\eta \in C$, Equation (2.20) ensures that $\gamma \in C$ and $\gamma_k \in D$ for $k \geq 1$.

For this assignment of γ and the $\{\gamma_k : k \geq 1\}$, we have

$$\left.\begin{aligned} \lim_{k\to\infty} d(\gamma_k, \gamma) &= \lim_{k\to\infty} d(\mathfrak{B}_j\{\eta_{kb}\}, \mathfrak{B}_j\{\eta\}) \\ &\leq \|\mathfrak{B}_j\{\eta_{kb}\}, \mathfrak{B}_j\{\eta\}\| \\ &= 0, \end{aligned}\right\} \tag{2.33}$$

by Equations (2.22)–(2.24) and (2.28). On the other hand, Equation (2.21) assumes that for arbitrary deterministic elements $\eta \in C$ and $\{\eta_n : n \geq 1\} \subset D$ with $\lim_{n\to\infty} d(\eta_n, \eta) = 0$, we have

$$\lim_{k\to\infty} \Delta_k(\gamma_k, w) = \lim_{k\to\infty} \Delta_k(\mathfrak{B}_j\{\eta_{kb}\}, w) \tag{2.34}$$

$$= \lim_{m\to\infty} \Delta_m(\mathfrak{B}_j\{\eta_n\}, w) \tag{2.35}$$

$$= \Delta(\mathfrak{B}_j\{\eta\}, w) \tag{2.36}$$

$$= \Delta(\gamma, w), \tag{2.37}$$

where: Equation (2.34) follows from the definition of γ_k; Equation (2.35) follows from the reindexing scheme $m \equiv k$ and $n \equiv bk$ in Equation (2.34); Equation (2.36) follows from Equation (2.21); and Equation (2.37) follows from the definition of γ. Since η is an arbitrary element of C, Equations (2.33) and (2.37) together imply $C \cap \mathfrak{F} = \varnothing$. Since the random element $\mathscr{B}$ belongs to C always, no realization of $\mathscr{B}$ belongs to $\mathfrak{F}$ so that in the underlying probability space,

$$\Pr\{\mathscr{B} \in \mathfrak{F}\} = \Pr(\varnothing) = 0. \tag{2.38}$$

In terms of the random elements $\{\mathscr{I}_{j,m}(t) : j = 1, \ldots, b\}$ defined in Equation (2.19), we can apply Equation (2.21), the FCLT for the indicator process adapted to batch sizes of length m,

$$\mathscr{I}_{j,m} \underset{m\to\infty}{\Longrightarrow} \mathscr{W}, \tag{2.39}$$

and the GCMT to conclude that

$$\left.\begin{array}{rcl} \mathfrak{X}_j\{\mathscr{I}_{j,m}\} & \underset{m\to\infty}{\Longrightarrow} & \mathfrak{X}_j\{\mathscr{W}\} \text{ in } D, \\ \mathfrak{B}_j\{\mathscr{I}_{j,m}\} & \underset{m\to\infty}{\Longrightarrow} & \mathfrak{B}_j\{\mathscr{W}\} \text{ in } D, \quad \text{and} \\ \Delta_m(\mathfrak{B}_j\{\mathscr{I}_{j,m}\}, w) & \underset{m\to\infty}{\Longrightarrow} & \Delta(\mathfrak{B}_j\{\mathscr{W}\}, w) \text{ in } \mathbb{R}, \end{array}\right\} \quad \text{for } j = 1, \ldots, b. \tag{2.40}$$

Basic properties of $\mathscr{W}$ ensure that

$$\left.\begin{array}{rcl} \left\{\mathfrak{X}_j\{\mathscr{W}\} : j = 1, \ldots, b\right\} & \overset{\text{i.i.d.}}{\sim} & \mathscr{W} \text{ in } D, \\ \left\{\mathfrak{B}_j\{\mathscr{W}\} : j = 1, \ldots, b\right\} & \overset{\text{i.i.d.}}{\sim} & \mathscr{B} \text{ in } D, \quad \text{and} \\ \left\{\Delta(\mathfrak{B}_j\{\mathscr{W}\}, w) : j = 1, \ldots, b\right\} & \overset{\text{i.i.d.}}{\sim} & Z \text{ in } \mathbb{R} \end{array}\right\} \tag{2.41}$$

because (i) the Brownian motion is self-similar with Hurst index $1/2$ so that $\mathfrak{X}_j\{\mathscr{W}\} \overset{\text{d}}{=} \mathscr{W}$ for $j = 1, \ldots, b$ (Whitt [50], §4.2.2); and (ii) by the independent-increments property of Brownian motion, the random elements $\left\{\mathfrak{X}_j\{\mathscr{W}\} : j = 1, \ldots, b\right\}$ are independent since they are respectively defined as rescaled increments of $\mathscr{W}$ on the disjoint subintervals $\left\{\left(\frac{j-1}{b}, \frac{j}{b}\right] : j = 1, \ldots, b\right\}$ of $[0, 1]$ (Whitt [50], §1.2.3). Note here that by definition

$$\sigma_p \mathfrak{B}_j\{\mathscr{I}_{j,m}\} \equiv \mathscr{T}_{j,m}, \quad \text{for } j = 1, \ldots, b, \quad \text{and so} \tag{2.42}$$

$$\sigma_p \Delta_m(\mathfrak{B}_j\{\mathscr{I}_{j,m}\}, w) \equiv \Delta_m(\mathscr{T}_{j,m}, w), \quad \text{for } j = 1, \ldots, b. \tag{2.43}$$

We will now show that

$$d(\mathscr{T}_{j,m}, T_{j,m}) \underset{m\to\infty}{\Longrightarrow} 0, \quad \text{for } j = 1, \ldots, b.$$

Theorem 2.3.1 ensures there are a.s. bounded r.v.'s $\mathscr{U}_j \in \mathbb{R}^+$ and $\mathscr{R}_j \in \mathbb{Z}^+$ such that the remainder $Q_{j,m}$ in the Bahadur representation (2.7) for the BQE $\widehat{y}_p(j, m)$ satisfies Equation

(2.8). The latter equation yields

$$\left| \frac{m^{1/2}}{f(y_p)} \left[\overline{I}(y_p; j, m) - p \right] - m^{1/2} \left[y_p - \widehat{y}_p(j, m) \right] \right| = \left| m^{1/2} Q_{j,m} \right| \le \mathscr{U}_j \frac{(\log m)^{3/2}}{m^{1/4}} \underset{m \to \infty}{\Longrightarrow} 0. \tag{2.44}$$

Using Equations (2.7), (2.8), (2.14), and (2.19), for $j = 1, \ldots, b$, we can write:

$$\begin{aligned}
\left| \mathscr{T}_{j,m}(t) - T_{j,m}(t) \right| \le \sup_{t \in [0,1]} & \left| \frac{\lfloor mt \rfloor}{m^{1/2}} \left(\frac{\overline{I}(y_p; j, \lfloor mt \rfloor) - p}{f(y_p)} \right) - t m^{1/2} \left(\frac{\overline{I}(y_p; j, m) - p}{f(y_p)} \right) \right. \\
& \left. - \frac{\lfloor mt \rfloor}{m^{1/2}} \left[\widehat{y}_p(j, m) - \widehat{y}_p(j, \lfloor mt \rfloor) \right] \right| \\
\le \sup_{t \in [0,1]} & \left| \frac{\lfloor mt \rfloor}{m^{1/2}} \left(\frac{\overline{I}(y_p; j, \lfloor mt \rfloor) - p}{f(y_p)} \right) \right. \\
& \left. - t m^{1/2} \left(\frac{\overline{I}(y_p; j, m) - p}{f(y_p)} \right) - \frac{\lfloor mt \rfloor}{m^{1/2}} \left[\widehat{y}_p(j, m) - y_p + y_p - \widehat{y}_p(j, \lfloor mt \rfloor) \right] \right| \\
\le \sup_{t \in [0,1]} & \left| \frac{\lfloor mt \rfloor}{m^{1/2}} \left(\frac{\overline{I}(y_p; j, \lfloor mt \rfloor) - p}{f(y_p)} + \widehat{y}_p(j, \lfloor mt \rfloor) - y_p \right) \right. \\
& - \frac{\lfloor mt \rfloor}{m^{1/2}} \left(\frac{\overline{I}(y_p; j, m) - p}{f(y_p)} + \widehat{y}_p(j, m) - y_p \right) \\
& \left. - \left(\frac{mt - \lfloor mt \rfloor}{m} \right) m^{1/2} \left[\overline{I}(y_p; j, m) - p \right] / f(y_p) \right| \\
\le \sup_{t \in [0,1]} & \left| \frac{\lfloor mt \rfloor}{m^{1/2}} \left(Q_{j, \lfloor mt \rfloor} - Q_{j,m} \right) \right. \\
& \left. - \left(\frac{mt - \lfloor mt \rfloor}{m} \right) m^{1/2} \left[\overline{I}(y_p; j, m) - p \right] / f(y_p) \right| \\
\le \frac{\lfloor mt \rfloor}{m^{1/2}} & \left(\left| Q_{j, \lfloor mt \rfloor} \right| + \left| Q_{j,m} \right| \right) + m^{-1} \left| m^{1/2} \left[\overline{I}(y_p; j, m) - p \right] / f(y_p) \right| \\
\le 2 \mathscr{U}_j & \frac{(\log m)^{3/2}}{m^{1/4}} + m^{-1} \left| m^{1/2} \left[\overline{I}(y_p; j, m) - p \right] / f(y_p) \right|,
\end{aligned} \tag{2.45}$$

for each $t \in [0, 1]$ and $m \ge \mathscr{R}$ a.s. Equation (2.45) and the definition of $\| \cdot \|$ imply that

$$\| \mathscr{T}_{j,m} - T_{j,m} \| \le 2 \mathscr{U}_j \frac{(\log m)^{3/2}}{m^{1/4}} + m^{-1} \left| m^{1/2} \left[\overline{I}(y_p; j, m) - p \right] / f(y_p) \right|, \tag{2.46}$$

for each $t \in [0, 1]$ and $m \ge \mathscr{R}_j$ a.s. By the FCLT in Equation (2.39) at $t = 1$, namely for

$j = 1, \ldots, b$.

$$\mathscr{I}_{j,m}(1) \equiv m^{1/2}\big[\bar{I}(y_p; j, m) - p\big] \big/ f(y_p) \underset{m \to \infty}{\Longrightarrow} \mathscr{W}(1),$$

and Slutsky's theorem (Bickel and Doksum [56], Theorem A.14.9), we have

$$m^{-1}\Big|m^{1/2}\big[\bar{I}(y_p; j, m) - p\big] \big/ f(y_p)\Big| \underset{m \to \infty}{\Longrightarrow} 0. \tag{2.47}$$

Equations (2.44), (2.46), and (2.47) ensure that

$$d(\mathscr{T}_{j,m}, T_{j,m}) \underset{m \to \infty}{\Longrightarrow} 0, \quad \text{for } j = 1, \ldots, b, \tag{2.48}$$

and as a result, from Equations (2.40)–(2.42) and (2.48) we obtain

$$\big[T_{1,m}, \ldots, T_{b,m}\big]^{\mathsf{T}} \underset{m \to \infty}{\Longrightarrow} \sigma_p\big[\mathfrak{B}_1\{\mathscr{W}\}, \ldots, \mathfrak{B}_b\{\mathscr{W}\}\big]^{\mathsf{T}}. \tag{2.49}$$

Now Equations (2.32), (2.38), (2.43), (2.49), the GCMT, and the basic properties of $\mathscr{W}$ used to obtain Equation (2.41) from Equations (2.39)–(2.40) ensure that

$$\begin{aligned}\big\{A_p(w; j, m) : j = 1, \ldots, b\big\} = \big\{\Delta_m(T_{j,m}, w) : j = 1, \ldots, b\big\} \underset{m \to \infty}{\Longrightarrow}& \\ \sigma_p\big\{\Delta(\mathfrak{B}_j\{\mathscr{W}\}, w) : j = 1, \ldots, b\big\} \overset{\text{i.i.d.}}{\sim} \sigma_p Z \ \text{ in } \mathbb{R}.&\end{aligned} \tag{2.50}$$

Equation (2.50) implies that

$$\Delta_m^2(T_{j,m}, w) \underset{m \to \infty}{\Longrightarrow} \sigma_p^2\Delta^2(\mathfrak{B}_j\{\mathscr{W}\}, w) \overset{\text{d}}{=} \sigma_p^2\chi_1^2, \quad \text{for } j = 1, \ldots, b,$$

which together with the definition of $\mathscr{A}_p(w; b, m)$ yields

$$\mathscr{A}_p(w; b, m) \underset{m \to \infty}{\Longrightarrow} \sigma_p^2\chi_b^2/b,$$

which completes the proof. $\square$

We also define the average BQE as

$$\overline{\overline{y}}_p(b,m) = b^{-1}\sum_{j=1}^{b}\widehat{y}_p(j,m), \tag{2.51}$$

and the "average" squared deviations of the BQEs away from the average batch quantile estimator $\overline{\overline{y}}_p(b,m)$ and the full-sample quantile estimator $\widetilde{y}_p(n)$ respectively,

$$S_p^2(b,m) \equiv (b-1)^{-1}\sum_{j=1}^{b}\left[\widehat{y}_p(j,m) - \overline{\overline{y}}_p(b,m)\right]^2, \quad \text{and} \tag{2.52}$$

$$\widetilde{S}_p^2(b,m) \equiv (b-1)^{-1}\sum_{j=1}^{b}\left[\widehat{y}_p(j,m) - \widetilde{y}_p(n)\right]^2. \tag{2.53}$$

Notice that the value of q that minimizes $\sum_{j=1}^{b}\left[\widehat{y}_p(j,m)-q\right]^2$ is the average BQE $\overline{\overline{y}}_p(b,m)$, hence

$$S_p^2(b,m) \le \widetilde{S}_p^2(b,m). \tag{2.54}$$

Finally, we set

$$\mathscr{N}_p(b,m) = mS_p^2(b,m), \quad \text{and} \tag{2.55}$$

$$\widetilde{\mathscr{N}_p}(b,m) = m\widetilde{S}_p^2(b,m), \tag{2.56}$$

and we define the combined estimators of the variance parameter σ_p^2:

$$\mathscr{V}_p(w;b,m) \equiv \frac{b\mathscr{A}_p(w;b,m) + (b-1)\mathscr{N}_p(b,m)}{2b-1}, \quad \text{and} \tag{2.57}$$

$$\widetilde{\mathscr{V}_p}(w;b,m) \equiv \frac{b\mathscr{A}_p(w;b,m) + (b-1)\widetilde{\mathscr{N}_p}(b,m)}{2b-1}. \tag{2.58}$$

Theorem 2.3.5. *(Alexopoulos* et al. *[39]) If* $\{Y_k : k \ge 1\}$ *satisfies the assumptions of*

Theorem 2.3.1, then

$$n^{1/2}\big[\widetilde{y}_p(n) - y_p\big] \underset{m\to\infty}{\Longrightarrow} \sigma_p Z, \tag{2.59}$$

$$\mathscr{N}_p(b,m) \underset{m\to\infty}{\Longrightarrow} \sigma_p^2 \chi^2_{b-1}/(b-1), \tag{2.60}$$

$$\widetilde{\mathscr{N}_p}(b,m) \underset{m\to\infty}{\Longrightarrow} \sigma_p^2 \chi^2_{b-1}/(b-1), \tag{2.61}$$

$$\mathscr{V}_p(w;b,m) \underset{m\to\infty}{\Longrightarrow} \sigma_p^2 \chi^2_{2b-1}\big/(2b-1), \tag{2.62}$$

$$\widetilde{\mathscr{V}_p}(w;b,m) \underset{m\to\infty}{\Longrightarrow} \sigma_p^2 \chi^2_{2b-1}\big/(2b-1), \tag{2.63}$$

the limiting r.v.'s in Equations (2.18), (2.59), and (2.60) are independent, and the limiting r.v.'s in Equations (2.59) and (2.62) are also independent. In addition, the limiting r.v.'s in Equations (2.18), (2.59), and (2.61) are independent, and the limiting r.v.'s in Equations (2.59) and (2.63) are also independent. Further, for fixed b,

$$\widetilde{y}_p(n) \pm t_{1-\alpha/2,b}\big[\mathscr{A}_p(w;b,m)/n\big]^{1/2}, \tag{2.64}$$

$$\widetilde{y}_p(n) \pm t_{1-\alpha/2,b-1}\big[\mathscr{N}_p(b,m)/n\big]^{1/2}, \tag{2.65}$$

$$\widetilde{y}_p(n) \pm t_{1-\alpha/2,b-1}\big[\widetilde{\mathscr{N}_p}(b,m)/n\big]^{1/2}, \tag{2.66}$$

$$\widetilde{y}_p(n) \pm t_{1-\alpha/2,2b-1}\big[\mathscr{V}_p(w;b,m)/n\big]^{1/2}, \tag{2.67}$$

and

$$\widetilde{y}_p(n) \pm t_{1-\alpha/2,2b-1}\big[\widetilde{\mathscr{V}_p}(w;b,m)/n\big]^{1/2} \tag{2.68}$$

are asymptotically valid $100(1-\alpha)\%$ *CIs of* y_p *as* $m \to \infty$.

Theorem 2.3.6. *(Alexopoulos* et al. *[39]) The analogues of the CIs in Equations (2.64)–(2.68) are also asymptotically valid if the overall point estimator* $\widetilde{y}_p(n)$ *is replaced by the average BQE* $\overline{\overline{y}}_p(b,m)$.

Hereafter, we refer to $\widetilde{\mathscr{N}_p}(b,m)$ as the main nonoverlapping batched quantile (NBQ) variance estimator and to $\widetilde{\mathscr{V}}_p(w; b, m)$ as the main combined variance estimator. We also define the relative precision of a CI as the ratio of its HL over the absolute value of the point estimate (assuming that the latter is nonzero).

The CI in Equation (2.66) has been used in the Sequest method (Alexopoulos *et al.* [7]). The benefits of the combined variance estimator $\widetilde{\mathscr{V}}_p(w; b, m)$ should be apparent: since its distributional limit as $m \to \infty$ has nearly double d.f. compared to its constituents $\mathscr{A}_p(w; b, m)$ and $\widetilde{\mathscr{N}_p}(b, m)$, for large m the CI in Equation (2.68) will have a significantly less variable HL (by a factor of about $\sqrt{2}$) than each of the two competitors in Equations (2.64) and (2.66); this typically results in better sampling efficiency. The empirical evaluation in Sections 2.6-2.7 will highlight the benefits of the combined variance estimator.

STS area estimators tailored to the estimation of the steady-state mean are known to have noticeable small-sample bias; see Aktaran-Kalaycı *et al.* [57] and the citations therein. Preliminary experimental evaluation in Sections 2.6–2.7 with test processes from Section 2.5 has revealed that for small batch sizes m, the batched area estimator $\mathscr{A}_p(w_0; b, m)$ based on the constant weight function $w_0(t) = \sqrt{12}$ is substantially more biased than its NBQ counterpart $\widetilde{\mathscr{N}_p}(b, m)$; actually, the small-batch-bias problem for STS-based estimators appears to be more pronounced with regard to quantile estimation. The combined estimator $\widetilde{\mathscr{V}}_p(w; b, m)$ partially rectifies this problem.

Remark 2.3.2. We briefly elaborate on the suitability of the aforementioned weight functions $w_2(t) = \sqrt{840}(3t^2 - 3t + 1/2)$ and $\{w_{\cos,\ell}(t) = \sqrt{8}\pi\ell\cos(2\pi\ell t)\colon \ell = 1, 2, \ldots\}$ for the quantile estimation problem. Notably, these alternative weights yield first-order unbiased estimators for the variance parameter $\sigma^2 \equiv \lim_{n\to\infty} n\mathrm{Var}(\overline{Y}_n)$ related to the sample mean $\overline{Y}_n \equiv n^{-1}\sum_{k=1}^{n} Y_k$ of the base process $\{Y_k : k \geq 1\}$ (Foley and Goldsman [54], Goldsman *et al.* [33]); hence they were tailored to the estimation of the steady-state mean.

An open question is: does this property carry over to quantile estimation? This problem is very challenging because the derivation of analytical expressions for the expectation of the estimators $\widetilde{\mathscr{N}_p}(b, m)$, $\mathscr{A}_p(w; b, m)$, and $\widetilde{\mathscr{V}}_p(w; b, m)$ of $\sigma_p^2 = \lim_{n\to\infty} n\mathrm{Var}\big[\widetilde{y}_p(n)\big]$

involves joint moments of order statistics, which are often hard to obtain even for i.i.d. sequences; and this task is compounded in the presence of autocorrelation. So far it has been shown that the bias of all aforementioned estimators is $O(m^{-1/4})$ (Dingeç *et al.* [58]), but obtaining exact analytic expressions remains an open problem. Chapter 3 elaborates more on this topic by conducting a comparison of the variance-parameter estimators for the sample-quantile process based on calculations of their expected values for the special case of i.i.d. samples.

Further, extensive numerical and Monte Carlo experimentation in Section 2.8 has so far failed to provide firm evidence that the STS area and combined estimators based on the alternative weights from the literature $w_2(\cdot)$ and $\{w_{\cos,\ell}(\cdot)\}$ improve on $\mathscr{A}_p(w_0; b, m)$ and $\widetilde{\mathscr{V}}_p(w_0; b, m)$ with respect to small-sample bias and mean-squared error (MSE). This has motivated the search for new alternative weight functions in Sections 2.9–2.10 below that could be more tailored towards the estimation of steady-state quantiles.

Experimental evaluation of the bias and MSE of the variance parameter estimators presented in this chapter based on stationary versions of the processes in Section 2.5 below can be found in Sections 2.6–2.7 below.

2.4 Computational Complexity

In this section we elaborate on the effort required to compute the batched STS area estimator $\mathscr{A}_p(w; b, m)$ in Equation (2.16). It should be clear that the dominant component involves sorting both within each batch and for the entire sample. To simplify the discussion, we first consider the case with a single batch of size n. Since the evaluation of the STS quantile-estimation process $\{T_n(t) : t \in [0, 1]\}$ defined by Equation (2.10) at the points $t \in \{1/n, 2/n, \dots, (n-1)/n, 1\}$ involves the computation of p-quantile estimates from all partial samples of sizes $1, \dots, n$, one practically needs to start with a complete sort of the sample $\{Y_1, \dots, Y_n\}$. We implemented the procedures in Chapters 4–6 in Java, with the ultimate goal their incorporation into the Sequest application (Alexopoulos *et al.* [7]).

For reasons that will become apparent later in this section, we used an object-oriented paradigm to sort this non-primitive list using the default timsort algorithm of Tim Peters, a stable hybrid between merge sort and insertion sort with $O(n \log_2 n)$ average and worst-time complexity based on techniques from McIlroy [59].

It should be clear that once we have evaluated the STS quantile-estimation process $\{T_n(t) : t \in [0, 1]\}$ defined by Equation (2.10) at the points $t \in \{1/n, 2/n, \ldots, (n-1)/n, 1\}$, the evaluation of $\mathscr{A}_p(w; 1, n)$ using Equation (2.11) takes $O(n)$ extra time. For clarity, we temporarily adopt the classical notation $Y_{\ell:k}$ for the ℓth order statistic from the kth partial sample $\{Y_1, \ldots, Y_k\}$ for $1 \leq \ell \leq k \leq n$ so that $\widetilde{y}_p(k) = Y_{\lceil kp \rceil:k}$ for $1 \leq k \leq n$. Then the evaluation of $T_n(k/n)$ reduces to the computation of $Y_{\lceil kp \rceil:k}$ for $k = 1, \ldots, n$. Below we show how this task can be accomplished recursively in $O(n)$ time using object orientation and proceeding backwards to compute $Y_{\lceil kp \rceil:k}$ in stage k for $k = n, n-1, \ldots, 1$.

We store the original dataset $\{Y_1, \ldots, Y_n\}$ in a list comprised of n instances of an object. The kth instance has the following properties: the value Y_k, a reference (property) to the predecessor of that object in the original list having the value Y_{k-1}, and references to the predecessor and successor of that object in the sorted list. For brevity, we will often refer to the kth object by the usual symbol Y_k for its value.

We proceed by sorting the original list to obtain the sorted list $Y_{1:n} \leq Y_{2:n} \leq \cdots \leq Y_{n:n}$ and setting the predecessor/successor references for each object in the sorted list (essentially forming a doubly linked list of object instances). Starting at stage n, we obtain the value $Y_{\lceil np \rceil:n}$ from the $\lceil np \rceil$th object in the sorted list in $O(n)$ time.

We now focus on the recursive computation of $Y_{\lceil kp \rceil:k}$ from $Y_{\lceil (k+1)p \rceil:k+1}$ for $k \leq n-1$. The location of Y_{k+1} in the sorted list can be identified directly (in $O(1)$ time) using the predecessor reference of Y_{k+2} in the original list. Since $p \in (0, 1)$, we have only two potential cases:

- $\lceil kp \rceil = \lceil (k+1)p \rceil$: If the value $Y_{k+1} \leq Y_{\lceil (k+1)p \rceil:k+1}$, then we set $Y_{\lceil kp \rceil:k}$ equal to the successor of $Y_{\lceil (k+1)p \rceil:k+1}$ in the sorted list; otherwise, we set $Y_{\lceil kp \rceil:k} = Y_{\lceil (k+1)p \rceil:k+1}$.

- $\lceil kp \rceil = \lceil (k+1)p \rceil - 1$: If the value $Y_{k+1} \geq Y_{\lceil (k+1)p \rceil : k+1}$, then we set $Y_{\lceil kp \rceil : k}$ equal to the predecessor of $Y_{\lceil (k+1)p \rceil : k+1}$ in the sorted list; otherwise, we set $Y_{\lceil kp \rceil : k} = Y_{\lceil (k+1)p \rceil : k+1}$.

After the update, we "remove" Y_{k+1} from the sorted list by adjusting the predecessor and successor references from and to its previous successor and predecessor elements, respectively, in the sorted list (essentially, the list now contains k items because there are no references to/from Y_{k+1}). Since this recursive evaluation of $Y_{\lceil kp \rceil : k}$ from $Y_{\lceil (k+1)p \rceil : k+1}$ takes $O(1)$ time, the evaluation of $Y_{\lceil kp \rceil : k}$ for $k = n, n-1, \ldots, 1$ takes a total of $O(n)$ time. It follows that the computation of $\mathscr{A}_p(w; 1, n)$ takes a total of $O(n)$ time on top of the time to sort the entire sample.

Remark 2.4.1. Clearly, the use of objects results in higher memory usage. If one uses traditional (primitive) arrays instead of objects, the location of Y_{k+1} in the sorted array can be found in $O(\log_2(k+1))$ time (e.g., using a binary search); therefore the total time required for the evaluation of the values $Y_{\lceil kp \rceil : k}$ jumps to $O(n \log_2 n)$.

In the case of $b > 1$ batches, the average and worst-case time for sorting the batches and computing the full-sample point estimator remains $O(n \log_2 n)$ and the additional time for computing $\mathscr{A}_p(w; b, m)$ remains linear in n because $bO(m) = O(n)$. It should be clear that variance estimators based solely on BQEs (e.g., $\widetilde{\mathscr{N}_p}(b, m)$ defined by Equation (2.53)) can be computed in parallel with $\mathscr{A}_p(w; b, m)$.

Remark 2.4.2. We close this section by noting that the calculation of a BQE-based estimator alone can be achieved in $O(n)$ average time using a quickselect algorithm that does not sort observations that are less than a desired order statistic; cf. Section 9.2 of Cormen *et al.* [60].

2.5 Test Processes for Performance Evaluation

This section contains the descriptions of seven challenging processes from Alexopoulos *et al.* [7]. Throughout this paper we will use these processes or close variations of them.

2.5.1 First-Order Autoregressive Process

The first test process is the Gaussian first-order autoregressive [AR(1)] process defined by the recursion $Y_k = \mu_Y + \phi(Y_{k-1} - \mu_Y) + \epsilon_k$, for $k \geq 1$, where $\phi \in (-1, 1)$ and the residuals $\{\epsilon_k : k \geq 1\}$ are i.i.d. $N(0, \sigma_\epsilon^2)$. The steady-state marginal distribution of this process is $N[\mu_Y, \sigma_\epsilon^2/(1 - \phi^2)]$.

2.5.2 Autoregressive-to-Pareto Process

The second test process is an AR(1)-to-Pareto (ARTOP) process with a location parameter $\gamma > 0$, a shape parameter $\theta > 0$, and an autoregressive parameter $\phi \in (-1, 1)$; see Lada *et al.* [61] for details.

To generate this process, one starts with a stationary Gaussian AR(1) process $\{Z_k : k \geq 1\}$ defined by the iterative relation $Z_k = \phi Z_{k-1} + \epsilon_k$ for $k \geq 1$, where Z_0 is the initial state and the residuals $\{\epsilon_k : k \geq 1\}$ are i.i.d. $N(0, \sigma_\epsilon^2)$ with $\sigma_\epsilon^2 = 1 - \phi^2$. The next step obtains a dependent sequence of random numbers U_k that are uniformly distributed on $(0, 1)$ by feeding the Gaussian process $\{Z_k : k \geq 1\}$ into the standard normal c.d.f. $\Phi(\cdot)$ (i.e., $U_k = \Phi(Z_k)$, for $k \geq 1$). Finally, the sequence $\{U_k : k \geq 1\}$ is used as input to the inverse of the Pareto c.d.f.

$$F(y) = \begin{cases} 1 - (\gamma/y)^\theta & \text{if } y \geq \gamma, \\ 0 & \text{if } y < \gamma, \end{cases} \tag{2.69}$$

to obtain the ARTOP process

$$Y_k = F^{-1}(U_k) = F^{-1}[\Phi(Z_k)] = \gamma/[1 - \Phi(Z_k)]^{1/\theta}, \quad \text{for } k \geq 1.$$

The steady-state marginal mean and variance of this process are $\mu_Y = \gamma\theta(\theta - 1)^{-1}$ (for $\theta > 1$) and $\sigma_Y^2 = \gamma^2\theta(\theta - 1)^{-2}(\theta - 2)^{-1}$ (for $\theta > 2$).

2.5.3 M/M/1 Waiting-Time Process

The third test process is the waiting-time sequence in an M/M/1 queueing system with arrival rate λ, service rate ω (traffic intensity $\rho = \lambda/\omega$) and first-in, first-out (FIFO) service discipline. Let Y_k be the time spent by the kth entity in queue (prior to service). The steady-state c.d.f. of Y_k is

$$F(y) = \begin{cases} 0 & \text{if } y < 0, \\ 1 - \rho & \text{if } y = 0, \\ 1 - \rho e^{-\omega(1-\rho)y} & \text{if } y > 0, \end{cases} \tag{2.70}$$

with respective expected value $\mu_Y = \rho/(\omega - \lambda)$, and the quantiles of this distribution are readily computed by inverting Equation (2.70). This distribution is distinctly nonnormal, having an atom at zero, an exponential tail, and a skewness of $2(3 - 3\rho + \rho^2)/[\rho^{1/2}(2 - \rho)^{3/2}]$. The pronounced autocorrelation function of $\{Y_k :\geq 1\}$ in steady-state has made this process a gold-standard test bed for steady-state simulation analysis methods; see Section 4.2 of Alexopoulos *et al.* [7] for a more-detailed discussion.

2.5.4 M/H_2/1 Waiting-Time Process

The fourth test process is the sequence $\{Y_k : k \geq 1\}$ of entity delays in an M/H_2/1 queueing system with FIFO queue discipline, an empty-and-idle initial state, arrival rate $\lambda = 1$; and i.i.d. service times from the hyperexponential distribution that is a mixture of two other exponential distributions with mixing probabilities $g = (5 + \sqrt{15})/10 \approx 0.887$ and $1 - g$ and associated service rates $\omega_1 = 2g\tau$ and $\omega_2 = 2(1 - g)\tau$, with $\tau = 1.25$. The mean service time is 0.8 and the steady-state server utilization is $\rho = 0.8$. Using the Pollaczek-Khinchine formula in Equation (5.105) of Kleinrock [62] one can obtain the Laplace transform of the steady-state marginal c.d.f. $F(\cdot)$ of the waiting time

$$\mathscr{L}\{F;s\} = (1-\rho)\Big/\left\{s-\lambda+\lambda\left[\frac{g\omega_1}{\omega_1+s}+\frac{(1-g)\omega_2}{\omega_2+s}\right]\right\};$$

see Section 4.4 Alexopoulos *et al.* [7]. Using the first three derivatives of $\mathscr{L}\{F;s\}$ at $s=0$, one obtains the marginal steady-state mean $\mu_Y = 8$, the marginal steady-state standard deviation $\sigma_Y = 10.733$, and the respective marginal skewness of 2.5568 (Equation (A.3) in Lada *et al.* [63]). Accurate numerical approximations of the selected quantiles y_p were obtained by numerical inversion of $\mathscr{L}\{F;s\}$ using Euler's algorithm from Abate and Whitt [64] to obtain a piecewise-linear approximation of $F(\cdot)$, followed by a direct inversion of the latter approximation.

2.5.5 M/M/1/LIFO Waiting-Time Process

The fifth test process is the sequence of entity delays $\{Y_k : k \geq 1\}$ in a single-server queueing system with non-preemptive LIFO service discipline, empty-and-idle initial state, arrival rate $\lambda = 1$, and service rate $\omega = 1.25$. The steady-state server utilization is $\rho = 0.8$ and the marginal mean waiting time is $\mu_Y = 3.2$. This test process was selected because it presents challenges to sequential methods for estimating the steady-state mean (Tafazzoli *et al.* [65], Alexopoulos *et al.* [40]).

Accurate approximations for y_p were obtained by computing the Laplace transform $\mathscr{L}\{F;s\}$ of the marginal c.d.f., numerical inversion of $\mathscr{L}\{F;s\}$ using Euler's algorithm in Abate and Whitt [64] to obtain a piecewise-linear approximation of $F(\cdot)$, and direct inversion of the latter approximation; see Section 4.3 of Alexopoulos *et al.* [7] for details.

2.5.6 M/M/1/M/1 Waiting-Time Process

The sixth test process is constructed from the sequence $\{Y_k : k \geq 1\}$ of the total waiting times (prior to service) in a tandem network of two M/M/1 queues. The system has an arrival rate of $\lambda = 1$, service rates $\omega = 1.25$ at each station, and is initialized in the empty and idle state. Transitions between the two stations are instantaneous. The steady-state utilization for each server is $\rho = \lambda/\omega = 0.8$ and the mean total delay on the system is equal to 8. It is well known that the c.d.f. $F^*(\cdot)$ of the total waiting time in steady state is the convolution of two identical copies of the c.d.f. in Equation (2.70); hence the Laplace transform $\mathscr{L}\{F^*; s\}$ of $F^*(\cdot)$ is the square of the Laplace transform $\mathscr{L}\{F; s\}$. We computed accurate approximations of y_p by obtaining a piecewise-linear approximation of $F^*(\cdot)$ using numerical inversion of $\mathscr{L}\{F^*; s\}$ by means of Euler's algorithm in Abate and Whitt [64], followed by direct inversion of the latter approximation of $F^*(\cdot)$.

2.5.7 Central Server Model 3

The last test process is generated by a small computer network comprised of three stations, namely the Central Server Model 3 from Law and Carson [66]. The system contains a central processing unit (CPU), labeled as station 3, and two peripheral units, labeled as stations 1 and 2. The system always contains eight jobs. At time zero, station 1 contains one job, station 2 contains two jobs, and the CPU contains five jobs. A job arriving at the CPU joins the CPU queue if the CPU is busy; otherwise it moves immediately into service. Once service is completed at the CPU, the respective job moves instantaneously to station 1 with probability 0.9 or station 2 with probability 0.1. After service completion at a peripheral server, the job departs from the system and is immediately replaced by a new job that arrives at the CPU. Stations 1–3 are G/M/1 queueing systems with FIFO service discipline and service rates 0.45, 0.05, and 1, respectively. The *response time* Y_k of the kth departing job is the total time the job spent in the system, and the objective of our study is to estimate marginal steady-state quantiles of the sequence $\{Y_k : k \geq 1\}$.

The estimation of the marginal steady-state distribution of this process entails a variety of challenges. The histogram in Figure 4 of Alexopoulos *et al.* [7] based on a sample of size $n = 10^8$ revealed the following findings: (i) the steady-state marginal density $f(\cdot)$ of the response time exhibits substantial departure from normality with large skewness and kurtosis; (ii) $f(\cdot)$ is tightly concentrated in a narrow neighborhood of its mode, which is close to $y = 10$; (iii) $f(\cdot)$ dropped rapidly over its right-hand "cliff," which ended near $y = 40$; and (iv) $f(\cdot)$ declined very slowly in the portion of its right tail past $y = 40$. Nearly "exact" values of y_p were computed from the aforementioned large sample by inversion of the empirical c.d.f., i.e., $y_p \approx Y_{(\lceil np \rceil)}$.

2.6 An Initial Empirical Evaluation of the Performance of the Main Variance-Parameter Estimators

In this section we conduct an initial empirical evaluation of the performance of the following variance-parameter estimators:

- the batched STS area estimator $\mathscr{A}_p(w; b, m)$ defined by Equation (2.16);
- the main NBQ estimator $\widetilde{\mathscr{N}_p}(b, m)$ defined in Equation (2.56) based on the BQEs $\big\{\widehat{y}_p(j, m)\big\}$ and the full-sample point estimator $\widetilde{y}_p(n)$; and
- the main combined estimator $\widetilde{\mathscr{V}_p}(w; b, m)$ defined in Equation (2.58) composed of the batched STS area estimator $\mathscr{A}_p(w; b, m)$ and the main NBQ estimator $\widetilde{\mathscr{N}_p}(b, m)$.

The evaluation will be based on the bias, standard deviation, root mean squared error (RMSE), and the coverage probability of the 95% CIs for y_p defined by Equations (2.64), (2.66), and (2.68), respectively. The main NBQ estimator $\widetilde{\mathscr{N}_p}(b, m)$ is used in the Sequest procedure of Alexopoulos *et al.* [7].

The goal of this study is the validation of our theoretical findings and, in particular, to showcase the superiority of the combined estimator $\widetilde{\mathscr{V}_p}(w; b, m)$ with regard to its efficiency, as its asymptotic variance $\lim_{m\to\infty} \operatorname{Var}\big[\widetilde{\mathscr{V}_p}(w; b, m)\big]$ is nearly 50% smaller than the asymptotic variances $\lim_{m\to\infty} \operatorname{Var}\big[\mathscr{A}_p(w; b, m)\big]$ and $\lim_{m\to\infty} \operatorname{Var}\big[\widetilde{\mathscr{N}_p}(b, m)\big]$ of its respective constituents. (Note that the three asymptotic variances in the preceding statementis different from the variance parameter σ_p^2 of the quantile process.) The combined estimator

$\widetilde{\mathscr{V}}_p(w; b, m)$ will be used in the sequential and fixed-sample-size procedures in Chapters 4–6 for steady-state quantile estimation. For reasons mentioned in Remark 2.3.2, our analysis focuses on the constant weight function $w_0(t) = \sqrt{12}$, $t \in [0, 1]$.

We consider two stationary test processes: a variation of the AR(1) process in Section 2.5.1 with mean zero and correlation coefficient 0.9 and the waiting-time process from an M/M/1 queueing system as described in Section 2.5.3 with traffic intensity 0.8. For each process and value of p under study, we fix the number of batches at $b = 32$ and consider an increasing sequence of batch sizes $m = 2^{\mathcal{L}}$, where $\mathcal{L} \in \{10, 11, \ldots, 20\}$. We note that batch sizes with $\mathcal{L} \leq 15$ are often inadequate for variance-parameter estimation in these problems (Alexopoulos *et al.* [7]).

All experiments were coded in Java using common random numbers generated by the RngStreams package of L'Ecuyer *et al.* [67]. The numerical results were based on 2,500 independent replications for each process; and those results are summarized in Tables 2.1 and 2.2 below. In each table, column 1 contains the values of p, y_p, and σ_p^2 (the latter quantity is set in **bold red typeface**); column 2 contains the value of $\mathcal{L} = \log_2(m)$; columns 3, 8, and 13 contain the average values of the selected variance-parameter estimators computed from 2,500 i.i.d. observations of those estimators; columns 4, 9, and 14 contain the average bias of the selected variance-parameter estimators; and columns 5, 10, and 15 contain the sample standard deviations of the selected variance-parameter estimators. For nominal 95% CIs of y_p that are respectively defined by Equations (2.64), (2.66), and (2.68), columns 6, 11, and 16 have the heading "95% CI $\overline{H}$" and respectively contain the average CI HLs computed from 2,500 i.i.d. realizations of those CIs; moreover columns 7, 12, and 17 have the heading "95% CI Cover." and contain the corresponding empirical CI coverage probabilities. Finally, Figures 2.1 and 2.2 in Sections 2.6.1 and 2.6.2 below summarize the accuracy and precision of each variance-parameter estimator as the batch size increases by plotting estimates of the respective relative biases (as a percentage) and estimated RMSEs. In the figures we labeled $\widetilde{\mathscr{N}}_p(b, m)$ as "NBQ (tilde)" and $\widetilde{\mathscr{V}}_p(w_0; b, m)$

as "Combined (tilde)."

2.6.1 First-Order Autoregressive Process

The first test process is a variation of the stationary AR(1) time-series model described in Section 2.5.1. This regression model is $Y_k = \phi Y_{k-1} + \varepsilon_k$ for $k \geq 1$, where the autoregressive parameter is $\phi \in (-1, 1)$, the initial state Y_0 follows the $N(0, 1)$ distribution, and the residuals $\{\varepsilon_k : k \geq 1\}$ are i.i.d. $N(0, 1 - \phi^2)$ and independent of Y_0. Since the marginal distribution of the Y_k is $N(0, 1)$, the p-quantile can be computed by $y_p = \Phi^{-1}(p)$, where $\Phi(\cdot)$ denotes the standard normal c.d.f.

The asymptotic variance parameter for the AR(1) process was evaluated as follows (Dingeç *et al.* [68]). Let $\mathscr{T}(h, a)$ denote Owen's T-function:

$$\mathscr{T}(h, a) = \frac{1}{2\pi} \int_0^a \frac{\exp\left[-\frac{1}{2}h^2(1 + x^2)\right]}{1 + x^2}\, dx, \quad \text{for } h, a \in \mathbb{R}.$$

For two standard normal variates Z_1 and Z_2 with correlation $\varphi = \text{Corr}(Z_1, Z_2) \in (-1, 1)$, one has

$$P\left\{Z_1 \leq \Phi^{-1}(p), Z_2 \leq \Phi^{-1}(p)\right\} = p - 2\mathscr{T}\left[\Phi^{-1}(p), \left(\frac{1 - \varphi}{1 + \varphi}\right)^{1/2}\right], \quad \text{for } p \in (0, 1);$$

see Equation (3.12) of Meyer [69]. Since $\text{Corr}(Y_k, Y_{k+\ell}) = \phi^\ell$ for $\ell \geq 0$, we have

$$P\{Y_k \leq y_p, Y_{k+\ell} \leq y_p\} = p - 2\mathscr{T}\left[\Phi^{-1}(p), \left(\frac{1 - \phi^\ell}{1 + \phi^\ell}\right)^{1/2}\right], \quad \text{for } \ell \geq 0.$$

Using the definition of correlation, one can obtain the following expression for the autocorrelation function $\{\rho_I(\ell) : \ell \geq 0\}$ of the indicator process at lag ℓ:

$$\rho_I(\ell) = 1 - \frac{2}{p(1 - p)} \mathscr{T}\left[\Phi^{-1}(p), \left(\frac{1 - \phi^\ell}{1 + \phi^\ell}\right)^{1/2}\right], \quad \text{for } p \in (0, 1) \text{ and } \ell \geq 0.$$

Owen's T-function was computed using the R package and the implementation of Azzalini

[70], which is based on a series expansion. Then the variance parameter $\sigma^2_{I(y_p)}$ for the indicator process $\{I_k(y_p) : k \geq 1\}$ was approximated by truncating the infinite sum $\sigma^2_{I(y_p)} = p(1-p)\left[\,1 + 2\sum_{\ell=1}^{\infty} \rho_I(\ell)\,\right]$. Since for the $N(0,1)$ p.d.f. we have $f(y_p) = (2\pi)^{-1/2}\exp\left(-y_p^2/2\right)$, the approximation of $\sigma_p^2 = \sigma^2_{I(y_p)}\big/ f^2(y_p)$ follows immediately.

For experimentation we selected the values $\phi = 0.9$ and $p \in \{0.75, 0.95, 0.99\}$. Because of the symmetry of the marginal $N(0,1)$ distribution, we did not consider values of $p < 1/2$. The results are summarized in Table 2.1, which clearly indicates that all three estimators of the variance parameter σ_p^2 and their respective estimated standard deviations converged to their asymptotic limits reasonably fast, albeit with speed that diminishes as p approaches 1. Further, the estimated coverage probabilities of the three CIs for y_p respectively based on Equations (2.64), (2.66), and (2.68) hovered near the nominal value of 0.95. Of equal importance, the lower standard deviation of the combined estimator $\widetilde{\mathscr{V}}_p(w_0; b, m)$ becomes evident from the plots of the RMSEs in Figure 2.1. Among the three values of p, the near-extreme case of $p = 0.99$ provides a few insights, the first of which will become more prominent with the second example in Section 2.6.2.

- For small batch sizes, the batched STS area estimator $\mathscr{A}_p(w_0; b, m)$ has significantly more bias than the NBQ estimator $\widetilde{\mathscr{N}_p}(b, m)$, while the bias of the combined estimator $\widetilde{\mathscr{V}}_p(w_0; b, m)$ typically falls between the biases of its constituents (see Figure 2.1).
- For small batch sizes, the batched STS area estimator $\mathscr{A}_p(w_0; b, m)$ has noticeably larger standard deviation than the NBQ estimator $\widetilde{\mathscr{N}_p}(b, m)$. Notice that the asymptotic standard deviation of the batched STS area estimator, namely $\lim_{m\to\infty}\left\{\mathrm{Var}\left[\mathscr{A}_p(w_0; b, m)\right]\right\}^{1/2} = \left[2\sigma_p^4/b\right]^{1/2}$, is a bit smaller that the respective value for the NBQ estimator $\lim_{m\to\infty}\left\{\mathrm{Var}\left[\widetilde{\mathscr{N}_p}(b, m)\right]\right\}^{1/2} = \left[2\sigma_p^4/(b-1)\right]^{1/2}$.

2.6.2 M/M/1 Waiting-Time Process

Our second stationary test process $\{Y_k : k \geq 1\}$ was generated by the M/M/1 queueing system in Section 2.5.3 with FIFO service discipline, arrival rate $\lambda = 0.8$, and service rate $\omega = 1$. In this system the steady-state server utilization is $\rho = \lambda/\omega = 0.8$ and the steady-state distribution of Y_k has mean $\mu_Y = \rho/(\omega - \lambda) = 4$.

The steady-state distribution (2.70) is markedly nonnormal, having an atom at zero, an exponential tail, and a skewness of $2(3 - 3\rho + \rho^2)/[\rho^{1/2}(2 - \rho)^{3/2}] \approx 2.1093$. These properties can induce a significant skewness in the corresponding BQEs $\{\widehat{y}_p(j, m) : j = 1, \ldots, b\}$ that can degrade the performance of the CI defined by Equation (2.66), resulting in a coverage probability that can be substantially below the nominal level (Alexopoulos *et al.* [23]). Because of the atom at zero in the c.d.f. in Equation (2.70), we only considered values of $p > 1 - \rho = 0.20$.

The variance parameter σ_I^2 of the indicator process was computed from Equation (22) of Blomqvist [71]. After some algebra, we obtained the following analytical expression for the asymptotic variance parameter corresponding to $\widetilde{y}_p(n)$:

$$\sigma_p^2 = \frac{1}{\omega^2(1-\rho)^4}\left\{\frac{[-2 + p(3-\rho) + 2\rho](1+\rho)}{1-p} - 4\rho \ln\left(\frac{\rho}{1-p}\right)\right\}.$$

We generated the stationary version $\{Y_k : k \geq 1\}$ of this waiting-time process by sampling Y_1 using Equation (2.70), and then using Lindley's recursion. Table 2.2 below lists the numerical experimental outcomes. We selected the values $p = 0.25$ (near the value $1 - \rho = 0.2$), $p = 0.75$, and the extreme value $p = 0.99$.

A careful examination of Table 2.2 confirms that all three variance-parameter estimators and their standard deviations converge to the respective theoretical limits, but at a significantly lower rate than for the AR(1) process in Section 2.6.1. Most importantly, it reveals the presence of substantial bias in the variance-parameter estimators for small batch sizes m; this bias apparently becomes more prominent for $p = 0.99$. We believe that this bias is primarily explained by the bias of the point estimator $\widetilde{y}_p(n)$ that is evident in the Bahadur representation (2.6). Ongoing work includes a comprehensive study of the relationship between the bias of $\widetilde{y}_p(n)$ and the bias of the batched STS area estimator $\mathscr{A}_p(w_0; b, m)$.

Notably, the magnitude of this small-batch bias of the variance-parameter estimators corresponding to the full-sample quantile estimator $\widetilde{y}_p(n)$ is more pronounced than the bias of the respective variance-parameter estimators corresponding to the sample mean $\overline{Y}_n$; see Table 4 of Alexopoulos *et al.* [34].

Among the three variance-parameter estimators, the NBQ estimator $\widetilde{\mathscr{N}_p}(b, m)$ exhibited the lowest small-sample bias, while the batched STS area estimator $\mathscr{A}_p(w_0; b, m)$ exhibited the largest. Since the combined estimator $\widetilde{\mathscr{V}_p}(w_0; b, m)$ is roughly the average of its constituents, its average bias tends to fall in the middle; see Figure 2.2. For example, when $p = 0.25$, all three estimators exhibited substantial positive bias for small batch sizes ($m \leq 2^{14}$): the average percent relative bias of the batched STS area estimator decreased from an overwhelming 272.43% for $m = 2^{10}$ to under 1% at approximately $m = 2^{17}$; the relative bias of the NBQ estimator dipped from roughly 40.83% at $m = 2^{10}$ to below 1% at $m = 2^{15}$; and the relative bias of the combined estimator dropped from roughly 158.47% at $m = 2^{10}$ to under 1% near $m = 2^{17}$.

When $p = 0.75$ all three variance-parameter estimators exhibited bias with nearly similar behavior. In particular, the average relative bias of the batched STS area estimator decreased slowly from 47.12% above the asymptotic variance parameter for $m = 2^{10}$ to about 0.19% below for $m = 2^{20}$. When $p = 0.99$, the variance-parameter estimators approached their limit more slowly, with a relative bias that started at nearly 86% below the asymptotic variance parameter for $m = 2^{10}$, became positive near $m = 2^{15}$, and then dropped slowly.

Notice that for $m = 2^{20}$ ($n = 2^{25} \approx 33$ million), the average relative bias of the batched STS area estimator is 1.17%, while the average relative bias of the NBQ estimator is a bit lower (0.94%) and the average relative bias of the combined estimator is about 1.05%. Overall, the behavior of the bias of the three estimators exhibits no clear patterns as the batch size increases. Detailed analysis of the bias is a very hard problem. A rudimentary analysis for i.i.d. processes is conducted in Chapter 3 (of this thesis).

At this juncture, we would like to caution the reader that for this output process and

$p = 0.99$, the Sequest procedure of Alexopoulos *et al.* [7], which is based on the NBQ estimator $\widetilde{\mathcal{N}_p}(b, m)$ defined in Equation (2.56), often delivered CIs that exhibited significant undercoverage while requiring excessive sample sizes. This discovery was one of the motivations for the development of the Sequem procedure (Alexopoulos *et al.* [23]) for the more-challenging problem of estimating near-extreme quantiles.

We now turn to the remaining statistics in Table 2.2. The standard deviation of each variance-parameter estimator converged to its respective theoretical limit. In particular, the standard deviation of the batched STS area estimator (column 5) converged to $\left[2\sigma_p^4/b\right]^{1/2} = (2/b)^{1/2}\sigma_p^2$, based on Equation (2.18). For instance, when $p = 0.99$ and $m = 2^{20}$, the average standard deviation of 49780.2 is only 4.11% larger than the theoretical limit $\sigma_p^2/4 = 47815.2$. In comparison, the average standard deviation 35608.7 of the combined estimator is only 4.49% larger than the theoretical limit $\left[2\sigma_p^4/(2b-1)\right]^{1/2} = [2/(2b-1)]^{1/2}\sigma_p^2 = 34077.8$. The dominance of the combined estimator with respect to its variance, and hence its mean squared error (MSE), is evident from the plots of the estimated RMSEs in Figure 2.2, in particular once the variance-parameter estimates approach the value σ_p^2.

The estimated coverage probabilities of the CIs obtained from Equations (2.64), (2.66), and (2.68) echo the respective small-batch-size issues. When $p = 0.25$ or 0.75, the estimated coverage probability of the approximate 95% CIs was near the nominal level for all batch sizes; this is due to the convergence of the variance-parameter estimators to σ_p^2 from above. Unfortunately, this was not the case for $p = 0.99$, when the approximate 95% CIs exhibited substantial undercoverage for moderate sample sizes; indeed, the estimated coverage probabilities started approach 0.95 only as $m \geq 2^{15}$. Overall, all three variance-parameter estimators appear to be equally competitive when $p = 0.75$, while the NBQ estimator $\widetilde{\mathcal{N}_p}(b, m)$ appears to dominate with regard to CI estimated coverage probability when $p = 0.99$ and $m \leq 2^{14}$ followed by the combined estimator and the batched STS area estimator. As we stated earlier, such batch sizes are grossly inadequate for estimating such extreme quantiles.

Table 2.1: Experimental results for the AR(1) process with $\mu_Y = 0$ and $\phi = 0.9$. All estimates are based on 2,500 independent replications with $b = 32$ batches and batch sizes $m = 2^{\mathcal{L}}$, $\mathcal{L} \in \{10, 11, \ldots, 20\}$, where for nominal 95% CIs for y_p, the average CI HLs and coverage probabilities are denoted by "95% CI $\overline{H}$" and "95% CI Cover.", respectively.

		Batched STS Area Estimator $\mathscr{A}_p(w_0; b, m)$					NBQ Estimator $\widetilde{\mathscr{N}_p}(b, m)$					Combined Estimator $\widetilde{\mathscr{V}_p}(w; b, m)$				
p (y_p) **Var. Par.**	$\mathcal{L}$	Avg.	Bias	Std. Dev.	95% CI $\overline{H}$	95% CI Cover.	Avg.	Bias	Std. Dev.	95% CI $\overline{H}$	95% CI Cover.	Avg.	Bias	Std. Dev.	95% CI $\overline{H}$	95% CI Cover.
0.75	10	22.3	−0.6	6.0	0.0527	93.64	22.8	−0.1	5.8	0.0533	94.36	22.5	−0.4	4.2	0.0522	94.44
(0.6745)	11	22.7	−0.2	5.8	0.0376	94.60	22.8	−0.1	5.8	0.0377	94.32	22.8	−0.1	4.0	0.0371	94.44
22.9	12	22.9	0.0	5.7	0.0267	95.32	22.7	−0.2	5.8	0.0266	95.24	22.8	−0.1	4.1	0.0263	95.60
	13	22.7	−0.2	5.9	0.0188	94.76	22.8	−0.1	5.9	0.0189	94.96	22.7	−0.2	4.1	0.0185	95.24
	14	22.9	0.0	5.8	0.0134	95.12	22.8	−0.1	5.8	0.0134	95.44	22.9	0.0	4.1	0.0131	95.16
	15	22.8	−0.1	5.8	0.0094	94.80	22.8	−0.1	5.9	0.0094	95.12	22.8	−0.1	4.1	0.0093	94.80
	16	22.8	−0.1	5.7	0.0067	94.76	22.9	0.0	5.8	0.0067	95.08	22.9	0.0	4.1	0.0066	95.00
	17	22.7	−0.2	5.7	0.0047	95.24	22.9	0.0	5.8	0.0047	95.08	22.8	−0.1	4.0	0.0046	95.48
	18	22.9	0.0	5.7	0.0033	95.68	23.0	0.1	5.9	0.0034	96.16	22.9	0.0	4.1	0.0033	95.76
	19	22.8	−0.1	5.6	0.0024	94.92	23.0	0.1	5.8	0.0024	94.00	22.9	0.0	4.0	0.0023	94.12
	20	23.0	0.1	5.8	0.0017	95.00	22.8	−0.1	5.7	0.0017	95.52	22.9	0.0	4.0	0.0016	95.16
0.95	10	37.8	−0.5	11.4	0.0684	94.32	38.1	−0.2	10.1	0.0689	95.00	38.0	−0.3	7.9	0.0677	94.88
(1.6449)	11	38.4	0.1	10.8	0.0488	93.96	38.0	−0.3	9.8	0.0487	94.40	38.2	−0.1	7.4	0.0480	94.40
38.3	12	38.7	0.4	10.4	0.0347	95.28	38.1	−0.2	9.8	0.0345	94.56	38.4	0.1	7.2	0.0340	94.84
	13	38.1	−0.2	10.0	0.0243	94.36	38.1	−0.2	9.9	0.0244	95.00	38.1	−0.2	7.1	0.0240	94.64
	14	38.3	0.0	9.9	0.0173	95.12	38.3	0.0	9.7	0.0173	95.68	38.3	0.0	7.0	0.0170	95.40
	15	38.4	0.1	9.9	0.0122	94.68	38.1	−0.2	10.0	0.0122	94.40	38.3	0.0	7.0	0.0120	94.36
	16	38.2	−0.1	9.9	0.0086	95.32	38.3	0.0	9.8	0.0086	95.44	38.2	−0.1	7.1	0.0085	95.40
	17	38.2	−0.1	9.5	0.0061	95.72	38.4	0.1	9.9	0.0061	95.52	38.3	0.0	6.8	0.0060	95.56
	18	38.5	0.2	9.6	0.0043	95.16	38.7	0.4	9.9	0.0043	95.44	38.6	0.3	6.9	0.0043	95.24
	19	38.4	0.1	9.5	0.0031	94.40	38.7	0.4	9.8	0.0031	94.28	38.5	0.2	6.7	0.0030	94.52
	20	38.8	0.5	9.7	0.0022	94.96	38.3	0.0	9.7	0.0022	95.12	38.6	0.3	6.8	0.0021	95.08
0.99	10	76.4	−5.2	32.0	0.0964	92.92	79.6	−2.0	22.8	0.0995	94.52	77.9	−3.7	21.4	0.0966	93.96
(2.3263)	11	81.8	0.2	29.7	0.0709	94.32	81.2	−0.4	21.8	0.0712	94.84	81.5	−0.1	19.9	0.0700	94.56
81.6	12	84.0	2.4	26.1	0.0509	94.60	81.8	0.2	21.6	0.0505	94.32	82.9	1.3	17.4	0.0500	94.84
	13	82.6	1.0	23.8	0.0358	94.00	81.4	−0.2	21.7	0.0356	94.48	82.0	0.4	16.6	0.0352	94.12
	14	82.4	0.8	22.7	0.0253	95.36	81.4	−0.2	20.8	0.0252	95.44	81.9	0.3	15.4	0.0249	95.40
	15	81.8	0.2	21.2	0.0178	94.88	81.5	−0.1	20.3	0.0178	95.28	81.6	0.0	14.9	0.0176	95.12
	16	82.1	0.5	21.3	0.0126	94.92	81.1	−0.5	20.4	0.0126	94.92	81.6	0.0	14.7	0.0124	95.00
	17	81.8	0.2	20.7	0.0089	95.72	81.5	−0.1	20.6	0.0089	95.00	81.7	0.1	14.5	0.0088	95.04
	18	81.5	−0.1	21.3	0.0063	95.04	82.3	0.7	20.8	0.0063	94.92	81.9	0.3	14.9	0.0062	94.80
	19	82.1	0.5	20.9	0.0045	95.28	82.6	1.0	20.9	0.0045	94.52	82.3	0.7	14.7	0.0044	94.68
	20	83.0	1.4	20.8	0.0032	94.80	82.2	0.6	20.9	0.0032	95.00	82.6	1.0	14.4	0.0031	95.04

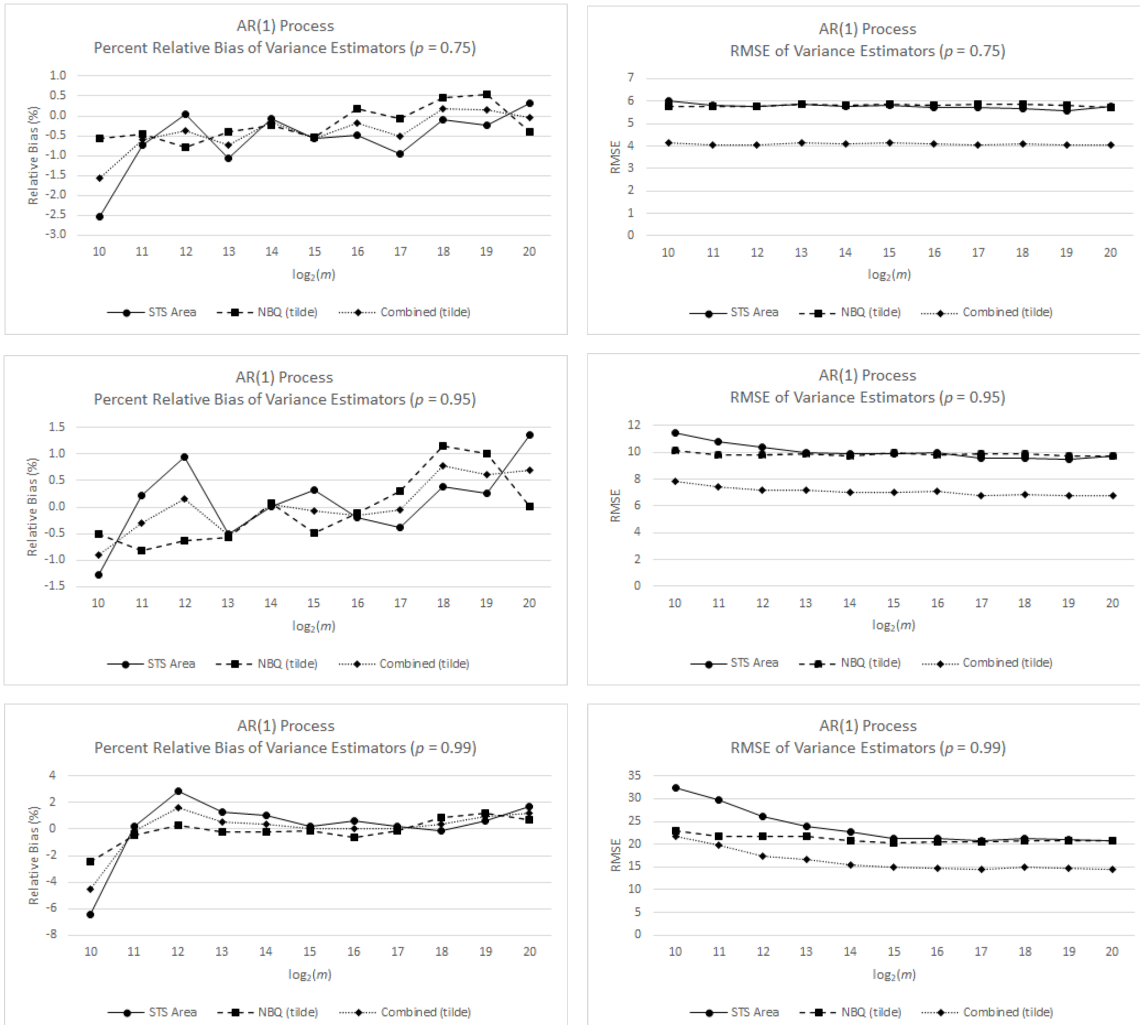

Figure 2.1: Estimated percent relative bias and RMSE of the variance-parameter estimators for selected marginal quantiles of a stationary AR(1) process with $\mu_Y = 0$ and $\phi = 0.9$. All estimates are based on 2,500 independent replications with $b = 32$ batches and batch sizes $m = 2^{\mathcal{L}}$, $\mathcal{L} \in \{10, 11, \ldots, 20\}$.

Table 2.2: Experimental results for a stationary waiting-time process in an M/M/1 queueing system with traffic intensity $\rho = 0.8$. All estimates are based on 2,500 independent replications with $b = 32$ batches and batch sizes $m = 2^{\mathcal{L}}$, $\mathcal{L} = 10, 11, \ldots, 20$, where for nominal 95% CIs for y_p, the average CI HLs and coverage probabilities are denoted by "95% CI $\overline{H}$" and "95% CI Cover.", respectively.

		STS Area Estimator $\mathscr{A}_p(w_0; b, m)$					NBQ Estimator $\widetilde{\mathscr{N}}_p(b, m)$					Combined Estimator $\widetilde{\mathscr{V}}_p(w; b, m)$				
p (y_p) **Var. Par.**	$\mathcal{L}$	Avg.	Bias	Std. Dev.	95% CI $\overline{H}$	95% CI Cover.	Avg.	Bias	Std. Dev.	95% CI $\overline{H}$	95% CI Cover.	Avg.	Bias	Std. Dev.	95% CI $\overline{H}$	95% CI Cover.
0.25	10	357.2	261.3	522.4	0.1923	99.24	135.1	39.2	92.6	0.1266	96.04	247.9	152.0	278.4	0.1626	98.48
(0.3227)	11	192.1	96.1	175.4	0.1047	97.52	113.2	17.3	44.0	0.0834	96.00	153.3	57.3	96.4	0.0939	97.56
95.9	12	127.2	31.3	57.0	0.0622	96.84	104.7	8.8	31.4	0.0570	96.12	116.1	20.2	34.8	0.0589	96.60
	13	108.8	12.9	34.5	0.0410	95.96	100.2	4.3	28.0	0.0395	95.84	104.6	8.7	22.8	0.0397	96.28
	14	102.4	6.5	28.4	0.0282	95.88	97.4	1.5	25.7	0.0276	94.96	100.0	4.0	19.5	0.0275	95.60
	15	98.6	2.6	26.6	0.0196	94.64	96.8	0.8	25.3	0.0194	95.04	97.7	1.8	18.6	0.0192	94.88
	16	97.5	1.6	25.3	0.0138	95.00	96.3	0.4	24.2	0.0137	95.04	96.9	1.0	17.4	0.0135	95.12
	17	96.7	0.8	24.4	0.0097	94.72	96.3	0.4	23.9	0.0097	94.84	96.5	0.6	17.0	0.0096	94.96
	18	96.4	0.5	24.4	0.0069	93.84	95.4	−0.5	23.8	0.0068	94.16	95.9	0.0	17.0	0.0067	93.80
	19	96.5	0.6	24.6	0.0048	94.76	95.3	−0.7	24.6	0.0048	95.12	95.9	0.0	17.3	0.0048	94.76
	20	95.5	−0.4	23.6	0.0034	94.84	95.9	0.0	24.5	0.0034	94.96	95.7	−0.2	16.9	0.0034	94.88
0.75	10	4853.0	1554.3	3419.9	0.7503	95.92	4798.4	1499.7	3211.7	0.7495	96.12	4826.1	1527.4	2831.1	0.7425	96.52
(5.8158)	11	4992.9	1694.2	3657.9	0.5402	96.56	4113.1	814.4	2162.2	0.4981	95.80	4560.0	1261.3	2449.3	0.5143	96.60
3298.7	12	4242.5	943.8	2046.1	0.3583	96.16	3703.1	404.4	1329.6	0.3379	95.96	3977.1	678.4	1361.7	0.3438	96.20
	13	3819.2	520.5	1402.5	0.2423	96.32	3466.6	167.9	1036.7	0.2320	95.68	3645.7	347.0	944.1	0.2338	96.20
	14	3547.5	248.8	1045.6	0.1658	95.36	3366.1	67.4	905.0	0.1620	95.16	3458.3	159.6	726.8	0.1614	95.24
	15	3412.5	113.8	936.5	0.1152	94.64	3345.8	47.1	878.2	0.1142	94.72	3379.7	81.0	652.7	0.1129	94.76
	16	3356.4	57.7	873.3	0.0808	94.60	3337.2	38.5	861.3	0.0807	94.80	3347.0	48.3	617.7	0.0795	94.64
	17	3332.1	33.4	859.7	0.0569	94.48	3327.3	28.6	839.2	0.0570	94.68	3329.7	31.0	605.0	0.0561	94.48
	18	3316.1	17.4	814.8	0.0402	94.60	3312.8	14.1	829.5	0.0402	94.76	3314.5	15.8	578.2	0.0396	94.60
	19	3310.2	11.5	838.5	0.0284	94.36	3306.4	7.7	856.2	0.0284	94.68	3308.3	9.6	593.9	0.0279	94.88
	20	3292.4	−6.3	813.3	0.0200	94.64	3316.4	17.7	853.0	0.0201	95.04	3304.2	5.5	580.6	0.0198	94.76
0.99	10	27618.0	−163642.9	17700.9	1.7889	54.88	53584.8	−137676.1	30487.4	2.5205	71.00	40395.4	−150865.5	20481.1	2.1576	62.72
(21.9101)	11	54706.7	−136554.2	37687.2	1.7710	67.96	80128.0	−111132.9	37863.4	2.2007	80.12	67215.6	−124045.3	31916.3	1.9742	74.88
191260.9	12	92768.8	−98492.1	66686.8	1.6278	79.08	123087.5	−68173.4	56786.8	1.9309	89.04	107687.5	−83573.4	52972.3	1.7657	85.16
	13	135781.4	−55479.5	93622.5	1.3998	87.72	179439.6	−11821.3	87474.8	1.6448	93.52	157264.0	−33996.9	76578.9	1.5096	91.16
	14	179612.2	−11648.7	128351.8	1.1440	91.20	218074.5	26813.6	117142.2	1.2789	94.56	198538.1	7277.2	106052.3	1.1979	93.00
	15	204721.9	13461.0	110567.3	0.8759	94.40	213376.8	22115.9	109485.9	0.9002	94.88	208980.7	17719.8	91853.7	0.8764	94.92
	16	209708.5	18447.6	106715.1	0.6301	95.44	202610.7	11349.8	77118.1	0.6250	95.84	206215.9	14955.0	75154.4	0.6190	95.80
	17	203575.5	12314.6	70787.1	0.4429	95.32	195545.3	4284.4	55570.2	0.4361	95.00	199624.1	8363.2	48901.2	0.4329	95.00
	18	199606.7	8345.8	57125.7	0.3111	95.24	193632.8	2371.9	53765.4	0.3070	94.84	196667.2	5406.3	41549.9	0.3043	95.00
	19	196112.6	4851.7	52084.9	0.2183	95.52	192647.7	1386.8	51991.8	0.2166	95.20	194407.7	3146.8	38005.1	0.2141	95.04
	20	193492.2	2231.3	49780.2	0.1534	95.52	193054.5	1793.6	48724.2	0.1535	95.16	193276.8	2015.9	35608.7	0.1510	95.16

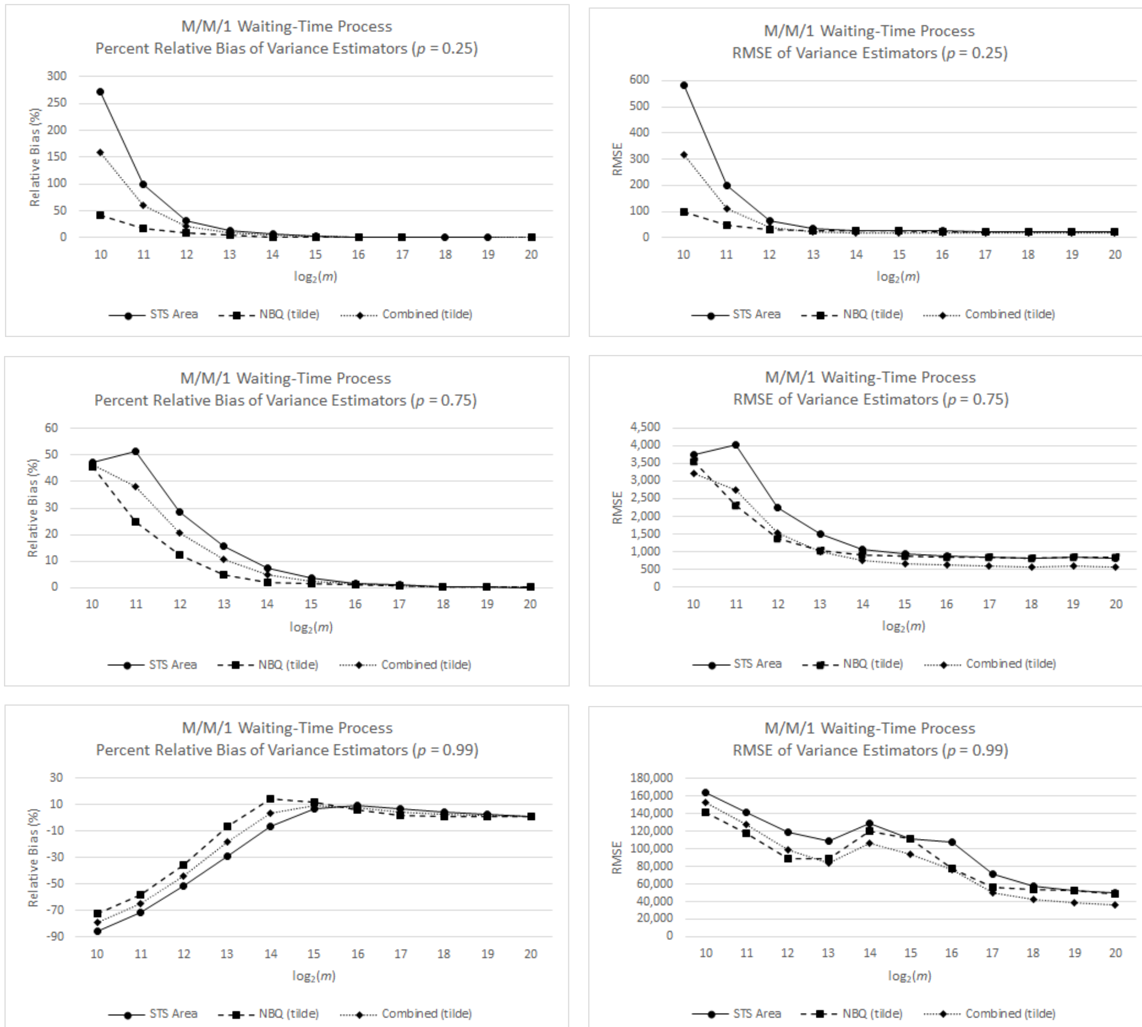

Figure 2.2: Estimated percent relative bias and RMSE of the variance-parameter estimators for selected marginal quantiles of a stationary waiting-time process in an M/M/1 queueing system with traffic intensity $\rho = 0.8$. All estimates are based on 2500 independent replications with $b = 32$ batches and batch sizes $m = 2^{\mathcal{L}}$, $\mathcal{L} = 10, 11, \ldots, 20$.

2.7 Extended Empirical Evaluation of the Performance of Several Variance-Parameter Estimators

In this section we build on Section 2.6 and we conduct an extended empirical evaluation of the performance of the following estimators for σ_p^2:

- the batched STS area estimator $\mathscr{A}_p(w; b, m)$ defined in Equation (2.16);
- the main NBQ estimator $\widetilde{\mathscr{N}_p}(b, m)$ defined in Equation (2.56) based on the BQEs $\{\widehat{y}_p(j, m)\}$ and the full-sample point estimator $\widetilde{y}_p(n)$;
- the NBQ estimator $\mathscr{N}_p(b, m)$ defined in Equation (2.55) based on the BQEs $\{\widehat{y}_p(j, m)\}$ and the average BQE $\overline{\widehat{y}}_p(b, m)$;
- the main combined estimator $\widetilde{\mathscr{V}_p}(w; b, m)$ defined by Equation (2.58) composed of the batched STS area estimator $\mathscr{A}_p(w; b, m)$ and the main NBQ estimator $\widetilde{\mathscr{N}_p}(b, m)$; and
- the combined estimator $\mathscr{V}_p(w; b, m)$ defined in Equation (2.57) composed of the batched STS area estimator $\mathscr{A}_p(w; b, m)$ and the NBQ estimator $\mathscr{N}_p(b, m)$.

The evaluation will be based on the bias, standard deviation, RMSE, and the coverage probability of the 95% CIs for y_p defined by Equations (2.64)–(2.68). Similarly to Section 2.6, our analysis focuses on the constant weight function $w_0(t) = \sqrt{12}$, $t \in [0, 1]$. Our goal is to validate our theoretical findings and, in particular, to showcase the superiority of the combined estimator $\widetilde{\mathscr{V}_p}(w; b, m)$ with regard to its efficiency and make clear why this is incorporated in the proposed sequential and fixed-sample-size procedures for steady-state quantile estimation in Chapters 4–6.

We consider three stationary test processes: the AR(1) process in Section 2.6.1 with mean zero and correlation coefficient 0.9, the waiting-time process from an M/M/1 queueing system as described in Section 2.6.2 with traffic intensity 0.8, the ARTOP process with location parameter $\gamma = 1$, shape parameter $\theta = 2.1$, and autoregressive parameter $\phi = 0.995$. For each process and value of p under study, we fix the number of batches at $b = 32$ and consider an increasing sequence of batch sizes $m = 2^{\mathcal{L}}$, $\mathcal{L} \in \{7, 8, \ldots, 20\}$. We note that batch sizes with $\mathcal{L} \leq 15$ are often inadequate for variance-parameter estimation in these problems (Alexopoulos *et al.* [7]).

Essentially, in comparison with Section 2.6, we consider more variance-parameter estimators, we add one more test process, and we increase the range of the batch sizes that we use. In some situations the number of significant digits displayed may also vary.

All experiments were coded in Java using common random numbers generated by the RngStreams package of L'Ecuyer *et al.* [67]. The numerical results were computed from 2,500 independent replications of each test process; and those results are summarized in Tables 2.3–2.8 below. In each table, column 1 contains the values of p, y_p, and σ_p^2 (the latter quantity is set in **bold red typeface**); column 2 contains the value of $\mathcal{L} = \log_2(m)$; columns 3, 7, 11, 15, and 19 respectively contain the average values of the selected variance-parameter estimators computed from 2,500 i.i.d. observations of those estimators; columns 4, 8, 12, 16, and 20 respectively contain the average bias of the selected variance-parameter estimators; columns 5, 9, 13, 17, and 21 respectively contain the sample standard deviations of the selected variance-parameter estimators; and columns 6, 10, 14, 18, and 22 respectively contain the corresponding empirical CI coverage probabilities. Finally, Figures 2.3–2.5 summarize the accuracy and precision of each variance-parameter estimator for each test process in Sections 2.7.1–2.7.3, respectively, as the batch size increases by plotting estimates of the respective average relative biases (as a percentage) and estimated RMSEs. In the figures we refer to $\widetilde{\mathscr{N}}_p(b, m)$ as "NBQ (tilde)" and to $\widetilde{\mathscr{V}}_p(w_0; b, m)$ as "Combined (tilde)."

2.7.1 First-Order Autoregressive Process

The first test process is the stationary AR(1) time-series model described in Section 2.6.1. For experimentation we selected the values $\phi = 0.9$ and $p \in \{0.5, 0.75, 0.95, 0.99\}$. The results are summarized in Tables 2.3–2.4 and in Figure 2.3. Notice here that there is some overlap with the experimental results presented in Section 2.6, thus we will not discuss here any findings already presented in the previous section.

Tables 2.3–2.4 indicate that all five estimators of σ_p^2 and their respective estimated standard deviations converged to their asymptotic limits reasonably fast (for values $\mathcal{L} > 10$). They also reveal that the BQE-based estimators $\widetilde{\mathcal{N}_p}(b,m)$ and $\mathcal{N}_p(b,m)$ converged faster compared to the batched STS area estimator $\mathcal{A}_p(w_0;b,m)$. Typically, the batched STS area estimator $\mathcal{A}_p(w_0;b,m)$ was more biased than $\widetilde{\mathcal{N}_p}(b,m)$ and $\mathcal{N}_p(b,m)$, especially for small batch sizes. There were a few exceptions. Specifically, in Table of 2.4 for $p = 0.99$ and $\mathcal{L} = 10, 11$, $\mathcal{A}_p(w_0;b,m)$ exhibited an average bias of -38.589 and -18.068, respectively, while $\mathcal{N}_p(b,m)$ exhibited an average bias of -41.419 and -25.188, respectively. Further, for $p = 0.99$ columns 5 and 9 show that the estimated standard deviation of $\widetilde{\mathcal{N}_p}(b,m)$ approached its asymptotic value more quickly than the estimated standard deviation of $\mathcal{A}_p(w_0;b,m)$.

For this test process, Tables 2.3 and 2.4 indicate that $\widetilde{\mathcal{N}_p}(b,m)$ is less biased than $\mathcal{N}_p(b,m)$, especially for small batch sizes. Of course, as we expected, the bias of the combined estimators $\widetilde{\mathcal{V}_p}(w_0;b,m)$ and $\mathcal{V}_p(w_0;b,m)$ fell between the biases of their constituents. Moreover, among $\mathcal{A}_p(w;b,m)$, $\widetilde{\mathcal{N}_p}(b,m)$, and $\mathcal{N}_p(b,m)$, the standard deviation of $\widetilde{\mathcal{N}_p}(b,m)$ usually converged more quickly to its asymptotic value. Figure 2.3 illustrates that the main NBQ estimator $\widetilde{\mathcal{N}_p}(b,m)$ outperformed its competitors with regard to percent relative bias, especially for small batch sizes. Further, Figure 2.3 clearly shows the advantage of the combined estimators $\widetilde{\mathcal{V}_p}(w_0;b,m)$ and $\mathcal{V}_p(w_0;b,m)$ with regard to RMSE.

It is important to note here that comparisons between variance parameter estimators based on average bias can be misleading because the respective estimates may "oscillate" about zero. Specifically, in several cases the bias of the batched STS area estimator $\mathcal{A}_p(w_0;b,m)$ may be low for small samples, and then increase significantly for larger sample sizes. This issue is more pronounced in the next two examples.

2.7.2 M/M/1 Waiting-Time Process

Our second stationary test process was generated by the M/M/1 queueing system in Section 2.6.2 with FIFO service discipline, arrival rate $\lambda = 0.8$, and service rate $\omega = 1$.

The results are summarized in Tables 2.5–2.6 and in Figure 2.4. Tables 2.5–2.6 illustrate that all five variance-parameter estimators and their standard deviations converged to the respective theoretical limits, but at a significantly lower rate than for the AR(1) process in Section 2.7.1; these findings are extensions to those in Section 2.6. Again, this example clearly indicated the presence of substantial bias in the variance-parameter estimators for small batch sizes m, and this bias became more prominent for large values of p (near-extreme quantiles).

Among the five variance-parameter estimators, the NBQ estimators $\widetilde{\mathscr{N}_p}(b,m)$ and $\mathscr{N}_p(b,m)$ exhibited the lowest absolute bias for $2^{10} \le m \le 2^{17}$. Although. there was no a clear winner between the two NBQ estimators, there seems to be an indication that NBQ $\widetilde{\mathscr{N}_p}(b,m)$ exhibits lower absolute bias for larger values of p ($p \ge 0.95$) and larger bias for $p \le 0.75$ compared to $\mathscr{N}_p(b,m)$. Verifying this "trend" requires experimentation using a wider set of p values and more test processes. On the other hand, most frequently the batched STS area estimator $\mathscr{A}_p(w_0;b,m)$ exhibited the largest absolute small-sample bias. There were a few exceptions, e.g., for $p = 0.5$ and $m < 2^9$, where $\mathscr{A}_p(w_0;b,m)$ reported the smallest absolute bias. Again, since the combined estimators $\widetilde{\mathscr{V}_p}(w_0;b,m)$ and $\mathscr{V}_p(w_0;b,m)$ are roughly the average of their constituents, their estimated average bias tends to fall in the middle; see Figure 2.4. For $p = 0.5$ and $m \le 2^{10}$, all five variance-parameter estimators induced CIs that exhibited slight overcoverage. On the other hand, for $p \ge 0.75$ all five variance-parameter estimators, induced CIs with significant undercoverage for small values of m, and this issue was more pronounced in larger values of p. In all cases, for $p \ge 0.75$, the NBQ estimator $\widetilde{\mathscr{N}_p}(b,m)$ resulted in CIs for y_p with coverage probabilities that converged faster to the nominal value of 95%, followed by the NBQ estimator $\mathscr{N}_p(b,m)$. This was expected as $\widetilde{\mathscr{N}_p}(b,m) \ge \mathscr{N}_p(b,m)$, so that the NBQ estimator $\widetilde{\mathscr{N}_p}(b,m)$ yields wider CIs.

Additionally, in these cases, the batched STS area estimator $\mathscr{A}_p(w_0; b, m)$ usually required larger batch sizes to achieve estimated CI coverage probabilities close to the nominal value compared to the NBQ estimators. Specifically, for $p = 0.99$ and $m = 2^{12}$, $\mathscr{A}_p(w_0; b, m)$ yielded a CI with estimated coverage probability of 79.08%, the NBQ estimator $\widetilde{\mathscr{N}_p}(b, m)$ resulted in a CI coverage probability of 89.04%, and the NBQ estimator $\mathscr{N}_p(b, m)$ resulted in a CI coverage probability of 87.88%.

The combined estimators resulted in CIs with estimated coverage probabilities analogously to the estimated CI coverage probabilities of their constituents. In particular, the combined estimator $\widetilde{\mathscr{V}}_p(w_0; b, m)$ yielded CIs with estimated coverage probabilities that are closer to the nominal value of 95% compared to $\mathscr{V}_p(w_0; b, m)$. This is one of the main reasons why we chose to incorporate $\widetilde{\mathscr{V}}_p(w_0; b, m)$ in the newly developed procedures in Chapters 4-6.

The plots of the RMSEs in Figure 2.4 once more highlight the importance of the combined estimators, especially for reasonably large batch sizes ($m \geq 2^{15}$).

2.7.3 Autoregressive-to-Pareto Process

The third test process is the ARTOP process described in Section 2.5.2 with location parameter $\gamma = 1$, shape parameter $\theta = 2.1$, and autoregressive parameter $\phi = 0.995$. The initial state Z_0 is generated from a $N(0, 1)$. The results are summarized in Tables 2.7–2.8 and in Figure 2.5.

Tables 2.7–2.8 indicate that all five variance-parameter estimators and their standard deviations converged to the respective theoretical limits. For $p \leq 0.95$ and $2^{10} \leq m \leq 2^{16}$, the NBQ estimators outperform ed the batched STS area estimator $\mathscr{A}_p(w_0; b, m)$ with regard to bias. In this example, we also see that in most cases the NBQ estimator $\mathscr{N}_p(b, m)$ reported smaller absolute bias than the NBQ estimator $\widetilde{\mathscr{N}_p}(b, m)$. On the other hand, especially for small batch sizes, $\widetilde{\mathscr{N}_p}(b, m)$ resulted in CIs with coverage probabilities that are closer to the nominal value compared to $\mathscr{N}_p(b, m)$. Further, the estimated coverage probabilities of the

CIs based on the batched STS area estimator $\mathscr{A}_p(w_0; b, m)$ converged to the nominal value at a lower rate. We see again that the estimated bias of the combined estimators $\widetilde{\mathscr{V}_p}(w_0; b, m)$ and $\mathscr{V}_p(w_0; b, m)$ fell between the biases of their constituents and the respective estimated standard deviations have smaller asymptotic values compared to the other three. Also, the combined estimator $\widetilde{\mathscr{V}_p}(w_0; b, m)$ resulted in CIs with estimated coverage probabilities that are closer to the nominal value of 95% compared to $\mathscr{V}_p(w_0; b, m)$. Figure 2.5 reveals that the RMSEs of the NBQ estimators $\mathscr{N}_p(b, m)$ and $\widetilde{\mathscr{N}_p}(b, m)$ appear to reach a peak for relatively small batch sizes, and then converge faster to their theoretical limit than the RMSE of the batched STS area estimator $\mathscr{A}_p(w_0; b, m)$. Further, the plots of the estimated relative bias highlight the benefits of the combined estimators.

Table 2.3: Experimental results for the AR(1) process with $\mu_Y = 0$ and $\phi = 0.9$ for $p \in \{0.5, 0.75\}$. All estimates are based on 2,500 independent replications with $b = 32$ batches and batch sizes $m = 2^{\mathcal{L}}$, $\mathcal{L} \in \{7, 8, \ldots, 20\}$, where for nominal 95% CIs for y_p, the coverage probabilities are denoted by "95% CI Cover."

		STS area $\mathscr{A}_p(w_0; b, m)$				NBQ $\widetilde{\mathscr{N}}_p(b, m)$				NBQ $\mathscr{N}_p(b, m)$				Combined $\widetilde{\mathscr{V}}_p(w; b, m)$				Combined $\mathscr{V}_p(w; b, m)$			
p (y_p) **Var. Par.**	$\mathcal{L}$	Avg.	Bias	Std. Dev.	95% CI Cover.	Avg.	Bias	Std. Dev.	95% CI Cover.	Avg.	Bias	Std. Dev.	95% CI Cover.	Avg.	Bias	Std. Dev.	95% CI Cover.	Avg.	Bias	Std. Dev.	95% CI Cover.
0.5	7	16.961	−3.897	5.004	92.20	19.183	−1.675	4.870	94.32	19.125	−1.733	4.861	94.24	18.054	−2.804	3.544	93.12	18.026	−2.832	3.541	93.12
(0.0000)	8	19.025	−1.833	5.116	93.12	19.831	−1.027	5.041	93.92	19.794	−1.064	5.033	93.80	19.422	−1.436	3.616	93.28	19.403	−1.455	3.613	93.28
20.858	9	19.939	−0.919	5.389	94.40	20.304	−0.554	5.250	94.44	20.281	−0.577	5.246	94.44	20.119	−0.739	3.826	94.60	20.107	−0.751	3.825	94.60
	10	20.370	−0.488	5.340	94.32	20.671	−0.187	5.239	94.52	20.657	−0.201	5.237	94.52	20.518	−0.340	3.759	94.56	20.511	−0.347	3.758	94.56
	11	20.638	−0.220	5.141	94.16	20.697	−0.161	5.183	94.44	20.688	−0.170	5.181	94.44	20.667	−0.191	3.614	93.88	20.662	−0.196	3.614	93.88
	12	20.751	−0.107	5.309	95.08	20.705	−0.153	5.197	94.92	20.699	−0.159	5.196	94.92	20.728	−0.130	3.667	94.88	20.725	−0.133	3.667	94.88
	13	20.525	−0.333	5.292	94.48	20.809	−0.049	5.327	94.84	20.805	−0.053	5.326	94.80	20.664	−0.194	3.738	94.80	20.662	−0.196	3.738	94.80
	14	20.813	−0.045	5.165	94.80	20.893	0.035	5.374	95.16	20.890	0.032	5.374	95.16	20.852	−0.006	3.751	94.88	20.851	−0.007	3.750	94.88
	15	20.660	−0.198	5.137	94.96	20.936	0.078	5.356	94.72	20.934	0.076	5.355	94.72	20.796	−0.062	3.716	95.52	20.795	−0.063	3.716	95.52
	16	20.797	−0.061	5.233	95.28	21.028	0.170	5.197	95.68	21.027	0.169	5.197	95.68	20.911	0.053	3.698	95.24	20.910	0.052	3.698	95.24
	17	20.682	−0.176	5.228	95.40	20.907	0.049	5.286	95.24	20.907	0.049	5.285	95.24	20.793	−0.065	3.680	95.32	20.793	−0.065	3.680	95.32
	18	20.918	0.060	5.254	95.80	20.997	0.139	5.430	95.80	20.996	0.138	5.430	95.80	20.957	0.099	3.763	95.88	20.956	0.098	3.763	95.88
	19	20.815	−0.043	5.171	95.04	20.909	0.051	5.314	94.68	20.908	0.050	5.314	94.68	20.861	0.003	3.734	95.00	20.861	0.003	3.734	95.00
	20	20.930	0.072	5.387	94.72	20.908	0.050	5.226	95.04	20.907	0.049	5.226	95.04	20.919	0.061	3.730	94.80	20.919	0.061	3.730	94.80
0.75	7	18.803	−4.055	6.246	91.28	21.135	−1.723	5.431	93.52	20.804	−2.054	5.321	93.28	19.950	−2.908	4.263	92.52	19.787	−3.071	4.236	92.52
(0.6745)	8	21.005	−1.853	6.095	93.76	21.999	−0.859	5.629	95.00	21.825	−1.033	5.567	94.84	21.494	−1.364	4.292	94.48	21.409	−1.449	4.275	94.40
22.858	9	22.127	−0.731	6.260	94.32	22.393	−0.465	5.829	93.96	22.295	−0.563	5.797	93.92	22.258	−0.600	4.310	94.12	22.209	−0.649	4.299	94.04
	10	22.317	−0.541	5.974	93.64	22.771	−0.087	5.776	94.36	22.718	−0.140	5.760	94.36	22.541	−0.317	4.152	94.44	22.515	−0.343	4.146	94.40
	11	22.733	−0.125	5.810	94.60	22.798	−0.060	5.779	94.32	22.768	−0.090	5.771	94.24	22.765	−0.093	4.042	94.44	22.750	−0.108	4.039	94.44
	12	22.912	0.054	5.749	95.32	22.719	−0.139	5.761	95.24	22.703	−0.155	5.757	95.24	22.817	−0.041	4.071	95.60	22.809	−0.049	4.070	95.60
	13	22.654	−0.204	5.884	94.76	22.808	−0.050	5.863	94.96	22.799	−0.059	5.860	94.96	22.730	−0.128	4.150	95.24	22.725	−0.133	4.149	95.24
	14	22.887	0.029	5.779	95.12	22.844	−0.014	5.832	95.44	22.838	−0.020	5.831	95.44	22.866	0.008	4.099	95.16	22.863	0.005	4.098	95.16
	15	22.771	−0.087	5.801	94.80	22.775	−0.083	5.868	95.12	22.771	−0.087	5.867	95.12	22.773	−0.085	4.140	94.80	22.771	−0.087	4.140	94.80
	16	22.787	−0.071	5.718	94.76	22.938	0.080	5.810	95.08	22.936	0.078	5.809	95.08	22.862	0.004	4.107	95.00	22.860	0.002	4.107	95.00
	17	22.682	−0.176	5.707	95.24	22.881	0.023	5.845	95.08	22.880	0.022	5.845	95.08	22.780	−0.078	4.024	95.48	22.779	−0.079	4.024	95.48
	18	22.875	0.017	5.654	95.68	23.007	0.149	5.876	96.16	23.006	0.148	5.875	96.16	22.940	0.082	4.106	95.76	22.940	0.082	4.106	95.72
	19	22.844	−0.014	5.593	94.92	23.025	0.167	5.801	94.00	23.025	0.167	5.801	94.00	22.933	0.075	4.044	94.12	22.933	0.075	4.044	94.12
	20	22.972	0.114	5.779	95.00	22.810	−0.048	5.725	95.52	22.810	−0.048	5.725	95.52	22.893	0.035	4.030	95.16	22.892	0.034	4.030	95.16

Table 2.4: Experimental results for the AR(1) process with $\mu_Y = 0$ and $\phi = 0.9$ for $p \in \{0.95, 0.99\}$. All estimates are based on 2,500 independent replications with $b = 32$ batches and batch sizes $m = 2^{\mathcal{L}}$, $\mathcal{L} \in \{7, 8, \ldots, 20\}$, where for nominal 95% CIs for y_p, the coverage probabilities are denoted by "95% CI Cover."

		STS area $\mathscr{A}_p(w_0; b, m)$				NBQ $\widetilde{\mathscr{N}}_p(b, m)$				NBQ $\mathscr{N}_p(b, m)$				Combined $\widetilde{\mathscr{V}}_p(w; b, m)$				Combined $\mathscr{V}_p(w; b, m)$			
p (y_p) Var. Par.	$\mathcal{L}$	Avg.	Bias	Std. Dev.	95% CI Cover.	Avg.	Bias	Std. Dev.	95% CI Cover.	Avg.	Bias	Std. Dev.	95% CI Cover.	Avg.	Bias	Std. Dev.	95% CI Cover.	Avg.	Bias	Std. Dev.	95% CI Cover.
0.95	7	30.912	−7.353	14.120	90.48	33.950	−4.315	9.300	93.28	31.275	−6.990	8.311	92.28	32.407	−5.858	9.081	92.52	31.091	−7.174	8.907	92.12
(1.6449)	8	36.479	−1.786	15.062	93.40	36.504	−1.761	9.666	93.80	35.610	−2.655	9.306	93.64	36.491	−1.774	9.600	94.04	36.051	−2.214	9.545	94.00
38.265	9	37.594	−0.671	13.516	94.32	37.580	−0.685	10.070	95.08	37.028	−1.237	9.842	94.88	37.587	−0.678	8.791	94.64	37.315	−0.950	8.754	94.60
	10	37.812	−0.453	11.414	94.32	38.109	−0.156	10.105	95.00	37.698	−0.567	9.961	94.88	37.958	−0.307	7.855	94.88	37.756	−0.509	7.820	94.88
	11	38.386	0.121	10.799	93.96	37.984	−0.281	9.849	94.40	37.804	−0.461	9.783	94.28	38.188	−0.077	7.425	94.40	38.099	−0.166	7.405	94.36
	12	38.662	0.397	10.384	95.28	38.054	−0.211	9.797	94.56	37.986	−0.279	9.769	94.52	38.363	0.098	7.214	94.84	38.330	0.065	7.206	94.84
	13	38.104	−0.161	10.008	94.36	38.085	−0.180	9.928	95.00	38.040	−0.225	9.911	95.00	38.094	−0.171	7.141	94.64	38.072	−0.193	7.136	94.64
	14	38.306	0.041	9.899	95.12	38.326	0.061	9.737	95.68	38.291	0.026	9.726	95.68	38.316	0.051	7.016	95.40	38.299	0.034	7.013	95.40
	15	38.422	0.157	9.894	94.68	38.115	−0.150	9.956	94.40	38.098	−0.167	9.950	94.40	38.271	0.006	7.035	94.36	38.262	−0.003	7.034	94.36
	16	38.226	−0.039	9.943	95.32	38.255	−0.010	9.836	95.44	38.246	−0.019	9.834	95.44	38.240	−0.025	7.091	95.40	38.236	−0.029	7.090	95.40
	17	38.153	−0.112	9.532	95.72	38.418	0.153	9.878	95.52	38.412	0.147	9.877	95.52	38.283	0.018	6.806	95.56	38.280	0.015	6.805	95.56
	18	38.451	0.186	9.582	95.16	38.743	0.478	9.878	95.44	38.738	0.473	9.877	95.44	38.595	0.330	6.887	95.24	38.592	0.327	6.886	95.24
	19	38.399	0.134	9.496	94.40	38.682	0.417	9.760	94.28	38.679	0.414	9.759	94.28	38.538	0.273	6.748	94.52	38.537	0.272	6.748	94.52
	20	38.819	0.554	9.716	94.96	38.306	0.041	9.747	95.12	38.304	0.039	9.747	95.12	38.566	0.301	6.788	95.08	38.566	0.301	6.788	95.08
0.99	7	43.023	−38.589	19.888	82.72	59.836	−21.776	19.167	90.56	40.193	−41.419	10.956	83.60	51.296	−30.316	14.885	87.40	41.630	−39.982	12.478	82.96
(2.3263)	8	63.544	−18.068	29.612	90.48	64.789	−16.823	18.939	91.92	56.424	−25.188	15.541	90.04	64.157	−17.455	19.384	91.12	60.040	−21.572	18.620	90.20
81.612	9	69.221	−12.391	33.086	91.60	74.505	−7.107	21.540	94.16	68.185	−13.427	19.802	93.08	71.821	−9.791	21.641	92.76	68.712	−12.900	21.333	91.92
	10	76.350	−5.262	31.978	92.92	79.563	−2.049	22.842	94.52	76.832	−4.780	22.154	94.08	77.931	−3.681	21.385	93.96	76.587	−5.025	21.288	93.84
	11	81.773	0.161	29.693	94.32	81.200	−0.412	21.763	94.84	80.209	−1.403	21.445	94.64	81.491	−0.121	19.890	94.56	81.003	−0.609	19.845	94.52
	12	83.965	2.353	26.111	94.60	81.832	0.220	21.628	94.32	81.558	−0.054	21.525	94.32	82.915	1.303	17.379	94.84	82.780	1.168	17.357	94.80
	13	82.641	1.029	23.842	94.00	81.407	−0.205	21.678	94.48	81.241	−0.371	21.616	94.44	82.034	0.422	16.566	94.12	81.952	0.340	16.549	94.12
	14	82.426	0.814	22.724	95.36	81.423	−0.189	20.838	95.44	81.307	−0.305	20.796	95.44	81.933	0.321	15.450	95.40	81.876	0.264	15.436	95.40
	15	81.767	0.155	21.163	94.88	81.482	−0.130	20.288	95.28	81.401	−0.211	20.263	95.24	81.627	0.015	14.903	95.12	81.587	−0.025	14.895	95.12
	16	82.122	0.510	21.256	94.92	81.094	−0.518	20.445	94.92	81.030	−0.582	20.427	94.92	81.616	0.004	14.667	95.00	81.585	−0.027	14.662	95.00
	17	81.788	0.176	20.670	95.72	81.524	−0.088	20.606	95.00	81.494	−0.118	20.599	95.00	81.658	0.046	14.482	95.04	81.644	0.032	14.480	95.04
	18	81.523	−0.089	21.343	95.04	82.320	0.708	20.759	94.92	82.299	0.687	20.754	94.92	81.916	0.304	14.887	94.80	81.905	0.293	14.886	94.80
	19	82.083	0.471	20.924	95.28	82.607	0.995	20.864	94.52	82.594	0.982	20.862	94.52	82.341	0.729	14.732	94.68	82.334	0.722	14.731	94.68
	20	82.971	1.359	20.830	94.80	82.194	0.582	20.854	95.00	82.185	0.573	20.852	95.00	82.589	0.977	14.409	95.04	82.584	0.972	14.409	95.04

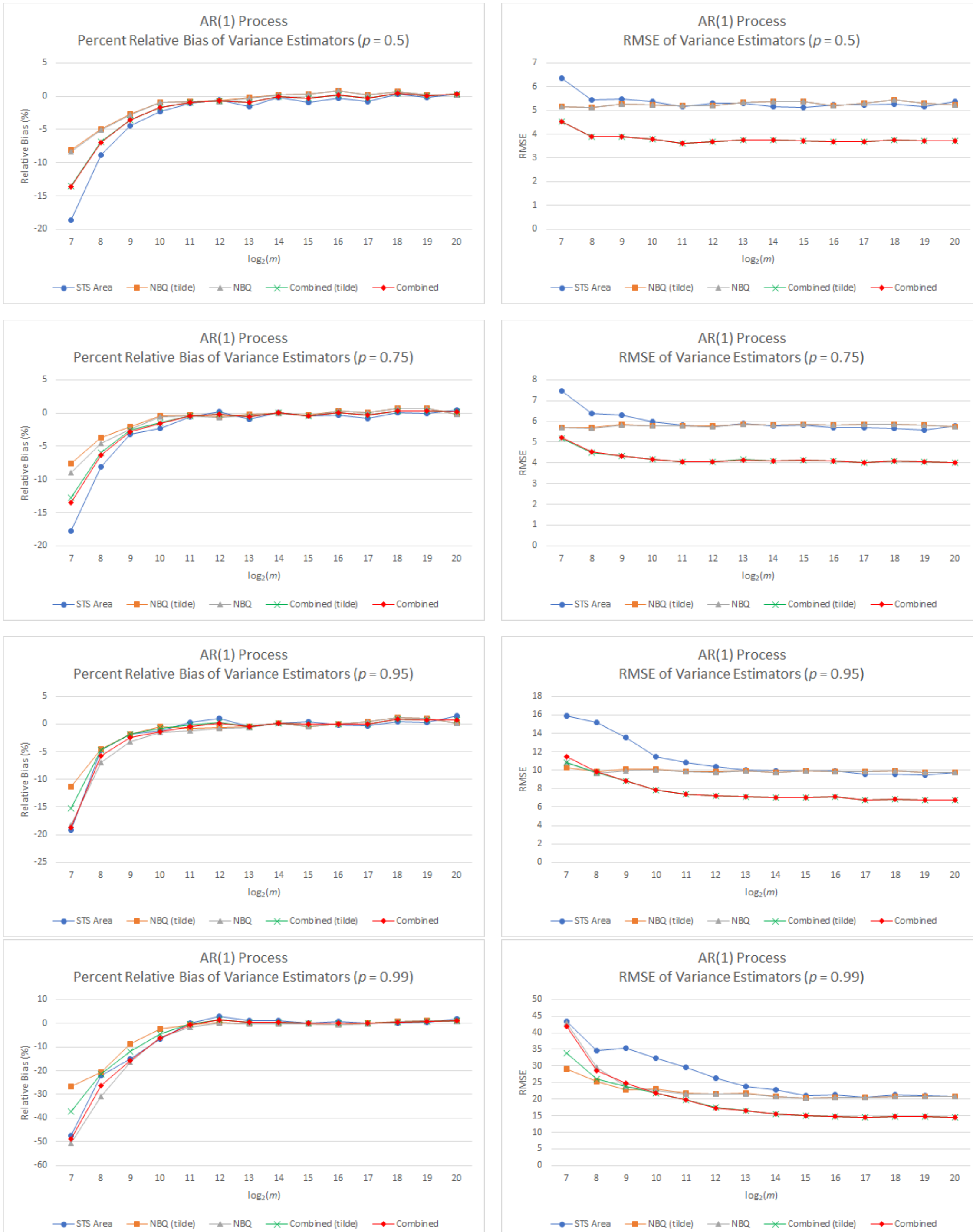

Figure 2.3: Estimated percent relative bias and RMSE of the variance-parameter estimators for selected marginal quantiles of a stationary AR(1) process with $\mu_Y = 0$ and $\phi = 0.9$ based on Tables 2.3–2.4. All estimates are based on 2,500 independent replications with $b = 32$ batches and batch sizes $m = 2^{\mathcal{L}}$, $\mathcal{L} \in \{7, 8, \ldots, 20\}$.

Table 2.5: Experimental results for a stationary waiting-time process in an M/M/1 queueing system with traffic intensity $\rho = 0.8$ for $p \in \{0.5, 0.75\}$. All estimates are based on 2,500 independent replications with $b = 32$ batches and batch sizes $m = 2^{\mathcal{L}}$, $\mathcal{L} = 7, 8, \ldots, 20$, where for nominal 95% CIs for y_p, the coverage probabilities are denoted by "95% CI Cover."

p (y_p) Var. Par.	$\mathcal{L}$	STS area $\mathscr{A}_p(w_0; b, m)$ Avg.	Bias	Std. Dev.	95% CI Cover.	NBQ $\widetilde{\mathscr{N}}_p(b, m)$ Avg.	Bias	Std. Dev.	95% CI Cover.	NBQ $\mathscr{N}_p(b, m)$ Avg.	Bias	Std. Dev.	95% CI Cover.	Combined $\widetilde{\mathscr{V}}_p(w; b, m)$ Avg.	Bias	Std. Dev.	95% CI Cover.	Combined $\mathscr{V}_p(w; b, m)$ Avg.	Bias	Std. Dev.	95% CI Cover.
0.5	7	812.2	177.2	529.5	94.56	1,566.0	931.0	1,395.1	97.32	1,451.3	816.3	1,266.3	97.08	1,183.1	548.1	848.0	97.00	1,126.7	491.7	786.7	96.72
(2.3500)	8	1,409.7	774.7	1,128.4	97.92	1,708.9	1,073.9	1,576.5	97.88	1,608.1	973.1	1,470.1	97.68	1,556.9	921.9	1,143.3	98.56	1,507.3	872.3	1,095.1	98.52
635.0	9	1,697.4	1,062.4	1,537.4	98.32	1,366.9	731.9	1,405.9	97.32	1,308.9	673.9	1,340.9	97.16	1,534.8	899.8	1,210.1	98.20	1,506.2	871.2	1,183.6	98.16
	10	1,489.4	854.4	1,440.2	98.08	928.3	293.3	626.1	96.60	903.9	268.9	602.7	96.40	1,213.3	578.3	869.1	97.76	1,201.3	566.3	862.0	97.64
	11	1,110.6	475.6	808.9	97.36	769.7	134.7	343.3	96.04	758.6	123.6	334.8	95.88	942.9	307.9	484.1	97.04	937.4	302.4	481.6	97.00
	12	836.0	201.0	352.9	96.92	698.9	63.9	221.6	96.04	693.7	58.7	218.4	95.96	768.5	133.5	227.5	96.52	766.0	131.0	226.4	96.48
	13	729.9	94.9	236.3	95.76	664.2	29.2	187.6	95.56	661.6	26.6	186.3	95.52	697.5	62.5	157.2	95.88	696.3	61.3	156.8	95.88
	14	682.8	47.8	192.7	95.88	643.7	8.7	170.3	95.64	642.4	7.4	169.7	95.52	663.5	28.5	132.1	95.96	662.9	27.9	131.9	95.96
	15	654.3	19.3	176.3	94.36	640.1	5.1	167.0	94.52	639.4	4.4	166.7	94.48	647.3	12.3	122.6	94.52	647.0	12.0	122.5	94.52
	16	646.4	11.4	166.6	95.16	639.1	4.1	163.1	95.36	638.8	3.8	163.0	95.36	642.8	7.8	116.9	95.40	642.7	7.7	116.9	95.40
	17	639.1	4.1	161.9	94.72	640.0	5.0	163.5	94.80	639.8	4.8	163.5	94.80	639.5	4.5	114.4	94.32	639.5	4.5	114.4	94.32
	18	638.9	3.9	159.6	94.40	634.7	-0.3	159.3	94.76	634.6	−0.4	159.2	94.72	636.8	1.8	112.4	94.64	636.8	1.8	112.4	94.64
	19	639.4	4.4	163.0	94.64	632.8	−2.2	164.1	94.72	632.8	−2.2	164.1	94.72	636.2	1.2	114.5	94.64	636.2	1.2	114.5	94.64
	20	632.5	−2.5	157.6	94.84	637.6	2.6	163.6	94.88	637.6	2.6	163.6	94.88	635.0	0.0	112.2	95.20	635.0	0.0	112.2	95.20
0.75	7	1,125.4	−2,173.3	682.2	73.60	2,527.5	−771.2	1,727.4	89.20	2,497.1	−801.6	1,692.4	88.96	1,815.3	−1,483.4	1,060.7	83.12	1,800.3	−1,498.4	1,043.6	82.96
(5.8158)	8	2,351.4	−947.3	1,727.0	86.56	4,027.8	729.1	2,721.3	94.80	3,940.8	642.1	2,624.7	94.68	3,176.3	−122.4	1,960.0	92.20	3,133.5	−165.2	1,911.9	92.16
3, 298.7	9	3,785.6	486.9	2,732.4	93.00	5,064.1	1,765.4	3,548.2	95.64	4,940.3	1,641.6	3,416.8	95.52	4,414.7	1,116.0	2,682.6	95.00	4,353.8	1,055.1	2,620.3	94.84
	10	4,853.0	1,554.3	3,419.9	95.92	4,798.4	1,499.7	3,211.7	96.12	4,707.5	1,408.8	3,111.5	96.04	4,826.1	1,527.4	2,831.1	96.52	4,781.4	1,482.7	2,787.7	96.48
	11	4,992.9	1,694.2	3,657.9	96.56	4,113.1	814.4	2,162.2	95.80	4,066.2	767.5	2,113.7	95.64	4,560.0	1,261.3	2,449.3	96.60	4,536.9	1,238.2	2,431.2	96.56
	12	4,242.5	943.8	2,046.1	96.16	3,703.1	404.4	1,329.6	95.96	3,681.0	382.3	1,312.2	95.88	3,977.1	678.4	1,361.7	96.20	3,966.2	667.5	1,355.5	96.20
	13	3,819.2	520.5	1,402.5	96.32	3,466.6	167.9	1,036.7	95.68	3,456.0	157.3	1,029.9	95.68	3,645.7	347.0	944.1	96.20	3,640.5	341.8	941.7	96.20
	14	3,547.5	248.8	1,045.6	95.36	3,366.1	67.4	905.0	95.16	3,360.9	62.2	902.2	95.16	3,458.3	159.6	726.8	95.24	3,455.7	157.0	725.8	95.24
	15	3,412.5	113.8	936.5	94.64	3,345.8	47.1	878.2	94.72	3,343.1	44.4	876.9	94.72	3,379.7	81.0	652.7	94.76	3,378.4	79.7	652.3	94.76
	16	3,356.4	57.7	873.3	94.60	3,337.2	38.5	861.3	94.80	3,335.9	37.2	860.7	94.80	3,347.0	48.3	617.7	94.64	3,346.3	47.6	617.5	94.64
	17	3,332.1	33.4	859.7	94.48	3,327.3	28.6	839.2	94.68	3,326.6	27.9	838.9	94.68	3,329.7	31.0	605.0	94.48	3,329.4	30.7	604.9	94.48
	18	3,316.1	17.4	814.8	94.60	3,312.8	14.1	829.5	94.76	3,312.5	13.8	829.3	94.76	3,314.5	15.8	578.2	94.60	3,314.3	15.6	578.1	94.60
	19	3,310.2	11.5	838.5	94.36	3,306.4	7.7	856.2	94.68	3,306.2	7.5	856.1	94.68	3,308.3	9.6	593.9	94.88	3,308.2	9.5	593.9	94.88
	20	3,292.4	−6.3	813.3	94.64	3,316.4	17.7	853.0	95.04	3,316.3	17.6	853.0	95.04	3,304.2	5.5	580.6	94.76	3,304.1	5.4	580.6	94.76

Table 2.6: Experimental results for a stationary waiting-time process in an M/M/1 queueing system with traffic intensity $\rho = 0.8$ for $p \in \{0.95, 0.99\}$. All estimates are based on 2,500 independent replications with $b = 32$ batches and batch sizes $m = 2^{\mathcal{L}}$, $\mathcal{L} = 7, 8, \ldots, 20$, where for nominal 95% CIs for y_p, the coverage probabilities are denoted by "95% CI Cover."

		STS area $\mathscr{A}_p(w_0;b,m)$				NBQ $\widetilde{\mathscr{N}}_p(b,m)$				NBQ $\mathscr{N}_p(b,m)$				Combined $\widetilde{\mathscr{V}}_p(w;b,m)$				Combined $\mathscr{V}_p(w;b,m)$			
p (y_p) **Var. Par.**	$\mathcal{L}$	Avg.	Bias	Std. Dev.	95% CI Cover.	Avg.	Bias	Std. Dev.	95% CI Cover.	Avg.	Bias	Std. Dev.	95% CI Cover.	Avg.	Bias	Std. Dev.	95% CI Cover.	Avg.	Bias	Std. Dev.	95% CI Cover.
0.95	7	1,884	−30,596	1,038	37.00	5,839	−26,641	5,100	58.76	3,606	−28,874	2,032	49.52	3,830	−28,650	2,749	49.20	2,731	−29,749	1,347	43.24
(13.8629)	8	4,611	−27,869	2,770	54.80	9,082	−23,398	5,698	71.16	7,382	−25,098	3,787	66.56	6,811	−25,669	3,651	62.92	5,974	−26,506	2,867	60.72
32,480	9	9,503	−22,977	6,386	68.56	14,877	−17,603	7,458	81.20	13,965	−18,515	6,732	80.00	12,147	−20,333	6,009	75.80	11,699	−20,781	5,751	75.04
	10	16,816	−15,664	12,658	80.96	24,106	−8,374	11,553	90.60	23,806	−8,674	11,450	90.48	20,403	−12,077	10,560	87.24	20,256	−12,224	10,535	87.00
	11	26,142	−6,338	19,292	88.84	34,970	2,490	18,686	94.44	34,807	2,327	18,554	94.44	30,486	−1,994	16,199	92.92	30,406	−2,074	16,133	92.92
	12	33,519	1,039	22,209	93.96	39,307	6,827	22,823	95.44	39,103	6,623	22,503	95.44	36,367	3,887	19,361	95.08	36,267	3,787	19,213	95.08
	13	37,166	4,686	18,578	95.52	37,129	4,649	18,450	95.80	37,006	4,526	18,232	95.76	37,148	4,668	15,334	96.20	37,087	4,607	15,238	96.16
	14	36,801	4,321	17,075	94.76	34,516	2,036	11,262	94.68	34,464	1,984	11,218	94.68	35,676	3,196	11,496	94.80	35,651	3,171	11,478	94.80
	15	35,003	2,523	12,155	94.80	33,469	989	9,686	95.04	33,444	964	9,669	95.04	34,249	1,769	8,505	94.72	34,236	1,756	8,498	94.72
	16	33,714	1,234	10,240	95.16	33,148	668	8,827	95.84	33,135	655	8,821	95.84	33,436	956	7,193	95.36	33,429	949	7,191	95.36
	17	33,065	585	8,831	94.84	32,693	213	8,363	94.76	32,686	206	8,360	94.76	32,882	402	6,177	95.00	32,878	398	6,177	95.00
	18	32,996	516	8,343	94.76	32,556	76	8,460	94.72	32,552	72	8,459	94.72	32,779	299	5,911	94.76	32,778	298	5,910	94.76
	19	32,564	84	8,239	94.88	32,570	90	8,315	95.20	32,568	88	8,314	95.20	32,567	87	5,859	94.80	32,566	86	5,858	94.80
	20	32,462	−18	7,978	94.68	32,593	113	8,318	94.56	32,592	112	8,317	94.56	32,526	46	5,705	94.56	32,526	46	5,705	94.56
0.99	7	2,255	−189,006	1,170	18.92	16,809	−174,452	17,586	49.36	3,846	−187,415	2,095	25.12	9,416	−181,845	8,861	37.52	3,038	−188,223	1,424	21.60
(21.9101)	8	6,001	−185,260	3,245	31.68	26,575	−164,686	26,786	57.36	8,256	−183,005	4,024	37.24	16,125	−175,136	13,839	46.40	7,111	−184,150	3,177	33.60
191,261	9	13,214	−178,047	7,919	41.56	38,974	−152,287	32,980	62.80	17,133	−174,128	7,526	47.92	25,890	−165,371	18,023	53.40	15,143	−176,118	6,765	44.48
	10	27,618	−163,643	17,701	54.88	53,585	−137,676	30,487	71.00	34,675	−156,586	14,418	61.48	40,395	−150,866	20,481	62.72	31,091	−160,170	14,065	57.92
	11	54,707	−136,554	37,687	67.96	80,128	−111,133	37,863	80.12	67,239	−124,022	28,074	76.24	67,216	−124,045	31,916	74.88	60,874	−130,387	28,645	72.64
	12	92,769	−98,492	66,687	79.08	123,088	−68,173	56,787	89.04	117,742	−73,519	54,211	87.88	107,688	−83,573	52,972	85.16	105,057	−86,204	52,186	84.84
	13	135,781	−55,480	93,623	87.72	179,440	−11,821	87,475	93.52	177,898	−13,363	87,261	93.44	157,264	−33,997	76,579	91.16	156,506	−34,755	76,546	91.04
	14	179,612	−11,649	128,352	91.20	218,074	26,813	117,142	94.56	217,213	25,952	116,265	94.56	198,538	7,277	106,052	93.00	198,114	6,853	105,703	93.00
	15	204,722	13,461	110,567	94.40	213,377	22,116	109,486	94.88	212,818	21,557	108,149	94.88	208,981	17,720	91,854	94.92	208,706	17,445	91,319	94.88
	16	209,709	18,448	106,715	95.44	202,611	11,350	77,118	95.84	202,367	11,106	76,595	95.80	206,216	14,955	75,154	95.80	206,096	14,835	74,931	95.80
	17	203,576	12,315	70,787	95.32	195,545	4,284	55,570	95.00	195,433	4,172	55,513	95.00	199,624	8,363	48,901	95.00	199,569	8,308	48,876	95.00
	18	199,607	8,346	57,126	95.24	193,633	2,372	53,765	94.84	193,573	2,312	53,742	94.84	196,667	5,406	41,550	95.00	196,638	5,377	41,538	95.00
	19	196,113	4,852	52,085	95.52	192,648	1,387	51,992	95.20	192,617	1,356	51,983	95.20	194,408	3,147	38,005	95.04	194,392	3,131	38,001	95.04
	20	193,492	2,231	49,780	95.52	193,054	1,793	48,724	95.16	193,036	1,775	48,720	95.16	193,277	2,016	35,609	95.16	193,268	2,007	35,607	95.16

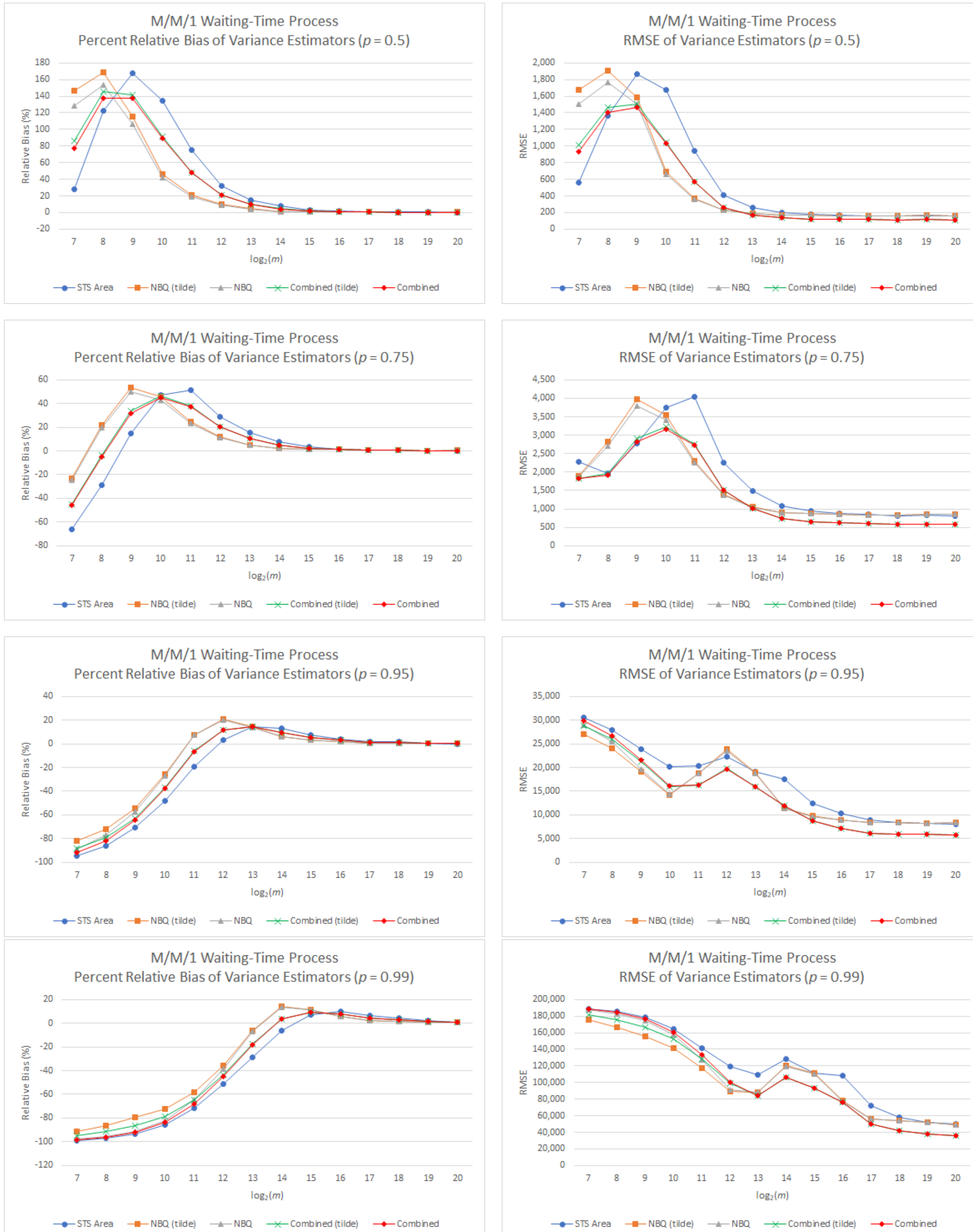

Figure 2.4: Estimated percent relative bias and RMSE of the variance-parameter estimators for selected marginal quantiles of a stationary waiting-time process in an M/M/1 queueing system with traffic intensity $\rho = 0.8$ based on Tables 2.5–2.6. All estimates are based on 2500 independent replications with $b = 32$ batches and batch sizes $m = 2^{\mathcal{L}}$, $\mathcal{L} = 7, 8, \ldots, 20$.

Table 2.7: Experimental results of an ARTOP process with $\gamma = 1, \theta = 2.1,$ and $\beta = 0.995$ for $p \in \{0.5, 0.75\}$. All estimates are based on 2,500 independent replications with $b = 32$ batches and batch sizes $m = 2^{\mathcal{L}}$, $\mathcal{L} = 7, 8, \ldots, 20$, where for nominal 95% CIs for y_p, the coverage probabilities are denoted by "95% CI Cover."

		STS area $\mathscr{A}_p(w_0; b, m)$				NBQ $\widetilde{\mathscr{N}}_p(b, m)$				NBQ $\mathscr{N}_p(b, m)$				Combined $\widetilde{\mathscr{V}}_p(w; b, m)$				Combined $\mathscr{V}_p(w; b, m)$			
p (y_p) **Var. Par.**	$\mathcal{L}$	Avg.	Bias	Std. Dev.	95% CI Cover.	Avg.	Bias	Std. Dev.	95% CI Cover.	Avg.	Bias	Std. Dev.	95% CI Cover.	Avg.	Bias	Std. Dev.	95% CI Cover.	Avg.	Bias	Std. Dev.	95% CI Cover.
0.5	7	101.6	−19.8	447.0	64.16	299.3	177.9	983.7	87.56	269.4	148.0	906.7	86.60	198.9	77.5	623.2	81.00	184.2	62.8	586.9	79.60
(1.3911)	8	198.5	77.1	651.3	84.36	327.8	206.4	714.2	94.36	296.8	175.4	662.3	93.32	262.2	140.8	603.7	91.64	246.9	125.5	581.0	90.60
121.4	9	322.5	201.1	1,078.2	93.20	325.6	204.2	850.9	96.76	298.0	176.6	809.7	96.24	324.0	202.6	743.2	96.16	310.4	189.0	728.3	95.72
	10	370.4	249.0	2,242.1	96.64	225.3	103.9	198.7	96.88	208.4	87.0	184.7	96.16	299.0	177.6	1,148.9	97.56	290.7	169.3	1,147.7	97.40
	11	250.3	128.9	243.5	96.68	171.9	50.5	92.8	96.32	162.9	41.5	86.7	95.96	211.7	90.3	140.8	97.12	207.3	85.9	139.2	96.88
	12	192.2	70.8	116.1	97.16	144.9	23.5	56.4	96.00	140.2	18.8	53.7	95.72	168.9	47.5	70.0	96.48	166.6	45.2	69.2	96.40
	13	156.2	34.8	68.1	96.16	133.5	12.1	44.1	95.60	131.1	9.7	42.7	95.48	145.0	23.6	43.8	96.04	143.9	22.5	43.4	96.00
	14	138.3	16.9	46.4	95.52	128.1	6.7	37.8	95.44	126.9	5.5	37.1	95.40	133.3	11.9	31.9	95.28	132.7	11.3	31.6	95.24
	15	129.6	8.2	38.0	94.92	124.9	3.5	34.5	95.32	124.3	2.9	34.2	95.16	127.3	5.9	26.3	95.32	127.0	5.6	26.2	95.28
	16	125.7	4.3	34.4	94.92	124.1	2.7	32.4	95.60	123.8	2.4	32.2	95.60	124.9	3.5	24.2	95.60	124.7	3.3	24.1	95.60
	17	122.6	1.2	31.7	95.36	122.5	1.1	31.9	95.12	122.4	1.0	31.9	95.12	122.6	1.2	22.3	95.76	122.5	1.1	22.3	95.76
	18	122.6	1.2	31.6	95.08	122.5	1.1	31.1	95.28	122.4	1.0	31.1	95.28	122.6	1.2	22.1	95.20	122.5	1.1	22.1	95.20
	19	121.3	−0.1	30.3	94.96	122.2	0.8	31.1	94.60	122.2	0.8	31.1	94.60	121.7	0.3	21.8	95.00	121.7	0.3	21.8	95.00
	20	122.1	0.7	31.0	94.96	121.4	0.0	30.5	94.92	121.4	0.0	30.5	94.92	121.7	0.3	21.9	94.68	121.7	0.3	21.9	94.68
0.75	7	223.7	−428.6	2,080.3	43.92	799.7	147.4	3,461.1	74.60	769.9	117.6	3,305.7	74.20	507.1	−145.2	2,479.0	64.80	492.5	−159.8	2,404.2	64.44
(1.9351)	8	519.1	−133.2	2,332.2	68.08	1,155.8	503.5	3,689.9	87.28	1,112.7	460.4	3,533.4	87.12	832.4	180.1	2,707.8	81.68	811.2	158.9	2,633.6	81.52
652.3	9	1,044.8	392.5	4,834.3	84.76	1,477.7	825.4	5,288.2	94.00	1,420.5	768.2	5,101.8	93.84	1,257.8	605.5	4,113.0	91.04	1,229.7	577.4	4,033.9	90.88
	10	1,988.2	1,335.9	33,099.7	92.44	1,318.0	665.7	2,936.4	95.72	1,268.6	616.3	2,830.3	95.60	1,658.4	1,006.1	16,985.5	94.96	1,634.1	981.8	16,975.2	94.84
	11	1,315.0	662.7	3,118.3	95.56	935.6	283.3	632.1	95.68	909.3	257.0	606.0	95.40	1,128.3	476.0	1,684.1	96.00	1,115.3	463.0	1,678.6	95.96
	12	1,029.1	376.8	913.9	96.88	779.8	127.5	341.5	96.04	766.3	114.0	330.9	95.84	906.4	254.1	531.7	96.60	899.8	247.5	528.6	96.60
	13	845.0	192.7	435.7	96.56	719.4	67.1	255.3	95.28	712.4	60.1	250.7	95.28	783.2	130.9	278.9	96.20	779.7	127.4	277.2	96.08
	14	744.2	91.9	256.0	95.44	688.1	35.8	212.5	94.92	684.5	32.2	210.5	94.76	716.6	64.3	178.7	95.56	714.8	62.5	178.0	95.52
	15	693.6	41.3	205.0	95.16	671.9	19.6	190.6	95.32	670.2	17.9	189.6	95.32	683.0	30.7	145.9	95.40	682.1	29.8	145.6	95.40
	16	673.8	21.5	181.9	95.20	668.8	16.5	179.3	95.12	667.9	15.6	178.8	95.12	671.4	19.1	130.6	95.32	670.9	18.6	130.4	95.32
	17	659.9	7.6	171.2	95.32	659.7	7.4	173.3	95.48	659.2	6.9	173.1	95.44	659.8	7.5	123.3	95.08	659.6	7.3	123.2	95.08
	18	658.6	6.3	169.0	95.60	659.5	7.2	174.7	95.96	659.3	7.0	174.5	95.96	659.0	6.7	123.0	95.60	658.9	6.6	122.9	95.60
	19	653.2	0.9	165.0	94.52	658.7	6.4	170.1	94.84	658.6	6.3	170.1	94.84	655.9	3.6	119.0	94.60	655.8	3.5	119.0	94.60
	20	656.1	3.8	169.6	94.92	657.4	5.1	165.1	95.12	657.4	5.1	165.1	95.12	656.8	4.5	119.3	94.92	656.7	4.4	119.3	94.92

Table 2.8: Experimental results of an ARTOP process with $\gamma = 1, \theta = 2.1,$ and $\beta = 0.995$ for $p \in \{0.95, 0.99\}$. All estimates are based on 2,500 independent replications with $b = 32$ batches and batch sizes $m = 2^{\mathcal{L}}$, $\mathcal{L} = 7, 8, \ldots, 20$, where for nominal 95% CIs for y_p, the coverage probabilities are denoted by "95% CI Cover."

		STS area $\mathscr{A}_p(w_0; b, m)$				NBQ $\widetilde{\mathscr{N}}_p(b, m)$				NBQ $\mathscr{N}_p(b, m)$				Combined $\widetilde{\mathscr{V}}_p(w; b, m)$				Combined $\mathscr{V}_p(w; b, m)$			
p (y_p) **Var. Par.**	$\mathcal{L}$	Avg.	Bias	Std. Dev.	95% CI Cover.	Avg.	Bias	Std. Dev.	95% CI Cover.	Avg.	Bias	Std. Dev.	95% CI Cover.	Avg.	Bias	Std. Dev.	95% CI Cover.	Avg.	Bias	Std. Dev.	95% CI Cover.
0.95	7	668	−12,533	5,867	17.32	3,157	−10,044	14,408	44.20	2,597	−10,604	13,634	36.92	1,893	−11,308	9,516	32.44	1,617	−11,584	9,185	28.40
(4.1643)	8	2,370	−10,831	17,984	34.32	6,986	−6,215	32,553	61.84	6,571	−6,630	32,197	58.08	4,641	−8,560	21,543	51.92	4,437	−8,764	21,376	49.24
13,201	9	5,132	−8,069	16,862	55.92	15,200	1,999	72,014	77.68	14,861	1,660	70,781	76.52	10,086	−3,115	39,342	70.76	9,920	−3,281	38,758	69.80
	10	46,958	33,757	1,749,162	75.28	31,114	17,913	372,607	87.80	30,534	17,333	360,870	87.64	39,162	25,961	1,065,953	83.68	38,876	25,675	1,060,252	83.60
	11	23,951	10,750	77,224	88.80	27,023	13,822	66,947	93.72	26,578	13,377	64,979	93.68	25,463	12,262	67,137	92.16	25,244	12,043	66,246	92.12
	12	27,807	14,606	77,432	93.60	23,532	10,331	34,623	95.36	23,153	9,952	33,674	95.32	25,704	12,503	48,888	95.16	25,517	12,316	48,570	95.16
	13	26,155	12,954	69,351	95.48	17,562	4,361	10,935	95.76	17,382	4,181	10,672	95.72	21,927	8,726	37,065	96.16	21,838	8,637	36,988	96.08
	14	19,033	5,832	14,175	96.12	15,090	1,889	6,331	95.32	15,012	1,811	6,250	95.32	17,093	3,892	8,591	96.32	17,054	3,853	8,563	96.28
	15	15,890	2,689	7,031	96.28	14,168	967	4,620	95.36	14,131	930	4,594	95.28	15,043	1,842	4,664	95.92	15,024	1,823	4,653	95.92
	16	14,544	1,343	4,646	96.28	13,787	586	3,987	95.92	13,767	566	3,976	95.92	14,172	971	3,277	96.12	14,162	961	3,272	96.12
	17	13,785	584	3,807	95.04	13,505	304	3,655	95.32	13,496	295	3,651	95.32	13,647	446	2,730	95.44	13,643	442	2,728	95.40
	18	13,560	359	3,617	96.08	13,453	252	3,597	96.08	13,448	247	3,594	96.08	13,507	306	2,615	96.24	13,505	304	2,614	96.24
	19	13,403	202	3,452	95.56	13,301	100	3,427	95.72	13,299	98	3,426	95.72	13,353	152	2,489	95.52	13,352	151	2,488	95.52
	20	13,297	96	3,447	95.28	13,364	163	3,414	95.36	13,362	161	3,413	95.36	13,330	129	2,437	95.32	13,329	128	2,436	95.32
0.99	7	1,061	−213,216	8,256	6.16	15,922	−198,355	79,647	27.28	4,032	−210,245	21,183	13.92	8,374	−205,903	42,129	19.92	2,523	−211,754	13,995	10.36
(8.9615)	8	5,149	−209,128	36,627	12.80	28,450	−185,827	119,126	37.20	13,379	−200,898	71,217	23.12	16,615	−197,662	69,166	27.88	9,199	−205,078	47,770	18.92
214,277	9	13,456	−200,821	63,685	25.52	55,124	−159,153	238,687	51.36	38,664	−175,613	197,717	40.28	33,960	−180,317	130,912	39.92	25,860	−188,417	112,048	33.96
	10	63,961	−150,316	774,835	43.68	341,692	127,415	10,855,637	66.72	325,339	111,062	10,632,413	60.80	200,622	−13,655	5,721,547	57.80	192,576	−21,701	5,611,750	54.12
	11	149,196	−65,081	1,008,149	67.04	359,839	145,562	5,863,407	82.04	350,163	135,886	5,717,035	80.48	252,846	38,569	3,121,658	77.40	248,085	33,808	3,050,694	76.24
	12	389,911	175,634	2,852,610	82.24	542,259	327,982	4,877,664	91.72	532,850	318,573	4,740,608	91.56	464,876	250,599	3,644,191	88.80	460,246	245,969	3,579,002	88.72
	13	524,018	309,741	4,731,970	91.16	521,692	307,415	1,533,489	95.24	512,116	297,839	1,480,442	95.20	522,874	308,597	2,861,910	94.24	518,162	303,885	2,845,187	94.24
	14	540,122	325,845	1,636,833	95.04	389,527	175,250	563,378	96.32	383,525	169,248	545,855	96.32	466,020	251,743	973,150	96.20	463,066	248,789	967,598	96.16
	15	433,001	218,724	829,837	95.92	282,290	68,013	167,006	95.84	279,890	65,613	163,576	95.84	358,842	144,565	451,512	96.12	357,661	143,384	450,683	96.12
	16	323,008	108,731	323,937	96.52	249,888	35,611	105,017	96.04	248,792	34,515	103,842	96.04	287,028	72,751	182,098	96.88	286,489	72,212	181,769	96.88
	17	266,306	52,029	146,212	96.04	230,223	15,946	73,093	95.32	229,724	15,447	72,753	95.32	248,551	34,274	88,058	96.00	248,305	34,028	87,933	96.00
	18	236,186	21,909	77,113	95.56	224,068	9,791	64,519	95.44	223,826	9,549	64,376	95.44	230,223	15,946	53,780	95.44	230,104	15,827	53,724	95.44
	19	225,507	11,230	63,720	95.08	217,850	3,573	60,228	94.24	217,728	3,451	60,162	94.24	221,739	7,462	45,877	94.88	221,679	7,402	45,851	94.88
	20	217,120	2,843	57,690	95.40	218,651	4,374	56,898	95.16	218,588	4,311	56,869	95.16	217,873	3,596	41,702	95.64	217,842	3,565	41,691	95.64

Figure 2.5: Estimated percent relative bias and RMSE of the variance-parameter estimators for selected marginal quantiles of an ARTOP process with $\gamma = 1, \theta = 2.1,$ and $\beta = 0.995$ based on Tables 2.7–2.8. All estimates are based on 2500 independent replications with $b = 32$ batches and batch sizes $m = 2^{\mathcal{L}}$, $\mathcal{L} = 7, 8, \ldots, 20$.

2.8 Experimentation with Weight Functions from the Literature

In this section we conduct a limited experimental evaluation of the bias and MSE of the NBQ estimator $\widetilde{\mathscr{N}_p}(b, m)$ in Equation (2.61) and the batched STS area estimators $\mathscr{A}_p(w; b, m)$ for the variance parameter $\sigma_p^2 = \lim_{n\to\infty} n\mathrm{Var}\big[\widetilde{y}_p(n)\big]$ based on the weight functions $w_0(t) = \sqrt{12}$, $w_2(t) = \sqrt{840}(3t^2-3t+1/2)$ (Goldsman *et al.* [33]), and $\{w_{\cos,\ell}(t) = \sqrt{8}\pi\ell\cos(2\pi\ell t)$: $\ell = 1, 2\}$ (Foley and Goldsman [54]) by means of the stationary AR(1) process in Section 2.6.1 and the M/M/1 waiting-time process in Section 2.6.2. Our objective is to illustrate our (temporary) decision to use the constant weight function $w_0(\cdot)$ in the procedures in Chapters 4–6.

Recall that the weights $w_2(\cdot)$ and $w_{\cos,\ell}(\cdot)$ were tailored to the estimation of the steady-state mean of the base process $\{Y_k : k \geq 1\}$ and yield first-order unbiased estimators for the respective variance parameter $\sigma^2 = \lim_{n\to\infty} n\mathrm{Var}(\overline{Y}_n)$. In particular, the STS area estimators for σ^2 obtained from the orthonormal sequence $\{w_{\cos,\ell}(\cdot) : \ell = 1, 2, \ldots\}$ are asymptotically independent as $m \to \infty$ for fixed b; hence they can be averaged to yield an estimator with smaller variance.

At this junction we wish to review a few findings regarding the bias of the estimators of σ^2 in the last paragraph. The main competitor of the STS area estimators for σ^2 is the NBM estimator $\mathscr{N}(b, m) \equiv \frac{m}{b-1}\sum_{j=1}^{b}(\overline{Y}_{j,m} - \overline{Y}_n)^2$, where $\overline{Y}_{j,m}$ the sample average from batch j. (Notice that the NBQ estimator $\mathscr{N}_p(b, m)$ is an analogue of $\mathscr{N}(b, m)$.) Aktaran-Kalaycı *et al.* [57] obtained detailed expressions for the expected value of various estimators of σ^2, including the ones mentioned in this section. Specifically, the NBM estimator has first-order bias equal to $-\gamma_1(b + 1)/n$, where $\gamma_1 \equiv 2\sum_{i=1}^{\infty} i\mathrm{Cov}[Y_1, Y_{1+i}]$ (assuming that the infinite series is summable). Analytical results in Aktaran-Kalaycı *et al.* [57] for the two stochastic processes under study herein revealed that, for fixed b, the STS area estimator of σ^2 based on the quadratic weight $w_2(\cdot)$ has more prominent bias than the NBM estimator $\mathscr{N}(b, m)$ for very small batch sizes m until it "catches up" as m increases, and eventually outperforms the NBM estimator with regard to the rate of convergence to σ^2. Further, Example 1 in Alexopoulos *et al.* [40] (corresponding to the Example in Section 2.8.2 below) illustrated that for processes with positive autocorrelation and for fixed (b, m), the bias of the estimator for σ^2 based on the weights $\{w_{\cos,\ell}(\cdot)\} : \ell = 1, 2, \ldots\}$ can become more pronounced as ℓ increases. (Of course, this effect diminishes as m increases.)

Unfortunately, as stated in Remark 2.3.2, the derivation of analytical expressions for the expected value of the estimators for σ_p^2 is a very difficult problem, even for i.i.d. processes (for more details see Chapter 3). A key question is: do the properties of the STS area estimators based on the weights $w_2(t) = \sqrt{840}(3t^2 - 3t + 1/2)$ (Goldsman *et al.* [33]) and $\{w_{\cos,\ell}(t) = \sqrt{8}\pi\ell\cos(2\pi\ell t)\text{: } \ell = 1, 2, \ldots\}$ carry over to the quantile-estimation setting? The following two examples attempt to provide a preliminary answer with regard to the small-sample bias of the NBQ variance estimator $\widetilde{\mathcal{N}_p}(b, m)$ and the STS area variance estimators $\mathscr{A}_p(w; b, m)$ corresponding to the weight functions $w_0(\cdot)$, $w_2(\cdot)$, and $\{w_{\cos,\ell}(\cdot) : \ell = 1, 2\}$.

2.8.1 First-Order Autoregressive Process

Consider the stationary Gaussian AR(1) time-series from Section 2.6.1. We take $Y_0 \sim N(0, 1)$, $\phi = 0.9$, and $\sigma_\epsilon^2 = 1 - \phi^2 = 0.19$; hence the process is stationary with a standard normal marginal distribution.

Figure 2.6 displays plots of the five estimated expeced values $\widetilde{\mathcal{N}_p}(b, m)$ ("NBQ (tilde)") and $\mathscr{A}_p(w; b, m)$ for the weight functions w_0 ("STS Const"), w_2 ("STS Quad"), $w_{\cos,1}$ ("STS Cos,1"), and $w_{\cos,2}$ ("STS Cos,2") computed from 2,500 independent replications for a fixed batch count $b = 32$, values $p \in \{0.75, 0.9, 0.95, 0.99, 0.995\}$, and increasing batch sizes $m = 2^{\mathcal{L}}$, $\mathcal{L} \in \{10, 11, \ldots, 20\}$. Figure 2.7 displays plots of the respective estimated relative bias (as a percentage) of the variance estimators and Figure 2.8 contains plots of the respective estimated RMSEs.

An examination of Figures 2.6–2.8 reveals the following findings: (i) All variance estimators converge to the value σ_p^2, as anticipated by theory. Indeed, for $m = 2^{20}$ all averages are within 2% of σ_p^2. (ii) The NBQ variance estimator $\widetilde{\mathscr{N}_p}(b, m)$ typically has the lowest small-sample estimated absolute bias; this is illustrated best for $p = 0.99$ or 0.995. (iii) There is no evidence in this experiment that any of the alternative weights $w_2(\cdot)$ and $\{w_{\cos,\ell} : \ell = 1, 2\}$ induces a variance estimator with lower small-sample absolute bias than $w_0(\cdot)$. Although for $p = 0.995$ the estimator $\mathscr{A}_p(w_0; b, m)$ has the most-pronounced estimated bias at $m = 2^{10}$, it catches up to the NBQ estimator $\widetilde{\mathscr{N}_p}(b, m)$ near $m = 2^{12}$, while the STS area estimators corresponding to $w_2(\cdot)$ and $\{w_{\cos,\ell} : \ell = 1, 2\}$ bounce from negative to excessive positive estimated bias before settling near σ_p^2 for $m \approx 2^{17}$. (iv) Among the five competing estimators of σ_p^2, the NBQ estimator $\widetilde{\mathscr{N}_p}(b, m)$ appears to exhibit the quickest convergence to a small neighborhood of σ_p^2 (within 2%) followed by $\mathscr{A}_p(w_0; b, m)$.

2.8.2 M/M/1 Waiting-Time Process

Consider the waiting-time process $\{Y_k : k \geq 1\}$ in an M/M/1 queueing system in steady-state with arrival rate $\lambda = 0.8$, service rate $\omega = 1$ (traffic intensity $\rho = 0.8$) and FIFO service discipline.

Figures 2.9–2.11 depict the experimental results based on 2,500 independent replications for a fixed batch count $b = 32$, values $p \in \{0.5, 0.75, 0.9, 0.95, 0.99, 0.995\}$, and increasing batch sizes $m = 2^{\mathcal{L}}$, $\mathcal{L} \in \{10, 11, \ldots, 20\}$.

For this test process, the dominance of the NBQ estimator $\widetilde{\mathscr{N}_p}(b, m)$ (primarily) and the STS area estimator $\mathscr{A}_p(w_0; b, m)$ (secondarily) over their competitors with regard to the rate of convergence to a narrow neighborhood of σ_p^2 (say, within 2%) is more evident than in the example of Section 2.8.1.

Remark 2.8.1. Based on the limited experimentation in Sections 2.8.1 and 2.8.2 and the early stage of our theoretical study of the bias of the aforementioned variance estimators, which may eventually lead to better weight functions adapted to quantile estimation, we adopted the constant weight $w_0(\cdot)$ in our experimental evaluation of the quantile-estimation

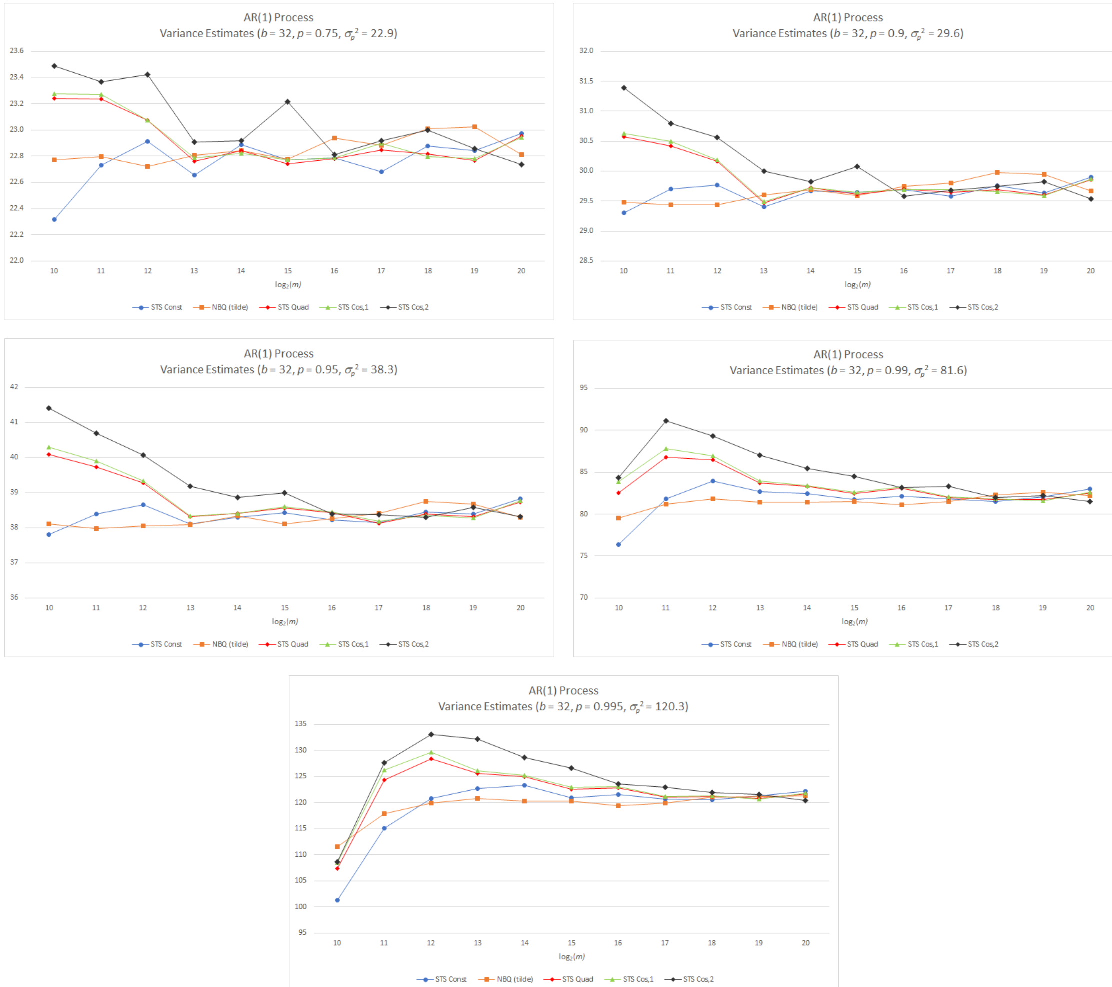

Figure 2.6: Estimated expected values of the variance estimators $\widetilde{\mathcal{N}}_p(b,m)$ ("NBQ (tilde)") and $\mathscr{A}_p(w;b,m)$ for the weight functions w_0 ("STS Const"), w_2 ("STS Quad"), $w_{\cos,1}$ ("STS Cos,1"), and $w_{\cos,2}$ ("STS Cos,2") for selected marginal quantiles of the AR(1) process in Section 2.8.1 with correlation coefficient $\phi = 0.9$. All estimates are based on 2,500 independent replications with $b = 32$ batches and batch sizes $m = 2^{\mathcal{L}}$, $\mathcal{L} \in \{10, 11, \ldots, 20\}$.

procedures in Chapters 4–6.

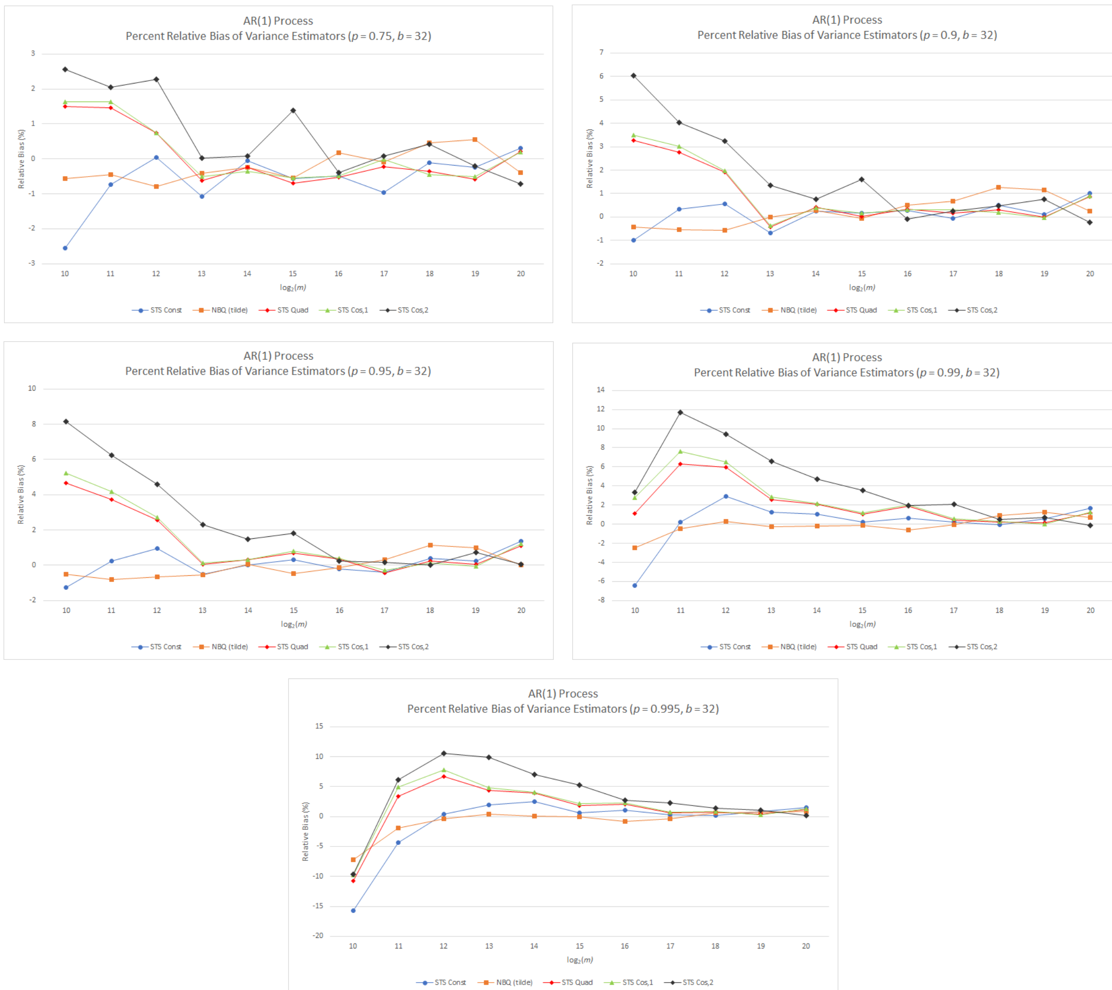

Figure 2.7: Estimated percent relative bias of the variance estimators $\widetilde{\mathcal{N}}_p(b,m)$ ("NBQ (tilde)") and $\mathscr{A}_p(w;b,m)$ for the weight functions w_0 ("STS Const"), w_2 ("STS Quad"), $w_{\cos,1}$ ("STS Cos,1"), and $w_{\cos,2}$ ("STS Cos,2") for selected marginal quantiles of the stationary AR(1) process in Section 2.8.1 with correlation coefficient $\phi = 0.9$. All estimates are based on 2,500 independent replications with $b = 32$ batches and batch sizes $m = 2^{\mathcal{L}}$, $\mathcal{L} \in \{10, 11, \ldots, 20\}$.

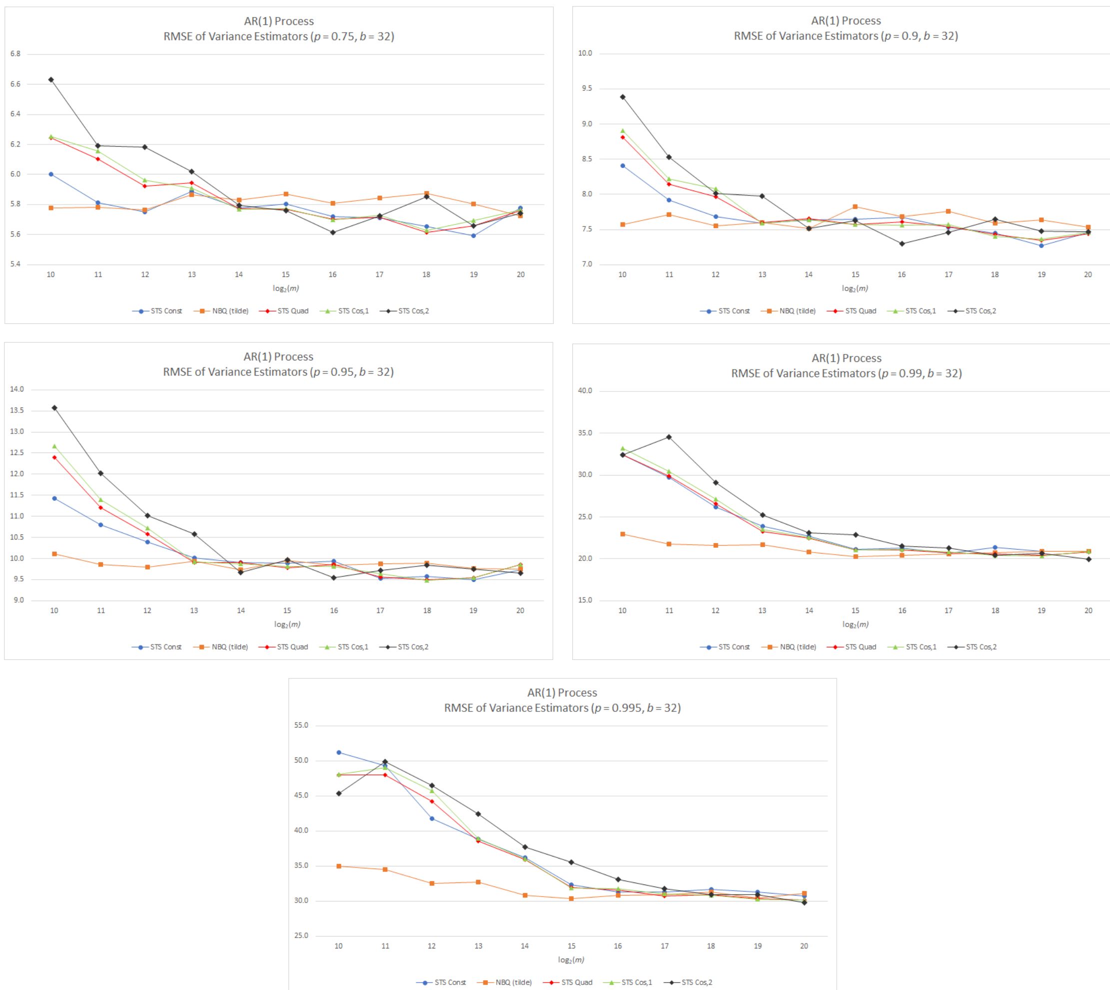

Figure 2.8: Estimated RMSEs of the variance estimators $\widetilde{\mathscr{N}}_p(b,m)$ ("NBQ (tilde)") and $\mathscr{A}_p(w;b,m)$ for the weight functions w_0 ("STS Const"), w_2 ("STS Quad"), $w_{\cos,1}$ ("STS Cos,1"), and $w_{\cos,2}$ ("STS Cos,2") for selected marginal quantiles of the stationary AR(1) process in Section 2.8.1 with correlation coefficient $\phi = 0.9$. All estimates are based on 2,500 independent replications with $b = 32$ batches and batch sizes $m = 2^{\mathcal{L}}$, $\mathcal{L} \in \{10, 11, \ldots, 20\}$.

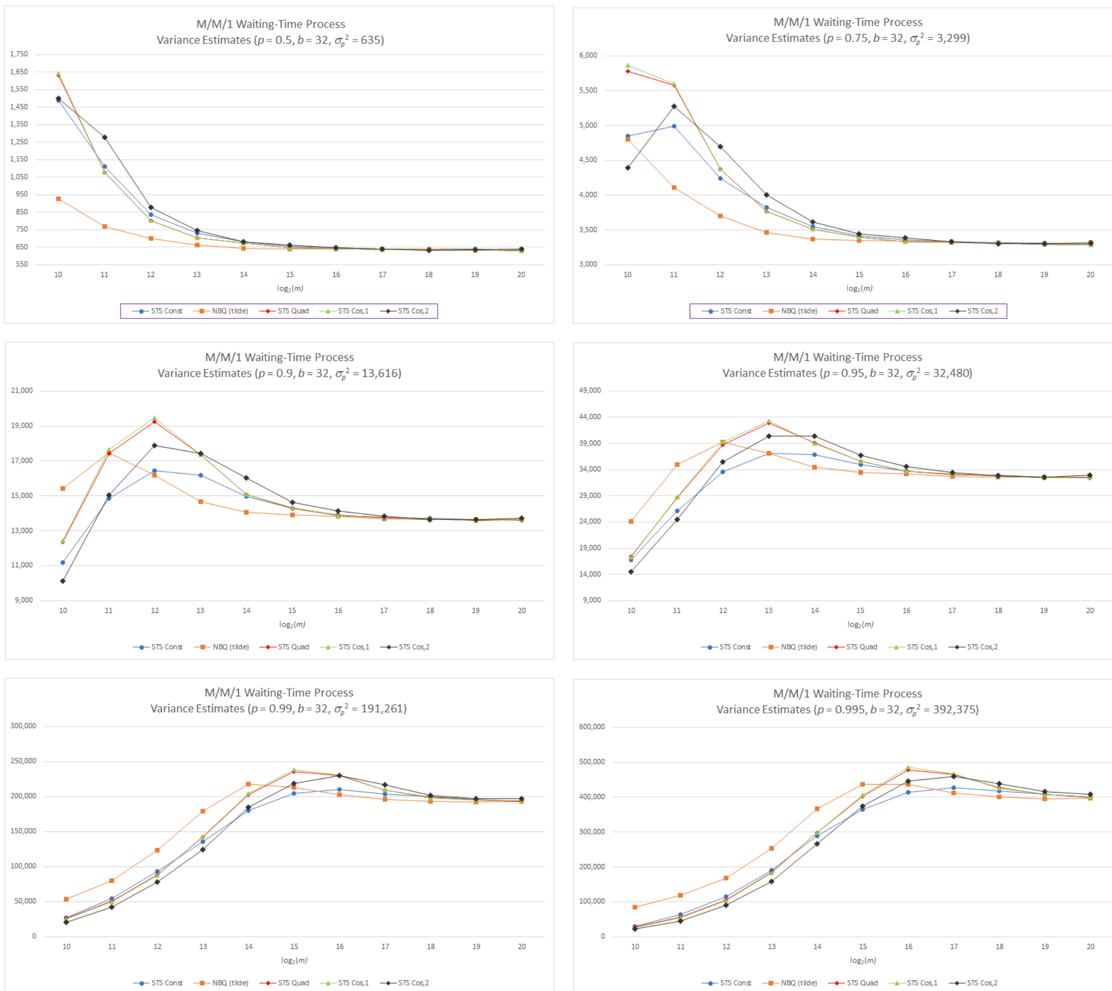

Figure 2.9: Estimated expected values of the variance estimators $\widetilde{\mathcal{N}}_p(b,m)$ ("NBQ (tilde)") and $\mathscr{A}_p(w;b,m)$ for the weight functions w_0 ("STS Const"), w_2 ("STS Quad"), $w_{\cos,1}$ ("STS Cos,1"), and $w_{\cos,2}$ ("STS Cos,2") for selected marginal quantiles of the stationary waiting-time process in the M/M/1 queueing system in Section 2.8.2 with traffic intensity $\rho = 0.8$. All estimates are based on 2,500 independent replications with $b = 32$ batches and batch sizes $m = 2^{\mathcal{L}}$, $\mathcal{L} \in \{10, 11, \ldots, 20\}$.

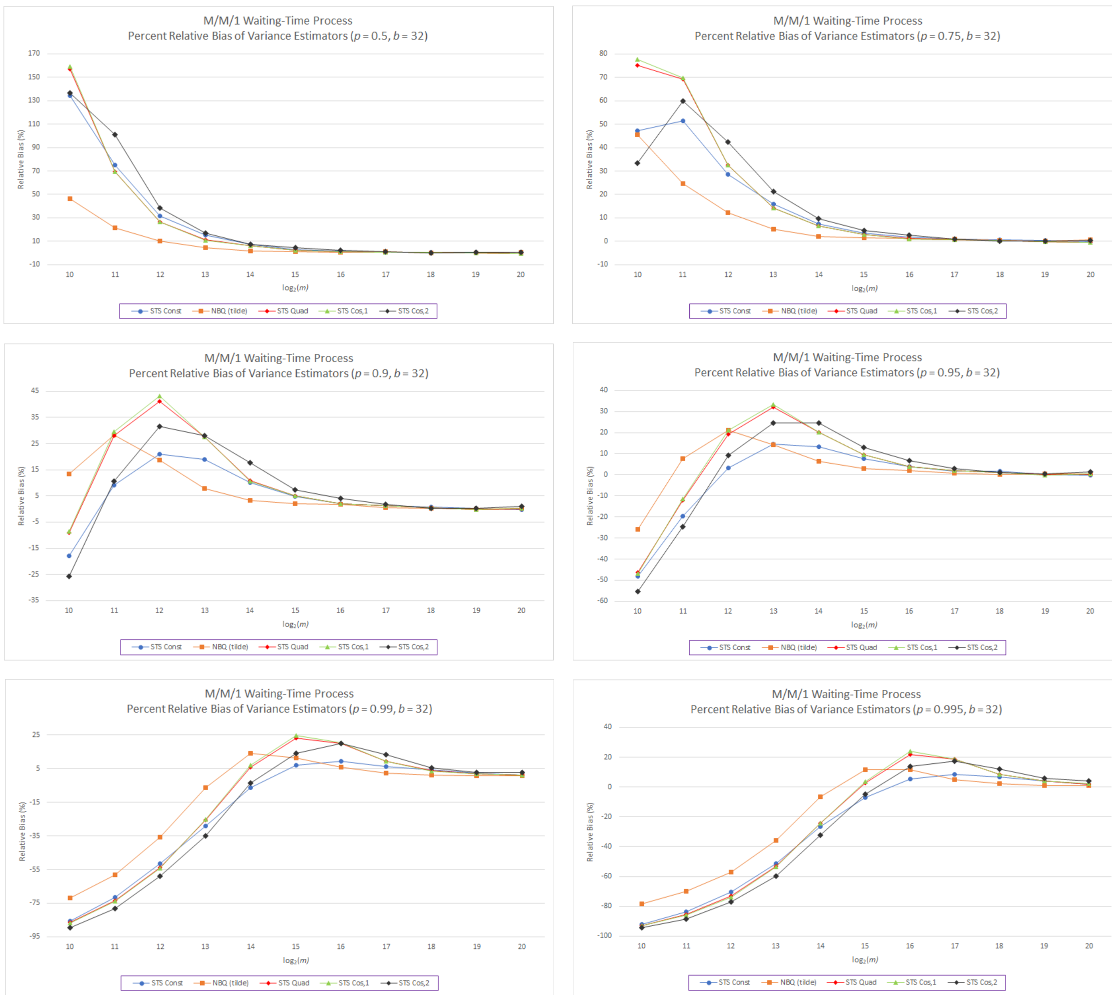

Figure 2.10: Estimated percent relative bias of the variance estimators $\widetilde{\mathcal{N}_p}(b,m)$ ("NBQ (tilde)") and $\mathscr{A}_p(w;b,m)$ for the weight functions w_0 ("STS Const"), w_2 ("STS Quad"), $w_{\cos,1}$ ("STS Cos,1"), and $w_{\cos,2}$ ("STS Cos,2") for selected marginal quantiles of the stationary waiting-time process in the M/M/1 queueing system in Section 2.8.2 with traffic intensity $\rho = 0.8$. All estimates are based on 2,500 independent replications with $b = 32$ batches and batch sizes $m = 2^{\mathcal{L}}$, $\mathcal{L} \in \{10, 11, \ldots, 20\}$.

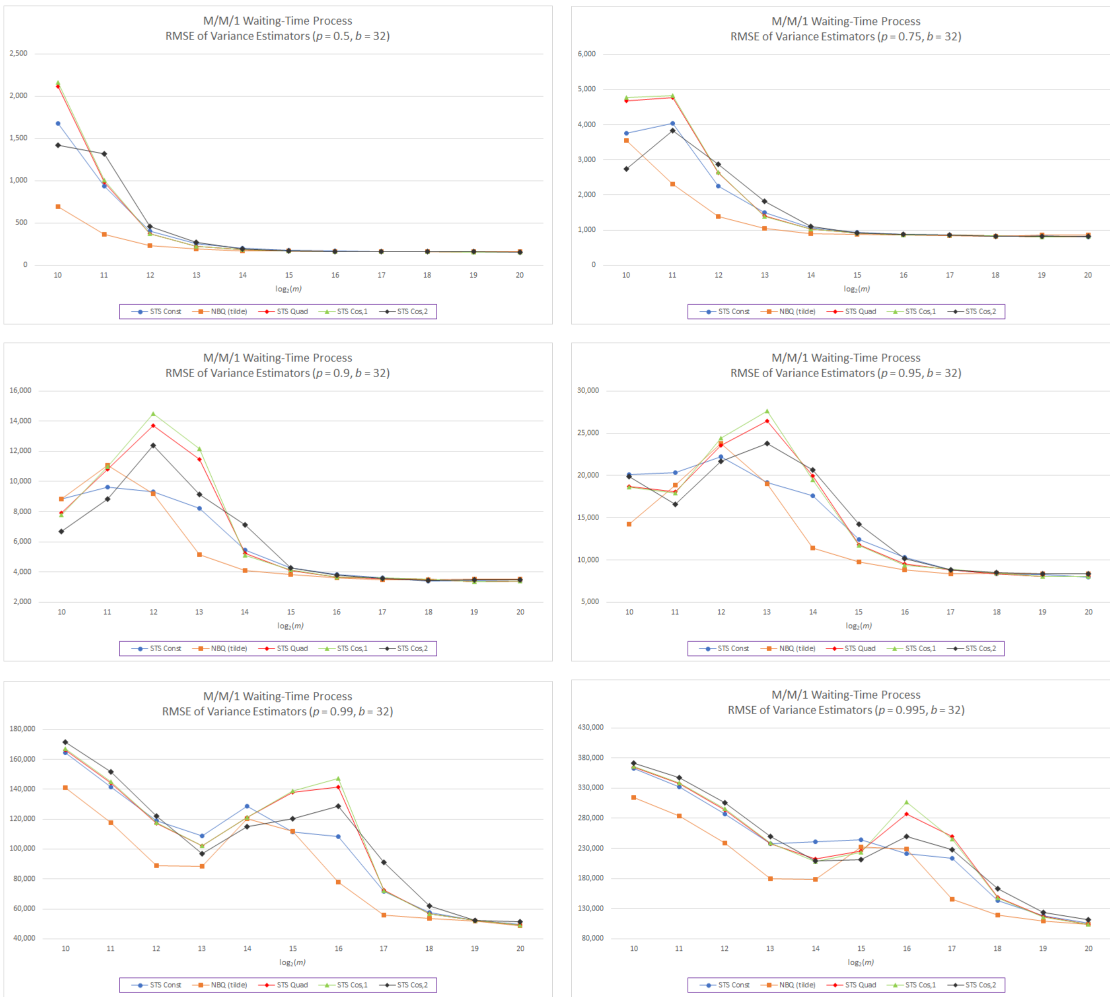

Figure 2.11: Estimated RMSEs of the variance estimators $\widetilde{\mathscr{N}}_p(b,m)$ ("NBQ (tilde)") and $\mathscr{A}_p(w;b,m)$ for the weight functions w_0 ("STS Const"), w_2 ("STS Quad"), $w_{\cos,1}$ ("STS Cos,1"), and $w_{\cos,2}$ ("STS Cos,2") for selected marginal quantiles of the stationary waiting-time process in the M/M/1 queueing system in Section 2.8.2 with traffic intensity $\rho = 0.8$. All estimates are based on 2,500 independent replications with $b = 32$ batches and batch sizes $m = 2^{\mathcal{L}}$, $\mathcal{L} \in \{10, 11, \ldots, 20\}$.

2.9 Alternative Weight Functions

In this section, we explore a methodology that leads to the construction of alternative weight functions which can be more effective with regard to small-sample bias primarily and MSE than the ones reviewed in Section 2.8.

2.9.1 Requirements for the Weight Function

As we mentioned in Section 2.3, the full-sample STS area estimator of the variance parameter σ_p^2 is $A_p^2(w;n)$, where

$$A_p(w;n) \equiv n^{-1} \sum_{k=1}^{n} w(k/n) T_n(k/n), \quad \text{for } n \geq 1$$

and $w(\cdot)$ is a deterministic weight function that is bounded and continuous almost everywhere in $[0,1]$ (so that $w(t)\mathscr{B}(t)$ is Riemann integrable on $[0,1]$); and the r.v.

$$Z(w) \equiv \int_0^1 w(t)\mathscr{B}(t)\,dt \sim N(0,1).$$

Recall that $\mathscr{W}$ denotes a standard Brownian motion on $[0,1]$ and $\mathscr{B}(t) \equiv \mathscr{W}(t) - t\mathscr{W}(1)$ for $t \in [0,1]$ is a standard Brownian bridge process that is independent of $\mathscr{W}(1)$. Clearly, $w_0(t) = \sqrt{12}$ for $t \in [0,1]$, is a valid weight function because

$$Z(w_0) = \int_0^1 \sqrt{12}\mathscr{B}(t)\,dt = \sqrt{12}\int_0^1 \mathscr{B}(t)\,dt$$

and

$$\int_0^1 \mathscr{B}(t)\,dt \sim N\left(0, \frac{1}{12}\right)$$

together imply $Z(w_0) \sim N(0,1)$.

2.9.2 Partial Weight Functions

In this subsection, we discuss the first set of alternative weight functions, referred to as "partial" because they assign a constant positive weight on a subinterval of $[0, 1]$.

Since $\mathscr{B}(t), t \in [0, 1]$ is a Brownian bridge, then the integrated Brownian bridge defined as $\int_0^s \mathscr{B}(t)\,dt$ for $s \in [0, 1]$ is a Gaussian process with zero mean and covariance function

$$\operatorname{Cov}\left[\int_0^{u_1} \mathscr{B}(t)\,dt, \int_0^{u_2} \mathscr{B}(t)\,dt\right] = \frac{u_1 u_2 \min(u_1, u_2)}{2} - \frac{\min(u_1, u_2)^3}{6} - \frac{u_1^2 u_2^2}{4}, \quad (2.71)$$

for $u_1, u_2 \in [0, 1]$ (Henze and Nikitin [72]). From Equation (2.71) with $u_1 = u_2 = u$ we have

$$\operatorname{Var}\left[\int_0^{u} \mathscr{B}(t)\,dt\right] = \frac{u^3}{3} - \frac{u^4}{4} = \frac{4u^3 - 3u^4}{12},$$

which implies

$$\int_0^{u} \mathscr{B}(t)\,dt \sim N\left(0, \frac{4u^3 - 3u^4}{12}\right). \quad (2.72)$$

Equation (2.72) allows us to construct the first type of partial weight functions, with $w(t) = c_u$ for $t \in [0, u]$ and $w(t) = 0$ for $t \in [u, 1]$. To ensure that $Z(w) \sim N(0, 1)$, we should set

$$c_u = \sqrt{\frac{12}{4u^3 - 3u^4}}. \quad (2.73)$$

For example, the weight function that corresponds to a constant weight only for the first half of the interval $[0, 1]$, i.e.,

$$w(t) = \begin{cases} \sqrt{\frac{192}{5}} & \text{if } t \in [0, 1/2], \\ 0 & \text{otherwise.} \end{cases}$$

We can easily verify this result using Equation (2.73) with $u = 1$.

Our next goal is to construct weight functions that are positive constants on an arbitrary subinterval of $[0, 1]$. First, we show that

$$\int_l^u \mathscr{B}(t)\,dt \sim N\left(0, \frac{4u^3 - 3u^4 + 8l^3 - 3l^4 - 12ul^2 + 6l^2u^2}{12}\right). \tag{2.74}$$

We start with

$$\int_l^u \mathscr{B}(t)\,dt = \int_0^u \mathscr{B}(t)\,dt - \int_0^l \mathscr{B}(t)\,dt. \tag{2.75}$$

By Equation (2.72), $\int_0^u \mathscr{B}(t)\,dt \sim N\left(0, \frac{4u^3-3u^4}{12}\right)$ and $\int_0^l \mathscr{B}(t)\,dt \sim N\left(0, \frac{4l^3-3l^4}{12}\right)$. Recall that for $X \sim N\left(\mu_X, \sigma_X^2\right)$ and $Y \sim N\left(\mu_Y, \sigma_Y^2\right)$, we have $X \pm Y \sim N(\mu_X \pm \mu_Y, \sigma_X^2 + \sigma_Y^2 \pm 2\mathrm{Cov}[X, Y])$. Using Equation (2.75) we obtain

$$\int_l^u \mathscr{B}(t)\,dt \sim N\left(0, \frac{4u^3 - 3u^4}{12} + \frac{4l^3 - 3l^4}{12} - 2\mathrm{Cov}\left[\int_0^u \mathscr{B}(t)\,dt, \int_0^l \mathscr{B}(t)\,dt\right]\right),$$

while Equation (2.71) yields

$$\begin{aligned}\int_l^u \mathscr{B}(t)\,dt &\sim N\left(0, \frac{4u^3 - 3u^4}{12} + \frac{4l^3 - 3l^4}{12} - 2\left(\frac{ul^2}{2} - \frac{l^3}{6} - \frac{u^2l^2}{4}\right)\right)\\ &\stackrel{\mathrm{d}}{=} N\left(0, \frac{4u^3 - 3u^4}{12} + \frac{4l^3 - 3l^4}{12} - ul^2 + \frac{l^2u^2}{2}\right).\end{aligned}$$

The latter two equations imply

$$\int_l^u \mathscr{B}(t)\,dt \sim N\left(0, \frac{4u^3 - 3u^4 + 8l^3 - 3l^4 - 12ul^2 + 6l^2u^2}{12}\right).$$

Equation (2.74) allows us to construct the second type of partial weight functions, where

$$w(t) = \begin{cases} c_{l,u} & \text{if } t \in [l, u], \\ 0 & \text{otherwise.} \end{cases}$$

To ensure that $Z(w) \sim N(0,1)$, we should set

$$c_{l,u} = \sqrt{\frac{12}{4u^3 - 3u^4 + 8l^3 - 3l^4 - 12ul^2 + 6l^2u^2}}. \tag{2.76}$$

We can easily verify the result in Equation (2.76) by setting $l = 0$, under $u = 1$ to obtain $w(t) = \sqrt{12}$ for $t \in [0,1]$. For example, the weight function that corresponds to a constant weight only for $t \in [1/4, 3/4]$ (and zero elsewhere), is

$$w(t) = \begin{cases} \sqrt{24} & \text{if } t \in [1/4, 3/4], \\ 0 & \text{otherwise.} \end{cases}$$

Remark 2.9.1. This new class of weight functions has spawned the idea of assigning a zero weight to small intervals close to 0 or 1. Potentially, the length of these intervals could depend on the sample size n, This is the subject of future work.

Another interesting special set of weight functions is created when we set $u = 1$. In this case,

$$\int_l^1 \mathscr{B}(t)\, dt \sim N\left(0, \frac{1 + 8l^3 - 3l^4 - 6l^2}{12}\right), \tag{2.77}$$

which yields the constant

$$c_{l,1} = \sqrt{\frac{12}{1 + 8l^3 - 3l^4 - 6l^2}}. \tag{2.78}$$

The first two alternative weight functions that we will evaluate in Section 2.10 belong to the set of weight functions that we just mentioned. Specifically, the first weight function will be given by

$$w_{s,1}(t) = \begin{cases} \sqrt{\frac{1024}{63}} & \text{if } t \in [1/4, 1], \\ 0 & \text{otherwise.} \end{cases} \tag{2.79}$$

We calculated the weight for the second interval by setting $l = 1/4$ in Equation (2.78) above.

The second weight function is

$$w_{s,2}(t) = \begin{cases} \sqrt{\frac{192}{5}} & \text{if } t \in [1/2, 1], \\ 0 & \text{otherwise.} \end{cases} \tag{2.80}$$

Again we calculated the weight for the interval $[1/2, 1]$ by setting $l = 1/2$ in Equation (2.78) above.

2.9.3 Stepwise Weight Functions

This subsection will present how to construct even more general weight functions, that assign different constant weights in different intervals of $[0, 1]$. We will call these "stepwise" weight functions.

Our first goal is to calculate the expression for

$$\text{Cov}\left[\int_{l_1}^{u_1} \mathscr{B}(t)\,dt, \int_{l_2}^{u_2} \mathscr{B}(t)\,dt\right], \quad \text{for } l_1 \le u_1 \le l_2 \le u_2.$$

We start by writing

$$\begin{aligned}\text{Cov}&\left[\int_{l_1}^{u_1} \mathscr{B}(t)\,dt, \int_{l_2}^{u_2} \mathscr{B}(t)\,dt\right] = \\ &= \text{E}\left[\left(\int_{l_1}^{u_1} \mathscr{B}(t)\,dt - \text{E}\left[\int_{l_1}^{u_1} \mathscr{B}(t)\,dt\right]\right)\left(\int_{l_2}^{u_2} \mathscr{B}(t)\,dt - \text{E}\left[\int_{l_2}^{u_2} \mathscr{B}(t)\,dt\right]\right)\right],\end{aligned}$$

Using Equation (2.74) we get

$$\text{Cov}\left[\int_{l_1}^{u_1} \mathscr{B}(t)\,dt, \int_{l_2}^{u_2} \mathscr{B}(t)\,dt\right] = \text{E}\left[\int_{l_1}^{u_1} \mathscr{B}(t)\,dt \int_{l_2}^{u_2} \mathscr{B}(t)\,dt\right].$$

Using the same mechanism as in Equation (2.75) yields

$$
\begin{aligned}
\operatorname{Cov}\left[\int_{l_1}^{u_1} \mathscr{B}(t)\,dt, \int_{l_2}^{u_2} \mathscr{B}(t)\,dt\right] = & \\
&= \mathrm{E}\left[\left(\int_0^{u_1} \mathscr{B}(t)\,dt - \int_0^{l_1} \mathscr{B}(t)\,dt\right)\left(\int_0^{u_2} \mathscr{B}(t)\,dt - \int_0^{l_2} \mathscr{B}(t)\,dt\right)\right] \\
&= \mathrm{E}\left[\int_0^{u_1} \mathscr{B}(t)\,dt \int_0^{u_2} \mathscr{B}(t)\,dt - \int_0^{l_1} \mathscr{B}(t)\,dt \int_0^{u_2} \mathscr{B}(t)\,dt\right. \\
&\quad \left. - \int_0^{u_1} \mathscr{B}(t)\,dt \int_0^{l_2} \mathscr{B}(t)\,dt + \int_0^{l_1} \mathscr{B}(t)\,dt \int_0^{l_2} \mathscr{B}(t)\,dt\right] \\
&= \mathrm{E}\left[\int_0^{u_1} \mathscr{B}(t)\,dt \int_0^{u_2} \mathscr{B}(t)\,dt\right] - \mathrm{E}\left[\int_0^{l_1} \mathscr{B}(t)\,dt \int_0^{u_2} \mathscr{B}(t)\,dt\right] \\
&\quad - \mathrm{E}\left[\int_0^{u_1} \mathscr{B}(t)\,dt \int_0^{l_2} \mathscr{B}(t)\,dt\right] + \mathrm{E}\left[\int_0^{l_1} \mathscr{B}(t)\,dt \int_0^{l_2} \mathscr{B}(t)\,dt\right].
\end{aligned}
$$

Equation (2.71) leads to

$$
\begin{aligned}
\operatorname{Cov}\left[\int_{l_1}^{u_1} \mathscr{B}(t)\,dt, \int_{l_2}^{u_2} \mathscr{B}(t)\,dt\right] = & \\
&= \frac{u_1^2 u_2}{2} - \frac{u_1^3}{6} - \frac{u_1^2 u_2^2}{4} - \frac{l_1^2 u_2}{2} + \frac{l_1^3}{6} + \frac{l_1^2 u_2^2}{4} \\
&\quad - \frac{u_1^2 l_2}{2} + \frac{u_1^3}{6} + \frac{u_1^2 l_2^2}{4} + \frac{l_1^2 l_2}{2} - \frac{l_1^3}{6} - \frac{l_1^2 l_2^2}{4}, \\
&= \frac{(u_2 - l_2)(u_1 - l_1)(u_1 + l_1)(2 - u_2 - l_2)}{4}. \qquad (2.81)
\end{aligned}
$$

We will introduce now the methodology for constructing stepwise weight functions based on the result in Equation (2.81). We will start with an easy case, where we have two nonzero constant weights c_1 and c_2 for the intervals $[0, v)$ and $[v, 1]$, respectively. By setting $l_1 = 0$, $u_1 = l_2 = v$, and $u_2 = 1$ in Equation (2.81) we get

$$
\operatorname{Cov}\left[\int_0^{v} \mathscr{B}(t)\,dt, \int_v^{1} \mathscr{B}(t)\,dt\right] = \frac{v^2(1-v)^2}{4}. \qquad (2.82)
$$

We will calculate the constants c_1 and c_2 using $Z(w) \equiv \int_0^1 w(t)\mathscr{B}(t)\,dt \sim N(0, 1)$. We write

$$\int_0^1 w(t)\mathscr{B}(t)\,dt = \int_0^v c_1\mathscr{B}(t)\,dt + \int_v^1 c_2\mathscr{B}(t)\,dt.$$

Equations (2.72) and (2.77) imply $\int_0^v c_1\mathscr{B}(t)\,dt \sim N(0, c_1^2(4v^3 - 3v^4)/12)$ and $\int_v^1 c_2\mathscr{B}(t)\,dt \sim N(0, c_2^2(1 + 8v^3 - 3v^4 - 6v^2)/12)$, respectively. Using Equation (2.82) we can write

$$\int_0^v c_1\mathscr{B}(t)\,dt + \int_v^1 c_2\mathscr{B}(t)\,dt$$
$$\sim N\left(0, c_1^2\frac{4v^3 - 3v^4}{12} + c_2^2\frac{1 + 8v^3 - 3v^4 - 6v^2}{12} + c_1c_2\frac{v^2(1-v)^2}{2}\right).$$

To identify appropriate pairs (c_1, c_2), we need to solve

$$c_1^2\frac{4v^3 - 3v^4}{12} + c_2^2\frac{1 + 8v^3 - 3v^4 - 6v^2}{12} + c_1c_2\frac{v^2(1-v)^2}{2} = 1,$$

which can be satisfied for infinitely many pairs of c_1 and c_2. To find a unique solution, we impose an additional relationship, e.g., $c_2 = 2c_1$. Solving the resulting equation

$$c_1^2\frac{4v^3 - 3v^4}{12} + 4c_1^2\frac{1 + 8v^3 - 3v^4 - 6v^2}{12} + 2c_1^2\frac{v^2(1-v)^2}{2} = 1$$

leads to

$$c_1 = \sqrt{\frac{12}{12v^3 - 3v^4 - 12v^2 + 4}}, \quad \text{and} \tag{2.83}$$

$$c_2 = 2\sqrt{\frac{12}{12v^3 - 3v^4 - 12v^2 + 4}} \tag{2.84}$$

This leads to the third weight function that we will consider for the empirical evaluation in Section 2.10, namely

$$w_{s,3}(t) = \begin{cases} \sqrt{\frac{192}{37}} & \text{if } t \in [0, 1/2), \\ 2\sqrt{\frac{192}{37}} & \text{if } t \in [1/2, 1]. \end{cases} \tag{2.85}$$

We will also do the calculations for one more general case, where

$$w(t) = \begin{cases} c_1 & \text{if } t \in [l_1, u_1), \\ c_2 & \text{if } t \in [l_2, u_2), \\ 0 & \text{otherwise.} \end{cases}$$

for $l_1 \leq u_1 \leq l_2 \leq u_2$. In this case we can write

$$\int_0^1 w(t)\mathscr{B}(t)\,dt = \int_{l_1}^{u_1} c_1\mathscr{B}(t)\,dt + \int_{l_2}^{u_2} c_2\mathscr{B}(t)\,dt.$$

Following a similar analysis as above, we get

$$\int_{l_1}^{u_1} c_1\mathscr{B}(t)\,dt + \int_{l_2}^{u_2} c_2\mathscr{B}(t)\,dt \sim N(0, \sigma_c^2),$$

where

$$\begin{aligned}\sigma_c^2 = {} & c_1^2\frac{4u_1^3 - 3u_1^4 + 8l_1^3 - 3l_1^4 - 12u_1l_1^2 + 6l_1^2u_1^2}{12} \\ & + c_2^2\frac{4u_2^3 - 3u_2^4 + 8l_2^3 - 3l_2^4 - 12u_2l_2^2 + 6l_2^2u_2^2}{12} \\ & + c_1c_2\frac{(u_2 - l_2)(u_1 - l_1)(u_1 + l_1)(2 - u_2 - l_2)}{2}.\end{aligned}$$

By a linear relationship between c_1 and c_2 and solving $\sigma_c^2 = 1$, we can calculate an appropriate pair (c_1, c_2).

The fourth weight function that we will consider for the empirical evaluation in Section

2.10 is a special case of this category, where

$$w_{s,4}(t) = \begin{cases} 2\sqrt{\frac{1024}{207}} & \text{if } t \in [1/4, 3/4), \\ \sqrt{\frac{1024}{207}} & \text{if } t \in [3/4, 1], \\ 0 & \text{otherwise.} \end{cases} \tag{2.86}$$

We can extend the methodology described in this section for constructing stepwise functions that assign a set of nonzero weights in multiple subintervals within $[0, 1]$. For example, for $l_1 \leq u_1 \leq l_2 \leq u_2 \leq l_3 \leq u_3$ we can set

$$w(t) = \begin{cases} c_1 & \text{if } t \in [l_1, u_1), \\ c_2 & \text{if } t \in [l_2, u_2), \\ c_3 & \text{if } t \in [l_3, u_3), \\ 0 & \text{otherwise.} \end{cases}$$

Since

$$\int_0^1 w(t)\mathscr{B}(t)\,dt = \int_{l_1}^{u_1} c_1\mathscr{B}(t)\,dt + \int_{l_2}^{u_2} c_2\mathscr{B}(t)\,dt + \int_{l_3}^{u_3} c_3\mathscr{B}(t)\,dt,$$

appropriate constants c_1, c_2 and c_3 can be identified by using: (i) the properties of summation of normal random variables; and (ii) Equations (2.74) and (2.81).

2.9.4 Continuous Weight Functions

An alternative set of weights is continuous functions on $[0, 1]$. Goldsman *et al.* [33] have provided the formulas for constructing such weight functions on $[0, 1]$ with the goal of estimating the variance parameter σ^2 associated with based on STS. Their work also applies for the construction of continuous weight functions on $[0, 1]$ for quantile estimation. We will present here their methodology in short.

First, we start with $g(t)$, a continuous function on $[0, 1]$. Then we calculate an appropriate constant c so that $cg(t)$ is an appropriate weight function $w(t)$. To find c, we calculate

$$f = \int_0^1 \left(\int_0^x g(y)\,dy - \int_0^1 \int_0^z g(y)\,dy\,dz \right)^2 dx \tag{2.87}$$

and then we set

$$c = \frac{1}{\sqrt{f}}.$$

Our notation is analogous to Goldsman *et al.* [33] who used $w(\cdot)$ in place of $g(\cdot)$ and V in place of f. Equation (2.87) above is a direct analogue of Equation (2) of Goldsman *et al.* [33].

Initial experimentation using a variety of new alternative polynomial weight functions (constructed through the methodology above) based on a limited set of test processes, did not reveal any significant insights on how to construct efficient weight functions tailored to quantile estimation.

2.10 Experimental Evaluation of the Alternative STS Weight Area Estimators

In this section we conduct an extended empirical evaluation of the performance of the following estimators for σ_p^2:

- the batched STS area estimator $\mathscr{A}_p(w_0; b, m)$, with $w_0(t) = \sqrt{12}$ for $t \in [0, 1]$;
- the batched STS area estimator $\mathscr{A}_p(w_{s,1}; b, m)$, where $w_{s,1}(\cdot)$ is defined in Equation (2.79);
- the batched STS area estimator $\mathscr{A}_p(w_{s,2}; b, m)$, where $w_{s,2}(\cdot)$ is defined in Equation (2.80);
- the batched STS area estimator $\mathscr{A}_p(w_{s,3}; b, m)$, where $w_{s,3}(\cdot)$ is defined in Equation (2.85); and

- the batched STS area estimator $\mathscr{A}_p(w_{s,4}; b, m)$, where $w_{s,4}(\cdot)$ is defined in Equation (2.86).

The evaluation will be based on the bias, standard deviation, RMSE, and the coverage probability of the 95% CIs for y_p defined in Equation (2.64). Our goal is to validate the new alternative weights constructed in Section 2.9 and examine whether any of the newly constructed weight functions has clear advantages over the constant weight function $w_0(\cdot)$.

We consider two stationary test processes: the AR(1) process in Section 2.6.1 with mean zero and correlation coefficient 0.9 and the waiting-time process from an M/M/1 queueing system as described in Section 2.6.2 with traffic intensity 0.8. For each process and value of p under study, we fix the number of batches at $b = 32$ and consider an increasing sequence of batch sizes $m = 2^{\mathcal{L}}$, $\mathcal{L} \in \{10, 11, \ldots, 20\}$. Again, we note that batch sizes with $\mathcal{L} \leq 15$ are often inadequate for variance-parameter estimation in these problems (Alexopoulos *et al.* [7]).

All experiments were coded in Java using common random numbers generated by the RngStreams package of L'Ecuyer *et al.* [67]. The numerical results were computed from 2,500 independent replications of each test process; and those results are summarized in Tables 2.9–2.12 below. In each table, column 1 contains the values of p, y_p, and σ_p^2 (the latter quantity is set in **bold red typeface**); column 2 contains the value of $\mathcal{L} = \log_2(m)$; columns 3, 7, 11, 15, and 19 respectively contain the average values of the selected variance-parameter estimators computed from 2,500 i.i.d. observations of those estimators; columns 4, 8, 12, 16, and 20 respectively contain the average bias of the selected variance-parameter estimators; columns 5, 9, 13, 17, and 21 respectively contain the sample standard deviations of the selected variance-parameter estimators; and columns 6, 10, 14, 18, and 22 respectively contain the corresponding empirical CI coverage probabilities. Finally, Figures 2.12–2.13 summarize the accuracy and precision of each variance-parameter estimator for each test process in Sections 2.10.1 and 2.10.2, respectively, as the batch size increases by plotting estimates of the respective average relative biases (as a percentage) and estimated RMSEs.

2.10.1 First-Order Autoregressive Process

The first test process is the stationary AR(1) time-series model described in Section 2.6.1. For experimentation we selected the values $\phi = 0.9$ and $p \in \{0.5, 0.75, 0.95, 0.99\}$. The results are summarized in Tables 2.9–2.10 and in Figure 2.12 and they reveal several findings:

(i) All five estimators of σ_p^2 and their respective estimated standard deviations converged to their asymptotic limits reasonably fast (the respective estimated standard deviations of all five estimators seem to converge to the same asymptotic limit).

(ii) For $p = 0.5$ and $\mathcal{L} \leq 13$, $\mathscr{A}_p(w_{s,2}; b, m)$ reported the smallest (absolute) bias. However, for $p = 0.5$ and $\mathcal{L} \geq 19$, $\mathscr{A}_p(w_0; b, m)$ reported the smallest (absolute) bias, while $\mathscr{A}_p(w_{s,2}; b, m)$ reported the largest (absolute) bias.

(iii) For $p = 0.75$ and the smallest value $\mathcal{L} = 10$, again $\mathscr{A}_p(w_{s,2}; b, m)$ reported the smallest (absolute) bias, while $\mathscr{A}_p(w_{s,1}; b, m)$ delivered an estimated coverage probability of 94.04%, which was closest to the nominal value in comparison with the other estimators of σ_p^2. Notably, for $\mathcal{L} = 10$, all variance-parameter estimators yielded CIs with estimated coverage probabilities near the nominal value. $\mathscr{A}_p(w_0; b, m)$ reported the smallest value which was 93.63%. For $p = 0.75$ and $\mathcal{L} \geq 18$, $\mathscr{A}_p(w_0; b, m)$ reported again the smallest (absolute) bias, while $\mathscr{A}_p(w_{s,2}; b, m)$ reported the largest (absolute) bias.

(iv) For $p = 0.95$ and $\mathcal{L} \leq 13$, $\mathscr{A}_p(w_{s,2}; b, m)$ reported the largest (absolute) bias.

(v) For $p = 0.99$ and $\mathcal{L} = 10$, $\mathscr{A}_p(w_{s,1}; b, m)$ reported the smallest (absolute) bias, while $\mathscr{A}_p(w_{s,2}; b, m)$ delivered an estimated coverage probability of 93.88%, which was closest to the nominal value. The estimator $\mathscr{A}_p(w_{s,4}; b, m)$ delivered an estimated coverage probability of 93.84%, while $\mathscr{A}_p(w_0; b, m)$ resulted in the CI with the smallest estimated coverage probability of 92.92%.

(vi) The standard deviation of $\mathscr{A}_p(w_0; b, m)$ usually appeared to converge more rapidly to its asymptotic value.

(vii) Figure 2.12 indicates that there was no clear winner among the five estimators of σ_p^2 with respect to estimated relative bias. For $p = 0.95, 0.99$ and $\mathcal{L} \leq 13$, $\mathscr{A}_p(w_{s,2}; b, m)$ exhibited the largest estimated (absolute) relative bias.

(viii) Figure 2.12 revealed also that there was no clear winner among the five estimators of σ_p^2 with respect to estimated RMSE. For $p = 0.95, 0.99$ and $\mathcal{L} \leq 13$, $\mathscr{A}_p(w_{s,2}; b, m)$ reported the largest estimated RMSE, followed by $\mathscr{A}_p(w_{s,3}; b, m)$ and $\mathscr{A}_p(w_{s,1}; b, m)$, while $\mathscr{A}_p(w_0; b, m)$ reported the smallest estimated RMSE.

These experimental results did not yield any valid reasons for replacing the constant weight function $w_0(\cdot)$ with one of the newly constructed weight functions in Section 2.9.

2.10.2 M/M/1 Waiting-Time Process

Our second stationary test process was generated by the M/M/1 queueing system in Section 2.6.2 with FIFO service discipline, arrival rate $\lambda = 0.8$, and service rate $\omega = 1$. The results are summarized in Tables 2.11–2.12 and in Figure 2.13, and they reveal several findings:

(i) All five variance-parameter estimators and their standard deviations seem to converge to the respective theoretical limits, but at a significantly lower rate than for the AR(1) process in Section 2.10.1. This example clearly indicated the presence of substantial bias in these variance-parameter estimators for small batch sizes m, and this bias became more prominent for large values of p (near-extreme quantiles).

(ii) For $p = 0.5$ and $\mathcal{L} \leq 14$, $\mathscr{A}_p(w_{s,2}; b, m)$ reported the smallest estimated (absolute) bias and its estimated standard deviation converged more rapidly to its asymptotic value. For $\mathcal{L} \leq 10$, all five variance-parameter estimators resulted in CIs that exhibited some overcoverage.

(iii) For $p = 0.75, 0.95$ and 0.99, there was no clear winner among the five variance-parameter estimators with respect to the estimated bias and standard deviation. This conclusion is further strengthened by Figure 2.13 as no variance-parameter estimator stands out with regard to estimated relative bias and RMSE.

Again, these experimental results did not provide any valid reasons for replacing the constant weight function $w_0(\cdot)$ with one of the newly constructed weight functions in Section 2.9. Further, these results showcased the importance of identifying alternative weight functions for computing STS area estimators inducing lower small-sample bias than the constant weight $w_0(t) = \sqrt{12}$, $t \in [0, 1]$. This will be an interesting direction for future work. Further, the performance evaluation of an alternative weight function should be based on an expanded experimental test bed.

Table 2.9: Performance evaluation of the batched STS area estimators in Section 2.10 for the AR(1) process with $\mu_Y = 0$ and $\phi = 0.9$ for $p \in \{0.5, 0.75\}$. All estimates are based on 2,500 independent replications with $b = 32$ batches and batch sizes $m = 2^{\mathcal{L}}$, $\mathcal{L} \in \{10, 11, \ldots, 20\}$, where for nominal 95% CIs for y_p, the coverage probabilities are denoted by “95% CI Cover.”

		STS area $\mathscr{A}_p(w_0; b, m)$				STS area $\mathscr{A}_p(w_{s,1}; b, m)$				STS area $\mathscr{A}_p(w_{s,2}; b, m)$				STS area $\mathscr{A}_p(w_{s,3}; b, m)$				STS area $\mathscr{A}_p(w_{s,4}; b, m)$			
p (y_p) **Var. Par.**	$\mathcal{L}$	Avg.	Bias	Std. Dev.	95% CI Cover.	Avg.	Bias	Std. Dev.	95% CI Cover.	Avg.	Bias	Std. Dev.	95% CI Cover.	Avg.	Bias	Std. Dev.	95% CI Cover.	Avg.	Bias	Std. Dev.	95% CI Cover.
0.5	10	20.370	−0.488	5.340	94.32	20.643	−0.215	5.424	94.36	20.750	−0.108	5.384	94.68	20.508	−0.350	5.353	94.36	20.678	−0.180	5.449	94.56
(0.0000)	11	20.638	−0.220	5.141	94.16	20.780	−0.078	5.159	94.48	20.862	0.004	5.234	94.44	20.726	−0.132	5.155	94.44	20.799	−0.059	5.172	94.36
20.858	12	20.751	−0.107	5.309	95.08	20.813	−0.045	5.349	94.92	20.851	−0.007	5.332	94.96	20.793	−0.065	5.328	95.08	20.811	−0.047	5.339	95.00
	13	20.525	−0.333	5.292	94.48	20.612	−0.246	5.343	94.64	20.793	−0.065	5.407	94.56	20.615	−0.243	5.330	94.56	20.578	−0.280	5.324	94.52
	14	20.813	−0.045	5.165	94.80	20.838	−0.020	5.162	94.68	20.827	−0.031	5.219	94.92	20.812	−0.046	5.171	94.84	20.829	−0.029	5.157	94.68
	15	20.660	−0.198	5.137	94.96	20.718	−0.140	5.139	95.08	20.742	−0.116	5.153	95.04	20.689	−0.169	5.126	94.96	20.708	−0.150	5.153	95.00
	16	20.797	−0.061	5.233	95.28	20.841	−0.017	5.185	95.24	20.775	−0.083	5.115	95.48	20.793	−0.065	5.186	95.48	20.843	−0.015	5.188	94.96
	17	20.682	−0.176	5.228	95.40	20.699	−0.159	5.233	95.20	20.694	−0.164	5.212	95.56	20.681	−0.177	5.226	95.44	20.709	−0.149	5.236	95.24
	18	20.918	0.060	5.254	95.80	20.961	0.103	5.313	95.92	21.032	0.174	5.361	96.12	20.972	0.114	5.310	96.00	20.917	0.059	5.289	95.84
	19	20.815	−0.043	5.171	95.04	20.780	−0.078	5.194	94.96	20.730	−0.128	5.209	94.68	20.771	−0.087	5.177	95.00	20.791	−0.067	5.187	94.92
	20	20.930	0.072	5.387	94.72	20.939	0.081	5.356	94.84	20.997	0.139	5.267	94.80	20.955	0.097	5.364	94.76	20.939	0.081	5.357	94.76
0.75	10	22.317	−0.541	5.974	93.64	22.642	−0.216	6.010	94.04	22.768	−0.090	6.017	93.84	22.478	−0.380	5.996	94.00	22.677	−0.181	6.035	93.96
(0.6745)	11	22.733	−0.125	5.810	94.60	22.919	0.061	5.866	94.72	23.054	0.196	5.929	94.52	22.860	0.002	5.842	94.64	22.932	0.074	5.889	94.68
22.858	12	22.912	0.054	5.749	95.32	23.014	0.156	5.821	95.52	23.071	0.213	5.885	95.68	22.985	0.127	5.808	95.52	22.996	0.138	5.807	95.36
	13	22.654	−0.204	5.884	94.76	22.740	−0.118	5.955	94.92	22.858	0.000	6.027	95.28	22.725	−0.133	5.925	94.80	22.706	−0.152	5.945	94.76
	14	22.887	0.029	5.779	95.12	22.904	0.046	5.802	95.08	22.883	0.025	5.810	94.84	22.878	0.020	5.781	95.00	22.890	0.032	5.793	95.00
	15	22.771	−0.087	5.801	94.80	22.819	−0.039	5.808	94.92	22.852	−0.006	5.774	94.64	22.810	−0.048	5.790	94.84	22.792	−0.066	5.808	95.00
	16	22.787	−0.071	5.718	94.76	22.829	−0.029	5.717	94.56	22.788	−0.070	5.703	94.68	22.790	−0.068	5.704	94.48	22.818	−0.040	5.725	94.60
	17	22.682	−0.176	5.707	95.24	22.713	−0.145	5.703	95.36	22.750	−0.108	5.730	95.16	22.694	−0.164	5.711	95.32	22.720	−0.138	5.702	95.32
	18	22.875	0.017	5.654	95.68	22.928	0.070	5.710	95.80	23.001	0.143	5.794	95.76	22.934	0.076	5.715	95.68	22.890	0.032	5.672	95.68
	19	22.844	−0.014	5.593	94.92	22.799	−0.059	5.644	95.04	22.711	−0.147	5.682	94.88	22.787	−0.071	5.616	94.92	22.814	−0.044	5.634	94.96
	20	22.972	0.114	5.779	95.00	23.016	0.158	5.751	95.12	23.090	0.232	5.635	95.52	23.018	0.160	5.739	95.16	23.009	0.151	5.766	95.28

Table 2.10: Performance evaluation of the batched STS area estimators in Section 2.10 for the AR(1) process with $\mu_Y = 0$ and $\phi = 0.9$ for $p \in \{0.95, 0.99\}$. All estimates are based on 2,500 independent replications with $b = 32$ batches and batch sizes $m = 2^{\mathcal{L}}$, $\mathcal{L} \in \{10, 11, \ldots, 20\}$, where for nominal 95% CIs for y_p, the coverage probabilities are denoted by "95% CI Cover."

		STS area $\mathscr{A}_p(w_0; b, m)$				STS area $\mathscr{A}_p(w_{s,1}; b, m)$				STS area $\mathscr{A}_p(w_{s,2}; b, m)$				STS area $\mathscr{A}_p(w_{s,3}; b, m)$				STS area $\mathscr{A}_p(w_{s,4}; b, m)$			
p (y_p) **Var. Par.**	$\mathcal{L}$	Avg.	Bias	Std. Dev.	95% CI Cover.	Avg.	Bias	Std. Dev.	95% CI Cover.	Avg.	Bias	Std. Dev.	95% CI Cover.	Avg.	Bias	Std. Dev.	95% CI Cover.	Avg.	Bias	Std. Dev.	95% CI Cover.
0.95	10	37.812	−0.453	11.414	94.32	38.859	0.594	11.961	94.68	39.639	1.374	13.132	95.08	38.464	0.199	12.120	94.76	38.797	0.532	11.720	95.00
(1.6449)	11	38.386	0.121	10.799	93.96	39.083	0.818	11.142	94.56	39.683	1.418	11.944	94.80	38.878	0.613	11.242	94.44	39.008	0.743	10.948	94.52
38.265	12	38.662	0.397	10.384	95.28	39.105	0.840	10.620	95.32	39.474	1.209	11.227	95.36	38.978	0.713	10.715	95.12	38.999	0.734	10.449	95.28
	13	38.104	−0.161	10.008	94.36	38.400	0.135	10.206	94.36	38.885	0.620	10.696	94.68	38.396	0.131	10.265	94.52	38.258	−0.007	10.041	94.24
	14	38.306	0.041	9.899	95.12	38.444	0.179	9.941	95.24	38.439	0.174	9.952	94.92	38.357	0.092	9.942	95.24	38.399	0.134	9.931	95.28
	15	38.422	0.157	9.894	94.68	38.613	0.348	9.893	94.76	38.782	0.517	9.892	94.92	38.574	0.309	9.881	94.60	38.557	0.292	9.877	94.60
	16	38.226	−0.039	9.943	95.32	38.416	0.151	9.909	95.32	38.552	0.287	9.907	95.16	38.342	0.077	9.951	95.36	38.370	0.105	9.914	95.32
	17	38.153	−0.112	9.532	95.72	38.149	−0.116	9.498	95.80	38.243	−0.022	9.589	96.00	38.174	−0.091	9.559	95.84	38.128	−0.137	9.489	95.80
	18	38.451	0.186	9.582	95.16	38.506	0.241	9.530	94.92	38.591	0.326	9.604	94.92	38.513	0.248	9.549	95.16	38.471	0.206	9.514	95.08
	19	38.399	0.134	9.496	94.40	38.424	0.159	9.543	94.32	38.397	0.132	9.550	94.20	38.402	0.137	9.502	94.36	38.407	0.142	9.551	94.40
	20	38.819	0.554	9.716	94.96	38.873	0.608	9.727	95.16	38.893	0.628	9.614	95.20	38.878	0.613	9.711	95.08	38.872	0.607	9.765	95.16
0.99	10	76.350	−5.262	31.978	92.92	80.905	−0.707	34.921	93.68	87.162	5.550	42.497	93.88	80.187	−1.425	36.589	93.32	79.885	−1.727	32.387	93.84
(2.3263)	11	81.773	0.161	29.693	94.32	85.380	3.768	32.221	94.72	89.164	7.552	38.633	94.84	84.575	2.963	33.403	94.60	84.578	2.966	30.145	94.88
81.612	12	83.965	2.353	26.111	94.60	86.266	4.654	27.257	94.96	88.490	6.878	30.573	95.04	85.778	4.166	27.904	95.08	85.603	3.991	26.310	95.08
	13	82.641	1.029	23.842	94.00	84.200	2.588	24.887	94.28	86.271	4.659	27.518	94.60	84.025	2.413	25.335	94.20	83.496	1.884	23.972	94.12
	14	82.426	0.814	22.724	95.36	83.343	1.731	23.141	95.40	84.277	2.665	24.474	95.36	83.148	1.536	23.424	95.28	83.004	1.392	22.737	95.40
	15	81.767	0.155	21.163	94.88	82.546	0.934	21.346	95.08	83.357	1.745	21.838	95.16	82.340	0.728	21.374	95.08	82.254	0.642	21.195	95.00
	16	82.122	0.510	21.256	94.92	82.601	0.989	21.312	95.12	83.016	1.404	21.557	95.20	82.452	0.840	21.433	94.80	82.532	0.920	21.266	95.16
	17	81.788	0.176	20.670	95.72	81.900	0.288	20.796	95.36	82.206	0.594	21.088	95.44	81.927	0.315	20.855	95.60	81.845	0.233	20.738	95.56
	18	81.523	−0.089	21.343	95.04	81.804	0.192	21.227	94.96	82.092	0.480	21.121	94.80	81.743	0.131	21.313	95.00	81.694	0.082	21.147	94.96
	19	82.083	0.471	20.924	95.28	82.283	0.671	20.820	95.16	82.386	0.774	20.842	95.20	82.236	0.624	20.862	95.44	82.161	0.549	20.819	95.08
	20	82.971	1.359	20.830	94.80	83.056	1.444	20.823	94.64	82.970	1.358	20.709	94.60	83.047	1.435	20.860	94.72	83.040	1.428	20.820	94.76

Figure 2.12: Estimated percent relative bias and RMSE of the variance-parameter estimators for selected marginal quantiles of a stationary AR(1) process with $\mu_Y = 0$ and $\phi = 0.9$ based on Tables 2.9–2.10. All estimates are based on 2,500 independent replications with $b = 32$ batches and batch sizes $m = 2^{\mathcal{L}}$, $\mathcal{L} \in \{10, 11, \ldots, 20\}$.

Table 2.11: Performance evaluation of the batched STS area estimators in Section 2.10 for a stationary waiting-time process in an M/M/1 queueing system with traffic intensity $\rho = 0.8$ for $p \in \{0.5, 0.75\}$. All estimates are based on 2,500 independent replications with $b = 32$ batches and batch sizes $m = 2^{\mathcal{L}}$, $\mathcal{L} = 10, 11, \ldots, 20$, where for nominal 95% CIs for y_p, the coverage probabilities are denoted by "95% CI Cover."

		STS area $\mathscr{A}_p(w_0; b, m)$				STS area $\mathscr{A}_p(w_{s,1}; b, m)$				STS area $\mathscr{A}_p(w_{s,2}; b, m)$				STS area $\mathscr{A}_p(w_{s,3}; b, m)$				STS area $\mathscr{A}_p(w_{s,4}; b, m)$			
p (y_p) **Var. Par.**	$\mathcal{L}$	Avg.	Bias	Std. Dev.	95% CI Cover.	Avg.	Bias	Std. Dev.	95% CI Cover.	Avg.	Bias	Std. Dev.	95% CI Cover.	Avg.	Bias	Std. Dev.	95% CI Cover.	Avg.	Bias	Std. Dev.	95% CI Cover.
0.5	10	1,489.4	854.4	1,440.2	98.08	1,438.0	803.0	1,471.6	97.84	1,218.0	583.0	1,166.8	97.32	1,377.5	742.5	1,325.9	97.80	1,501.1	866.1	1,575.3	98.04
(2.3500)	11	1,110.6	475.6	808.9	97.36	1,007.0	372.0	716.1	97.00	879.8	244.8	593.3	96.92	1,009.2	374.2	662.1	97.08	1,039.2	404.2	773.3	97.08
635.0	12	836.0	201.0	352.9	96.92	773.8	138.8	296.3	96.52	730.3	95.3	242.2	96.20	788.9	153.9	294.4	96.68	785.0	150.0	312.6	96.56
	13	729.9	94.9	236.3	95.76	697.3	62.3	206.7	95.32	678.1	43.1	189.7	95.44	707.4	72.4	212.5	95.60	701.9	66.9	211.6	95.40
	14	682.8	47.8	192.7	95.88	669.3	34.3	184.2	95.72	664.5	29.5	180.3	95.72	674.5	39.5	186.2	95.64	671.0	36.0	185.6	95.84
	15	654.3	19.3	176.3	94.36	649.9	14.9	171.7	94.20	652.3	17.3	168.8	94.60	652.8	17.8	172.9	94.32	649.5	14.5	172.5	94.16
	16	646.4	11.4	166.6	95.16	644.9	9.9	166.6	95.12	645.0	10.0	168.2	95.04	645.6	10.6	167.0	95.00	644.3	9.3	165.8	95.08
	17	639.1	4.1	161.9	94.72	637.5	2.5	161.6	94.40	638.9	3.9	162.0	94.68	638.9	3.9	162.4	94.56	637.4	2.4	161.5	94.36
	18	638.9	3.9	159.6	94.40	638.6	3.6	160.2	94.48	639.9	4.9	159.0	94.76	639.2	4.2	159.8	94.36	638.6	3.6	160.6	94.40
	19	639.4	4.4	163.0	94.64	638.8	3.8	162.4	94.56	639.6	4.6	163.4	94.68	639.6	4.6	163.2	94.48	638.5	3.5	161.8	94.56
	20	632.5	−2.5	157.6	94.84	631.0	−4.0	155.3	94.72	631.7	−3.3	153.6	94.60	632.0	−3.0	155.5	94.76	631.0	−4.0	155.9	94.80
0.75	10	4,853.0	1,554.3	3,419.9	95.92	5,224.9	1,926.2	3,780.1	96.08	5,232.5	1,933.8	4,075.5	96.08	5,012.4	1,713.7	3,695.7	95.80	5,304.4	2,005.7	3,734.2	96.44
(5.8158)	11	4,992.9	1,694.2	3,657.9	96.56	5,098.9	1,800.2	3,927.7	96.76	4,817.0	1,518.3	4,274.0	96.52	4,917.4	1,618.7	3,788.6	96.52	5,205.2	1,906.5	3,935.4	96.76
3,298.7	12	4,242.5	943.8	2,046.1	96.16	4,134.4	835.7	1,948.8	95.96	3,878.9	580.2	1,597.0	95.96	4,083.1	784.4	1,797.6	96.00	4,203.8	905.1	2,064.5	96.12
	13	3,819.2	520.5	1,402.5	96.32	3,692.3	393.6	1,236.2	96.20	3,562.6	263.9	1,067.5	96.00	3,709.4	410.7	1,231.5	96.36	3,726.4	427.7	1,283.2	96.20
	14	3,547.5	248.8	1,045.6	95.36	3,482.2	183.5	983.5	95.44	3,454.4	155.7	962.2	95.20	3,504.0	205.3	996.7	95.28	3,492.7	194.0	993.5	95.40
	15	3,412.5	113.8	936.5	94.64	3,390.0	91.3	907.1	94.84	3,387.4	88.7	893.1	94.92	3,400.2	101.5	912.6	94.72	3,391.3	92.6	910.5	94.76
	16	3,356.4	57.7	873.3	94.60	3,349.8	51.1	872.5	94.52	3,354.2	55.5	884.5	94.28	3,353.3	54.6	875.5	94.60	3,346.7	48.0	867.5	94.48
	17	3,332.1	33.4	859.7	94.48	3,321.5	22.8	859.4	94.36	3,328.2	29.5	862.0	94.28	3,330.6	31.9	862.9	94.24	3,320.9	22.2	859.9	94.40
	18	3,316.1	17.4	814.8	94.60	3,311.9	13.2	819.2	94.48	3,317.6	18.9	817.1	94.64	3,315.1	16.4	814.9	94.56	3,311.9	13.2	822.8	94.44
	19	3,310.2	11.5	838.5	94.36	3,309.4	10.7	837.1	94.28	3,319.7	21.0	846.7	94.76	3,313.5	14.8	842.0	94.40	3,305.5	6.8	832.0	94.20
	20	3,292.4	−6.3	813.3	94.64	3,287.4	−11.3	806.7	94.72	3,290.6	−8.1	802.4	95.04	3,290.9	−7.8	806.9	94.76	3,287.7	−11.0	808.3	94.76

Table 2.12: Performance evaluation of the batched STS area estimators in Section 2.10 for a stationary waiting-time process in an M/M/1 queueing system with traffic intensity $\rho = 0.8$ for $p \in \{0.95, 0.99\}$. All estimates are based on 2,500 independent replications with $b = 32$ batches and batch sizes $m = 2^{\mathcal{L}}$, $\mathcal{L} = 10, 11, \ldots, 20$, where for nominal 95% CIs for y_p, the coverage probabilities are denoted by "95% CI Cover."

		STS area $\mathscr{A}_p(w_0; b, m)$				STS area $\mathscr{A}_p(w_{s,1}; b, m)$				STS area $\mathscr{A}_p(w_{s,2}; b, m)$				STS area $\mathscr{A}_p(w_{s,3}; b, m)$				STS area $\mathscr{A}_p(w_{s,4}; b, m)$			
p (y_p) **Var. Par.**	$\mathcal{L}$	Avg.	Bias	Std. Dev.	95% CI Cover.	Avg.	Bias	Std. Dev.	95% CI Cover.	Avg.	Bias	Std. Dev.	95% CI Cover.	Avg.	Bias	Std. Dev.	95% CI Cover.	Avg.	Bias	Std. Dev.	95% CI Cover.
0.95	10	16,816	−15,664	12,658	80.96	18,250	−14,230	14,218	82.28	20,163	−12,317	17,800	83.08	18,248	−14,232	15,001	81.72	17,863	−14,617	12,897	82.40
(13.8629)	11	26,142	−6,338	19,292	88.84	28,747	−3,733	21,842	90.52	31,840	−640	28,313	91.20	28,485	−3,995	23,197	89.56	28,199	−4,281	19,478	90.36
32,480	12	33,519	1,039	22,209	93.96	36,984	4,504	25,196	94.88	39,951	7,471	31,669	95.12	36,032	3,552	26,110	94.20	36,577	4,097	22,943	95.12
	13	37,166	4,686	18,578	95.52	39,632	7,152	20,792	96.12	39,937	7,457	22,995	96.24	38,277	5,797	20,014	95.88	39,850	7,370	20,711	96.16
	14	36,801	4,321	17,075	94.76	37,392	4,912	16,831	94.80	36,583	4,103	15,221	95.32	36,685	4,205	16,147	94.80	37,632	5,152	17,259	94.88
	15	35,003	2,523	12,155	94.80	34,959	2,479	11,141	95.04	34,573	2,093	10,722	95.08	34,793	2,313	11,117	94.88	35,075	2,595	11,312	95.08
	16	33,714	1,234	10,240	95.16	33,549	1,069	9,787	95.20	33,471	991	9,677	95.24	33,574	1,094	9,888	95.12	33,573	1,093	9,773	95.20
	17	33,065	585	8,831	94.84	32,905	425	8,710	94.88	32,807	327	8,709	94.84	32,950	470	8,723	94.68	32,953	473	8,731	94.88
	18	32,996	516	8,343	94.76	32,924	444	8,348	95.00	32,977	497	8,387	95.20	32,977	497	8,344	94.92	32,905	425	8,331	95.04
	19	32,564	84	8,239	94.88	32,612	132	8,131	94.68	32,789	309	8,143	94.64	32,646	166	8,161	94.60	32,559	79	8,116	94.72
	20	32,462	−18	7,978	94.68	32,400	−80	7,901	94.84	32,277	−203	7,883	94.56	32,392	−88	7,935	94.76	32,432	−48	7,892	94.84
0.99	10	27,618	−163,643	17,701	54.88	28,851	−162,410	19,742	55.68	30,801	−160,460	24,659	56.00	29,258	−162,003	20,883	55.76	28,254	−163,007	17,953	55.36
(21.9101)	11	54,707	−136,554	37,687	67.96	57,858	−133,403	42,382	68.84	63,179	−128,082	54,767	69.12	58,747	−132,514	45,242	68.48	56,192	−135,069	37,620	69.00
191,261	12	92,769	−98,492	66,687	79.08	99,087	−92,174	75,008	79.88	109,502	−81,759	97,461	80.16	100,134	−91,127	80,154	79.44	95,872	−95,389	66,034	80.40
	13	135,781	−55,480	93,623	87.72	146,984	−44,277	104,752	88.44	161,829	−29,432	132,776	88.72	146,551	−44,710	110,923	88.20	144,020	−47,241	95,028	89.00
	14	179,612	−11,649	128,352	91.20	197,294	6,033	144,902	91.72	216,109	24,848	184,611	92.40	194,135	2,874	152,860	91.28	194,203	2,942	130,054	92.00
	15	204,722	13,461	110,567	94.40	222,011	30,750	124,641	95.12	231,261	40,000	146,642	94.96	215,280	24,019	125,004	94.56	221,184	29,923	119,390	95.12
	16	209,709	18,448	106,715	95.44	217,362	26,101	112,770	95.56	214,930	23,669	107,089	95.40	211,760	20,499	107,237	95.40	218,422	27,161	114,314	95.60
	17	203,576	12,315	70,787	95.32	203,675	12,414	66,934	95.44	199,868	8,607	63,503	94.88	202,000	10,739	65,835	95.32	204,745	13,484	67,958	95.44
	18	199,607	8,346	57,126	95.24	198,737	7,476	56,057	94.96	197,947	6,686	56,585	95.20	198,792	7,531	56,283	95.04	198,870	7,609	55,832	94.96
	19	196,113	4,852	52,085	95.52	195,583	4,322	51,580	95.40	195,410	4,149	52,288	95.24	195,807	4,546	51,860	95.52	195,514	4,253	51,450	95.56
	20	193,492	2,231	49,780	95.52	192,720	1,459	48,830	95.48	191,263	2	48,458	95.28	192,646	1,385	49,061	95.48	193,072	1,811	48,960	95.48

Figure 2.13: Estimated percent relative bias and RMSE of the variance-parameter estimators for selected marginal quantiles of a stationary waiting-time process in an M/M/1 queueing system with traffic intensity $\rho = 0.8$ based on Tables 2.11–2.12. All estimates are based on 2500 independent replications with $b = 32$ batches and batch sizes $m = 2^{\mathcal{L}}$, $\mathcal{L} = 10, 11, \ldots, 20$.

CHAPTER 3

COMPARISON OF SEVERAL VARIANCE-PARAMETER ESTIMATORS BASED ON EXACT CALCULATIONS OF THEIR EXPECTED VALUES FOR THE SPECIAL CASE OF I.I.D. SAMPLES

In this chapter, we derive exact (or nearly exact) calculations for the expected values of the variance-parameter estimators of σ_p^2 in Chapter 2; and we compare these estimators with regard to small-sample bias and rate of convergence to their asymptotic limits. The exact calculations of the expected values of the variance parameter estimators involve the evaluations of joint moments of order statistics. Unfortunately, the computation of such joint moments of order statistics is hard even for i.i.d. data, as we will show in the following sections using four illustrative examples.

3.1 Analytical Expressions for Order Statistics and Joint Moments of Order Statistics for Specific Distributions for the Special Case of I.I.D. Data

We consider i.i.d. samples from the following four distributions: (i) the uniform distribution on $[0, 1]$; (ii) the exponential distribution with parameter one; (iii) the Pareto distribution with parameters $\gamma = 1$ and $\theta = 2.1$; and (iv) the Laplace distribution with zero mean and unit scale parameter. For the exact calculations of the expected values of the variance parameter estimators $\mathscr{N}_p(b, m)$, $\widetilde{\mathscr{N}_p}(b, m)$, and $\mathscr{A}_p(w; b, m)$ in the special case of i.i.d. observations, we need analytical expressions for $\mathrm{E}\big[\widetilde{y}_p^2(i)\big]$ and $\mathrm{E}\big[\widetilde{y}_p(i)\widetilde{y}_p(j)\big]$, as we will show in Sections 3.2–3.3. We will use the notation $Y_{k:n}$ for the kth order statistics of a sample $\{Y_1, \ldots, Y_n\}$. Then $\widetilde{y}_p(i) = Y_{k:i}$ for $k = \lceil pi \rceil$ and $i = 1, \ldots, n$.

Below, we will derive analytical expressions for $\mathrm{E}\big[\widetilde{y}_p^2(i)\big]$ and $\mathrm{E}\big[\widetilde{y}_p(i)\widetilde{y}_p(j)\big]$ for the four distributions under study. We have

$$\mathrm{E}\big[\widetilde{y}_p^2(i)\big] = \mathrm{E}[Y_{k:i}^2], \quad \text{for } k = \lceil pi \rceil \text{ and } i = 1, \dots, n,$$

and

$$\mathrm{E}\big[\widetilde{y}_p(i)\widetilde{y}_p(j)\big] = \mathrm{E}[Y_{k:i}Y_{\ell:j}] = \sum_{r=k}^{j-i+k} \frac{\binom{r-1}{k-1}\binom{j-r}{i-k}}{\binom{j}{i}} \mathrm{E}[Y_{r:j}Y_{\ell:j}], \tag{3.1}$$

for $k = \lceil pi \rceil$, $\ell = \lceil pj \rceil$, and $i < j$. The last equality follows from Equation (2) in Dołęgowski and Wesołowski [73]. The second moment of order statistics can be calculated by evaluating the single-dimensional integral

$$\mathrm{E}[Y_{k:i}^2] = \frac{i!}{(i-1)!(i-k)!} \int_{-\infty}^{\infty} x^2 F^{k-1}(x)(1 - F(x))^{i-k} f(x)\, dx;$$

see Equation (7.3), Ahsanullah *et al.* [74]. Also, the product moments $\mathrm{E}[Y_{r:j}Y_{\ell:j}]$ for $1 \le r < \ell \le j$ can be calculated by computing the double integral

$$\begin{aligned} \mathrm{E}[Y_{r:j}Y_{\ell:j}] = {} & \frac{j!}{(r-1)!(\ell-r-1)!(j-\ell)!} \\ & \times \int_{-\infty}^{\infty} \int_{-\infty}^{x} x^r y^\ell F^{r-1}(x)[F(y) - F(x)]^{\ell-r-1}[1 - F(y)]^{j-\ell} f(x)(y)\, dy\, dx; \end{aligned}$$

see Equations (7.4) and (7.5), Ahsanullah *et al.* [74]. Furthermore, for uniform, exponential, and Pareto distributions, there are closed formulas for the raw and product moments of order statistics.

3.1.1 Uniform Distribution

For i.i.d. observations from the uniform distribution on $[0, 1]$, the second moments and the product moments of the order statistics are

$$\mathrm{E}[Y_{k:i}^2] = \frac{k(k+1)}{(i+1)(i+2)} \quad \text{and} \quad \mathrm{E}[Y_{r:j}Y_{\ell:j}] = \frac{r(\ell+1)}{(j+1)(j+2)}, \quad \text{for } r < \ell, \tag{3.2}$$

respectively (see Equations (8.4) and (8.9) in Section 8.1 of Ahsanullah *et al.* [74]). Further, for $i < j$, we can use Equations (3.1)–(3.2) and Mathematica from Wolfram Research, Inc. [75] to write

$$
\begin{aligned}
\mathrm{E}[Y_{k:i}Y_{\ell:j}] &= \frac{1}{\binom{j}{i}}\left[\left\{\sum_{r=k}^{\ell}+\sum_{r=\ell+1}^{j-i+k}\right\}\binom{r-1}{k-1}\binom{j-r}{i-k}\mathrm{E}[Y_{r:j}Y_{\ell:j}]\right] \\
&= \frac{1}{\binom{j}{i}}\left[\sum_{r=k}^{\ell}\binom{r-1}{k-1}\binom{j-r}{i-k}\frac{r(\ell+1)}{(j+1)(j+2)}\right. \\
&\quad \left.+\sum_{r=\ell+1}^{j-i+k}\binom{r-1}{k-1}\binom{j-r}{i-k}\frac{\ell(r+1)}{(j+1)(j+2)}\right] \\
&= \frac{1}{(j+1)(j+2)\binom{j}{i}}\left[\ell\sum_{r=k}^{j-i+k}r\binom{r-1}{k-1}\binom{j-r}{i-k}+\sum_{r=k}^{\ell}r\binom{r-1}{k-1}\binom{j-r}{i-k}\right. \\
&\quad \left.+\ell\sum_{r=\ell+1}^{j-i+k}\binom{r-1}{k-1}\binom{j-r}{i-k}\right] \\
&= \frac{i!(j-i)!}{(j+1)(j+2)j!}\left[\frac{k\ell(j+1)!}{(i+1)!(j-i)!}+\sum_{r=k}^{\ell}r\binom{r-1}{k-1}\binom{j-r}{i-k}\right. \\
&\quad \left.+\ell\sum_{r=\ell+1}^{j-i+k}\binom{r-1}{k-1}\binom{j-r}{i-k}\right] \\
&= \frac{k\ell}{(i+1)(j+2)}+\frac{i!(j-i)!}{(j+2)!}\left[\sum_{r=k}^{\ell}r\binom{r-1}{k-1}\binom{j-r}{i-k}+\ell\sum_{r=\ell+1}^{j-i+k}\binom{r-1}{k-1}\binom{j-r}{i-k}\right].
\end{aligned}
\tag{3.3}
$$

3.1.2 Exponential Distribution

For i.i.d. observations from an exponential distribution with unit rate parameter, the mean and variance of order statistics are

$$
\mathrm{E}[Y_{k:i}] = \sum_{s=1}^{k}\frac{1}{i-s+1} \quad \text{and} \quad \mathrm{Var}[Y_{k:i}] = \sum_{s=1}^{k}\frac{1}{(i-s+1)^2}\,, \tag{3.4}
$$

respectively (see Equations (8.25) and (8.26) in Section 8.2 of Ahsanullah *et al.* [74]). Thus the second moment of $Y_{k:i}$ is

$$\mathrm{E}[Y_{k:i}^2] = \mathrm{Var}[Y_{k:i}] + \mathrm{E}[Y_{k:i}]^2 = \sum_{s=1}^{k} \frac{1}{(i-s+1)^2} + \left(\sum_{s=1}^{k} \frac{1}{i-s+1}\right)^2, \tag{3.5}$$

and the covariance between the order statistics $Y_{r:j}$ and $Y_{\ell:j}$ is

$$\mathrm{Cov}[Y_{r:j}, Y_{\ell:j}] = \mathrm{Var}[Y_{r:j}] = \sum_{s=1}^{r} \frac{1}{(j-s+1)^2}, \quad \text{for } r \le \ell;$$

see the solution of Exercise 8.9 in Section 8.2 of Ahsanullah *et al.* [74]. Thus

$$\begin{aligned}
\mathrm{E}[Y_{r:j}Y_{\ell:j}] &= \mathrm{Cov}[Y_{r:j}, Y_{\ell:j}] + \mathrm{E}[Y_{r:j}]\mathrm{E}[Y_{\ell:j}] \\
&= \sum_{s=1}^{r} \frac{1}{(j-s+1)^2} + \left(\sum_{s=1}^{r} \frac{1}{j-s+1}\right)\left(\sum_{s=1}^{\ell} \frac{1}{j-s+1}\right), \quad \text{for } r \le \ell.
\end{aligned} \tag{3.6}$$

Using Equations (3.1) and (3.6) we have

$$\begin{aligned}
\mathrm{E}[Y_{k:i}Y_{\ell:j}] &= \left\{\sum_{r=k}^{\ell} + \sum_{r=\ell+1}^{j-i+k}\right\} \frac{\binom{r-1}{k-1}\binom{j-r}{i-k}}{\binom{j}{i}} \mathrm{E}[Y_{r:j}Y_{\ell:j}] \\
&= \sum_{r=k}^{\ell} \frac{\binom{r-1}{k-1}\binom{j-r}{i-k}}{\binom{j}{i}} \left[\sum_{s=1}^{r} \frac{1}{(j-s+1)^2} + \left(\sum_{s=1}^{r} \frac{1}{j-s+1}\right)\left(\sum_{s=1}^{\ell} \frac{1}{j-s+1}\right)\right] \\
&\quad + \sum_{r=\ell+1}^{j-i+k} \frac{\binom{r-1}{k-1}\binom{j-r}{i-k}}{\binom{j}{i}} \left[\sum_{s=1}^{\ell} \frac{1}{(j-s+1)^2} + \left(\sum_{s=1}^{r} \frac{1}{j-s+1}\right)\left(\sum_{s=1}^{\ell} \frac{1}{j-s+1}\right)\right] \\
&= \sum_{r=k}^{\ell} \frac{\binom{r-1}{k-1}\binom{j-r}{i-k}}{\binom{j}{i}} \sum_{s=1}^{r} \frac{1}{(j-s+1)^2} \\
&\quad + \left(\sum_{s=1}^{\ell} \frac{1}{j-s+1}\right)\left(\sum_{r=k}^{j-i+k} \frac{\binom{r-1}{k-1}\binom{j-r}{i-k}}{\binom{j}{i}} \sum_{s=1}^{r} \frac{1}{j-s+1}\right) \\
&\quad + \left(\sum_{r=\ell+1}^{j-i+k} \frac{\binom{r-1}{k-1}\binom{j-r}{i-k}}{\binom{j}{i}}\right)\left(\sum_{s=1}^{\ell} \frac{1}{(j-s+1)^2}\right).
\end{aligned} \tag{3.7}$$

3.1.3 Pareto Distribution

For i.i.d. observations from a Pareto distribution with parameters γ and θ and the density $f(x) = \theta\gamma^{\theta}x^{-\theta-1}$, for $x \geq \gamma$, the moments of the order statistics are given by

$$\mathrm{E}[Y_{k:i}^{\eta}] = \gamma^{\eta}\frac{i!}{(i-k)!}\frac{\Gamma(i-k+1-\eta/\theta)}{\Gamma(i+1-\eta/\theta)}, \quad \text{for } \eta < (i-k+1)\theta; \tag{3.8}$$

see Equation (4) of Huang [76]. For $\theta \geq 2$ and $j \geq 2$, the product moments are

$$\mathrm{E}[Y_{r:j}Y_{\ell:j}] = \gamma^{2}\frac{j!}{(j-\ell)!}\frac{\Gamma(j-\ell+1-1/\theta)\,\Gamma(j-r+1-2/\theta)}{\Gamma(j-r+1-1/\theta)\,\Gamma(j+1-2/\theta)}, \quad \text{for } r < \ell; \tag{3.9}$$

see Equation (4.5) of Malik [77].

3.1.4 Laplace Distribution

For i.i.d. data $\{Y_1, \ldots, Y_n\}$ from the Laplace (double exponential) distribution with density function $f(x) = e^{-|x|}/2$, for $-\infty < x < \infty$, the second and product moments of order statistics can be calculated by using the moment formulas of order statistics for the exponential distribution (Section 4 of Govindarajulu [78]). Let $\{Z_1, \ldots, Z_i\}$, $i = 1, \ldots, n$, be i.i.d. exponential r.v.'s with unit rate and let $Z_{i:n}$, $i = 1, \ldots, n$, denote the respective order statistics. Then, by Formula 2.1 in Govindarajulu [78], the first and second moment of the order statistic $Y_{k:i}$ is given by

$$\begin{aligned}\mathrm{E}[Y_{k:i}] &= 2^{-i}\left\{\sum_{m=0}^{k-1}\binom{i}{m}\mathrm{E}[Z_{(k-m):(i-m)}] - \sum_{m=k}^{i}\binom{i}{m}\mathrm{E}[Z_{(m-k+1):m}]\right\}\\ &= 2^{-i}\left\{\sum_{m=0}^{k-1}\binom{i}{m}\sum_{s=1}^{k-m}\frac{1}{i-m-s+1} - \sum_{m=k}^{i}\binom{i}{m}\sum_{s=1}^{m-k+1}\frac{1}{m-s+1}\right\}.\end{aligned} \tag{3.10}$$

$$
\begin{aligned}
\mathrm{E}[Y_{k:i}^2] &= 2^{-i}\left\{\sum_{m=0}^{k-1}\binom{i}{m}\mathrm{E}[Z_{(k-m):(i-m)}^2] + \sum_{m=k}^{i}\binom{i}{m}\mathrm{E}[Z_{(m-k+1):m}^2]\right\} \\
&= 2^{-i}\left\{\sum_{m=0}^{k-1}\binom{i}{m}\left[\sum_{s=1}^{k-m}\frac{1}{(i-m-s+1)^2} + \left(\sum_{s=1}^{k-m}\frac{1}{i-m-s+1}\right)^2\right]\right. \\
&\quad \left. + \sum_{m=k}^{i}\binom{i}{m}\left[\sum_{s=1}^{m-k+1}\frac{1}{(m-s+1)^2} + \left(\sum_{s=1}^{m-k+1}\frac{1}{m-s+1}\right)^2\right]\right\}.
\end{aligned} \tag{3.11}
$$

The last equality follows from Equation (3.5). Also, by Formula 2.2 in Govindarajulu [78], the product moment $\mathrm{E}[Y_{r:j}Y_{\ell:j}]$ for $r < \ell$ can be computed as follows:

$$
\begin{aligned}
\mathrm{E}[Y_{r:j}Y_{\ell:j}] &= 2^{-j}\left\{\sum_{m=0}^{r-1}\binom{j}{m}\mathrm{E}[Z_{(r-m):(j-m)}Z_{(\ell-m):(j-m)}]\right. \\
&\quad \left. - \sum_{m=r}^{\ell-1}\binom{j}{m}\mathrm{E}[Z_{(m-r+1):m}]\mathrm{E}[Z_{(\ell-m):(j-m)}] + \sum_{m=\ell}^{j}\binom{j}{m}\mathrm{E}[Z_{(m+1-\ell):m}Z_{(m+1-r):m}]\right\} \\
&= 2^{-j}\left\{\sum_{m=0}^{r-1}\binom{j}{m}\left[\sum_{s=1}^{r-m}\frac{1}{(j-m-s+1)^2}\right.\right. \\
&\quad \left. + \left(\sum_{s=1}^{r-m}\frac{1}{j-m-s+1}\right)\left(\sum_{s=1}^{\ell-m}\frac{1}{j-m-s+1}\right)\right] \\
&\quad - \sum_{m=r}^{\ell-1}\binom{j}{m}\left(\sum_{s=1}^{m-r+1}\frac{1}{m-s+1}\right)\left(\sum_{s=1}^{\ell-m}\frac{1}{j-m-s+1}\right) \\
&\quad \left. + \sum_{m=\ell}^{j}\binom{j}{m}\left[\sum_{s=1}^{m+1-\ell}\frac{1}{(m-s+1)^2} + \left(\sum_{s=1}^{m+1-\ell}\frac{1}{m-s+1}\right)\left(\sum_{s=1}^{m+1-r}\frac{1}{m-s+1}\right)\right]\right\}.
\end{aligned} \tag{3.12}
$$

The last equality follows from Equations(3.4) and (3.6).

3.1.5 Asymptotic Variance Parameter σ_p^2

In this subsection, we calculate the asymptotic variance parameter σ_p^2 for the four distributions under consideration. We will use these values to calculate the bias of the variance-parameter estimators in the numerical results for the exact (or nearly exact) calculations in Section 3.5.

For the uniform distribution on $[0, 1]$, the asymptotic variance parameter is

$$\sigma_p^2 = p(1-p). \tag{3.13}$$

For the exponential distribution with rate $\lambda > 0$ and density $f(x) = \lambda e^{-\lambda x}$, $x > 0$ the asymptotic variance parameter is

$$\sigma_p^2 = \frac{p(1-p)}{f^2(y_p)} = \frac{p}{\lambda^2(1-p)}, . \tag{3.14}$$

For the Pareto distribution with parameters γ and θ and density $f(x) = \theta\gamma^\theta x^{-\theta-1}$, $x \geq \gamma$, the asymptotic variance parameter is given by

$$\sigma_p^2 = p(1-p)\left[\frac{\gamma}{\theta(1-p)^{\frac{(\theta+1)}{\theta}}}\right]^2 = \frac{\gamma^2 p}{\theta^2(1-p)^{1+2/\theta}}\,. \tag{3.15}$$

Finally, the Laplace distribution with parameters $\mu \in \mathbb{R}$ $b > 0$ and density $f(x) = \frac{1}{2b}e^{-\frac{|x-\mu|}{b}}$, $-\infty < x < \infty$, the p-quantile is

$$y_p = F^{-1}(p) = \begin{cases} \mu + b\log(2p) & \text{if } 0 < p \leq 1/2 \\ \mu - b\log(2(1-p)) & \text{if } 1/2 < p \leq 1, \end{cases}$$

and so the asymptotic variance parameter is

$$\sigma_p^2 = \frac{p(1-p)}{f^2(y_p)} = b^2 \times \begin{cases} \frac{1-p}{p}, & \text{if } 0 < p \leq 1/2 \\ \frac{p}{1-p}, & \text{if } 1/2 < p \leq 1. \end{cases} \tag{3.16}$$

3.2 Expected Value of the STS Area Variance-Parameter Estimator

For now, consider a single batch $\{Y_1, Y_2, \ldots, Y_n\}$ of observations. Recall that the STS area quantile-estimation process is defined as

$$T_n(t) \equiv \frac{\lfloor nt \rfloor}{n^{1/2}} \big[\, \widetilde{y}_p(n) - \widetilde{y}_p(\lfloor nt \rfloor) \big], \quad \text{for } n \geq 1 \text{ and } t \in [0,1],$$

where $\widetilde{y}_p(\lfloor nt \rfloor)$ is the point estimator of the p-quantile y_p based on the partial sample $\{Y_1, \ldots, Y_{\lfloor nt \rfloor}\}$, and the STS area variance estimator is $A_p^2(w;n)$, where

$$\begin{aligned} A_p(w;n) &\equiv n^{-1} \sum_{k=1}^{n} w(k/n) T_n(k/n) = n^{-3/2} \sum_{k=1}^{n} k\, w(k/n) \big[\, \widetilde{y}_p(n) - \widetilde{y}_p(k) \big] \\ &= n^{-3/2} \sum_{k=1}^{n} \alpha_k \widetilde{y}_p(k), \end{aligned}$$

and

$$\alpha_k \equiv -k w(k/n), \text{ for } k = 1, \ldots, n-1 \quad \text{and} \quad \alpha_n \equiv -\sum_{k=1}^{n-1} \alpha_k. \tag{3.17}$$

Thus, we can write

$$\begin{aligned} n^3 \mathrm{E}\big[A_p^2(w;n)\big] &= \mathrm{E}\Bigg[\bigg(\sum_{k=1}^{n} \alpha_k \widetilde{y}_p(k)\bigg)^2\Bigg] = \sum_{i=1}^{n} \sum_{j=1}^{n} \alpha_i \alpha_j \mathrm{E}[\widetilde{y}_p(i) \widetilde{y}_p(j)]. \\ &= \sum_{i=1}^{n} \alpha_i^2 \mathrm{E}\big[\widetilde{y}_p^2(i)\big] + 2 \sum_{i=1}^{n-1} \sum_{j=i+1}^{n} \alpha_i \alpha_j \mathrm{E}\big[\widetilde{y}_p(i) \widetilde{y}_p(j)\big]. \end{aligned} \tag{3.18}$$

3.3 Expected Values of the NBQ Variance-Parameter Estimators for the Special Case of I.I.D. Data

In this section, we undertake some analytical work related to the expected values of the NBQ variance-parameter estimators $\mathscr{N}_p(b,m)$ and $\widetilde{\mathscr{N}_p}(b,m)$ based on b batches of size m, for the special case of i.i.d. data. Recall that given a fixed batch count $b \geq 2$, for $j = 1, \ldots, b$, the jth nonoverlapping batch of size $m \geq 1$ consists of the subsequence $\{Y_{(j-1)m+1}, \ldots, Y_{jm}\}$.

First, we will derive an analytical expression for the expected value of the NBQ variance-parameter estimator $\mathscr{N}_p(b,m)$ defined in Equation (2.55). Note that the BQEs $\widehat{y}_p(j,m)$ are i.i.d. Thus we have

$$
\begin{aligned}
\mathrm{E}\big[\mathscr{N}_p(b,m)\big] &= \frac{mb}{b-1}\Big(\mathrm{Var}\big[\widehat{y}_p(1,m)\big] - \mathrm{Var}\big[\overline{\widehat{y}}_p(b,m)\big]\Big) \\
&= \frac{mb}{b-1}\left(\mathrm{Var}\big[\widehat{y}_p(1,m)\big] - \mathrm{Var}\left[\frac{1}{b}\sum_{j=1}^{b}\widehat{y}_p(j,m)\right]\right) \\
&= \frac{mb}{b-1}\left(\mathrm{Var}\big[\widehat{y}_p(1,m)\big] - \frac{1}{b}\mathrm{Var}\big[\widehat{y}_p(1,m)\big]\right) \\
&= \frac{mb(b-1)}{(b-1)b}\mathrm{Var}\big[\widehat{y}_p(1,m)\big] \\
&= m\mathrm{Var}\big[\widehat{y}_p(1,m)\big] \\
&= m\mathrm{Var}\big[\widetilde{y}_p(m)\big]. \qquad (3.19)
\end{aligned}
$$

It is worth noting that the expected value and the bias for the NBQ variance-parameter estimator $\mathscr{N}_p(b,m)$ in the i.i.d. case depend only on m (and not on j).

Second, we will derive the analytical expression for the expected value of the NBQ variance-parameter estimator $\widetilde{\mathscr{N}_p}(b,m)$ defined in Equation (2.56). Again, the $\widehat{y}_p(j,m)$ are i.i.d. due to the i.i.d. data, which allows us to write that $\mathrm{E}\big[\widehat{y}_p(1,m)\widetilde{y}_p(n)\big] = \mathrm{E}\big[\widehat{y}_p(2,m)\widetilde{y}_p(n)\big] = \cdots = \mathrm{E}\big[\widehat{y}_p(b,m)\widetilde{y}_p(n)\big]$. It follows that

$$
\begin{aligned}
\mathrm{E}\big[\widetilde{\mathscr{N}_p}(b,m)\big] &= \frac{m}{b-1}\sum_{j=1}^{b}\mathrm{E}\big[(\widehat{y}_p(j,m)-\widetilde{y}_p(n))^2\big] \\
&= \frac{m}{b-1}\sum_{j=1}^{b}\mathrm{E}\big[\widehat{y}_p^2(j,m) - 2\widehat{y}_p(j,m)\widetilde{y}_p(n) + \widetilde{y}_p^2(n)\big] \\
&= \frac{mb}{b-1}\big(\mathrm{E}\big[\widehat{y}_p^2(j,m)\big] - 2\mathrm{E}\big[\widehat{y}_p(j,m)\widetilde{y}_p(n)\big] + \mathrm{E}\big[\widetilde{y}_p^2(n)\big]\big). \qquad (3.20)
\end{aligned}
$$

Next, we wish to obtain a relation between the expected values of the NBQ variance-parameter estimators $\mathscr{N}_p(b,m)$ and $\widetilde{\mathscr{N}_p}(b,m)$ for the i.i.d. case. Starting with Equation

(3.20), we can write

$$
\begin{aligned}
\mathrm{E}\big[\widetilde{\mathcal{N}_p}(b,m)\big] &= \frac{mb}{b-1}\Big(\mathrm{E}\big[\widehat{y}_p^2(1,m)\big] - 2\mathrm{E}\big[\widehat{y}_p(1,m)\widetilde{y}_p(n)\big] + \mathrm{E}\big[\widetilde{y}_p^2(n)\big]\Big) \\
&= \frac{mb}{b-1}\Big(\mathrm{E}\big[\widehat{y}_p^2(1,m)\big] - \mathrm{E}\big[\widehat{y}_p(1,m)\big]^2 + \mathrm{E}\big[\widehat{y}_p(1,m)\big]^2 \\
&\quad - 2\mathrm{E}\big[\widehat{y}_p(1,m)\widetilde{y}_p(n)\big] + \mathrm{E}\big[\widetilde{y}_p^2(n)\big] - \mathrm{E}\big[\widetilde{y}_p(n)\big]^2 + \mathrm{E}\big[\widetilde{y}_p(n)\big]^2\Big) \\
&= \frac{mb}{b-1}\Big(\mathrm{E}\big[\widehat{y}_p^2(1,m)\big] - \mathrm{E}\big[\widehat{y}_p(1,m)\big]^2\Big) + \frac{mb}{b-1}\Big(\mathrm{E}\big[\widetilde{y}_p^2(n)\big] - \mathrm{E}\big[\widetilde{y}_p(n)\big]^2\Big) \\
&\quad + \frac{mb}{b-1}\Big(\mathrm{E}\big[\widetilde{y}_p(n)\big]^2 - 2\mathrm{E}\big[\widehat{y}_p(1,m)\widetilde{y}_p(n)\big] + \mathrm{E}\big[\widehat{y}_p(1,m)\big]^2\Big).
\end{aligned}
$$

Then using Equation (3.19) and the fact that $\mathrm{E}\big[\widetilde{y}_p(n)\big] = \mathrm{E}\big[\widehat{y}_p(1,n)\big]$, we obtain

$$
\begin{aligned}
\mathrm{E}\big[\widetilde{\mathcal{N}_p}(b,m)\big] &= \frac{b}{b-1}\mathrm{E}\big[\mathcal{N}_p(b,m)\big] + \frac{1}{b-1}\mathrm{E}\big[\mathcal{N}_p(b,n)\big] \\
&\quad + \frac{mb}{b-1}\Big(\mathrm{E}\big[\widetilde{y}_p(n)\big]^2 - 2\mathrm{E}\big[\widehat{y}_p(1,m)\widetilde{y}_p(n)\big] + \mathrm{E}\big[\widehat{y}_p(1,m)\big]^2\Big).
\end{aligned}
$$

Using the inequality

$$
\mathrm{E}\big[\widetilde{y}_p(n)\big]^2 + \mathrm{E}\big[\widehat{y}_p(1,m)\big]^2 \geq 2\mathrm{E}\big[\widehat{y}_p(1,m)\big]\mathrm{E}\big[\widetilde{y}_p(n)\big],
$$

we obtain

$$
\begin{aligned}
\mathrm{E}\big[\widetilde{\mathcal{N}_p}(b,m)\big] &\geq \frac{b}{b-1}\mathrm{E}\big[\mathcal{N}_p(b,m)\big] + \frac{1}{b-1}\mathrm{E}\big[\mathcal{N}_1(b,n)\big] \\
&\quad + \frac{mb}{b-1}\Big(2\mathrm{E}\big[\widehat{y}_p(1,m)\big]\mathrm{E}\big[\widetilde{y}_p(n)\big] - 2\mathrm{E}\big[\widehat{y}_p(1,m)\widetilde{y}_p(n)\big]\Big),
\end{aligned}
$$

which yields

$$
\mathrm{E}\big[\widetilde{\mathcal{N}_p}(b,m)\big] \geq \frac{b}{b-1}\mathrm{E}\big[\mathcal{N}_p(b,m)\big] + \frac{1}{b-1}\mathrm{E}\big[\mathcal{N}_p(b,n)\big] - \frac{2mb}{b-1}\mathrm{Cov}[\widehat{y}_p(1,m)\widetilde{y}_p(n)].
$$

3.4 Analytical Expressions of the Expected Value of Variance-Parameter Estimators for Four Specific Distributions for the Special Case of I.I.D. Data

In this section we will derive analytical expressions for the expected values of the NBQ and STS area variance-parameter estimators in the case of i.i.d. observations from the four distributions under consideration.

3.4.1 Uniform Distribution

The kth order statistic of n i.i.d. observations from the uniform distribution on $[0, 1]$ is a beta r.v. with parameters k and $n + 1 - k$, denoted as $B(k, n + 1 - k)$. Thus, $\widehat{y}_p(1, m) \sim B(\lceil mp \rceil, m + 1 - \lceil mp \rceil)$ (Gentle [79]) and

$$\mathrm{Var}\big[\widehat{y}_p(j, m)\big] = \frac{\lceil mp \rceil(m + 1 - \lceil mp \rceil)}{(m + 1)^2(m + 2)}. \tag{3.21}$$

Equation (3.21) can also be obtained directly by using the expressions in Equation (3.2). Using Equation (3.19), we obtain

$$\mathrm{E}\big[\mathcal{N}_p(b, m)\big] = \frac{m\lceil mp \rceil(m + 1 - \lceil mp \rceil)}{(m + 1)^2(m + 2)}. \tag{3.22}$$

Further, using Equation (3.21), we can write

$$\mathrm{E}\big[\widehat{y}_p^2(1, m)\big] = \mathrm{E}\big[Y^2_{\lceil mp \rceil:m}\big] = \frac{\lceil mp \rceil(\lceil mp \rceil + 1)}{(m + 1)(m + 2)}, \tag{3.23}$$

$$\mathrm{E}\big[\widetilde{y}_p^2(n)\big] = \mathrm{E}\big[Y^2_{\lceil np \rceil:n}\big] = \frac{\lceil np \rceil(\lceil np \rceil + 1)}{(n + 1)(n + 2)}, \tag{3.24}$$

and

$$\mathrm{E}\big[\widehat{y}_p(1,m)\widetilde{y}_p(n)\big] = \mathrm{E}\big[Y_{\lceil mp\rceil:m}Y_{\lceil np\rceil:n}\big] = \sum_{r=\lceil mp\rceil}^{n-m+\lceil mp\rceil} \frac{\binom{r-1}{\lceil mp\rceil-1}\binom{n-r}{m-\lceil mp\rceil}}{\binom{n}{m}}\mathrm{E}[Y_{r:n}Y_{\lceil np\rceil:n}]$$

$$= \sum_{r=\lceil mp\rceil}^{n-m+\lceil mp\rceil} \frac{\binom{r-1}{\lceil mp\rceil-1}\binom{n-r}{m-\lceil mp\rceil}}{\binom{n}{m}} \frac{\min(r,\lceil np\rceil)(\max(r,\lceil np\rceil)+1)}{(n+1)(n+2)}$$

$$= \sum_{r=\lceil mp\rceil}^{n-m+\lceil mp\rceil} \frac{\binom{r-1}{\lceil mp\rceil-1}\binom{n-r}{m-\lceil mp\rceil}}{\binom{n}{m}} \frac{\min(r,\lceil np\rceil)+r\lceil np\rceil}{(n+1)(n+2)}. \tag{3.25}$$

Remark 3.4.1. We can also obtain an expression for $\mathrm{E}\big[\widehat{y}_p(j,m)\widetilde{y}_p(n)\big]$ using Equation (3.3)

$$\mathrm{E}\big[\widehat{y}_p(1,m)\widetilde{y}_p(n)\big] = \mathrm{E}\big[Y_{\lceil mp\rceil:m}Y_{\lceil np\rceil:n}\big] = \frac{\lceil mp\rceil\lceil np\rceil}{(m+1)(n+2)}$$
$$+ \frac{m!(n-m)!}{(n+2)!}\Bigg[\sum_{r=\lceil mp\rceil}^{\lceil np\rceil} r\binom{r-1}{\lceil mp\rceil-1}\binom{n-r}{m-\lceil mp\rceil}$$
$$+ \lceil np\rceil \sum_{r=\lceil np\rceil+1}^{n-m+\lceil mp\rceil}\binom{r-1}{\lceil mp\rceil-1}\binom{n-r}{m-\lceil mp\rceil}\Bigg] \tag{3.26}$$

Equation (3.26) could be potentially used for more-efficient calculations from the computational point of view as it avoids the use of min.

Using Equations (3.20) and (3.23)–(3.25) we obtain

$$\mathrm{E}\big[\widetilde{\mathcal{N}_p}(b,m)\big] = \frac{mb}{b-1}\Bigg(\frac{\lceil mp\rceil(\lceil mp\rceil+1)}{(m+1)(m+2)} + \frac{\lceil np\rceil(\lceil np\rceil+1)}{(n+1)(n+2)}$$
$$- 2\sum_{r=\lceil mp\rceil}^{n-m+\lceil mp\rceil} \frac{\binom{r-1}{\lceil mp\rceil-1}\binom{n-r}{m-\lceil mp\rceil}}{\binom{n}{m}} \frac{\min(r,\lceil np\rceil)+r\lceil np\rceil}{(n+1)(n+2)}\Bigg). \tag{3.27}$$

Equations (3.18) and (3.23)–(3.25) yield

$$\begin{aligned}
\mathrm{E}\big[A_p^2(w;n)\big] &= 1/n^3\bigg(\sum_{i=1}^{n}\alpha_i^2\mathrm{E}\big[\widetilde{y}_p^2(i)\big] + 2\sum_{i=1}^{n-1}\sum_{j=i+1}^{n}\alpha_i\alpha_j\mathrm{E}\big[\widetilde{y}_p(i)\widetilde{y}_p(j)\big]\bigg)\\
&= 1/n^3\bigg(\sum_{i=1}^{n}\alpha_i^2\frac{\lceil ip\rceil(\lceil ip\rceil+1)}{(i+1)(i+2)}\\
&\quad + 2\sum_{i=1}^{n-1}\sum_{j=i+1}^{n}\alpha_i\alpha_j\sum_{r=\lceil ip\rceil}^{j-i+\lceil ip\rceil}\frac{\binom{r-1}{\lceil ip\rceil-1}\binom{j-r}{i-\lceil ip\rceil}}{\binom{j}{i}}\frac{\min(r,\lceil jp\rceil)(\max(r,\lceil jp\rceil)+1)}{(j+1)(j+2)}\bigg),
\end{aligned} \tag{3.28}$$

where the constants α_k are define in Equation (3.17).

Remark 3.4.2. In this special case, we can also use the work of Ahsanullah and Nevzorov [80] to write

$$\begin{aligned}
\mathrm{E}\big[\widetilde{y}_p(i)\widetilde{y}_p(j)\big] = \mathrm{E}\big[\widetilde{y}_p^2(j)\big]&\bigg(k\sum_{r=k}^{\ell-1}\frac{q_r}{r+1} + p_0 + (i-k+1)\sum_{s=1}^{j-i-\ell+k}\frac{p_s}{s+i-k+1}\bigg)\\
&+ \mathrm{E}\big[\widetilde{y}_p(j)\big]\sum_{s=1}^{j-i-\ell+k}\frac{p_s s}{s+i-k+1},
\end{aligned}$$

where $k = \lceil pi\rceil$, $\ell = \lceil pj\rceil$, and

$$q_r = \frac{(\ell-1)!\,i!\,(-\ell+j+1)!(j-i)!}{j!r!(\ell-r-1)!(i-r)!(-\ell-i+j+r+1)!},$$

$$p_0 = \frac{(\ell-1)!\,i!\,(j-\ell)!(j-i)!}{(k-1)!j!(\ell-k)!(i-k)!(k-\ell-i+j)!},$$

and

$$p_s = \frac{\ell!\,i!\,(j-\ell)!(j-i)!}{j!(k-s)!(-k+\ell+s)!(-k+i+s)!(k-\ell-i+j-s)!}.$$

We could use these closed-form formulas to rewrite the expressions in Equations (3.27) and (3.28).

3.4.2 Exponential Distribution

In the case of the exponential distribution, Equation (3.4) implies

$$\mathrm{Var}\big[\widehat{y}_p(1,m)\big] = \mathrm{Var}[Y_{\lceil mp\rceil:m}] = \sum_{s=1}^{\lceil mp\rceil} \frac{1}{(m-s+1)^2},$$

which in association with Equation (3.19) leads to

$$\mathrm{E}\big[\mathscr{N}_p(b,m)\big] = m \sum_{s=1}^{\lceil mp\rceil} \frac{1}{(m-s+1)^2}. \tag{3.29}$$

Using Equations (3.5) and (3.6), we can write

$$\mathrm{E}\big[\widehat{y}_p^2(1,m)\big] = \mathrm{E}\big[Y_{\lceil mp\rceil:m}^2\big] = \sum_{s=1}^{\lceil mp\rceil} \frac{1}{(m-s+1)^2} + \left(\sum_{s=1}^{\lceil mp\rceil} \frac{1}{m-s+1}\right)^2, \tag{3.30}$$

$$\mathrm{E}\big[\widetilde{y}_p^2(n)\big] = \mathrm{E}\big[Y_{\lceil np\rceil:n}^2\big] = \sum_{s=1}^{\lceil np\rceil} \frac{1}{(n-s+1)^2} + \left(\sum_{s=1}^{\lceil np\rceil} \frac{1}{n-s+1}\right)^2, \tag{3.31}$$

and

$$\begin{aligned}\mathrm{E}\big[\widehat{y}_p(1,m)\widetilde{y}_p(n)\big] = \mathrm{E}\big[Y_{\lceil mp\rceil:m}Y_{\lceil np\rceil:n}\big] &= \sum_{r=\lceil mp\rceil}^{n-m+\lceil mp\rceil} \frac{\binom{r-1}{\lceil mp\rceil-1}\binom{n-r}{m-\lceil mp\rceil}}{\binom{n}{m}} \mathrm{E}[Y_{r:n}Y_{\lceil np\rceil:n}] \\ &= \sum_{r=\lceil mp\rceil}^{n-m+\lceil mp\rceil} \frac{\binom{r-1}{\lceil mp\rceil-1}\binom{n-r}{m-\lceil mp\rceil}}{\binom{n}{m}} \\ &\quad \cdot \left(\sum_{s=1}^{\min(r,\lceil np\rceil)} \frac{1}{(n-s+1)^2} + \left(\sum_{s=1}^{r} \frac{1}{n-s+1}\right)\left(\sum_{s=1}^{\lceil np\rceil} \frac{1}{n-s+1}\right)\right).\end{aligned} \tag{3.32}$$

Remark 3.4.3. We can also obtain an expression for $\mathrm{E}\big[\widehat{y}_p(1,m)\widetilde{y}_p(n)\big]$ using Equation

(3.7)

$$
\begin{aligned}
\mathrm{E}\big[\widehat{y}_p(j,m)\widetilde{y}_p(n)\big] &= \mathrm{E}\big[Y_{\lceil mp\rceil:m}Y_{\lceil np\rceil:n}\big] \\
&= \sum_{r=\lceil mp\rceil}^{\lceil np\rceil} \frac{\binom{r-1}{\lceil mp\rceil-1}\binom{n-r}{m-\lceil mp\rceil}}{\binom{n}{m}} \Bigg[\sum_{s=1}^{r} \frac{1}{(n-s+1)^2} \\
&\quad + \Bigg(\sum_{s=1}^{\lceil np\rceil} \frac{1}{n-s+1} \Bigg) \Bigg(\sum_{r=\lceil mp\rceil}^{n-m+\lceil mp\rceil} \frac{\binom{r-1}{\lceil mp\rceil-1}\binom{n-r}{m-\lceil mp\rceil}}{\binom{j}{m}} \sum_{s=1}^{r} \frac{1}{n-s+1} \Bigg) \\
&\quad + \Bigg(\sum_{r=\lceil np\rceil+1}^{n-m+\lceil mp\rceil} \frac{\binom{r-1}{\lceil mp\rceil-1}\binom{n-r}{m-\lceil mp\rceil}}{\binom{n}{m}} \Bigg) \Bigg(\sum_{s=1}^{\lceil np\rceil} \frac{1}{(n-s+1)^2} \Bigg) \Bigg]. \qquad (3.33)
\end{aligned}
$$

Equation (3.33) could be potentially used for more efficient calculations from the computational point of view as it avoids the use of min.

Using Equations (3.20) and (3.30)–(3.32) we obtain

$$
\begin{aligned}
\mathrm{E}\big[\widetilde{\mathcal{N}_p}(b,m)\big] &= \frac{mb}{b-1} \Bigg(\sum_{s=1}^{\lceil mp\rceil} \frac{1}{(m-s+1)^2} + \Bigg(\sum_{s=1}^{\lceil mp\rceil} \frac{1}{m-s+1} \Bigg)^2 \\
&\quad - 2 \sum_{r=\lceil mp\rceil}^{n-m+\lceil mp\rceil} \frac{\binom{r-1}{\lceil mp\rceil-1}\binom{n-r}{m-\lceil mp\rceil}}{\binom{n}{m}} \\
&\quad \cdot \Bigg(\sum_{s=1}^{\min(r,\lceil np\rceil)} \frac{1}{(n-s+1)^2} + \Bigg(\sum_{s=1}^{r} \frac{1}{n-s+1} \Bigg) \Bigg(\sum_{s=1}^{\lceil np\rceil} \frac{1}{n-s+1} \Bigg) \Bigg) \\
&\quad + \sum_{s=1}^{\lceil np\rceil} \frac{1}{(n-s+1)^2} + \Bigg(\sum_{s=1}^{\lceil np\rceil} \frac{1}{n-s+1} \Bigg)^2 \Bigg). \qquad (3.34)
\end{aligned}
$$

Finally, Equations (3.18) and (3.30)–(3.32) yield

$$
\begin{aligned}
\mathrm{E}\big[A_p^2(w;n)\big] &= 1/n^3\Bigg(\sum_{i=1}^{n}\alpha_i^2\mathrm{E}\big[\widetilde{y}_p^2(i)\big] + 2\sum_{i=1}^{n-1}\sum_{j=i+1}^{n}\alpha_i\alpha_j\mathrm{E}\big[\widetilde{y}_p(i)\widetilde{y}_p(j)\big]\Bigg)\\
&= 1/n^3\Bigg(\sum_{i=1}^{n}\alpha_i^2\Bigg(\sum_{s=1}^{\lceil ip\rceil}\frac{1}{(i-s+1)^2} + \Bigg(\sum_{s=1}^{\lceil ip\rceil}\frac{1}{i-s+1}\Bigg)^2\Bigg)\\
&\quad + 2\sum_{i=1}^{n-1}\sum_{j=i+1}^{n}\alpha_i\alpha_j\sum_{r=\lceil ip\rceil}^{j-i+\lceil ip\rceil}\frac{\binom{r-1}{\lceil ip\rceil-1}\binom{j-r}{i-\lceil ip\rceil}}{\binom{j}{i}}\\
&\quad \cdot\Bigg(\sum_{s=1}^{\min(r,\lceil jp\rceil)}\frac{1}{(j-s+1)^2} + \Bigg(\sum_{s=1}^{r}\frac{1}{j-s+1}\Bigg)\Bigg(\sum_{s=1}^{\lceil jp\rceil}\frac{1}{j-s+1}\Bigg)\Bigg)\Bigg),
\end{aligned}
\tag{3.35}
$$

where the constants α_k are defined in Equation (3.17).

3.4.3 Pareto Distribution

In the case of the Pareto distribution, Equation (3.8) yields

$$
\mathrm{E}\big[\widehat{y}_p(1,m)\big] = \mathrm{E}\big[Y_{\lceil mp\rceil:m}\big] = \gamma\frac{m!}{(m-\lceil mp\rceil)!}\frac{\Gamma(m-\lceil mp\rceil+1-1/\theta)}{\Gamma(m+1-1/\theta)}, \tag{3.36}
$$

for $1 < (m-\lceil mp\rceil+1)\theta$, and

$$
\mathrm{E}\big[\widehat{y}_p^2(j,m)\big] = \mathrm{E}\big[Y_{\lceil mp\rceil:m}^2\big] = \gamma^2\frac{m!}{(m-\lceil mp\rceil)!}\frac{\Gamma(m-\lceil mp\rceil+1-2/\theta)}{\Gamma(m+1-2/\theta)}, \tag{3.37}
$$

for $2 < (m-\lceil mp\rceil+1)\theta$.

Remark 3.4.4. For the numerical results in Section 3.5 we are considering the Pareto(1, 2.1) distribution, where $\gamma = 1$ and $\theta = 2.1$. We can easily verify that both conditions mentioned above are satisfied for these parameters.

Using Equations (3.36) and (3.37) we can write

$$\begin{aligned}\mathrm{E}\big[\mathscr{N}_p(b,m)\big] &= m\mathrm{Var}\big[\widehat{y}_p(1,m)\big] = m\Big(\mathrm{E}\big[\widehat{y}_p^2(1,m)\big] - \big(\mathrm{E}\big[\widehat{y}_p(1,m)\big]\big)^2\Big)\\ &= m\gamma^2\frac{m!}{(m-\lceil mp\rceil)!}\left[\frac{\Gamma(m-\lceil mp\rceil+1-2/\theta)}{\Gamma(m+1-2/\theta)}\right.\\ &\quad\left. - \frac{m!}{(m-\lceil mp\rceil)!}\left(\frac{\Gamma(m-\lceil mp\rceil+1-1/\theta)}{\Gamma(m+1-1/\theta)}\right)^2\right].\end{aligned} \tag{3.38}$$

Further, Equation (3.8) implies

$$\mathrm{E}\big[\widetilde{y}_p^2(n)\big] = \mathrm{E}\big[Y^2_{\lceil np\rceil:n}\big] = \gamma^2\frac{n!}{(n-\lceil np\rceil)!}\frac{\Gamma(n-\lceil np\rceil+1-2/\theta)}{\Gamma(n+1-2/\theta)}, \tag{3.39}$$

for $2 < (n-\lceil np\rceil+1)\theta$, while Equation (3.9) yields

$$\begin{aligned}\mathrm{E}\big[\widehat{y}_p(1,m)\widetilde{y}_p(n)\big] &= \mathrm{E}\big[Y_{\lceil mp\rceil:m}Y_{\lceil np\rceil:n}\big]\\ &= \sum_{r=\lceil mp\rceil}^{n-m+\lceil mp\rceil}\frac{\binom{r-1}{\lceil mp\rceil-1}\binom{n-r}{m-\lceil mp\rceil}}{\binom{n}{m}}\mathrm{E}[Y_{r:n}Y_{\lceil np\rceil:n}]\\ &= \sum_{r=\lceil mp\rceil}^{n-m+\lceil mp\rceil}\left(\frac{\binom{r-1}{\lceil mp\rceil-1}\binom{n-r}{m-\lceil mp\rceil}}{\binom{n}{m}}\cdot\frac{\gamma^2\cdot n!}{(n-\max(r,\lceil np\rceil)!}\right.\\ &\quad\left.\cdot\frac{\Gamma(n-\max(r,\lceil np\rceil)+1-1/\theta)\,\Gamma(n-\min(r,\lceil np\rceil)+1-2/\theta)}{\Gamma(n-\min(r,\lceil np\rceil)+1-1/\theta)\Gamma(n+1-2/\theta)}\right).\end{aligned} \tag{3.40}$$

Using Equations (3.20) and (3.37)–(3.40) we obtain

$$\begin{aligned}\mathrm{E}\big[\widetilde{\mathscr{N}_p}(b,m)\big] &= \frac{mb}{b-1}\left(\gamma^2\frac{m!}{(m-\lceil mp\rceil)!}\frac{\Gamma(m-\lceil mp\rceil+1-2/\theta)}{\Gamma(m+1-2/\theta)}\right.\\ &\quad - 2\sum_{r=\lceil mp\rceil}^{n-m+\lceil mp\rceil}\frac{\binom{r-1}{\lceil mp\rceil-1}\binom{n-r}{m-\lceil mp\rceil}}{\binom{n}{m}}\frac{\gamma^2\cdot n!}{(n-\max(r,\lceil np\rceil)!}\\ &\quad\cdot\frac{\Gamma(n-\max(r,\lceil np\rceil)+1-1/\theta)\,\Gamma(n-\min(r,\lceil np\rceil)+1-2/\theta)}{\Gamma(n-\min(r,\lceil np\rceil)+1-1/\theta)\Gamma(n+1-2/\theta)}\\ &\quad\left.+\gamma^2\frac{n!}{(n-\lceil np\rceil)!}\frac{\Gamma(n-\lceil np\rceil+1-2/\theta)}{\Gamma(n+1-2/\theta)}\right).\end{aligned} \tag{3.41}$$

Finally, Equations (3.18) and (3.37)–(3.40) imply

$$\begin{aligned}
\mathrm{E}\big[A_p^2(w;n)\big] &= 1/n^3\bigg(\sum_{i=1}^{n}\alpha_i^2\mathrm{E}\big[\widetilde{y}_p^2(i)\big] + 2\sum_{i=1}^{n-1}\sum_{j=i+1}^{n}\alpha_i\alpha_j\mathrm{E}\big[\widetilde{y}_p(i)\widetilde{y}_p(j)\big]\bigg) \\
&= 1/n^3\bigg(\sum_{i=1}^{n}\alpha_i^2\gamma^2\frac{i!}{(i-\lceil ip\rceil)!}\frac{\Gamma(i-\lceil ip\rceil+1-2/\theta)}{\Gamma(i+1-2/\theta)} \\
&\quad + 2\sum_{i=1}^{n-1}\sum_{j=i+1}^{n}\alpha_i\alpha_j\sum_{r=\lceil ip\rceil}^{j-i+\lceil ip\rceil}\frac{\binom{r-1}{\lceil ip\rceil-1}\binom{j-r}{i-\lceil ip\rceil}}{\binom{j}{i}}\cdot\frac{\gamma^2\cdot j!}{(j-\max(r,\lceil jp\rceil))!} \\
&\quad \cdot\frac{\Gamma(j-\max(r,\lceil jp\rceil)+1-1/\theta)\,\Gamma(j-\min(r,\lceil jp\rceil)+1-2/\theta)}{\Gamma(j-\min(r,\lceil jp\rceil)+1-1/\theta)\Gamma(j+1-2/\theta)}\bigg),
\end{aligned} \tag{3.42}$$

where the constants α_k are defined in Equation (3.17).

3.4.4 Laplace Distribution

In the case of the Laplace distribution, Equations (3.10) and (3.11), allows us to write

$$\begin{aligned}
\mathrm{E}\big[\widehat{y}_p(1,m)\big] &= \mathrm{E}\big[Y_{\lceil mp\rceil:m}\big] \\
&= 2^{-m}\bigg\{\sum_{r=0}^{\lceil mp\rceil-1}\binom{m}{r}\sum_{s=1}^{\lceil mp\rceil-r}\frac{1}{m-r-s+1} - \sum_{r=\lceil mp\rceil}^{m}\binom{m}{r}\sum_{s=1}^{r-\lceil mp\rceil+1}\frac{1}{r-s+1}\bigg\},
\end{aligned} \tag{3.43}$$

$$\begin{aligned}
\mathrm{E}\big[\widehat{y}_p^2(1,m)\big] &= \mathrm{E}\big[Y_{\lceil mp\rceil:m}^2\big] \\
&= 2^{-m}\bigg\{\sum_{r=0}^{\lceil mp\rceil-1}\binom{m}{r}\bigg[\sum_{s=1}^{\lceil mp\rceil-r}\frac{1}{(m-r-s+1)^2} + \bigg(\sum_{s=1}^{\lceil mp\rceil-r}\frac{1}{m-r-s+1}\bigg)^2\bigg] \\
&\quad + \sum_{r=\lceil mp\rceil}^{m}\binom{m}{r}\bigg[\sum_{s=1}^{r-\lceil mp\rceil+1}\frac{1}{(r-s+1)^2} + \bigg(\sum_{s=1}^{r-\lceil mp\rceil+1}\frac{1}{r-s+1}\bigg)^2\bigg]\bigg\}.
\end{aligned} \tag{3.44}$$

Using Equations (3.43) and (3.44) we can write

$$
\begin{aligned}
\mathrm{E}\big[\mathscr{N}_p(b,m)\big] &= m\mathrm{Var}\big[\widehat{y}_p(1,m)\big] = m\Big(\mathrm{E}\big[\widehat{y}_p^2(1,m)\big] - \big(\mathrm{E}\big[\widehat{y}_p(1,m)\big]\big)^2\Big) \\
&= m\Bigg(2^{-m}\Bigg\{\sum_{r=0}^{\lceil mp\rceil-1}\binom{m}{r}\Bigg[\sum_{s=1}^{\lceil mp\rceil-r}\frac{1}{(m-r-s+1)^2} + \Bigg(\sum_{s=1}^{\lceil mp\rceil-r}\frac{1}{m-r-s+1}\Bigg)^2 \\
&\quad + \sum_{r=\lceil mp\rceil}^{m}\binom{m}{r}\Bigg[\sum_{s=1}^{r-\lceil mp\rceil+1}\frac{1}{(r-s+1)^2} + \Bigg(\sum_{s=1}^{r-\lceil mp\rceil+1}\frac{1}{r-s+1}\Bigg)^2\Bigg]\Bigg\} \\
&\quad - \Bigg(2^{-m}\Bigg\{\sum_{r=0}^{\lceil mp\rceil-1}\binom{m}{r}\sum_{s=1}^{\lceil mp\rceil-r}\frac{1}{m-r-s+1} \\
&\quad - \sum_{r=\lceil mp\rceil}^{m}\binom{m}{r}\sum_{s=1}^{r-\lceil mp\rceil+1}\frac{1}{r-s+1}\Bigg\}\Bigg)^2\Bigg).
\end{aligned}
\tag{3.45}
$$

Further, Equation (3.11) implies

$$
\begin{aligned}
\mathrm{E}\big[\widetilde{y}_p^2(n)\big] = \mathrm{E}\big[Y_{\lceil np\rceil:n}^2\big] = 2^{-n}\Bigg\{&\sum_{r=0}^{\lceil np\rceil-1}\binom{n}{r}\Bigg[\sum_{s=1}^{\lceil np\rceil-r}\frac{1}{(n-r-s+1)^2} \\
&+ \Bigg(\sum_{s=1}^{\lceil np\rceil-r}\frac{1}{n-r-s+1}\Bigg)^2\Bigg] \\
&+ \sum_{r=\lceil np\rceil}^{n}\binom{n}{r}\Bigg[\sum_{s=1}^{r-\lceil np\rceil+1}\frac{1}{(r-s+1)^2} + \Bigg(\sum_{s=1}^{r-\lceil np\rceil+1}\frac{1}{r-s+1}\Bigg)^2\Bigg]\Bigg\}.
\end{aligned}
\tag{3.46}
$$

From Equation (3.12), we have

$$
\begin{aligned}
\mathrm{E}\left[\widehat{y}_p(1,m)\widetilde{y}_p(n)\right] &= \mathrm{E}\left[Y_{\lceil mp\rceil:m}Y_{\lceil np\rceil:n}\right] \\
&= \sum_{r=\lceil mp\rceil}^{n-m+\lceil mp\rceil} \frac{\binom{r-1}{\lceil mp\rceil-1}\binom{n-r}{m-\lceil mp\rceil}}{\binom{n}{m}} \mathrm{E}[Y_{r:n}Y_{\lceil np\rceil:n}] \\
&= \sum_{r=\lceil mp\rceil}^{n-m+\lceil mp\rceil} \frac{\binom{r-1}{\lceil mp\rceil-1}\binom{n-r}{m-\lceil mp\rceil}}{\binom{n}{m}} \\
&\quad \times 2^{-n}\Bigg\{ \sum_{k=0}^{\min(r,\lceil np\rceil)-1} \binom{n}{k}\Bigg[\sum_{s=1}^{\min(r,\lceil np\rceil)-k} \frac{1}{(n-k-s+1)^2} \\
&\quad + \left(\sum_{s=1}^{\min(r,\lceil np\rceil)-k} \frac{1}{n-k-s+1} \right)\left(\sum_{s=1}^{\max(r,\lceil np\rceil)-k} \frac{1}{n-k-s+1} \right)\Bigg] \\
&\quad - \sum_{k=\min(r,\lceil np\rceil)}^{\max(r,\lceil np\rceil)-1} \binom{n}{k}\left(\sum_{s=1}^{k-\min(r,\lceil np\rceil)+1} \frac{1}{k-s+1} \right) \\
&\quad \times \left(\sum_{s=1}^{\max(r,\lceil np\rceil)-k} \frac{1}{n-k-s+1} \right) \\
&\quad + \sum_{k=\max(r,\lceil np\rceil)}^{n} \binom{n}{k}\Bigg[\sum_{s=1}^{k+1-\max(r,\lceil np\rceil)} \frac{1}{(k-s+1)^2} \\
&\quad + \left(\sum_{s=1}^{k+1-\max(r,\lceil np\rceil)} \frac{1}{k-s+1} \right)\left(\sum_{s=1}^{k+1-\min(r,\lceil np\rceil)} \frac{1}{k-s+1} \right)\Bigg]\Bigg\}. \quad (3.47)
\end{aligned}
$$

Using Equations (3.20) and (3.44)–(3.47), we obtain

$$
\begin{aligned}
\mathrm{E}\big[\widetilde{\mathscr{N}_p}(b,m)\big] = \frac{mb}{b-1}\Bigg(2^{-m}\Bigg\{ & \sum_{r=0}^{\lceil mp\rceil-1}\binom{m}{r}\Bigg[\sum_{s=1}^{\lceil mp\rceil-r}\frac{1}{(m-r-s+1)^2} \\
& + \Bigg(\sum_{s=1}^{\lceil mp\rceil-r}\frac{1}{m-r-s+1}\Bigg)^2\Bigg] \\
& + \sum_{r=\lceil mp\rceil}^{m}\binom{m}{r}\Bigg[\sum_{s=1}^{r-\lceil mp\rceil+1}\frac{1}{(r-s+1)^2} + \Bigg(\sum_{s=1}^{r-\lceil mp\rceil+1}\frac{1}{r-s+1}\Bigg)^2\Bigg]\Bigg\} \\
& - 2\sum_{r=\lceil mp\rceil}^{n-m+\lceil mp\rceil}\frac{\binom{r-1}{\lceil mp\rceil-1}\binom{n-r}{m-\lceil mp\rceil}}{\binom{n}{m}} \\
& \times 2^{-n}\Bigg\{\sum_{k=0}^{\min(r,\lceil np\rceil)-1}\binom{n}{k}\Bigg[\sum_{s=1}^{\min(r,\lceil np\rceil)-k}\frac{1}{(n-k-s+1)^2} \\
& + \Bigg(\sum_{s=1}^{\min(r,\lceil np\rceil)-k}\frac{1}{n-k-s+1}\Bigg)\Bigg(\sum_{s=1}^{\max(r,\lceil np\rceil)-k}\frac{1}{n-k-s+1}\Bigg) \\
& - \sum_{k=\min(r,\lceil np\rceil)}^{\max(r,\lceil np\rceil)-1}\binom{n}{k}\Bigg(\sum_{s=1}^{k-\min(r,\lceil np\rceil)+1}\frac{1}{k-s+1}\Bigg)\Bigg(\sum_{s=1}^{\max(r,\lceil np\rceil)-k}\frac{1}{n-k-s+1}\Bigg) \\
& + \sum_{k=\max(r,\lceil np\rceil)}^{n}\binom{n}{k}\Bigg[\sum_{s=1}^{k+1-\max(r,\lceil np\rceil)}\frac{1}{(k-s+1)^2} \\
& + \Bigg(\sum_{s=1}^{k+1-\max(r,\lceil np\rceil)}\frac{1}{k-s+1}\Bigg)\Bigg(\sum_{s=1}^{k+1-\min(r,\lceil np\rceil)}\frac{1}{k-s+1}\Bigg)\Bigg]\Bigg\} \\
& + 2^{-n}\Bigg\{\sum_{r=0}^{\lceil np\rceil-1}\binom{n}{r}\Bigg[\sum_{s=1}^{\lceil np\rceil-r}\frac{1}{(n-r-s+1)^2} + \Bigg(\sum_{s=1}^{\lceil np\rceil-r}\frac{1}{n-r-s+1}\Bigg)^2\Bigg] \\
& + \sum_{r=\lceil np\rceil}^{n}\binom{n}{r}\Bigg[\sum_{s=1}^{r-\lceil np\rceil+1}\frac{1}{(r-s+1)^2} + \Bigg(\sum_{s=1}^{r-\lceil np\rceil+1}\frac{1}{r-s+1}\Bigg)^2\Bigg]\Bigg\}\Bigg).
\end{aligned}
\tag{3.48}
$$

Finally, Equations (3.18) and (3.44)–(3.47) imply

$$
\begin{aligned}
\mathrm{E}\big[A_p^2(w;n)\big] &= 1/n^3\bigg(\sum_{i=1}^{n}\alpha_i^2\mathrm{E}\big[\widetilde{y}_p^2(i)\big] + 2\sum_{i=1}^{n-1}\sum_{j=i+1}^{n}\alpha_i\alpha_j\mathrm{E}\big[\widetilde{y}_p(i)\widetilde{y}_p(j)\big]\bigg) \\
&= 1/n^3\bigg(\sum_{i=1}^{n}\alpha_i^2 2^{-i}\bigg\{\sum_{r=0}^{\lceil ip\rceil-1}\binom{i}{r}\bigg[\sum_{s=1}^{\lceil ip\rceil-r}\frac{1}{(i-r-s+1)^2} \\
&\quad + \bigg(\sum_{s=1}^{\lceil ip\rceil-r}\frac{1}{i-r-s+1}\bigg)^2\bigg] \\
&\quad + \sum_{r=\lceil ip\rceil}^{i}\binom{i}{r}\bigg[\sum_{s=1}^{r-\lceil ip\rceil+1}\frac{1}{(r-s+1)^2} + \bigg(\sum_{s=1}^{r-\lceil ip\rceil+1}\frac{1}{r-s+1}\bigg)^2\bigg]\bigg\} \\
&\quad + 2\sum_{i=1}^{n-1}\sum_{j=i+1}^{n}\alpha_i\alpha_j\sum_{r=\lceil ip\rceil}^{j-i+\lceil ip\rceil}\frac{\binom{r-1}{\lceil ip\rceil-1}\binom{j-r}{i-\lceil ip\rceil}}{\binom{j}{i}} \\
&\quad \times 2^{-j}\bigg\{\sum_{k=0}^{\min(r,\lceil jp\rceil)-1}\binom{j}{k}\bigg[\sum_{s=1}^{\min(r,\lceil jp\rceil)-k}\frac{1}{(j-k-s+1)^2} \\
&\quad + \bigg(\sum_{s=1}^{\min(r,\lceil jp\rceil)-k}\frac{1}{j-k-s+1}\bigg)\bigg(\sum_{s=1}^{\max(r,\lceil jp\rceil)-k}\frac{1}{j-k-s+1}\bigg)\bigg] \\
&\quad - \sum_{k=\min(r,\lceil jp\rceil)}^{\max(r,\lceil jp\rceil)-1}\binom{j}{k}\bigg(\sum_{s=1}^{k-\min(r,\lceil jp\rceil)+1}\frac{1}{k-s+1}\bigg)\bigg(\sum_{s=1}^{\max(r,\lceil jp\rceil)-k}\frac{1}{j-k-s+1}\bigg) \\
&\quad + \sum_{k=\max(r,\lceil jp\rceil)}^{n}\binom{j}{k}\bigg[\sum_{s=1}^{k+1-\max(r,\lceil np\rceil)}\frac{1}{(k-s+1)^2} \\
&\quad + \bigg(\sum_{s=1}^{k+1-\max(r,\lceil np\rceil)}\frac{1}{k-s+1}\bigg)\bigg(\sum_{s=1}^{k+1-\min(r,\lceil np\rceil)}\frac{1}{k-s+1}\bigg)\bigg]\bigg\}\bigg), \qquad (3.49)
\end{aligned}
$$

where the constants α_k are given in Equation (3.17).

3.5 Exact Numerical Results for the Expected Values of Several Variance-Parameter Estimators

In this section we present exact (or nearly exact) numerical results based on i.i.d. observations for the expected values of the variance-parameter estimators that we also evaluated in Section 2.7, i.e., we will consider (i) the STS area estimator $\mathscr{A}_p(w_0;b,m)$; (ii) the NBQ estimator

$\mathscr{N}_p(b,m)$; (iii) the NBQ estimator $\widetilde{\mathscr{N}_p}(b,m)$; (iv) the combined estimator $\mathscr{V}_p(w_0;b,m)$; and (v) the combined estimator $\widetilde{\mathscr{V}_p}(w_0;b,m)$.

Remark 3.5.1. Recall that our analysis in Sections 2.8 and 2.10 did not reveal any compelling reasons for using a weight function other than the constant $w_0(\cdot)$. However, future work could include a direct comparison between the constant and alternative weight functions based on exact numerical results for i.i.d. observations, based on the work in Sections 3.1–3.4.

The exact numerical results for the distributions under consideration are presented in Tables 3.1–3.5. In each table we provide the exact expected values and biases of one of the variance-parameter estimators for each distribution and for $p \in \{0.5, 0.95, 0.99\}$. The last row for each distribution corresponds to the asymptotic variance parameter σ_p^2 ($m \to \infty$). The column with label "m" contains the batch sizes and the column with label "n" contains the total sample sizes. However, since the number of batches that we use is irrelevant for the exact calculations of the STS area estimator $\mathscr{A}_p(w_0;b,m)$ and $\mathscr{N}_p(b,m)$, we dropped column "n" from Tables 3.1 and 3.2. The exact numerical results in Tables 3.3–3.5, were computed with $b = 16$ batches. In all experiments we used batch sizes $m = 2^{\mathcal{L}}$, $\mathcal{L} \in \{2, 3, \ldots, 11\}$. However, in some tables corresponding to the Laplace distribution, the maximum batch size was much smaller than 2^{11} due to time limitations.

Table 3.1 reports the exact expected values and biases of the STS area estimator $A_p^2(w_0;n)$ from Equations (3.28)–(3.49). Table 3.2 reports the exact expected values and biases of the NBQ estimator $\mathscr{N}_p(b,m)$ using Equations (3.22)–(3.45). Table 3.3 reports the exact expected values and biases of the NBQ estimator $\widetilde{\mathscr{N}_p}(b,m)$ based on Equations (3.27)–(3.48). Tables 3.4 and 3.5 report the exact expected values and biases of the combined estimators $\mathscr{V}_p(w_0;b,m)$ and $\widetilde{\mathscr{V}_p}(w_0;b,m)$, respectively.

Some tabulated results are summarized in Figures 3.1–3.3. Specifically, we considered three cases: (i) the uniform distribution with $p = 0.99$ (Figure 3.1); (ii) the exponential distribution with $p = 0.95$ (Figure 3.2); and (iii) the Pareto distribution with $p = 0.95$

(Figure 3.3). Figure 3.3 contains two plots, with the second plot using a logarithmic scale.

Tables 3.1–3.5 and Figures 3.1–3.3 reveal a variety of interesting findings:

(i) All five estimators of σ_p^2 converged to their asymptotic limits reasonably fast.

(ii) The STS area estimator reported larger (absolute) bias in most cases and it converged more slowly to its asymptotic limit than its competitors.

(iii) There is no clear winner between the two NBQ estimators $\mathcal{N}_p(b,m)$ and $\widetilde{\mathcal{N}_p}(b,m)$ with regard to small-sample bias and rate of convergence to σ_p^2. In some cases $\mathcal{N}_p(b,m)$ performed better, e.g., see Figure 3.1 for $p = 0.99$ and the uniform distribution, while in others $\widetilde{\mathcal{N}_p}(b,m)$ performed better, e.g., for $p = 0.5$ and the exponential distribution.

(iv) The performance of the combined estimators was commensurate with the performance of their constituents.

The numerical results did not reveal any additional major findings, but validated our observations in Chapter 2.

Tables 3.6–3.8 contain experimental results to verify the exact calculations in Tables 3.1–3.3. The results are based on 100,000 replications with $b = 16$ batches of size $m = 2^{\mathcal{L}}$, $\mathcal{L} \in \{2, 3, \ldots, 11\}$. All experiments were coded in Java using common random numbers generated by the RngStreams package of L'Ecuyer *et al.* [67]. The simulation results were very closed to the exact results, with a few exceptions, e.g., for small batch sizes and $p = 0.95$ or 0.99 for the Pareto distribution. This discrepancy is potentially due to the pronounced small-sample (absolute) bias of the variance-parameter estimators; this conjecture could be verified by rerunning the simulation experiments with many more replications, e.g., 1,000,000.

Table 3.1: Exact expected values and biases of the STS area estimator $A_p^2(w_0;n)$.

		$p = 0.5$		$p = 0.95$		$p = 0.99$	
	m	Expected Value	Bias	Expected Value	Bias	Expected Value	Bias
Uniform(0, 1)	4	0.1625	−0.0875	0.2250	0.1775	0.2250	0.2151
	8	0.2017	−0.0483	0.2403	0.1928	0.2403	0.2304
	16	0.2294	−0.0206	0.1921	0.1446	0.1921	0.1822
	32	0.2454	−0.0046	0.1115	0.0640	0.1276	0.1177
	64	0.2531	0.0031	0.0718	0.0243	0.0754	0.0655
	128	0.2559	0.0059	0.0644	0.0169	0.0260	0.0161
	256	0.2562	0.0062	0.0632	0.0157	0.0213	0.0114
	512	0.2555	0.0055	0.0549	0.0074	0.0145	0.0046
	1,024	0.2545	0.0045	0.0511	0.0036	0.0125	0.0026
	2,048	0.2534	0.0034	0.0500	0.0025	0.0117	0.0018
	∞	0.2500		0.0475		0.0099	
Expo(1)	4	1.2500	0.2500	5.2188	−13.7813	5.2188	−93.7813
	8	1.1776	0.1776	12.8765	−6.1235	12.8765	−86.1235
	16	1.1389	0.1389	28.3060	9.3060	28.3060	−70.6940
	32	1.1077	0.1077	22.1858	3.1858	59.2348	−39.7652
	64	1.0813	0.0813	13.9750	−5.0250	121.1333	22.1333
	128	1.0602	0.0602	21.3233	2.3233	133.5575	34.5575
	256	1.0439	0.0439	21.2966	2.2966	114.8635	15.8635
	512	1.0317	0.0317	20.3529	1.3529	125.0791	26.0791
	1,024	1.0227	0.0227	20.0736	1.0736	112.0033	13.0033
	2,048	1.0162	0.0162	19.7029	0.7029	106.6767	7.6767
	∞	1.0000		19.0000		99.0000	
Pareto(1, 2.1)	4	4.5216	4.0828	145.5091	70.7970	145.5091	−1,657.3364
	8	1.3143	0.8755	612.5504	537.8383	612.5504	−1,190.2951
	16	0.7325	0.2937	2,422.0966	2,347.3845	2,422.0966	619.2511
	32	0.5782	0.1394	2,126.6643	2,051.9522	9,428.4047	7,625.5592
	64	0.5169	0.0781	458.1188	383.4067	36,550.5299	34,747.6844
	128	0.4859	0.0471	156.6993	81.9872	104,452.8501	102,650.0046
	256	0.4683	0.0295	101.8110	27.0989	17,021.9880	15,219.1425
	512	0.4579	0.0191	87.9547	13.2425	5,511.0072	3,708.1617
	1,024	0.4514	0.0126	83.4814	8.7692	2,881.1354	1,078.2899
	2,048	0.4472	0.0084	79.4565	4.7444	2,217.8375	414.9920
	∞	0.4388		74.7121		1,802.8455	
Laplace(0, 1)	4	2.8359	1.8359	6.2422	−12.7578	6.2422	−92.7578
	8	2.3423	1.3423	13.3708	−5.6292	13.3708	−85.6292
	16	1.9338	0.9338	28.5260	9.5260	28.5260	−70.4740
	32	1.6437	0.6437	22.2178	3.2178	59.3364	−39.6636
	64	1.4446	0.4446	23.9702	4.9702	121.1821	22.1821
	128	1.3084	0.3084	21.3235	2.3235	133.5531	34.5531
	256	1.2149	0.2149	21.2974	2.2974	114.8647	15.8647
	∞	1.0000		19.0000		99.0000	

Table 3.2: Exact expected values and biases of the NBQ estimator $\mathscr{N}_p(b, m)$.

		$p = 0.5$		$p = 0.95$		$p = 0.99$	
	m	Expected Value	Bias	Expected Value	Bias	Expected Value	Bias
Uniform$(0, 1)$	4	0.1600	−0.0900	0.1067	0.0592	0.1067	0.0968
	8	0.1975	−0.0525	0.0790	0.0315	0.0790	0.0691
	16	0.2215	−0.0285	0.0492	0.0017	0.0492	0.0393
	32	0.2351	−0.0149	0.0536	0.0061	0.0277	0.0178
	64	0.2424	−0.0076	0.0560	0.0085	0.0147	0.0048
	128	0.2461	−0.0039	0.0505	0.0030	0.0150	0.0051
	256	0.2481	−0.0019	0.0477	0.0002	0.0114	0.0015
	512	0.2490	−0.0010	0.0479	0.0004	0.0115	0.0016
	1,024	0.2495	−0.0005	0.0481	0.0006	0.0106	0.0007
	2,048	0.2498	−0.0002	0.0477	0.0002	0.0101	0.0002
	∞	0.2500		0.0475		0.0099	
Expo(1)	4	0.6944	−0.3056	5.6944	−13.3056	5.6944	−93.3056
	8	0.8305	−0.1695	12.2194	−6.7806	12.2194	−86.7806
	16	0.9108	−0.0892	25.3495	6.3495	25.3495	−73.6505
	32	0.9543	−0.0457	19.6534	0.6534	51.6534	−47.3467
	64	0.9768	−0.0232	17.1724	−1.8276	104.2836	5.2836
	128	0.9883	−0.0117	18.6577	−0.3423	81.5555	−17.4445
	256	0.9942	−0.0058	19.4711	0.4711	100.1051	1.1051
	512	0.9971	−0.0029	19.0168	0.0168	91.8383	−7.1617
	1,024	0.9985	−0.0015	18.8834	−0.1166	96.4508	−2.5492
	2,048	0.9993	−0.0007	18.9806	−0.0194	98.8829	−0.1171
	∞	1.0000		19.0000		99.0000	
Pareto$(1, 2.1)$	4	0.4093	−0.0295	262.6510	187.9389	262.6510	−1,540.1945
	8	0.4255	−0.0133	1,018.3200	943.6079	1,018.3200	−784.5255
	16	0.4326	−0.0062	3,944.5600	3,869.8479	3,944.5600	2,141.7145
	32	0.4358	−0.0030	158.0330	83.3209	15,272.8000	13,469.9545
	64	0.4373	−0.0015	80.3721	5.6600	59,120.9000	57,318.0545
	128	0.4381	−0.0007	82.7581	8.0460	2,420.3300	617.4845
	256	0.4384	−0.0004	83.9088	9.1967	2,676.4745	873.6290
	512	0.4386	−0.0002	77.8614	3.1492	1,826.6021	23.7566
	1,024	0.4387	−0.0001	75.0719	0.3598	1,858.1757	55.3302
	2,048	0.4387	−0.0001	75.1866	0.4744	1,873.5939	70.7484
	∞	0.4388		74.7121		1,802.8455	
Laplace$(0, 1)$	4	2.0829	1.0829	5.7669	−13.2331	5.7669	−93.2331
	8	1.6825	0.6825	12.2228	−6.7772	12.2280	−86.7720
	16	1.4521	0.4521	25.3496	6.3496	25.3496	−73.6504
	32	1.3072	0.3072	19.6534	0.6534	51.6534	−47.3466
	64	1.2117	0.2117	17.1724	−1.8276	104.2840	5.2840
	128	1.1471	0.1471	18.6577	−0.3423	81.5555	−17.4445
	256	1.1027	0.1027	19.4711	0.4711	100.1051	1.1051
	512	1.0720	0.0720	19.0768	0.0768	91.8383	−7.1617
	1,024	1.0506	0.0506	18.8834	−0.1166	96.4508	−2.5492
	2,048	1.0356	0.0356	18.9806	−0.0194	98.8829	−0.1171
	∞	1.0000		19.0000		99.0000	

Table 3.3: Exact expected values and biases of the NBQ estimator $\widetilde{\mathcal{N}_p}(b, m)$ using $b = 16$ batches.

			$p = 0.5$		$p = 0.95$		$p = 0.99$	
	n	m	Expected Value	Bias	Expected Value	Bias	Expected Value	Bias
Uniform(0, 1)	64	4	0.2025	−0.0475	0.1937	0.1462	0.2586	0.2487
	128	8	0.2257	−0.0243	0.1101	0.0626	0.1615	0.1516
	256	16	0.2388	−0.0112	0.0526	0.0051	0.0898	0.0799
	512	32	0.2455	−0.0045	0.0587	0.0112	0.0408	0.0309
	1,024	64	0.2486	−0.0014	0.0654	0.0179	0.0168	0.0069
	2,048	128	0.2500	0.0000	0.0537	0.0062	0.0193	0.0094
	4,096	256	0.2505	0.0005	0.0484	0.0009	0.0125	0.0026
	8,192	512	0.2506	0.0006	0.0486	0.0011	0.0133	0.0034
	16,384	1,024	0.2505	0.0005	0.0489	0.0014	0.0113	0.0014
	32,768	2,048	0.2504	0.0004	0.0481	0.0006	0.0104	0.0005
	∞	∞	0.2500		0.0475		0.0099	
Expo(1)	64	4	0.7672	−0.2328	9.1084	−9.8916	41.2349	−57.7651
	128	8	0.8803	−0.1197	13.3306	−5.6694	40.5842	−58.4158
	256	16	0.9441	−0.0559	28.4606	9.4606	55.0795	−43.9205
	512	32	0.9765	−0.0235	20.3131	1.3131	61.8404	−37.1596
	1,024	64	0.9918	−0.0082	17.9843	−1.0158	109.7608	10.7608
	2,048	128	0.9985	−0.0015	18.9890	−0.0110	88.0001	−10.9999
	4,096	256	1.0011	0.0011	19.8736	0.8736	102.4672	3.4672
	8,192	512	1.0019	0.0019	19.2658	0.2658	96.7640	−2.2360
	16,384	1,024	1.0019	0.0019	19.0393	0.0393	98.5628	−0.4372
	32,768	2,048	1.0016	0.0016	19.0750	0.0750	99.8848	0.8848
	∞	∞	1.0000		19.0000		99.0000	
Pareto(1, 2.1)	64	4	0.4331	−0.0057	282.2080	207.4959	4,049.4300	2,246.5845
	128	8	0.4422	0.0034	1,083.6000	1,008.8879	1,330.3300	−472.5155
	256	16	0.4443	0.0055	4,275.9900	4,201.2779	4,409.2200	2,606.3745
	512	32	0.4440	0.0052	170.6320	95.9199	16,226.7000	14,423.8545
	1,024	64	0.4431	0.0043	82.4016	7.6895	63,648.8000	61,845.9545
	2,048	128	0.4421	0.0033	84.5105	9.7984	2,505.8800	703.0345
	4,096	256	0.4413	0.0025	86.8946	12.1825	2,805.2842	1,002.4387
	8,192	512	0.4406	0.0018	78.9740	4.2619	1,875.2114	72.3659
	16,384	1,024	0.4401	0.0013	75.5977	0.8856	1,885.4866	82.6411
	32,768	2,048	0.4397	0.0009	75.5791	0.8670	1,896.8248	93.9793
	∞	∞	0.4388		74.7121		1,802.8455	
Laplace(0, 1)	64	4	2.6083	1.6083	9.2169	−9.7831	41.4180	−57.5820
	128	8	1.9209	0.9209	13.3345	−5.6655	40.5904	−58.4096
	256	16	1.5667	0.5667	28.4606	9.4606	55.0795	−43.9205
	512	32	1.3657	0.3657	20.3131	1.3131	61.8404	−37.1596
	1,024	64	1.2433	0.2433	17.9843	−1.0157	109.7608	10.7608
	2,048	128	1.1650	0.1650	18.9890	−0.0110	88.0001	−10.9999
	∞	∞	1.0000		19.0000		99.0000	

Table 3.4: Exact expected values and biases of the combined estimator $\mathscr{V}_p(w_0; b, m)$ using $b = 16$ batches.

	n	m	$p = 0.5$ Expected Value	Bias	$p = 0.95$ Expected Value	Bias	$p = 0.99$ Expected Value	Bias
Uniform(0, 1)	64	4	0.1613	−0.0887	0.1677	0.1202	0.1677	0.1578
	128	8	0.1997	−0.0503	0.1623	0.1148	0.1623	0.1524
	256	16	0.2256	−0.0244	0.1230	0.0755	0.1230	0.1131
	512	32	0.2404	−0.0096	0.0835	0.0360	0.0792	0.0693
	1,024	64	0.2479	−0.0021	0.0642	0.0167	0.0460	0.0361
	2,048	128	0.2512	0.0012	0.0577	0.0102	0.0207	0.0108
	4,096	256	0.2523	0.0023	0.0557	0.0082	0.0165	0.0066
	8,192	512	0.2524	0.0024	0.0515	0.0040	0.0131	0.0032
	16,384	1,024	0.2521	0.0021	0.0496	0.0021	0.0116	0.0017
	32,768	2,048	0.2516	0.0016	0.0489	0.0014	0.0109	0.0010
	∞	∞	0.2500		0.0475		0.0099	
Expo(1)	64	4	0.9812	−0.0188	5.4489	−13.5511	5.4489	−93.5511
	128	8	1.0096	0.0096	12.5585	−6.4415	12.5585	−86.4415
	256	16	1.0285	0.0285	26.8754	7.8754	26.8755	−72.1245
	512	32	1.0335	0.0335	20.9604	1.9604	55.5664	−43.4336
	1,024	64	1.0307	0.0307	15.5221	−3.4779	112.9802	13.9802
	2,048	128	1.0254	0.0254	20.0335	1.0335	108.3952	9.3952
	4,096	256	1.0199	0.0199	20.4133	1.4133	107.7223	8.7223
	8,192	512	1.0150	0.0150	19.7064	0.7064	108.9949	9.9949
	16,384	1,024	1.0110	0.0110	19.4977	0.4977	104.4779	5.4779
	32,768	2,048	1.0080	0.0080	19.3534	0.3534	102.9055	3.9055
	∞	∞	1.0000		19.0000		99.0000	
Pareto(1, 2.1)	64	4	2.5318	2.0930	202.1907	127.4785	202.1907	−1,600.6548
	128	8	0.8842	0.4454	808.8905	734.1784	808.8905	−993.9550
	256	16	0.5874	0.1486	3,158.7724	3,084.0603	3,158.7724	1,355.9269
	512	32	0.5093	0.0705	1,174.1008	1,099.3886	12,256.3379	10,453.4924
	1,024	64	0.4784	0.0396	275.3381	200.6260	47,471.6767	45,668.8312
	2,048	128	0.4628	0.0240	120.9213	46.2092	55,082.2759	53,279.4304
	4,096	256	0.4538	0.0150	93.1486	18.4365	10,080.6105	8,277.7650
	8,192	512	0.4486	0.0098	83.0708	8.3587	3,728.2305	1,925.3850
	16,384	1,024	0.4453	0.0065	79.4123	4.7001	2,386.1549	583.3094
	32,768	2,048	0.4431	0.0043	77.3904	2.6783	2,051.2680	248.4225
	∞	∞	0.4388		74.7121		1802.8455	
Laplace(0, 1)	64	4	2.4715	1.4715	6.0122	−12.9878	6.0122	−92.9878
	128	8	2.0230	1.0230	12.8153	−6.1847	12.8178	−86.1822
	256	16	1.7007	0.7007	26.9890	7.9890	26.9890	−72.0110
	512	32	1.4809	0.4809	20.9770	1.9770	55.6188	−43.3812
	1,024	64	1.3319	0.3319	20.6809	1.6809	113.0056	14.0056
	2,048	128	1.2303	0.2303	20.0336	1.0336	108.3929	9.3929
	∞	∞	1.0000		19.0000		99.0000	

Table 3.5: Exact expected values and biases of the combined estimator $\widetilde{\mathscr{V}}_p(w_0; b, m)$ using $b = 16$ batches.

			$p = 0.5$		$p = 0.95$		$p = 0.99$	
	n	m	Expected Value	Bias	Expected Value	Bias	Expected Value	Bias
Uniform(0, 1)	64	4	0.1819	−0.0681	0.2098	0.1623	0.2413	0.2314
	128	8	0.2133	−0.0367	0.1773	0.1298	0.2022	0.1923
	256	16	0.2340	−0.0160	0.1246	0.0771	0.1426	0.1327
	512	32	0.2454	−0.0046	0.0860	0.0385	0.0856	0.0757
	1,024	64	0.2509	0.0009	0.0687	0.0212	0.0471	0.0372
	2,048	128	0.2530	0.0030	0.0592	0.0117	0.0228	0.0129
	4,096	256	0.2534	0.0034	0.0560	0.0085	0.0171	0.0072
	8,192	512	0.2531	0.0031	0.0519	0.0044	0.0139	0.0040
	16,384	1,024	0.2526	0.0026	0.0500	0.0025	0.0119	0.0020
	32,768	2,048	0.2520	0.0020	0.0491	0.0016	0.0111	0.0012
	∞	∞	0.2500		0.0475		0.0099	
Expo(1)	64	4	1.0164	0.0164	7.1008	−11.8992	22.6459	−76.3541
	128	8	1.0337	0.0337	13.0962	−5.9038	26.2835	−72.7165
	256	16	1.0446	0.0446	28.3808	9.3808	41.2609	−57.7391
	512	32	1.0442	0.0442	21.2797	2.2797	60.4956	−38.5044
	1,024	64	1.0380	0.0380	15.9149	−3.0851	115.6305	16.6305
	2,048	128	1.0303	0.0303	20.1938	1.1938	111.5136	12.5136
	4,096	256	1.0232	0.0232	20.6080	1.6080	108.8653	9.8653
	8,192	512	1.0173	0.0173	19.8269	0.8269	111.3782	12.3782
	16,384	1,024	1.0126	0.0126	19.5731	0.5731	105.4998	6.4998
	32,768	2,048	1.0091	0.0091	19.3991	0.3991	103.3903	4.3903
	∞	∞	1.0000		19.0000		99.0000	
Pareto(1, 2.1)	64	4	2.5433	2.1045	211.6537	136.9416	2,034.5031	231.6576
	128	8	0.8923	0.4535	840.4776	765.7655	959.8631	−842.9824
	256	16	0.5930	0.1542	3,319.1418	3,244.4296	3,383.6079	1,580.7624
	512	32	0.5133	0.0745	1,180.1971	1,105.4849	12,717.9024	10,915.0569
	1,024	64	0.4812	0.0424	276.3202	201.6080	49,662.5961	47,859.7506
	2,048	128	0.4647	0.0259	121.7692	47.0571	55,123.6710	53,320.8255
	4,096	256	0.4552	0.0164	94.5934	19.8812	10,142.9378	8,340.0923
	8,192	512	0.4495	0.0107	83.6092	8.8970	3,751.7512	1,948.9057
	16,384	1,024	0.4459	0.0071	79.6667	4.9545	2,399.3698	596.5243
	32,768	2,048	0.4436	0.0048	77.5803	2.8682	2,062.5088	259.6633
	∞	∞	0.4388		74.7121		1,802.8455	
Laplace(0, 1)	64	4	2.7258	1.7258	7.6815	−11.3185	23.2628	−75.7372
	128	8	2.1384	1.1384	13.3532	−5.6468	26.5416	−72.4584
	256	16	1.7562	0.7562	28.4943	9.4943	41.3745	−57.6255
	512	32	1.5092	0.5092	21.2962	2.2962	60.5480	−38.4520
	1,024	64	1.3472	0.3472	21.0738	2.0738	115.6556	16.6556
	2,048	128	1.2390	0.2390	20.1939	1.1939	111.5113	12.5113
	∞	∞	1.0000		19.0000		99.0000	

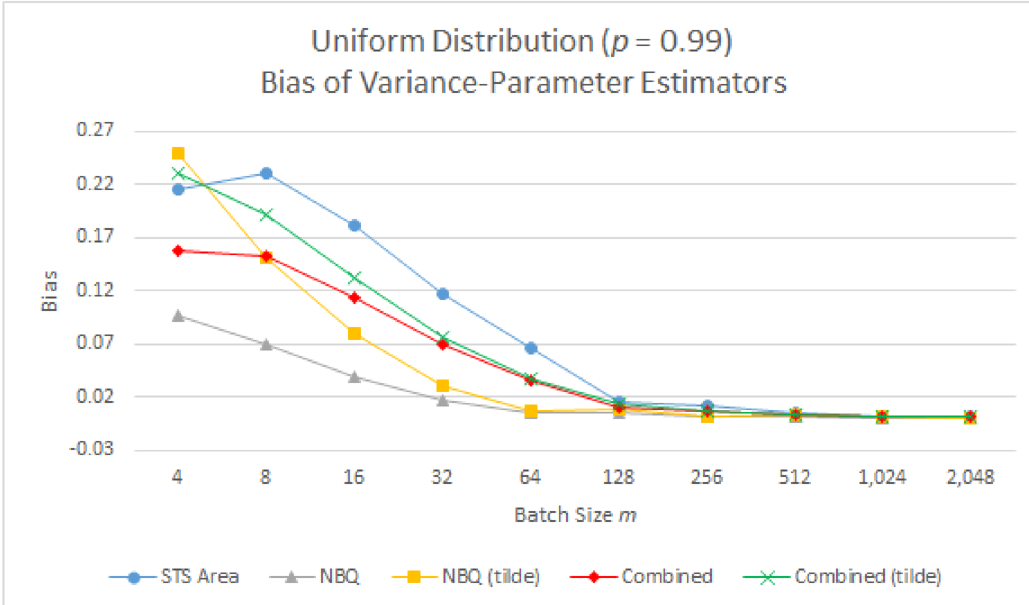

Figure 3.1: Bias of the variance-parameter estimators for the uniform distribution on $[0, 1]$ and $p = 0.99$, in the special case of i.i.d. observations. The results are based on Tables 3.1–3.5, with batch sizes $m = 2^{\mathcal{L}}$, $\mathcal{L} = 2, 3, \ldots, 11$.

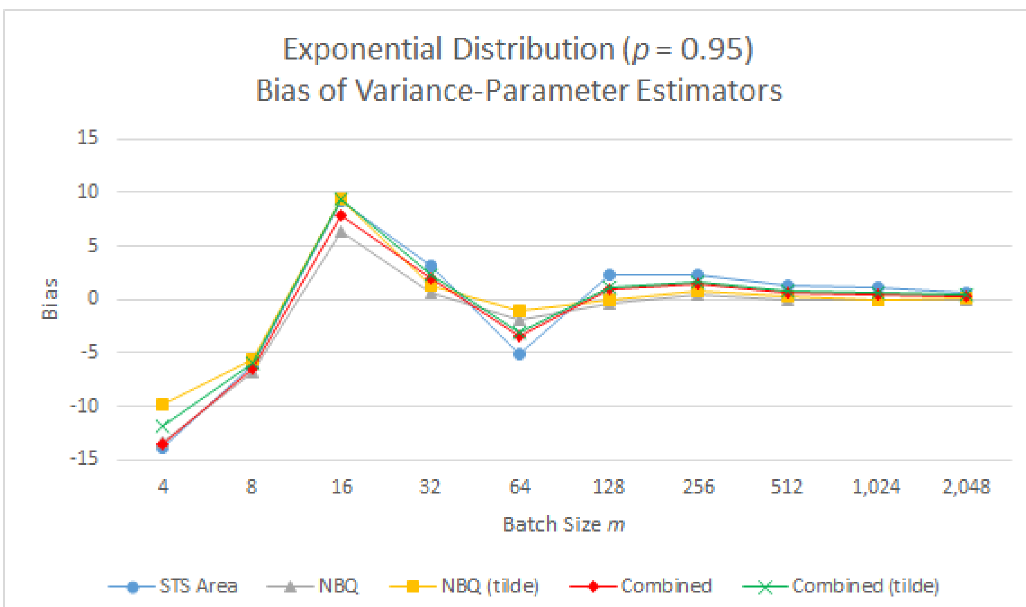

Figure 3.2: Bias of the variance-parameter estimators for the exponential distribution with unit rate parameter and $p = 0.95$, in the special case of i.i.d. observations. The results are based on Tables 3.1–3.5, with batch sizes $m = 2^{\mathcal{L}}$, $\mathcal{L} = 2, 3, \ldots, 11$.

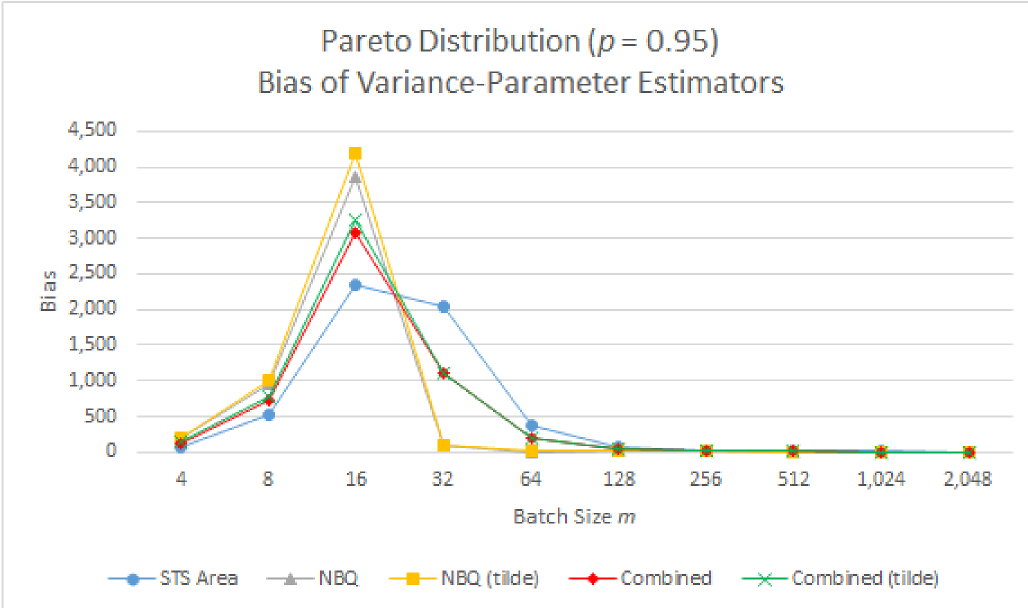

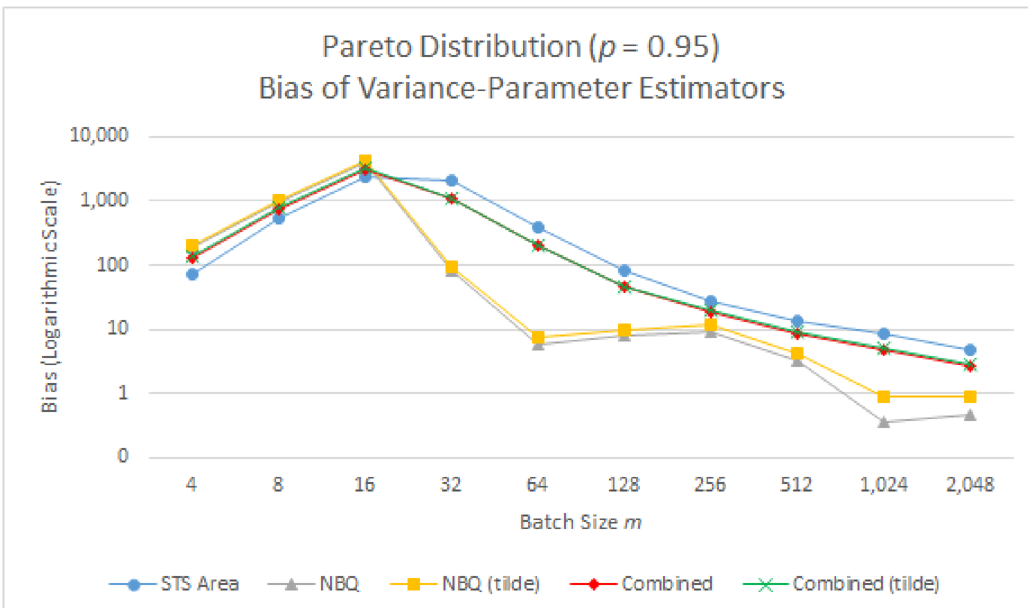

Figure 3.3: Bias of the variance-parameter estimators for the Pareto distribution with parameters $\gamma = 1$ and $\theta = 2.1$ and $p = 0.95$, in the special case of i.i.d. observations. The results are based on Tables 3.1–3.5, with batch sizes $m = 2^{\mathcal{L}}$, $\mathcal{L} = 2, 3, \ldots, 11$. The second graph plots the same values as the first one, but we use a logarithmic scale for the vertical axis.

Table 3.6: Verification of the exact results in Table 3.1 for the expected values and biases of the STS area estimator $\widetilde{\mathscr{A}_p}(w_0; b, m)$. The results are based on 100,000 replications with $b = 16$ batches of size m.

			$p = 0.5$		$p = 0.95$		$p = 0.99$	
	n	m	Expected Value	Bias	Expected Value	Bias	Expected Value	Bias
Uniform(0, 1)	64	4	0.1624	−0.0876	0.2251	0.1776	0.2251	0.2152
	128	8	0.2017	−0.0483	0.2409	0.1934	0.2409	0.231
	256	16	0.2295	−0.0205	0.1922	0.1447	0.1922	0.1823
	512	32	0.2450	−0.0050	0.1113	0.0638	0.1277	0.1178
	1024	64	0.2535	0.0035	0.0716	0.0241	0.0755	0.0656
	2048	128	0.2561	0.0061	0.0643	0.0168	0.0260	0.0161
	4096	256	0.2557	0.0057	0.0632	0.0157	0.0213	0.0114
	8192	512	0.2556	0.0056	0.0549	0.0074	0.0145	0.0046
	16384	1024	0.2546	0.0046	0.0511	0.0036	0.0126	0.0027
	32768	2048	0.2535	0.0035	0.0501	0.0026	0.0117	0.0018
	∞	∞	0.2500		0.0475		0.0099	
Expo(1)	64	4	1.2504	0.2504	5.2023	−13.7977	5.2023	−93.7977
	128	8	1.1772	0.1772	12.9122	−6.0878	12.9122	−86.0878
	256	16	1.1396	0.1396	28.3053	9.3053	28.3053	−70.6947
	512	32	1.1065	0.1065	22.1531	3.1531	59.3864	−39.6136
	1024	64	1.0829	0.0829	23.9586	4.9586	121.0511	22.0511
	2048	128	1.0608	0.0608	21.3112	2.3112	133.1777	34.1777
	4096	256	1.0423	0.0423	21.3414	2.3414	115.0248	16.0248
	8192	512	1.0315	0.0315	20.3520	1.3520	125.2362	26.2362
	16384	1024	1.0228	0.0228	20.0783	1.0783	112.0425	13.0425
	32768	2048	1.0163	0.0163	19.7304	0.7304	107.0313	8.0313
	∞	∞	1.0000		19.0000		99.0000	
Pareto(1, 2.1)	64	4	4.3157	3.8769	76.7433	2.0312	76.7433	−1,726.1022
	128	8	1.2957	0.8569	285.4158	210.7037	285.4158	−1,517.4297
	256	16	0.7173	0.2785	939.0643	864.3522	939.0643	−863.7812
	512	32	0.5738	0.1350	988.7529	914.0408	4,460.3143	2,657.4688
	1024	64	0.5174	0.0786	469.6862	394.9741	16,806.1935	15,003.3480
	2048	128	0.4856	0.0468	184.1516	109.4395	96,463.9087	94,661.0632
	4096	256	0.4675	0.0287	102.0384	27.3263	13,119.5019	11,316.6564
	8192	512	0.4578	0.0190	88.0488	13.3367	5,025.5242	3,222.6787
	16384	1024	0.4515	0.0127	83.4638	8.7517	2,746.5135	943.6680
	32768	2048	0.4472	0.0084	79.5687	4.8566	2,208.9441	406.0986
	∞	∞	0.4388		74.7121		1,802.8455	
Laplace(0, 1)	64	4	2.8360	1.8360	6.2371	−12.7629	6.2371	−92.7629
	128	8	2.3415	1.3415	13.3564	−5.6436	13.3564	−85.6436
	256	16	1.9327	0.9327	28.3851	9.3851	28.3851	−70.6149
	512	32	1.6453	0.6453	22.2273	3.2273	59.2076	−39.7924
	1024	64	1.4425	0.4425	23.9929	4.9929	121.4868	22.4868
	2048	128	1.3082	0.3082	21.3155	2.3155	133.3865	34.3865
	4096	256	1.2167	0.2167	21.3015	2.3015	114.6917	15.6917
	8192	512	1.1489	0.1489	20.4139	1.4139	124.9536	25.9536
	16384	1024	1.1061	0.1061	20.1183	1.1183	112.1394	13.1394
	32768	2048	1.0733	0.0733	19.7135	0.7135	106.6866	7.6866
	∞	∞	1.0000		19.0000		99.0000	

Table 3.7: Verification of the exact results in Table 3.2 for the expected values and biases of the NBQ estimator $\mathcal{N}_p(b,m)$. The results are based on 100,000 replications with $b = 16$ batches of size m.

			$p = 0.5$		$p = 0.95$		$p = 0.99$	
	n	m	Expected Value	Bias	Expected Value	Bias	Expected Value	Bias
Uniform(0, 1)	64	4	0.1601	−0.0899	0.1066	0.0591	0.1066	0.0967
	128	8	0.1979	−0.0521	0.0791	0.0316	0.0791	0.0692
	256	16	0.2217	−0.0283	0.0492	0.0017	0.0492	0.0393
	512	32	0.2356	−0.0144	0.0536	0.0061	0.0277	0.0178
	1024	64	0.2427	−0.0073	0.0561	0.0086	0.0147	0.0048
	2048	128	0.2459	−0.0041	0.0506	0.0031	0.0151	0.0052
	4096	256	0.2478	−0.0022	0.0477	0.0002	0.0114	0.0015
	8192	512	0.2492	−0.0008	0.0480	0.0005	0.0115	0.0016
	16384	1024	0.2496	−0.0004	0.0481	0.0006	0.0106	0.0007
	32768	2048	0.2493	−0.0007	0.0477	0.0002	0.0101	0.0002
	∞	∞	0.2500		0.0475		0.0099	
Expo(1)	64	4	0.6948	−0.3052	5.6993	−13.3007	5.6993	−93.3007
	128	8	0.8310	−0.1690	12.2491	−6.7509	12.2491	−86.7509
	256	16	0.9099	−0.0901	25.3988	6.3988	25.3988	−73.6012
	512	32	0.9565	−0.0435	19.6816	0.6816	51.8084	−47.1916
	1024	64	0.9780	−0.0220	17.1900	−1.8100	104.4081	5.4081
	2048	128	0.9873	−0.0127	18.6847	−0.3153	81.6047	−17.3953
	4096	256	0.9934	−0.0066	19.4602	0.4602	100.0662	1.0662
	8192	512	0.9977	−0.0023	19.0956	0.0956	91.9019	−7.0981
	16384	1024	0.9987	−0.0013	18.8861	−0.1139	96.5214	−2.4786
	32768	2048	0.9973	−0.0027	18.9812	−0.0188	98.9691	−0.0309
	∞	∞	1.0000		19.0000		99.0000	
Pareto(1, 2.1)	64	4	0.4069	−0.0319	147.9965	73.2844	147.9965	−1,654.8490
	128	8	0.4251	−0.0137	484.1441	409.4320	484.1441	−1,318.7014
	256	16	0.4331	−0.0057	1,780.1279	1,705.4158	1,780.1279	−22.7176
	512	32	0.4369	−0.0019	157.2442	82.5321	6,644.2400	4,841.3945
	1024	64	0.4379	−0.0009	80.5462	5.8341	36,623.8829	34,821.0374
	2048	128	0.4376	−0.0012	82.8637	8.1516	2,428.4070	625.5615
	4096	256	0.4380	−0.0008	83.8321	9.1200	2,675.7794	872.9339
	8192	512	0.4389	0.0001	77.9031	3.1910	1,827.7987	24.9532
	16384	1024	0.4387	−0.0001	75.0747	0.3626	1,860.6216	57.7761
	32768	2048	0.4379	−0.0009	75.1760	0.4639	1,875.0958	72.2503
	∞	∞	0.4388		74.7121		1,802.8455	
Laplace(0, 1)	64	4	2.0831	1.0831	5.7598	−13.2402	5.7598	−93.2402
	128	8	1.6824	0.6824	12.2000	−6.8000	12.2000	−86.8000
	256	16	1.4530	0.4530	25.3410	6.3410	25.3410	−73.6590
	512	32	1.3095	0.3095	19.6770	0.6770	51.6760	−47.3240
	1024	64	1.2142	0.2142	17.1742	−1.8258	104.3546	5.3546
	2048	128	1.1493	0.1493	18.6739	−0.3261	81.5766	−17.4234
	4096	256	1.1040	0.1040	19.5123	0.5123	100.0925	1.0925
	8192	512	1.0725	0.0725	19.0747	0.0747	91.8258	−7.1742
	16384	1024	1.0506	0.0506	18.8852	−0.1148	96.4822	−2.5178
	32768	2048	1.0352	0.0352	18.9450	−0.0550	98.9591	−0.0409
	∞	∞	1.0000		19.0000		99.0000	

Table 3.8: Verification of the exact results in Table 3.3 for the expected values and biases of the NBQ estimator $\widetilde{\mathscr{N}_p}(b, m)$. The results are based on 100,000 replications with $b = 16$ batches of size m.

			$p = 0.5$		$p = 0.95$		$p = 0.99$	
	n	m	Expected Value	Bias	Expected Value	Bias	Expected Value	Bias
Uniform(0, 1)	64	4	0.2027	−0.0473	0.1936	0.1461	0.2586	0.2487
	128	8	0.2262	−0.0238	0.1102	0.0627	0.1615	0.1516
	256	16	0.2391	−0.0109	0.0525	0.0050	0.0899	0.0800
	512	32	0.2460	−0.0040	0.0588	0.0113	0.0409	0.0310
	1024	64	0.2490	−0.0010	0.0654	0.0179	0.0169	0.0070
	2048	128	0.2498	−0.0002	0.0538	0.0063	0.0194	0.0095
	4096	256	0.2502	0.0002	0.0484	0.0009	0.0125	0.0026
	8192	512	0.2508	0.0008	0.0487	0.0012	0.0133	0.0034
	16384	1024	0.2505	0.0005	0.0489	0.0014	0.0113	0.0014
	32768	2048	0.2499	−0.0001	0.0481	0.0006	0.0104	0.0005
	∞	∞	0.2500		0.0475		0.0099	
Expo(1)	64	4	0.7678	−0.2322	9.1011	−9.8989	41.4232	−57.5768
	128	8	0.8808	−0.1192	13.3593	−5.6407	40.6656	−58.3344
	256	16	0.9434	−0.0566	28.5165	9.5165	55.1407	−43.8593
	512	32	0.9787	−0.0213	20.3415	1.3415	62.0076	−36.9924
	1024	64	0.9930	−0.0070	18.0052	−0.9948	109.8971	10.8971
	2048	128	0.9975	−0.0025	19.0128	0.0128	88.0655	−10.9345
	4096	256	1.0004	0.0004	19.8616	0.8616	102.4331	3.4331
	8192	512	1.0026	0.0026	19.2851	0.2851	96.8201	−2.1799
	16384	1024	1.0020	0.0020	19.0414	0.0414	98.6367	−0.3633
	32768	2048	0.9996	−0.0004	19.0752	0.0752	99.9691	0.9691
	∞	∞	1.0000		19.0000		99.0000	
Pareto(1, 2.1)	64	4	0.4307	−0.0081	159.8003	85.0882	2217.0827	414.2372
	128	8	0.4419	0.0031	513.8276	439.1155	766.6884	−1,036.1571
	256	16	0.4448	0.0060	1,967.2317	1,892.5196	2,099.1771	296.3316
	512	32	0.4450	0.0062	169.7745	95.0624	7,022.0654	5,219.2199
	1024	64	0.4436	0.0048	82.5926	7.8805	3,9645.0957	3,7842.2502
	2048	128	0.4417	0.0029	84.6089	9.8968	2,514.5563	711.7108
	4096	256	0.4408	0.0020	86.8118	12.0997	2,804.3265	1,001.4810
	8192	512	0.4409	0.0021	79.0190	4.3069	1,876.3340	73.4885
	16384	1024	0.4401	0.0013	75.5988	0.8867	1,887.9799	85.1344
	32768	2048	0.4389	0.0001	75.5652	0.8531	1,898.3584	95.5129
	∞	∞	0.4388		74.7121		1,802.8455	
Laplace(0, 1)	64	4	2.6096	1.6096	9.1994	−9.8006	41.3127	−57.6873
	128	8	1.9212	0.9212	13.3021	−5.6979	40.5058	−58.4942
	256	16	1.5678	0.5678	28.4508	9.4508	55.0313	−43.9687
	512	32	1.3679	0.3679	20.3421	1.3421	61.8744	−37.1256
	1024	64	1.2457	0.2457	17.9814	−1.0186	109.8195	10.8195
	2048	128	1.1673	0.1673	19.0049	0.0049	88.0347	−10.9653
	4096	256	1.1148	0.1148	19.9145	0.9145	102.4663	3.4663
	8192	512	1.0791	0.0791	19.2634	0.2634	96.7777	−2.2223
	16384	1024	1.0548	0.0548	19.0415	0.0415	98.6023	−0.3977
	32768	2048	1.0380	0.0380	19.0396	0.0396	99.9643	0.9643
	∞	∞	1.0000		19.0000		99.0000	

CHAPTER 4

SQSTS: A SEQUENTIAL PROCEDURE FOR ESTIMATING STEADY-STATE QUANTILES USING STANDARDIZED TIME SERIES

This chapter builds on the theoretical foundations laid out in Chapter 2 to develop and assess SQSTS, an automated sequential procedure for computing point estimators and CIs for steady-state quantiles based on the simulation analysis methods of STS and sectioning as the latter method is applied to batch quantile estimators and the full-sample quantile estimator. The variance parameter σ_p^2 associated with the full-sample quantile estimator is estimated by a combination of variance-parameter estimators that are based on the two aforementioned methods of simulation analysis and are asymptotically independent as the batch size increases with a fixed number of batches (Alexopoulos *et al.* [7]).

SQSTS is the first sequential procedure to incorporate STS-based variance-parameter estimators for steady-state quantile estimation. Theorem 2.3.4 forms the basis for some of the key steps in SQSTS that control the growth of the batch size on successive iterations of the procedure. Our SQSTS method borrows elements from two recent sequential methods having different objectives: the SPSTS method of Alexopoulos *et al.* [40] for estimation of the steady-state mean and the Sequest method of Alexopoulos *et al.* [7] for estimation of steady-state quantiles. The key differences of SQSTS with Sequest and SPSTS will be detailed in Section 4.1 below. The remainder of this chapter is organized as follows. Section 4.1 contains a formal algorithmic statement of SQSTS. Section 4.2 includes an experimental evaluation of SQSTS using a test bed of seven challenging processes and a direct comparison to the Sequest and Sequem methods (Alexopoulos *et al.* [7, 23]), which are the state-of-the-art methods for sequential steady-state quantile estimation. Section 4.3 contains a short summary of this chapter and the findings in Section 4.2.

4.1 SQSTS Algorithm

In this section we present our STS-based sequential procedure for estimating a steady-state quantile of a stochastic sequence. Figure 4.1 contains a high-level flowchart of the procedure. The user provides the probability associated with the quantile p and the nominal error probability $\alpha \in (0,1)$ for the CI for y_p. Further, the user has the option to impose an upper bound for the absolute or relative precision of the CI.

We start with a cursory overview of the procedure. The core of SQSTS consists of three loops. Step **[2]** of SQSTS (the first loop) progressively increases the batch size m until the signed (weighted) areas $A_p(w; j, m)$ under the STSs based on b nonoverlapping batches pass the two-sided randomness test of von Neumann [43], while Step **[3]** (the second loop) increases the batch size until the signed areas pass the one-sided test of Shapiro and Wilk [81] for testing the hypothesis that the approximately i.i.d. $\{A_p(w; j, m) : j = 1, \ldots, b\}$ sample has a univariate normal distribution, whose mean and variance are not specified. To control the growth of the batch size, both loops use a rapidly decreasing sequence of significance levels. We focus on the signed areas in an attempt to ameliorate the pronounced bias of the batched STS area estimator $\mathscr{A}_p(w; b, m)$ relative to the NBQ variance estimator (Alexopoulos *et al.* [39]). At the end of the two loops, the signed areas $A_p(w; j, m)$ in Equation (2.15) approximately satisfy the asymptotic properties in Theorem 2.3.4 as they are approximately i.i.d. normal r.v.'s. In Step **[4]** the first batch of size m is removed because the (near) independence of $A_p(w; 1, m)$ and the remaining signed areas $\{A_p(w; j, m) : j = 2, \ldots, b\}$ based on the successful completion of Step **[2]** indicates that any initialization bias due to warm-up effects is mostly confined to the first batch; and the simulation is restarted to generate another batch of the current size m and compute another BQE and signed area that are almost free of initialization bias. In Step **[5]** the batch size is quadrupled so that the batch count is reduced by a factor of $1/4$, and the signed areas and BQEs $\{\widehat{y}_p(j, m)\}$ are recomputed. The scope of this rebatching is to increase the reliability of the CI for y_p

in the case where there are no precision requirements for the CI HL; this is typical for most commercial simulation packages and a reasonable starting point for estimating the sample size required to achieve a given precision requirement. If the user has specified a finite upper bound on the HL of the CI for y_p, Step **[6]**, the last loop of SQSTS, performs iterative increases of the batch count b or batch size m until the CI for y_p in Equation (2.68) meets the target relative-precision requirement.

In comparison with the Sequest and Sequem procedures (Alexopoulos *et al.* [23, 7]), the SQSTS procedure is structurally less complicated. For instance: (i) while Sequest starts with a smaller initial batch size (128 versus 512 or 4096), it contains an intricate loop that increases the batch size in a progressively cautious fashion until the estimated absolute skewness of the BQEs $\{\widehat{y}_p(j,m)\}$, drops below an upper bound that is a function of p; (ii) the CI for y_p delivered by Sequest incorporates adjustments for residual skewness and autocorrelation in the BQEs; and (iii) Sequem adds more complexity to Sequest because it uses two-dimensional blocks of batches in order to apply the maximum transformation. On another front, whereas SQSTS has similar core logic akin to the SPSTS procedure of Alexopoulos *et al.* [40] for estimating the steady-state mean, it has key differences from the latter. Specifically, (i) SPSTS attempts to control the excessive small-sample bias of the STS-based estimates of the associated variance parameter $\sigma^2 = \lim_{n\to\infty} n\mathrm{Var}\big[\overline{Y}_n\big]$ by means of an ad hoc variance estimator computed as the maximum of the area estimators based on the cosine weights $w_{\cos,1}(\cdot)$ and $w_{\cos,2}(\cdot)$ and an estimator arising from the method of overlapping batch means (Meketon and Schmeiser [82]); and (ii) SQSTS provides an additional safeguard against small-sample bias with the aggressive rebatching in Step **[5]**. The next few paragraphs contain a detailed description of each step of SQSTS.

Steps **[0]**–**[1]** initialize the experimental parameters and generate the initial dataset comprised of $b = 64$ batches of size 512 when $p \in [0.05, 0.95]$ or 4096 otherwise. The values of p, α, and the CI precision requirement (if any) are specified by the user. The level of significance for the statistical tests in Steps **[2]**–**[3]** is set according to the sequence

$\{\beta\psi(\ell) : \ell = 1, 2, \ldots\}$, where $\beta = 0.3$, $\psi(\ell) \equiv \exp\left[-\eta(\ell-1)^{\theta}\right]$, $\eta = 0.2$, and $\theta = 2.3$. Step **[2]** consists of a loop that tests for the randomness (i.i.d. property) of the signed areas $A_p(w; j, m)$ using a two-sided test based on von Neumann's ratio (von Neumann [43], Young [83]) with progressively decreasing size $\beta\psi(\ell)$ on iteration ℓ. Let $\overline{A}_p(w; b, m) = b^{-1}\sum_{j=1}^{b} A_p(w; j, m)$ be the average of the sample $\{A_p(w; j, m) : j = 1, \ldots, b\}$, and let

$$\widehat{\tau}_1 = \frac{\sum_{j=1}^{b-1}[A_p(w; j, m) - \overline{A}_p(w; b, m)][A_p(w; j+1, m) - \overline{A}_p(w; b, m)]}{\sum_{j=1}^{b}[A_p(w; j, m) - \overline{A}_p(w; b, m)]^2}$$

be the estimate of the respective lag-1 sample autocorrelation. The (rescaled) von Neumann test statistic is

$$U_b \equiv \sqrt{\frac{b^2-1}{b-2}}\left\{\widehat{\tau}_1 + \frac{[A_p(w; 1, m) - \overline{A}_p(w; b, m)]^2 + [A_p(w; b, m) - \overline{A}_p(w; b, m)]^2}{2\sum_{j=1}^{b}[A_p(w; j, m) - \overline{A}_p(w; b, m)]^2}\right\}. \tag{4.1}$$

Notice that the quantity inside the square brackets of Equation (4.1) is equal to the estimate $\widehat{\tau}_1$ plus end effects that diminish as b increases. If the data are nearly normal, for sufficiently large b, the distribution of U_b under the null hypothesis is approximately $N(0, 1)$; hence the two-sided test rejects the i.i.d. property at level of significance β when $|U_b| > z_{1-\beta/2}$.

At this juncture, a few additional comments on the application of von Neumann's test are in order. First, the test should have sufficient power to avoid passing to the Shapiro–Wilk test in Step **[3]** a sample dataset $\{A_p(w; j, m) : j = 1, \ldots, b\}$ that is contaminated by significant statistical dependencies. Since the power of the test increases with increasing batch count b, we chose the initial value $b = 64$ in Step **[1]** of SQSTS. Second, the null distribution of von Neumann's test can be badly distorted by departures from normality in the dataset $\{A_p(w; j, m) : j = 1, \ldots, b\}$; and the distortion is pronounced when the underlying distribution is heavy-tailed (Bartels [84], §1, 1st para.). This is the basis for setting the initial batch size in Step **[1]** as

$$m_0 = \begin{cases} 512 & \text{if } p \in [0.05, 0.95], \\ 4096 & \text{otherwise.} \end{cases}$$

The values of these β, η, and θ were chosen after careful experimentation to balance the tradeoff between the rate of convergence of the vector $[A_p(w;1,m),\ldots,A_p(w;b,m)]^\mathsf{T}$ to a vector of i.i.d. normal r.v.'s and the explosion of the batch size; indeed, on iteration 4 the significance level drops $\beta\psi(4) = 0.025$, thus facilitating the acceptance of the null hypothesis. If the signed areas fail the randomness test, the batch size is incremented by the factor of $\sqrt{2}$ and $b\big(\llbracket m\sqrt{2}\rrbracket - m\big)$ additional data are generated, where $\llbracket\cdot\rrbracket$ is the rounding function to the nearest integer.

Step **[3]** contains a second loop that assesses the univariate normality of the signed areas $A_p(w;j,m)$ using the one-sided Shapiro–Wilk test again with level of significance $\beta\psi(\ell)$ on iteration ℓ. Let $A_p(w;(1),m) \le A_p(w;(2),m) \le \cdots \le A_p(w;(b),m)$ be the order statistics of the sample $\{A_p(w;j,m) : j = 1,\ldots,b\}$. The Shapiro–Wilk test statistic is

$$W_b \equiv \frac{\big[\sum_{j=1}^{b} a_j A_p(w;(j),m)\big]^2}{\sum_{j=1}^{b}\big[A_p(w;j,m) - \overline{A}_p(w;b,m)\big]^2}, \tag{4.2}$$

with the coefficients a_j computed from

$$\boldsymbol{a} \equiv (a_1,\ldots,a_b) = \frac{\boldsymbol{q}^\mathsf{T}\boldsymbol{V}^{-1}}{\big(\boldsymbol{q}^\mathsf{T}\boldsymbol{V}^{-1}\boldsymbol{V}^{-1}\boldsymbol{q}\big)^{1/2}}, \tag{4.3}$$

where $\boldsymbol{q} \equiv (q_1,\ldots,q_b)^\mathsf{T}$ is the vector of the expected values of the order statistics corresponding to an i.i.d. sample from the standard normal distribution and $\boldsymbol{V}$ is the covariance matrix of these order statistics. The vector $\boldsymbol{a}$ of coefficients was selected to satisfy the following properties: (i) $\boldsymbol{a}^\mathsf{T}\boldsymbol{a} = 1$ and $a_j = -a_{b-j+1}$ for $1 \le j \le b$. (ii) the null distribution of W_b depends only on b; (iii) the value of W_b ranges from $ba_1^2/(b-1)$ to unity; and (iv) the closer W_b is to unity, the better the data conform to normality. For a test of size γ, the null hypothesis is rejected when $W_b < w^*_{1-\gamma,b}$ with the critical value chosen so that $\Pr(W_b \ge w^*_{1-\gamma,b}) = 1 - \gamma$. Tables containing the elements of the vector of coefficients $\boldsymbol{a}$ and critical values $w^*_{1-\gamma,b}$ for $3 \le b \le 5000$ are contained in Royston [85] and references therein. The Shapiro–Wilk test for univariate normality is widely recognized as having the highest power when compared to several alternative tests (Fishman [2], §2.10). In particular, it is the most powerful test when the data have a continuous, skewed, and short- or long-tailed distribution.

By now, it should be clear that the von Neumann and Shapiro–Wilk tests are intertwined: the initial batch-size assignment aims at supplying signed areas $A_p(w; j, m)$ that do not exhibit pronounced departures from normality, while the loop in Step **[3]** starts with near i.i.d. data and increases the batch size until the signed areas $A_p(w; j, m)$ can be considered as an i.i.d. sample from the normal distribution.

Step **[4]** deals with the initial transient phase. Specifically, after the signed areas pass both the independence and normality tests, the first of the 64 batches is removed and a new batch is generated in anticipation that once the latter statistical tests are passed any transient effects are confined to the first batch. We realize that this truncation may be excessive, and plan to address it in the future. Step **[5]** rebatches the current sample into 16 batches of quadruple batch size. In the absence of a user-specified CI precision requirement for the CI's HL, the algorithm skips to Step **[7]**. Otherwise, Step **[6]** sequentially increases the batch count b (up to $b^* = 64$) or the batch size m until the HL of the CI for y_p meets the precision requirement. The value b' corresponds to the typical formula for increasing the sample size. If the batch count cannot be increased all the way to b', the batch size is increased by a relatively small factor (between 5% and 30%) to avoid an explosion of the sample size. Step **[7]** delivers the final CI for y_p defined in Equation (2.68), based on the combined variance-parameter estimator $\widetilde{\mathscr{V}}_p(w; b, m)$.

The formal algorithmic statement of SQSTS follows. We state the algorithm for a general weight function $w(\cdot)$ satisfying Equation (2.12) and in terms of a relative precision of the CI for y_p. If the user wishes to impose a finite upper bound h^* on the absolute precision (half-length) of the CI, then the condition $h(b,m,\alpha) > r^*|\widetilde{y}_p(n)|$ of the loop in Step **[6]** should be replaced by $h(b,m,\alpha) > h^*$.

Algorithm SQSTS

---

[0] Initialization: Set $\beta = 0.30$, $b^* = 64$, $p \in (0,1)$ and $\alpha \in (0,1)$. If the user specifies an upper bound on the CI's relative precision, set r^* to the value of the bound. Let $w(t)$, $t \in [0,1]$ be the weight function, and define the significance level for the hypothesis tests as $\beta\psi(\ell)$, where $\psi(\ell) \equiv \exp\left[-\eta(\ell-1)^\theta\right]$, $\ell = 1, 2, \ldots$, with $\eta = 0.2$ and $\theta = 2.3$.

[1] Generate $b = 64$ batches of size $m_0 = 512$ for $p \in [0.05, 0.95]$ or 4096 for $p \in [0.005, 0.05) \cup (0.95, 0.995]$. Let $\ell = 1$.

[2] **Until** von Neumann's test fails to reject randomness $\left(|U_b| \le z_{1-\beta\psi(\ell)/2}\right)$:

- Compute the signed areas $\{A_p(w; j, m) : j = 1, \ldots, b\}$;
- Assess the randomness of $\{A_p(w; j, m) : j = 1, \ldots, b\}$ using von Neumann's two-sided randomness test based on the statistic U_b in Equation (4.1) and the significance level $\beta\psi(\ell)$;
- Set $\ell \leftarrow \ell + 1$, generate $b\left(\llbracket m\sqrt{2}\rrbracket - m\right)$ additional observations, and set $m \leftarrow \llbracket m\sqrt{2}\rrbracket$.

End

[3] Reset $\ell \leftarrow 1$.

Until the Shapiro–Wilk test fails to reject normality $\left(W_b > w^*_{1-\beta\psi(\ell),b}\right)$:

- Compute the signed areas $\{A_p(w;j,m) : j = 1, \ldots, b\}$;
- Assess the univariate normality of $\{A_p(w;j,m) : j = 1, \ldots, b\}$ using the Shapiro–Wilk test based on the statistic W_b in Equations (4.2)–(4.3) and the significance level $\beta\psi(\ell)$;
- Set $\ell \leftarrow \ell + 1$, generate $b\big(\llbracket m\sqrt{2}\rrbracket - m\big)$ additional observations, and set $m \leftarrow \llbracket m\sqrt{2}\rrbracket$.

End

[4] Remove the first batch and append a new batch of size m.

[5] Rebatch the data with $b \leftarrow b/4 = 16$ and batches of size $m \leftarrow 4m$. If the user has not specified an upper bound on the CI's relative precision, go to Step **[7]**.

[6] **Until** the relative CI HL $h(b,m,\alpha) = t_{1-\alpha/2,2b-1}\big[\widetilde{\mathscr{V}}_p(w;b,m)/n\big]^{1/2}$ satisfies $h(b,m,\alpha) \le r^*|\widetilde{y}_p(n)|$:

- Compute the CI midpoint $\widetilde{y}_p(n)$ and the HL $h(b,m,\alpha)$ using the combined variance-parameter estimator

$$\widetilde{\mathscr{V}}_p(w;b,m) \equiv \frac{b\mathscr{A}_p(w;b,m) + (b-1)\widetilde{\mathscr{N}}_p(b,m)}{2b-1}$$

in Equation (2.58), where

$$\mathscr{A}_p(w;b,m) = b^{-1}\sum_{j=1}^{b} A_p^2(w;j,m) \quad \text{and}$$

$$\widetilde{\mathscr{N}}_p(b,m) = m(b-1)^{-1}\sum_{j=1}^{b}\big[\widehat{y}_p(j,m) - \widetilde{y}_p(n)\big]^2;$$

- Estimate the number of batches of the current size required to satisfy the precision requirement,

$$b' = \left\lceil b \left\{ \frac{h(b, m, \alpha)}{r^* \widetilde{y}_p(n)} \right\}^2 \right\rceil;$$

- Update the batch count b, the batch size m, and the total sample size n as follows:

$$\begin{aligned}
b &\leftarrow \min\{b', b^*\}, \\
m &\leftarrow \begin{cases} m & \text{if } b = b', \\ \lceil m \times \text{mid}\{1.05, (b'/b), 1.3\} \rceil & \text{if } b < b', \end{cases} \\
n &\leftarrow bm,
\end{aligned}$$

where the function mid$(\cdot)$ computes the median of its arguments;

- Generate the necessary additional data.

End

[7] Deliver the $100(1-\alpha)\%$ CI: $\widetilde{y}_p(n) \pm t_{1-\alpha/2,2b-1} \left[\widetilde{\mathscr{V}}_p(w; b, m)/n \right]^{1/2}$.

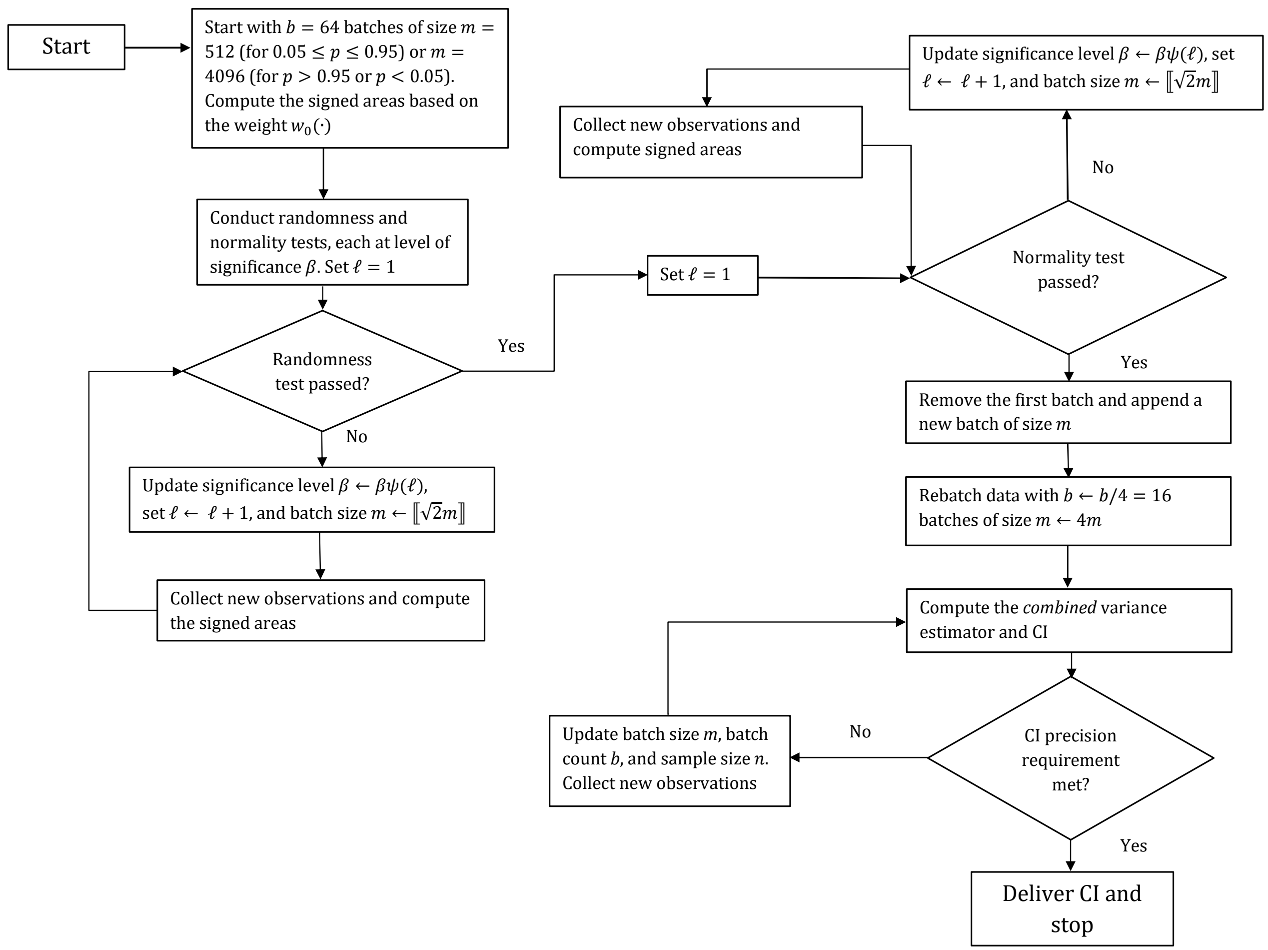

Figure 4.1: High-Level Flowchart of SQSTS.

4.2 Experimental Results

This section contains an extensive empirical study designed to assess the performance of SQSTS using a test bed of seven challenging processes from Alexopoulos *et al.* [7] and Alexopoulos *et al.* [23]. Specifically, the test bed is related to two time-series models, three single-server queueing systems, and two small queueing networks, described in Sections 2.5.1–2.5.7 of this thesis. For each test problem, the analysis considered two levels of 95% ($\alpha = 0.05$) CI relative precision: (i) no CI precision requirement (denoted for brevity by "$r^* = \infty$"), and (ii) a model-dependent values of r^* that was usually selected at least 10% lower than the smallest estimated CI relative precision observed in Sequest under no precision requirement. We chose the value of r^* to evaluate the effectiveness of Step **[6]** of SQSTS, especially when relatively little additional sampling is required compared to the case of no CI precision requirement; this is the case where sequential methods tend to exhibit substantial loss of CI coverage probability. All experiments were coded in Java using common random numbers generated by the RngStreams package of L'Ecuyer *et al.* [67]. Since the experimentation in Sections 2.8 and 2.10, and the analytical calculations in Chapter 3 failed to provide firm evidence for the dominance of the STS area estimators for σ_p^2 based on alternative weight functions, including $w_2(t) = \sqrt{840}(3t^2 - 3t + 1/2)$ (Goldsman *et al.* [33]), and $\{w_{\cos,\ell}(t) = \sqrt{8}\pi\ell\cos(2\pi\ell t)\colon\ \ell = 1, 2\}$ (Foley and Goldsman [54]), over $\mathscr{A}_p(w_0; b, m)$ with respect to small-sample bias and MSE, we used the constant weight function $w_0(\cdot) = \sqrt{12}, 0 \le t \le 1$ in our experimentation.

Each table contains experimental results for SQSTS, Sequest (in bold typeface), and Sequem (in italic typeface). All estimates are averages computed from 1,000 independent trials; the entries for Sequest were taken from Alexopoulos *et al.* [7], whereas most entries for Sequem were taken from Alexopoulos *et al.* [23] and are limited to the extreme values $p \ge 0.95$. Specifically, column 1 of Tables 4.1–4.7 lists selected values of p from the tables in Alexopoulos *et al.* [23, 7], and columns 2 and 3 list the (nearly) exact value of the associated quantile y_p and the average value of the absolute bias of the associated point estimator, respectively. Columns 4–6 contain the average value of the HL of the 95% CI, the average value of the CI's relative precision expressed as a percentage, and the estimated coverage probability of the CI as a percentage, respectively. The standard errors of the latter estimates are approximately $\sqrt{(0.95 \times 0.05)/1000} = 0.007$. Finally columns 7 and 8 of Tables 4.1–4.7 display the average final batch size ($\overline{m}$) and average final sample size ($\overline{n}$), respectively. The experimental results for Sequem do not include the average batch sizes because the method of maximum transformation (Heidelberger and Lewis [30]) forms two-dimensional blocks of batches, as outlined in the next paragraph.

Further, below each table we provide a set of graphs based on the respective table for both levels of 95% ($\alpha = 0.05$) CI relative precision for the list of selected values of p depicting the three most important metrics for SQSTS' performance evaluation: (i) the average sample sizes; (ii) the average 95% CI relative precision, defined as the ratio of the CI HL over $|\widetilde{y}_p(n)|$; and (iii) the estimated 95% CI coverage probability. Essentially, Figures 4.2–4.9 illustrate SQSTS' performance (against its competitors) on these fronts in a more intelligible way by plotting the estimates of the 95% CI relative precision and coverage probability, and the average sample sizes in columns 5, 6, and 8, respectively, of Tables 4.1–4.7.

We close this preamble with a few comments regarding the simpler structure of SQSTS compared to its Sequest and Sequem competitors, as well as the potential effects of the initial batch sizes used in SQSTS. Recall that SQSTS starts with $b = 64$ batches of size $m = 512$ when $p \in [0.05, 0.95]$ or $m = 4096$ when $p \in [0.005, 0.05) \cup (0.95, 0.995]$; hence its initial sample size is equal to 2^{15} for nonextreme quantiles and 2^{18} for extreme quantiles. On the other hand, Sequest was designed for $p \in [0.05, 0.95]$ and is initialized with 64 batches of size 128; hence it starts with the substantially smaller sample size of 2^{13}. While in many cases Sequest performs well with regard to estimated CI coverage probability, the relatively small initial batch size can cause the method to perform poorly for extreme quantiles in the absence of a CI precision requirement, as illustrated by the respective table entries. On the other hand, Sequem was designed for extreme quantiles and starts with 64 adjacent blocks of data, each consisting of $c = \lfloor \ln(0.9)/\ln(p) \rfloor$ rows of adjacent batches of size $m_0 = 256$ (cf. Fig. 1 Alexopoulos *et al.* [23]). For example $p = 0.99$ yields $c = 10$ and an initial sample size of $2^6 \times (10 \times 2^8) = 10 \times 2^{14}$, which is 1.6 times smaller than the initial sample size of SQSTS for this value of p. Under no CI precision requirement, the smaller initial sample size of Sequest may result in noticeably smaller final sample sizes when the BQEs $\{\widehat{y}_p(j, m) : j = 1, \ldots, b\}$ pass von Neumann's randomness test early on and the absolute value of the estimated skewness of the BQEs drops below a threshold for relatively small batch sizes; we anticipate that this potential advantage of Sequest will vanish due to the potential effectiveness of von Neumann's and Shapiro–Wilk tests applied to the signed areas $\{A_p(w; j, m) : j = 1, \ldots, b\}$. In the presence of tight CI precision requirements, SQSTS may receive an additional boost with regard to the average sample-size requirement due to (i) the lack of adjustments to the CI for y_p for compensation against residual skewness and autocorrelation in the BQEs $\{\widehat{y}_p(j, m)\}$; and (ii) the smaller limiting (as $m \to \infty$) standard deviation of the combined variance estimator $\widetilde{\mathscr{V}}_p(w_0; b, m)$.

4.2.1 First-Order Autoregressive Processes

The first test process is the Gaussian AR(1) process defined in Section 2.5.1 with $\mu_Y = 100$, $\phi = 0.995$, $\sigma_\epsilon = 1$, and $Y_0 = 0$. Since the steady-state marginal standard deviation is $\sigma_Y = \sigma_\epsilon/(1 - \phi^2)^{1/2} = 10.01$, the process was initialized nearly 10 standard deviations below its steady-state mean. On top of the pronounced initialization bias, this process exhibits strong stochastic dependence with a lag-ℓ conditional correlation given Y_0 given by

$$\operatorname{Corr}[Y_k, Y_{k+\ell} \,|\, Y_0] = \phi^\ell \left[\frac{1 - \phi^{2k}}{1 - \phi^{2(k+\ell)}} \right]^{1/2}, \quad \text{for } \ell \geq 1 \text{ and } k \geq 1$$

(Fishman [86], Equation (6)), so that in our case $\mathrm{Corr}[Y_{10}, Y_{11} \,|\, Y_0] \approx 0.95$ and the $\mathrm{Corr}[Y_k, Y_{k+1}]$ converges monotonically to $\phi = 0.995$ as $k \to \infty$. Hence, this case study is a good test for evaluating the ability of SQSTS to overcome the effects of initialization bias and pronounced serial correlation between successive observations of the base process.

The experimental results are displayed in Table 4.1 and in Figure 4.2. The selected quantiles were computed by inverting the normal steady-state c.d.f. An examination of column 3 reveals that the point estimates of y_p delivered by SQSTS exhibit little average absolute bias (typically under 1% relative to the true value of y_p). Under no CI precision requirements and for $p \leq 0.95$, SQSTS was outperformed by Sequest with regard to the average sample size required to compute 95% CIs for y_p with near-nominal estimated coverage probability. As we elaborated earlier, this dominance is due to the significantly larger (by a factor of 4) initial sample size used by SQSTS. As it becomes clear from Figure 4.2, this victory for Sequest vanishes for extreme quantiles ($p > 0.95$) because of the noticeable undercoverage of the CIs it delivered (e.g., 90.2% for $p = 0.995$). Under the tight CI relative precision requirement of $r^* = 0.5\%$, SQSTS clearly outperformed Sequest for $p \leq 0.95$ and both Sequest and Sequem for $p > 0.95$ with regard to the reported average sample sizes required to obtain 95% CIs for y_p with near-nominal coverage probability. This reduction in average sample size is primarily due to the additional d.f. of the combined variance estimator $\widetilde{\mathscr{V}}_p(w_0; b, m)$ used in Step **[6]** of SQSTS. It should be noted that SQSTS requires little additional sampling effort in the transition from the no-precision case to $r^* = 0.5\%$. Overall, we judge the performance of SQSTS in this problem as satisfactory.

4.2.2 Autoregressive-to-Pareto Process

The second test process is a version of the ARTOP process described in Section 2.5.2. We considered the case with $\gamma = 1$, $\theta = 2.1$, and $\phi = 0.995$. These assignments yield $\mu_Y = 1.9091$, $\sigma_Y^2 = 17.3554$, marginal skewness $\mathrm{E}\{[(Y_k - \mu_Y)/\sigma_Y]^3\} = +\infty$, and marginal kurtosis $\mathrm{E}\{[(Y_k - \mu_Y)/\sigma_Y]^4\} = \infty$. We also initialized the original AR(1) process with the value $Z_0 = 3.4$; this assignment yields the initial observation $Y_0 = F^{-1}[\Phi(Z_0)] = 43.5689$ for the ARTOP process which is approximately 10 standard deviations above its steady-state mean. On top of the initialization problem and the strong stochastic dependence, this process has a marginal distribution with a fat tail (Mandelbrot [87]), which is reflected by the infinite marginal skewness and kurtosis.

Table 4.2 and Figure 4.3 summarize the experimental results for this process for the CI relative precision levels of $r^* = \infty$ and $r^* = 2.5\%$. The selected quantiles y_p were computed by inverting the c.d.f. in Equation (2.69). Despite the relatively small range for the values y_p (from 1.185 to 12.466), the large average sample sizes reflect the aforementioned challenges with regard to the initialization of the process far away from the steady-state mean μ_Y, the strong autocorrelation between $\{Y_k : i \geq 1\}$ caused by the large autoregressive coefficient $\phi = 0.995$ of the initial AR(1) process, and the infinite marginal skewness and kurtosis. In spite of these challenges, as it can be clearly seen in Figure 4.3, SQSTS substantially outperformed its competitors by delivering CIs for y_p with estimated coverage probabilities near the nominal value 0.95 based on substantially smaller average sample sizes, especially in the absence of a CI precision requirement. For instance, for $r^* = \infty$ and $p = 0.99$, SQSTS required an average sample size that is smaller by a factor of $18{,}133{,}822/2{,}578{,}084 \approx 7.03$ than the average sample size required by Sequest and smaller by a factor of about 3.84 than the average sample size required by Sequem. It should also be noted that for $r^* = 2.5\%$ and $p = 0.99$, SQSTS reported an approximately 50% smaller sample size on average than Sequem despite starting with a larger sample size by a a factor of $2^4/10 = 1.6$ than its competitor.

4.2.3 M/M/1 Waiting-Time Process

The third test process is the waiting-time sequence in an M/M/1 queueing system described in Section 2.5.3 with arrival rate $\lambda = 0.9$, service rate $\omega = 1$ (traffic intensity $\rho = \lambda/\omega = 0.9$) and FIFO service discipline. Y_k is the time spent by the kth entity in queue (prior to service).

The respective expected value is $\mu_X = \rho/(\omega - \lambda) = 9$.

To assess the ability of the heuristic approach in Step **[4]** that removes the first batch after completion of the loops in Steps **[2]**–**[3]**, we initialized the system with one entity in service and 112 entities in queue. The steady-state probability of this initial state is $(1 - \rho)\rho^{113} \approx 6.752 \times 10^{-7}$, implying a high probability for a prolonged transient phase.

For this process Sequest and Sequem outperformed their earlier competitors, such as the two-phase QI procedure of Chen and Kelton [25], with regard to sampling efficiency, but required substantial average sample sizes to deliver reliable CIs for quantiles with $p \geq 0.9$ (even in the absence of a CI precision requirement).

Table 4.3 and Figure 4.4 contain the experimental results for two levels of CI relative precision, $r^* = \infty$ and $r^* = 2\%$. A close examination of Figure 4.4 reveals that, in this test problem, SQSTS substantially outmatched its competitors, in particular under no CI precision requirement: while all methods delivered CIs with estimated coverage probabilities near the nominal value of 0.95, with the exception of Sequest for $p > 0.95$, SQSTS required substantially smaller sample sizes. For example, from Table 4.3 for $r^* = \infty$ and $p = 0.95$, we see that Sequest required 9,809,640/378,815 $\approx$ 25.9 more samples on average than SQSTS. The sample size reduction is less pronounced for $p \leq 0.7$, but remains significant. As we mentioned earlier, a partial explanation for the dominance of SQSTS in this experimental setting pertains to the effectiveness of the von Neumann and Shapiro–Wilk tests applied to the signed areas. Under the stringent $r^* = 2\%$ CI relative precision requirement, the ratio of the average sample sizes reflects the smaller asymptotic variance of the combined variance estimator $\widetilde{\mathscr{V}}_p(w_0; b, m)$.

4.2.4 M/H$_2$/1 Waiting-Time Process

The fourth test process is the sequence $\{Y_k : k \geq 1\}$ of entity waiting times in an M/H$_2$/1 queueing system described in Section 2.5.4 with FIFO queue discipline, an empty-and-idle initial state, arrival rate $\lambda = 1$; and i.i.d. service times from the hyperexponential distribution that is a mixture of two other exponential distributions with mixing probabilities $g = (5+\sqrt{15})/10 \approx 0.887$ and $1-g$ and associated service rates $\omega_1 = 2g\tau$ and $\omega_2 = 2(1-g)\tau$, with $\tau = 1.25$. The mean service time is 0.8 and the steady-state server utilization is $\rho = 0.8$.

Table 4.4 and Figure 5.7 display the experimental findings for two cases of CI relative precision, $r^* = \infty$ and $r^* = 2\%$. Figure 5.7 clearly indicates that under no precision requirement, SQSTS outshined its competitors with substantially smaller sample sizes required to obtain CIs with near-nominal estimated coverage probability. For instance, in Table 4.4 with $p = 0.95$, SQSTS reported an average sample size of 314,152, which is 5,352,998/314,152 = 17.04 times lower than the average sample size reported by Sequest and 5.41 times smaller than the average sample size required by Sequem. (As in the M/M/1 system, Sequest exhibited substantial CI undercoverage for $p = 0.99$ and 0.995 despite the very large average sample sizes.) This dominance of SQSTS with regard to average sample size is less noticeable under the $r^* = 2\%$ CI relative precision requirement. For example, when $p = 0.995$, SQSTS reported an average sample size of 17,775,197, which is nearly half the average sample size reported by Sequest and approximately 2.21 time smaller than the average sample size reported by Sequem (despite the lower initial sample sizes employed by the latter two methods).

4.2.5 M/M/1/LIFO Waiting-Time Process

The fifth test process is the sequence of entity delays $\{Y_k : k \geq 1\}$ in a single-server queueing system described in Section 2.5.5 with non-preemptive LIFO service discipline, empty-and-idle initial state, arrival rate $\lambda = 1$, and service rate $\omega = 1.25$. The steady-state server utilization is $\rho = 0.8$ and the marginal mean waiting time is $\mu_Y = 3.2$. This test process has caused trouble in the past to sequential methods for estimating the steady-state mean (Tafazzoli *et al.* [65], Alexopoulos *et al.* [40]).

Accurate approximations for y_p were obtained by computing the Laplace transform

$\mathscr{L}\{F; s\}$ of the marginal c.d.f., numerical inversion of $\mathscr{L}\{F; s\}$ using Euler's algorithm in Abate and Whitt [64] to obtain a piecewise-linear approximation of $F(\cdot)$, and direct inversion of the latter approximation; see Section 4.3 of Alexopoulos *et al.* [7] for details.

Table 4.5 and Figure 4.6 display the experimental outcomes for two levels of CI relative precision requirements, $r^* = \infty$ and $r^* = 2\%$. For this test process all three methods delivered 95% CIs with estimated coverage probabilities near the nominal value. Table 4.5 showcases that under no CI precision requirement, SQSTS outperformed its competitors with regard to average sample size, with the exception of $p \in \{0.3, 0.5\}$; in these cases the large initial batch size of SQSTS seems to be detrimental. It should be noted that such sample sizes are typically low for estimating quantiles of dependent processes. An examination of Figure 4.6 illustrates that under the tight 2% CI relative precision requirement, SQSTS dominated its competitors with noticeably smaller average sample sizes.

4.2.6 M/M/1/M/1 Waiting-Time Process

The sixth test process is constructed from the sequence $\{Y_k : k \geq 1\}$ of the total waiting times (prior to service) in a tandem network of two M/M/1 queues; see Section 2.5.6 for details. The system has an arrival rate of $\lambda = 1$, service rates $\omega = 1.25$ at each station, and is initialized in the empty and idle state. The steady-state utilization for each server is $\rho = \lambda/\omega = 0.8$ and the mean total delay on the system is equal to 8.

Table 4.6 and Figure 4.7 display the experimental results for two levels of CI relative precision, $r^* = \infty$ and $r^* = 2\%$. As noted in Section 4.3 of Alexopoulos *et al.* [23], under no CI precision requirement Sequest exhibited substantial slippage with regard to the estimated CI coverage probability for $p > 0.95$: despite the larger average sample sizes than Sequem, the estimated CI coverage probability dropped from 94.7% for $p = 0.95$ to 87% for $p = 0.99$ and to the unacceptable rate of 81.1% for $p = 0.995$.

An examination of Table 4.6 and Figure 4.7 reveals that SQSTS clearly outperformed its competitors with near-nominal estimated CI coverage rates and lower average sample sizes. The slightly low estimates of the CI coverage probabilities for $p = 0.995$ are within three standard errors off the nominal value.

4.2.7 Central Server Model 3

The last test process is described in Section 2.5.7 and is generated by a small computer network comprised of three stations, namely the Central Server Model 3 from Law and Carson [66].

Table 4.7 and Figures 4.8–4.9 display experimental results for two levels of CI precision, no precision and $r^* = 2\%$. The estimates reveal a variety of interesting findings:

(i) The accuracy of the point estimates delivered by SQSTS was on par with its competitors.

(ii) Under no CI precision requirement and for $p \leq 0.87$, we see from Table 4.7 that SQSTS required noticeably larger average sample sizes than Sequest; this is due to its larger initial batch size of 512 (versus 128). However, such sample sizes are not exorbitant for steady-state quantile estimation.

(iii) Under no CI precision requirement and for $p = 0.5$, Table 4.7 indicates that SQSTS exhibited a noticeable CI undercoverage rate with an estimate of 93%; we postulate that this is due to the skewness and kurtosis of the marginal density $f(\cdot)$. Section EC.3 of the e-companion of Alexopoulos *et al.* [7] contains a heuristic argument that attempts to explain the dependence of the marginal skewness of the BQEs $\{\widehat{y}_p(j,m) : j = 1, \ldots, b\}$ on p, $f(y_p)$, $f'(y_p)$, and on the structure of the stochastic dependence of the base process $\{Y_k : k \geq 1\}$. The close proximity of the estimated CI coverage probability (94.1%) of Sequest to the nominal value is likely due the adjustments employed by Sequest to the CI for y_p to compensate for excess skewness and kurtosis in the BQEs.

(iv) Under no CI precision requirement, the average sample sizes reported by SQSTS and Sequest exhibited an incline as p increased from 0.87 to 0.91 and a decline as p increased from 0.91 to 0.95; this variation was more prominent for Sequest. We believe that the heuristic discussion in item (iii) above provides a partial explanation for this sample-size variability, in particular with regard to Sequest.

(v) Under no CI precision requirement and for $p \in \{0.99, 0.995\}$, we see from Figure 4.8 that SQSTS reported average sample sizes which are larger by nearly an order of magnitude from the respective averages reported by Sequest.

(vi) Under the tight relative precision requirement of $r^* = 2\%$, SQSTS outperformed its competitors with respect to average sample size. In a few cases ($p \in \{0.5, 0.93, 0.99\}$), Figure 4.9 indicates that the CIs delivered by SQSTS exhibit slight undercoverage; this issue is a subject of ongoing investigation.

Overall, we judge the performance of SQSTS in this challenging test case as adequate.

4.3 Summary

In this chapter, we described SQSTS, the first fully automated sequential procedure for computing point estimators and CIs for steady-state quantiles of a stochastic process based on STSs. SQSTS estimates the variance parameter for the quantile process $\{\widetilde{y}_p(n) : n \geq 1\}$ by a linear combination of estimators computed from nonoverlapping batches: the first estimator is computed from the associated BQEs while the second estimator is obtained from STSs based on the batches. The core of SQSTS keeps the batch count constant and progressively increases the batch size until both the von Neumann and Shapiro–Wilk tests fail to reject the hypothesis that the signed areas associated with the batched STSs are i.i.d. normal r.v.'s. As detailed in Chapter 2 of this dissertation, the asymptotic i.i.d. normality of the signed areas, as the batch size $m \to \infty$, was established mainly under the GMC condition of Wu [8] and regularity conditions for the marginal density function.

Extensive experimentation with the test bed of output processes from Alexopoulos *et al.* [23, 7] highlighted the potential benefits of SQSTS over Sequest and Sequem: (i) under no CI precision requirement, SQSTS was frequently able to curtail excessive average sample sizes, often by an order of magnitude, despite its larger initial batch size—we believe that this dominance was partially due to the effectiveness of the von Neumann and Shapiro–Wilk tests for the signed areas; and (ii) under tight CI relative precision requirements, the lack of CI adjustments and lower standard deviation of the combined variance estimator allowed SQSTS to outperform its competitors with regard to average sample size in most cases. Moreover, SQSTS performed comparatively well against Sequest and Sequem with regard to average absolute bias of the point estimator and estimated CI coverage probability.

Table 4.1: Performance evaluation of SQSTS against Sequest (in bold typeface) and Sequem (in italic typeface) with regard to point and 95% CIs of y_p for the AR(1) process in Section 4.2.1 based on 1,000 independent replications.

p	y_p	Avg. |Bias|	Avg. 95% CI HL	Avg. 95% CI rel. prec. (%)	Avg. 95% CI cov. (%)	$\overline{m}$	$\overline{n}$
No CI prec. req.							
0.3	94.749	0.459	1.126	1.188	94.0	9,722	157,977
		0.580	**1.497**	**1.579**	**94.7**	**3,016**	**98,551**
0.5	100.000	0.519	1.261	1.261	93.7	7,320	118,956
		0.561	**1.458**	**1.457**	**94.9**	**2,997**	**97,752**
0.7	105.251	0.509	1.252	1.190	93.7	7,700	125,118
		0.559	**1.499**	**1.424**	**95.6**	**3,046**	**99,245**
0.9	112.832	0.471	1.156	1.024	94.2	12,245	198,985
		0.649	**1.716**	**1.521**	**95.6**	**3,138**	**102,220**
0.95	116.469	0.472	1.177	1.010	94.7	15,217	247,276
		0.737	**1.901**	**1.633**	**95.3**	**3,271**	**106,485**
		0.614	*1.594*	*1.369*	*93.4*		*207,766*
0.99	123.293	0.286	0.715	0.580	94.5	87,749	1,425,914
		1.056	**2.457**	**1.995**	**91.0**	**3,661**	**119,018**
		0.385	*0.975*	*0.791*	*95.2*		*1,789,741*
0.995	125.791	0.305	0.765	0.608	94.5	111,485	1,811,627
		1.276	**2.780**	**2.213**	**90.2**	**4,121**	**133,743**
		0.308	*0.772*	*0.614*	*94.1*		*4,324,081*
CI prec. req. $r^* = 0.5\%$							
0.3	94.749	0.182	0.450	0.475	95.3	13,464	839,705
		0.163	**0.428**	**0.452**	**96.4**	**34,929**	**1,119,707**
0.5	100.000	0.198	0.477	0.477	94.1	11,109	698,901
		0.183	**0.452**	**0.452**	**94.3**	**29,508**	**946,075**
0.7	105.251	0.209	0.500	0.475	94.1	10,825	670,115
		0.191	**0.475**	**0.451**	**95.4**	**28,177**	**903,434**
0.9	112.832	0.223	0.529	0.469	95.5	14,220	818,735
		0.199	**0.510**	**0.452**	**95.8**	**32,720**	**1,048,849**
0.95	116.469	0.226	0.545	0.468	94.8	17,344	1,001,216
		0.196	**0.523**	**0.450**	**96.3**	**40,111**	**1,285,409**
		0.212	*0.530*	*0.455*	*94.7*		*1,421,778*
0.99	123.293	0.238	0.567	0.460	94.4	87,757	2,013,577
		0.216	**0.556**	**0.451**	**95.0**	**74,491**	**2,385,618**
		0.229	*0.545*	*0.442*	*93.6*		*3,734,704*
0.995	125.791	0.238	0.579	0.461	93.6	111,543	2,781,998
		0.224	**0.564**	**0.448**	**95.6**	**106,578**	**3,412,348**
		0.225	*0.540*	*0.430*	*93.7*		*6,178,909*

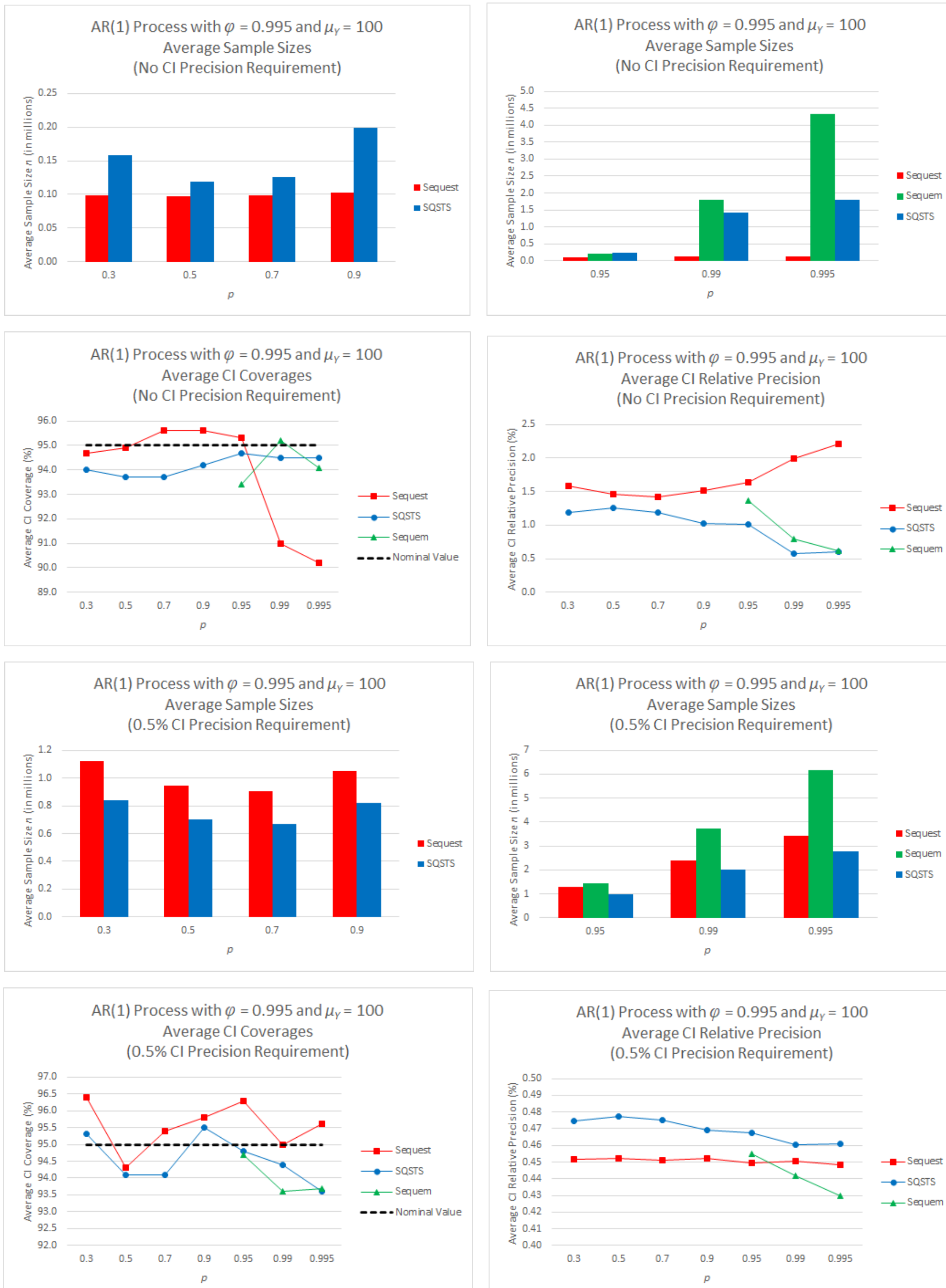

Figure 4.2: Plots of the estimates for sample sizes, CI relative precision, and coverage probability for the AR(1) process from Table 4.1.

Table 4.2: Performance evaluation of SQSTS against Sequest (in bold typeface) and Sequem (in italic typeface) with regard to point and 95% CIs of y_p for the ARTOP process in Section 4.2.2 based on 1,000 independent replications.

p	y_p	Avg. |Bias|	Avg. 95% CI HL	Avg. 95% CI rel. prec. (%)	Avg. 95% CI cov. (%)	$\overline{m}$	$\overline{n}$
No CI prec. req.							
0.300	1.185	0.009	0.024	2.038	95.0	20,848	338,776
		0.004	**0.013**	**1.116**	**97.1**	**41,866**	**1,341,069**
0.500	1.391	0.017	0.045	3.244	94.8	19,429	315,726
		0.009	**0.025**	**1.832**	**96.9**	**36,858**	**1,180,865**
0.700	1.774	0.032	0.083	4.654	94.7	21,161	343,862
		0.016	**0.044**	**2.482**	**97.6**	**43,999**	**1,409,450**
0.900	2.994	0.079	0.211	7.021	95.8	29,202	474,533
		0.032	**0.087**	**2.903**	**95.8**	**96,589**	**3,092,677**
0.950	4.164	0.135	0.368	8.811	96.1	33,958	551,823
		0.046	**0.125**	**3.001**	**96.3**	**159,321**	**5,100,396**
		0.085	*0.247*	*5.943*	*96.7*		*1,903,394*
0.990	8.962	0.245	0.662	7.382	94.8	158,651	2,578,084
		0.100	**0.268**	**2.991**	**96.0**	**566,595**	**18,133,822**
		0.177	*0.471*	*5.253*	*95.7*		*9,894,374*
0.995	12.466	0.412	1.107	8.886	94.5	188,485	3,062,888
		0.136	**0.376**	**3.017**	**95.1**	**917,832**	**29,373,651**
		0.243	*0.636*	*5.101*	*96.2*		*19,341,046*
CI prec. req. $r^* = 2.5\%$							
0.300	1.185	0.008	0.020	1.721	95.1	20,861	408,985
		0.004	**0.013**	**1.113**	**97.1**	**41,884**	**1,341,637**
0.500	1.391	0.010	0.026	1.855	95.7	20,066	767,613
		0.009	**0.024**	**1.734**	**96.6**	**37,862**	**1,212,989**
0.700	1.774	0.013	0.033	1.878	96.0	27,645	1,579,259
		0.013	**0.037**	**2.080**	**96.9**	**51,603**	**1,652,781**
0.900	2.994	0.024	0.057	1.902	94.2	72,412	4,589,273
		0.025	**0.065**	**2.157**	**95.2**	**137,164**	**4,391,066**
0.950	4.164	0.033	0.079	1.904	95.9	127,335	8,126,953
		0.036	**0.091**	**2.175**	**95.2**	**237,505**	**7,602,293**
		0.038	*0.094*	*2.257*	*94.0*		*7,838,045*
0.990	8.962	0.085	0.212	2.366	95.2	300,817	18,832,429
		0.076	**0.195**	**2.180**	**95.4**	**833,521**	**26,675,482**
		0.085	*0.200*	*2.234*	*94.1*		*36,308,107*
0.995	12.466	0.120	0.295	2.365	94.3	507,755	32,340,386
		0.107	**0.273**	**1.193**	**95.4**	**1,387,032**	**44,388,041**
		0.117	*0.278*	*2.229*	*94.0*		*67,186,848*

Figure 4.3: Plots of the estimates for sample sizes, CI relative precision, and coverage probability for the ARTOP process from Table 4.2.

Table 4.3: Performance evaluation of SQSTS against Sequest (in bold typeface) and Sequem (in italic typeface) with regard to point and 95% CIs of y_p for the M/M/1 waiting-time process in Section 4.2.3 based on 1,000 independent replications.

p	y_p	Avg. |Bias|	Avg. 95% CI HL	Avg. 95% CI rel. prec. (%)	Avg. 95% CI cov. (%)	$\overline{m}$	$\overline{n}$
No CI prec. req.							
0.300	2.513	0.055	0.150	5.974	96.3	37,483	609,093
		0.034	**0.095**	**3.801**	**96.6**	**56,354**	**1,806,090**
0.500	5.878	0.124	0.348	5.901	96.0	30,694	498,777
		0.007	**0.185**	**3.149**	**96.6**	**64,229**	**2,058,446**
0.700	10.986	0.291	0.808	7.277	96.0	27,231	442,498
		0.111	**0.311**	**2.839**	**96.0**	**81,992**	**2,627,562**
0.900	21.972	0.717	1.948	8.827	95.3	22,018	357,785
		0.204	**0.527**	**2.400**	**96.0**	**183,093**	**5,864,109**
0.950	28.904	1.031	2.634	9.088	93.7	23,312	378,815
		0.274	**0.654**	**2.268**	**95.0**	**306,385**	**9,809,640**
		0.584	*1.529*	*5.314*	*95.0*		*2,960,055*
0.990	44.998	0.983	2.472	5.498	93.8	152,099	2,471,614
		0.777	**1.055**	**2.371**	**90.0**	**1,008,926**	**32,290,677**
		0.680	*1.737*	*3.866*	*96.3*		*15,309,534*
0.995	51.930	1.262	3.128	6.027	92.7	176,113	2,861,834
		1.322	**1.357**	**2.666**	**86.0**	**1,467,551**	**46,966,504**
		0.715	*1.776*	*3.424*	*95.4*		*30,444,573*
CI prec. req. $r^* = 2\%$							
0.300	2.513	0.020	0.048	1.896	95.1	71,132	4,528,399
		0.017	**0.045**	**1.777**	**95.6**	**186,504**	**5,970,862**
0.500	5.878	0.047	0.111	1.893	94.6	56,470	3,576,460
		0.039	**0.105**	**1.783**	**95.6**	**148,044**	**4,740,512**
0.700	10.986	0.087	0.208	1.891	94.6	58,612	3,731,135
		0.075	**0.194**	**1.768**	**95.8**	**156,768**	**5,020,393**
0.900	21.972	0.169	0.416	1.893	94.6	85,310	5,461,971
		0.146	**0.377**	**1.717**	**95.1**	**257,961**	**8,259,880**
0.950	28.904	0.226	0.547	1.892	94.1	117,098	7,500,116
		0.184	**0.483**	**1.671**	**95.9**	**384,836**	**12,320,089**
		0.209	*0.522*	*1.808*	*95.7*		*11,158,913*
0.990	44.998	0.357	0.845	1.879	93.0	290,332	18,479,751
		0.266	**0.700**	**1.556**	**96.1**	**1,177,202**	**37,675,497**
		0.318	*0.795*	*1.767*	*95.5*		*37,861,128*
0.995	51.930	0.417	0.974	1.877	93.6	441,517	28,290,323
		0.312	**0.808**	**1.558**	**95.8**	**1,796,989**	**57,508,525**
		0.368	*0.900*	*1.734*	*95.1*		*64,312,254*

Figure 4.4: Plots of the estimates for sample sizes, CI relative precision, and coverage probability for the M/M/1 waiting-time process from Table 4.3.

Table 4.4: Performance evaluation of SQSTS against Sequest (in bold typeface) and Sequem (in italic typeface) with regard to point and 95% CIs of y_p for the M/H_2/1 waiting-time process in Section 4.2.4 based on 1,000 independent replications.

p	y_p	Avg. |Bias|	Avg. 95% CI HL	Avg. 95% CI rel. prec. (%)	Avg. 95% CI cov. (%)	$\overline{m}$	$\overline{n}$
No CI prec. req.							
0.300	0.669	0.032	0.094	13.973	96.0	22,650	368,063
		0.013	**0.036**	**5.360**	**95.7**	**85,629**	**2,740,816**
0.500	3.847	0.150	0.399	10.349	94.6	16,062	261,001
		0.072	**0.200**	**5.207**	**96.8**	**39,164**	**1,254,058**
0.700	9.606	0.326	0.868	8.998	95.5	14,621	237,598
		0.126	**0.353**	**3.678**	**96.0**	**46,571**	**1,491,189**
0.900	22.011	0.736	1.895	8.595	95.0	15,422	250,613
		0.223	**0.607**	**2.763**	**96.1**	**98,903**	**3,166,001**
0.950	29.837	0.972	2.491	8.355	94.0	19,332	314,152
		0.312	**0.755**	**2.536**	**95.0**	**167,246**	**5,352,998**
		0.594	*1.708*	*5.751*	*96.1*		*1,698,441*
0.990	48.010	0.939	2.371	4.936	94.9	122,859	1,996,451
		0.903	**1.209**	**2.551**	**88.9**	**575,488**	**18,416,822**
		0.755	*1.886*	*3.940*	*95.0*		*8,859,686*
0.995	55.837	1.149	2.924	5.229	94.5	158,175	2,570,337
		1.358	**1.487**	**2.713**	**86.0**	**895,356**	**28,652,597**
		0.795	*2.048*	*3.675*	*94.9*		*17,162,987*
CI prec. req. $r^* = 2\%$							
0.300	0.669	0.005	0.013	1.910	94.7	210,335	13,467,079
		0.005	**0.012**	**1.797**	**94.7**	**559,132**	**17,892,922**
0.500	3.847	0.030	0.074	1.913	94.5	87,509	5,604,582
		0.027	**0.069**	**1.794**	**94.9**	**233,039**	**7,458,036**
0.700	9.606	0.074	0.183	1.905	95.2	53,214	3,408,128
		0.066	**0.172**	**1.794**	**94.9**	**140,522**	**4,497,635**
0.900	22.011	0.170	0.418	1.900	95.2	60,084	3,847,939
		0.148	**0.386**	**1.754**	**95.4**	**171,509**	**5,489,375**
0.950	29.837	0.233	0.566	1.898	95.8	78,268	5,013,977
		0.200	**0.511**	**1.713**	**95.2**	**240,091**	**7,684,059**
		0.214	*0.538*	*1.805*	*94.5*		*7,631,701*
0.990	48.010	0.365	0.900	1.875	94.9	188,828	11,784,581
		0.272	**0.758**	**1.579**	**95.9**	**703,708**	**22,519,866**
		0.339	*0.848*	*1.767*	*94.1*		*23,491,128*
0.995	55.837	0.436	1.049	1.878	94.2	279,123	17,775,197
		0.325	**0.870**	**1.559**	**95.7**	**1,099,249**	**35,177,170**
		0.386	*0.972*	*1.741*	*93.8*		*39,279,619*

Figure 4.5: Plots of the estimates for sample sizes, CI relative precision, and coverage probability for the $M/H_2/1$ waiting-time process from Table 4.4.

Table 4.5: Performance evaluation of SQSTS against Sequest (in bold typeface) and Sequem (in italic typeface) with regard to point and 95% CIs of y_p for the M/M/1/LIFO waiting-time process in Section 4.2.5 based on 1,000 independent replications.

p	y_p	Avg. |Bias|	Avg. 95% CI HL	Avg. 95% CI rel. prec. (%)	Avg. 95% CI cov. (%)	$\overline{m}$	$\overline{n}$
No CI prec. req.							
0.300	0.113	0.005	0.013	11.504	95.0	3,616	58,757
		0.007	**0.019**	**16.587**	**96.3**	**1,039**	**33,630**
0.500	0.469	0.009	0.024	5.102	94.5	3,375	54,842
		0.013	**0.036**	**7.657**	**97.1**	**964**	**31,227**
0.700	1.358	0.022	0.056	4.120	94.7	4,413	71,716
		0.023	**0.063**	**4.612**	**96.0**	**2,355**	**75,709**
0.900	6.718	0.125	0.324	4.829	95.9	7,523	122,251
		0.083	**0.234**	**3.477**	**95.9**	**9,040**	**289,601**
0.950	14.405	0.292	0.773	5.366	95.8	9,931	161,386
		0.169	**0.490**	**3.403**	**96.7**	**15,617**	**500,097**
		0.307	*0.871*	*6.056*	*96.4*		*208,045*
0.990	49.582	0.795	2.015	4.062	95.6	45,073	732,442
		0.561	**1.575**	**3.179**	**96.1**	**47,679**	**1,526,164**
		0.902	*2.513*	*5.067*	*97.0*		*1,038,381*
0.995	71.844	1.218	3.186	4.430	95.1	56,246	913,998
		0.826	**2.158**	**3.004**	**95.3**	**80,022**	**2,561,157**
		1.166	*3.263*	*4.541*	*97.2*		*2,088,031*
CI prec. req. $r^* = 2\%$							
0.300	0.113	0.001	0.002	1.914	94.0	27,493	1,760,476
		0.001	**0.002**	**1.803**	**95.9**	**73,070**	**2,338,645**
0.500	0.469	0.004	0.009	1.898	95.8	5,209	321,943
		0.003	**0.008**	**1.790**	**95.6**	**13,108**	**419,824**
0.700	1.358	0.010	0.026	1.883	95.5	5,121	277,689
		0.009	**0.024**	**1.796**	**95.7**	**10,839**	**347,201**
0.900	6.718	0.051	0.127	1.888	95.2	10,341	624,688
		0.046	**0.120**	**1.785**	**95.3**	**24,780**	**793,280**
0.950	14.405	0.111	0.274	1.899	95.2	16,222	1,022,400
		0.097	**0.257**	**1.782**	**95.4**	**41,617**	**1,332,079**
		0.104	*0.261*	*1.815*	*95.4*		*1,513,981*
0.990	49.582	0.386	0.931	1.877	95.1	52,032	2,792,264
		0.342	**0.883**	**1.781**	**96.2**	**112,097**	**3,587,515**
		0.370	*0.888*	*1.792*	*94.1*		*5,514,620*
0.995	71.844	0.543	1.350	1.880	95.7	70,315	4,070,692
		0.488	**1.267**	**1.764**	**95.9**	**168,645**	**5,397,092**
		0.537	*1.287*	*1.792*	*94.3*		*8,827,362*

Figure 4.6: Plots of the estimates for sample sizes, CI relative precision, and coverage probability for the M/M/1/LIFO waiting-time process from Table 4.5.

Table 4.6: Performance evaluation of SQSTS against Sequest (in bold typeface), and Sequem (in italic typeface) with regard to point and 95% CIs of y_p for the M/M/1/M/1 total waiting-time process in Section 4.2.6 based on 1,000 independent replications.

p	y_p	Avg. |Bias|	Avg. 95% CI HL	Avg. 95% CI rel. prec. (%)	Avg. 95% CI cov. (%)	$\overline{m}$	$\overline{n}$
No CI prec. req.							
0.300	2.748	0.058	0.152	5.544	95.3	9,214	149,724
		0.041	**0.111**	**4.057**	**96.4**	**10,571**	**338,750**
0.500	5.079	0.098	0.260	5.113	95.0	8,439	137,135
		0.063	**0.172**	**3.391**	**96.5**	**11,505**	**368,704**
0.700	8.126	0.152	0.438	5.379	96.1	7,995	129,921
		0.088	**0.240**	**2.961**	**96.4**	**15,734**	**504,095**
0.900	13.931	0.288	0.754	5.407	94.8	10,271	166,906
		0.138	**0.347**	**2.493**	**95.4**	**35,988**	**1,152,326**
0.950	17.349	0.351	0.917	5.290	95.4	13,662	222,008
		0.183	**0.430**	**2.481**	**94.7**	**59,728**	**1,912,034**
		0.304	*0.833*	*4.812*	*95.0*		*652,442*
0.990	24.928	0.319	0.788	3.161	95.4	91,639	1,489,131
		0.501	**0.703**	**2.858**	**87.6**	**201,486**	**6,448,335**
		0.324	*0.816*	*3.280*	*94.9*		*3,701,075*
0.995	28.096	0.384	0.943	3.355	93.4	118,687	1,928,664
		0.771	**0.864**	**3.142**	**81.1**	**329,066**	**10,530,896**
		0.329	*0.834*	*2.969*	*94.8*		*7,224,510*
CI prec. req. $r^* = 2\%$							
0.300	2.748	0.022	0.052	1.896	94.5	15,495	976,761
		0.019	**0.049**	**1.793**	**96.7**	**38,778**	**1,241,390**
0.500	5.079	0.041	0.096	1.889	94.7	12,430	756,582
		0.034	**0.091**	**1.787**	**95.2**	**30,275**	**969,348**
0.700	8.126	0.064	0.154	1.890	95.1	12,447	759,540
		0.053	**0.144**	**1.771**	**96.0**	**31,373**	**1,004,546**
0.900	13.931	0.109	0.263	1.887	93.8	17,007	1,059,133
		0.088	**0.237**	**1.703**	**96.2**	**50,537**	**1,617,912**
0.950	17.349	0.136	0.328	1.890	94.7	22,851	1,433,861
		0.108	**0.286**	**1.649**	**96.5**	**76,926**	**2,462,381**
		0.123	*0.312*	*1.799*	*95.1*		*2,158,319*
0.990	24.928	0.191	0.462	1.853	94.0	84,576	3,692,005
		0.142	**0.374**	**1.503**	**96.0**	**250,911**	**8,029,952**
		0.176	*0.436*	*1.747*	*94.3*		*7,493,148*
0.995	28.096	0.208	0.520	1.853	93.8	124,712	5,640,097
		0.155	**0.413**	**1.472**	**94.8**	**414,067**	**13,250,919**
		0.191	*0.482*	*1.717*	*94.3*		*12,731,353*

Figure 4.7: Plots of the estimates for sample sizes, CI relative precision, and coverage probability for the M/M/1/M/1 total waiting-time process from Table 4.6.

Table 4.7: Performance evaluation of SQSTS against Sequest (in bold typeface) and Sequem (in italic typeface) with regard to point and 95% CIs of y_p for the Response-Time process in the Central Server Model 3 in Section 4.2.7 based on 1,000 independent replications.

p	y_p	Avg. |Bias|	Avg. 95% CI HL	Avg. 95% rel. prec. (%)	Avg. 95% CI cov. (%)	$\overline{m}$	$\overline{n}$
No CI prec. req.							
0.300	7.078	0.178	0.435	6.140	93.0	3,972	64,549
		0.230	**0.572**	**8.036**	**94.4**	**1,244**	**40,502**
0.500	10.771	0.222	0.527	4.891	93.0	3,233	52,532
		0.263	**0.641**	**5.931**	**94.1**	**1,190**	**38,760**
0.700	15.364	0.188	0.470	3.061	93.7	4,355	70,764
		0.260	**0.686**	**4.460**	**95.1**	**1,142**	**37,168**
0.800	18.868	0.159	0.399	2.114	93.6	5,592	90,868
		0.250	**0.720**	**3.816**	**97.1**	**1,048**	**34,093**
0.850	21.631	0.138	0.364	1.683	95.3	5,823	94,626
		0.232	**0.731**	**3.382**	**98.0**	**948**	**30,675**
0.870	23.236	0.115	0.309	1.329	95.9	7,554	122,751
		0.155	**0.477**	**2.052**	**97.4**	**2,032**	**65,372**
0.890	25.514	0.095	0.251	0.985	96.1	15,798	256,720
		0.091	**0.255**	**0.999**	**96.9**	**9,582**	**306,988**
0.900	27.181	0.108	0.300	1.102	96.3	21,398	347,722
		0.071	**0.193**	**0.709**	**96.2**	**30,581**	**979,010**
0.910	29.648	0.188	0.576	1.940	96.4	22,543	366,316
		0.067	**0.185**	**0.624**	**96.2**	**99,104**	**3,171,779**
0.930	44.766	2.041	4.594	10.163	92.8	7,032	114,271
		0.871	**2.046**	**4.551**	**93.2**	**30,613**	**980,176**
0.950	74.481	3.052	7.323	9.838	93.7	4,134	67,176
		3.304	**8.339**	**11.105**	**94.9**	**1,839**	**59,421**
		3.290	*8.565*	*11.523*	*95.4*		*76,294*
0.990	166.528	1.562	4.041	2.430	94.2	27,104	440,432
		4.954	**13.090**	**7.854**	**96.1**	**1,478**	**47,958**
		2.231	*6.398*	*3.850*	*97.0*		*421,463*
0.995	196.230	1.781	4.546	2.319	95.5	31,020	504,081
		5.748	**15.039**	**7.658**	**95.9**	**1,758**	**56,950**
		1.762	*5.182*	*2.643*	*97.0*		*1,036,913*
CI prec. req. $r^* = 2\%$							
0.300	7.078	0.056	0.136	1.916	94.3	8,741	556,478
		0.052	**0.128**	**1.809**	**95.0**	**23,744**	**760,490**
0.500	10.771	0.090	0.206	1.913	92.3	4,764	293,162
		0.080	**0.195**	**1.805**	**93.5**	**12,783**	**409,717**
0.700	15.364	0.120	0.287	1.865	93.9	4,415	153,859
		0.108	**0.276**	**1.795**	**95.0**	**6,122**	**196,531**
0.800	18.868	0.135	0.331	1.752	93.9	5,594	111,179
		0.129	**0.334**	**1.771**	**96.0**	**3,681**	**118,358**
0.850	21.631	0.131	0.339	1.564	95.3	5,823	100,013
		0.141	**0.381**	**1.762**	**96.1**	**2,563**	**82,370**
0.870	23.236	0.115	0.307	1.319	95.9	7,554	123,237
		0.141	**0.392**	**1.689**	**97.3**	**2,492**	**80,072**
0.890	25.514	0.095	0.251	0.985	96.1	15,798	256,720
		0.091	**0.254**	**0.995**	**96.9**	**9,590**	**307,241**
0.900	27.181	0.108	0.298	1.095	96.3	21,400	348,987
		0.071	**0.193**	**0.709**	**96.2**	**30,581**	**979,010**
0.910	29.648	0.166	0.483	1.631	96.3	22,605	443,819
		0.067	**0.185**	**0.624**	**96.2**	**99,104**	**3,171,779**
0.930	44.766	0.372	0.855	1.915	93.7	44,045	2,820,610
		0.321	**0.804**	**1.801**	**95.2**	**124,853**	**3,995,832**
0.950	74.481	0.592	1.425	1.916	94.0	24,869	1,592,628
		0.535	**1.342**	**1.803**	**95.1**	**67,765**	**2,169,067**
		0.533	*1.355*	*1.822*	*96.1*		*2,530,587*
0.990	166.528	1.244	3.069	1.845	93.6	27,104	661,011
		1.235	**2.988**	**1.797**	**94.2**	**24,203**	**775,168**
		1.162	*2.979*	*1.791*	*96.1*		*1,284,382*
0.995	196.230	1.413	3.568	1.820	94.9	31,023	701,700
		1.400	**3.527**	**1.799**	**96.0**	**24,247**	**776,614**
		1.328	*3.430*	*1.749*	*95.0*		*1,594,629*

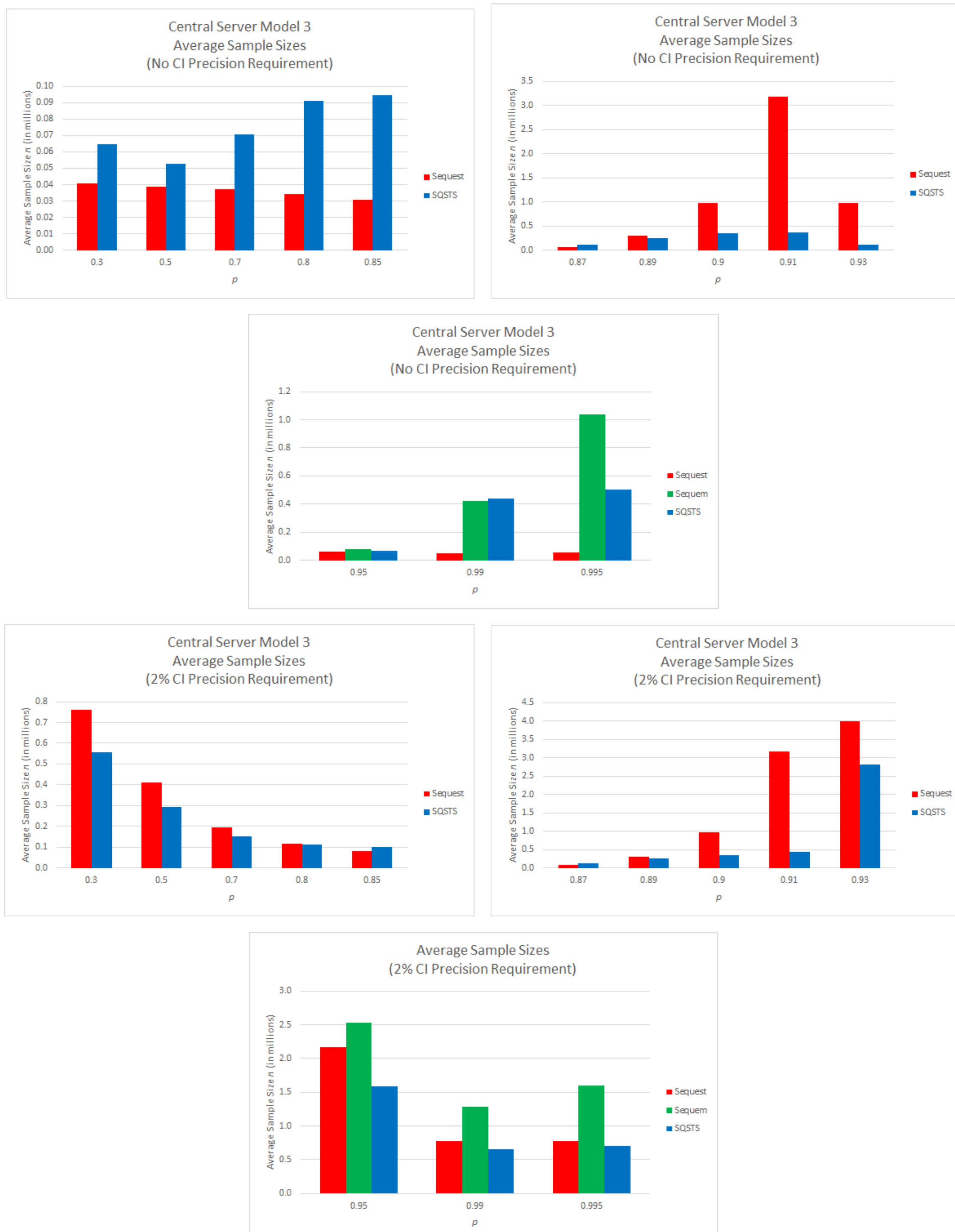

Figure 4.8: Plots of the estimates for sample sizes for the response-time process in the Central Server Model 3 from Table 4.7.

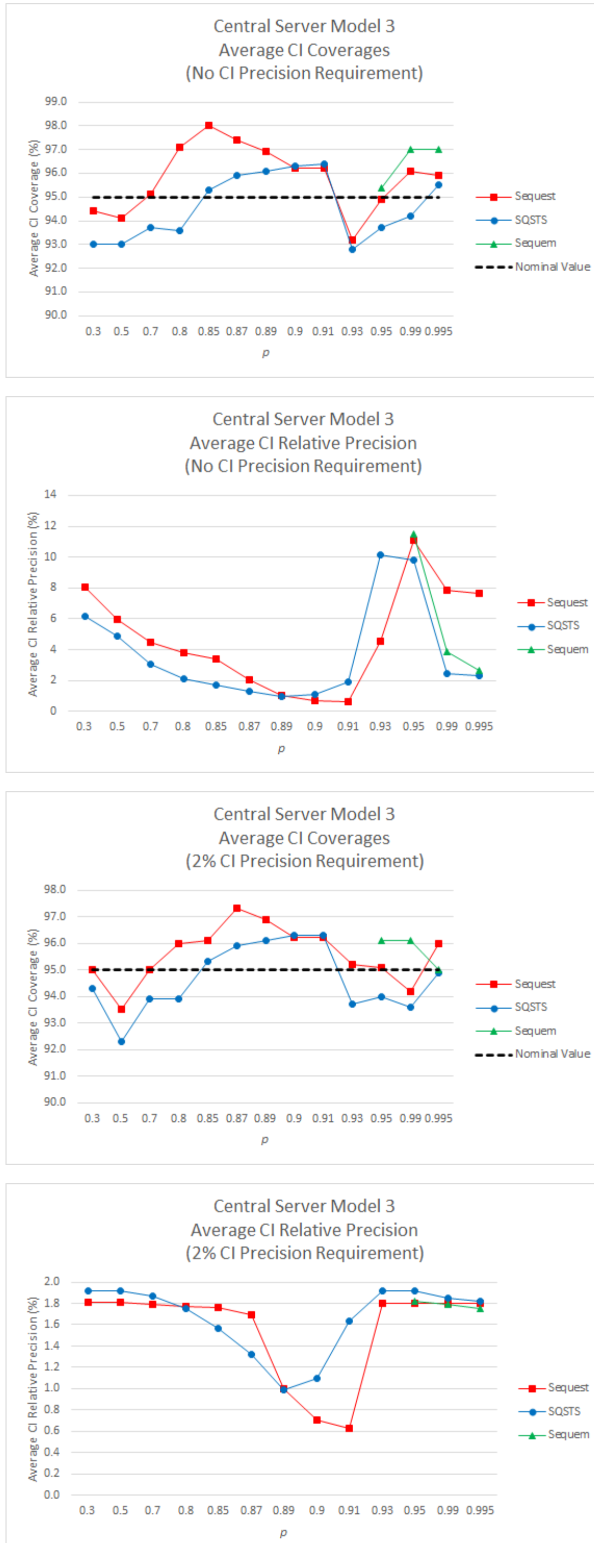

Figure 4.9: Plots of the estimates for CI relative precision and coverage probability for the response-time process in the Central Server Model 3 from Table 4.7.

CHAPTER 5

FQUEST: A FIXED-SAMPLE-SIZE METHOD FOR ESTIMATING STEADY-STATE QUANTILES BASED ON A SINGLE SAMPLE PATH

While sequential estimation methods have their own merit, users are often constrained by simulation models that are not integrated with the underlying sequential method or by datasets that are limited due to budget limitations. For example, when the implementation of the Sequest method (Alexopoulos *et al.* [7]) in the Sequest app [41] encounters a failed statistical test or an insufficient sample size to compute a CI with a given precision, it reports an estimate of the additional observations that should be generated and halts. When the data are generated by a simulation model, the user may have to restart the model and rerun Sequest from scratch; and this cycle may need to be repeated multiple times until the method can terminate successfully.

As noted in Chapter 1, the literature contains a few fixed-sample-size procedures for estimating the steady-state mean; see Law [4]. The most efficient is the N-Skart procedure of Tafazzoli *et al.* [42] which is based on a single run and applies the randomness test of von Neumann [43] to batch means computed from dynamically reconstructed batches with intervening "spacers." If the method determines that additional data are required, it seeks permission from the user to proceed with the computation of a CI that employs adjustments for the residual lag-1 autocorrelation and skewness between the batch means. The latter CI is delivered by default when the sample size is sufficient to pass the randomness test with an appropriate set of spaced batch means.

To the best of our knowledge, no commercial simulation software contains a fixed-sample-size procedure for computing CIs for steady-state quantiles. Both Arena [44] and Simio [45] incorporate a rudimentary procedure for estimating the steady-state *mean* based on a single replication with a given length. The procedure uses the method of nonoverlapping batch means (Fishman [2]) and a simple rebatching scheme that ends up with a batch count between 20 and 39. The respective batch means are subjected to the one-sided randomness test of von Neumann [43] with type-I error 0.10 (to guard against positive autocorrelation among the batch means). If the batch means pass the test, the method delivers a CI based on Student's t ratio; otherwise, it delivers an exorbitant CI HL indicating that the batch means failed the randomness test. Unfortunately, neither package incorporates a method for computing CIs for steady-state quantiles based on a sufficiently long run or replicated sample paths. Simio computes nonparametric CIs from replicate statistics, such as the average cycle time or average waiting time in a buffer, but, to this day, it does not even have a function that computes a sample quantile from a tally statistic collected during a replication.

In this chapter, we present and assess FQUEST, a fully automated fixed-sample-size procedure for computing CIs for steady-state quantiles based on a single run. To the best of our knowledge, FQUEST is the first such method that (i) uses the STS methodology; (ii) addresses the simulation initialization problem; and (iii) warns the user when the dataset is insufficient and, subject to user's approval, delivers a heuristic CI. We substantiate our claim with a synopsis of a few methods from the literature. Methods based on regenerative cycles (Iglehart [9], Moore [10], Seila [11], Seila [12]) can address the simulation initialization problem but do not lie within our scope because the number of cycles that can be completed within a finite limit N on the sample size may be insufficient so as to ensure good performance of the point estimators and CIs for the quantile of interest. This challenge escalates for extreme quantiles Seila [12].

Heidelberger and Lewis [30] presented three procedures for estimating steady-state quantiles, the first based on the spectral method and the last two based on empirical quantiles computed from groups of nonoverlapping batches. The estimation of the p-quantile was reduced to the estimation of the p^v-quantile of a sequence composed of the maxima of v spaced observations, where $v \approx \lfloor \ln(q)/\ln(p) \rfloor$ and q is a value away from 0 or 1. The authors provided no recommendations for the spacing between the observations or the number of groups. Although their experimentation was based on stationary processes, the CIs generated by all methods exhibited substantial undercoverage for waiting-time processes generated by single-server queues with traffic intensity 0.9 and large values of the associated probability p.

The indirect method of Bekki *et al.* [13] also assumes that the initial transient phase has been eliminated and computes point estimators and CIs for a set of selected quantiles. This fixed-sample-size method estimates a given quantile by a four-term Cornish-Fisher expansion (Fisher and Cornish [14]) based on the respective standard normal quantile and the first four sample moments of the time series. The method has the advantage of estimating multiple quantiles simultaneously without storing or sorting data. However, a sample moment computed from strongly correlated data often requires a large sample for accurate estimation of the associated true moment, and this problem worsens for higher-order moments. The impact of this problem is evident with use of sample sizes of 30 and 60 million to estimate job cycle times in simple queueing systems with server utilizations below and above 90%, respectively. In addition, this method may yield unreliable point estimates of quantiles if the marginal density exhibits highly nonnormal behavior. This issue was partially rectified in Bekki *et al.* [15] by combining the Cornish-Fisher expansion with a Box-Cox transformation. Furthermore, the Cornish-Fisher expansion is known to produce less reliable approximations as the probability p approaches zero or one (extreme quantile estimation), cf. Bekki *et al.* [13]. Notably, the latter three methods do not address the issues in items (ii) and (iii) above.

The user provides a (simulation-generated) dataset of arbitrary size and specifies the required quantile and nominal coverage probability of the anticipated CI. FQUEST incorporates the simulation analysis methods of batching, STS, and sectioning. When the sample size is sufficiently large, FQUEST delivers (i) the empirical quantile from a truncated dataset that is nearly free of initialization bias; and (ii) a CI based on an estimator for the variance parameter associated with the quantile process computed from the batched STSs, the BQEs, and the empirical quantile in item (i) above. Otherwise, the method returns a warning message and, subject to the user's agreement, computes a point estimate and a heuristic CI formed by a set of CIs based on the empirical quantile of the truncated sample, the BQEs, and the batched STSs.

The theoretical foundations of FQUEST are in Chapter 2, with Theorem 2.3.4 forming the basis for some of the statistical tests in FQUEST. The method draws elements from three procedures: (i) the SQSTS method introduced in Chapter 4 of this dissertation; (ii) the Sequest method of Alexopoulos *et al.* [7]; and (iii) the N-Skart method of Tafazzoli *et al.* [42]. However, since the aforementioned methods have different objectives, FQUEST delineates from all three and has significant differences with regard to its scope, structure, and the computation of the final CI. These differences will become transparent in Section 5.2. The remainder of this chapter is organized as follows. Section 5.1 presents and describes an approximate CI from the BQEs $\{\widehat{y}_p(j,m) : j = 1,\dots,b\}$ computed from b nonoverlapping batches and the full-sample estimator $\widetilde{y}_p(n)$ using adjustments for residual skewness and lag-1 autocorrelation in the BQEs that FQUEST may incorporate in its final stage. Section 5.2 contains a formal algorithmic statement of FQUEST. Section 5.3 contains an experimental performance evaluation of FQUEST using a test bed of seven challenging processes (two of them with two sets of parameters, for a total of nine experiments) as well as an informal comparison of FQUEST against the SQSTS procedure. Section 5.4 concludes with a short summary of the contributions and performance of FQUEST.

5.1 An Approximate Correlation- and Skewness-Adjusted Confidence Interval

FQUEST employs statistical tests to assess the asymptotic properties related to Equations (2.9) and (2.17). When any of the statistical tests fails and the size of the dataset limits the ability to increase the batch size (subject to approval by the user), FQUEST may also construct an approximate CI from the BQEs $\{\widehat{y}_p(j,m) : j = 1,\dots,b\}$ and the full-sample estimator $\widetilde{y}_p(n^*)$ based on a truncated sample of size n^* using adjustments for residual skewness and lag-1 autocorrelation in the BQEs. The steps below are based on Willink [88], Tafazzoli *et al.* [42], and Alexopoulos *et al.* [7].

First, we calculate the sample skewness of the BQEs

$$\widehat{B}_{\widehat{y}_p}(b,m) \equiv \frac{b}{(b-1)(b-2)} \sum_{j=1}^{b} \left[\frac{\widehat{y}_p(j,m) - \overline{\overline{y}}_p(b,m)}{S_p(b,m)} \right]^3,$$

where $S_p^2(b,m)$ is the sample variance of the BQEs in Equation (2.52).Then we compute the skewness-adjustment parameter

$$\vartheta \equiv \frac{\widehat{B}_{\widehat{y}_p}(b,m)}{6\sqrt{b}}$$

and define the skewness-adjustment function

$$G(\zeta) \equiv \begin{cases} \zeta & \text{if } |\vartheta| \leq 0.001, \\ \frac{[1+6\vartheta(\zeta-\vartheta)]^{1/3}-1}{2\vartheta} & \text{if } |\vartheta| > 0.001, \end{cases}$$

for all real ζ. The sample lag-1 autocorrelation of the BQEs is estimated by

$$\widehat{\phi}_{\widehat{y}_p}(b,m) \equiv \frac{1}{b-1} \sum_{j=1}^{b-1} \frac{[\widehat{y}_p(j,m) - \overline{\overline{y}}_p(b,m)][\widehat{y}_p(j+1,m) - \overline{\overline{y}}_p(b,m)]}{S_p^2(b,m)},$$

and the correlation-adjustment factor is computed from

$$\varphi = \max\left(\frac{1+\widehat{\phi}_{\widehat{y}_p}(b,m)}{1-\widehat{\phi}_{\widehat{y}_p}(b,m)}, 1 \right).$$

Finally we set

$$G_1 \equiv G(t_{1-\alpha/2,b-1})\sqrt{\varphi \widetilde{S}_p^2(b,m)/b}, \quad \text{and} \quad G_2 \equiv G(t_{\alpha/2,b-1})\sqrt{\varphi \widetilde{S}_p^2(b,m)/b}. \tag{5.1}$$

The (asymmetric) correlation- and skewness-adjusted CI for y_p is given by

$$\left[\min\left(\widetilde{y}_p(n^*) - G_1, \widetilde{y}_p(n^*) - G_2\right), \max\left(\widetilde{y}_p(n^*) - G_1, \widetilde{y}_p(n^*) - G_2\right)\right]. \tag{5.2}$$

This CI differs from the symmetric CI delivered by the Sequest method of Alexopoulos *et al.* [7]. We will elaborate more on this adjusted CI in Section 5.2 below.

5.2 FQUEST Algorithm

In this section we present the proposed procedure for estimating a steady-state quantile based on a single run of fixed length. Figure 5.1 contains a high-level flowchart of the procedure. At a high level, FQUEST is comprised of four main blocks. The first block consists of Steps **[0]**–**[2]** which initialize the experimental parameters. The second block includes Steps **[3]**–**[5]** and deals with the potential transient effects in the data sample. At the end of this block the observations comprising the first batch are removed. The third block consists of Steps **[6]**–**[9]**, which conduct randomness and normality tests to assess the statistical conformance of the signed areas $\{A_p(w; j, m) : j = 1, \ldots, b\}$ and the BQEs $\{\widehat{y}_p(j, m) : j = 1, \ldots, b\}$ to the asymptotic properties in Equations (2.17) and (2.9), respectively. Finally, the last block consists of Step **[10]**: If the statistical tests within the third block are passed, the procedure delivers the CI in Equation (2.68) based on the combined variance estimator. Otherwise, it potentially delivers a conservative CI, subject to user approval. The following paragraphs contain an elaborate description of each step of FQUEST.

In Step **[0]**, the simulation model or user provides a sample path $\{Y_1, \ldots, Y_N\}$ of fixed size N, the probability associated with the quantile p, and the nominal error probability $\alpha \in (0, 1)$ for the CI for y_p. Step **[1]** initializes the experimental parameters. The initial number of batches is set at $b = 50$ to enhance the power of von Neumann's randomness test in Step **[3]**, and the initial batch size is set at $m = 500$. We also define the array of batch counts $\boldsymbol{s} = [32, 24, 16, 10]$ for Steps **[5]**–**[9]**. Further, we initialize the counters $l = 1$ and

$v = 1$, and set `flag` = `false`. At this point the algorithm sets the weight function that will be used for the calculation of the signed areas and the STS variance-parameter estimator. For the reasons stated at the start of Section 4.1, we used the constant weight function w_0 for the experiments in Section 5.3 but state the algorithm using a general weight function satisfying Equation (2.12). The level of significance for the statistical test in Step **[3]** is set according to the sequence $\{\beta\psi(\ell) : \ell = 1, 2, \ldots\}$, where $\beta = 0.3$, $\psi(\ell) \equiv \exp\left[-\eta(\ell-1)^{\theta}\right]$, $\eta = 0.2$, and $\theta = 2.3$. For the statistical tests in Steps **[6]**–**[9]** we fix the significance level at β. The values of the parameters β, η, and θ were chosen after careful experimentation to control the growth of the batch size and to avoid excessive truncation during Step **[5]** which can be detrimental given the sample-size limitation. Notice that on a potential fourth iteration within Step **[3]** one has $\beta\psi(4) = 0.025$, which makes passing the test easier.

Since the sample size N is fixed, it is possible that it is less than the initial assignment $bm = 25{,}000$. In this case Step **[2]** sets $m = \lfloor N/b \rfloor$, which is the largest allowable value for the current batch count b. Step **[3]** consists of a loop that tests for the randomness of the signed areas $\{A_p(w; j, m) : j = 1, \ldots, b\}$ computed from the first bm observations (the tail $N - bm$ observations are ignored, but not discarded) using a two-sided test based on von Neumann's ratio (von Neumann [43], Young [83]) with progressively decreasing significance level $\beta\psi(\ell)$ on iteration ℓ; see Section 4.1 of this thesis for a detailed discussion of the test statistic and its power. If the randomness test fails, we increase the batch size to $[\![m\sqrt{2}]\!]$, where $[\![\cdot]\!]$ is the rounding function to the nearest integer. If the updated sample size exceeds N, we set $m = \lfloor N/b \rfloor$, which is the largest allowable value for the current batch count b. If the randomness test fails with the largest allowable batch size $\lfloor N/b \rfloor$, FQUEST exits Step **[3]** and moves to Step **[4]**, where it issues a warning to the user regarding the insufficiency of the sample. Then it seeks permission from the user to continue with the construction of a CI. As with the sequential SQSTS method in Chapter 4, we focus on the signed areas in an attempt to ameliorate the pronounced small-sample bias of the batched STS area estimator $\mathscr{A}_p(w; b, m)$ relative to the NBQ variance estimator (Alexopoulos *et al.*

[39]).

If the randomness test in Step **[3]** is passed or the user decides to proceed with the construction of the CI despite the failure of the randomness test, in Step **[5]** FQUEST removes the first batch, sets the new sample size to $N^* = N - m$, and reindexes the truncated dataset. Assuming the successful completion of Step **[3]**, the (approximate) independence between $A_p(w; 1, m)$ and the remaining signed areas $\{A_p(w; j, m) : j = 2, \ldots, b\}$ indicates that any initialization bias due to warmup effects is mostly confined to the first batch. In the worst-case scenario where the randomness test in Step **[3]** fails, Step **[5]** ends up removing $\lfloor N/b \rfloor$ data points.

Remark 5.2.1. At this junction, a few comments are in order. We avoid decreasing the batch count b in Step **[3]** to limit the size of the truncated set. Also the initial batch size is set at $m = 500$ to address situations where the provided sample has a short transient phase. For example, if $N = 500{,}000$, FQUEST will remove only 500 data points if the randomness test in Step **[3]** is passed on the first attempt. On the other hand, if we had started with 50 batches of size 10,000 each (i.e., all the data) in Step **[3]** and the randomness test was successful in the first iteration (which is highly likely given that the randomness test was successful with $m = 500$), the algorithm would end up removing the excessive number of 10,000 initial observations.

Step **[5]** restarts with $b = s[1] = 32$ and $m = \lfloor N^*/b \rfloor$. Notice that we may have to ignore (but not remove) a few initial observations in the updated sample. We chose the entries of the vector $\boldsymbol{s} = [32, 24, 16, 10]$ after extensive experimentation. Notice that the elements of $\boldsymbol{s}$ decrease at a rate of about $\sqrt{2}$. Further, 32 batches typically suffice for effective estimation of the variance parameter σ_p^2, while fewer than 10 batches may result in unreliable CIs.

In Steps **[6]**–**[9]** we conduct the two-sided randomness test of von Neumann [43] and the one-sided test of Shapiro and Wilk [81] for univariate normality to assess whether the signed areas $\{A_p(w; j, m) : j = 1, \ldots, b\}$ and the BQEs $\{\widehat{y}_p(j, m) : j = 1, \ldots, b\}$ satisfy the asymptotic properties in Equations (2.17) and (2.9), respectively. A detailed presentation of the Shapiro–Wilk test and its interconnection with von Neumann's test is given in Section 4.1 of this thesis. Each of the Steps **[6]–[9]** has a very similar structure. First we compute the signed areas $\{A_p(w; j, m) : j = 1, \ldots, b\}$ or the BQEs $\{\widehat{y}_p(j, m) : j = 1, \ldots, b\}$ and conduct the pertinent statistical test using the fixed significance level of $\beta = 0.3$. The significance level is kept constant and high to avoid passing a test with an inadequately small batch size leading to unreliable CIs. If the test is passed, FQUEST proceeds to the next step; otherwise, the batch count decreases to the next element of the array $\boldsymbol{s}$. For example, if we fail a test with 24 batches, we set the batch count to 16, recompute the batch size m, and ignore any leftover initial observations. Since $\boldsymbol{s}$ contains only four values, we can have up to four failed attempts to pass any of the statistical tests in Steps **[6]–[9]**. If at any point a statistical test fails with $b = 10$, then FQUEST skips the remaining statistical tests and moves to Step **[10]**.

In Step **[10]**, if all the statistical tests have been passed, FQUEST computes the combined variance estimator $\widetilde{\mathscr{V}_p}(w; b, m)$ and returns the CI in Equation (2.68). Otherwise, it issues a warning mentioning that some of the statistical tests failed (with the significance level of $\beta = 0.3$) and asks the user for permission to continue with the construction of a CI for y_p. If the user chooses to continue, then FQUEST computes the quantity

$$h_{\alpha,b,m} \equiv \max\left\{t_{1-\alpha/2,b}\left[\mathscr{A}_p(w; b, m)/n^*\right]^{1/2}, t_{1-\alpha/2,b-1}\left[\widetilde{\mathscr{N}_p}(b, m)/n^*\right]^{1/2}\right\}, \tag{5.3}$$

with $n^* = bm$ using Equations (2.16) and (2.56), and constructs two new intervals with HL $h_{\alpha,b,m}$: the first CI is centered around the full-sample point estimator $\widetilde{y}_p(n^*)$ defined in Section 2.1 of this thesis, while the second CI is centered around the average (batch quantile) point estimator $\overline{\widehat{y}}_p(b, m)$ defined in Equation (2.51). Then FQUEST reports the point estimate $\widetilde{y}_p(n^*)$ computed from the truncated sample of $n^* = bm$ observations (with the initial $N^* - n^*$ observations ignored) and the smallest interval containing both newly constructed intervals and the correlation- and skewness-adjusted CI in Equation (5.2) with

n^*, and stops.

Remark 5.2.2. By the inequality $S_p^2(b,m) \leq \widetilde{S}_p^2(b,m)$, as noted in Equation (2.54), we have $\mathcal{N}_p(b,m) \leq \widetilde{\mathcal{N}_p}(b,m)$. Since the FQUEST procedure relies on conservative CIs when one of the statistical tests fails, we will ignore the alternative batched estimator $\mathcal{N}_p(b,m)$ of σ_p^2.

Remark 5.2.3. Passing a single pair of the statistical tests in Steps **[6]**–**[9]** (i.e., **[6]**–**[7]** or **[8]**–**[9]**) could provide on its own the theoretical basis for using the respective CIs in Equations (2.64) or (2.66). However, due to the sample-size limitations, FQUEST often resolves to batch counts $b \leq 16$, which typically reduce the power of von Neumann's and Shapiro–Wilk tests. Preliminary experimentation with two output processes from Sections 2.5.3 and 2.5.4 with $p = 0.95$ and $N = 50{,}000$ revealed that FQUEST frequently delivered CIs with substantial undercoverage. This explains why FQUEST is designed to incorporate the heuristic CI in Step **[10]** even if only one of the statistical tests failed during Steps **[6]**–**[9]**.

The formal algorithmic statement of FQUEST follows. As we stated earlier, we present the algorithm for a general weight function $w(\cdot)$ satisfying Equation (2.12).

Algorithm FQUEST

---

[0] User-Initialization: Provide a sample of fixed size N, the probability p corresponding to the quantile, and the error probability $\alpha \in (0,1)$.

[1] Parameter-Initialization: Set the number of batches $b = 50$, batch size $m = 500$, $\ell = 1$, $v = 1$, and `flag` = `false`. Also set $\beta = 0.30$ and $\boldsymbol{s} = [32, 24, 16, 10]$. Let $w(t)$, $t \in [0,1]$, be the weight function and define the initial significance level for the first hypothesis test in Step **[3]** as $\beta\psi(\ell) \equiv \exp\big[-\eta(\ell-1)^\theta\big]$, $\ell = 1, 2, \ldots$, with $\eta = 0.2$ and $\theta = 2.3$.

[2] **If** $N < bm$:

Set $m \leftarrow \lfloor N/b \rfloor$;

End If

[3] **Until** von Neumann's test fails to reject randomness **or** `flag` = `true`:

- Compute the signed areas $\{A_p(w; j, m) : j = 1, \ldots, b\}$ from the initial bm observations;
- Assess the randomness of $\{A_p(w; j, m) : j = 1, \ldots, b\}$ using von Neumann's two-sided randomness test with significance level $\beta\psi(\ell)$;
- Set $\ell \leftarrow \ell + 1$ and $m \leftarrow [\![m\sqrt{2}]\!]$;
- **If** $N < bm$ **and** $m \neq \lfloor N/b \rfloor$:

  Set $m \leftarrow \lfloor N/b \rfloor$;

  Else

  Set `flag` $\leftarrow$ `true`;

  End If

End

[4] If the randomness test in Step **[3]** failed, then issue a warning that the randomness test failed due to insufficient size of the dataset and seek permission from the user to continue with the construction of a CI. If the user declines, then exit without delivering a CI.

[5] Remove the first batch, reindex the truncated dataset, and set N^* equal to the size of the truncated sample. Set the number of batches $b \leftarrow s[v]$ and calculate the batch size as $m \leftarrow \lfloor N^*/b \rfloor$. Ignore the initial $N^* - bm$ observations.

[6] Until von Neumann's test fails to reject randomness **or** $v = 5$ (a test has failed with $b = 10$):

- Compute the signed areas $\{A_p(w; j, m) : j = 1, \dots, b\}$;
- Assess the randomness of the signed areas $\{A_p(w; j, m) : j = 1, \dots, b\}$ using von Neumann's two-sided randomness test with significance level β;
- Set $v \leftarrow v + 1$. Update $b \leftarrow s[v]$ and $m \leftarrow \lfloor N^*/b \rfloor$. Ignore the initial $N^* - bm$ observations.

End

[7] Until the Shapiro-Wilk test fails to reject normality **or** $v = 5$ (a test has failed with $b = 10$):

- Compute the signed areas $\{A_p(w; j, m) : j = 1, \dots, b\}$;
- Assess the univariate normality of the signed areas $\{A_p(w; j, m) : j = 1, \dots, b\}$ using the Shapiro–Wilk test with significance level β;
- Set $v \leftarrow v + 1$. Update $b \leftarrow s[j]$ and $m \leftarrow \lfloor N^*/b \rfloor$. Ignore the initial $N^* - bm$ observations.

End

[8] Until von Neumann's test fails to reject randomness **or** $v = 5$ (a test has failed with $b = 10$):

- Compute the BQEs $\{\widehat{y}_p(j, m) : j = 1, \dots, b\}$;
- Assess the randomness of the BQEs $\{\widehat{y}_p(j, m) : j = 1, \dots, b\}$ using von Neumann's two-sided randomness test with significance level β;
- Set $v \leftarrow v + 1$. Update $b \leftarrow s[v]$ and $m \leftarrow \lfloor N^*/b \rfloor$. Ignore the initial $N^* - bm$ observations.

End

[9] **Until** the Shapiro–Wilk test fails to reject normality **or** $v = 5$ (a test has failed with $b = 10$):

- Compute the BQEs $\{\widehat{y}_p(j, m) : j = 1, \ldots, b\}$;
- Assess the univariate normality of the BQEs $\{\widehat{y}_p(j, m) : j = 1, \ldots, b\}$ using the Shapiro–Wilk test with significance level β;
- Set $v \leftarrow v + 1$. Update $b \leftarrow s[v]$ and $m \leftarrow \lfloor N^*/b \rfloor$. Ignore the initial $N^* - bm$ observations.

End

[10] Set $n^* \leftarrow bm$.

If $v < 5$ (no statistical test in Steps **[6]**–**[9]** failed):

- Compute the combined variance estimator

$$\widetilde{\mathscr{V}}_p(w; b, m) = \frac{b\mathscr{A}_p(w; b, m) + (b - 1)\widetilde{\mathscr{N}_p}(b, m)}{2b - 1}$$

in Equation (2.58), deliver the $100(1 - \alpha)\%$ CI for y_p,

$$\widetilde{y}_p(n^*) \pm t_{1-\alpha/2, 2b-1}\left(\widetilde{\mathscr{V}}_p(w; b, m)/n^*\right)^{1/2},$$

and exit;

Else

- Issue a warning that a statistical test failed due to insufficient size of the dataset and seek permission from the user to continue with the construction of a CI. If the user declines, then exit without delivering a CI;

- Compute

$$h_{\alpha,b,m} = \max\left\{t_{1-\alpha/2,b}\left[\mathscr{A}_p(w;b,m)/n^*\right]^{1/2}, t_{1-\alpha/2,b-1}\left[\widetilde{\mathscr{N}_p}(b,m)/n^*\right]^{1/2}\right\},$$

where

$$\mathscr{A}_p(w;b,m) = b^{-1}\sum_{j=1}^{b} A_p^2(w;j,m) \quad \text{and}$$

$$\widetilde{\mathscr{N}_p}(b,m) = m(b-1)^{-1}\sum_{j=1}^{b}\left[\widehat{y}_p(j,m) - \widetilde{y}_p(n)\right]^2.$$

Then, construct the following (auxiliary) CIs for y_p with HL $h_{\alpha,b,m}$:

$$\widetilde{y}_p(n^*) \pm h_{\alpha,b,m} \quad \text{and} \quad \overline{\widehat{y}}_p(b,m) \pm h_{\alpha,b,m}, \tag{5.4}$$

where the first CI centered around the full-sample point estimator $\widetilde{y}_p(n^*)$ and the second centered around the average BQE $\overline{\widehat{y}}_p(b,m) = b^{-1}\sum_{j=1}^{b}\widehat{y}_p(j,m)$;

- Construct the (asymmetric) correlation- and skewness-adjusted CI

$$\left[\min\left(\widetilde{y}_p(n^*) - G_1, \widetilde{y}_p(n^*) - G_2\right), \max\left(\widetilde{y}_p(n^*) - G_1, \widetilde{y}_p(n^*) - G_2\right)\right] \tag{5.5}$$

with G_1 and G_2 defined in Equation (5.1);

- Deliver the full-sample point estimator $\widetilde{y}_p(n^*)$ and the smallest interval containing the CIs in Equations (5.4) and (5.5), and exit.

End If

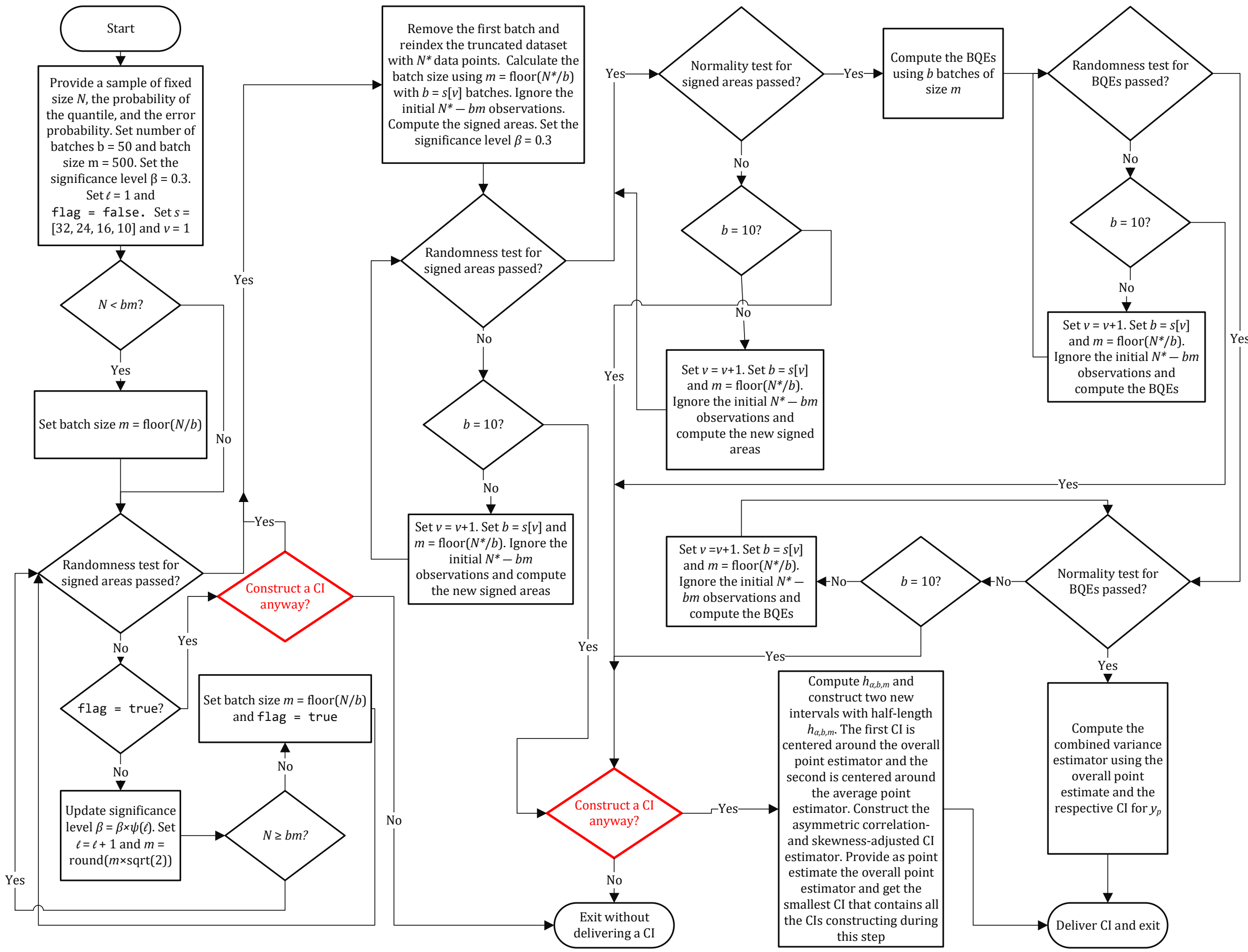

Figure 5.1: High-Level Flowchart of FQUEST.

5.3 Experimental Results

In this section we present an extensive empirical study designed to assess the performance of the FQUEST procedure. Our test bed includes the seven challenging stochastic processes from Alexopoulos *et al.* [23] and Alexopoulos *et al.* [7], involving two time-series models, three single-server queueing systems, and two small queueing networks. For two processes we present results for different choices of parameters, hence we consider a total of nine test problems. We have already introduced these stochastic processes in Sections 2.5.1–2.5.7. All experiments were coded in Java using common random numbers generated by the RngStreams package of L'Ecuyer *et al.* [67]. As mentioned earlier, we constructed the STS area variance estimators using the constant weight function $w_0(\cdot)$.

For each experimental setting we present three different sets of experimental results: (i) an initial table with numerical results for the FQUEST method using five different sample sizes $N \in \mathscr{S} \equiv \{50{,}000, 100{,}000, 200{,}000, 500{,}000, 1{,}000{,}000\}$ and a nominal 95% ($\alpha = 0.05$) CI coverage probability; (ii) a set of graphs based on the aforementioned table, each for a specific probability p depicting the average 95% CI relative precision, defined as the ratio of the CI HL over $|\widetilde{y}_p(n)|$, and the estimated 95% CI coverage probability; and (iii) a second table containing results for an informal comparison of FQUEST against the sequential SQSTS from Chapter 4 of this thesis. The sample sizes in $\mathscr{S}$ are larger than those used for the experimental evaluation of the N-Skart procedure (Tafazzoli *et al.* [42]) (namely 10,000; 20,000; 50,000; and 200,000), but quantile estimation typically requires substantially larger sample sizes than mean estimation. Notably, the smaller values in $\mathscr{S}$ are typically insufficient for estimating marginal quantiles for the stationary processes with a high degree of autocorrelation of departures from normality (Chen and Kelton [25], Alexopoulos *et al.* [23], Alexopoulos *et al.* [7]), in particular extreme ones.

Tables 5.1, 5.3, 5.5, 5.7, 5.9, 5.11, 5.13, 5.15, 5.17, and 5.18 contain experimental results for the FQUEST method with all estimates being averages computed from 1,000 independent trials. Specifically, column 1 lists selected values of p and column 2 contains the (nearly) exact value of the associated quantile y_p. Column 3 lists the sample size N. Columns 4 and 5 contain the average value of the point estimate $\widetilde{y}_p(n)$ and the average value of the absolute error $\left|\widetilde{y}_p(n) - y_p\right|$, respectively. Columns 6–8 contain the average value of the HL of the 95% CI for y_p, the average value of the CI's relative precision expressed as a percentage and the estimated coverage of the CI as a percentage, respectively. We report the average CI HL and average relative precision despite the fact that the final CI delivered in Step **[10]** of FQUEST may be asymmetric for small samples (when a statistical test in Steps **[6]**–**[9]** fails with $b = 10$ batches). The standard errors of the estimated coverage probabilities are approximately $\sqrt{(0.95 \times 0.05)/1000} = 0.007$. Columns 9 and 10 display the average final batch size ($\overline{m}$) and average final batch count ($\overline{b}$), respectively, after the truncation of the initial subset of observations in Step **[5]**. Finally, Columns 11 and 12 list the standard deviation of the CI HL and the average truncated sample size ($N - n^*$), respectively.

Given the nonsequential nature of FQUEST, the two most important metrics for its performance evaluation are the estimated coverage probability of the CI and the average value of the CI's relative precision. There is always a tradeoff between these two metrics. A reliable fixed-sample-size procedure should achieve the requested CI coverage probability, while keeping the average value of the CI's relative precision as low as possible. Figures 5.2–5.11 illustrate FQUEST's performance on this front in a more intelligible way by plotting the estimates of the 95% CI relative precision and coverage probability in columns 7–8 of Tables 5.1, 5.3, 5.5, 5.7, 5.9, 5.11, 5.13, 5.15, 5.17, and 5.18.

Tables 5.2, 5.4, 5.6, 5.8, 5.10, 5.12, 5.14, 5.16, and 5.19 aim at an ad hoc comparison between FQUEST and the sequential SQSTS procedure, presented in Chapter 4 of this thesis, when the latter is executed without a CI precision requirement. They have a very similar format with the tables in the first set, but do not report the average final number of batches ($\overline{b}$) and the average truncated sample size. The entries from SQSTS are provided in italic typeface. The selected sample size for FQUEST was obtained by rounding the average final sample size requested by the SQSTS method to the nearest 1,000. All results are based on 1,000 replications. The main purpose of this comparison is to evaluate the behavior of FQUEST when the provided sample size is close to what a cutting-edge sequential procedure like SQSTS requests: ideally, as the sample size N increases, FQUEST should be able to deliver CIs with similar reliability and relative precision as those delivered by SQSTS. Because of the computation of the heuristic CI in Step **[10]** of FQUEST when a statistical test in Steps **[6]**–**[9]** cannot be passed, the average relative precision of the CIs delivered by FQUEST will typically be larger that the respective CIs obtained from SQSTS for the (nearly) same sample size; this gap (and the frequency of the heuristic CI) should diminish as N becomes very large.

Finally, Figure 5.12 reports the frequency of the heuristic CI in Step **[10]** in a few selected cases and for $N \in \{50{,}000, 100{,}000, 200{,}000, 500{,}000, 1{,}000{,}000\}$. These results are also based on 1,000 independent replications.

5.3.1 First-Order Autoregressive Processes

The first test process is the Gaussian AR(1) process defined in Section 2.5.1. We considered two sets of parameters. In the first case we chose $\mu_Y = 100$, $\phi = 0.995$, $\sigma_\epsilon = 1$, and $Y_0 = 0$. Since the steady-state marginal standard deviation is $\sigma_Y = \sigma_\epsilon/(1 - \phi^2)^{1/2} = 10.01$, this process was initialized nearly 10 standard deviations below its steady-state mean. As we have already mentioned in Section 4.2.1, on top of the pronounced initialization bias, this process exhibits strong stochastic dependence. These traits will allow us to evaluate the ability of FQUEST to overcome the effects of initialization bias and pronounced serial correlation between successive observations of the base process.

The experimental results are displayed in Tables 5.1 and 5.2, and Figure 5.2. We start our analysis with Table 5.1. An examination of columns 4 and 5 reveals that the point estimates of y_p delivered by FQUEST are close to the exact value, with small average absolute bias, which significantly decreases as the sample size increases. The 95% CIs exhibit slight undercoverage for $p \in \{0.3, 0.5, 0.99, 0.995\}$ and small values of N (50,000 and 100,000). For example, for $N = 50{,}000$ and $p = 0.5$ or $p = 0.995$, the estimated CI coverage probabilities are 92.9% and 90.9%, respectively. This effect vanishes for $N \geq 200{,}000$. The estimated CI relative precision is reasonable in all cases and decreases significantly as the sample size increases. The average size of the truncated sample was near 620, which seems reasonable. From Table 5.2 we see that when FQUEST was executed with sample sizes near the average sample sizes required by the sequential SQSTS procedure, it delivered CIs with estimated coverage probabilities typically close to the nominal value and slightly higher CI relative precision. This is expected due to the adjustments in Step **[10]** of FQUEST. In a few cases the estimated CI coverage probability was closer to the nominal value compared to SQSTS. For example, for $p = 0.7$ FQUEST delivered CIs with an estimated coverage probability of 94.6% and relative precision of 1.285, while SQSTS delivered CIs with an estimated coverage coverage probability of 93.7% and relative precision of 1.156. Overall, we judge the performance of FQUEST in this problem as satisfactory.

In the second (less challenging) case we took $\mu_Y = 0$, $\phi = 0.9$, $\sigma_\epsilon = 1$, and $Y_0 = 0$. The stationary version of this process was used to compare the Sequest method (Alexopoulos *et al.* [7]) against the two-phase procedure of Chen and Kelton [25]. The experimental results are displayed in Tables 5.3 and 5.4, and Figure 5.3. In Table 5.3, the estimated CI coverage probabilities were close to the nominal value, with some small overcoverage in a few cases. Specifically, for $p = 0.45$ and $N = 500{,}000$ FQUEST delivered CIs with estimated coverage probability 97.4%. Further, the estimated CI relative precision was reasonable for all the probabilities except for $p = 0.45$, where it was quite large at 39.432% for $N = 50{,}000$ and dropped to 8.325% for $N = 1{,}000{,}000$. The high CI relative precision at $p = 0.45$ is partially attributable to the exact value of $y_p = -0.288$, which is close to zero. The average truncated sample size was close to 600, which is deemed as reasonable. We conclude that FQUEST performed well in this case.

The outcome of the informal comparison between FQUEST and SQSTS in Table 5.4, for this example, clearly confirmed FQUEST's ability to yield CI coverage probabilities close to the nominal value while keeping the CI relative precision slightly higher than what SQSTS yielded.

5.3.2 Autoregressive-to-Pareto Process

The second test process is the ARTOP process described in Section 2.5.2. For this example we used $\gamma = 1$, $\theta = 2.1$, and $\phi = 0.995$. Recall that these assignments yield $\mu_Y = 1.9091$, $\sigma_Y^2 = 17.3554$, marginal skewness $\mathrm{E}\{[(Y_k - \mu_Y)/\sigma_Y]^3\} = +\infty$, and marginal kurtosis $\mathrm{E}\{[(Y_k - \mu_Y)/\sigma_Y]^4\} = +\infty$. We also initialized the original AR(1) process with the value $Z_0 = 3.4$; which results to an initial observation $Y_0 = F^{-1}[\Phi(Z_0)] = 43.5689$ for the ARTOP process, which is approximately 10 standard deviations above its steady-state mean. On top of the initialization problem and the strong stochastic dependence, this process has a marginal distribution with a fat tail (Mandelbrot [87]), which is reflected by the infinite marginal skewness and kurtosis.

The experimental results for this process are displayed in Tables 5.5 and 5.6, and Figure 5.4. We start our analysis with Table 5.5. Columns 4 and 5 illustrate that FQUEST delivered reasonably accurate point estimates for y_p. For $p < 0.9$, FQUEST performed reasonably well with regard to CI coverage probability and relative precision, with a few cases of noticeable CI overcoverage in small samples (e.g., for $p = 0.3$ and $N \leq 200{,}000$). For $p \geq 0.9$ and small samples, FQUEST underperformed, in particular with regard to estimated CI relative precision; this issue became more pronounced as p approached 0.995. For instance, at $p = 0.995$, the average CI relative precision dropped from the unacceptable value of nearly 106% for $N = 50{,}000$ to about 24% for $N = 1{,}000{,}000$. This behavior is not unexpected: a close examination of Table 5.6 reveals that for $p = 0.99$ and 0.995 the largest sample size used in the experimental evaluation of FQUEST was lower by a factor of about 2.5 and 3, respectively, than the average sample sizes requested by the sequential SQSTS method. In particular, for $N \leq 100{,}000$ FQUEST reported excessively wide CIs. An examination of Figure 5.12 below (for $p = 0.99$) reveals that FQUEST failed a statistical test in Steps **[6]–[9]** with a frequency near 91% with $N = 50{,}000$ and 87% with $N = 100{,}000$. Such failures caused the use of the heuristic CI in Step **[10]**. The warning issued to the user in those cases should be an indicator for potential problems associated with the insufficiency of the sample size for delivering a CI based on a sound theoretical foundation. In these cases, the user should probably rerun FQUEST using a larger sample size. A potential recipe for determining an appropriate sample size is discussed in Section 5.4.

The entries of Table 5.6 clearly demonstrate that when FQUEST was fed with the average sample size reported by SQSTS, it caught up with the latter procedure by delivering CIs whose estimated coverage probabilities were close to the nominal value and similar average relative precision (within 2%). We deem that FQUEST performed well in this test problem.

5.3.3 M/M/1 Waiting-Time Process

The third test process is the waiting-time sequence in an M/M/1 queueing system described in Section 2.5.3 with FIFO service discipline. We considered two examples for this process. For the first example we used an arrival rate $\lambda = 0.9$ and a service rate $\omega = 1$ (traffic intensity $\rho = \lambda/\omega = 0.9$). Let Y_k be the time spent by the kth entity in queue (prior to service).

To assess the ability of the FQUEST method to deal with excessive initialization bias, we initialized the system with one entity beginning service and 112 entities in queue. Recall that the steady-state probability of this initial state is $(1 - \rho)\rho^{113} \approx 6.752 \times 10^{-7}$, implying a high probability for a prolonged transient phase.

The experimental results for this case are displayed in Tables 5.7 and 5.8, and Figure 5.5. We start our analysis with Table 5.7. FQUEST managed to provide satisfactory estimated CI coverage probabilities, with the worst one being 90.1% for $p = 0.995$ and $N = 50{,}000$. There were a few cases with noticeable CI overcoverage for $p \leq 0.7$ and $N \leq 200{,}000$. As illustrated in Figure 5.5, the near proximity of the estimated CI coverage probability to the nominal value of 95% often came at the expense of high estimated CI relative precision, in particular for relatively small samples and large values of p where the average batch counts in column 10 indicates that FQUEST failed the statistical tests in Steps **[6]–[9]** with high frequency and resorted to the computation of the heuristic CI in Step **[10]** with approximately 10 batches. This trait diminished substantially as N increased. An examination of Table 5.8 reveals that when FQUEST was supplied with a sample size near the one required by SQSTS, it performed well with regard to both primary performance metrics of interest. As with the ARTOP process in Section 2.5.2, the values of N in our experimentation were significantly smaller than those required by the sequential SQSTS method (under no CI precision requirement) for $p \geq 0.99$. The value of FQUEST is evident from its ability to provide usable CIs for smaller fixed sample sizes N that are smaller than those required by SQSTS and Sequest (Table 4.3 of this thesis), e.g., for $p = 0.3$ and $N \in \{200{,}000, 500{,}000\}$ or $p = 0.99$ and $N \in \{500{,}000, 1{,}000{,}000\}$.

For the second, less-challenging example we only lowered the arrival rate to $\lambda = 0.8$, so that $\rho = 0.8$. The experimental results are displayed in Tables 5.9 and 5.10, and Figure 5.6. Based on these results we conclude that FQUEST encountered fewer issues in this less-challenging setting. Overall, FQUEST performed adequately in both difficult settings.

5.3.4 M/H_2/1 Waiting-Time Process

The fourth test process is the sequence $\{Y_k : k \geq 1\}$ of entity waiting times in an M/H_2/1 queueing system as described in Section 2.5.4 with FIFO queue discipline, an empty-and-idle initial state, arrival rate $\lambda = 1$, and i.i.d. service times from the hyperexponential distribution that is a mixture of two other exponential distributions with mixing probabilities $g = (5 + \sqrt{15})/10 \approx 0.887$ and $1 - g$ and associated service rates $\omega_1 = 2g\tau$ and $\omega_2 = 2(1 - g)\tau$, with $\tau = 1.25$. As a result, we have a mean service time of 0.8 and a steady-state server utilization of $\rho = 0.8$. Recall that for this process and under no CI precision requirement, the Sequest sequential method of Alexopoulos *et al.* [7] reported average sample sizes ranging from 1.2 to 28.7 million, and yet delivered CIs with significant undercoverage for $p \geq 0.99$ (see Table 4.4 in this thesis). Most importantly, it was outshined by SQSTS for all values of p under study.

The experimental results for this process are displayed in Tables 5.11 and 5.12, and Figure 5.7. We start our analysis with Table 5.11. For $p \in \{0.3, 0.5, 0.7\}$, the 95% CIs for y_p exhibited noticeable overcoverage. On the other hand, for $p \geq 0.99$ FQUEST delivered CIs with significant undercoverage for sample sizes $N \leq 100{,}000$. However, Figure 5.7 illustrates clearly that this issue was resolved as the sample size approached 1 million. Column 7 also reveals cases with excessive estimated CI relative precision, especially for small sample sizes $N \leq 100{,}000$. Figure 5.7 clearly showcases the significant improvements in the reported estimated CI relative precision as the sample size N increased beyond 200,000. For $p = 0.3$ and $N = 50{,}000$ FQUEST's excessive estimate of 90.834% for the estimated CI relative precision is partially attributable to the small value of the actual quantile $y_p = 0.669$.

Table 5.12 reveals once again that when FQUEST was supplied with sample sizes close to those requested by SQSTS, it performed well with regard to both estimated CI coverage probability and relative precision. Notice that for $p \geq 0.99$, SQSTS required sample sizes that exceeded the largest value of N in Table 5.11 by a factor of 2 or more. Overall, we believe that FQUEST handled this challenging process effectively for reasonably low sample sizes N depending on the value of p.

5.3.5 M/M/1/LIFO Waiting-Time Process

The fifth test process is the sequence of entity waiting times $\{Y_k : k \geq 1\}$ in a single-server queueing system as described in Section 2.5.5 with non-preemptive LIFO service discipline, empty-and-idle initial state, arrival rate $\lambda = 1$, and service rate $\omega = 1.25$. The steady-state server utilization is $\rho = 0.8$ and the marginal mean waiting time is $\mu_Y = 3.2$.

The experimental results for this process are displayed in Tables 5.13 and 5.14, and Figure 5.8. Table 5.13 and Figure 5.8 reveal that the 95% CIs for y_p exhibited noticeable overcoverage for all values of p under study and excessive average relative precision for tail probabilities $p \geq 0.99$ and small samples $N \leq 100{,}000$. A perusal of Table 5.14 clearly showcases the issue of excessive CI overcoverage; this is due to the heuristic used in Step **[10]** of FQUEST. However, column 7 reveals that the reported estimates of CI relative precision delivered by FQUEST and SQSTS were reasonably close. Overall, FQUEST performed adequately in this example.

5.3.6 M/M/1/M/1 Waiting-Time Process

The sixth test process, detailed in Section 2.5.6, is constructed from the sequence $\{Y_k : k \geq 1\}$ of the total waiting times (prior to service) in a tandem network of two M/M/1 queues. The system has an arrival rate of $\lambda = 1$, service rates $\omega = 1.25$ at each station, and is initialized in the empty and idle state. The steady-state utilization for each server is $\rho = \lambda/\omega = 0.8$ and the mean total waiting time in the system is equal to 8.

The experimental results for this process are displayed in Tables 5.15 and 5.16, and Figure 5.9. Based on Table 5.15 and Figure 5.9, FQUEST performed exceptionally well with respect to all metrics for all $p \leq 0.95$. The estimated CI coverage probabilities were very close to the nominal values without resulting in excessive estimated CI relative precision. However, for $p \geq 0.99$ and $N = 50{,}000$ FQUEST delivered CIs with noticeable undercoverage. Table 5.16 reveals that FQUEST performed very well once it was supplied with sample sizes near those required by SQSTS. Overall, we assess that FQUEST performed well in this case study despite the sample size limitations.

5.3.7 Central Server Model 3

The seventh test process, described in Section 2.5.7, is generated by the sequence $\{Y_k : k \geq 1\}$ of response times (cycle times) in a small computer network comprised of three stations, namely the Central Server Model 3 from Law and Carson [66].

The experimental results for this process are displayed in Tables 5.17–5.19 and Figures 5.10–5.11. Recall from the discussion in Section 4.2.7 that in the absence of a CI precision requirement and for $p \in \{0.85, \ldots, 0.93\}$, the Sequest method (Alexopoulos *et al.* [7]) experienced substantial sample-size variation and delivered CIs with noticeable variation around the nominal 95% level (see Table 4.7 in this thesis) while SQSTS delivered CIs with minor undercoverage in a few cases ($p \in \{0.3, 0.5, 0.93\}$). For this response-time process FQUEST performed well, with a few exceptions: the CIs delivered by FQUEST exhibited noticeable overcoverage for $p \in \{0.87, 0.89, 0.90, 0.91\}$ and noticeable undercoverage for $p = 0.95$ and $N \leq 100{,}000$.

The experimental results in Table 5.19 indicate that FQUEST managed to deliver CIs with estimated coverage probability very close to the nominal value and reasonable estimated relative precision when it was supplied with sample sizes close to the respective averages required by the sequential SQSTS method. Overall, we judge the performance of FQUEST in this test case as solid.

5.4 Summary

In this chapter, we presented FQUEST, a completely automated procedure for computing point estimators and CIs for steady-state quantiles based on a single sample path with fixed length. The user provides the sample and specifies the probability of the quantile and the required coverage probability of the requested CI. FQUEST incorporates the analysis methods of batching, STS, and sectioning. If the sample size suffices to identify a set of signed weighted areas $\{A_p(w; j, m) : j = 1, \ldots, b\}$ and BQEs $\{\widehat{y}_p(j, m) : j = 1, \ldots, b\}$ that pass the von Neumman and Shapiro-Wilk tests, FQUEST reports a CI for the quantile y_p under consideration centered at the empirical quantile from a truncated subset of the sample path and based on the combined estimator $\widetilde{\mathscr{V}}_p(w; b, m)$ of σ_p^2. Otherwise, the procedure issues a warning and, upon user's approval, formulates a wider CI from a set of CIs based on the quantile estimator computed from the entire truncated sample, the BQEs, and the batched area estimator $\mathscr{A}_p(w; b, m)$ obtained from the nonoverlapping batches.

Experimentation with an extensive test bed of output processes in Section 5.3 showed that FQUEST delivered CIs with coverage probabilities close to the nominal level. This feat is quite remarkable, considering that the state-of-the-art sequential methods Sequest and SQSTS required substantial sample sizes for the same processes under no CI precision requirement (Alexopoulos *et al.* [7], Chapter 4 of this thesis).

In difficult cases, such as the ARTOP process in Section 5.3.2 or the waiting-time process in an M/M/1 queue in Section 5.3.3, and with small samples, FQUEST may report a CI with an excessive HL or relative precision. This should be an indicator (especially in practical applications) for potential problems associated with the delivered CI or insufficiency of the sample size. In these cases, the user should probably rerun FQUEST with a larger sample size. Such an estimate can be obtained by a pilot study with sequential methods executed without a CI precision requirement. For instance, the Sequest method supplied with the same sample will either deliver a CI or (most likely) will provide an estimate of the augmented size of the sample that should be collected and resubmitted to FQUEST.

Table 5.1: Experimental results for FQUEST with regard to point and 95% CI estimation of y_p for the AR(1) process in Section 5.3.1 with $\mu_Y = 100$ and $\phi = 0.995$ based on 1,000 independent replications.

p	y_p	N	Point Est.	Avg. |Bias|	Avg. 95% CI HL	Avg. 95% CI rel. prec. (%)	Avg. 95% CI cov. (%)	$\overline{m}$	$\overline{b}$	St. Dev. HL	Avg. Trunc. Point
0.3	94.749	50,000	94.753	0.739	2.067	2.183	93.2	3,467	17.16	0.936	625
		100,000	94.773	0.554	1.488	1.570	93.2	6,451	18.69	0.604	639
		200,000	94.751	0.385	1.091	1.151	94.8	12,598	19.28	0.414	639
		500,000	94.765	0.237	0.682	0.720	95.7	30,304	20.10	0.225	640
		1,000,000	94.751	0.165	0.497	0.524	97.0	60,715	20.11	0.190	640
0.5	100.000	50,000	99.997	0.723	2.024	2.025	92.9	3,388	17.73	0.973	629
		100,000	100.021	0.543	1.430	1.430	93.0	6,309	19.14	0.544	635
		200,000	100.001	0.381	1.052	1.052	95.6	12,541	19.41	0.393	636
		500,000	100.015	0.232	0.673	0.673	95.9	30,957	19.74	0.226	636
		1,000,000	100.002	0.162	0.470	0.470	96.9	59,908	20.36	0.143	636
0.7	105.251	50,000	105.238	0.745	2.135	2.029	94.7	3,559	16.63	0.968	628
		100,000	105.264	0.549	1.514	1.439	94.2	6,504	18.59	0.603	639
		200,000	105.252	0.392	1.071	1.017	94.8	12,478	19.46	0.376	640
		500,000	105.262	0.240	0.700	0.665	95.8	31,587	19.36	0.248	640
		1,000,000	105.250	0.168	0.489	0.465	96.8	60,234	20.37	0.157	640
0.9	112.832	50,000	112.808	0.879	2.785	2.468	94.5	4,169	13.26	1.351	612
		100,000	112.830	0.626	1.856	1.644	94.3	7,502	15.64	0.850	622
		200,000	112.820	0.455	1.280	1.134	95.1	13,620	17.63	0.522	623
		500,000	112.835	0.277	0.811	0.718	96.1	32,712	18.60	0.303	624
		1,000,000	112.829	0.197	0.568	0.504	95.9	62,065	19.66	0.183	625
0.95	116.469	50,000	116.424	1.027	3.385	2.905	94.1	4,518	11.66	1.657	613
		100,000	116.451	0.706	2.251	1.932	93.9	8,351	13.32	1.048	622
		200,000	116.445	0.511	1.498	1.286	94.9	15,085	15.61	0.682	624
		500,000	116.466	0.309	0.928	0.797	96.0	33,607	18.04	0.371	626
		1,000,000	116.462	0.219	0.651	0.559	96.0	63,258	19.27	0.236	627
0.99	123.293	50,000	123.112	1.489	5.125	4.152	93.2	4,842	10.34	2.507	603
		100,000	123.198	0.988	3.653	2.962	95.7	9,486	10.84	1.882	611
		200,000	123.217	0.712	2.501	2.029	95.0	18,043	11.86	1.364	612
		500,000	123.263	0.441	1.415	1.147	95.9	39,219	14.86	0.674	615
		1,000,000	123.273	0.321	0.976	0.791	95.5	72,252	16.63	0.450	616
0.995	125.791	50,000	125.483	1.795	6.079	4.823	90.9	4,891	10.17	3.188	602
		100,000	125.630	1.199	4.365	3.468	93.8	9,673	10.47	2.251	608
		200,000	125.674	0.863	3.098	2.463	94.6	18,910	10.94	1.655	609
		500,000	125.741	0.537	1.808	1.437	96.6	43,201	12.77	0.919	611
		1,000,000	125.757	0.388	1.226	0.975	95.0	78,190	14.92	0.630	613

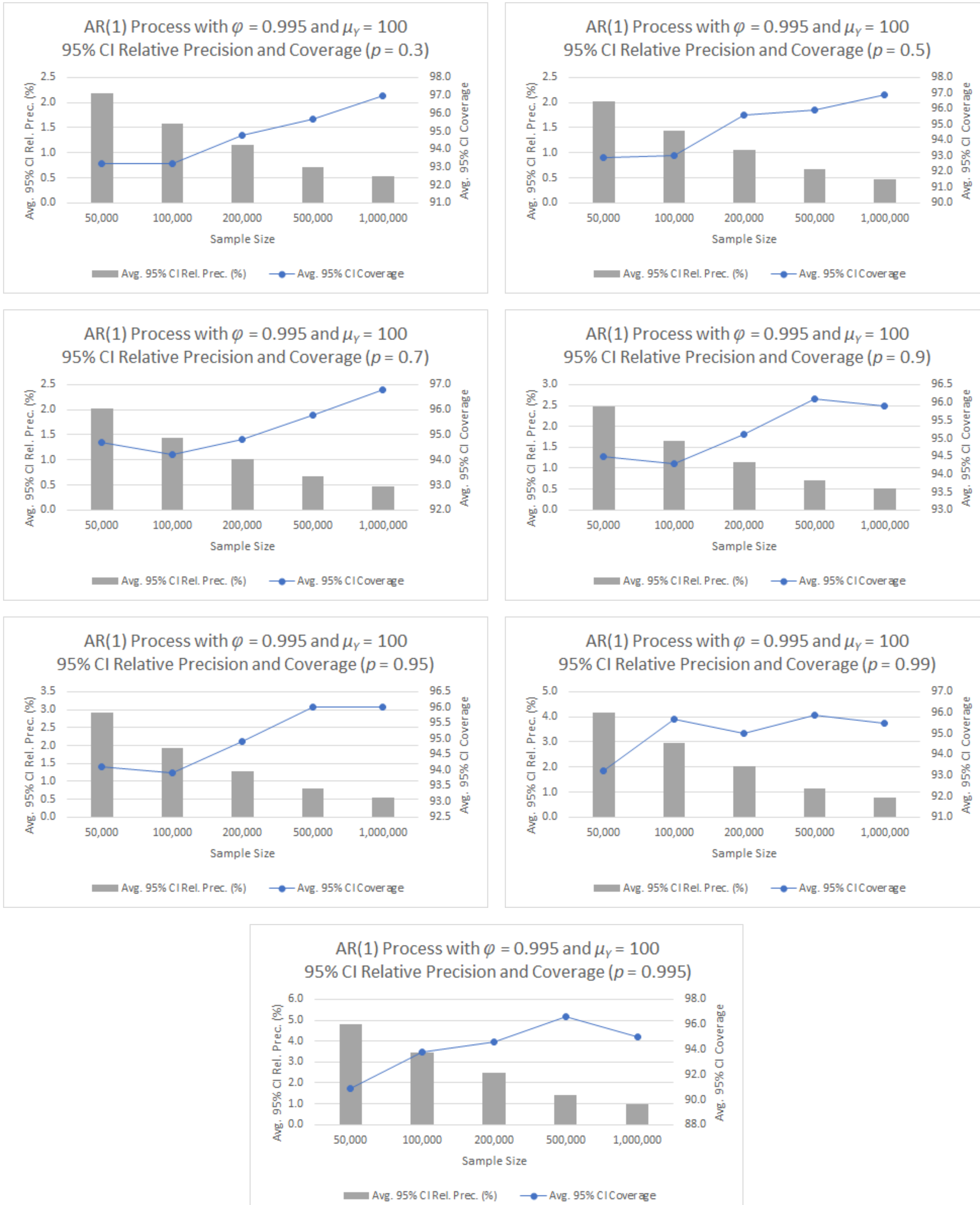

Figure 5.2: Plots for the average 95% CI relative precision and estimated coverage probability for the AR(1) process from Table 5.1.

Table 5.2: Comparison between FQUEST and SQSTS (in italic typeface) without a CI precision requirement for the AR(1) process in Section 5.3.1 with $\mu_Y = 100$ and $\phi = 0.995$ based on approximately equal sample sizes (rounded to the nearest 1,000 for FQUEST) and 1,000 independent replications.

p	y_p	N	Point Est.	Avg. |Bias|	Avg. 95% CI HL	Avg. 95% CI rel. prec. (%)	Avg. 95% CI cov. (%)	$\overline{m}$	St. Dev. HL
0.3	94.749	158,000	94.762	0.427	1.217	1.285	94.3	10,018	0.496
		157,977	*94.767*	*0.459*	*1.126*	*1.188*	*94.0*	*9,722*	*0.246*
0.5	100.000	119,000	100.015	0.486	1.323	1.323	94.3	7,417	0.502
		118,956	*100.023*	*0.519*	*1.261*	*1.261*	*93.7*	*7,320*	*0.290*
0.7	105.251	125,000	105.270	0.485	1.352	1.285	94.6	8,058	0.532
		125,118	*105.278*	*0.509*	*1.252*	*1.190*	*93.7*	*7,700*	*0.277*
0.9	112.832	199,000	112.820	0.455	1.288	1.141	95.3	13,770	0.550
		198,985	*112.828*	*0.471*	*1.156*	*1.024*	*94.2*	*12,245*	*0.241*
0.95	116.469	247,000	116.443	0.455	1.370	1.176	94.7	18,156	0.623
		247,276	*116.454*	*0.472*	*1.177*	*1.010*	*94.7*	*15,217*	*0.243*
0.99	123.293	1,426,000	123.274	0.266	0.829	0.673	96.6	99,337	0.366
		1,425,914	*123.274*	*0.286*	*0.715*	*0.580*	*94.5*	*87,749*	*0.149*
0.995	125.791	1,812,000	125.776	0.282	0.866	0.688	95.0	129,654	0.378
		1,811,627	*125.773*	*0.305*	*0.765*	*0.608*	*94.5*	*111,485*	*0.168*

Table 5.3: Experimental results for FQUEST with regard to point and 95% CI estimation of y_p for the AR(1) process in Section 5.3.1 with $\mu_Y = 0$ and $\phi = 0.9$ based on 1,000 independent replications.

p	y_p	N	Point Est.	Avg. |Bias|	Avg. 95% CI HL	Avg. 95% CI rel. prec. (%)	Avg. 95% CI cov. (%)	$\overline{m}$	$\overline{b}$	St. Dev. HL	Avg. Trunc. Point
0.25	−1.547	50,000	−1.545	0.038	0.116	7.520	96.7	3,058	19.74	0.042	595
		100,000	−1.545	0.028	0.079	5.146	95.9	6,006	20.17	0.024	600
		200,000	−1.547	0.020	0.057	3.710	96.5	12,228	20.04	0.019	600
		500,000	−1.547	0.012	0.036	2.306	96.2	30,907	19.71	0.011	600
		1,000,000	-1.548	0.008	0.026	1.667	96.6	61,322	20.04	0.009	600
0.45	−0.288	50,000	−0.287	0.037	0.110	39.432	96.2	2,986	20.18	0.040	597
		100,000	−0.286	0.027	0.077	27.200	96.1	6,019	20.12	0.025	599
		200,000	−0.288	0.019	0.054	19.009	96.1	12,191	19.99	0.017	599
		500,000	−0.288	0.011	0.035	12.105	97.4	30,772	19.89	0.012	599
		1,000,000	-0.288	0.008	0.024	8.325	96.9	60,066	20.28	0.007	600
0.75	1.547	50,000	1.548	0.039	0.114	7.351	95.2	3,020	20.04	0.038	598
		100,000	1.548	0.029	0.082	5.274	95.4	6,182	19.72	0.029	601
		200,000	1.548	0.020	0.056	3.648	96.3	11,988	20.26	0.017	602
		500,000	1.548	0.012	0.036	2.297	96.5	29,709	20.33	0.011	602
		1,000,000	1.548	0.009	0.026	1.661	97.3	61,236	19.92	0.008	602
0.9	2.940	50,000	2.939	0.046	0.132	4.506	96.3	3,090	19.48	0.051	593
		100,000	2.940	0.033	0.092	3.121	96.0	6,201	19.53	0.029	596
		200,000	2.941	0.023	0.066	2.228	96.2	12,229	20.05	0.023	596
		500,000	2.941	0.014	0.042	1.434	96.3	31,110	19.58	0.016	595
		1,000,000	2.940	0.010	0.030	1.011	96.6	62,215	19.66	0.011	596
0.95	3.774	50,000	3.772	0.052	0.150	3.976	95.7	3,181	18.98	0.057	603
		100,000	3.774	0.037	0.103	2.740	95.0	6,292	19.07	0.034	604
		200,000	3.774	0.026	0.073	1.931	96.5	12,168	19.93	0.023	605
		500,000	3.774	0.016	0.047	1.257	97.4	31,346	19.42	0.017	605
		1,000,000	3.774	0.012	0.033	0.881	95.7	62,371	19.64	0.011	605
0.99	5.337	50,000	5.336	0.076	0.229	4.294	95.0	3,606	16.43	0.100	594
		100,000	5.336	0.052	0.156	2.913	95.3	6,780	17.77	0.061	597
		200,000	5.338	0.037	0.108	2.024	95.4	12,918	18.80	0.037	597
		500,000	5.337	0.024	0.067	1.265	96.5	31,028	19.70	0.023	598
		1,000,000	5.337	0.017	0.048	0.902	95.7	60,577	20.22	0.015	599
0.995	5.909	50,000	5.905	0.092	0.284	4.813	95.0	3,827	15.01	0.132	590
		100,000	5.907	0.064	0.192	3.253	96.0	7,114	16.62	0.086	595
		200,000	5.909	0.045	0.134	2.260	95.6	13,310	18.24	0.054	595
		500,000	5.909	0.029	0.081	1.377	96.9	30,934	19.67	0.026	597
		1,000,000	5.909	0.021	0.058	0.987	95.4	61,451	19.82	0.021	597

Figure 5.3: Plots of the estimates for CI relative precision and coverage probability for the AR(1) process from Table 5.3.

Table 5.4: Comparison between FQUEST and SQSTS (in italic typeface) without a CI precision requirement for the AR(1) process in Section 5.3.1 with $\mu_Y = 0$ and $\phi = 0.9$ based on approximately equal sample sizes (rounded to the nearest 1,000 for FQUEST) and 1,000 independent replications.

p	y_p	N	Point Est.	Avg. |Bias|	Avg. 95% CI HL	Avg. 95% CI rel. prec. (%)	Avg. 95% CI cov. (%)	$\overline{m}$	St. Dev. HL
0.25	−1.547	49,000	−1.545	0.039	0.117	7.579	97.5	3,017	0.043
		48,556	*−1.544*	*0.041*	*0.106*	*6.881*	*95.2*	*2,988*	*0.021*
0.45	−0.288	46,000	−0.288	0.038	0.116	41.500	96.7	2,841	0.043
		46,403	*−0.286*	*0.040*	*0.104*	*37.678*	*95.5*	*2,856*	*0.020*
0.75	1.547	49,000	1.547	0.039	0.115	7.453	95.9	3,053	0.038
		48,798	*1.548*	*0.042*	*0.105*	*6.808*	*94.5*	*3,003*	*0.021*
0.9	2.940	57,000	2.940	0.043	0.122	4.133	95.7	3,549	0.041
		56,556	*2.941*	*0.046*	*0.113*	*3.834*	*94.3*	*3,480*	*0.025*
0.95	3.774	66,000	3.772	0.046	0.128	3.398	95.9	4,150	0.043
		65,655	*3.771*	*0.048*	*0.120*	*3.180*	*94.9*	*4,040*	*0.030*
0.99	5.337	438,000	5.337	0.025	0.073	1.375	96.6	27,156	0.027
		437,898	*5.337*	*0.026*	*0.067*	*1.260*	*95.2*	*26,948*	*0.015*
0.995	5.909	499,000	5.909	0.029	0.083	1.409	96.1	31,032	0.030
		498,559	*5.908*	*0.030*	*0.077*	*1.307*	*94.9*	*30,681*	*0.018*

Table 5.5: Experimental results for FQUEST with regard to point and 95% CI estimation of y_p for the ARTOP process in Section 5.3.2 based on 1,000 independent replications.

p	y_p	N	Point Est.	Avg. |Bias|	Avg. 95% CI HL	Avg. 95% CI rel. prec. (%)	Avg. 95% CI cov. (%)	$\overline{m}$	$\overline{b}$	St. Dev. HL	Avg. Trunc. Point
0.3	1.185	50,000	1.188	0.021	0.103	8.648	98.0	4,719	10.77	0.061	739
		100,000	1.187	0.016	0.062	5.208	97.3	8,989	11.78	0.035	871
		200,000	1.186	0.011	0.038	3.225	97.1	16,710	13.36	0.019	885
		500,000	1.186	0.007	0.021	1.812	96.8	35,771	16.70	0.008	887
		1,000,000	1.185	0.005	0.015	1.240	97.5	67,890	17.75	0.006	888
0.5	1.391	50,000	1.395	0.039	0.176	12.589	97.1	4,619	11.14	0.112	766
		100,000	1.394	0.029	0.107	7.669	96.4	8,759	12.28	0.060	914
		200,000	1.392	0.020	0.067	4.837	96.4	16,144	14.11	0.033	927
		500,000	1.392	0.012	0.039	2.795	96.1	35,563	16.76	0.016	930
		1,000,000	1.391	0.009	0.026	1.880	97.1	65,144	18.53	0.009	931
0.7	1.774	50,000	1.780	0.073	0.330	18.460	97.5	4,648	11.00	0.223	786
		100,000	1.779	0.054	0.206	11.529	96.2	8,740	12.33	0.126	970
		200,000	1.776	0.038	0.129	7.246	96.0	16,006	14.19	0.067	995
		500,000	1.776	0.023	0.074	4.137	96.7	35,868	16.55	0.030	997
		1,000,000	1.774	0.016	0.050	2.792	96.9	65,123	18.63	0.018	998
0.9	2.994	50,000	3.014	0.223	1.145	37.296	97.2	4,811	10.38	0.895	793
		100,000	3.006	0.157	0.675	22.313	95.6	9,321	11.06	0.447	1,019
		200,000	2.997	0.114	0.425	14.112	96.5	17,331	12.61	0.279	1,068
		500,000	2.997	0.069	0.233	7.777	96.6	38,526	15.09	0.127	1,070
		1,000,000	2.994	0.049	0.152	5.070	96.4	68,538	17.65	0.062	1,072
0.95	4.164	50,000	4.205	0.428	2.393	55.444	95.7	4,854	10.25	2.041	758
		100,000	4.184	0.290	1.410	33.363	95.7	9,574	10.59	1.045	933
		200,000	4.168	0.209	0.878	20.878	96.7	18,261	11.57	0.629	973
		500,000	4.168	0.126	0.461	11.044	95.9	41,294	13.72	0.274	975
		1,000,000	4.164	0.089	0.290	6.954	96.6	73,992	15.87	0.134	977
0.99	8.962	50,000	9.112	1.741	9.631	98.912	93.2	4,926	10.02	9.566	662
		100,000	9.011	1.136	7.257	77.372	94.0	9,869	10.10	6.566	736
		200,000	8.955	0.810	4.802	52.634	95.8	19,568	10.31	4.039	747
		500,000	8.958	0.500	2.365	26.132	96.3	47,897	10.73	1.682	747
		1,000,000	8.955	0.365	1.443	16.050	96.0	89,404	12.04	0.929	749
0.995	12.466	50,000	12.751	3.197	14.953	106.177	90.7	4,938	10.01	15.592	601
		100,000	12.552	2.080	12.777	95.946	93.1	9,910	10.04	12.796	635
		200,000	12.451	1.485	9.518	73.741	95.5	19,647	10.25	8.832	643
		500,000	12.451	0.919	4.963	39.181	96.6	48,821	10.40	3.804	643
		1,000,000	12.444	0.664	3.041	24.255	96.1	94,027	11.10	2.170	644

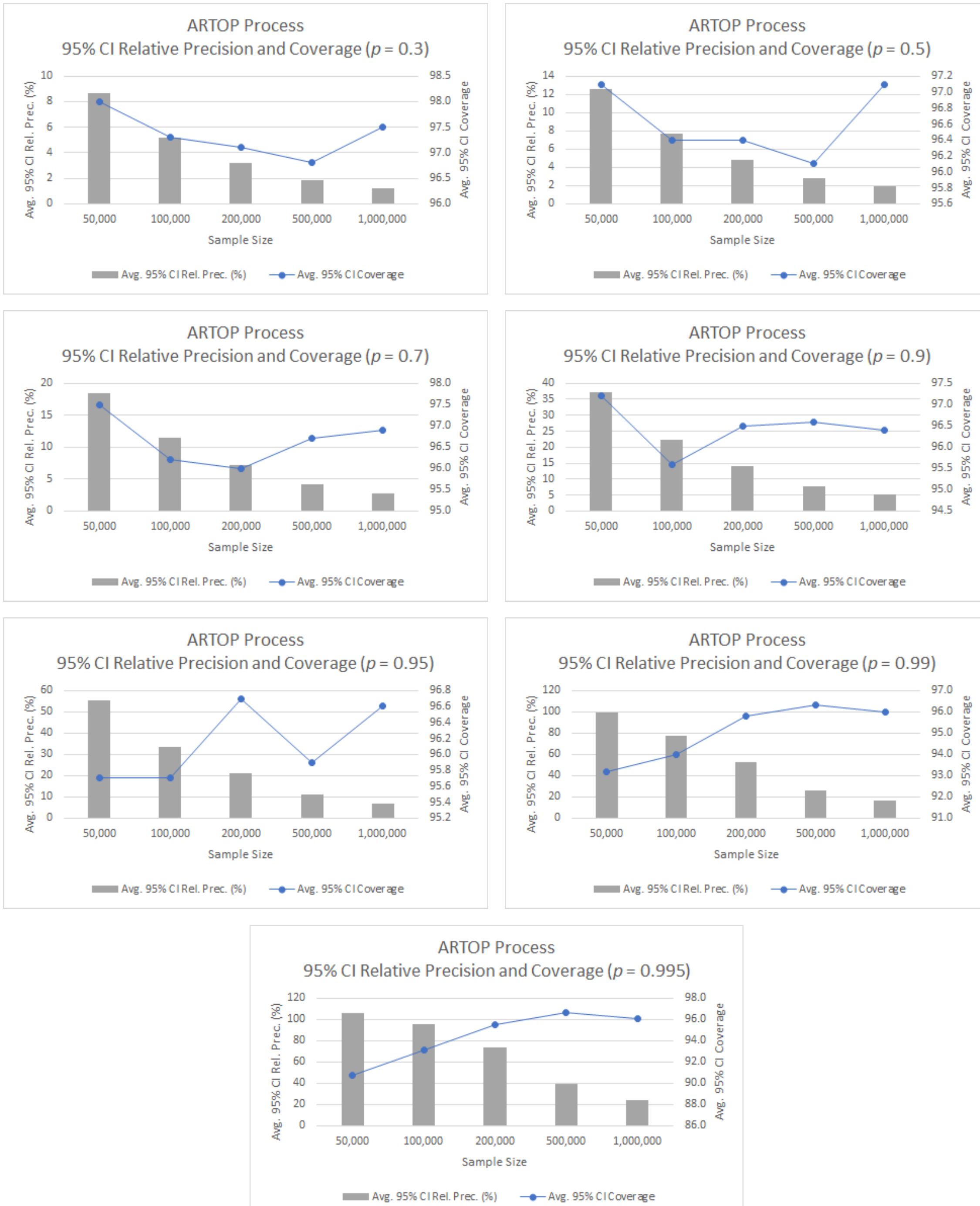

Figure 5.4: Plots of the estimates for CI relative precision and coverage probability for the ARTOP process from Table 5.5.

Table 5.6: Comparison between FQUEST and SQSTS (in italic typeface) without a CI precision requirement for the ARTOP process in Section 5.3.2 based on approximately equal sample sizes (rounded to the nearest 1,000 for FQUEST) and 1,000 independent replications.

p	y_p	N	Point Est.	Avg. |Bias|	Avg. 95% CI HL	Avg. 95% CI rel. prec. (%)	Avg. 95% CI cov. (%)	$\overline{m}$	St. Dev. HL
0.3	1.185	339,000	1.186	0.008	0.027	2.295	97.0	26,148	0.012
		338,776	*1.186*	*0.009*	*0.024*	*2.038*	*95.0*	*20,848*	*0.007*
0.5	1.391	316,000	1.392	0.015	0.051	3.640	96.4	23,559	0.023
		315,726	*1.393*	*0.017*	*0.045*	*3.244*	*94.8*	*19,429*	*0.014*
0.7	1.774	344,000	1.776	0.028	0.092	5.155	97.0	25,314	0.042
		343,862	*1.778*	*0.032*	*0.083*	*4.654*	*94.7*	*21,161*	*0.025*
0.9	2.994	475,000	2.998	0.072	0.243	8.091	96.5	37,185	0.129
		474,533	*2.998*	*0.079*	*0.211*	*7.021*	*95.8*	*29,202*	*0.067*
0.95	4.164	552,000	4.168	0.123	0.440	10.550	97.0	44,732	0.246
		551,823	*4.168*	*0.135*	*0.368*	*8.811*	*96.1*	*33,958*	*0.118*
0.99	8.962	2,578,000	8.960	0.227	0.778	8.677	96.4	203,651	0.428
		2,578,084	*8.954*	*0.245*	*0.662*	*7.382*	*94.8*	*158,651*	*0.191*
0.995	12.466	3,063,000	12.467	0.373	1.346	10.782	96.6	251,432	0.749
		3,062,888	*12.441*	*0.412*	*1.107*	*8.886*	*94.5*	*188,485*	*0.313*

Table 5.7: Experimental results for FQUEST with regard to point and 95% CI estimation of y_p for the M/M/1 waiting-time process in Section 5.3.3 with traffic intensity 0.9 based on 1000 independent replications.

p	y_p	N	Point Est.	Avg. |Bias|	Avg. 95% CI HL	Avg. 95% CI rel. prec. (%)	Avg. 95% CI cov. (%)	$\overline{m}$	$\overline{b}$	St. Dev. HL	Avg. Trunc. Point
0.3	2.513	50,000	2.541	0.186	1.045	40.769	97.4	4,809	10.42	0.711	765
		100,000	2.533	0.129	0.599	23.530	98.0	9,316	11.08	0.371	1,031
		200,000	2.525	0.091	0.357	14.130	97.8	17,276	12.72	0.190	1,088
		500,000	2.520	0.056	0.188	7.442	97.6	37,209	15.80	0.072	1,091
		1,000,000	2.516	0.040	0.128	5.076	96.8	68,747	17.42	0.050	1,093
0.5	5.878	50,000	5.946	0.386	2.166	36.056	97.6	4,790	10.52	1.733	674
		100,000	5.925	0.263	1.211	20.350	98.0	9,252	11.22	0.785	755
		200,000	5.906	0.183	0.720	12.187	97.8	17,474	12.50	0.380	765
		500,000	5.894	0.114	0.387	6.569	97.2	37,968	15.36	0.157	768
		1,000,000	5.884	0.081	0.262	4.447	96.7	69,099	17.46	0.097	769
0.7	10.986	50,000	11.145	0.750	4.419	39.082	97.9	4,761	10.65	4.226	646
		100,000	11.090	0.508	2.391	21.410	97.3	9,231	11.30	1.748	666
		200,000	11.046	0.348	1.384	12.518	98.4	17,617	12.38	0.797	668
		500,000	11.017	0.220	0.746	6.765	96.7	37,801	15.39	0.335	671
		1,000,000	10.998	0.156	0.499	4.539	97.0	69,797	17.28	0.185	672
0.9	21.972	50,000	22.578	1.908	11.376	49.271	96.6	4,822	10.41	9.492	659
		100,000	22.342	1.258	6.885	30.346	97.0	9,408	10.97	6.174	675
		200,000	22.160	0.871	3.908	17.532	96.5	18,159	11.74	2.925	677
		500,000	22.061	0.545	1.951	8.826	96.8	41,262	13.81	1.159	679
		1,000,000	22.007	0.379	1.274	5.781	97.2	75,474	15.69	0.602	680
0.95	28.904	50,000	30.108	3.099	15.268	49.204	95.5	4,822	10.42	11.617	656
		100,000	29.606	2.053	11.057	36.538	96.5	9,612	10.60	9.494	676
		200,000	29.240	1.393	6.709	22.652	96.3	18,611	11.25	5.867	677
		500,000	29.045	0.857	3.302	11.314	96.3	44,391	12.30	2.285	678
		1,000,000	28.963	0.590	2.090	7.202	96.7	80,608	14.22	1.210	680
0.99	44.998	50,000	49.730	8.917	28.705	51.357	92.6	4,907	10.10	27.367	653
		100,000	47.619	5.882	20.448	40.031	93.9	9,821	10.21	18.106	668
		200,000	46.054	3.691	15.032	31.680	94.9	19,583	10.31	11.375	668
		500,000	45.416	2.164	10.379	22.538	95.8	47,266	10.98	8.282	669
		1,000,000	45.131	1.490	6.894	15.132	95.2	92,147	11.46	5.667	670
0.995	51.930	50,000	57.240	11.541	36.435	55.529	90.1	4,924	10.04	34.815	661
		100,000	55.654	8.615	27.125	43.841	91.4	9,880	10.09	26.090	676
		200,000	53.680	5.549	19.006	33.343	92.5	19,636	10.25	16.403	676
		500,000	52.644	3.186	13.465	25.022	95.2	48,511	10.49	10.124	676
		1,000,000	52.155	2.180	10.277	19.437	95.7	94,553	10.99	7.988	677

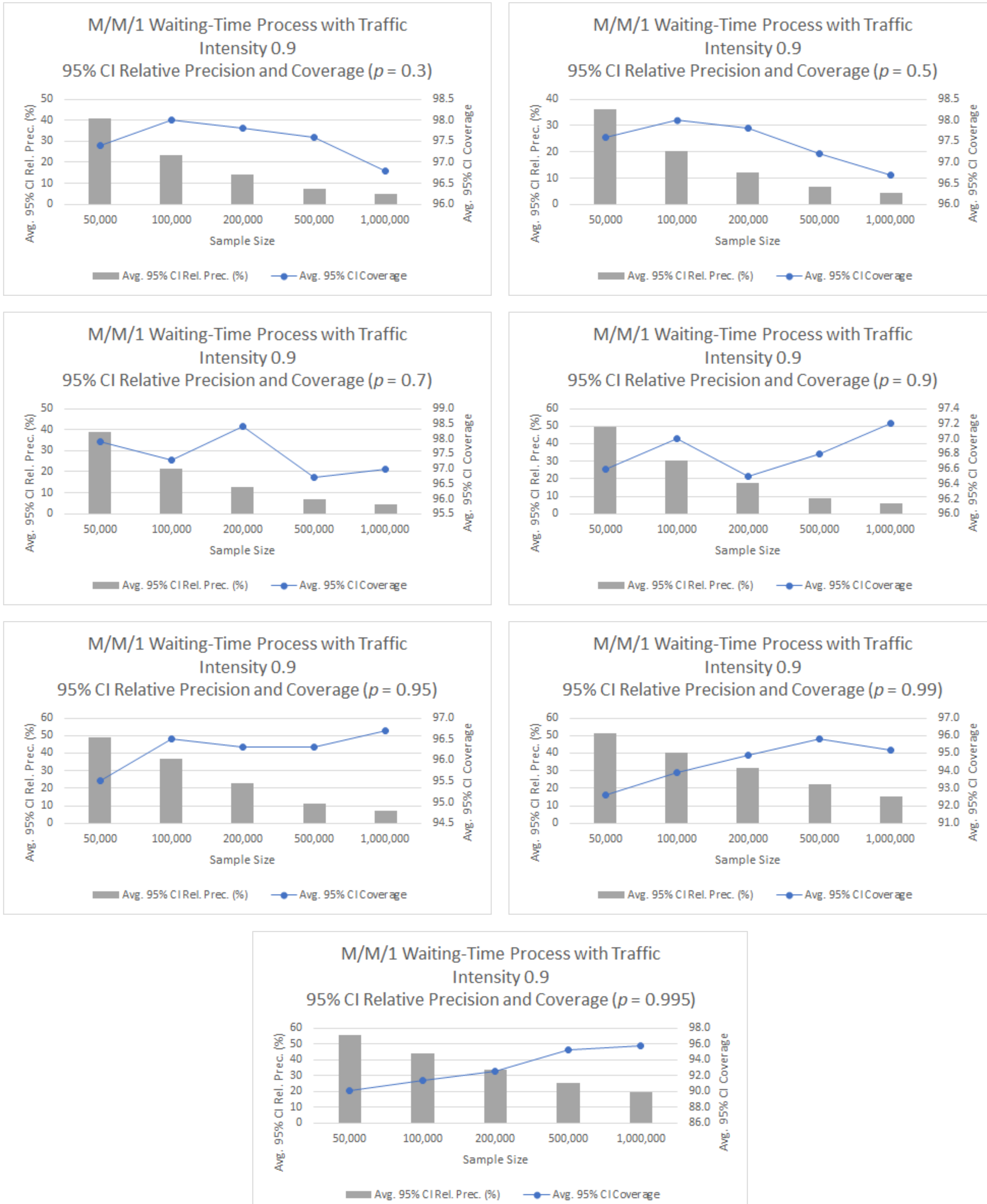

Figure 5.5: Plots of the estimates for CI relative precision and coverage probability for the M/M/1 waiting-time process from Table 5.7.

Table 5.8: Comparison between FQUEST and SQSTS (in italic typeface) without a CI precision requirement for the M/M/1 waiting-time process in Section 5.3.3 with traffic intensity 0.9 based on approximately equal sample sizes (rounded to the nearest 1,000 for FQUEST) and 1,000 independent replications.

p	y_p	N	Point Est.	Avg. |Bias|	Avg. 95% CI HL	Avg. 95% CI rel. prec. (%)	Avg. 95% CI cov. (%)	$\overline{m}$	St. Dev. HL
0.3	2.513	609,000	2.520	0.052	0.167	6.639	97.4	44,317	0.067
		609,093	*2.518*	*0.055*	*0.150*	*5.974*	*96.3*	*37,483*	*0.043*
0.5	5.878	499,000	5.894	0.114	0.394	6.685	97.2	37,796	0.175
		498,777	*5.894*	*0.124*	*0.348*	*5.901*	*96.0*	*30,694*	*0.129*
0.7	10.986	442,000	11.016	0.234	0.816	7.397	97.5	34,744	0.390
		442,498	*11.030*	*0.291*	*0.808*	*7.277*	*96.0*	*27,231*	*0.595*
0.9	21.972	358,000	22.089	0.660	2.341	10.568	97.1	30,795	1.415
		357,785	*22.008*	*0.717*	*1.948*	*8.827*	*95.3*	*22,018*	*0.735*
0.95	28.904	379,000	29.081	1.001	4.080	13.929	96.3	33,988	3.045
		378,815	*28.879*	*1.031*	*2.634*	*9.088*	*93.7*	*23,312*	*0.885*
0.99	44.998	2,472,000	45.052	0.935	3.494	7.729	96.9	212,102	2.402
		2,471,614	*44.894*	*0.983*	*2.472*	*5.498*	*93.8*	*152,099*	*0.690*
0.995	51.930	2,862,000	51.965	1.226	5.109	9.774	96.0	256,190	4.113
		2,861,834	*51.777*	*1.262*	*3.128*	*6.027*	*92.7*	*176,113*	*0.875*

Table 5.9: Experimental results for FQUEST with regard to point and 95% CI estimation of y_p for the M/M/1 waiting-time process in Section 5.3.3 with traffic intensity 0.8 based on 1000 independent replications.

p	y_p	N	Point Est.	Avg. |Bias|	Avg. 95% CI HL	Avg. 95% CI rel. prec. (%)	Avg. 95% CI cov. (%)	$\overline{m}$	$\overline{b}$	St. Dev. HL	Avg. Trunc. Point
0.3	0.668	50,000	0.667	0.044	0.160	24.030	97.3	4,098	13.49	0.080	1,002
		100,000	0.669	0.030	0.105	15.774	96.8	7,431	15.45	0.051	1,950
		200,000	0.669	0.021	0.071	10.582	97.3	13,665	17.37	0.031	2,460
		500,000	0.669	0.013	0.042	6.348	97.1	31,526	19.25	0.015	2,461
		1,000,000	0.668	0.010	0.030	4.429	96.9	62,711	19.48	0.009	2,463
0.5	2.350	50,000	2.348	0.090	0.335	14.223	96.9	4,099	13.37	0.180	986
		100,000	2.352	0.062	0.215	9.149	96.9	7,388	15.52	0.100	1,897
		200,000	2.352	0.044	0.143	6.070	97.3	13,807	17.20	0.059	2,336
		500,000	2.352	0.028	0.085	3.626	97.2	31,159	19.32	0.026	2,338
		1,000,000	2.350	0.020	0.060	2.545	96.6	61,917	19.72	0.019	2,340
0.7	4.904	50,000	4.905	0.173	0.658	13.368	97.1	4,170	13.08	0.401	880
		100,000	4.910	0.120	0.418	8.497	97.2	7,548	15.13	0.208	1,553
		200,000	4.909	0.083	0.276	5.623	97.9	14,031	16.93	0.120	1,881
		500,000	4.908	0.052	0.166	3.378	97.7	32,139	18.77	0.063	1,883
		1,000,000	4.905	0.038	0.113	2.304	97.8	62,625	19.47	0.033	1,885
0.9	10.397	50,000	10.431	0.416	1.784	17.005	96.5	4,437	11.95	1.289	628
		100,000	10.428	0.288	1.108	10.592	96.8	8,369	13.37	0.667	667
		200,000	10.415	0.206	0.702	6.730	96.7	15,466	15.04	0.367	673
		500,000	10.408	0.129	0.404	3.880	96.6	34,019	17.68	0.162	676
		1,000,000	10.400	0.094	0.277	2.661	96.7	64,571	18.84	0.099	677
0.95	13.863	50,000	13.922	0.638	3.064	21.803	96.6	4,585	11.37	2.302	604
		100,000	13.914	0.442	1.916	13.691	97.0	8,806	12.35	1.306	612
		200,000	13.886	0.321	1.140	8.186	96.8	16,442	13.82	0.650	613
		500,000	13.879	0.199	0.641	4.615	96.4	35,872	16.70	0.293	616
		1,000,000	13.868	0.146	0.435	3.137	96.3	66,674	18.22	0.163	617
0.99	21.910	50,000	22.107	1.607	6.700	29.648	94.9	4,827	10.43	4.864	602
		100,000	22.061	1.129	5.151	23.043	95.4	9,537	10.74	3.801	607
		200,000	21.972	0.792	3.546	16.019	95.7	18,488	11.45	2.708	608
		500,000	21.949	0.498	1.794	8.152	96.1	42,812	12.93	1.103	610
		1,000,000	21.918	0.344	1.209	5.509	96.3	79,373	14.65	0.670	611
0.995	25.376	50,000	25.630	2.317	8.272	31.061	93.3	4,888	10.20	6.109	599
		100,000	25.581	1.614	6.503	24.989	93.7	9,711	10.43	4.507	603
		200,000	25.470	1.143	5.137	19.937	95.2	19,066	10.80	3.833	604
		500,000	25.435	0.714	2.946	11.532	95.4	45,271	11.88	2.147	605
		1,000,000	25.388	0.492	1.895	7.441	95.6	85,392	13.04	1.212	607

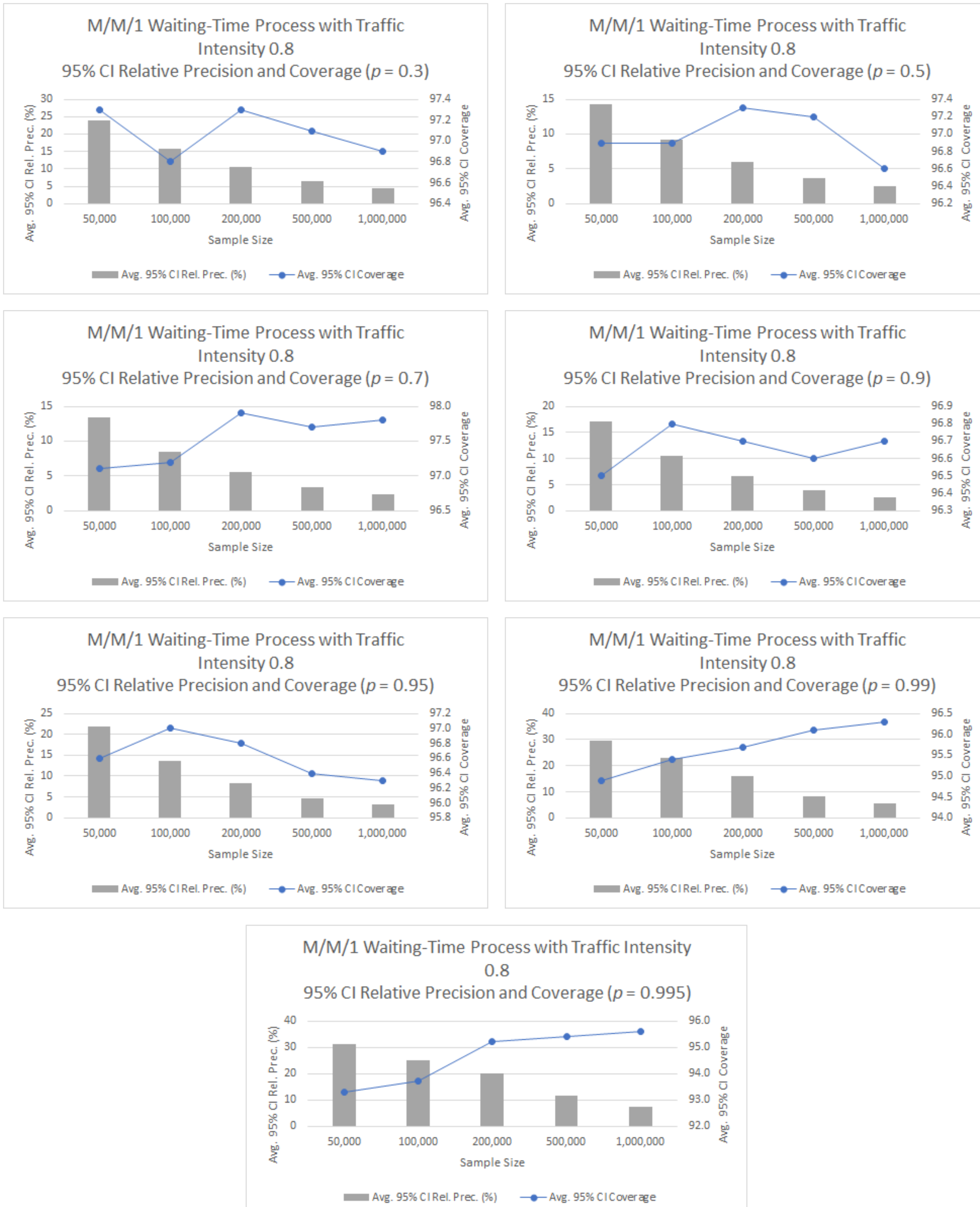

Figure 5.6: Plots of the estimates for CI relative precision and coverage probability for the M/M/1 waiting-time process from Table 5.9.

Table 5.10: Comparison between FQUEST and SQSTS (in italic typeface) without a CI precision requirement for the M/M/1 waiting-time process in Section 5.3.3 with traffic intensity 0.8 based on approximately equal sample sizes (rounded to the nearest 1,000 for FQUEST) and 1,000 independent replications.

p	y_p	N	Point Est.	Avg. |Bias|	Avg. 95% CI HL	Avg. 95% CI rel. prec. (%)	Avg. 95% CI cov. (%)	$\overline{m}$	St. Dev. HL
0.3	0.668	799,000	0.668	0.011	0.033	4.908	97.2	50,685	0.010
		798,681	*0.668*	*0.012*	*0.030*	*4.559*	*95.8*	*49,150*	*0.008*
0.5	2.350	760,000	2.351	0.022	0.069	2.936	96.7	46,032	0.022
		759,669	*2.352*	*0.025*	*0.064*	*2.728*	*96.1*	*46,749*	*0.018*
0.7	4.904	725,000	4.907	0.044	0.135	2.754	97.2	45,462	0.044
		725,428	*4.908*	*0.048*	*0.126*	*2.561*	*96.6*	*44,642*	*0.036*
0.9	10.397	620,000	10.407	0.119	0.361	3.463	96.9	42,313	0.138
		619,642	*10.412*	*0.140*	*0.358*	*3.432*	*95.3*	*38,132*	*0.197*
0.95	13.863	546,000	13.876	0.192	0.616	4.436	97.1	39,395	0.287
		546,450	*13.871*	*0.243*	*0.626*	*4.509*	*94.9*	*33,628*	*0.303*
0.99	21.910	4,013,000	21.917	0.177	0.541	2.468	96.9	274,623	0.238
		4,012,767	*21.922*	*0.195*	*0.527*	*2.402*	*95.2*	*246,940*	*0.254*
0.995	25.376	3,361,000	25.378	0.272	0.896	3.529	96.1	250,979	0.478
		3,361,373	*25.381*	*0.321*	*0.826*	*3.250*	*94.9*	*206,854*	*0.328*

Table 5.11: Experimental results for FQUEST with regard to point and 95% CI estimation of y_p for the M/H$_2$/1 waiting-time process in Section 5.3.4 based on 1,000 independent replications.

p	y_p	N	Point Est.	Avg. |Bias|	Avg. 95% CI HL	Avg. 95% CI rel. prec. (%)	Avg. 95% CI cov. (%)	$\overline{m}$	$\overline{b}$	St. Dev. HL	Avg. Trunc. Point
0.3	0.669	50,000	0.675	0.086	0.616	90.834	98.8	4,861	10.26	0.387	615
		100,000	0.676	0.062	0.334	49.245	99.0	9,591	10.61	0.203	620
		200,000	0.674	0.043	0.188	27.839	98.0	17,994	11.87	0.105	622
		500,000	0.671	0.027	0.096	14.382	97.8	39,649	14.52	0.043	625
		1,000,000	0.670	0.019	0.062	9.311	97.6	71,368	16.79	0.026	626
0.5	3.847	50,000	3.854	0.316	1.472	38.055	97.9	4,621	11.17	0.918	666
		100,000	3.865	0.228	0.901	23.229	97.7	8,807	12.20	0.517	682
		200,000	3.864	0.161	0.557	14.412	97.0	15,773	14.51	0.275	685
		500,000	3.853	0.100	0.316	8.206	97.0	35,000	17.17	0.127	687
		1,000,000	3.851	0.072	0.217	5.631	97.0	65,682	18.50	0.080	687
0.7	9.606	50,000	9.603	0.601	2.762	28.587	96.3	4,563	11.42	1.874	680
		100,000	9.631	0.432	1.742	18.024	97.3	8,639	12.56	1.077	710
		200,000	9.634	0.306	1.058	10.957	96.8	15,751	14.52	0.536	712
		500,000	9.618	0.193	0.609	6.328	97.6	35,249	16.95	0.247	714
		1,000,000	9.613	0.139	0.411	4.278	97.1	66,149	18.30	0.142	715
0.9	22.011	50,000	22.013	1.468	7.123	32.021	95.2	4,674	10.96	5.626	663
		100,000	22.039	1.044	4.575	20.623	95.6	8,934	12.01	3.526	689
		200,000	22.041	0.734	2.750	12.434	96.4	16,754	13.31	1.739	690
		500,000	22.019	0.469	1.496	6.788	95.4	37,574	15.69	0.740	693
		1,000,000	22.025	0.341	1.012	4.595	96.3	70,256	16.94	0.431	693
0.95	29.837	50,000	29.873	2.266	10.388	34.251	94.2	4,776	10.60	7.812	651
		100,000	29.900	1.630	7.716	25.467	94.7	9,268	11.27	6.178	667
		200,000	29.880	1.143	4.609	15.310	95.7	17,764	12.16	3.464	669
		500,000	29.844	0.726	2.468	8.252	95.6	40,734	14.13	1.410	670
		1,000,000	29.860	0.520	1.663	5.568	95.7	73,636	16.10	0.867	672
0.99	48.010	50,000	48.090	5.432	17.728	35.163	88.7	4,909	10.09	13.143	644
		100,000	48.178	3.934	14.617	29.619	91.4	9,718	10.39	10.276	653
		200,000	48.060	2.825	11.495	23.602	93.1	19,185	10.72	8.237	653
		500,000	48.029	1.792	7.613	15.726	93.5	46,407	11.38	5.892	654
		1,000,000	48.092	1.261	4.789	9.918	95.3	87,155	12.62	3.404	655
0.995	55.837	50,000	55.517	7.327	22.459	37.773	84.9	4,918	10.06	18.149	638
		100,000	55.962	5.523	17.943	30.710	88.4	9,811	10.23	13.492	645
		200,000	55.854	4.033	14.261	25.006	90.6	19,548	10.35	9.880	645
		500,000	55.893	2.592	10.788	19.104	93.8	47,938	10.70	7.801	645
		1,000,000	55.983	1.819	7.478	13.275	94.8	91,968	11.60	5.629	646

Figure 5.7: Plots of the estimates for CI relative precision and coverage probability for the M/H$_2$/1 waiting-time process from Table 5.11.

Table 5.12: Comparison between FQUEST and SQSTS (in italic typeface) without a CI precision requirement for the $M/H_2/1$ waiting-time process in Section 5.3.4 based on approximately equal sample sizes (rounded to the nearest 1,000 for FQUEST) and 1,000 independent replications.

p	y_p	N	Point Est.	Avg. |Bias|	Avg. 95% CI HL	Avg. 95% CI rel. prec. (%)	Avg. 95% CI cov. (%)	$\overline{m}$	St. Dev. HL
0.3	0.669	368,000	0.672	0.031	0.120	17.899	97.8	30,289	0.063
		368,063	*0.672*	*0.032*	*0.094*	*13.973*	*96.0*	*22,650*	*0.027*
0.5	3.847	261,000	3.861	0.138	0.473	12.228	96.4	20,170	0.223
		261,001	*3.860*	*0.150*	*0.399*	*10.349*	*94.6*	*16,062*	*0.128*
0.7	9.606	238,000	9.633	0.281	0.948	9.826	96.6	18,517	0.435
		237,598	*9.624*	*0.326*	*0.868*	*8.998*	*95.5*	*14,621*	*0.375*
0.9	22.011	251,000	22.038	0.663	2.330	10.555	97.0	20,864	1.361
		250,613	*21.995*	*0.736*	*1.895*	*8.595*	*95.0*	*15,422*	*0.622*
0.95	29.837	314,000	29.852	0.912	3.227	10.768	95.8	26,459	2.080
		314,152	*29.760*	*0.972*	*2.491*	*8.355*	*94.0*	*19,332*	*0.723*
0.99	48.010	1,996,000	48.054	0.898	2.946	6.121	95.7	161,440	1.647
		1,996,451	*47.993*	*0.939*	*2.371*	*4.936*	*94.9*	*122,859*	*0.649*
0.995	55.837	2,570,000	55.894	1.117	3.980	7.099	95.6	215,430	2.658
		2,570,337	*55.823*	*1.149*	*2.924*	*5.229*	*94.5*	*158,175*	*0.773*

Table 5.13: Experimental results for FQUEST with regard to point and 95% CI estimation of y_p for the M/M/1/LIFO waiting-time process in Section 5.3.5 based on 1,000 independent replications.

p	y_p	N	Point Est.	Avg. |Bias|	Avg. 95% CI HL	Avg. 95% CI rel. prec. (%)	Avg. 95% CI cov. (%)	$\overline{m}$	$\overline{b}$	St. Dev. HL	Avg. Trunc. Point
0.3	0.113	50,000	0.113	0.005	0.017	15.080	97.7	3,148	19.13	0.005	615
		100,000	0.113	0.004	0.012	10.499	97.6	6,143	19.62	0.004	622
		200,000	0.113	0.003	0.008	7.240	97.1	12,390	19.63	0.002	621
		500,000	0.113	0.002	0.005	4.537	98.1	30,089	20.25	0.002	622
		1,000,000	0.113	0.001	0.004	3.119	97.4	61,709	19.75	0.001	622
0.5	0.469	50,000	0.468	0.009	0.030	6.493	97.9	3,155	19.13	0.009	606
		100,000	0.469	0.006	0.021	4.416	97.5	6,177	19.59	0.006	610
		200,000	0.469	0.005	0.014	3.071	97.3	12,270	19.80	0.004	610
		500,000	0.469	0.003	0.009	1.943	98.2	30,846	20.00	0.003	610
		1,000,000	0.469	0.002	0.006	1.314	97.4	59,793	20.39	0.002	610
0.7	1.358	50,000	1.357	0.024	0.080	5.879	97.9	3,277	18.33	0.025	610
		100,000	1.358	0.017	0.055	4.022	96.8	6,399	18.99	0.017	612
		200,000	1.358	0.012	0.038	2.792	96.8	12,646	19.22	0.012	613
		500,000	1.358	0.008	0.024	1.752	98.1	30,382	20.25	0.008	613
		1,000,000	1.358	0.005	0.016	1.213	97.2	61,895	19.66	0.005	613
0.9	6.718	50,000	6.713	0.174	0.654	9.743	98.5	3,860	14.84	0.269	593
		100,000	6.724	0.126	0.428	6.367	98.1	6,924	17.16	0.167	598
		200,000	6.724	0.089	0.290	4.312	97.4	13,214	18.47	0.105	598
		500,000	6.722	0.055	0.176	2.617	98.0	31,029	19.54	0.056	600
		1,000,000	6.718	0.039	0.123	1.825	97.5	61,393	19.88	0.040	600
0.95	14.405	50,000	14.395	0.481	1.931	13.403	99.0	4,117	13.46	0.885	578
		100,000	14.420	0.350	1.252	8.670	98.2	7,549	15.37	0.589	583
		200,000	14.426	0.246	0.826	5.728	97.4	13,573	17.74	0.338	585
		500,000	14.416	0.152	0.498	3.452	97.9	32,257	18.92	0.177	585
		1,000,000	14.408	0.111	0.339	2.354	96.6	60,983	20.09	0.110	587
0.99	49.582	50,000	49.500	2.685	13.716	27.565	98.6	4,571	11.39	8.233	592
		100,000	49.680	1.905	8.358	16.783	98.6	8,634	12.62	4.515	598
		200,000	49.656	1.347	5.186	10.438	98.1	16,034	14.17	2.398	599
		500,000	49.588	0.859	2.895	5.834	97.4	35,027	17.14	1.120	602
		1,000,000	49.567	0.607	2.003	4.039	97.8	66,015	18.35	0.729	603
0.995	71.844	50,000	71.632	4.700	28.478	39.366	98.9	4,772	10.65	19.253	586
		100,000	72.028	3.371	17.138	23.697	98.8	9,089	11.67	10.416	595
		200,000	71.932	2.390	10.005	13.894	98.8	16,936	13.08	5.264	597
		500,000	71.876	1.512	5.402	7.510	98.0	37,375	15.69	2.311	599
		1,000,000	71.835	1.080	3.487	4.853	97.8	67,535	17.72	1.233	601

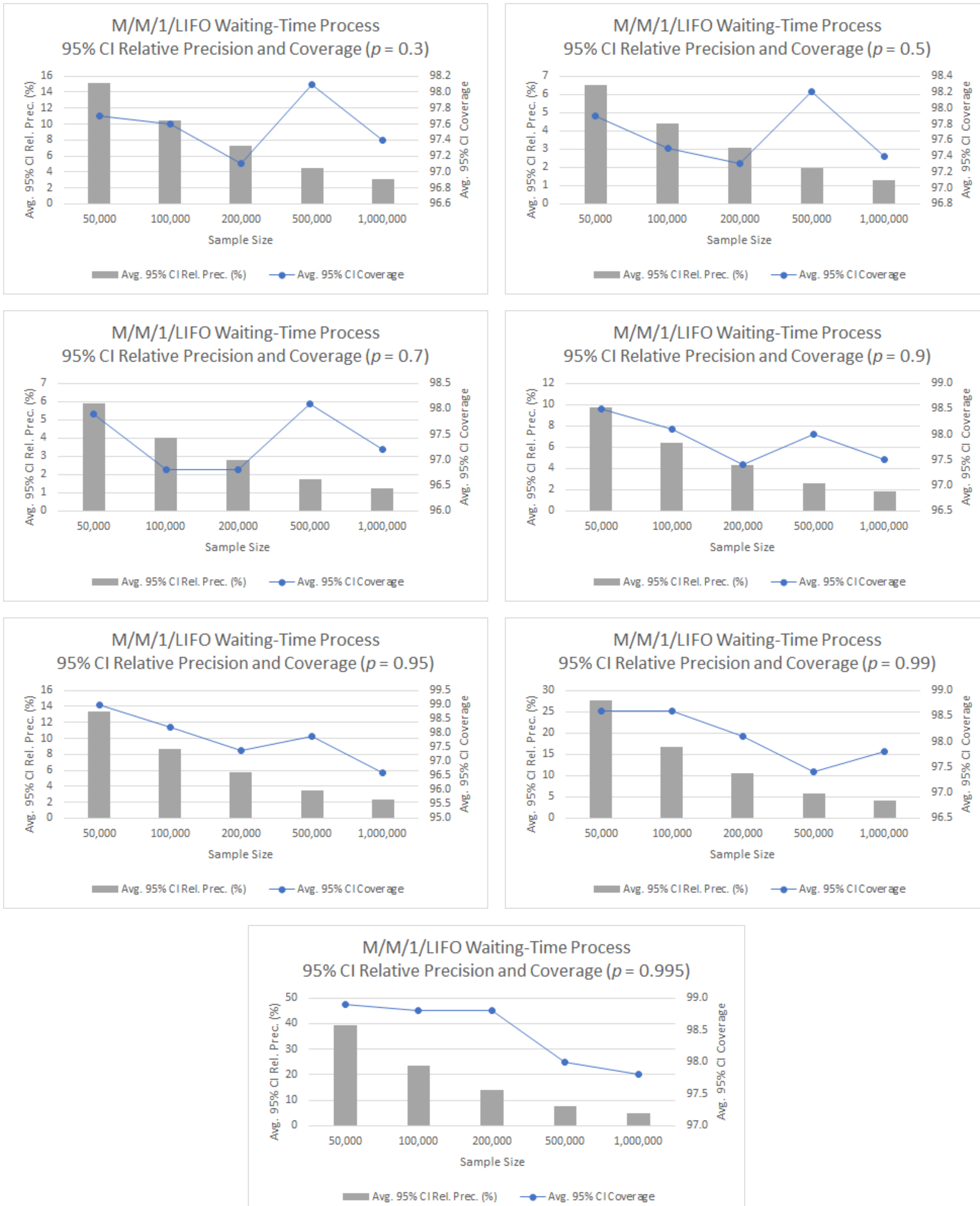

Figure 5.8: Plots of the estimates for CI relative precision and coverage probability for the M/M/1/LIFO waiting-time process from Table 5.13.

Table 5.14: Comparison between FQUEST and SQSTS (in italic typeface) without a CI precision requirement for the M/M/1/LIFO waiting-time process in Section 5.3.5 based on approximately equal sample sizes (rounded to the nearest 1,000 for FQUEST) and 1,000 independent replications.

p	y_p	N	Point Est.	Avg. |Bias|	Avg. 95% CI HL	Avg. 95% CI rel. prec. (%)	Avg. 95% CI cov. (%)	$\overline{m}$	St. Dev. HL
0.3	0.113	59,000	0.113	0.005	0.016	13.939	97.7	3,683	0.005
		58,757	*0.113*	*0.005*	*0.013*	*11.504*	*95.0*	*3,616*	*0.003*
0.5	0.469	55,000	0.468	0.009	0.029	6.167	97.7	3,463	0.009
		54,842	*0.468*	*0.009*	*0.024*	*5.102*	*94.5*	*3,375*	*0.005*
0.7	1.358	72,000	1.357	0.020	0.066	4.837	97.7	4,732	0.022
		71,716	*1.357*	*0.022*	*0.056*	*4.120*	*94.7*	*4,413*	*0.014*
0.9	6.718	122,000	6.728	0.116	0.381	5.659	97.6	8,319	0.138
		122,251	*6.717*	*0.125*	*0.324*	*4.829*	*95.9*	*7,523*	*0.090*
0.95	14.405	161,000	14.427	0.277	0.938	6.498	97.4	11,264	0.387
		161,386	*14.405*	*0.292*	*0.773*	*5.366*	*95.8*	*9,931*	*0.212*
0.99	49.582	732,000	49.577	0.734	2.361	4.762	96.9	48,807	0.926
		732,442	*49.594*	*0.795*	*2.015*	*4.062*	*95.6*	*45,073*	*0.540*
0.995	71.844	914,000	71.867	1.142	3.770	5.243	97.5	63,322	1.454
		913,998	*71.871*	*1.218*	*3.186*	*4.430*	*95.1*	*56,246*	*0.894*

Table 5.15: Experimental results for FQUEST with regard to point and 95% CI estimation of y_p for the M/M/1/M/1 total waiting-time process in Section 5.3.6 based on 1,000 independent replications.

p	y_p	N	Point Est.	Avg. |Bias|	Avg. 95% CI HL	Avg. 95% CI rel. prec. (%)	Avg. 95% CI cov. (%)	$\overline{m}$	$\overline{b}$	St. Dev. HL	Avg. Trunc. Point
0.3	2.748	50,000	2.745	0.092	0.335	12.203	97.4	4,065	13.80	0.174	626
		100,000	2.748	0.065	0.221	8.026	97.1	7,450	15.69	0.104	637
		200,000	2.749	0.045	0.144	5.236	95.2	13,430	17.97	0.058	639
		500,000	2.749	0.030	0.086	3.121	96.0	31,238	19.37	0.027	640
		1,000,000	2.748	0.021	0.062	2.254	96.0	62,833	19.46	0.023	639
0.5	5.079	50,000	5.075	0.145	0.521	10.264	97.1	4,035	13.85	0.269	641
		100,000	5.080	0.103	0.346	6.810	96.7	7,361	15.85	0.163	651
		200,000	5.082	0.072	0.232	4.571	96.5	13,647	17.51	0.094	653
		500,000	5.082	0.047	0.141	2.775	96.1	32,472	18.67	0.047	653
		1,000,000	5.080	0.034	0.101	1.981	97.0	63,327	19.32	0.038	653
0.7	8.126	50,000	8.119	0.223	0.844	10.383	97.1	4,051	13.83	0.483	641
		100,000	8.129	0.164	0.563	6.920	96.7	7,536	15.53	0.287	651
		200,000	8.133	0.115	0.379	4.655	96.3	13,824	17.50	0.181	653
		500,000	8.131	0.075	0.224	2.759	96.3	31,896	18.98	0.076	655
		1,000,000	8.128	0.053	0.159	1.954	97.0	62,403	19.56	0.052	654
0.9	13.931	50,000	13.929	0.468	1.900	13.577	95.9	4,308	12.61	1.305	645
		100,000	13.941	0.341	1.164	8.329	96.6	7,971	14.23	0.696	660
		200,000	13.939	0.236	0.780	5.586	96.6	15,031	15.55	0.382	661
		500,000	13.933	0.152	0.470	3.372	95.0	33,091	18.25	0.207	663
		1,000,000	13.931	0.111	0.322	2.314	96.6	63,294	19.12	0.125	664
0.95	17.349	50,000	17.344	0.681	2.966	16.990	95.1	4,541	11.58	2.164	632
		100,000	17.362	0.495	1.802	10.328	96.3	8,564	12.79	1.205	645
		200,000	17.351	0.351	1.188	6.833	96.1	16,023	14.31	0.690	646
		500,000	17.348	0.222	0.690	3.971	94.9	35,396	16.87	0.333	649
		1,000,000	17.346	0.164	0.478	2.756	96.9	66,141	18.37	0.206	650
0.99	24.928	50,000	24.903	1.536	5.555	21.919	91.9	4,834	10.37	3.696	623
		100,000	24.924	1.111	4.422	17.527	94.1	9,549	10.72	3.142	631
		200,000	24.920	0.810	3.183	12.670	94.2	18,214	11.74	2.453	632
		500,000	24.920	0.510	1.831	7.324	94.7	42,380	13.14	1.262	634
		1,000,000	24.918	0.366	1.167	4.676	95.6	78,415	14.79	0.654	636
0.995	28.096	50,000	27.966	2.124	6.814	23.574	87.9	4,858	10.31	4.858	621
		100,000	28.068	1.566	5.477	19.163	92.5	9,729	10.36	3.748	626
		200,000	28.071	1.145	4.291	15.131	92.0	19,038	10.83	3.053	627
		500,000	28.075	0.704	2.772	9.823	93.8	44,989	12.00	2.074	628
		1,000,000	28.081	0.503	1.813	6.441	95.9	84,986	13.23	1.222	629

Figure 5.9: Plots of the estimates for CI relative precision and coverage probability for the M/M/1/M/1 total waiting-time process from Table 5.15.

Table 5.16: Comparison between FQUEST and SQSTS (in italic typeface) without a CI precision requirement for the M/M/1/M/1 total waiting-time process in Section 5.3.6 based on approximately equal sample sizes (rounded to the nearest 1,000 for FQUEST) and 1,000 independent replications.

p	y_p	N	Point Est.	Avg. |Bias|	Avg. 95% CI HL	Avg. 95% CI rel. prec. (%)	Avg. 95% CI cov. (%)	$\overline{m}$	St. Dev. HL
0.3	2.748	150,000	2.749	0.053	0.164	5.966	96.6	10,564	0.057
		149,724	*2.750*	*0.058*	*0.152*	*5.544*	*95.3*	*9,214*	*0.045*
0.5	5.079	137,000	5.084	0.088	0.288	5.656	97.0	9,553	0.129
		137,135	*5.083*	*0.098*	*0.260*	*5.113*	*95.0*	*8,439*	*0.081*
0.7	8.126	130,000	8.137	0.144	0.464	5.697	96.6	8,923	0.213
		129,921	*8.133*	*0.152*	*0.438*	*5.379*	*96.1*	*7,995*	*0.150*
0.9	13.931	167,000	13.940	0.263	0.882	6.314	95.8	12,659	0.513
		166,906	*13.931*	*0.288*	*0.754*	*5.407*	*94.8*	*10,271*	*0.226*
0.95	17.349	222,000	17.350	0.332	1.122	6.459	96.1	17,475	0.655
		222,008	*17.328*	*0.351*	*0.917*	*5.290*	*95.4*	*13,662*	*0.255*
0.99	24.928	1,489,000	24.924	0.297	0.934	3.745	95.6	113,373	0.495
		1,489,131	*24.913*	*0.319*	*0.788*	*3.161*	*95.4*	*91,639*	*0.208*
0.995	28.096	1,929,000	28.090	0.351	1.186	4.218	95.9	154,282	0.665
		1,928,664	*28.077*	*0.384*	*0.943*	*3.355*	*93.4*	*118,687*	*0.237*

Table 5.17: Experimental results for FQUEST with regard to point and 95% CI estimation of y_p for the response-time process in the Central Server Model 3 in Section 5.3.7 for $p \in \{0.3, 0.5, 0.7, 0.8, 0.85, 0.87, 0.89\}$ based on 1,000 independent replications.

p	y_p	N	Point Est.	Avg. |Bias|	Avg. 95% CI HL	Avg. 95% CI rel. prec. (%)	Avg. 95% CI cov. (%)	$\overline{m}$	$\overline{b}$	St. Dev. HL	Avg. Trunc. Point
0.3	7.078	50,000	7.090	0.190	0.533	7.531	95.2	3,168	18.84	0.174	662
		100,000	7.095	0.137	0.387	5.459	94.8	6,133	19.70	0.143	679
		200,000	7.092	0.095	0.276	3.898	95.7	12,779	19.10	0.094	678
		500,000	7.090	0.059	0.174	2.452	95.8	30,456	20.02	0.054	680
		1,000,000	7.087	0.043	0.123	1.732	96.0	61,169	19.87	0.040	679
0.5	10.771	50,000	10.783	0.211	0.567	5.265	94.0	2,990	20.09	0.178	660
		100,000	10.789	0.153	0.414	3.835	93.8	5,930	20.31	0.146	674
		200,000	10.786	0.106	0.302	2.802	94.9	12,273	19.83	0.109	674
		500,000	10.785	0.066	0.193	1.787	95.9	30,929	19.83	0.058	674
		1,000,000	10.782	0.047	0.136	1.265	95.7	61,396	19.92	0.043	674
0.7	15.364	50,000	15.375	0.204	0.584	3.798	95.1	3,321	18.00	0.220	645
		100,000	15.381	0.145	0.417	2.714	95.0	6,207	19.32	0.158	654
		200,000	15.379	0.102	0.297	1.933	96.1	12,423	19.59	0.113	654
		500,000	15.379	0.064	0.188	1.223	95.8	31,213	19.60	0.061	654
		1,000,000	15.376	0.046	0.131	0.851	95.9	61,158	19.98	0.039	654
0.8	18.868	50,000	18.879	0.192	0.570	3.021	96.0	3,516	16.73	0.237	619
		100,000	18.884	0.133	0.395	2.093	95.6	6,496	18.43	0.149	626
		200,000	18.881	0.094	0.283	1.498	96.3	12,909	18.80	0.114	626
		500,000	18.880	0.059	0.177	0.939	96.5	31,837	19.31	0.061	626
		1,000,000	18.878	0.042	0.123	0.650	96.6	62,613	19.42	0.043	626
0.85	21.631	50,000	21.642	0.180	0.548	2.532	96.9	3,502	16.87	0.204	585
		100,000	21.645	0.125	0.374	1.729	96.2	6,556	18.26	0.124	588
		200,000	21.643	0.087	0.259	1.199	96.7	12,283	19.76	0.089	588
		500,000	21.640	0.055	0.164	0.760	96.6	31,393	19.33	0.059	588
		1,000,000	21.638	0.039	0.116	0.536	96.1	62,836	19.35	0.043	588
0.87	23.236	50,000	23.246	0.176	0.604	2.598	97.6	3,566	16.60	0.215	560
		100,000	23.249	0.126	0.385	1.655	97.1	6,387	18.86	0.117	563
		200,000	23.245	0.087	0.264	1.136	97.0	12,375	19.61	0.095	562
		500,000	23.242	0.053	0.165	0.712	96.8	31,271	19.48	0.057	562
		1,000,000	23.240	0.039	0.115	0.495	96.1	63,539	19.18	0.042	563
0.89	25.514	50,000	25.529	0.207	1.009	3.951	98.7	4,453	11.95	0.574	561
		100,000	25.527	0.146	0.563	2.206	98.0	7,678	15.09	0.261	566
		200,000	25.520	0.103	0.346	1.355	97.2	13,429	18.01	0.136	567
		500,000	25.516	0.064	0.206	0.806	97.2	31,801	19.15	0.081	568
		1,000,000	25.515	0.046	0.141	0.553	96.9	62,827	19.45	0.054	569

Figure 5.10: Plots of the estimates for CI relative precision and coverage probability for the response-time process in the Central Server Model 3 from Table 5.17.

Table 5.18: Experimental results for FQUEST with regard to point and 95% CI estimation of y_p for the response-time process in the Central Server Model 3 in Section 5.3.7 for $p \in \{0.9, 0.91, 0.93, 0.95, 0.99, 0.995\}$ based on 1,000 independent replications.

p	y_p	N	Point Est.	Avg. |Bias|	Avg. 95% CI HL	Avg. 95% CI rel. prec. (%)	Avg. 95% CI cov. (%)	$\overline{m}$	$\overline{b}$	St. Dev. HL	Avg. Trunc. Point
0.9	27.181	50,000	27.199	0.280	1.890	6.939	98.8	4,768	10.63	1.234	575
		100,000	27.187	0.199	0.946	3.478	99.1	8,931	12.00	0.513	580
		200,000	27.179	0.141	0.533	1.960	97.8	16,179	14.07	0.241	582
		500,000	27.175	0.085	0.298	1.098	97.0	35,338	16.94	0.132	584
		1,000,000	27.175	0.062	0.192	0.708	96.8	65,556	18.53	0.069	586
0.91	29.648	50,000	29.690	0.500	4.411	14.798	99.4	4,899	10.14	2.754	593
		100,000	29.656	0.344	2.176	7.323	99.2	9,615	10.54	1.362	597
		200,000	29.639	0.241	1.181	3.979	98.4	18,229	11.65	0.653	598
		500,000	29.632	0.148	0.589	1.987	97.8	40,609	14.12	0.290	600
		1,000,000	29.633	0.108	0.366	1.234	97.6	72,436	16.31	0.152	603
0.93	44.766	50,000	44.883	2.778	8.988	20.170	94.4	4,480	11.70	4.757	615
		100,000	44.691	1.988	5.955	13.376	95.3	8,425	13.05	3.069	624
		200,000	44.640	1.381	4.139	9.276	94.3	15,441	14.88	1.849	626
		500,000	44.636	0.848	2.511	5.627	94.9	33,600	17.89	0.978	629
		1,000,000	44.658	0.598	1.783	3.993	96.4	66,094	18.27	0.676	629
0.95	74.481	50,000	74.440	3.387	8.725	11.739	91.6	3,246	18.30	3.404	632
		100,000	74.305	2.411	6.444	8.684	93.1	6,213	19.56	2.467	638
		200,000	74.300	1.685	4.692	6.318	95.0	12,572	19.33	1.619	638
		500,000	74.340	1.054	3.018	4.061	95.6	30,440	20.18	0.957	639
		1,000,000	74.381	0.734	2.167	2.914	95.6	62,433	19.59	0.666	638
0.99	166.528	50,000	166.402	4.300	13.277	7.976	95.0	3,458	17.23	5.676	636
		100,000	166.218	3.101	9.220	5.547	96.0	6,519	18.67	3.643	642
		200,000	166.261	2.261	6.529	3.926	96.0	12,843	18.95	2.532	643
		500,000	166.374	1.369	4.088	2.457	96.3	31,644	19.16	1.414	644
		1,000,000	166.441	0.973	2.917	1.753	95.9	60,817	19.98	1.044	644
0.995	196.230	50,000	195.971	5.254	16.823	8.584	95.9	3,838	15.00	7.756	641
		100,000	195.898	3.709	11.282	5.761	95.6	7,043	16.99	4.841	651
		200,000	195.965	2.654	7.898	4.029	96.4	13,205	18.37	3.247	653
		500,000	196.062	1.667	4.864	2.481	95.5	31,418	19.38	1.656	654
		1,000,000	196.122	1.172	3.482	1.775	96.1	61,576	19.78	1.324	654

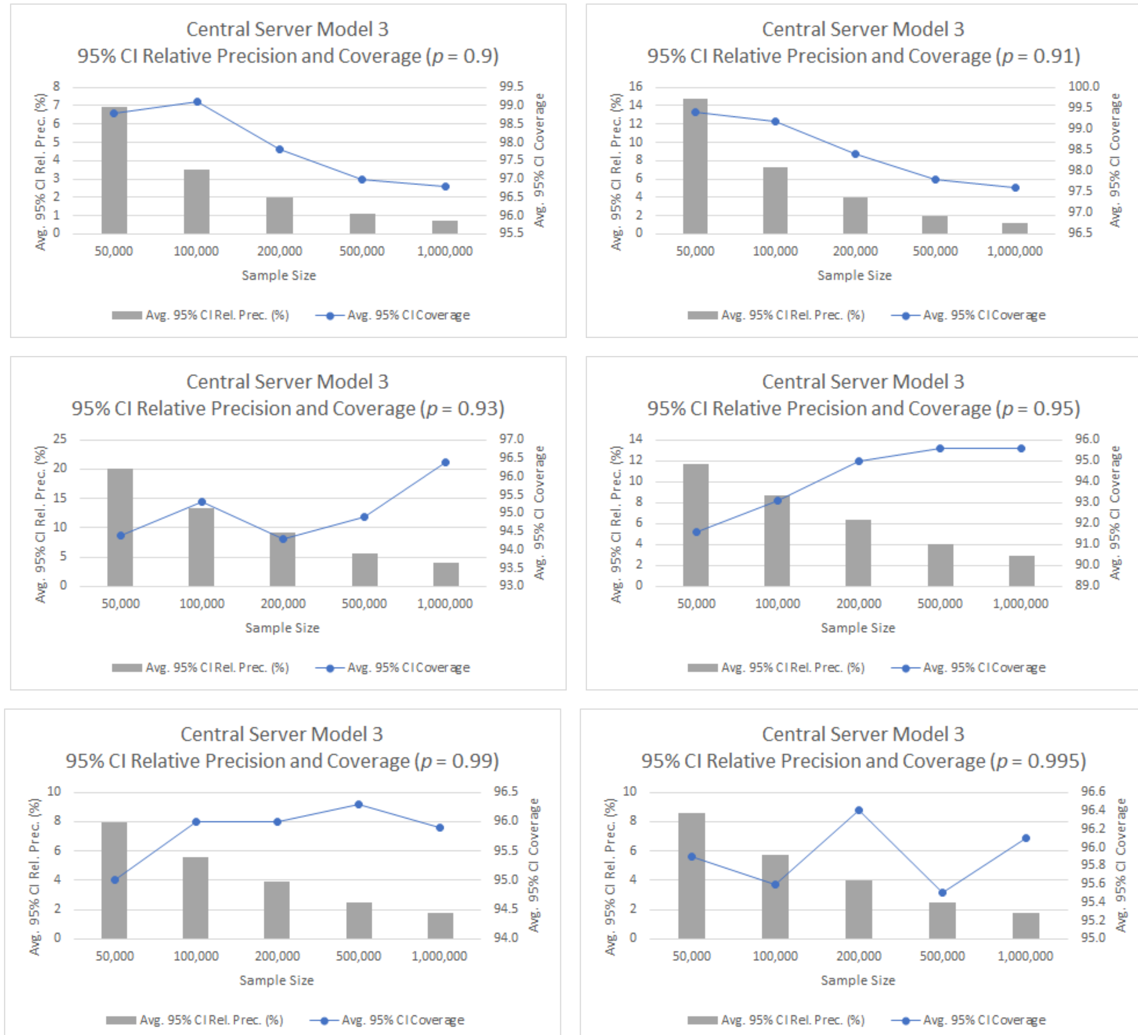

Figure 5.11: Plots of the estimates for CI relative precision and coverage probability for the response-time process in the Central Server Model 3 from Table 5.18.

Table 5.19: Comparison between FQUEST and SQSTS (in italic typeface) without a CI precision requirement for the response-time process in the Central Server Model 3 in Section 5.3.7 based on approximately equal sample sizes (rounded to the nearest 1,000 for FQUEST) and 1,000 independent replications.

p	y_p	N	Point Est.	Avg. |Bias|	Avg. 95% CI HL	Avg. 95% CI rel. prec. (%)	Avg. 95% CI cov. (%)	$\overline{m}$	St. Dev. HL
0.3	7.078	65,000	7.092	0.168	0.474	6.691	94.4	4,111	0.150
		64,549	*7.092*	*0.178*	*0.435*	*6.140*	*93.0*	*3,972*	*0.099*
0.5	10.771	53,000	10.780	0.205	0.560	5.200	94.8	3,226	0.190
		52,532	*10.784*	*0.222*	*0.527*	*4.891*	*93.0*	*3,233*	*0.106*
0.7	15.364	71,000	15.381	0.173	0.494	3.211	95.8	4,589	0.183
		70,764	*15.374*	*0.188*	*0.470*	*3.061*	*93.7*	*4,355*	*0.117*
0.8	18.868	91,000	18.885	0.142	0.422	2.233	94.8	6,122	0.166
		90,868	*18.884*	*0.159*	*0.399*	*2.114*	*93.6*	*5,592*	*0.117*
0.85	21.631	95,000	21.645	0.129	0.384	1.774	96.1	6,184	0.132
		94,626	*21.646*	*0.138*	*0.364*	*1.683*	*95.3*	*5,823*	*0.105*
0.87	23.236	123,000	23.247	0.111	0.340	1.461	97.5	7,883	0.099
		122,751	*23.249*	*0.115*	*0.309*	*1.329*	*95.9*	*7,554*	*0.072*
0.89	25.514	257,000	25.520	0.090	0.300	1.177	97.2	17,123	0.125
		256,720	*25.517*	*0.095*	*0.251*	*0.985*	*96.1*	*15,798*	*0.053*
0.9	27.181	348,000	27.179	0.104	0.368	1.352	97.6	25,468	0.153
		347,722	*27.180*	*0.108*	*0.300*	*1.102*	*96.3*	*21,398*	*0.079*
0.91	29.648	366,000	29.636	0.175	0.724	2.441	98.1	31,028	0.359
		366,316	*29.648*	*0.188*	*0.576*	*1.940*	*96.4*	*22,543*	*0.225*
0.93	44.766	114,000	44.677	1.841	5.724	12.845	95.6	9,553	2.874
		114,271	*45.030*	*2.041*	*4.594*	*10.163*	*92.8*	*7,032*	*1.322*
0.95	74.481	67,000	74.373	2.958	7.631	10.282	93.4	4,222	2.687
		67,176	*74.523*	*3.052*	*7.323*	*9.838*	*93.7*	*4,134*	*1.620*
0.99	166.528	440,000	166.360	1.434	4.339	2.609	97.3	27,811	1.347
		440,432	*166.345*	*1.562*	*4.041*	*2.430*	*94.2*	*27,104*	*0.903*
0.995	196.230	504,000	196.071	1.658	4.880	2.489	95.9	31,770	1.804
		504,081	*196.026*	*1.781*	*4.546*	*2.319*	*95.5*	*31,020*	*1.089*

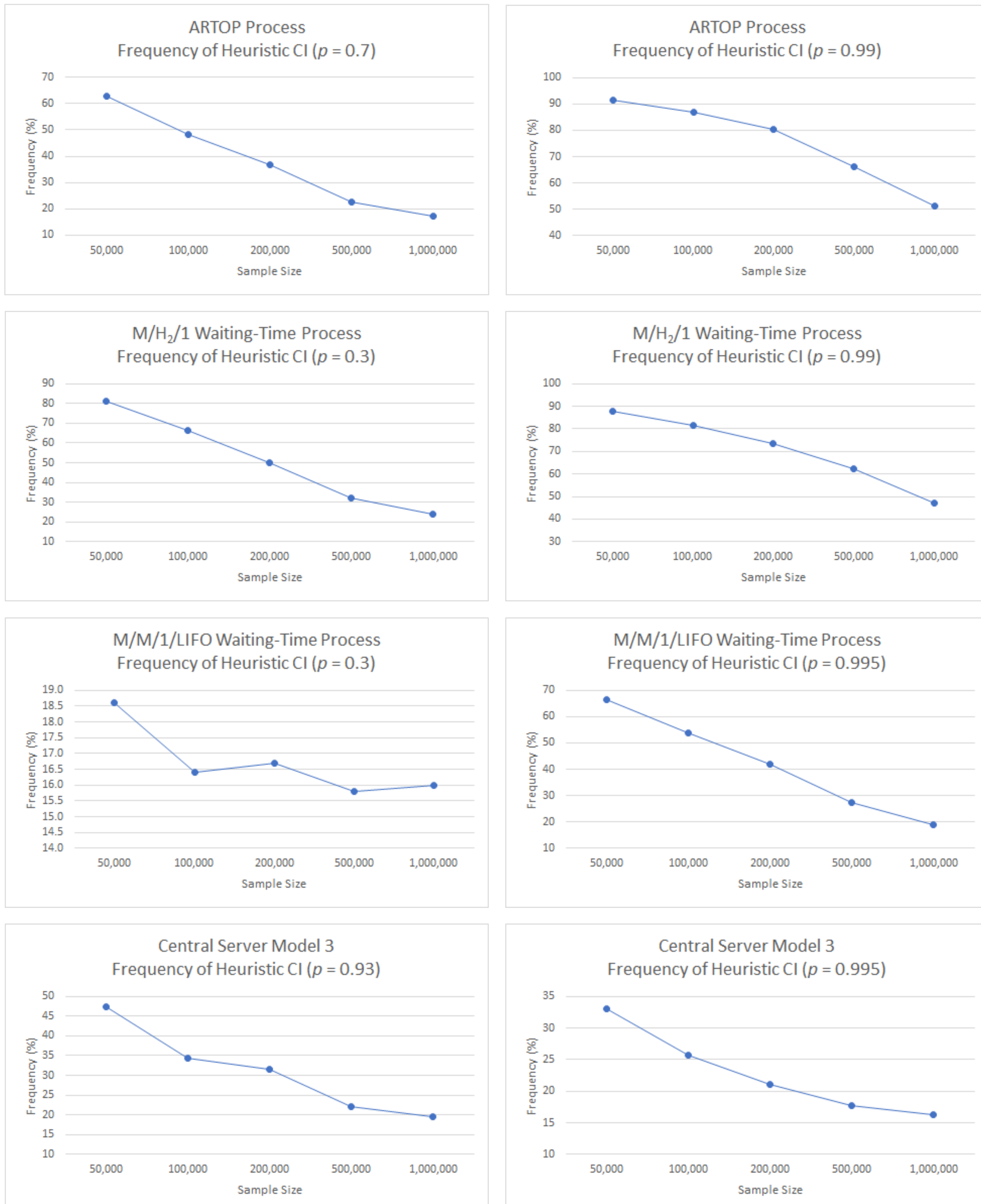

Figure 5.12: Frequency of Heuristic CI in Step **[10]** of FQUEST for selected examples. The results are based on 1,000 independent replications with sample sizes $N \in \{50{,}000, 100{,}000, 200{,}000, 500{,}000, 1{,}000{,}000\}$.

CHAPTER 6

FIRQUEST: A FIXED-SAMPLE-SIZE METHOD FOR ESTIMATING STEADY-STATE QUANTILES BASED ON INDEPENDENT REPLICATIONS

Steady-state analysis methods based on a single simulation run such as SQSTS in Chapter 4 and FQUEST in Chapter 5 are convenient since they usually diminish the effects of initialization bias by truncating only an initial portion of the sample. Unfortunately, the potential issues associated with pronounced autocorrelation in the underlying output process may require an excessively large sample path to attenuate this correlation effect and yield reliable CIs for the performance measure of interest. On the other hand, steady-state estimation methods based on independent replications are convenient and can potentially tackle these correlation issues. For practical purposes, the need for such tools is further enhanced by the fact that multiple replications can be made simultaneously on different cores/threads within a single computer or on different computers on a network, provided that the software being used for simulation supports this (Law [4]). On the negative side, independent replications can induce systematic bias in the replicated point estimates if insufficient truncation is applied at the onset of each replication, and this systematic bias can have deleterious effects on the reliability of a CI for a steady-state measure; see Section 6.4 in Fishman [48] and Alexopoulos and Goldsman [47] with regard to the estimation of the steady-state mean. Further, for fixed-sample-size procedures, one has to decide on the number of replications and the length of each replication.

In this chapter, we present and assess FIRQUEST, the first automated fixed-sample-size procedure for computing CIs for steady-state quantiles based on independent replications. The user provides a dataset comprised of $R \geq 2$ sample paths of finite length that are generated by independent replications, and specifies the required quantile and nominal coverage probability of the anticipated CI. We describe FIRQUEST assuming that each replication has the same length (number of observations) n, but it can also handle situations, in which the replications have different lengths. We will revisit this issue in Section 6.3 below. FIRQUEST is essentially an extension of the FQUEST procedure in Chapter 5 with adjustments to handle replicate sample paths and more-aggressive steps to remove any potential warm-up effects that can induce systematic bias across replicate estimates. The foundations for the statistical tests are laid out in an extension of Theorem 2.3.4 for multiple replications and in Section 6.1 below.

The remainder of this chapter is organized as follows. Section 6.1 extends results from Chapter 2 and presents (approximate) CIs for y_p computed from independent batched replications. Section 6.2 presents and describes an approximate CI from the replicate BQEs and the full-sample estimator using adjustments for residual skewness in the BQEs that FIRQUEST may incorporate in its final stage. Section 6.3 contains a formal algorithmic statement of FIRQUEST. Section 6.4 contains an experimental performance evaluation of FIRQUEST using a test bed of seven challenging processes (one of them with two sets of parameters, and another with three sets of parameters) for a total of ten experiments as well as an informal comparison of FIRQUEST against the FQUEST procedure. Section 6.5 concludes with a short summary of the contributions and performance of FIRQUEST.

6.1 Preliminaries

In this section we form the foundations for the statistical tests employed by FIRQUEST as well as approximate CIs for the quantile y_p under study. For simplicity, assume that we have generated R i.i.d. stationary sample paths of the process $\{Y_k : k \geq 1\}$, each of size bm, so that $N = Rbm$. We split each replicate path in b nonoverlapping batches of size m each. From each batch we compute the respective empirical quantile and weighted signed area. For the remainder of this chapter, we denote the replicate batched quantile estimator (RBQE) as $\left\{\widehat{y}_p(j,m) : j = 1,\ldots,Rb\right\}$ and the (replicate) signed areas as $\{A_p(w;j,m) : j = 1,\ldots,Rb\}$, where the subscript j in $\widehat{y}_p(j,m)$ or $A_p(w;j,m)$ denotes the ith RBQE or signed area, respectively, from replication $r+1$ with $r = \lfloor j/b \rfloor$ and $i \equiv j - rb$. For example, if $b = 20$, $\widehat{y}_p(43, m)$ is the 3rd RBQE from replication 3. Also, let $\widetilde{y}_p(N)$ be the empirical quantile from the entire dataset comprised of the R sample paths.

We define the replicated batched STS area estimator for σ_p^2 as

$$\mathscr{A}_p(w; R, b, m) \equiv (Rb)^{-1} \sum_{j=1}^{Rb} A_p^2(w; j, m). \tag{6.1}$$

We also define the average RBQE

$$\overline{\overline{y}}_p(R, b, m) \equiv (Rb)^{-1} \sum_{j=1}^{Rb} \widehat{y}_p(j, m) \tag{6.2}$$

and the "average" squared deviations of the RBQEs away from the average RBQE $\overline{\overline{y}}_p(R, b, m)$ and the full-sample quantile estimator $\widetilde{y}_p(N)$, respectively,

$$S_p^2(R, b, m) \equiv (Rb-1)^{-1} \sum_{j=1}^{Rb} \left[\widehat{y}_p(j, m) - \overline{\overline{y}}_p(R, b, m)\right]^2, \quad \text{and} \tag{6.3}$$

$$\widetilde{S}_p^2(R, b, m) \equiv (Rb-1)^{-1} \sum_{j=1}^{Rb} \left[\widehat{y}_p(j, m) - \widetilde{y}_p(N)\right]^2. \tag{6.4}$$

Finally, we let

$$\mathscr{N}_p(R, b, m) \equiv m S_p^2(R, b, m), \quad \text{and} \tag{6.5}$$

$$\widetilde{\mathscr{N}_p}(R, b, m) \equiv m \widetilde{S}_p^2(R, b, m), \tag{6.6}$$

and we define the combined estimators of the variance parameter σ_p^2

$$\mathscr{V}_p(w; R, b, m) \equiv \frac{Rb\mathscr{A}_p(w; R, b, m) + (Rb-1)\mathscr{N}_p(R, b, m)}{2Rb-1}, \quad \text{and} \tag{6.7}$$

$$\widetilde{\mathscr{V}_p}(w; R, b, m) \equiv \frac{Rb\mathscr{A}_p(w; R, b, m) + (Rb-1)\widetilde{\mathscr{N}_p}(R, b, m)}{2Rb-1}. \tag{6.8}$$

Under the assumptions of Theorem 2.3.1, we can easily show that each of the (Rb)-dimensional random vectors $\left[\widehat{y}_p(1,m),\ldots,\widehat{y}_p(Rb,m)\right]^{\mathsf{T}}$ and $\left[A_p(w;1,m),\ldots,A_p(w;Rb,m)\right]^{\mathsf{T}}$ converges to a vector of i.i.d. normal r.v.'s as $m \to \infty$. Hence, one can readily see that, for fixed R and b,

$$\mathscr{A}_p(w;R,b,m) \underset{m\to\infty}{\Longrightarrow} \sigma_p^2 \chi^2_{Rb}/(Rb).$$

We postulate that the following $100(1-\alpha)\%$ CIs for y_p are asymptotically valid as $m \to \infty$ with fixed R and b:

$$\widetilde{y}_p(N) \pm t_{1-\alpha/2,Rb}\left[\mathscr{A}_p(w;R,b,m)/N\right]^{1/2}, \tag{6.9}$$

$$\overline{\widetilde{y}}_p(R,b,m) \pm t_{1-\alpha/2,Rb}\left[\mathscr{A}_p(w;R,b,m)/N\right]^{1/2}, \tag{6.10}$$

$$\widetilde{y}_p(N) \pm t_{1-\alpha/2,Rb-1}\left[\widetilde{\mathscr{N}_p}(R,b,m)/N\right]^{1/2}, \tag{6.11}$$

$$\overline{\widehat{y}}_p(R,b,m) \pm t_{1-\alpha/2,Rb-1}\left[\widetilde{\mathscr{N}_p}(R,b,m)/N\right]^{1/2}, \tag{6.12}$$

and

$$\widetilde{y}_p(N) \pm t_{1-\alpha/2,2Rb-1}\left[\widetilde{\mathscr{V}_p}(w;R,b,m)/N\right]^{1/2}. \tag{6.13}$$

Remark 6.1.1. The asymptotic validity of CIs for the steady-state mean that are constructed from replicated batch means and are analogues of Equation (6.11) was established by Argon and Andradóttir [89].

6.2 An Approximate Skewness-Adjusted Confidence Interval

Similarly to FQUEST, FIRQUEST employs statistical tests to assess the extensions of asymptotic properties in Equations (2.9) and (2.17) for $R > 1$ replications. When any of the statistical tests fails and the size of the dataset limits the ability to increase the batch size, (subject to approval by the user) FIRQUEST may also construct an approximate CI from the

RBQEs $\{\widehat{y}_p(j,m) : j = 1, \ldots, Rb\}$ and the full-sample estimator $\widetilde{y}_p(N)$ using adjustments for residual skewness in the RBQEs. (Since the RBQEs are not computed from a single time series, we do not perform an adjustment for residual autocorrelation.) Essentially, the steps below are the same as in Section 5.1, but we skip the parts that correspond to the correlation-adjustment factor (Willink [88], Tafazzoli *et al.* [42], Alexopoulos *et al.* [7]).

Initially, we calculate the sample skewness of the RBQEs

$$\widehat{B}_{\widehat{y}_p}(R,b,m) \equiv \frac{Rb}{(Rb-1)(Rb-2)} \sum_{j=1}^{Rb} \left[\frac{\widehat{y}_p(j,m) - \overline{\widehat{y}}_p(R,b,m)}{S_p(R,b,m)} \right]^3,$$

we compute the skewness-adjustment parameter

$$\vartheta \equiv \frac{\widehat{B}_{\widehat{y}_p}(R,b,m)}{6\sqrt{Rb}},$$

and define the skewness-adjustment function

$$G(\zeta) \equiv \begin{cases} \zeta & \text{if } |\vartheta| \le 0.001, \\ \frac{[1+6\vartheta(\zeta-\vartheta)]^{1/3}-1}{2\vartheta} & \text{if } |\vartheta| > 0.001, \end{cases}$$

for all real ζ. Then we set

$$G_1 \equiv G(t_{1-\alpha/2,Rb-1})\sqrt{\widetilde{S}_p^2(R,b,m)/(Rb)}, \quad \text{and} \quad G_2 \equiv G(t_{\alpha/2,Rb-1})\sqrt{\widetilde{S}_p^2(R,b,m)/(Rb)}.$$

The (asymmetric) skewness-adjusted CI for y_p is given by

$$\left[\min\left(\widetilde{y}_p(N) - G_1, \widetilde{y}_p(N) - G_2\right), \max\left(\widetilde{y}_p(N) - G_1, \widetilde{y}_p(N) - G_2\right)\right]. \tag{6.14}$$

We will elaborate more on this adjusted CI in Section 6.3 below.

6.3 FIRQUEST Algorithm

In this section we present FIRQUEST, the first automated fixed-sample-size procedure for estimating a steady-state quantile based on independent replications. Figure 6.1 contains a high-level flowchart of the procedure. FIRQUEST uses the same batching scheme in each replication, specifically b batches of size m, to execute the statistical tests. At a high level, similarly to FQUEST, FIRQUEST is comprised of four main blocks. The first block consists of Steps **[0]–[2]** which initialize the experimental parameters. The second block includes Steps **[3]–[5]** and deals with the potential transient effects in each replication. At the end of this block we remove the same number of initial observations from every replication. The third block consists of Steps **[6]–[9]**, which conduct randomness and normality tests to assess the statistical conformance of each of the replicate signed areas $\{A_p(w; j, m) : j = 1, \ldots, Rb\}$ and the RBQEs $\{\widehat{y}_p(j, m) : j = 1, \ldots, Rb\}$ to asymptotic independence and normality. Finally, the last block consists of Step **[10]**: If the statistical tests within the third block are passed, the procedure delivers the CI in Equation (6.13) based on the combined variance estimator. Otherwise, it potentially delivers a conservative CI, subject to user approval. The following paragraphs contain a detailed description of each step of FIRQUEST.

In Step **[0]**, the simulation model or user provides the number of independent replications R, the fixed size n of each replication, the probability p, and the nominal error probability $\alpha \in (0, 1)$ for the CI for y_p. Step **[1]** initializes the experimental parameters. The initial number of batches is set at $b = 25$ and the initial batch size is set at $m = 500$.

Remark 6.3.1. In Step **[3]**, FIRQUEST performs the randomness test of von Neumann [43] for every replication independently (i.e., every time we finish with one replication, we reset the significance level to 0.3, and the batch size m to 500) and starts with fewer batches compared to FQUEST (which initially sets $b = 50$). This change lies in the scope of allowing FIRQUEST to take more aggressive steps towards removing any potential warm-up effects when the provided sample size for every replication is relatively small. For example, if the user provides $n = 20{,}000$ observations per replication, using $b = 25$ and keeping it constant can result in the removal of up to 800 initial observations from each replication. Alternatively, using $b = 50$ batches can lead to the the removal of up to 400 initial observations from each replication, which may be too small in some cases.

We also define the array of batch counts $\boldsymbol{s}$ for Steps **[5]**–**[9]** as a function of the number of independent replications R, and we set q equal to the number of elements in $\boldsymbol{s}$. The assignment of the elements of $\boldsymbol{s}$ is based on the following guidelines: (i) keep the total number of batches $Rb \geq 10$; (ii) start with at least 16 total number of batches Rb; (iii) use the same number of batches from every replication; (iv) use at least one batch from every replication; and (v) if $R < 33$, use $Rb \leq 66$ batches in total. Notice here that 32 batches typically suffice for effective estimation of a variance parameter (σ_p^2 in our setting), while fewer than 10 batches may result in unreliable CIs (see also Section 5.2 of this thesis). Further, we initialize the counters $l = 1$ and $v = 1$, and set `flag` = `false`. At this point the algorithm sets the weight function that will be used for the calculation of the signed areas and the STS variance-parameter estimator. Again, for the reasons stated at the start of Section 4.2, we used the constant weight function w_0 for the experiments in Section 6.4. The level of significance for the statistical test in Step **[3]** is set according to the sequence $\{\beta\psi(\ell) : \ell = 1, 2, \ldots\}$, where $\beta = 0.3$, $\psi(\ell) \equiv \exp\left[-\eta(\ell-1)^{\theta}\right]$, $\eta = 0.2$, and $\theta = 2.3$. For the statistical tests in Steps **[6]**–**[9]** we fix the significance level at β. The values of the parameters β, η, and θ were chosen after careful experimentation to control the growth of the batch size and to avoid excessive truncation during Step **[5]**, which can be detrimental given the sample-size limitation and the fact that FIRQUEST removes the same number of initial observations from every replication. Notice that on a potential fourth iteration one has $\beta\psi(4) = 0.025$, which makes passing the test easier.

Since the sample size n for each replication is fixed, it is possible that it is less than the initial assignment $bm = 25{,}000$. In this case, Step **[2]** sets $m = \lfloor n/b \rfloor$, which is the largest allowable value for the current batch count b. Step **[3]** consists of a loop that tests for the randomness of the signed areas $\{A_p(w; j, m)\}$ in each replication computed from the first bm observations (the tail $n - bm$ observations are ignored, but not discarded) using a two-sided test based on von Neumann's ratio (von Neumann [43], Young [83]) with progressively decreasing significance level $\beta\psi(\ell)$ on iteration ℓ; see Section 4.1 of this thesis for a detailed discussion of the test statistic when $R = 1$ and its power. If the randomness test fails, we increase the batch size to $[\![m\sqrt{2}]\!]$, where $[\![\cdot]\!]$ is the rounding function to the nearest integer. If the updated sample size exceeds n, we reset $m = \lfloor n/b \rfloor$. If the randomness test fails with the largest allowable batch size $\lfloor n/b \rfloor$ even for one of the independent replications, FIRQUEST exits Step **[3]** and moves to Step **[4]**, where it issues a warning to the user regarding the insufficiency of the length of each replication. Then it seeks permission from the user to continue with the construction of a CI. We focus on the signed areas in an attempt to ameliorate the pronounced small-sample bias of the batched STS area estimator in Equation (6.1) relative to variance estimators computed from RBQEs, e.g., $\widetilde{\mathscr{N}_p}(R, b, m)$ in Equation (6.6).

If the dataset of every replication passes the randomness test in Step **[3]** or the user decides to proceed with the construction of the CI despite the failure of the randomness test, FIRQUEST calculates $m_{\max}$, the maximum batch size m that was used across the independent replications in Step **[3]**. Then in Step **[5]** FIRQUEST removes the $m_{\max}$ first observations from every replication, sets the new run length to $n^* = n - m_{\max}$, and reindexes the truncated dataset in each replication. Assuming the successful completion of Step **[3]**, the (approximate) independence between the first and the remaining signed areas within every replication indicates that any initialization bias due to warmup effects is mostly confined to the first batch within every replication. In the worst-case scenario where the randomness test in Step **[3]** fails, even for one replication, Step **[5]** ends up removing $\lfloor n/b \rfloor$ data points from every replication.

Remark 6.3.2. At this junction, a few comments are in order. We avoid decreasing the batch count b in Step **[3]** to avoid reducing significantly the power of von Neumann's randomness test (displayed in Section 4.1 of this thesis for $R = 1$). Also the initial batch size is set at $m = 500$ to address situations where the provided samples have a short transient phase. For example, if $n = 500{,}000$, FIRQUEST will remove only 500 data points from every replication if the randomness test in Step **[3]** is passed on the first attempt. On the other hand, if we had started with 25 batches of size 20,000 each (i.e., with all data) in Step **[3]** and the randomness test was successful in the first iteration (which is highly likely given that the randomness test was successful with $m = 500$), the algorithm would end up removing the excessive number of 20,000 initial observations from every replication.

Step **[5]** restarts with $b = s[1]$ and $m = \lfloor n^*/b \rfloor$. Notice that we may have to ignore (but not remove) a few initial observations at the beginning of every replication. We choose the entries of the vector $\boldsymbol{s}$ according to the number of the provided independent replications R.

In Steps **[6]**–**[9]** we conduct the two-sided randomness test of von Neumann [43] and the one-sided test of Shapiro and Wilk [81] for univariate normality to assess the convergence of each of the replicate signed areas $\{A_p(w; j, m) : j = 1, \ldots, Rb\}$ and the RBQEs $\{\widehat{y}_p(j, m) : j = 1, \ldots, Rb\}$ to asymptotic independence and normality. Each of the Steps **[6]**–**[9]** has a very similar structure. First we compute the replicate signed areas $\{A_p(w; j, m) : j = 1, \ldots, Rb\}$ or the RBQEs $\{\widehat{y}_p(j, m) : j = 1, \ldots, Rb\}$ and conduct the pertinent statistical test using the fixed significance level of $\beta = 0.3$. The significance level is kept constant and high to avoid passing a test with an inadequately small batch size leading to unreliable CIs. If the test is passed, FIRQUEST proceeds to the next step; otherwise, the batch count in each replication decreases to the next element of the array $\boldsymbol{s}$. For example, if $R = 10$ and we fail a test with 3 batches in every replication (30 in total), we set the batch count to 2 per replication (20 in total), recompute the batch size m, and ignore any leftover initial observations at the beginning of each replication. Since q is equal to the number of elements in $\boldsymbol{s}$, we can have up to q failed attempts to pass any of the statistical tests in Steps **[6]**–**[9]**. If at any point a statistical test fails with $v = q$, then FIRQUEST skips the remaining statistical tests and moves to Step **[10]**.

In Step **[10]**, if all the statistical tests have been passed, FIRQUEST computes the combined variance estimator $\widetilde{\mathscr{V}}_p(w; R, b, m)$ in Equation (6.8) and returns the CI in Equation (6.13). Otherwise, it issues a warning mentioning that some of the statistical tests failed (with the significance level of $\beta = 0.3$) and asks the user for permission to continue with the construction of a CI for y_p. If the user chooses to continue, then FIRQUEST computes the quantity

$$h_{\alpha,R,b,m} = \max\left\{ t_{1-\alpha/2,Rb}\left[\frac{\mathscr{A}_p(w; R, b, m)}{N^*}\right]^{1/2}, t_{1-\alpha/2,Rb-1}\left[\frac{\widetilde{\mathscr{N}_p}(R, b, m)}{N^*}\right]^{1/2}\right\}, \quad (6.15)$$

with $N^* = Rbm$ using Equations (6.1) and (6.6), and constructs two new approximate CIs with HL $h_{\alpha,R,b,m}$: the first CI is centered around the full-sample point estimator $\widetilde{y}_p(N^*)$ computed from $N^* = Rbm$ total observations with $n^* - bm$ initial observations within each replication ignored, while the second CI is centered around the average RBQE $\overline{\overline{y}}_p(R, b, m)$ in Equation (6.2). Then FIRQUEST reports the point estimate $\widetilde{y}_p(N^*)$ and the smallest interval containing both two newly constructed intervals and the skewness-adjusted CI in Equation (6.14) with sample size N^*, and stops.

Since FIRQUEST also relies on conservative CIs when one of the statistical tests fail, by the same reasoning as in Remark 5.2.2, we will ignore the alternative estimator $\mathscr{N}_p(R, b, m)$ of σ_p^2 in Equation (6.5). Further, for the same reasons as in Remark 5.2.3, FIRQUEST avoids using the respective CIs in Equations (6.9) or (6.11) when a single pair of the statistical tests in Steps **[6]–[9]** (i.e., **[6]–[7]** or **[8]–[9]**) is passed.

Remark 6.3.3. We present the FIRQUEST algorithm assuming that the user provides the same run length n for every independent replication. However, we can easily modify the procedure to handle replications with different sample sizes. Specifically, at the beginning we can calculate the minimum number of observations in a single replication across all replications $n_{\min}$ and from each replication we consider only the $n_{\min}$ trailing observations.

For example, if replication i contains n_i observations, we will ignore the initial $n_i - n_{\min}$ observations.

Remark 6.3.4. It is important to note that currently FIRQUEST issues a warning to the user in Step **[4]** even if the randomness test in Step **[3]** fails only for one of the independent replications. We could modify FIRQUEST to inform the user about the number of replications that fail the test in Step **[3]** and if this number is small, the user could allow FIRQUEST to ignore these replications and continue. However, we should mention that due to the decreasing significance level in the randomness test of Step **[3]**, if the user provides a reasonably large dataset for each replication and the randomness test in Step **[3]** fails for one replication, most likely, this will be also the case for all supplied replicate paths.

The remarks above will be taken into consideration in the development of an industrial-strength version of FIRQUEST.

The formal algorithmic statement of FIRQUEST follows. We present the algorithm for a general weight function $w(\cdot)$ satisfying Equation (2.12).

Algorithm FIRQUEST

---

[0] User-Initialization: Provide a sample from R independent replications of size n (total sample size Rn), the probability of the quantile p, and the error probability $\alpha \in (0, 1)$.

[1] Parameter-Initialization: Set number of batches $b = 25$, batch size $m = 500$, $\ell = 1$, $v = 1$, and `flag` = `false`. Also set $\beta = 0.30$ and

$$\boldsymbol{s} = \begin{cases} [14, 11, 8, 5] & \text{if } R = 2, \\ [10, 8, 6, 4] & \text{if } R = 3, \\ [6, 5, 4, 3] & \text{if } R = 4, \\ [5, 4, 3, 2] & \text{if } 5 \le R < 10, \\ [4, 3, 2, 1] & \text{if } 10 \le R < 17, \\ [3, 2, 1] & \text{if } 17 \le R < 23, \\ [2, 1] & \text{if } 23 \le R < 33, \\ [1] & \text{if } 33 \le R. \end{cases}$$

Further, set q equal to the number of elements in $\boldsymbol{s}$. Let $w(t)$, $t \in [0, 1]$ be the weight function and define the initial significance level for the first hypothesis test in Step **[3]** as $\beta\psi(\ell) \equiv \exp\left[-\eta(\ell - 1)^{\theta} \right]$, $\ell = 1, 2, \ldots$, with $\eta = 0.2$ and $\theta = 2.3$.

[2] **If** $n < bm$:

Set $m \leftarrow \lfloor n/b \rfloor$;

End If

[3] For the observations of every independent replication repeat the following procedure and calculate the maximum batch size $m_{\max}$ (the maximum m that was used across the independent replications in this step):

Until von Neumann's test fails to reject randomness **or** `flag` = `true`:

- Compute the signed areas $\{A_p(w; j, m)\}$ from the current replication;
- Assess the randomness of the signed areas $\{A_p(w; j, m)\}$ from the current replication using von Neumann's two-sided randomness test with significance level $\beta\psi(\ell)$;
- Set $\ell \leftarrow \ell + 1$ and $m \leftarrow [\![m\sqrt{2}]\!]$;
- **If** $n < bm$ **and** $m \neq \lfloor n/b \rfloor$:

  Set $m \leftarrow \lfloor n/b \rfloor$;

  Else

  Set `flag` $\leftarrow$ `true`;

  End If

End

Set $\ell \leftarrow 1$ and $m \leftarrow 500$.

[4] If the randomness test in Step **[3]** failed for any of the independent replications, then issue a warning that the randomness test failed due to insufficient length of each replication and seek permission from the user to continue with the construction of a CI. If the user declines, then exit without delivering a CI.

[5] Remove the first $m_{\max}$ observations from each replication, reindex the truncated datasets, and set n^* equal to the size of the truncated sample of each replication ($n^* = n - m_{\max}$). Set the number of batches $b \leftarrow s[v]$ and calculate the batch size as $m \leftarrow \lfloor n^*/b \rfloor$. Ignore the initial $n^* - bm$ observations from each replication.

[6] **Until** von Neumann's test fails to reject randomness **or** $v = q + 1$ (a test has failed with minimum allowable number of batches in $\boldsymbol{s}$):

- Compute the replicate signed areas $\{A_p(w; j, m) : j = 1, \ldots, Rb\}$ [1];
- Assess the randomness of the replicate signed areas $\{A_p(w; j, m) : j = 1, \ldots, Rb\}$ using von Neumann's two-sided randomness test with significance level β;
- Set $v \leftarrow v + 1$. Update $b \leftarrow s[v]$ and $m \leftarrow \lfloor n^*/b \rfloor$. Ignore the initial $n^* - bm$ observations from each replication.

End

[7] Until the Shapiro-Wilk test fails to reject normality **or** $v = q + 1$ (a test has failed with minimum allowable number of batches in $\boldsymbol{s}$):

- Compute the replicate signed areas $\{A_p(w; j, m) : j = 1, \ldots, Rb\}$;
- Assess the univariate normality of the replicate signed areas $\{A_p(w; j, m) : j = 1, \ldots, Rb\}$ using the Shapiro–Wilk test with significance level β;
- Set $v \leftarrow v + 1$. Update $b \leftarrow s[v]$ and $m \leftarrow \lfloor n^*/b \rfloor$. Ignore the initial $n^* - bm$ observations from each replication.

End

[8] Until von Neumann's test fails to reject randomness **or** $v = q + 1$ (a test has failed with minimum allowable number of batches in $\boldsymbol{s}$):

- Compute the RBQEs $\{\widehat{y}_p(j, m) : j = 1, \ldots, Rb\}$;
- Assess the randomness of the RBQEs $\{\widehat{y}_p(j, m) : j = 1, \ldots, Rb\}$ using von Neumann's two-sided randomness test with significance level β;
- Set $v \leftarrow v + 1$. Update $b \leftarrow s[v]$ and $m \leftarrow \lfloor n^*/b \rfloor$. Ignore the initial $n^* - bm$ observations from each replication.

[1] across all replications

End

[9] **Until** the Shapiro–Wilk test fails to reject normality **or** $v = q + 1$ (a test has failed with minimum allowable number of batches in $\boldsymbol{s}$):

- Compute the RBQEs $\{\widehat{y}_p(j, m) : j = 1, \ldots, Rb\}$;
- Assess the univariate normality of the BQEs $\{\widehat{y}_p(j, m) : j = 1, \ldots, Rb\}$ using the Shapiro–Wilk test with significance level β;
- Set $v \leftarrow v + 1$. Update $b \leftarrow s[v]$ and $m \leftarrow \lfloor n^*/b \rfloor$. Ignore the initial $n^* - bm$ observations from each independent replication.

End

[10] Set $N^* \leftarrow Rbm$.

If $v < q + 1$ (no statistical test in Steps **[6]–[9]** failed):

- Compute the combined variance estimator

$$\widetilde{\mathscr{V}}_p(w; R, b, m) \equiv \frac{Rb\mathscr{A}_p(w; R, b, m) + (Rb - 1)\widetilde{\mathscr{N}_p}(R, b, m)}{2Rb - 1},$$

with

$$\mathscr{A}_p(w; R, b, m) = (Rb)^{-1} \sum_{j=1}^{Rb} A_p^2(w; j, m), \quad \text{and}$$

$$\widetilde{\mathscr{N}_p}(R, b, m) = m(Rb - 1)^{-1} \sum_{j=1}^{Rb} \left[\widehat{y}_p(j, m) - \widetilde{y}_p(N^*)\right]^2,$$

deliver the $100(1 - \alpha)\%$ CI for y_p,

$$\widetilde{y}_p(N^*) \pm t_{1-\alpha/2, 2Rb-1}\left(\widetilde{\mathscr{V}}_p(w; Rb, m)/N^*\right)^{1/2},$$

and exit;

Else

- Issue a warning that a statistical test failed due to insufficiency of the dataset and seek permission from the user to continue with the construction of a CI. If the user declines, then exit without delivering a CI;

- Compute

$$h_{\alpha,R,b,m} = \max\left\{t_{1-\alpha/2,Rb}\sqrt{\frac{\mathscr{A}_p(w;R,b,m)}{N^*}}, t_{1-\alpha/2,Rb-1}\sqrt{\frac{\widetilde{\mathscr{N}_p}(R,b,m)}{N^*}}\right\},$$

  where $\mathscr{A}_p(w;R,b,m)$ and $\widetilde{\mathscr{N}_p}(R,b,m)$ are displayed earlier in this step. Then, construct the following approximate CIs for y_p with HL $h_{\alpha,R,b,m}$:

$$\widetilde{y}_p(N^*) \pm h_{\alpha,R,b,m} \quad \text{and} \quad \overline{\overline{y}}_p(R,b,m) \pm h_{\alpha,R,b,m}, \tag{6.16}$$

  with the first CI centered around the full-sample point estimator $\widetilde{y}_p(N^*)$ and the second centered around the average RBQE $\overline{\overline{y}}_p(R,b,m) = (Rb)^{-1}\sum_{j=1}^{Rb}\widehat{y}_p(j,m)$;

- Construct the (asymmetric) skewness-adjusted CI

$$\left[\min\left(\widetilde{y}_p(N^*) - G_1, \widetilde{y}_p(N^*) - G_2\right), \max\left(\widetilde{y}_p(N^*) - G_1, \widetilde{y}_p(N^*) - G_2\right)\right] \tag{6.17}$$

  with G_1 and G_2 defined in Equation (6.14);

- Deliver the full-sample point estimator $\widetilde{y}_p(N^*)$ and the smallest interval containing the CIs in Equations (6.16) and (6.17), and exit.

End If

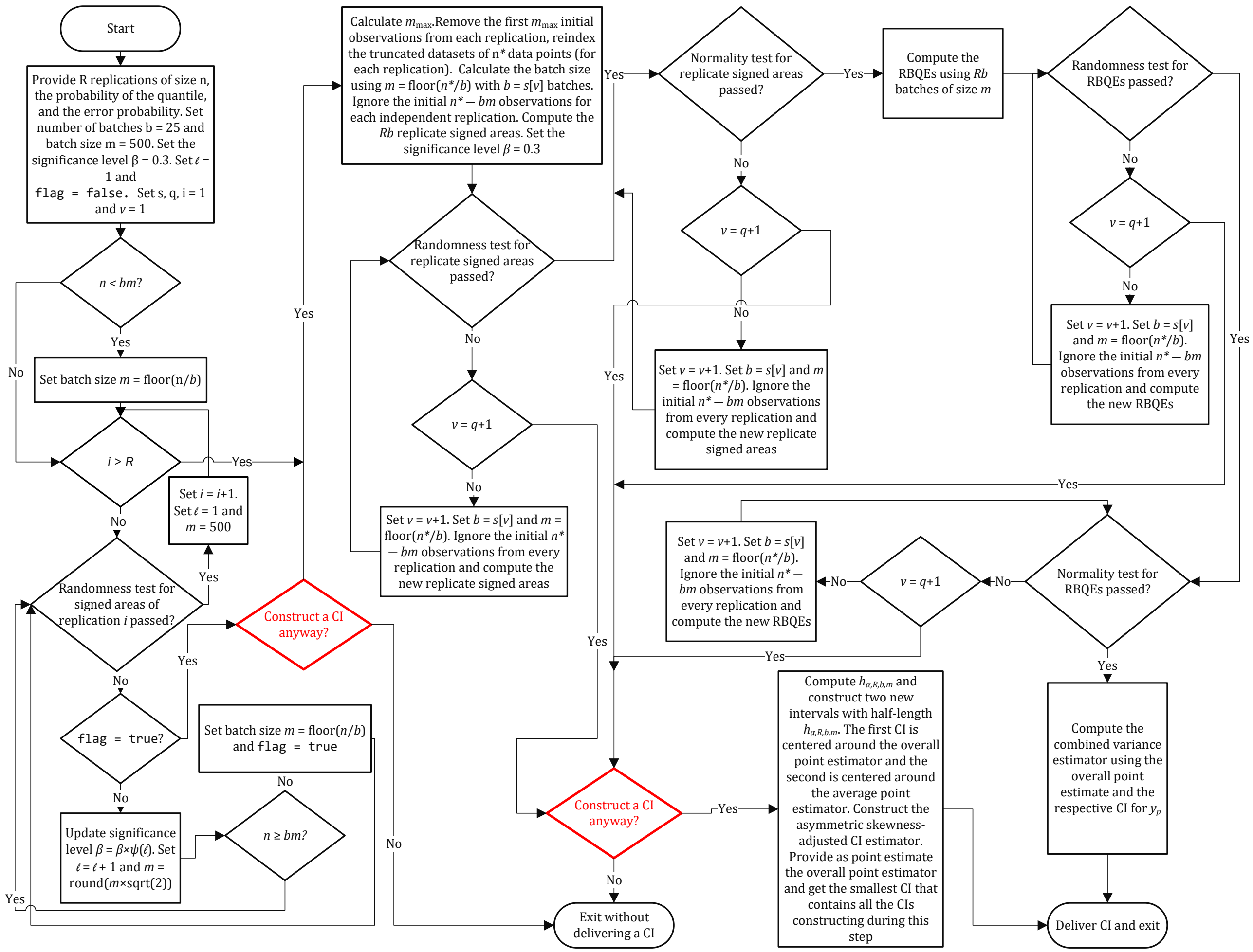

Figure 6.1: High-Level Flowchart of FIRQUEST.

6.4 Experimental Results

In this section we present an extensive empirical study designed to assess the performance of the FIRQUEST procedure. Our test bed includes the seven challenging stochastic processes from Alexopoulos *et al.* [23] and Alexopoulos *et al.* [7], involving two time-series models, three single-server queueing systems, and two small queueing networks. For some processes we present results for different choices of parameters, hence we consider a total of ten test problems. A detailed description of these processes is given in Sections 2.5.1–2.5.7. All experiments were coded in Java using common random numbers generated by the RngStreams package of L'Ecuyer *et al.* [67]. As mentioned earlier, we constructed the STS area variance estimators using the constant weight function $w_0(\cdot)$.

For each experimental setting we present two different sets of experimental results: (i) tables with numerical results for the FIRQUEST method with $R = 5$ and 10 independent replications and the FQUEST method using five different total sample sizes $N \in \mathscr{S} \equiv \{50{,}000, 100{,}000, 200{,}000, 500{,}000, 1{,}000{,}000\}$ and a nominal 95% ($\alpha = 0.05$) CI coverage probability; and (ii) a set of graphs based on the aforementioned tables, each for a specific probability p depicting the average 95% CI relative precision, defined as the ratio of the CI HL over the reported point estimate, and the estimated 95% CI coverage probability. Notably, the smaller values in $\mathscr{S}$ are typically insufficient for estimating marginal quantiles for the stationary processes with a high degree of autocorrelation of departures from normality (Chen and Kelton [25], Alexopoulos *et al.* [23], Alexopoulos *et al.* [7]), in particular extreme quantiles. For the remainder of this chapter, we will write FIRQUEST($R = R_0$) to denote the FIRQUEST method when executed with R_0 independent replications.

Tables 6.1–6.32 contain experimental results for the FIRQUEST and FQUEST methods with all estimates computed from 1,000 independent trials. Specifically, column 1 lists selected values of p and column 2 contains the (nearly) exact value of the associated quantile y_p. Column 3 lists the respective number of independent replications R. Column 4 lists the fixed-sample size n for every replication. Column 5 refers to the method used (FIRQUEST or FQUEST). Columns 6 and 7 contain the average value of the point estimate and the average value of the absolute error (the absolute value of the difference between the point estimate and the exact value of the associated quantile), respectively. Columns 8–10 contain the average value of the HL of the 95% CI for y_p, the average value of the CI's relative precision expressed as a percentage, and the estimated coverage probability of the CI as a percentage, respectively. We report the average CI HL and average relative precision despite the fact that the final CI delivered in Step **[10]** for both FIRQUEST and FQUEST may be asymmetric for small samples (when a statistical test in Steps **[6]**–**[9]** fails). The standard errors of the estimated coverage probabilities are approximately $\sqrt{(0.95 \times 0.05)/1000} = 0.007$. Columns 11 and 12 display the average final batch size ($\overline{m}$) and average final batch count ($\overline{b}$), respectively, after removing observations in Step **[5]**. Finally, Columns 13 and 14 list the standard deviation of the CI HL and the average truncated sample size from every replication, respectively.

Similarly to FQUEST, the two most important metrics for FIRQUEST's performance evaluation are the estimated coverage probability of the CI and the average value of the CI's relative precision. As we mentioned in Chapter 5, there is always a tradeoff between these two metrics. A reliable fixed-sample-size procedure should achieve the requested CI coverage probability, while keeping the average value of the CI's relative precision as low as possible. Figures 6.2–6.12 illustrate FIRQUEST's and FQUEST's performances on this front in a more intelligible way by plotting the estimates of the 95% CI relative precision and coverage probability in columns 9–10 of Tables 6.1–6.32.

Finally, Figure 6.13 reports the frequency of the heuristic CI in Step **[10]** in a few selected cases for the FIRQUEST and FQUEST methods. These results are also based on 1,000 independent replications.

6.4.1 First-Order Autoregressive Processes

The first test process is the Gaussian AR(1) process defined in Section 2.5.1. We considered two sets of parameters. In the first case we chose $\mu_Y = 100$, $\phi = 0.995$, $\sigma_\epsilon = 1$, and $Y_0 = 0$. Since the steady-state marginal standard deviation is $\sigma_Y = \sigma_\epsilon/(1 - \phi^2)^{1/2} = 10.01$, this process was initialized nearly 10 standard deviations below its steady-state mean. As we have already mentioned in Section 4.2.1, on top of the pronounced initialization bias, this process exhibits strong stochastic dependence. These traits will allow us to evaluate the ability of FIRQUEST to overcome the effects of initialization bias and pronounced serial correlation between successive observations of the base process.

The experimental results are displayed in Tables 6.1–6.3 and Figure 6.2. We start our analysis with Tables 6.1–6.3. An examination of columns 6 and 7 reveals that for small total sample sizes the point estimates of y_p delivered by FQUEST are closer to the exact value, with smaller average absolute bias, followed by FIRQUEST($R = 5$) and FIRQUEST($R = 10$) in that order. As the total sample size increased, the differences between those three became smaller. This phenomenon is expected as: (i) FIRQUEST tends to remove more data points in total due to the removal of the same number of observations from every replication in Step **[5]**; and (ii) column 14 reveals that when $R = 5$ FIRQUEST removed 400 observations from each replication on average, while when $R = 10$ the method removed only 200 observations from each replication on average; hence there is a higher chance to have remaining warm-up effects with $R = 10$. For replication length $n = 10{,}000$, the 95% CIs reported by FIRQUEST($R = 5$) exhibited slight undercoverage for $p \in \{0.3, 0.7, 0.9, 0.95\}$, and significant undercoverage for $p \in \{0.99, 0.995\}$. For example, for $p = 0.7$, FIRQUEST($R = 5$) reported an estimated CI coverage probability of 92.7% whereas for $p = 0.995$ it reported an estimated CI coverage probability of 88.4%. For the same n, the 95% CIs reported by FIRQUEST($R = 10$) exhibited significant undercoverage for all values of p. In the worst case, FIRQUEST($R = 10$) for $p = 0.3$ reported an estimated 71.7% CI coverage probability, which is unacceptable. Clearly a replication size $n = 10{,}000$

is too small for this case, so it would be better to use fewer independent replications with larger replication lengths.

FQUEST's dominance started diminishing for total sample sizes greater than 100,000, which showcases FIRQUEST's value. This effect is plainly illustrated in Figure 6.2 as the reported CI coverage probabilities approach the nominal value for larger total sample sizes, while in most cases the average CI relative precision reported by FQUEST is higher compared to the value FIRQUEST reported. In most cases, FIRQUEST($R = 10$) reported the smallest average CI relative precision, especially for large total sample sizes. However, we have to be careful with our conclusions here as the arrays of batch counts $\boldsymbol{s}$ are not the same for different values of R. The entries of column 14 of Tables 6.1–6.3 reveal that the truncated sample size per replication is larger for FQUEST when the total sample size is $N = 50{,}000$, which is reasonable as the maximum truncated sample size that FIRQUEST can remove when $R = 5$ and 10 is 400 and 200, respectively. However, as the total sample size increased, FIRQUEST reported larger truncated sample size per replication than what FQUEST reported. Further, for total sample sizes greater than 200,000, FIRQUEST($R = 10$) reported the largest truncated sample size per replication. This behavior is expected for two reasons: (i) FIRQUEST removes $m_{\max}$, the maximum batch size m that was used in Step **[3]**, from each replication, from every replication; and (ii) FIRQUEST performs the randomness test in Step **[3]** with $b = 25$ for every replication (instead of 50 for FQUEST), which increases the maximum allowable batch size in that step.

In the second (less challenging) case we took $\mu_Y = 0$, $\phi = 0.9$, $\sigma_\epsilon = 1$, and $Y_0 = 0$. The stationary version of this process was used by Chen and Kelton [25]. The experimental results are displayed in Tables 6.4–6.6 and Figure 6.3. In Tables 6.4–6.6, the estimated CI coverage probabilities were close to the nominal value both for FIRQUEST and FQUEST, with some small overcoverage in a few cases. Further, the estimated CI relative precision was reasonable for both procedures for all probabilities p, except for $p = 0.45$; in this case as we explained in Section 5.3.1, the high CI relative precision is partially attributable to the exact value of $y_p = -0.288$, which is close to zero. Figure 6.3 illustrates that in most cases (with very few exceptions) FIRQUEST($R = 10$) reported the smallest estimated CI relative precision, followed by FIRQUEST($R = 5$), and then FQUEST. In this example, FIRQUEST was not outperformed by FQUEST and in most cases it performed slightly better with regard to the estimated CI relative precision.

Overall, we conclude that FIRQUEST performed well in these test cases.

6.4.2 Autoregressive-to-Pareto Process

The second test process is the ARTOP process described in Section 2.5.2. For this example we used $\gamma = 1$, $\theta = 2.1$, and $\phi = 0.995$. Recall that these assignments yield $\mu_Y = 1.9091$, $\sigma_Y^2 = 17.3554$, marginal skewness $\mathrm{E}\{[(Y_k - \mu_Y)/\sigma_Y]^3\} = +\infty$, and marginal kurtosis $\mathrm{E}\{[(Y_k - \mu_Y)/\sigma_Y]^4\} = +\infty$. We initialized the original AR(1) process with the value $Z_0 = 3.4$; which results to an initial observation $Y_0 = F^{-1}[\Phi(Z_0)] = 43.5689$ for the ARTOP process, which is approximately 10 standard deviations above its steady-state mean. On top of the initialization problem and the strong stochastic dependence, this process has a marginal distribution with a fat tail (Mandelbrot [87]), which is reflected by the infinite marginal skewness and kurtosis.

The experimental results for this process are displayed in Tables 6.7–6.9 and Figure 6.4. Columns 6 and 7 of Tables 6.7–6.9 illustrate that FIRQUEST and FQUEST delivered reasonably accurate point estimates for y_p. For $p < 0.9$, FIRQUEST($R = 5$) and FIRQUEST($R = 10$) performed well with regard to CI coverage probability and relative precision, and their estimated metrics were closed to what FQUEST reported. Similarly to FQUEST, FIRQUEST encountered issues for $p \geq 0.95$ and small samples with regard to the estimated CI relative precision. This issue was more pronounced for FIRQUEST($R = 10$). Specifically, for $p = 0.995$ and replication length $n = 5{,}000$, FIRQUEST($R = 10$) reported the enormous value of 128.260% for average CI relative precision. When n was increased to

10,000, the average CI relative precision dropped to 109.043%, which is still unacceptable. It is worth noting that for $R = 5$ independent replications, $p = 0.995$, and replication size $n = 10{,}000$, FIRQUEST reported a lower average CI relative precision 104.159% (which is still unusable), but it also experienced a slight undercoverage reporting a CI coverage probability of 90.9%.

For extreme quantiles and more suitable sample sizes (greater than 200,000), both FIRQUEST and FQUEST performed well and the reported average CI relative precision dropped to values below 40%. However, even when we used a sample size of 1,000,000 for $p = 0.995$ the smallest CI relative precision was reported by FIRQUEST($R = 10$) and it was 22.324%. This behavior is not unexpected because for $p = 0.99$ and 0.995 the largest sample size used in the experimental evaluation in Table 6.9 was lower by a factor of about 2.5 and 3, respectively, than the average sample sizes requested by the sequential SQSTS method (see Section 5.3.2). Further, Figure 6.4 illustrates that as the total sample size increased, FIRQUEST outperformed FQUEST with respect to average CI relative precision. It is worth pointing out that for a total sample size $N = 1{,}000{,}000$, FIRQUEST($R = 10$) reported the smallest CI relative precision, followed by FIRQUEST($R = 5$).

An examination of Figure 6.13 reveals that, for $p = 0.99$, FIRQUEST and FQUEST failed a statistical test in Steps **[6]**–**[9]** with a frequency more than 90% with total sample size 50,000 and more than 80% with total sample size 100,000. Such failures caused FIRQUEST to use the heuristic CI in Step **[10]**. Similarly to FQUEST, FIRQUEST will issue a warning to the user in those cases, which should be an indicator for potential problems associated with the insufficiency of the replication length (and total sample size) for delivering a CI based on a sound theoretical foundation. In these cases, the user should probably rerun FIRQUEST using a larger replication size n. Figure 6.13 also showcases that FIRQUEST($R = 5$), FIRQUEST($R = 10$), and FQUEST used the heuristic CI with similar frequencies. However, for the ARTOP process, we see that in most cases, FIRQUEST($R = 5$) has the smallest frequency of the heuristic CI, while FIRQUEST($R = 10$) has the largest one.

Overall, we deem that FIRQUEST performed well in this test problem, in particular for appropriately large sample sizes.

6.4.3 M/M/1 Waiting-Time Process

The third test process is the waiting-time sequence in an M/M/1 queueing system described in Section 2.5.3 with FIFO service discipline. We considered three examples for this process. For the first example we used an arrival rate $\lambda = 0.9$, a service rate $\omega = 1$ (traffic intensity $\rho = \lambda/\omega = 0.9$), and we initialized the system in the empty-and-idle state. Again, Y_k be the time spent by the kth entity in queue (prior to service).

The experimental results for this case are displayed in Tables 6.10–6.12 and Figure 6.5. Tables 6.10–6.12 reveal that FIRQUEST performed well for $p < 0.95$ with respect to average CI relative precision and coverage probability, with only few exceptions where it experienced slight CI overcoverage. For example, for $p = 0.3$ and replication size $n = 10{,}000$, FIRQUEST($R = 5$) reported a CI coverage probability of 97.5%. However, FIRQUEST experienced less CI overcoverage than FQUEST, which in the same case reported a CI coverage probability of 98.4% (the highest value across Tables 6.10–6.12). Figure 6.5 clearly illustrates that for $p < 0.95$, FIRQUEST reported estimated CI coverage probabilities closer to the nominal value compared to FQUEST. However, Table 6.12 indicates that FIRQUEST encountered issues for the extreme values $p \in \{0.99, 0.995\}$ when the total sample size was less than 500,000, as it reported estimated CI coverage probabilities much smaller than the nominal value of 95%. For example, for $p = 0.995$ and replication size $n = 20{,}000$, FIRQUEST($R = 5$) reported an estimated CI coverage probability of 82.5%, while FIRQUEST($R = 10$) with replication size $n = 10{,}000$ reported an estimated CI coverage probability of 81.5%. FQUEST also experienced similar problems, but the issues were slightly more pronounced with FIRQUEST. This is expected for two reasons: (i) for smaller total sample sizes with larger number of independent replications, it is more difficult to effectively remove the warm-up effects due to limitations associated with the maximum allowable truncation size; and (ii) independent replications could induce systematic bias if insufficient truncation is applied. These observations indicate again the importance of using fewer independent replications with larger replication sizes, when the total sample size is relatively small.

In the second example, we used the same arrival rate $\lambda = 0.9$ and service rate $\omega = 1$, but we initialized the system with one entity beginning service and 112 entities in queue. Recall that the steady-state probability of this initial state is $(1 - \rho)\rho^{113} \approx 6.752 \times 10^{-7}$, implying a high probability for a prolonged transient phase.

The experimental results for this case are displayed in Tables 6.13–6.15 and Figure 6.6. Columns 6 and 7 of Tables 6.13–6.15 clearly illustrate that for small total sample sizes FIRQUEST reported point estimates that are much larger than the true value. This issue is more pronounced for $R = 10$ and values of p near 1. In this example FIRQUEST experienced systematic bias in many cases with relatively small total sample size. This explains the unacceptable CI coverage probabilities reported with $R = 10$ and total sample size $N = 50{,}000$. For example, for $p = 0.95$, FIRQUEST($R = 10$) reported an estimated CI coverage probability of 9%. This is directly explained by the reported average point estimate of 74.284, while the true value is 28.904. Clearly, the prolonged transient phase was detrimental to the performance of FIRQUEST in these cases. As with the ARTOP process in Section 6.4.2, the total sample sizes used in our experimentation were significantly smaller than those required by the sequential SQSTS method in Chapter 4 under no CI precision requirement for large values of p. Further, as Figure 6.6 illustrates, for sample sizes greater than 200,000, FIRQUEST reported estimated CI coverage probabilities close to the nominal value, and the average CI relative precision dropped significantly.

For the third, less-challenging example we only lowered the arrival rate to $\lambda = 0.8$, so that $\rho = 0.8$ (we initialized the system again with one entity beginning service and 112 entities in queue). The experimental results are displayed in Tables 6.16–6.18 and Figure 6.7. In this less-challenging setting, FIRQUEST encountered fewer issues, but there were still cases of significant CI undercoverage (especially with $R = 10$) and overcoverage.

Overall, FIRQUEST performed well in these three examples, especially for relatively large sample sizes.

6.4.4 M/H$_2$/1 Waiting-Time Process

The fourth test process is the sequence $\{Y_k : k \geq 1\}$ of entity waiting times in an M/H$_2$/1 queueing system as described in Section 2.5.4 with FIFO queue discipline, an empty-and-idle initial state, arrival rate $\lambda = 1$, and i.i.d. service times from the hyperexponential distribution that is a mixture of two other exponential distributions with mixing probabilities $g = (5 + \sqrt{15})/10 \approx 0.887$ and $1 - g$ and associated service rates $\omega_1 = 2g\tau$ and $\omega_2 = 2(1 - g)\tau$, with $\tau = 1.25$. As a result, we have a mean service time of 0.8 and a steady-state server utilization of $\rho = 0.8$. For this process and under no CI precision requirement, the Sequest sequential method of Alexopoulos *et al.* [7] reported average sample sizes ranging from 1.2 to 28.7 million, and yet delivered CIs with significant undercoverage for $p \geq 0.99$ (Table 4.4 of this thesis). Most importantly, it was outshined by SQSTS for all values of p under study.

The experimental results for this process are displayed in Tables 6.19–6.21 and Figure 6.8. We start our analysis with Table 6.19. For $p = 0.3$, the 95% CIs reported by FIRQUEST exhibited noticeable overcoverage for total sample sizes $N < 200{,}000$. Specifically, for $p = 0.3$ and replication size $n = 10{,}000$, FIRQUEST($R = 5$) reported an estimated CI coverage probability of 99.3%, while with replication size $n = 5{,}000$, FIRQUEST($R = 10$) reported an estimated CI coverage probability of 98.6%. Further, for $p = 0.3$ and total sample size 50,000, FIRQUEST delivered large average CI relative precisions. For example, with $R = 5$ and 10, it yielded average 84.594% and 78.030% CI relative precisions, respectively. Both these values were lower than 90.834%, the estimate reported by FQUEST. This issue is partially attributable to the actual value of $y_p = 0.669$, which is very close to zero. As Figure 6.8 illustrates, FIRQUEST performed well, for all values of p under study, with regard to average CI relative precision when it was supplied with total sample sizes greater than 100,000. Additionally, column 10 of Tables 6.19–6.20 reveals that FIRQUEST yielded estimated CI coverage probabilities close to the nominal value for $p \in \{0.5, 0.7, 0.9\}$, while it experienced some slight undercoverage for $p = 0.95$ and total sample size $N < 200{,}000$. Table 6.21 showcases that FIRQUEST experienced significant CI undercoverage for extreme quantiles for total sample sizes $N < 200{,}000$. FQUEST experienced similar issues, but provided slightly better estimated CI coverage probabilities than FIRQUEST. Both FIRQUEST and FQUEST performed well for $p \in \{0.99, 0.995\}$ when they were provided with total sample sizes $N > 200{,}000$, which are more suitable for extreme quantile estimation.

An examination of the plots in Figure 6.13 for $p = 0.3$ and 0.99 reveals that FIRQUEST and FQUEST failed a statistical test in Steps **[6]–[9]** with a frequency close to or more than 80% with $N = 50{,}000$. Further, we see that FIRQUEST($R = 5$), FIRQUEST($R = 10$), and FQUEST use the heuristic CI at similar frequencies. However, similarly to what we observed for the ARTOP process, we see that in most cases, FIRQUEST($R = 5$) used the heuristic CI with the lowest frequency, while FIRQUEST($R = 10$) used the heuristic CI most often.

Overall, we believe that FIRQUEST handled this challenging process effectively for reasonably low total sample sizes N.

6.4.5 M/M/1/LIFO Waiting-Time Process

The fifth test process is the sequence of entity waiting times $\{Y_k : k \geq 1\}$ in a single-server queueing system as described in Section 2.5.5 with non-preemptive LIFO service discipline, empty-and-idle initial state, arrival rate $\lambda = 1$, and service rate $\omega = 1.25$. The steady-state server utilization is $\rho = 0.8$ and the marginal mean waiting time is $\mu_Y = 3.2$.

The experimental results for this process are displayed in Tables 6.22–6.24 and Figure 6.9. These results reveal that the 95% CIs for y_p exhibited some noticeable overcoverage for total sample sizes $N \leq 100{,}000$ and all values of p under study. Figure 6.9 clearly illustrates that FIRQUEST outperformed FQUEST with regard to average CI relative precision; clearly, the total sample sizes N that we considered for this example are sufficient.

An examination of the plots of this example for $p = 0.99$ in Figure 6.13, showcases that FIRQUEST and FQUEST failed a statistical test in Steps **[6]**–**[9]** with a frequency close to 70% with total sample size $N = 50{,}000$, which quickly dropped as we increased the total sample size. Further, for $p = 0.3$, we see that the values of the frequency of the heuristic CI for all methods were around 17% for all the total sample sizes under consideration. Once again, we see that FIRQUEST($R = 5$), FIRQUEST($R = 10$), and FQUEST used the heuristic CI at similar frequencies.

Overall, FIRQUEST performed very well in this example.

6.4.6 M/M/1/M/1 Waiting-Time Process

The sixth test process, detailed in Section 2.5.6, is constructed from the sequence $\{Y_k : k \geq 1\}$ of the total waiting times (prior to service) in a tandem network of two M/M/1 queues. The system has an arrival rate of $\lambda = 1$, service rates $\omega = 1.25$ at each station, and is initialized in the empty and idle state. The steady-state utilization for each server is $\rho = \lambda/\omega = 0.8$ and the mean total waiting time in the system is equal to 8.

The experimental results for this process are displayed in Tables 6.25–6.27 and Figure 6.10. Based on Tables 6.25–6.27, and Figure 6.10, FIRQUEST performed exceptionally well with respect to all metrics for $p \leq 0.9$. The estimated CI coverage probabilities were very close to the nominal values without resulting in excessive estimated CI relative precision. However, for $p \geq 0.95$ and total sample size $N = 50{,}000$, FIRQUEST delivered CIs with noticeable undercoverage. In these cases, the estimated CI coverage probabilities were significantly improved once the used total sample size N exceeded 100,000.

Overall, we assess that FIRQUEST performed well in this case study despite the sample size limitations.

6.4.7 Central Server Model 3

The seventh test process, described in Section 2.5.7, is generated by the sequence $\{Y_k : k \geq 1\}$ of response times (cycle times) in a small computer network comprised of three stations, namely the Central Server Model 3 from Law and Carson [66].

The experimental results for this process are displayed in Tables 6.28–6.32 and Figures 6.11–6.12. Recall from the discussion in Section 4.2.7 that in the absence of a CI precision requirement and for $p \in \{0.85, \ldots, 0.93\}$, the Sequest method (Alexopoulos *et al.* [7]) experienced substantial sample-size variation and delivered CIs with noticeable variation around the nominal 95% level (see Table 4.7 of this thesis), while the sequential SQSTS method delivered CIs with minor undercoverage in a few cases ($p \in \{0.3, 0.5, 0.93\}$). For this response-time process, similarly to FQUEST, FIRQUEST performed well, with a few exceptions. FIRQUEST delivered CIs that exhibited noticeable overcoverage for $p \in \{0.89, 0.90, 0.91\}$ and total sample size $N \leq 100{,}000$. It is worth mentioning that for total sample size 50,000, FIRQUEST reported an estimated CI coverage probability of 93.4% (for both $R = 5$ and 10), which is closer to the nominal value than the estimate of 91.6% that FQUEST reported.

The graphs of this example in Figure 6.13 illustrate again that FIRQUEST($R = 5$), FIRQUEST($R = 10$), and FQUEST used the heuristic CI at similar frequencies. Unfortunately, these plots did not provide any additional insights.

Overall, we judge the performance of FIRQUEST in this test case as solid.

6.5 Summary

In this chapter, we presented FIRQUEST, the first completely automated procedure for computing point estimators and CIs for steady-state quantiles based on independent replications. The user provides a fixed number R of replicate sample paths, each with fixed length n, and specifies the probability of the quantile and the required coverage probability of the requested CI. FIRQUEST incorporates the analysis methods of batching, STS, and sectioning. If the total sample size and the replication length suffice to identify a set of replicate signed weighted areas $\{A_p(w; j, m) : j = 1, \ldots, Rb\}$ and RBQEs $\{\widehat{y}_p(j, m) : j = 1, \ldots, Rb\}$ that pass both the von Neumman and Shapiro-Wilk tests, FIRQUEST reports a CI for the quantile y_p under consideration that is centered at the overall empirical quantile computed from all sample paths and based on the combined estimator $\widetilde{\mathscr{V}}_p(w; R, b, m)$ of σ_p^2. Otherwise, the procedure issues a warning and, upon user's approval, formulates a wider CI from a set of CIs based on the aforementioned overall quantile estimator, the RBQEs, and the replicate signed areas obtained from the nonoverlapping batches.

Experimentation with an extensive test bed of output processes and 5 or 10 replications in Section 6.4 showed that for sufficiently large replicate paths FIRQUEST delivered CIs with coverage probabilities close to the nominal level. This feat is impressive, considering that the state-of-the-art sequential methods Sequest and SQSTS required substantial sample sizes for the same processes under no CI precision requirement (see Alexopoulos *et al.* [7] and Chapter 4 of this thesis). Our experimental analysis revealed that for relatively small sample sizes, it is preferable to use fewer independent replications with larger replication lengths (in these cases FQUEST outperformed FIRQUEST). However, in several experimental settings and with sufficiently large replication lengths, FIRQUEST outperformed FQUEST with regard to average CI relative precision. In these cases using more independent replications may be beneficial.

The last statements raise the possibilities of potential benefits from parallel executions (e.g., multi-treading). Such an implementation will not only permit an execution speed-up of various loops, in particular those in Steps **[6]–[7]**, but it will also allow faster execution of the underlying simulation model that generates the sample paths, thereby relaxing the computational and time-related constraints.

Table 6.1: Experimental results for FIRQUEST with $R = 5, 10$ and FQUEST with regard to point and 95% CI estimation of y_p for the AR(1) process in Section 6.4.1 with $\mu_Y = 100$ and $\phi = 0.995$ for $p \in \{0.3, 0.5, 0.7\}$ based on 1,000 independent replications.

p	y_p	R	Repl. Size	Method	Point Est.	Avg. |Bias|	Avg. 95% CI HL	Avg. 95% CI rel. prec. (%)	Avg. 95% CI cov. (%)	$\overline{m}$	$\overline{b}$	St. Dev. HL	Avg. Trunc. Point
0.3	94.749	5	10,000	FIRQUEST	94.486	0.787	2.039	2.159	93.3	3,426	15.85	0.800	400
		10	5,000	FIRQUEST	93.300	1.508	2.191	2.348	71.7	3,482	17.83	0.856	200
		1	50,000	FQUEST	94.753	0.739	2.067	2.183	93.2	3,467	17.16	0.936	625
		5	20,000	FIRQUEST	94.742	0.558	1.446	1.526	94.0	6,544	16.72	0.466	777
		10	10,000	FIRQUEST	94.466	0.583	1.422	1.506	93.2	6,003	21.23	0.501	400
		1	100,000	FQUEST	94.773	0.554	1.488	1.570	93.2	6,451	18.69	0.604	639
		5	40,000	FIRQUEST	94.775	0.382	1.042	1.100	94.3	13,192	16.68	0.302	1,074
		10	20,000	FIRQUEST	94.750	0.379	1.015	1.072	94.9	10,994	23.32	0.360	796
		1	200,000	FQUEST	94.751	0.385	1.091	1.151	94.8	12,598	19.28	0.414	639
		5	100,000	FIRQUEST	94.768	0.242	0.674	0.711	96.0	33,001	16.99	0.210	1,081
		10	50,000	FIRQUEST	94.768	0.230	0.644	0.680	95.4	26,901	23.96	0.187	1,224
		1	500,000	FQUEST	94.765	0.237	0.682	0.720	95.7	30,304	20.10	0.225	640
		5	200,000	FIRQUEST	94.754	0.166	0.482	0.508	95.8	66,104	17.08	0.152	1,081
		10	100,000	FIRQUEST	94.759	0.168	0.466	0.492	96.5	54,610	23.95	0.140	1,223
		1	1,000,000	FQUEST	94.751	0.165	0.497	0.524	97.0	60,715	20.11	0.190	640
0.5	100.000	5	10,000	FIRQUEST	99.764	0.769	1.951	1.956	93.6	3,385	16.08	0.729	400
		10	5,000	FIRQUEST	98.921	1.215	2.051	2.073	79.2	3,333	18.98	0.795	200
		1	50,000	FQUEST	99.997	0.723	2.024	2.025	92.9	3,388	17.73	0.973	629
		5	20,000	FIRQUEST	99.979	0.553	1.414	1.414	94.0	6,466	16.82	0.476	780
		10	10,000	FIRQUEST	99.754	0.566	1.350	1.354	93.1	5,756	22.34	0.455	400
		1	100,000	FQUEST	100.021	0.543	1.430	1.430	93.0	6,309	19.14	0.544	635
		5	40,000	FIRQUEST	100.023	0.374	1.030	1.030	94.9	13,187	16.72	0.349	1,027
		10	20,000	FIRQUEST	99.994	0.373	0.997	0.997	95.2	10,832	23.65	0.356	797
		1	200,000	FQUEST	100.001	0.381	1.052	1.052	95.6	12,541	19.41	0.393	636
		5	100,000	FIRQUEST	100.016	0.239	0.657	0.656	96.0	32,700	17.21	0.211	1,028
		10	50,000	FIRQUEST	100.015	0.222	0.633	0.632	96.2	27,523	23.71	0.185	1,142
		1	500,000	FQUEST	100.015	0.232	0.673	0.673	95.9	30,957	19.74	0.226	636
		5	200,000	FIRQUEST	100.003	0.167	0.463	0.463	95.7	66,346	16.95	0.128	1,029
		10	100,000	FIRQUEST	100.009	0.167	0.449	0.449	94.7	54,456	24.30	0.137	1,142
		1	1,000,000	FQUEST	100.002	0.162	0.470	0.470	96.9	59,908	20.36	0.143	636
0.7	105.251	5	10,000	FIRQUEST	105.037	0.797	2.049	1.951	92.7	3,452	15.70	0.879	400
		10	5,000	FIRQUEST	104.389	1.086	2.144	2.054	84.3	3,608	16.83	0.843	200
		1	50,000	FQUEST	105.238	0.745	2.135	2.029	94.7	3,559	16.63	0.968	628
		5	20,000	FIRQUEST	105.224	0.562	1.479	1.406	93.8	6,680	16.37	0.550	764
		10	10,000	FIRQUEST	105.038	0.572	1.424	1.356	92.6	6,060	21.18	0.529	400
		1	100,000	FQUEST	105.264	0.549	1.514	1.439	94.2	6,504	18.59	0.603	639
		5	40,000	FIRQUEST	105.269	0.384	1.066	1.013	95.3	13,294	16.63	0.389	943
		10	20,000	FIRQUEST	105.241	0.381	1.044	0.992	94.4	11,449	22.78	0.407	788
		1	200,000	FQUEST	105.252	0.392	1.071	1.017	94.8	12,478	19.46	0.376	640
		5	100,000	FIRQUEST	105.260	0.249	0.668	0.635	95.8	33,112	16.99	0.193	945
		10	50,000	FIRQUEST	105.262	0.229	0.644	0.612	95.5	27,286	24.07	0.194	1,052
		1	500,000	FQUEST	105.262	0.240	0.700	0.665	95.8	31,587	19.36	0.248	640
		5	200,000	FIRQUEST	105.253	0.174	0.471	0.447	95.5	65,835	17.11	0.130	945
		10	100,000	FIRQUEST	105.257	0.171	0.463	0.440	94.7	53,028	24.71	0.166	1,052
		1	1,000,000	FQUEST	105.250	0.168	0.489	0.465	96.8	60,234	20.37	0.157	640

Table 6.2: Experimental results for FIRQUEST with $R = 5, 10$ and FQUEST with regard to point and 95% CI estimation of y_p for the AR(1) process in Section 6.4.1 with $\mu_Y = 100$ and $\phi = 0.995$ for $p \in \{0.9, 0.95\}$ based on 1,000 independent replications.

p	y_p	R	Repl. Size	Method	Point Est.	Avg. |Bias|	Avg. 95% CI HL	Avg. 95% CI rel. prec. (%)	Avg. 95% CI cov. (%)	$\overline{m}$	$\overline{b}$	St. Dev. HL	Avg. Trunc. Point
0.9	112.832	5	10,000	FIRQUEST	112.626	0.930	2.594	2.302	92.5	3,952	13.36	1.132	400
		10	5,000	FIRQUEST	112.153	1.084	2.742	2.444	88.9	4,246	12.83	1.221	200
		1	50,000	FQUEST	112.808	0.879	2.785	2.468	94.5	4,169	13.26	1.351	612
		5	20,000	FIRQUEST	112.795	0.635	1.811	1.605	93.6	7,264	14.99	0.758	750
		10	10,000	FIRQUEST	112.645	0.652	1.830	1.624	93.5	7,718	15.22	0.842	400
		1	100,000	FQUEST	112.830	0.626	1.856	1.644	94.3	7,502	15.64	0.850	622
		5	40,000	FIRQUEST	112.839	0.446	1.254	1.111	95.9	13,844	16.03	0.482	891
		10	20,000	FIRQUEST	112.820	0.439	1.254	1.111	94.7	13,274	19.23	0.507	779
		1	200,000	FQUEST	112.820	0.455	1.280	1.134	95.1	13,620	17.63	0.522	623
		5	100,000	FIRQUEST	112.831	0.285	0.764	0.677	95.2	33,370	16.86	0.235	892
		10	50,000	FIRQUEST	112.838	0.277	0.749	0.664	94.9	29,435	22.29	0.220	1,001
		1	500,000	FQUEST	112.835	0.277	0.811	0.718	96.1	32,712	18.60	0.303	624
		5	200,000	FIRQUEST	112.829	0.203	0.561	0.497	95.2	67,084	16.92	0.204	892
		10	100,000	FIRQUEST	112.837	0.202	0.537	0.476	94.0	57,007	23.21	0.181	1,001
		1	1,000,000	FQUEST	112.829	0.197	0.568	0.504	95.9	62,065	19.66	0.183	625
0.95	116.469	5	10,000	FIRQUEST	116.252	1.070	3.149	2.706	92.0	4,274	11.99	1.440	400
		10	5,000	FIRQUEST	115.852	1.178	3.299	2.845	90.9	4,498	11.45	1.507	200
		1	50,000	FQUEST	116.451	0.706	2.251	1.932	93.9	8,351	13.32	1.048	622
		5	20,000	FIRQUEST	116.424	0.727	2.163	1.857	94.4	7,787	13.75	0.998	744
		10	10,000	FIRQUEST	116.295	0.745	2.207	1.897	93.9	8,454	12.97	1.074	400
		1	100,000	FQUEST	116.451	0.706	2.251	1.932	93.9	8,351	13.32	1.048	622
		5	40,000	FIRQUEST	116.471	0.505	1.434	1.231	95.1	14,763	14.97	0.575	875
		10	20,000	FIRQUEST	116.454	0.509	1.481	1.272	94.9	14,749	16.37	0.699	777
		1	200,000	FQUEST	116.445	0.511	1.498	1.286	94.9	15,085	15.61	0.682	624
		5	100,000	FIRQUEST	116.463	0.315	0.899	0.771	95.6	34,240	16.50	0.345	876
		10	50,000	FIRQUEST	116.471	0.319	0.867	0.745	94.4	31,914	20.10	0.307	991
		1	500,000	FQUEST	116.466	0.309	0.928	0.797	96.0	33,607	18.04	0.371	626
		5	200,000	FIRQUEST	116.462	0.225	0.643	0.552	96.1	68,861	16.50	0.245	876
		10	100,000	FIRQUEST	116.472	0.231	0.598	0.513	94.6	60,124	22.08	0.199	991
		1	1,000,000	FQUEST	116.462	0.219	0.651	0.559	96.0	63,258	19.27	0.236	627

Table 6.3: Experimental results for FIRQUEST with $R = 5, 10$ and FQUEST with regard to point and 95% CI estimation of y_p for the AR(1) process in Section 6.4.1 with $\mu_Y = 100$ and $\phi = 0.995$ for $p \in \{0.99, 0.995\}$ based on 1,000 independent replications.

p	y_p	R	Repl. Size	Method	Point Est.	Avg. |Bias|	Avg. 95% CI HL	Avg. 95% CI rel. prec. (%)	Avg. 95% CI cov. (%)	$\overline{m}$	$\overline{b}$	St. Dev. HL	Avg. Trunc. Point
0.99	123.293	5	10,000	FIRQUEST	122.963	1.524	4.730	3.838	90.7	4,622	10.62	2.267	400
		10	5,000	FIRQUEST	122.709	1.581	4.876	3.963	90.6	4,715	10.36	2.348	200
		1	50,000	FQUEST	123.112	1.489	5.125	4.152	93.2	4,842	10.34	2.507	603
		5	20,000	FIRQUEST	123.187	1.038	3.397	2.753	93.6	8,977	11.20	1.811	741
		10	10,000	FIRQUEST	123.103	1.079	3.577	2.901	92.4	9,334	10.61	1.871	400
		1	100,000	FQUEST	123.198	0.988	3.653	2.962	95.7	9,486	10.84	1.882	611
		5	40,000	FIRQUEST	123.256	0.726	2.360	1.914	94.4	17,241	12.22	1.280	865
		10	20,000	FIRQUEST	123.241	0.737	2.499	2.026	95.3	17,867	11.65	1.332	776
		1	200,000	FQUEST	123.217	0.712	2.501	2.029	95.0	18,043	11.86	1.364	612
		5	100,000	FIRQUEST	123.261	0.450	1.384	1.123	94.7	39,328	14.09	0.705	866
		10	50,000	FIRQUEST	123.270	0.464	1.443	1.170	94.5	40,259	14.51	0.744	983
		1	500,000	FQUEST	123.263	0.441	1.415	1.147	95.9	39,219	14.86	0.674	615
		5	200,000	FIRQUEST	123.274	0.323	0.936	0.759	95.5	73,445	15.32	0.401	866
		10	100,000	FIRQUEST	123.284	0.334	0.916	0.743	92.8	71,167	17.97	0.399	983
		1	1,000,000	FQUEST	123.273	0.321	0.976	0.791	95.5	72,252	16.63	0.450	616
0.995	125.791	5	10,000	FIRQUEST	125.365	1.840	5.579	4.433	88.4	4,696	10.36	2.691	400
		10	5,000	FIRQUEST	125.143	1.878	5.699	4.535	87.5	4,731	10.30	2.789	200
		1	50,000	FQUEST	125.483	1.795	6.079	4.823	90.9	4,891	10.17	3.188	602
		5	20,000	FIRQUEST	125.636	1.256	4.042	3.210	92.5	9,283	10.60	2.077	740
		10	10,000	FIRQUEST	125.556	1.297	4.144	3.292	90.5	9,486	10.26	2.125	400
		1	100,000	FQUEST	125.630	1.199	4.365	3.468	93.8	9,673	10.47	2.251	608
		5	40,000	FIRQUEST	125.713	0.881	2.936	2.333	93.9	18,273	11.21	1.603	865
		10	20,000	FIRQUEST	125.716	0.889	3.097	2.460	94.5	18,674	10.62	1.679	774
		1	200,000	FQUEST	125.674	0.863	3.098	2.463	94.6	18,910	10.94	1.655	609
		5	100,000	FIRQUEST	125.744	0.548	1.736	1.380	93.5	41,647	13.09	0.954	866
		10	50,000	FIRQUEST	125.750	0.564	1.857	1.476	94.7	44,955	11.94	1.007	978
		1	500,000	FQUEST	125.741	0.537	1.808	1.437	96.6	43,201	12.77	0.919	611
		5	200,000	FIRQUEST	125.767	0.391	1.183	0.940	94.9	78,513	14.13	0.591	866
		10	100,000	FIRQUEST	125.777	0.409	1.174	0.933	93.4	79,466	15.14	0.575	978
		1	1,000,000	FQUEST	125.757	0.388	1.226	0.975	95.0	78,190	14.92	0.630	613

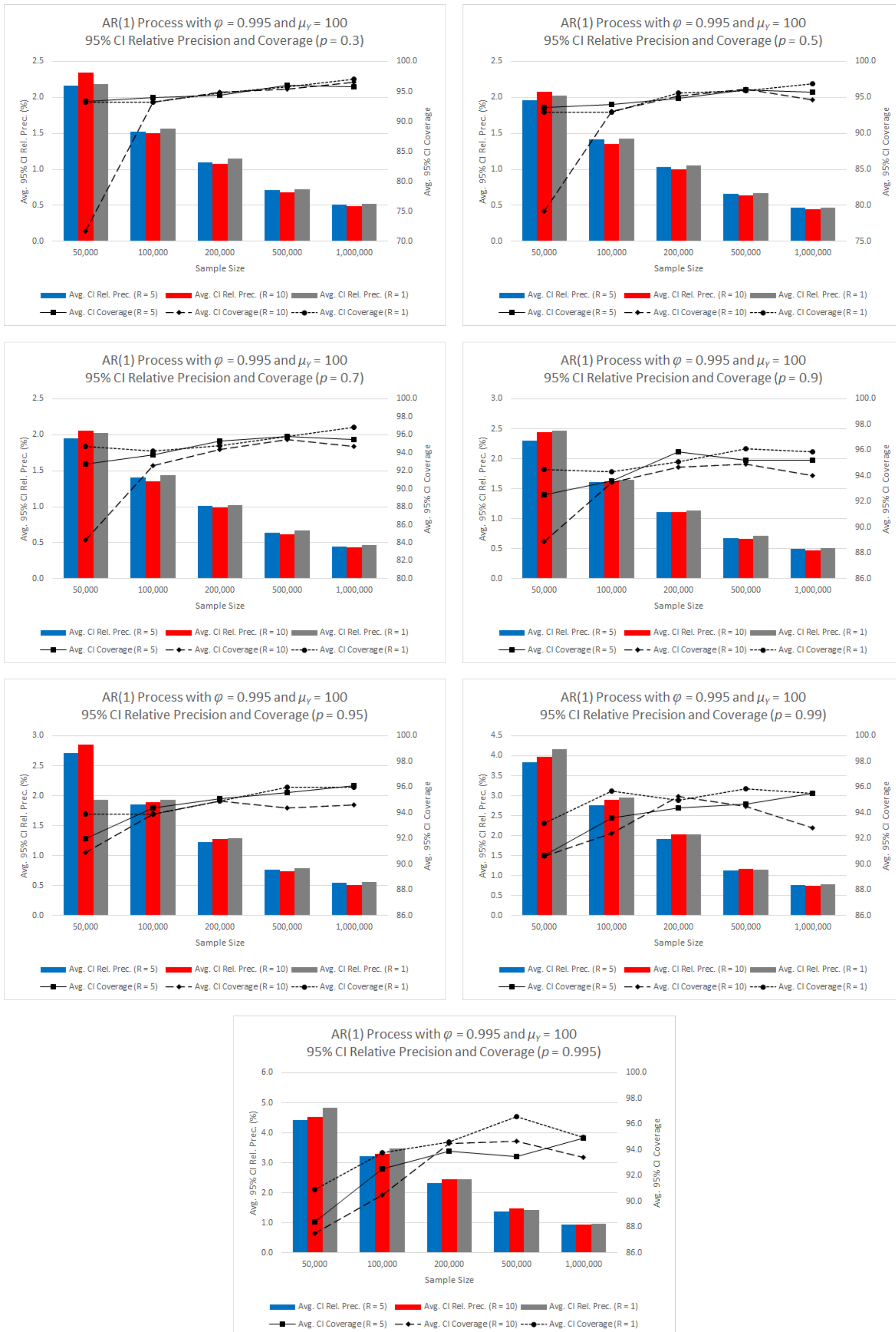

Figure 6.2: Plots for the average 95% CI relative precision and estimated coverage probability for the AR(1) process from Tables 6.1–6.3.

Table 6.4: Experimental results for FIRQUEST with $R = 5, 10$ and FQUEST with regard to point and 95% CI estimation of y_p for the AR(1) process in Section 6.4.1 with $\mu_Y = 0$ and $\phi = 0.9$ for $p \in \{0.25, 0.45, 0.75\}$ based on 1,000 independent replications.

p	y_p	R	Repl. Size	Method	Point Est.	Avg. |Bias|	Avg. 95% CI HL	Avg. 95% CI rel. prec. (%)	Avg. 95% CI cov. (%)	$\overline{m}$	$\overline{b}$	St. Dev. HL	Avg. Trunc. Point
0.25	-1.547	5	10,000	FIRQUEST	-1.546	0.039	0.110	7.142	96.3	3,129	17.25	0.029	400
		10	5,000	FIRQUEST	-1.548	0.039	0.110	7.123	95.2	2,700	23.83	0.036	200
		1	50,000	FQUEST	-1.545	0.038	0.116	7.520	96.7	3,058	19.74	0.042	595
		5	20,000	FIRQUEST	-1.547	0.029	0.079	5.128	95.5	6,430	17.01	0.024	707
		10	10,000	FIRQUEST	-1.546	0.027	0.077	5.009	97.0	5,046	25.12	0.024	400
		1	100,000	FQUEST	-1.545	0.028	0.079	5.146	95.9	6,006	20.17	0.024	600
		5	40,000	FIRQUEST	-1.546	0.020	0.055	3.565	95.6	12,865	17.23	0.016	796
		10	20,000	FIRQUEST	-1.546	0.019	0.055	3.529	96.1	10,544	24.42	0.017	753
		1	200,000	FQUEST	-1.547	0.020	0.057	3.710	96.5	12,228	20.04	0.019	600
		5	100,000	FIRQUEST	-1.547	0.012	0.035	2.267	96.1	33,473	16.81	0.010	796
		10	50,000	FIRQUEST	-1.546	0.012	0.034	2.170	96.1	27,273	23.95	0.009	900
		1	500,000	FQUEST	-1.547	0.012	0.036	2.306	96.2	30,907	19.71	0.011	600
		5	200,000	FIRQUEST	-1.547	0.009	0.025	1.596	96.6	66,681	16.98	0.007	796
		10	100,000	FIRQUEST	-1.547	0.009	0.024	1.553	95.4	55,292	24.12	0.008	900
		1	1,000,000	FQUEST	-1.548	0.008	0.026	1.667	96.6	61,322	20.04	0.009	600
0.45	-0.288	5	10,000	FIRQUEST	-0.287	0.038	0.108	38.612	96.7	3,124	17.33	0.032	400
		10	5,000	FIRQUEST	-0.289	0.038	0.104	36.965	95.1	2,600	24.68	0.030	200
		1	50,000	FQUEST	-0.287	0.037	0.110	39.432	96.2	2,986	20.18	0.040	597
		5	20,000	FIRQUEST	-0.288	0.028	0.076	26.736	95.9	6,352	17.26	0.022	708
		10	10,000	FIRQUEST	-0.287	0.026	0.074	26.054	97.0	5,152	24.64	0.020	400
		1	100,000	FQUEST	-0.286	0.027	0.077	27.200	96.1	6,019	20.12	0.025	599
		5	40,000	FIRQUEST	-0.287	0.019	0.053	18.619	95.9	13,015	17.13	0.015	792
		10	20,000	FIRQUEST	-0.287	0.019	0.052	18.383	96.1	10,770	23.92	0.017	753
		1	200,000	FQUEST	-0.288	0.019	0.054	19.009	96.1	12,191	19.99	0.017	599
		5	100,000	FIRQUEST	-0.287	0.012	0.033	11.630	95.5	33,162	16.98	0.010	792
		10	50,000	FIRQUEST	-0.287	0.011	0.032	11.188	95.7	26,786	24.51	0.009	893
		1	500,000	FQUEST	-0.288	0.011	0.035	12.105	97.4	30,772	19.89	0.012	599
		5	200,000	FIRQUEST	-0.288	0.008	0.024	8.187	96.5	65,393	17.27	0.007	792
		10	100,000	FIRQUEST	-0.288	0.008	0.023	8.051	95.5	54,640	24.15	0.007	894
		1	1,000,000	FQUEST	-0.288	0.008	0.024	8.325	96.9	60,066	20.28	0.007	600
0.75	1.547	5	10,000	FIRQUEST	1.549	0.040	0.113	7.329	95.5	3,213	17.00	0.035	400
		10	5,000	FIRQUEST	1.547	0.040	0.110	7.097	94.9	2,678	24.11	0.034	200
		1	50,000	FQUEST	1.548	0.039	0.114	7.351	95.2	3,020	20.04	0.038	598
		5	20,000	FIRQUEST	1.547	0.028	0.079	5.119	96.0	6,397	17.11	0.024	702
		10	10,000	FIRQUEST	1.549	0.028	0.076	4.892	94.4	5,147	24.86	0.018	400
		1	100,000	FQUEST	1.548	0.029	0.082	5.274	95.4	6,182	19.72	0.029	601
		5	40,000	FIRQUEST	1.549	0.020	0.056	3.588	95.3	12,974	17.18	0.017	784
		10	20,000	FIRQUEST	1.548	0.020	0.054	3.504	95.8	10,670	24.01	0.016	752
		1	200,000	FQUEST	1.548	0.020	0.056	3.648	96.3	11,988	20.26	0.017	602
		5	100,000	FIRQUEST	1.548	0.013	0.035	2.252	96.2	33,390	16.92	0.010	784
		10	50,000	FIRQUEST	1.548	0.011	0.034	2.188	96.5	26,148	24.79	0.010	900
		1	500,000	FQUEST	1.548	0.012	0.036	2.297	96.5	29,709	20.33	0.011	602
		5	200,000	FIRQUEST	1.548	0.009	0.025	1.602	95.9	66,529	16.97	0.008	784
		10	100,000	FIRQUEST	1.548	0.009	0.024	1.538	96.1	55,753	23.68	0.007	900
		1	1,000,000	FQUEST	1.548	0.009	0.026	1.661	97.3	61,236	19.92	0.008	602

Table 6.5: Experimental results for FIRQUEST with $R = 5, 10$ and FQUEST with regard to point and 95% CI estimation of y_p for the AR(1) process in Section 6.4.1 with $\mu_Y = 0$ and $\phi = 0.9$ for $p \in \{0.9, 0.95\}$ based on 1,000 independent replications.

p	y_p	R	Repl. Size	Method	Point Est.	Avg. |Bias|	Avg. 95% CI HL	Avg. 95% CI rel. prec. (%)	Avg. 95% CI cov. (%)	$\overline{m}$	$\overline{b}$	St. Dev. HL	Avg. Trunc. Point
0.9	2.940	5	10,000	FIRQUEST	2.941	0.045	0.130	4.414	96.3	3,221	16.95	0.044	400
		10	5,000	FIRQUEST	2.941	0.048	0.127	4.317	95.0	2,765	23.19	0.044	200
		1	50,000	FQUEST	2.939	0.046	0.132	4.506	96.3	3,090	19.48	0.051	593
		5	20,000	FIRQUEST	2.940	0.031	0.089	3.044	96.4	6,421	17.07	0.028	703
		10	10,000	FIRQUEST	2.941	0.032	0.088	3.009	95.2	5,509	23.54	0.027	400
		1	100,000	FQUEST	2.940	0.033	0.092	3.121	96.0	6,201	19.53	0.029	596
		5	40,000	FIRQUEST	2.941	0.022	0.063	2.136	96.2	12,924	17.21	0.019	789
		10	20,000	FIRQUEST	2.940	0.022	0.064	2.161	96.4	10,705	23.81	0.023	753
		1	200,000	FQUEST	2.941	0.023	0.066	2.228	96.2	12,229	20.05	0.023	596
		5	100,000	FIRQUEST	2.941	0.014	0.039	1.335	96.2	32,892	17.13	0.010	789
		10	50,000	FIRQUEST	2.941	0.013	0.039	1.318	96.6	26,155	24.79	0.012	906
		1	500,000	FQUEST	2.941	0.014	0.042	1.434	96.3	31,110	19.58	0.016	595
		5	200,000	FIRQUEST	2.940	0.010	0.028	0.946	96.1	66,215	17.02	0.007	789
		10	100,000	FIRQUEST	2.940	0.010	0.027	0.931	96.5	55,863	23.72	0.009	906
		1	1,000,000	FQUEST	2.940	0.010	0.030	1.011	96.6	62,215	19.66	0.011	596
0.95	3.774	5	10,000	FIRQUEST	3.774	0.051	0.149	3.948	96.2	3,292	16.55	0.053	400
		10	5,000	FIRQUEST	3.774	0.053	0.142	3.762	94.1	2,853	22.29	0.048	200
		1	50,000	FQUEST	3.772	0.052	0.150	3.976	95.7	3,181	18.98	0.057	603
		5	20,000	FIRQUEST	3.773	0.035	0.102	2.708	96.6	6,410	17.08	0.033	710
		10	10,000	FIRQUEST	3.775	0.036	0.101	2.667	95.2	5,584	22.92	0.030	400
		1	100,000	FQUEST	3.774	0.037	0.103	2.740	95.0	6,292	19.07	0.034	604
		5	40,000	FIRQUEST	3.774	0.025	0.073	1.931	96.9	13,400	16.64	0.023	799
		10	20,000	FIRQUEST	3.774	0.024	0.072	1.905	96.9	11,051	23.18	0.025	753
		1	200,000	FQUEST	3.774	0.026	0.073	1.931	96.5	12,168	19.93	0.023	605
		5	100,000	FIRQUEST	3.774	0.016	0.046	1.221	96.2	33,608	16.78	0.016	799
		10	50,000	FIRQUEST	3.774	0.015	0.044	1.161	96.1	26,834	24.29	0.012	895
		1	500,000	FQUEST	3.774	0.016	0.047	1.257	97.4	31,346	19.42	0.017	605
		5	200,000	FIRQUEST	3.774	0.011	0.032	0.843	95.8	66,301	17.05	0.009	799
		10	100,000	FIRQUEST	3.774	0.011	0.031	0.817	95.3	54,383	24.30	0.008	895
		1	1,000,000	FQUEST	3.774	0.012	0.033	0.881	95.7	62,371	19.64	0.011	605

Table 6.6: Experimental results for FIRQUEST with $R = 5, 10$ and FQUEST with regard to point and 95% CI estimation of y_p for the AR(1) process in Section 6.4.1 with $\mu_Y = 0$ and $\phi = 0.9$ for $p \in \{0.99, 0.995\}$ based on 1,000 independent replications.

p	y_p	R	Repl. Size	Method	Point Est.	Avg. |Bias|	Avg. 95% CI HL	Avg. 95% CI rel. prec. (%)	Avg. 95% CI cov. (%)	$\overline{m}$	$\overline{b}$	St. Dev. HL	Avg. Trunc. Point
0.99	5.337	5	10,000	FIRQUEST	5.335	0.075	0.214	4.014	95.2	3,487	15.61	0.076	400
		10	5,000	FIRQUEST	5.337	0.077	0.214	4.010	93.7	3,379	18.31	0.086	200
		1	50,000	FQUEST	5.336	0.076	0.229	4.294	95.0	3,606	16.43	0.100	594
		5	20,000	FIRQUEST	5.336	0.054	0.148	2.769	95.3	6,644	16.47	0.048	704
		10	10,000	FIRQUEST	5.339	0.053	0.150	2.806	95.4	6,131	20.74	0.057	400
		1	100,000	FQUEST	5.336	0.052	0.156	2.913	95.3	6,780	17.77	0.061	597
		5	40,000	FIRQUEST	5.339	0.038	0.106	1.993	96.2	13,485	16.52	0.039	786
		10	20,000	FIRQUEST	5.337	0.036	0.104	1.947	96.4	11,516	22.49	0.034	752
		1	200,000	FQUEST	5.338	0.037	0.108	2.024	95.4	12,918	18.80	0.037	597
		5	100,000	FIRQUEST	5.338	0.023	0.066	1.243	96.9	33,379	16.87	0.022	786
		10	50,000	FIRQUEST	5.338	0.023	0.065	1.222	95.2	28,078	23.45	0.021	892
		1	500,000	FQUEST	5.337	0.024	0.067	1.265	96.5	31,028	19.70	0.023	598
		5	200,000	FIRQUEST	5.338	0.017	0.046	0.861	96.7	66,095	17.14	0.013	786
		10	100,000	FIRQUEST	5.338	0.017	0.045	0.840	95.5	55,093	23.97	0.012	892
		1	1,000,000	FQUEST	5.337	0.017	0.048	0.902	95.7	60,577	20.22	0.015	599
0.995	5.909	5	10,000	FIRQUEST	5.905	0.091	0.268	4.540	95.6	3,634	14.89	0.114	400
		10	5,000	FIRQUEST	5.906	0.091	0.269	4.556	95.0	3,692	16.35	0.118	200
		1	50,000	FQUEST	5.905	0.092	0.284	4.813	95.0	3,827	15.01	0.132	590
		5	20,000	FIRQUEST	5.907	0.064	0.183	3.102	95.0	7,069	15.42	0.068	701
		10	10,000	FIRQUEST	5.910	0.063	0.186	3.140	96.2	6,704	18.53	0.075	400
		1	100,000	FQUEST	5.907	0.064	0.192	3.253	96.0	7,114	16.62	0.086	595
		5	40,000	FIRQUEST	5.911	0.046	0.130	2.200	95.6	13,685	16.21	0.052	770
		10	20,000	FIRQUEST	5.909	0.044	0.128	2.158	95.6	12,376	20.47	0.046	750
		1	200,000	FQUEST	5.909	0.045	0.134	2.260	95.6	13,310	18.24	0.054	595
		5	100,000	FIRQUEST	5.911	0.028	0.079	1.330	96.3	33,821	16.60	0.022	770
		10	50,000	FIRQUEST	5.910	0.029	0.079	1.337	94.8	28,609	23.07	0.026	876
		1	500,000	FQUEST	5.909	0.029	0.081	1.377	96.9	30,934	19.67	0.026	597
		5	200,000	FIRQUEST	5.910	0.020	0.056	0.954	96.7	66,135	17.10	0.017	770
		10	100,000	FIRQUEST	5.910	0.020	0.054	0.911	95.7	56,055	23.40	0.014	876
		1	1,000,000	FQUEST	5.909	0.021	0.058	0.987	95.4	61,451	19.82	0.021	597

Figure 6.3: Plots for the average 95% CI relative precision and estimated coverage probability for the AR(1) process from Tables 6.4–6.6.

Table 6.7: Experimental results for FIRQUEST with $R = 5, 10$ and FQUEST with regard to point and 95% CI estimation of y_p for the ARTOP process in Section 6.4.2 for $p \in \{0.3, 0.5, 0.7\}$ based on 1,000 independent replications.

p	y_p	R	Repl. Size	Method	Point Est.	Avg. |Bias|	Avg. 95% CI HL	Avg. 95% CI rel. prec. (%)	Avg. 95% CI cov. (%)	$\overline{m}$	$\overline{b}$	St. Dev. HL	Avg. Trunc. Point
0.3	1.185	5	10,000	FIRQUEST	1.190	0.022	0.099	8.336	97.7	4,563	10.86	0.058	400
		10	5,000	FIRQUEST	1.200	0.026	0.098	8.136	95.7	4,757	10.18	0.057	200
		1	50,000	FQUEST	1.188	0.021	0.103	8.648	98.0	4,719	10.77	0.061	739
		5	20,000	FIRQUEST	1.187	0.016	0.059	4.990	97.5	8,643	11.78	0.033	796
		10	10,000	FIRQUEST	1.189	0.016	0.059	4.918	97.2	9,102	11.11	0.033	400
		1	100,000	FQUEST	1.187	0.016	0.062	5.208	97.3	8,989	11.78	0.035	871
		5	40,000	FIRQUEST	1.186	0.011	0.037	3.079	96.2	15,619	13.69	0.016	1,337
		10	20,000	FIRQUEST	1.186	0.011	0.037	3.098	96.7	16,893	12.83	0.019	800
		1	200,000	FQUEST	1.186	0.011	0.038	3.225	97.1	16,710	13.36	0.019	885
		5	100,000	FIRQUEST	1.186	0.007	0.021	1.729	96.2	36,538	15.21	0.008	1,437
		10	50,000	FIRQUEST	1.186	0.006	0.021	1.764	96.7	36,199	16.71	0.009	1,613
		1	500,000	FQUEST	1.186	0.007	0.021	1.812	96.8	35,771	16.70	0.008	887
		5	200,000	FIRQUEST	1.185	0.005	0.014	1.190	96.0	69,758	16.08	0.005	1,437
		10	100,000	FIRQUEST	1.185	0.005	0.014	1.165	97.2	64,989	19.65	0.005	1,617
		1	1,000,000	FQUEST	1.185	0.005	0.015	1.240	97.5	67,890	17.75	0.006	888
0.5	1.391	5	10,000	FIRQUEST	1.400	0.040	0.168	11.954	96.8	4,471	11.19	0.105	400
		10	5,000	FIRQUEST	1.420	0.048	0.171	12.054	95.6	4,730	10.30	0.104	200
		1	50,000	FQUEST	1.395	0.039	0.176	12.589	97.1	4,619	11.14	0.112	766
		5	20,000	FIRQUEST	1.393	0.029	0.100	7.172	95.9	8,258	12.59	0.056	797
		10	10,000	FIRQUEST	1.398	0.029	0.105	7.488	96.7	8,758	11.95	0.064	400
		1	100,000	FQUEST	1.394	0.029	0.107	7.669	96.4	8,759	12.28	0.060	914
		5	40,000	FIRQUEST	1.393	0.020	0.065	4.684	96.5	15,182	14.16	0.032	1,369
		10	20,000	FIRQUEST	1.393	0.020	0.065	4.661	96.4	15,947	14.11	0.034	800
		1	200,000	FQUEST	1.392	0.020	0.067	4.837	96.4	16,144	14.11	0.033	927
		5	100,000	FIRQUEST	1.392	0.013	0.037	2.677	96.5	35,521	15.65	0.015	1,485
		10	50,000	FIRQUEST	1.392	0.012	0.037	2.675	96.4	33,672	18.45	0.016	1,668
		1	500,000	FQUEST	1.392	0.012	0.039	2.795	96.1	35,563	16.76	0.016	930
		5	200,000	FIRQUEST	1.391	0.009	0.026	1.841	95.6	69,876	16.08	0.009	1,485
		10	100,000	FIRQUEST	1.392	0.009	0.025	1.767	94.9	61,967	20.99	0.009	1,676
		1	1,000,000	FQUEST	1.391	0.009	0.026	1.880	97.1	65,144	18.53	0.009	931
0.7	1.774	5	10,000	FIRQUEST	1.790	0.078	0.318	17.690	96.3	4,460	11.23	0.218	400
		10	5,000	FIRQUEST	1.834	0.093	0.333	18.072	95.6	4,714	10.37	0.216	200
		1	50,000	FQUEST	1.780	0.073	0.330	18.460	97.5	4,648	11.00	0.223	786
		5	20,000	FIRQUEST	1.777	0.055	0.190	10.671	96.2	8,310	12.49	0.112	798
		10	10,000	FIRQUEST	1.787	0.055	0.201	11.215	95.9	8,913	11.65	0.123	400
		1	100,000	FQUEST	1.779	0.054	0.206	11.529	96.2	8,740	12.33	0.126	970
		5	40,000	FIRQUEST	1.778	0.038	0.122	6.877	96.0	15,105	14.20	0.062	1,418
		10	20,000	FIRQUEST	1.777	0.037	0.126	7.078	96.0	15,941	14.15	0.069	800
		1	200,000	FQUEST	1.776	0.038	0.129	7.246	96.0	16,006	14.19	0.067	995
		5	100,000	FIRQUEST	1.776	0.025	0.071	3.998	96.6	35,378	15.74	0.030	1,574
		10	50,000	FIRQUEST	1.776	0.023	0.070	3.962	95.8	34,423	18.04	0.030	1,759
		1	500,000	FQUEST	1.776	0.023	0.074	4.137	96.7	35,868	16.55	0.030	997
		5	200,000	FIRQUEST	1.775	0.017	0.049	2.764	95.5	69,485	16.11	0.018	1,574
		10	100,000	FIRQUEST	1.775	0.017	0.047	2.670	95.1	60,516	21.30	0.019	1,768
		1	1,000,000	FQUEST	1.774	0.016	0.050	2.792	96.9	65,123	18.63	0.018	998

Table 6.8: Experimental results for FIRQUEST with $R = 5, 10$ and FQUEST with regard to point and 95% CI estimation of y_p for the ARTOP process in Section 6.4.2 for $p \in \{0.9, 0.95\}$ based on 1,000 independent replications.

p	y_p	R	Repl. Size	Method	Point Est.	Avg. |Bias|	Avg. 95% CI HL	Avg. 95% CI rel. prec. (%)	Avg. 95% CI cov. (%)	$\overline{m}$	$\overline{b}$	St. Dev. HL	Avg. Trunc. Point
0.9	2.994	5	10,000	FIRQUEST	3.035	0.233	1.096	35.703	95.8	4,607	10.68	0.818	400
		10	5,000	FIRQUEST	3.186	0.283	1.215	37.708	97.9	4,754	10.19	0.865	200
		1	50,000	FQUEST	3.014	0.223	1.145	37.296	97.2	4,811	10.38	0.895	793
		5	20,000	FIRQUEST	3.003	0.159	0.643	21.309	95.0	8,865	11.34	0.432	798
		10	10,000	FIRQUEST	3.029	0.161	0.688	22.575	97.3	9,248	10.80	0.463	400
		1	100,000	FQUEST	3.006	0.157	0.675	22.313	95.6	9,321	11.06	0.447	1,019
		5	40,000	FIRQUEST	3.003	0.113	0.399	13.266	95.5	16,546	12.61	0.241	1,461
		10	20,000	FIRQUEST	3.002	0.110	0.416	13.800	96.2	17,475	12.11	0.265	800
		1	200,000	FQUEST	2.997	0.114	0.425	14.112	96.5	17,331	12.61	0.279	1,068
		5	100,000	FIRQUEST	2.996	0.072	0.225	7.509	95.6	37,553	14.69	0.122	1,663
		10	50,000	FIRQUEST	2.998	0.070	0.223	7.427	95.6	36,935	15.96	0.115	1,834
		1	500,000	FQUEST	2.997	0.069	0.233	7.777	96.6	38,526	15.09	0.127	1,070
		5	200,000	FIRQUEST	2.994	0.051	0.150	4.999	95.3	72,575	15.48	0.070	1,662
		10	100,000	FIRQUEST	2.996	0.051	0.146	4.874	94.9	67,614	18.83	0.067	1,840
		1	1,000,000	FQUEST	2.994	0.049	0.152	5.070	96.4	68,538	17.65	0.062	1,072
0.95	4.164	5	10,000	FIRQUEST	4.238	0.436	2.376	54.768	95.6	4,719	10.28	1.910	400
		10	5,000	FIRQUEST	4.527	0.534	2.852	61.925	98.3	4,778	10.09	2.801	200
		1	50,000	FQUEST	4.205	0.428	2.393	55.444	95.7	4,854	10.25	2.041	758
		5	20,000	FIRQUEST	4.181	0.298	1.374	32.494	95.0	9,119	10.87	1.026	797
		10	10,000	FIRQUEST	4.230	0.304	1.478	34.673	97.7	9,462	10.30	1.211	400
		1	100,000	FQUEST	4.184	0.290	1.410	33.363	95.7	9,574	10.59	1.045	933
		5	40,000	FIRQUEST	4.182	0.209	0.795	18.943	95.3	17,204	11.95	0.532	1,422
		10	20,000	FIRQUEST	4.180	0.209	0.836	19.887	96.3	18,274	11.10	0.577	800
		1	200,000	FQUEST	4.168	0.209	0.878	20.878	96.7	18,261	11.57	0.629	973
		5	100,000	FIRQUEST	4.168	0.129	0.434	10.383	96.0	39,396	13.90	0.252	1,599
		10	50,000	FIRQUEST	4.171	0.131	0.439	10.497	95.1	41,014	13.56	0.248	1,805
		1	500,000	FQUEST	4.168	0.126	0.461	11.044	95.9	41,294	13.72	0.274	975
		5	200,000	FIRQUEST	4.165	0.092	0.288	6.904	96.6	75,774	14.67	0.147	1,599
		10	100,000	FIRQUEST	4.169	0.094	0.282	6.764	95.7	73,393	16.76	0.143	1,806
		1	1,000,000	FQUEST	4.164	0.089	0.290	6.954	96.6	73,992	15.87	0.134	977

Table 6.9: Experimental results for FIRQUEST with $R = 5, 10$ and FQUEST with regard to point and 95% CI estimation of y_p for the ARTOP process in Section 6.4.2 for $p \in \{0.99, 0.995\}$ based on 1,000 independent replications.

p	y_p	R	Repl. Size	Method	Point Est.	Avg. |Bias|	Avg. 95% CI HL	Avg. 95% CI rel. prec. (%)	Avg. 95% CI cov. (%)	$\overline{m}$	$\overline{b}$	St. Dev. HL	Avg. Trunc. Point
0.99	8.962	5	10,000	FIRQUEST	9.228	1.727	9.780	99.251	94.3	4,785	10.05	9.508	400
		10	5,000	FIRQUEST	10.364	2.130	14.209	125.688	98.6	4,798	10.01	38.849	200
		1	50,000	FQUEST	9.112	1.741	9.631	98.912	93.2	4,926	10.02	9.566	662
		5	20,000	FIRQUEST	9.028	1.185	7.220	76.522	93.5	9,464	10.25	9.022	774
		10	10,000	FIRQUEST	9.217	1.249	8.184	84.632	96.0	9,576	10.05	10.628	400
		1	100,000	FQUEST	9.011	1.136	7.257	77.372	94.0	9,869	10.10	6.566	736
		5	40,000	FIRQUEST	9.012	0.833	4.611	50.140	94.9	18,831	10.52	4.135	1,185
		10	20,000	FIRQUEST	9.010	0.842	4.791	51.942	96.6	19,096	10.12	4.282	795
		1	200,000	FQUEST	8.955	0.810	4.802	52.634	95.8	19,568	10.31	4.039	747
		5	100,000	FIRQUEST	8.961	0.512	2.213	24.476	96.2	46,361	11.08	1.574	1,259
		10	50,000	FIRQUEST	8.973	0.531	2.282	25.170	95.2	47,310	10.52	1.761	1,478
		1	500,000	FQUEST	8.958	0.500	2.365	26.132	96.3	47,897	10.73	1.682	747
		5	200,000	FIRQUEST	8.958	0.367	1.353	15.046	95.4	86,517	12.39	0.875	1,259
		10	100,000	FIRQUEST	8.971	0.382	1.338	14.852	94.2	90,880	11.72	0.905	1,478
		1	1,000,000	FQUEST	8.955	0.365	1.443	16.050	96.0	89,404	12.04	0.929	749
0.995	12.466	5	10,000	FIRQUEST	12.988	3.203	14.894	104.159	90.9	4,790	10.03	15.082	400
		10	5,000	FIRQUEST	14.996	3.951	22.108	128.260	97.1	4,798	10.01	66.808	200
		1	50,000	FQUEST	12.751	3.197	14.953	106.177	90.7	4,938	10.01	15.592	601
		5	20,000	FIRQUEST	12.616	2.183	12.692	92.756	91.4	9,547	10.14	18.828	736
		10	10,000	FIRQUEST	12.922	2.297	15.387	109.043	94.2	9,590	10.02	37.440	400
		1	100,000	FQUEST	12.552	2.080	12.777	95.946	93.1	9,910	10.04	12.796	635
		5	40,000	FIRQUEST	12.538	1.520	9.377	72.060	95.1	19,116	10.33	10.405	988
		10	20,000	FIRQUEST	12.571	1.538	10.158	76.665	95.7	19,152	10.08	13.238	777
		1	200,000	FQUEST	12.451	1.485	9.518	73.741	95.5	19,647	10.25	8.832	643
		5	100,000	FIRQUEST	12.465	0.941	4.808	37.962	94.7	47,766	10.59	3.841	1,025
		10	50,000	FIRQUEST	12.484	0.967	4.955	39.117	96.0	48,103	10.29	3.972	1,240
		1	500,000	FQUEST	12.451	0.919	4.963	39.181	96.6	48,821	10.40	3.804	643
		5	200,000	FIRQUEST	12.465	0.671	2.861	22.806	96.0	91,560	11.43	2.010	1,025
		10	100,000	FIRQUEST	12.488	0.703	2.813	22.324	94.2	95,221	10.75	2.117	1,240
		1	1,000,000	FQUEST	12.444	0.664	3.041	24.255	96.1	94,027	11.10	2.170	644

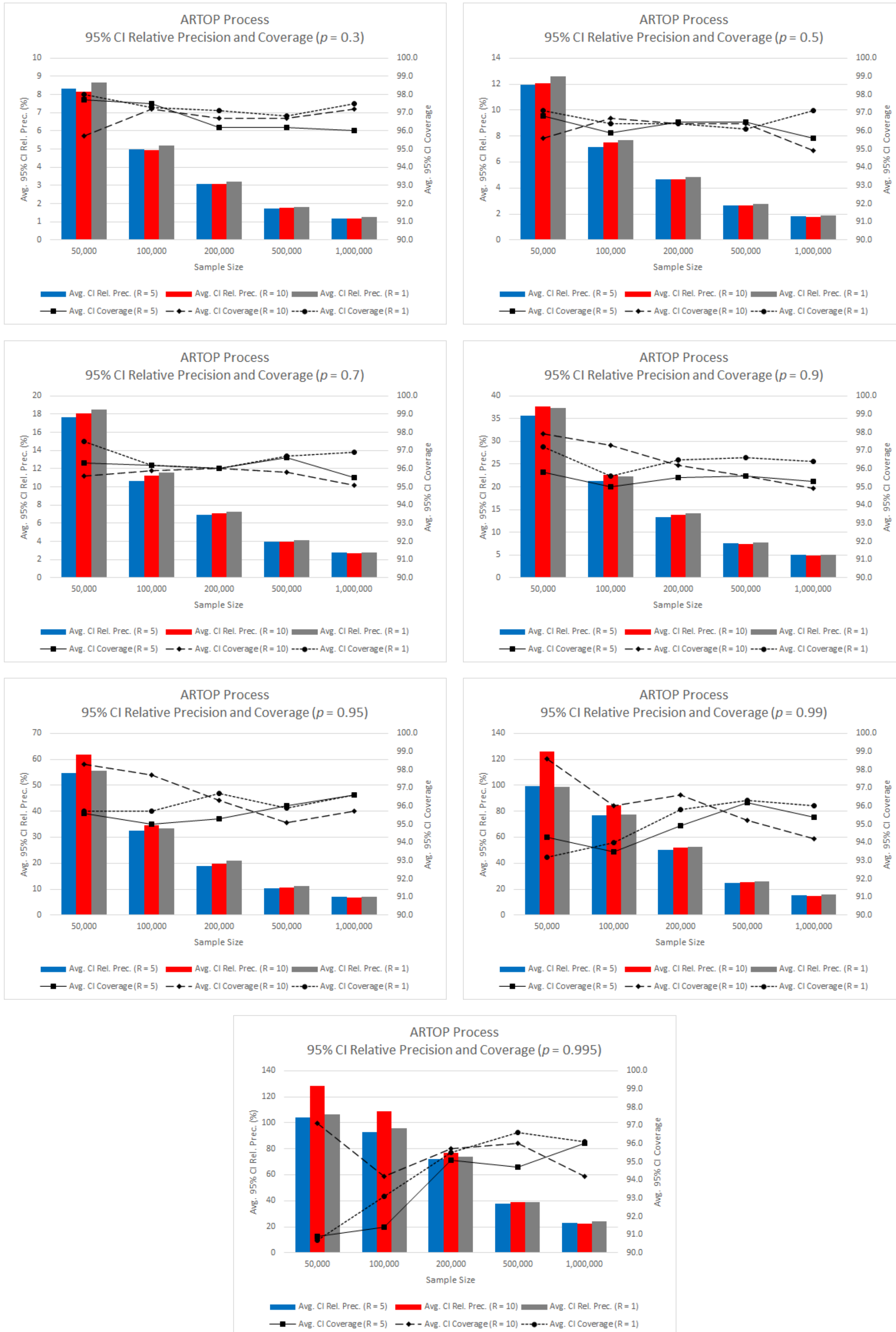

Figure 6.4: Plots for the average 95% CI relative precision and estimated coverage probability for the ARTOP process from Tables 6.7–6.9.

Table 6.10: Experimental results for FIRQUEST with $R = 5, 10$ and FQUEST with regard to point and 95% CI estimation of y_p for the waiting-time process in an M/M/1 system described in Section 6.4.3 with traffic intensity 0.9 initialized in the empty-and-idle state for $p \in \{0.3, 0.5, 0.7\}$ based on 1,000 independent replications.

p	y_p	R	Repl. Size	Method	Point Est.	Avg. |Bias|	Avg. 95% CI HL	Avg. 95% CI rel. prec. (%)	Avg. 95% CI cov. (%)	$\overline{m}$	$\overline{b}$	St. Dev. HL	Avg. Trunc. Point
0.3	2.513	5	10,000	FIRQUEST	2.513	0.179	0.929	36.618	97.9	4,561	10.83	0.661	400
		10	5,000	FIRQUEST	2.496	0.182	0.903	35.965	97.3	4,733	10.30	0.615	200
		1	50,000	FQUEST	2.513	0.184	0.990	39.027	97.8	4,756	10.62	0.679	685
		5	20,000	FIRQUEST	2.514	0.134	0.559	22.184	97.5	8,702	11.74	0.338	744
		10	10,000	FIRQUEST	2.509	0.133	0.543	21.562	96.4	9,152	11.00	0.351	400
		1	100,000	FQUEST	2.519	0.127	0.593	23.461	98.4	9,174	11.40	0.384	710
		5	40,000	FIRQUEST	2.517	0.091	0.326	12.930	97.0	16,157	13.30	0.173	891
		10	20,000	FIRQUEST	2.512	0.095	0.326	12.956	95.1	16,863	12.90	0.179	779
		1	200,000	FQUEST	2.519	0.090	0.341	13.538	97.3	16,963	13.03	0.177	712
		5	100,000	FIRQUEST	2.517	0.059	0.179	7.116	96.1	37,295	14.95	0.077	892
		10	50,000	FIRQUEST	2.514	0.061	0.182	7.216	94.9	37,488	16.21	0.089	1,009
		1	500,000	FQUEST	2.517	0.056	0.187	7.429	97.9	36,012	16.46	0.078	715
		5	200,000	FIRQUEST	2.517	0.042	0.120	4.754	94.6	68,906	16.39	0.044	892
		10	100,000	FIRQUEST	2.513	0.041	0.119	4.723	95.6	65,785	19.56	0.047	1,010
		1	1,000,000	FQUEST	2.515	0.040	0.126	4.995	96.8	68,110	17.62	0.045	716
0.5	5.878	5	10,000	FIRQUEST	5.879	0.370	1.858	31.286	96.9	4,542	10.92	1.364	400
		10	5,000	FIRQUEST	5.840	0.369	1.822	30.976	95.5	4,697	10.45	1.292	200
		1	50,000	FQUEST	5.873	0.373	2.000	33.724	97.0	4,734	10.70	1.545	723
		5	20,000	FIRQUEST	5.876	0.279	1.126	19.071	97.2	8,649	11.81	0.701	758
		10	10,000	FIRQUEST	5.869	0.275	1.108	18.810	95.8	9,103	11.13	0.738	400
		1	100,000	FQUEST	5.888	0.262	1.196	20.249	97.8	9,046	11.66	0.796	767
		5	40,000	FIRQUEST	5.886	0.191	0.671	11.377	96.5	16,125	13.28	0.388	955
		10	20,000	FIRQUEST	5.874	0.195	0.686	11.645	94.6	16,861	12.89	0.409	787
		1	200,000	FQUEST	5.891	0.186	0.708	12.021	96.7	17,098	12.93	0.399	768
		5	100,000	FIRQUEST	5.883	0.122	0.373	6.330	95.7	37,548	14.78	0.176	957
		10	50,000	FIRQUEST	5.880	0.126	0.375	6.371	94.8	37,382	16.27	0.186	1,094
		1	500,000	FQUEST	5.886	0.115	0.385	6.537	97.4	36,681	16.05	0.159	771
		5	200,000	FIRQUEST	5.885	0.085	0.249	4.238	95.2	70,601	15.89	0.093	957
		10	100,000	FIRQUEST	5.877	0.085	0.244	4.145	95.7	66,135	19.34	0.100	1,093
		1	1,000,000	FQUEST	5.880	0.083	0.261	4.434	97.2	68,127	17.70	0.105	771
0.7	10.986	5	10,000	FIRQUEST	10.983	0.700	3.555	31.935	96.0	4,482	11.17	3.005	400
		10	5,000	FIRQUEST	10.906	0.705	3.451	31.285	94.8	4,696	10.46	2.778	200
		1	50,000	FQUEST	10.975	0.710	3.842	34.454	96.4	4,719	10.76	3.158	725
		5	20,000	FIRQUEST	10.982	0.522	2.142	19.404	96.5	8,621	11.92	1.451	760
		10	10,000	FIRQUEST	10.969	0.521	2.103	19.062	94.9	8,995	11.42	1.519	400
		1	100,000	FQUEST	11.005	0.493	2.348	21.208	97.5	9,111	11.54	1.674	781
		5	40,000	FIRQUEST	10.999	0.365	1.296	11.748	95.9	16,284	13.17	0.788	969
		10	20,000	FIRQUEST	10.977	0.368	1.302	11.817	95.1	17,004	12.72	0.817	788
		1	200,000	FQUEST	11.008	0.348	1.364	12.368	96.9	17,373	12.68	0.796	783
		5	100,000	FIRQUEST	10.990	0.227	0.720	6.546	95.9	37,751	14.74	0.364	972
		10	50,000	FIRQUEST	10.988	0.236	0.711	6.467	94.9	37,858	16.03	0.357	1,116
		1	500,000	FQUEST	11.000	0.223	0.738	6.702	96.8	37,900	15.40	0.310	785
		5	200,000	FIRQUEST	10.996	0.162	0.479	4.355	95.4	72,044	15.52	0.186	972
		10	100,000	FIRQUEST	10.982	0.161	0.473	4.301	95.3	68,577	18.62	0.207	1,116
		1	1,000,000	FQUEST	10.987	0.158	0.498	4.529	96.9	67,787	17.78	0.204	786

Table 6.11: Experimental results for FIRQUEST with $R = 5, 10$ and FQUEST with regard to point and 95% CI estimation of y_p for the waiting-time process in an M/M/1 system described in Section 6.4.3 with traffic intensity 0.9 initialized in the empty-and-idle state for $p \in \{0.9, 0.95\}$ based on 1,000 independent replications.

p	y_p	R	Repl. Size	Method	Point Est.	Avg. |Bias|	Avg. 95% CI HL	Avg. 95% CI rel. prec. (%)	Avg. 95% CI cov. (%)	$\overline{m}$	$\overline{b}$	St. Dev. HL	Avg. Trunc. Point
0.9	21.972	5	10,000	FIRQUEST	21.976	1.705	8.095	36.193	94.4	4,538	10.96	6.303	400
		10	5,000	FIRQUEST	21.775	1.715	7.780	35.149	93.4	4,706	10.40	5.923	200
		1	50,000	FQUEST	21.960	1.754	8.723	38.759	93.4	4,770	10.62	7.228	704
		5	20,000	FIRQUEST	21.983	1.265	5.844	26.233	95.4	8,893	11.37	4.853	752
		10	10,000	FIRQUEST	21.930	1.253	5.700	25.655	94.3	9,198	10.94	4.680	400
		1	100,000	FQUEST	22.055	1.244	6.154	27.549	94.9	9,317	11.14	5.050	746
		5	40,000	FIRQUEST	22.008	0.902	3.493	15.764	94.9	17,318	12.09	2.700	922
		10	20,000	FIRQUEST	21.940	0.888	3.465	15.675	94.7	17,708	11.85	2.642	782
		1	200,000	FQUEST	22.023	0.861	3.630	16.380	95.2	17,900	11.99	2.696	747
		5	100,000	FIRQUEST	21.982	0.550	1.835	8.335	95.6	40,422	13.54	1.067	924
		10	50,000	FIRQUEST	21.969	0.571	1.856	8.438	94.1	41,260	13.93	1.111	1,049
		1	500,000	FQUEST	22.003	0.546	1.911	8.671	95.6	40,548	14.11	1.079	749
		5	200,000	FIRQUEST	21.993	0.389	1.183	5.378	94.9	75,094	14.93	0.558	924
		10	100,000	FIRQUEST	21.956	0.391	1.194	5.430	94.4	76,012	16.24	0.616	1,049
		1	1,000,000	FQUEST	21.974	0.385	1.275	5.798	96.6	76,453	15.44	0.625	750
0.95	28.904	5	10,000	FIRQUEST	28.941	2.640	10.559	35.648	92.6	4,648	10.55	7.562	400
		10	5,000	FIRQUEST	28.596	2.604	10.201	34.914	91.6	4,756	10.19	7.195	200
		1	50,000	FQUEST	28.983	2.748	10.974	36.721	91.4	4,820	10.42	8.472	679
		5	20,000	FIRQUEST	28.945	1.960	8.470	28.819	92.6	9,063	11.05	6.444	743
		10	10,000	FIRQUEST	28.852	1.957	8.465	28.892	93.4	9,382	10.51	6.250	400
		1	100,000	FQUEST	29.101	1.990	9.035	30.387	93.7	9,532	10.73	7.416	708
		5	40,000	FIRQUEST	28.964	1.380	6.028	20.616	94.2	17,958	11.51	4.972	890
		10	20,000	FIRQUEST	28.858	1.374	5.889	20.169	94.5	18,335	11.01	4.846	777
		1	200,000	FQUEST	29.001	1.373	6.128	20.903	94.2	18,607	11.27	4.922	709
		5	100,000	FIRQUEST	28.935	0.844	3.084	10.612	95.3	42,070	12.81	2.124	891
		10	50,000	FIRQUEST	28.898	0.881	3.007	10.383	94.1	43,657	12.57	1.920	1,006
		1	500,000	FQUEST	28.960	0.838	3.218	11.088	95.1	43,262	12.79	2.156	710
		5	200,000	FIRQUEST	28.940	0.596	1.896	6.546	95.6	79,224	13.99	0.963	891
		10	100,000	FIRQUEST	28.884	0.597	1.905	6.584	95.0	81,555	14.49	1.095	1,006
		1	1,000,000	FQUEST	28.907	0.589	2.029	7.013	96.4	81,317	14.06	1.154	711

Table 6.12: Experimental results for FIRQUEST with $R = 5, 10$ and FQUEST with regard to point and 95% CI estimation of y_p for the waiting-time process in an M/M/1 system described in Section 6.4.3 with traffic intensity 0.9 initialized in the empty-and-idle state for $p \in \{0.99, 0.995\}$ based on 1,000 independent replications.

p	y_p	R	Repl. Size	Method	Point Est.	Avg. |Bias|	Avg. 95% CI HL	Avg. 95% CI rel. prec. (%)	Avg. 95% CI cov. (%)	$\overline{m}$	$\overline{b}$	St. Dev. HL	Avg. Trunc. Point
0.99	44.998	5	10,000	FIRQUEST	44.754	6.177	16.022	33.680	82.1	4,752	10.16	11.484	400
		10	5,000	FIRQUEST	43.949	5.964	15.870	34.198	81.2	4,793	10.03	10.863	200
		1	50,000	FQUEST	44.758	6.372	18.781	38.650	84.8	4,917	10.05	16.746	664
		5	20,000	FIRQUEST	45.273	4.835	13.825	29.135	87.3	9,536	10.18	10.004	735
		10	10,000	FIRQUEST	44.895	4.693	13.920	29.800	89.3	9,562	10.08	9.440	400
		1	100,000	FQUEST	45.449	4.984	15.029	31.230	87.8	9,804	10.23	12.652	681
		5	40,000	FIRQUEST	45.171	3.349	12.026	25.964	90.8	18,953	10.56	8.621	858
		10	20,000	FIRQUEST	44.920	3.314	11.360	24.650	90.8	19,074	10.16	8.079	773
		1	200,000	FQUEST	45.146	3.416	12.160	26.256	92.0	19,530	10.35	8.686	681
		5	100,000	FIRQUEST	45.116	2.139	9.051	19.812	92.8	46,531	11.13	6.797	858
		10	50,000	FIRQUEST	44.950	2.138	8.900	19.577	94.2	47,671	10.63	6.387	969
		1	500,000	FQUEST	45.070	2.047	9.202	20.146	94.4	47,371	10.98	7.018	682
		5	200,000	FIRQUEST	45.083	1.484	6.206	13.669	94.5	90,607	11.66	4.806	858
		10	100,000	FIRQUEST	44.989	1.509	6.102	13.448	94.0	93,956	11.18	4.702	969
		1	1,000,000	FQUEST	44.979	1.434	6.584	14.521	95.3	91,417	11.71	5.326	683
0.995	51.930	5	10,000	FIRQUEST	50.551	7.994	18.986	35.024	74.4	4,772	10.10	13.130	400
		10	5,000	FIRQUEST	49.752	7.694	18.894	35.679	74.6	4,795	10.02	12.514	200
		1	50,000	FQUEST	50.464	8.036	23.078	41.694	78.5	4,929	10.02	20.676	655
		5	20,000	FIRQUEST	51.786	6.474	16.423	29.853	81.5	9,557	10.14	11.804	731
		10	10,000	FIRQUEST	51.491	6.351	16.684	30.708	82.5	9,581	10.04	11.323	400
		1	100,000	FQUEST	52.074	6.747	19.200	33.926	83.1	9,858	10.13	17.841	671
		5	40,000	FIRQUEST	52.213	4.830	14.505	26.688	88.1	19,212	10.31	10.331	847
		10	20,000	FIRQUEST	51.798	4.784	13.709	25.415	87.5	19,191	10.04	9.830	771
		1	200,000	FQUEST	52.047	4.807	15.102	27.659	87.6	19,660	10.22	12.290	671
		5	100,000	FIRQUEST	52.131	3.096	11.299	21.299	91.6	47,864	10.61	8.028	848
		10	50,000	FIRQUEST	51.875	3.043	11.231	21.294	92.7	48,353	10.30	7.607	961
		1	500,000	FQUEST	52.034	2.998	11.756	22.166	93.2	48,608	10.45	8.496	671
		5	200,000	FIRQUEST	52.067	2.129	8.816	16.760	93.3	93,409	11.10	6.607	848
		10	100,000	FIRQUEST	51.924	2.178	8.758	16.654	92.8	95,976	10.66	6.494	961
		1	1,000,000	FQUEST	51.888	2.064	9.270	17.654	94.2	95,448	10.87	7.230	672

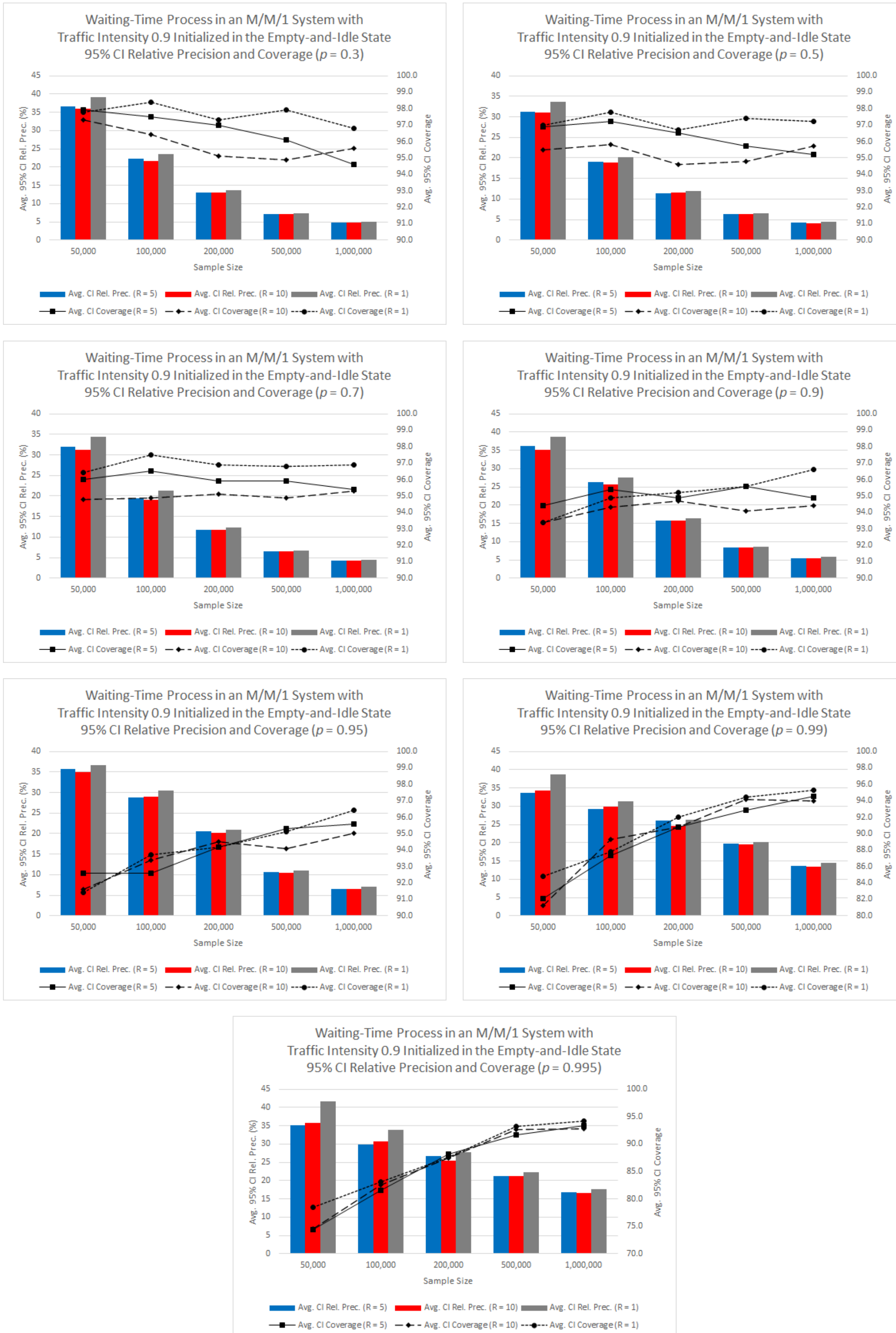

Figure 6.5: Plots for the average 95% CI relative precision and estimated coverage probability for the M/M/1 waiting-time process from Tables 6.10–6.12.

Table 6.13: Experimental results for FIRQUEST with $R = 5, 10$ and FQUEST with regard to point and 95% CI estimation of y_p for the waiting-time process in an M/M/1 system described in Section 6.4.3 with traffic intensity 0.9 initialized with 113 customers for $p \in \{0.3, 0.5, 0.7\}$ based on 1,000 independent replications.

p	y_p	R	Repl. Size	Method	Point Est.	Avg. |Bias|	Avg. 95% CI HL	Avg. 95% CI rel. prec. (%)	Avg. 95% CI cov. (%)	$\overline{m}$	$\overline{b}$	St. Dev. HL	Avg. Trunc. Point
0.3	2.513	5	10,000	FIRQUEST	2.767	0.297	1.352	48.348	98.0	4,789	10.04	1.012	400
		10	5,000	FIRQUEST	3.296	0.784	1.727	51.706	66.9	4,800	10.00	2.028	200
		1	50,000	FQUEST	2.541	0.186	1.045	40.769	97.4	4,809	10.42	0.711	765
		5	20,000	FIRQUEST	2.561	0.143	0.612	23.822	98.7	9,157	10.81	0.358	795
		10	10,000	FIRQUEST	2.761	0.262	0.671	24.291	88.0	9,595	10.01	0.456	400
		1	100,000	FQUEST	2.533	0.129	0.599	23.530	98.0	9,316	11.08	0.371	1,031
		5	40,000	FIRQUEST	2.520	0.094	0.333	13.177	97.1	16,319	12.84	0.174	1,482
		10	20,000	FIRQUEST	2.559	0.103	0.348	13.576	95.8	18,400	10.90	0.178	800
		1	200,000	FQUEST	2.525	0.091	0.357	14.130	97.8	17,276	12.72	0.190	1,088
		5	100,000	FIRQUEST	2.518	0.058	0.181	7.201	96.7	36,876	14.96	0.080	1,736
		10	50,000	FIRQUEST	2.514	0.060	0.183	7.283	96.2	36,610	16.14	0.086	1,899
		1	500,000	FQUEST	2.520	0.056	0.188	7.442	97.6	37,209	15.80	0.072	1,091
		5	200,000	FIRQUEST	2.518	0.041	0.120	4.755	95.0	69,238	16.24	0.043	1,736
		10	100,000	FIRQUEST	2.513	0.041	0.118	4.709	96.9	65,135	19.41	0.047	1,918
		1	1,000,000	FQUEST	2.516	0.040	0.128	5.076	96.8	68,747	17.42	0.050	1,093
0.5	5.878	5	10,000	FIRQUEST	6.475	0.671	3.077	46.957	97.8	4,789	10.04	2.382	400
		10	5,000	FIRQUEST	7.791	1.913	4.278	53.933	64.7	4,800	10.00	4.171	200
		1	50,000	FQUEST	5.946	0.386	2.166	36.056	97.6	4,790	10.52	1.733	674
		5	20,000	FIRQUEST	5.993	0.301	1.261	20.926	97.5	9,094	10.95	0.773	782
		10	10,000	FIRQUEST	6.463	0.608	1.499	23.121	87.1	9,586	10.03	1.206	400
		1	100,000	FQUEST	5.925	0.263	1.211	20.350	98.0	9,252	11.22	0.785	755
		5	40,000	FIRQUEST	5.904	0.199	0.692	11.696	96.8	16,624	12.67	0.383	1,264
		10	20,000	FIRQUEST	5.984	0.218	0.747	12.459	95.0	18,329	10.99	0.401	798
		1	200,000	FQUEST	5.906	0.183	0.720	12.187	97.8	17,474	12.50	0.380	765
		5	100,000	FIRQUEST	5.891	0.120	0.375	6.358	95.9	37,444	14.71	0.175	1,359
		10	50,000	FIRQUEST	5.884	0.125	0.378	6.425	96.0	37,802	15.67	0.185	1,586
		1	500,000	FQUEST	5.894	0.114	0.387	6.569	97.2	37,968	15.36	0.157	768
		5	200,000	FIRQUEST	5.888	0.085	0.246	4.182	95.5	69,541	16.25	0.090	1,359
		10	100,000	FIRQUEST	5.880	0.084	0.243	4.125	96.5	66,740	19.20	0.093	1,591
		1	1,000,000	FQUEST	5.884	0.081	0.262	4.447	96.7	69,099	17.46	0.097	769
0.7	10.986	5	10,000	FIRQUEST	12.377	1.495	7.738	61.316	98.3	4,782	10.06	6.801	400
		10	5,000	FIRQUEST	15.936	4.950	12.719	77.947	64.6	4,800	10.00	10.831	200
		1	50,000	FQUEST	11.145	0.750	4.419	39.082	97.9	4,761	10.65	4.226	646
		5	20,000	FIRQUEST	11.272	0.599	2.598	22.910	97.6	9,168	10.83	1.745	751
		10	10,000	FIRQUEST	12.365	1.406	3.316	26.627	85.6	9,590	10.02	2.627	400
		1	100,000	FQUEST	11.090	0.508	2.391	21.410	97.3	9,231	11.30	1.748	666
		5	40,000	FIRQUEST	11.093	0.392	1.372	12.340	96.3	17,218	12.19	0.810	972
		10	20,000	FIRQUEST	11.242	0.445	1.542	13.682	96.2	18,343	11.01	0.928	783
		1	200,000	FQUEST	11.046	0.348	1.384	12.518	98.4	17,617	12.38	0.797	668
		5	100,000	FIRQUEST	11.031	0.232	0.740	6.703	96.3	39,629	13.95	0.370	985
		10	50,000	FIRQUEST	11.034	0.245	0.735	6.654	95.0	40,134	14.57	0.370	1,160
		1	500,000	FQUEST	11.017	0.220	0.746	6.765	96.7	37,801	15.39	0.335	671
		5	200,000	FIRQUEST	11.014	0.167	0.479	4.349	95.7	72,466	15.59	0.175	985
		10	100,000	FIRQUEST	11.006	0.160	0.480	4.361	96.2	70,874	17.81	0.221	1,160
		1	1,000,000	FQUEST	10.998	0.156	0.499	4.539	97.0	69,797	17.28	0.185	672

Table 6.14: Experimental results for FIRQUEST with $R = 5, 10$ and FQUEST with regard to point and 95% CI estimation of y_p for the waiting-time process in an M/M/1 system described in Section 6.4.3 with traffic intensity 0.9 initialized with 113 customers for $p \in \{0.9, 0.95\}$ based on 1,000 independent replications.

p	y_p	R	Repl. Size	Method	Point Est.	Avg. |Bias|	Avg. 95% CI HL	Avg. 95% CI rel. prec. (%)	Avg. 95% CI cov. (%)	$\overline{m}$	$\overline{b}$	St. Dev. HL	Avg. Trunc. Point
0.9	21.972	5	10,000	FIRQUEST	27.681	5.796	24.641	88.476	97.9	4,767	10.12	14.174	400
		10	5,000	FIRQUEST	49.091	27.119	29.493	61.648	28.1	4,800	10.00	13.585	200
		1	50,000	FQUEST	22.578	1.908	11.376	49.271	96.6	4,822	10.41	9.492	659
		5	20,000	FIRQUEST	23.074	1.685	8.905	37.912	97.6	9,272	10.68	7.526	722
		10	10,000	FIRQUEST	27.544	5.590	16.970	60.672	91.7	9,576	10.05	12.005	400
		1	100,000	FQUEST	22.342	1.258	6.885	30.346	97.0	9,408	10.97	6.174	675
		5	40,000	FIRQUEST	22.450	1.020	4.210	18.608	97.4	18,251	11.25	3.086	838
		10	20,000	FIRQUEST	22.920	1.273	4.836	20.881	95.6	18,645	10.67	3.896	765
		1	200,000	FQUEST	22.160	0.871	3.908	17.532	96.5	18,159	11.74	2.925	677
		5	100,000	FIRQUEST	22.154	0.585	1.968	8.857	96.9	42,035	12.93	1.141	840
		10	50,000	FIRQUEST	22.229	0.629	1.999	8.963	95.0	43,648	12.66	1.161	951
		1	500,000	FQUEST	22.061	0.545	1.951	8.826	96.8	41,262	13.81	1.159	679
		5	200,000	FIRQUEST	22.075	0.411	1.220	5.520	95.3	77,001	14.50	0.568	840
		10	100,000	FIRQUEST	22.081	0.405	1.264	5.718	94.8	79,998	14.95	0.660	951
		1	1,000,000	FQUEST	22.007	0.379	1.274	5.781	97.2	75,474	15.69	0.602	680
0.95	28.904	5	10,000	FIRQUEST	41.514	12.688	32.397	78.284	97.4	4,787	10.04	15.894	400
		10	5,000	FIRQUEST	74.284	45.380	32.671	44.360	9.0	4,800	10.00	11.401	200
		1	50,000	FQUEST	30.108	3.099	15.268	49.204	95.5	4,822	10.42	11.617	656
		5	20,000	FIRQUEST	31.122	2.982	15.207	47.875	98.6	9,392	10.44	11.336	715
		10	10,000	FIRQUEST	41.369	12.473	28.561	69.018	91.1	9,590	10.02	14.521	400
		1	100,000	FQUEST	29.606	2.053	11.057	36.538	96.5	9,612	10.60	9.494	676
		5	40,000	FIRQUEST	29.850	1.691	8.344	27.539	97.9	18,519	11.00	6.811	819
		10	20,000	FIRQUEST	30.765	2.283	10.352	33.015	97.8	18,966	10.29	8.686	762
		1	200,000	FQUEST	29.240	1.393	6.709	22.652	96.3	18,611	11.25	5.867	677
		5	100,000	FIRQUEST	29.261	0.936	3.409	11.595	95.9	43,859	12.11	2.213	821
		10	50,000	FIRQUEST	29.397	1.034	3.639	12.301	96.5	45,653	11.72	2.558	938
		1	500,000	FQUEST	29.045	0.857	3.302	11.314	96.3	44,391	12.30	2.285	678
		5	200,000	FIRQUEST	29.093	0.650	2.076	7.115	96.8	81,715	13.49	1.143	821
		10	100,000	FIRQUEST	29.126	0.666	2.137	7.320	95.3	85,221	13.58	1.204	938
		1	1,000,000	FQUEST	28.963	0.590	2.090	7.202	96.7	80,608	14.22	1.210	680

Table 6.15: Experimental results for FIRQUEST with $R = 5, 10$ and FQUEST with regard to point and 95% CI estimation of y_p for the waiting-time process in an M/M/1 system described in Section 6.4.3 with traffic intensity 0.9 initialized with 113 customers for $p \in \{0.99, 0.995\}$ based on 1,000 independent replications.

p	y_p	R	Repl. Size	Method	Point Est.	Avg. |Bias|	Avg. 95% CI HL	Avg. 95% CI rel. prec. (%)	Avg. 95% CI cov. (%)	$\overline{m}$	$\overline{b}$	St. Dev. HL	Avg. Trunc. Point
0.99	44.998	5	10,000	FIRQUEST	78.782	33.838	50.217	62.325	98.6	4,797	10.01	22.070	400
		10	5,000	FIRQUEST	109.519	64.521	43.525	39.691	15.1	4,800	10.00	12.100	200
		1	50,000	FQUEST	49.730	8.917	28.705	51.357	92.6	4,907	10.10	27.367	653
		5	20,000	FIRQUEST	54.081	10.484	26.921	47.362	96.9	9,543	10.17	17.559	714
		10	10,000	FIRQUEST	81.797	36.799	43.863	53.525	87.8	9,600	10.00	15.583	400
		1	100,000	FQUEST	47.619	5.882	20.448	40.031	93.9	9,821	10.21	18.106	668
		5	40,000	FIRQUEST	48.573	5.136	19.002	37.906	96.8	19,187	10.35	12.904	814
		10	20,000	FIRQUEST	52.715	8.362	25.087	46.359	98.1	19,193	10.05	14.906	758
		1	200,000	FQUEST	46.054	3.691	15.032	31.680	94.9	19,583	10.31	11.375	668
		5	100,000	FIRQUEST	46.297	2.562	11.808	25.115	96.8	47,275	10.84	9.010	815
		10	50,000	FIRQUEST	46.851	2.926	13.593	28.514	98.1	47,700	10.63	10.389	918
		1	500,000	FQUEST	45.416	2.164	10.379	22.538	95.8	47,266	10.98	8.282	669
		5	200,000	FIRQUEST	45.625	1.670	7.102	15.422	96.1	91,315	11.55	5.703	815
		10	100,000	FIRQUEST	45.877	1.813	8.102	17.452	97.3	94,238	11.12	6.608	918
		1	1,000,000	FQUEST	45.131	1.490	6.894	15.132	95.2	92,147	11.46	5.667	670
0.995	51.930	5	10,000	FIRQUEST	90.449	38.574	57.001	61.287	99.2	4,795	10.02	24.044	400
		10	5,000	FIRQUEST	118.537	66.607	46.624	39.190	27.2	4,800	10.00	13.890	200
		1	50,000	FQUEST	57.240	11.541	36.435	55.529	90.1	4,924	10.04	34.815	661
		5	20,000	FIRQUEST	64.778	14.849	32.805	47.347	96.9	9,579	10.11	21.596	710
		10	10,000	FIRQUEST	95.613	43.684	50.424	52.382	90.6	9,600	10.00	16.847	400
		1	100,000	FQUEST	55.654	8.615	27.125	43.841	91.4	9,880	10.09	26.090	676
		5	40,000	FIRQUEST	58.102	8.388	23.597	38.682	96.3	19,359	10.20	15.593	805
		10	20,000	FIRQUEST	64.230	13.139	30.533	45.537	98.4	19,175	10.07	18.194	758
		1	200,000	FQUEST	53.680	5.549	19.006	33.343	92.5	19,636	10.25	16.403	676
		5	100,000	FIRQUEST	54.210	3.996	15.940	28.776	95.9	48,100	10.54	10.947	805
		10	50,000	FIRQUEST	55.225	4.771	18.341	32.429	96.7	48,692	10.18	12.263	915
		1	500,000	FQUEST	52.644	3.186	13.465	25.022	95.2	48,511	10.49	10.124	676
		5	200,000	FIRQUEST	52.990	2.474	10.968	20.417	96.0	93,988	11.00	8.401	805
		10	100,000	FIRQUEST	53.450	2.747	12.415	22.841	97.5	97,111	10.44	9.315	915
		1	1,000,000	FQUEST	52.155	2.180	10.277	19.437	95.7	94,553	10.99	7.988	677

Figure 6.6: Plots for the average 95% CI relative precision and estimated coverage probability for the M/M/1 waiting-time process from Tables 6.13–6.15.

Table 6.16: Experimental results for FIRQUEST with $R = 5, 10$ and FQUEST with regard to point and 95% CI estimation of y_p for the waiting-time process in an M/M/1 system described in Section 6.4.3 with traffic intensity 0.8 initialized with 113 customers for $p \in \{0.3, 0.5, 0.7\}$ based on 1,000 independent replications.

p	y_p	R	Repl. Size	Method	Point Est.	Avg. |Bias|	Avg. 95% CI HL	Avg. 95% CI rel. prec. (%)	Avg. 95% CI cov. (%)	$\overline{m}$	$\overline{b}$	St. Dev. HL	Avg. Trunc. Point
0.3	0.668	5	10,000	FIRQUEST	0.682	0.046	0.188	27.559	99.4	4,371	11.68	0.085	400
		10	5,000	FIRQUEST	0.774	0.109	0.193	25.021	77.7	4,800	10.00	0.097	200
		1	50,000	FQUEST	0.667	0.044	0.160	24.030	97.3	4,098	13.49	0.080	1,002
		5	20,000	FIRQUEST	0.667	0.032	0.104	15.664	97.8	7,303	14.75	0.039	800
		10	10,000	FIRQUEST	0.682	0.034	0.117	17.107	98.3	8,695	12.22	0.050	400
		1	100,000	FQUEST	0.669	0.030	0.105	15.774	96.8	7,431	15.45	0.051	1,950
		5	40,000	FIRQUEST	0.668	0.022	0.069	10.267	96.9	13,560	16.01	0.024	1,600
		10	20,000	FIRQUEST	0.667	0.022	0.069	10.404	96.2	12,698	19.62	0.026	800
		1	200,000	FQUEST	0.669	0.021	0.071	10.582	97.3	13,665	17.37	0.031	2,460
		5	100,000	FIRQUEST	0.668	0.014	0.041	6.077	96.5	33,564	16.51	0.012	2,023
		10	50,000	FIRQUEST	0.668	0.015	0.042	6.276	97.0	29,164	21.88	0.016	2,000
		1	500,000	FQUEST	0.669	0.013	0.042	6.348	97.1	31,526	19.25	0.015	2,461
		5	200,000	FIRQUEST	0.668	0.010	0.028	4.185	96.0	65,874	17.11	0.008	2,023
		10	100,000	FIRQUEST	0.668	0.010	0.028	4.137	97.2	56,421	23.05	0.008	2,048
		1	1,000,000	FQUEST	0.668	0.010	0.030	4.429	96.9	62,711	19.48	0.009	2,463
0.5	2.350	5	10,000	FIRQUEST	2.382	0.097	0.398	16.666	99.1	4,346	11.80	0.182	400
		10	5,000	FIRQUEST	2.599	0.253	0.434	16.706	77.0	4,800	10.00	0.226	200
		1	50,000	FQUEST	2.348	0.090	0.335	14.223	96.9	4,099	13.37	0.180	986
		5	20,000	FIRQUEST	2.349	0.065	0.221	9.431	97.9	7,311	14.70	0.098	800
		10	10,000	FIRQUEST	2.382	0.072	0.250	10.488	98.5	8,774	12.17	0.104	400
		1	100,000	FQUEST	2.352	0.062	0.215	9.149	96.9	7,388	15.52	0.100	1,897
		5	40,000	FIRQUEST	2.351	0.045	0.144	6.123	97.6	13,852	15.66	0.055	1,600
		10	20,000	FIRQUEST	2.349	0.045	0.145	6.173	96.7	12,926	19.19	0.056	800
		1	200,000	FQUEST	2.352	0.044	0.143	6.070	97.3	13,807	17.20	0.059	2,336
		5	100,000	FIRQUEST	2.351	0.028	0.083	3.548	96.1	33,779	16.40	0.026	2,016
		10	50,000	FIRQUEST	2.350	0.029	0.086	3.652	96.4	28,512	22.23	0.032	2,000
		1	500,000	FQUEST	2.352	0.028	0.085	3.626	97.2	31,159	19.32	0.026	2,338
		5	200,000	FIRQUEST	2.351	0.020	0.058	2.472	95.3	67,054	16.74	0.019	2,016
		10	100,000	FIRQUEST	2.350	0.020	0.057	2.405	96.7	56,460	22.98	0.016	2,037
		1	1,000,000	FQUEST	2.350	0.020	0.060	2.545	96.6	61,917	19.72	0.019	2,340
0.7	4.904	5	10,000	FIRQUEST	4.980	0.192	0.820	16.420	99.6	4,395	11.54	0.395	400
		10	5,000	FIRQUEST	5.504	0.601	1.002	18.142	77.0	4,800	10.00	0.540	200
		1	50,000	FQUEST	4.905	0.173	0.658	13.368	97.1	4,170	13.08	0.401	880
		5	20,000	FIRQUEST	4.903	0.125	0.426	8.679	97.5	7,428	14.40	0.203	800
		10	10,000	FIRQUEST	4.980	0.144	0.536	10.746	99.3	8,846	11.90	0.223	400
		1	100,000	FQUEST	4.910	0.120	0.418	8.497	97.2	7,548	15.13	0.208	1,553
		5	40,000	FIRQUEST	4.905	0.087	0.278	5.664	96.5	14,228	15.26	0.114	1,594
		10	20,000	FIRQUEST	4.903	0.087	0.281	5.719	97.1	13,365	18.33	0.112	800
		1	200,000	FQUEST	4.909	0.083	0.276	5.623	97.9	14,031	16.93	0.120	1,881
		5	100,000	FIRQUEST	4.905	0.054	0.160	3.263	96.0	33,258	16.61	0.050	1,998
		10	50,000	FIRQUEST	4.904	0.056	0.163	3.314	96.6	29,496	21.51	0.059	2,000
		1	500,000	FQUEST	4.908	0.052	0.166	3.378	97.7	32,139	18.77	0.063	1,883
		5	200,000	FIRQUEST	4.905	0.038	0.111	2.268	96.4	66,172	17.08	0.034	1,998
		10	100,000	FIRQUEST	4.903	0.037	0.109	2.226	97.1	55,880	23.28	0.033	2,024
		1	1,000,000	FQUEST	4.905	0.038	0.113	2.304	97.8	62,625	19.47	0.033	1,885

Table 6.17: Experimental results for FIRQUEST with $R = 5, 10$ and FQUEST with regard to point and 95% CI estimation of y_p for the waiting-time process in an M/M/1 system described in Section 6.4.3 with traffic intensity 0.8 initialized with 113 customers for $p \in \{0.9, 0.95\}$ based on 1,000 independent replications.

p	y_p	R	Repl. Size	Method	Point Est.	Avg. |Bias|	Avg. 95% CI HL	Avg. 95% CI rel. prec. (%)	Avg. 95% CI cov. (%)	$\overline{m}$	$\overline{b}$	St. Dev. HL	Avg. Trunc. Point
0.9	10.397	5	10,000	FIRQUEST	10.686	0.515	2.893	26.833	99.7	4,561	10.90	1.946	400
		10	5,000	FIRQUEST	13.034	2.637	7.368	55.534	94.9	4,800	10.00	6.121	200
		1	50,000	FQUEST	10.431	0.416	1.784	17.005	96.5	4,437	11.95	1.289	628
		5	20,000	FIRQUEST	10.413	0.305	1.100	10.545	96.7	7,920	13.43	0.632	748
		10	10,000	FIRQUEST	10.689	0.410	1.830	17.063	99.4	9,265	10.81	0.775	400
		1	100,000	FQUEST	10.428	0.288	1.108	10.592	96.8	8,369	13.37	0.667	667
		5	40,000	FIRQUEST	10.413	0.216	0.688	6.604	97.2	14,982	14.59	0.335	1,026
		10	20,000	FIRQUEST	10.404	0.211	0.727	6.983	97.4	15,155	15.43	0.377	784
		1	200,000	FQUEST	10.415	0.206	0.702	6.730	96.7	15,466	15.04	0.367	673
		5	100,000	FIRQUEST	10.402	0.134	0.400	3.840	96.6	35,642	15.66	0.157	1,069
		10	50,000	FIRQUEST	10.403	0.136	0.402	3.865	95.4	33,498	19.06	0.166	1,308
		1	500,000	FQUEST	10.408	0.129	0.404	3.880	96.6	34,019	17.68	0.162	676
		5	200,000	FIRQUEST	10.401	0.094	0.270	2.592	96.4	67,840	16.60	0.090	1,069
		10	100,000	FIRQUEST	10.396	0.091	0.268	2.576	95.2	60,517	21.65	0.101	1,309
		1	1,000,000	FQUEST	10.400	0.094	0.277	2.661	96.7	64,571	18.84	0.099	677
0.95	13.863	5	10,000	FIRQUEST	14.459	0.896	6.274	42.491	99.7	4,591	10.78	5.570	400
		10	5,000	FIRQUEST	21.374	7.511	23.386	109.054	99.0	4,800	10.00	11.289	200
		1	50,000	FQUEST	13.922	0.638	3.064	21.803	96.6	4,585	11.37	2.302	604
		5	20,000	FIRQUEST	13.905	0.469	1.925	13.787	96.7	8,331	12.55	1.257	710
		10	10,000	FIRQUEST	14.449	0.730	3.861	26.501	99.8	9,382	10.51	2.358	400
		1	100,000	FQUEST	13.914	0.442	1.916	13.691	97.0	8,806	12.35	1.306	612
		5	40,000	FIRQUEST	13.900	0.339	1.160	8.329	96.6	15,878	13.70	0.636	817
		10	20,000	FIRQUEST	13.878	0.322	1.197	8.607	97.3	16,276	13.81	0.640	758
		1	200,000	FQUEST	13.886	0.321	1.140	8.186	96.8	16,442	13.82	0.650	613
		5	100,000	FIRQUEST	13.872	0.206	0.642	4.623	96.9	37,476	14.84	0.273	821
		10	50,000	FIRQUEST	13.873	0.210	0.647	4.663	96.2	36,666	16.80	0.275	946
		1	500,000	FQUEST	13.879	0.199	0.641	4.615	96.4	35,872	16.70	0.293	616
		5	200,000	FIRQUEST	13.870	0.147	0.429	3.089	96.3	70,860	15.93	0.154	821
		10	100,000	FIRQUEST	13.860	0.142	0.422	3.040	95.8	65,013	20.05	0.160	947
		1	1,000,000	FQUEST	13.868	0.146	0.435	3.137	96.3	66,674	18.22	0.163	617

Table 6.18: Experimental results for FIRQUEST with $R = 5, 10$ and FQUEST with regard to point and 95% CI estimation of y_p for the waiting-time process in an M/M/1 system described in Section 6.4.3 with traffic intensity 0.8 initialized with 113 customers for $p \in \{0.99, 0.995\}$ based on 1,000 independent replications.

p	y_p	R	Repl. Size	Method	Point Est.	Avg. |Bias|	Avg. 95% CI HL	Avg. 95% CI rel. prec. (%)	Avg. 95% CI cov. (%)	$\overline{m}$	$\overline{b}$	St. Dev. HL	Avg. Trunc. Point
0.99	21.910	5	10,000	FIRQUEST	24.926	3.549	17.094	65.854	99.8	4,725	10.27	11.185	400
		10	5,000	FIRQUEST	62.465	40.555	42.929	69.427	77.8	4,800	10.00	10.533	200
		1	50,000	FQUEST	22.107	1.607	6.700	29.648	94.9	4,827	10.43	4.864	602
		5	20,000	FIRQUEST	22.031	1.127	5.389	24.149	95.9	9,164	10.90	4.028	698
		10	10,000	FIRQUEST	24.799	3.082	18.010	70.652	99.8	9,535	10.15	11.089	400
		1	100,000	FQUEST	22.061	1.129	5.151	23.043	95.4	9,537	10.74	3.801	607
		5	40,000	FIRQUEST	22.016	0.803	3.539	15.917	96.2	17,768	11.70	2.787	768
		10	20,000	FIRQUEST	21.956	0.789	3.850	17.422	98.0	18,477	10.88	2.946	747
		1	200,000	FQUEST	21.972	0.792	3.546	16.019	95.7	18,488	11.45	2.708	608
		5	100,000	FIRQUEST	21.929	0.501	1.853	8.415	96.4	41,867	12.99	1.163	769
		10	50,000	FIRQUEST	21.927	0.504	1.916	8.709	97.0	43,943	12.52	1.096	874
		1	500,000	FQUEST	21.949	0.498	1.794	8.152	96.1	42,812	12.93	1.103	610
		5	200,000	FIRQUEST	21.919	0.351	1.190	5.418	96.5	78,797	14.08	0.590	768
		10	100,000	FIRQUEST	21.905	0.353	1.222	5.571	96.5	81,167	14.62	0.663	874
		1	1,000,000	FQUEST	21.918	0.344	1.209	5.509	96.3	79,373	14.65	0.670	611
0.995	25.376	5	10,000	FIRQUEST	31.443	6.725	21.137	63.422	99.4	4,757	10.15	13.590	400
		10	5,000	FIRQUEST	75.286	49.911	49.519	66.322	81.5	4,800	10.00	10.998	200
		1	50,000	FQUEST	25.630	2.317	8.272	31.061	93.3	4,888	10.20	6.109	599
		5	20,000	FIRQUEST	25.586	1.646	6.812	26.044	95.4	9,391	10.46	5.023	697
		10	10,000	FIRQUEST	31.580	6.422	23.184	70.931	99.8	9,581	10.04	12.622	400
		1	100,000	FQUEST	25.581	1.614	6.503	24.989	93.7	9,711	10.43	4.507	603
		5	40,000	FIRQUEST	25.525	1.145	5.181	20.006	96.1	18,616	10.89	3.782	762
		10	20,000	FIRQUEST	25.441	1.134	5.370	20.925	97.5	18,753	10.58	3.664	749
		1	200,000	FQUEST	25.470	1.143	5.137	19.937	95.2	19,066	10.80	3.833	604
		5	100,000	FIRQUEST	25.400	0.717	2.970	11.620	96.4	44,177	12.03	2.175	762
		10	50,000	FIRQUEST	25.392	0.722	3.145	12.312	97.5	46,404	11.25	2.200	870
		1	500,000	FQUEST	25.435	0.714	2.946	11.532	95.4	45,271	11.88	2.147	605
		5	200,000	FIRQUEST	25.388	0.497	1.864	7.322	97.1	83,979	13.01	1.147	762
		10	100,000	FIRQUEST	25.368	0.502	1.930	7.592	96.7	86,937	13.02	1.148	870
		1	1,000,000	FQUEST	25.388	0.492	1.895	7.441	95.6	85,392	13.04	1.212	607

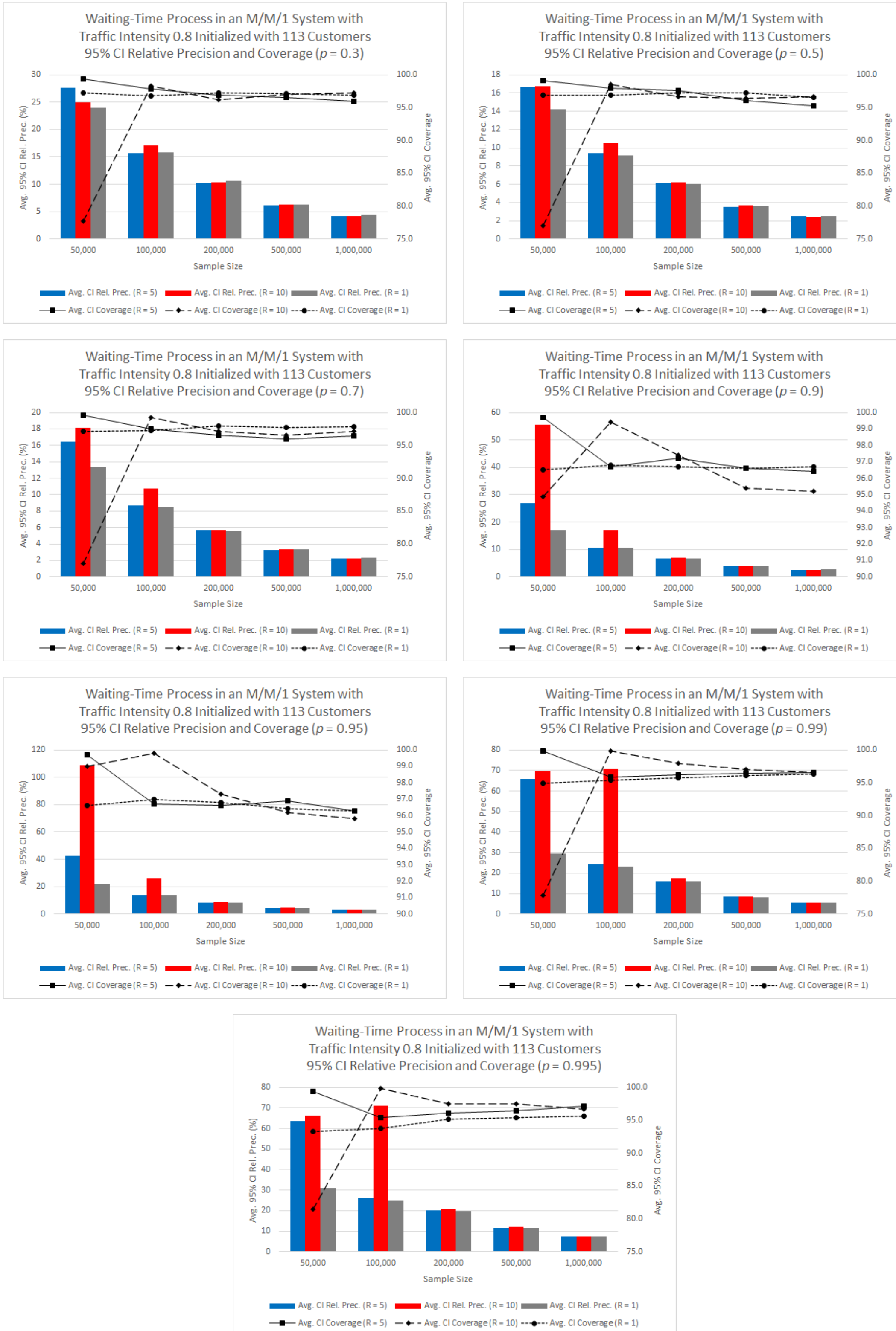

Figure 6.7: Plots for the average 95% CI relative precision and estimated coverage probability for the M/M/1 waiting-time process from Tables 6.16–6.18.

Table 6.19: Experimental results for FIRQUEST with $R = 5, 10$ and FQUEST with regard to point and 95% CI estimation of y_p for the M/H_2/1 waiting-time process in Section 6.4.4 for $p \in \{0.3, 0.5, 0.7\}$ based on 1,000 independent replications.

p	y_p	R	Repl. Size	Method	Point Est.	Avg. |Bias|	Avg. 95% CI HL	Avg. 95% CI rel. prec. (%)	Avg. 95% CI cov. (%)	$\overline{m}$	$\overline{b}$	St. Dev. HL	Avg. Trunc. Point
0.3	0.669	5	10,000	FIRQUEST	0.672	0.088	0.571	84.594	99.3	4,713	10.30	0.360	400
		10	5,000	FIRQUEST	0.669	0.090	0.522	78.030	98.6	4,781	10.08	0.326	200
		1	50,000	FQUEST	0.675	0.086	0.616	90.834	98.8	4,861	10.26	0.387	615
		5	20,000	FIRQUEST	0.669	0.064	0.308	45.761	97.5	9,140	10.90	0.188	710
		10	10,000	FIRQUEST	0.669	0.063	0.292	43.573	97.5	9,408	10.40	0.179	400
		1	100,000	FQUEST	0.676	0.062	0.334	49.245	99.0	9,591	10.61	0.203	620
		5	40,000	FIRQUEST	0.669	0.043	0.169	25.280	97.0	17,074	12.29	0.087	797
		10	20,000	FIRQUEST	0.669	0.045	0.172	25.703	96.3	18,108	11.24	0.095	757
		1	200,000	FQUEST	0.674	0.043	0.188	27.839	98.0	17,994	11.87	0.105	622
		5	100,000	FIRQUEST	0.671	0.027	0.088	13.124	96.6	38,579	14.34	0.038	797
		10	50,000	FIRQUEST	0.668	0.028	0.088	13.211	95.1	39,977	14.61	0.041	912
		1	500,000	FQUEST	0.671	0.027	0.096	14.382	97.8	39,649	14.52	0.043	625
		5	200,000	FIRQUEST	0.671	0.019	0.058	8.672	96.3	71,167	15.78	0.021	797
		10	100,000	FIRQUEST	0.669	0.019	0.057	8.573	95.6	71,499	17.66	0.022	913
		1	1,000,000	FQUEST	0.670	0.019	0.062	9.311	97.6	71,368	16.79	0.026	626
0.5	3.847	5	10,000	FIRQUEST	3.842	0.326	1.375	35.681	96.7	4,394	11.49	0.885	400
		10	5,000	FIRQUEST	3.831	0.334	1.330	34.691	96.7	4,631	10.77	0.834	200
		1	50,000	FQUEST	3.854	0.316	1.472	38.055	97.9	4,621	11.17	0.918	666
		5	20,000	FIRQUEST	3.840	0.239	0.839	21.825	96.6	8,259	12.61	0.490	734
		10	10,000	FIRQUEST	3.842	0.231	0.816	21.202	96.0	8,786	11.98	0.467	400
		1	100,000	FQUEST	3.865	0.228	0.901	23.229	97.7	8,807	12.20	0.517	682
		5	40,000	FIRQUEST	3.846	0.162	0.515	13.396	96.1	15,217	14.35	0.240	866
		10	20,000	FIRQUEST	3.845	0.166	0.532	13.811	94.6	15,628	14.63	0.261	775
		1	200,000	FQUEST	3.864	0.161	0.557	14.412	97.0	15,773	14.51	0.275	685
		5	100,000	FIRQUEST	3.854	0.101	0.299	7.750	95.6	35,706	15.65	0.105	867
		10	50,000	FIRQUEST	3.845	0.103	0.301	7.821	95.8	34,314	18.27	0.124	987
		1	500,000	FQUEST	3.853	0.100	0.316	8.206	97.0	35,000	17.17	0.127	687
		5	200,000	FIRQUEST	3.855	0.071	0.205	5.311	95.8	68,154	16.55	0.064	867
		10	100,000	FIRQUEST	3.849	0.072	0.199	5.171	95.5	61,921	20.92	0.064	987
		1	1,000,000	FQUEST	3.851	0.072	0.217	5.631	97.0	65,682	18.50	0.080	687
0.7	9.606	5	10,000	FIRQUEST	9.574	0.626	2.610	27.016	95.8	4,358	11.63	1.910	400
		10	5,000	FIRQUEST	9.570	0.626	2.512	26.081	95.9	4,582	11.00	1.739	200
		1	50,000	FQUEST	9.603	0.601	2.762	28.587	96.3	4,563	11.42	1.874	680
		5	20,000	FIRQUEST	9.581	0.454	1.633	16.972	95.2	8,237	12.71	1.027	742
		10	10,000	FIRQUEST	9.592	0.441	1.571	16.315	95.2	8,723	12.20	0.992	400
		1	100,000	FQUEST	9.631	0.432	1.742	18.024	97.3	8,639	12.56	1.077	710
		5	40,000	FIRQUEST	9.596	0.310	0.985	10.237	95.7	15,341	14.16	0.487	906
		10	20,000	FIRQUEST	9.599	0.312	1.025	10.655	95.5	15,851	14.37	0.548	779
		1	200,000	FQUEST	9.634	0.306	1.058	10.957	96.8	15,751	14.52	0.536	712
		5	100,000	FIRQUEST	9.615	0.195	0.590	6.132	96.2	36,012	15.57	0.255	907
		10	50,000	FIRQUEST	9.602	0.197	0.577	6.006	95.6	34,043	18.66	0.249	1,033
		1	500,000	FQUEST	9.618	0.193	0.609	6.328	97.6	35,249	16.95	0.247	714
		5	200,000	FIRQUEST	9.618	0.135	0.401	4.173	96.5	69,330	16.26	0.143	907
		10	100,000	FIRQUEST	9.608	0.138	0.391	4.074	95.7	62,868	20.78	0.143	1,033
		1	1,000,000	FQUEST	9.613	0.139	0.411	4.278	97.1	66,149	18.30	0.142	715

Table 6.20: Experimental results for FIRQUEST with $R = 5, 10$ and FQUEST with regard to point and 95% CI estimation of y_p for the M/H_2/1 waiting-time process in Section 6.4.4 for $p \in \{0.9, 0.95\}$ based on 1,000 independent replications.

p	y_p	R	Repl. Size	Method	Point Est.	Avg. |Bias|	Avg. 95% CI HL	Avg. 95% CI rel. prec. (%)	Avg. 95% CI cov. (%)	$\overline{m}$	$\overline{b}$	St. Dev. HL	Avg. Trunc. Point
0.9	22.011	5	10,000	FIRQUEST	21.983	1.546	6.928	30.985	93.1	4,473	11.21	5.762	400
		10	5,000	FIRQUEST	21.962	1.513	6.707	30.117	93.7	4,647	10.70	5.401	200
		1	50,000	FQUEST	22.013	1.468	7.123	32.021	95.2	4,674	10.96	5.626	663
		5	20,000	FIRQUEST	21.981	1.088	4.322	19.543	94.6	8,579	12.03	3.290	738
		10	10,000	FIRQUEST	22.001	1.068	4.237	19.082	94.2	8,944	11.57	3.237	400
		1	100,000	FQUEST	22.039	1.044	4.575	20.623	95.6	8,934	12.01	3.526	689
		5	40,000	FIRQUEST	21.998	0.755	2.628	11.915	95.1	16,316	13.13	1.660	881
		10	20,000	FIRQUEST	22.003	0.724	2.662	12.069	94.3	17,174	12.52	1.735	775
		1	200,000	FQUEST	22.041	0.734	2.750	12.434	96.4	16,754	13.31	1.739	690
		5	100,000	FIRQUEST	22.016	0.470	1.445	6.558	95.0	37,491	14.83	0.742	883
		10	50,000	FIRQUEST	22.007	0.471	1.436	6.514	96.2	38,174	15.79	0.728	1,002
		1	500,000	FQUEST	22.019	0.469	1.496	6.788	95.4	37,574	15.69	0.740	693
		5	200,000	FIRQUEST	22.032	0.328	1.012	4.591	95.7	71,536	15.78	0.472	883
		10	100,000	FIRQUEST	22.013	0.339	0.979	4.445	95.8	69,595	18.32	0.443	1,002
		1	1,000,000	FQUEST	22.025	0.341	1.012	4.595	96.3	70,256	16.94	0.431	693
0.95	29.837	5	10,000	FIRQUEST	29.857	2.415	9.948	32.638	92.2	4,556	10.90	7.875	400
		10	5,000	FIRQUEST	29.771	2.314	9.950	32.873	92.5	4,684	10.52	7.405	200
		1	50,000	FQUEST	29.873	2.266	10.388	34.251	94.2	4,776	10.60	7.812	651
		5	20,000	FIRQUEST	29.846	1.677	7.010	23.210	92.5	8,783	11.60	5.639	731
		10	10,000	FIRQUEST	29.825	1.669	7.095	23.486	93.8	9,207	10.92	5.552	400
		1	100,000	FQUEST	29.900	1.630	7.716	25.467	94.7	9,268	11.27	6.178	667
		5	40,000	FIRQUEST	29.855	1.153	4.441	14.779	94.0	17,147	12.28	3.302	849
		10	20,000	FIRQUEST	29.839	1.131	4.540	15.138	94.7	17,667	11.90	3.491	770
		1	200,000	FQUEST	29.880	1.143	4.609	15.310	95.7	17,764	12.16	3.464	669
		5	100,000	FIRQUEST	29.855	0.729	2.335	7.808	95.0	39,813	13.83	1.300	850
		10	50,000	FIRQUEST	29.846	0.718	2.329	7.785	95.3	41,001	14.18	1.384	971
		1	500,000	FQUEST	29.844	0.726	2.468	8.252	95.6	40,734	14.13	1.410	670
		5	200,000	FIRQUEST	29.870	0.509	1.594	5.332	95.9	74,146	15.17	0.816	850
		10	100,000	FIRQUEST	29.843	0.530	1.546	5.176	94.6	75,905	16.27	0.815	971
		1	1,000,000	FQUEST	29.860	0.520	1.663	5.568	95.7	73,636	16.10	0.867	672

Table 6.21: Experimental results for FIRQUEST with $R = 5, 10$ and FQUEST with regard to point and 95% CI estimation of y_p for the M/H_2/1 waiting-time process in Section 6.4.4 for $p \in \{0.99, 0.995\}$ based on 1,000 independent replications.

p	y_p	R	Repl. Size	Method	Point Est.	Avg. |Bias|	Avg. 95% CI HL	Avg. 95% CI rel. prec. (%)	Avg. 95% CI cov. (%)	$\overline{m}$	$\overline{b}$	St. Dev. HL	Avg. Trunc. Point
0.99	48.010	5	10,000	FIRQUEST	48.192	5.718	16.313	32.238	85.0	4,703	10.33	11.885	400
		10	5,000	FIRQUEST	47.781	5.365	15.938	32.080	87.4	4,786	10.06	10.813	200
		1	50,000	FQUEST	48.090	5.432	17.728	35.163	88.7	4,909	10.09	13.143	644
		5	20,000	FIRQUEST	48.147	4.053	13.452	27.198	90.0	9,370	10.47	9.394	726
		10	10,000	FIRQUEST	48.001	3.838	13.836	28.150	91.9	9,524	10.18	9.301	400
		1	100,000	FQUEST	48.178	3.934	14.617	29.619	91.4	9,718	10.39	10.276	653
		5	40,000	FIRQUEST	48.109	2.794	10.735	21.975	91.5	18,658	10.83	7.982	831
		10	20,000	FIRQUEST	48.015	2.713	11.099	22.771	92.1	18,862	10.44	8.015	766
		1	200,000	FQUEST	48.060	2.825	11.495	23.602	93.1	19,185	10.72	8.237	653
		5	100,000	FIRQUEST	48.024	1.805	7.060	14.560	93.2	44,866	11.75	5.506	832
		10	50,000	FIRQUEST	48.052	1.757	7.161	14.772	94.1	46,706	11.06	5.443	943
		1	500,000	FQUEST	48.029	1.792	7.613	15.726	93.5	46,407	11.38	5.892	654
		5	200,000	FIRQUEST	48.039	1.238	4.374	9.068	94.0	84,880	12.79	3.019	831
		10	100,000	FIRQUEST	48.025	1.246	4.625	9.600	94.3	90,432	12.02	3.288	944
		1	1,000,000	FQUEST	48.092	1.261	4.789	9.918	95.3	87,155	12.62	3.404	655
0.995	55.837	5	10,000	FIRQUEST	55.693	7.749	19.566	32.929	79.2	4,735	10.22	14.123	400
		10	5,000	FIRQUEST	55.272	7.397	19.298	32.931	80.5	4,794	10.03	13.323	200
		1	50,000	FQUEST	55.517	7.327	22.459	37.773	84.9	4,918	10.06	18.149	638
		5	20,000	FIRQUEST	55.923	5.748	16.226	27.842	86.7	9,465	10.30	11.241	724
		10	10,000	FIRQUEST	55.912	5.479	16.623	28.576	88.6	9,570	10.07	11.286	400
		1	100,000	FQUEST	55.962	5.523	17.943	30.710	88.4	9,811	10.23	13.492	645
		5	40,000	FIRQUEST	55.956	4.045	13.531	23.613	90.7	19,092	10.44	9.434	821
		10	20,000	FIRQUEST	55.861	3.945	13.613	23.766	90.4	19,060	10.19	9.485	764
		1	200,000	FQUEST	55.854	4.033	14.261	25.006	90.6	19,548	10.35	9.880	645
		5	100,000	FIRQUEST	55.873	2.602	10.118	17.878	92.5	46,933	10.99	7.444	821
		10	50,000	FIRQUEST	55.914	2.524	10.344	18.284	93.4	47,870	10.56	7.568	924
		1	500,000	FQUEST	55.893	2.592	10.788	19.104	93.8	47,938	10.70	7.801	645
		5	200,000	FIRQUEST	55.882	1.793	6.930	12.302	92.8	89,992	11.80	5.425	821
		10	100,000	FIRQUEST	55.862	1.788	7.264	12.918	93.0	94,255	11.11	5.409	924
		1	1,000,000	FQUEST	55.983	1.819	7.478	13.275	94.8	91,968	11.60	5.629	646

Figure 6.8: Plots for the average 95% CI relative precision and estimated coverage probability for the M/H_2/1 waiting-time process from Tables 6.19–6.21.

Table 6.22: Experimental results for FIRQUEST with $R = 5, 10$ and FQUEST with regard to point and 95% CI estimation of y_p for the M/M/1/LIFO waiting-time process in Section 6.4.5 for $p \in \{0.3, 0.5, 0.7\}$ based on 1,000 independent replications.

p	y_p	R	Repl. Size	Method	Point Est.	Avg. |Bias|	Avg. 95% CI HL	Avg. 95% CI rel. prec. (%)	Avg. 95% CI cov. (%)	$\overline{m}$	$\overline{b}$	St. Dev. HL	Avg. Trunc. Point
0.3	0.113	5	10,000	FIRQUEST	0.113	0.005	0.017	14.809	97.3	3,237	16.79	0.005	400
		10	5,000	FIRQUEST	0.112	0.005	0.016	14.112	97.0	2,779	22.79	0.004	200
		1	50,000	FQUEST	0.113	0.005	0.017	15.080	97.7	3147.6	19.13	0.005	615
		5	20,000	FIRQUEST	0.113	0.004	0.012	10.392	97.8	6,462	16.92	0.003	707
		10	10,000	FIRQUEST	0.113	0.004	0.011	10.035	96.9	5,291	24.02	0.003	400
		1	100,000	FQUEST	0.113	0.004	0.012	10.499	97.6	6142.6	19.62	0.004	622
		5	40,000	FIRQUEST	0.113	0.003	0.008	7.234	97.2	13,254	16.77	0.003	793
		10	20,000	FIRQUEST	0.113	0.003	0.008	7.065	95.7	10,334	24.67	0.002	759
		1	200,000	FQUEST	0.113	0.003	0.008	7.240	97.1	12389.9	19.63	0.002	621
		5	100,000	FIRQUEST	0.113	0.002	0.005	4.357	96.9	32,491	17.22	0.001	793
		10	50,000	FIRQUEST	0.113	0.002	0.005	4.275	95.7	27,697	23.86	0.001	918
		1	500,000	FQUEST	0.113	0.002	0.005	4.537	98.1	30088.6	20.25	0.002	622
		5	200,000	FIRQUEST	0.113	0.001	0.003	3.041	96.6	66,436	17.03	0.001	793
		10	100,000	FIRQUEST	0.113	0.001	0.003	2.983	95.6	54,758	23.97	0.001	918
		1	1,000,000	FQUEST	0.113	0.001	0.004	3.119	97.4	61709.4	19.75	0.001	622
0.5	0.469	5	10,000	FIRQUEST	0.469	0.009	0.030	6.389	97.4	3,311	16.42	0.009	400
		10	5,000	FIRQUEST	0.468	0.009	0.029	6.152	97.0	2,836	22.64	0.009	200
		1	50,000	FQUEST	0.468	0.009	0.030	6.493	97.9	3155.2	19.13	0.009	606
		5	20,000	FIRQUEST	0.469	0.007	0.021	4.447	97.6	6,410	16.99	0.006	712
		10	10,000	FIRQUEST	0.469	0.007	0.020	4.270	96.5	5,428	23.42	0.006	400
		1	100,000	FQUEST	0.469	0.006	0.021	4.416	97.5	6177.0	19.59	0.006	610
		5	40,000	FIRQUEST	0.469	0.005	0.014	3.030	96.8	13,317	16.70	0.004	800
		10	20,000	FIRQUEST	0.469	0.005	0.014	2.931	96.1	10,911	23.53	0.004	759
		1	200,000	FQUEST	0.469	0.005	0.014	3.071	97.3	12270.4	19.80	0.004	610
		5	100,000	FIRQUEST	0.469	0.003	0.009	1.844	97.1	33,356	16.89	0.003	800
		10	50,000	FIRQUEST	0.469	0.003	0.008	1.792	95.6	26,867	24.47	0.002	916
		1	500,000	FQUEST	0.469	0.003	0.009	1.943	98.2	30845.8	20.00	0.003	610
		5	200,000	FIRQUEST	0.469	0.002	0.006	1.291	95.8	66,306	17.00	0.002	800
		10	100,000	FIRQUEST	0.469	0.002	0.006	1.246	96.5	54,961	24.01	0.002	916
		1	1,000,000	FQUEST	0.469	0.002	0.006	1.314	97.4	59792.7	20.39	0.002	610
0.7	1.358	5	10,000	FIRQUEST	1.356	0.025	0.079	5.787	97.0	3,367	16.15	0.026	400
		10	5,000	FIRQUEST	1.356	0.025	0.077	5.662	96.9	3,115	20.08	0.026	200
		1	50,000	FQUEST	1.357	0.024	0.080	5.879	97.9	3277.0	18.33	0.025	610
		5	20,000	FIRQUEST	1.357	0.018	0.055	4.036	97.6	6,487	16.83	0.018	706
		10	10,000	FIRQUEST	1.357	0.018	0.052	3.840	96.7	5,810	21.92	0.016	400
		1	100,000	FQUEST	1.358	0.017	0.055	4.022	96.8	6398.5	18.99	0.017	612
		5	40,000	FIRQUEST	1.358	0.012	0.037	2.751	96.8	13,385	16.66	0.012	792
		10	20,000	FIRQUEST	1.357	0.013	0.037	2.691	97.1	11,131	23.18	0.011	756
		1	200,000	FQUEST	1.358	0.012	0.038	2.792	96.8	12646.2	19.22	0.012	613
		5	100,000	FIRQUEST	1.358	0.008	0.023	1.676	96.7	32,976	17.06	0.006	794
		10	50,000	FIRQUEST	1.358	0.008	0.022	1.652	96.2	27,527	23.94	0.007	910
		1	500,000	FQUEST	1.358	0.008	0.024	1.752	98.1	30382.5	20.25	0.008	613
		5	200,000	FIRQUEST	1.358	0.005	0.016	1.168	95.7	65,218	17.30	0.005	793
		10	100,000	FIRQUEST	1.358	0.005	0.016	1.146	97.5	56,352	23.36	0.005	910
		1	1,000,000	FQUEST	1.358	0.005	0.016	1.213	97.2	61895.4	19.66	0.005	613

Table 6.23: Experimental results for FIRQUEST with $R = 5, 10$ and FQUEST with regard to point and 95% CI estimation of y_p for the M/M/1/LIFO waiting-time process in Section 6.4.5 for $p \in \{0.9, 0.95\}$ based on 1,000 independent replications.

p	y_p	R	Repl. Size	Method	Point Est.	Avg. |Bias|	Avg. 95% CI HL	Avg. 95% CI rel. prec. (%)	Avg. 95% CI cov. (%)	$\overline{m}$	$\overline{b}$	St. Dev. HL	Avg. Trunc. Point
0.9	6.718	5	10,000	FIRQUEST	6.707	0.183	0.629	9.371	97.6	3,728	14.31	0.256	400
		10	5,000	FIRQUEST	6.707	0.181	0.623	9.291	97.0	3,875	14.92	0.270	200
		1	50,000	FQUEST	6.713	0.174	0.654	9.743	98.5	3859.9	14.84	0.269	593
		5	20,000	FIRQUEST	6.712	0.133	0.426	6.345	97.4	7,051	15.43	0.159	691
		10	10,000	FIRQUEST	6.710	0.132	0.411	6.123	97.3	6,774	18.17	0.159	400
		1	100,000	FQUEST	6.724	0.126	0.428	6.367	98.1	6923.6	17.16	0.167	598
		5	40,000	FIRQUEST	6.718	0.090	0.281	4.184	97.7	13,693	16.17	0.091	760
		10	20,000	FIRQUEST	6.714	0.095	0.281	4.189	96.4	12,010	21.29	0.096	745
		1	200,000	FQUEST	6.724	0.089	0.290	4.312	97.4	13213.9	18.47	0.105	598
		5	100,000	FIRQUEST	6.720	0.055	0.172	2.554	97.1	33,387	16.85	0.053	760
		10	50,000	FIRQUEST	6.717	0.058	0.168	2.501	96.6	28,792	22.98	0.059	873
		1	500,000	FQUEST	6.722	0.055	0.176	2.617	98.0	31028.6	19.54	0.056	600
		5	200,000	FIRQUEST	6.719	0.040	0.117	1.743	96.2	66,179	17.10	0.034	760
		10	100,000	FIRQUEST	6.717	0.039	0.114	1.703	96.4	55,663	23.56	0.033	873
		1	1,000,000	FQUEST	6.718	0.039	0.123	1.825	97.5	61392.5	19.88	0.040	600
0.95	14.405	5	10,000	FIRQUEST	14.384	0.489	1.820	12.637	96.9	3,953	13.34	0.807	400
		10	5,000	FIRQUEST	14.371	0.497	1.791	12.451	98.0	4,221	12.81	0.801	200
		1	50,000	FQUEST	14.395	0.481	1.931	13.403	99.0	4117.0	13.46	0.885	578
		5	20,000	FIRQUEST	14.393	0.364	1.203	8.361	98.2	7,251	14.92	0.475	697
		10	10,000	FIRQUEST	14.382	0.357	1.191	8.274	97.0	7,298	16.11	0.517	400
		1	100,000	FQUEST	14.420	0.350	1.252	8.670	98.2	7549.0	15.37	0.589	583
		5	40,000	FIRQUEST	14.410	0.250	0.783	5.428	98.0	13,978	15.86	0.248	776
		10	20,000	FIRQUEST	14.393	0.256	0.791	5.494	97.5	13,192	18.76	0.290	747
		1	200,000	FQUEST	14.426	0.246	0.826	5.728	97.4	13572.9	17.74	0.338	585
		5	100,000	FIRQUEST	14.410	0.157	0.478	3.319	96.8	34,180	16.47	0.158	776
		10	50,000	FIRQUEST	14.405	0.164	0.467	3.245	96.0	28,858	22.41	0.164	878
		1	500,000	FQUEST	14.416	0.152	0.498	3.452	97.9	32257.3	18.92	0.177	585
		5	200,000	FIRQUEST	14.410	0.108	0.334	2.316	96.6	67,972	16.62	0.119	775
		10	100,000	FIRQUEST	14.401	0.111	0.323	2.241	96.6	57,437	23.00	0.110	879
		1	1,000,000	FQUEST	14.408	0.111	0.339	2.354	96.6	60983.1	20.09	0.110	587

Table 6.24: Experimental results for FIRQUEST with $R = 5, 10$ and FQUEST with regard to point and 95% CI estimation of y_p for the M/M/1/LIFO waiting-time process in Section 6.4.5 for $p \in \{0.99, 0.995\}$ based on 1,000 independent replications.

p	y_p	R	Repl. Size	Method	Point Est.	Avg. |Bias|	Avg. 95% CI HL	Avg. 95% CI rel. prec. (%)	Avg. 95% CI cov. (%)	$\overline{m}$	$\overline{b}$	St. Dev. HL	Avg. Trunc. Point
0.99	49.582	5	10,000	FIRQUEST	49.543	2.767	12.837	25.767	98.2	4,452	11.28	7.317	400
		10	5,000	FIRQUEST	49.385	2.831	12.684	25.580	98.1	4,600	10.86	7.272	200
		1	50,000	FQUEST	49.500	2.685	13.716	27.565	98.6	4570.8	11.39	8.233	592
		5	20,000	FIRQUEST	49.538	1.997	7.939	15.986	98.1	8,211	12.78	4.037	705
		10	10,000	FIRQUEST	49.519	1.997	8.083	16.274	98.1	8,738	12.01	4.365	400
		1	100,000	FQUEST	49.680	1.905	8.358	16.783	98.6	8634.1	12.62	4.515	598
		5	40,000	FIRQUEST	49.628	1.416	5.019	10.107	98.5	15,462	14.10	2.293	789
		10	20,000	FIRQUEST	49.572	1.442	4.996	10.063	97.3	15,647	14.75	2.217	751
		1	200,000	FQUEST	49.656	1.347	5.186	10.438	98.1	16033.9	14.17	2.398	599
		5	100,000	FIRQUEST	49.600	0.873	2.789	5.621	97.7	36,334	15.46	0.959	791
		10	50,000	FIRQUEST	49.613	0.893	2.786	5.615	97.6	34,273	18.48	1.137	895
		1	500,000	FQUEST	49.588	0.859	2.895	5.834	97.4	35026.8	17.14	1.120	602
		5	200,000	FIRQUEST	49.600	0.607	1.895	3.818	96.2	68,912	16.36	0.605	791
		10	100,000	FIRQUEST	49.584	0.633	1.843	3.717	96.9	62,061	21.01	0.576	895
		1	1,000,000	FQUEST	49.567	0.607	2.003	4.039	97.8	66014.7	18.35	0.729	603
0.995	71.844	5	10,000	FIRQUEST	71.734	4.767	26.868	37.213	98.2	4,541	10.92	17.575	400
		10	5,000	FIRQUEST	71.506	4.989	26.025	36.201	98.2	4,692	10.50	16.847	200
		1	50,000	FQUEST	71.632	4.700	28.478	39.366	98.9	4771.9	10.65	19.253	586
		5	20,000	FIRQUEST	71.764	3.456	15.310	21.260	98.9	8,629	11.89	8.312	699
		10	10,000	FIRQUEST	71.776	3.525	15.445	21.445	98.4	9,086	11.18	8.613	400
		1	100,000	FQUEST	72.028	3.371	17.138	23.697	98.8	9088.6	11.67	10.416	595
		5	40,000	FIRQUEST	71.917	2.442	9.533	13.228	98.5	16,304	13.24	4.890	778
		10	20,000	FIRQUEST	71.814	2.557	9.366	13.001	98.0	16,887	12.90	4.640	748
		1	200,000	FQUEST	71.932	2.390	10.005	13.894	98.8	16935.7	13.08	5.264	597
		5	100,000	FIRQUEST	71.874	1.548	5.074	7.054	97.7	36,989	15.05	1.926	778
		10	50,000	FIRQUEST	71.874	1.568	5.103	7.098	97.9	37,406	16.32	2.054	885
		1	500,000	FQUEST	71.876	1.512	5.402	7.510	98.0	37375.1	15.69	2.311	599
		5	200,000	FIRQUEST	71.863	1.064	3.427	4.768	97.4	70,930	15.83	1.248	778
		10	100,000	FIRQUEST	71.851	1.115	3.342	4.649	96.8	67,291	19.00	1.103	885
		1	1,000,000	FQUEST	71.835	1.080	3.487	4.853	97.8	67534.5	17.72	1.233	601

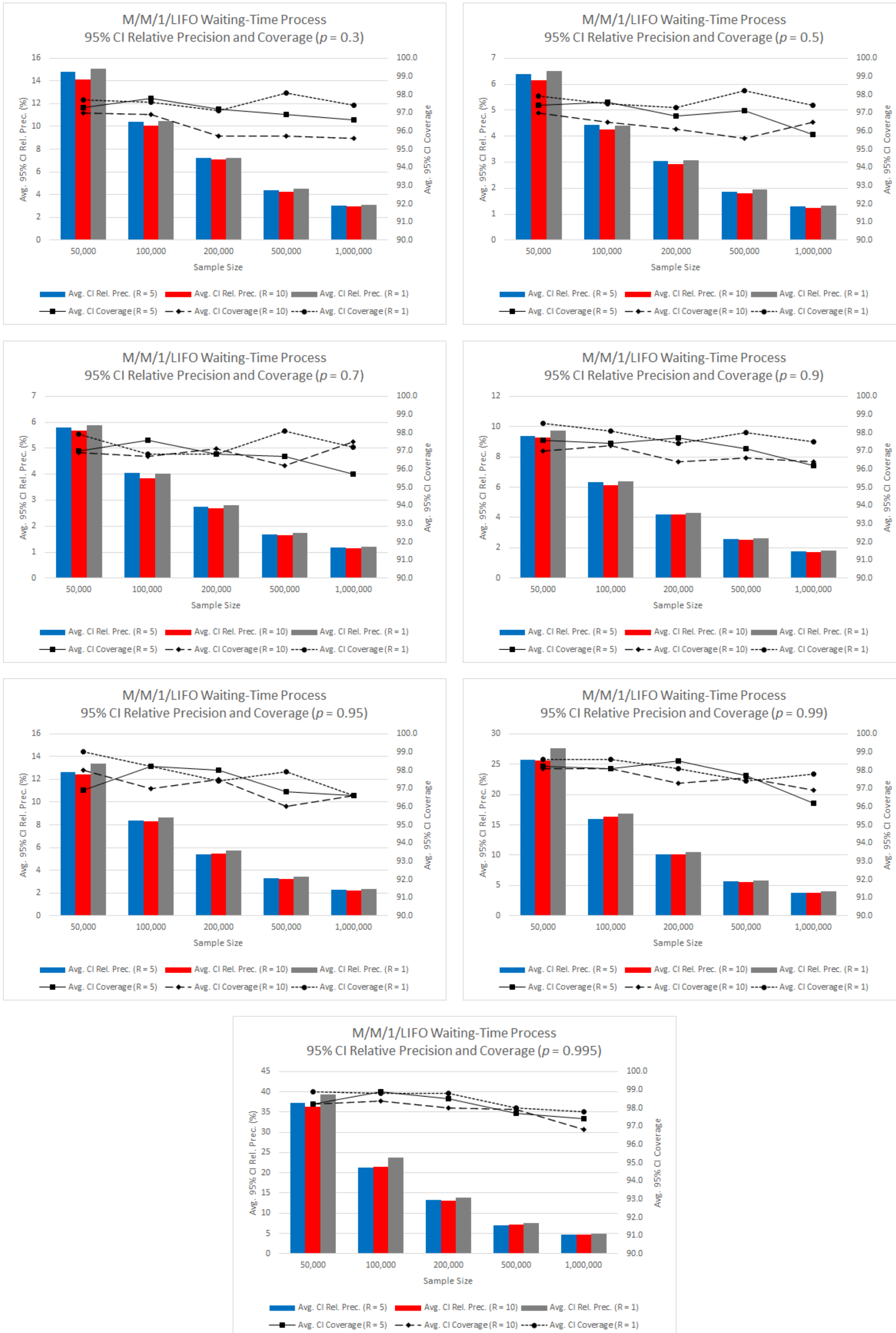

Figure 6.9: Plots for the average 95% CI relative precision and estimated coverage probability for the M/M/1/LIFO waiting-time process from Tables 6.22–6.24.

Table 6.25: Experimental results for FIRQUEST with $R = 5, 10$ and FQUEST with regard to point and 95% CI estimation of y_p for the M/M/1/M/1 total waiting-time process in Section 6.4.6 for $p \in \{0.3, 0.5, 0.7\}$ based on 1,000 independent replications.

p	y_p	R	Repl. Size	Method	Point Est.	Avg. |Bias|	Avg. 95% CI HL	Avg. 95% CI rel. prec. (%)	Avg. 95% CI cov. (%)	$\overline{m}$	$\overline{b}$	St. Dev. HL	Avg. Trunc. Point
0.3	2.748	5	10,000	FIRQUEST	2.744	0.092	0.318	11.602	97.7	3,845	13.82	0.157	400
		10	5,000	FIRQUEST	2.740	0.092	0.303	11.055	96.2	4,003	14.08	0.154	200
		1	50,000	FQUEST	2.745	0.092	0.335	12.203	97.4	4,065	13.80	0.174	626
		5	20,000	FIRQUEST	2.745	0.067	0.207	7.532	95.7	7,128	15.24	0.087	711
		10	10,000	FIRQUEST	2.745	0.066	0.204	7.438	96.3	7,094	16.96	0.090	400
		1	100,000	FQUEST	2.748	0.065	0.221	8.026	97.1	7,450	15.69	0.104	637
		5	40,000	FIRQUEST	2.747	0.047	0.142	5.176	97.1	13,967	15.83	0.053	804
		10	20,000	FIRQUEST	2.746	0.048	0.138	5.041	95.3	12,980	19.26	0.055	759
		1	200,000	FQUEST	2.749	0.045	0.144	5.236	95.2	13,430	17.97	0.058	639
		5	100,000	FIRQUEST	2.748	0.030	0.084	3.050	96.0	33,761	16.74	0.023	805
		10	50,000	FIRQUEST	2.747	0.030	0.082	2.986	96.4	29,809	21.88	0.025	924
		1	500,000	FQUEST	2.749	0.030	0.086	3.121	96.0	31,238	19.37	0.027	640
		5	200,000	FIRQUEST	2.749	0.020	0.059	2.135	95.7	67,747	16.68	0.018	805
		10	100,000	FIRQUEST	2.747	0.021	0.057	2.084	96.0	56,023	23.53	0.017	924
		1	1,000,000	FQUEST	2.748	0.021	0.062	2.254	96.0	62,833	19.46	0.023	639
0.5	5.079	5	10,000	FIRQUEST	5.073	0.146	0.512	10.075	96.5	3,797	14.03	0.283	400
		10	5,000	FIRQUEST	5.065	0.149	0.485	9.580	95.4	3,968	14.24	0.260	200
		1	50,000	FQUEST	5.075	0.145	0.521	10.264	97.1	4,035	13.85	0.269	641
		5	20,000	FIRQUEST	5.074	0.108	0.337	6.632	96.3	7,161	15.13	0.149	715
		10	10,000	FIRQUEST	5.074	0.106	0.331	6.525	95.9	7,264	16.48	0.162	400
		1	100,000	FQUEST	5.080	0.103	0.346	6.810	96.7	7,361	15.85	0.163	651
		5	40,000	FIRQUEST	5.078	0.076	0.226	4.458	96.9	13,831	16.05	0.086	818
		10	20,000	FIRQUEST	5.076	0.076	0.225	4.428	96.1	13,087	19.15	0.093	761
		1	200,000	FQUEST	5.082	0.072	0.232	4.571	96.5	13,647	17.51	0.094	653
		5	100,000	FIRQUEST	5.078	0.048	0.135	2.667	95.9	34,161	16.45	0.041	819
		10	50,000	FIRQUEST	5.078	0.048	0.133	2.619	95.2	29,733	21.93	0.043	937
		1	500,000	FQUEST	5.082	0.047	0.141	2.775	96.1	32,472	18.67	0.047	653
		5	200,000	FIRQUEST	5.080	0.033	0.094	1.854	95.0	65,934	17.03	0.031	819
		10	100,000	FIRQUEST	5.077	0.033	0.092	1.812	96.4	56,288	23.48	0.026	937
		1	1,000,000	FQUEST	5.080	0.034	0.101	1.981	97.0	63,327	19.32	0.038	653
0.7	8.126	5	10,000	FIRQUEST	8.117	0.236	0.821	10.102	95.5	3,815	13.96	0.500	400
		10	5,000	FIRQUEST	8.104	0.240	0.785	9.677	93.8	4,095	13.65	0.449	200
		1	50,000	FQUEST	8.119	0.223	0.844	10.383	97.1	4,051	13.83	0.483	641
		5	20,000	FIRQUEST	8.120	0.168	0.547	6.733	96.6	7,260	14.93	0.264	724
		10	10,000	FIRQUEST	8.119	0.169	0.533	6.558	95.2	7,379	16.11	0.280	400
		1	100,000	FQUEST	8.129	0.164	0.563	6.920	96.7	7,536	15.53	0.287	651
		5	40,000	FIRQUEST	8.125	0.119	0.364	4.476	97.3	14,028	15.85	0.146	830
		10	20,000	FIRQUEST	8.123	0.119	0.357	4.399	96.2	13,143	18.95	0.152	767
		1	200,000	FQUEST	8.133	0.115	0.379	4.655	96.3	13,824	17.50	0.181	653
		5	100,000	FIRQUEST	8.125	0.076	0.222	2.728	95.6	34,388	16.37	0.081	831
		10	50,000	FIRQUEST	8.125	0.077	0.214	2.630	95.7	29,886	21.76	0.074	956
		1	500,000	FQUEST	8.131	0.075	0.224	2.759	96.3	31,896	18.98	0.076	655
		5	200,000	FIRQUEST	8.128	0.053	0.153	1.881	94.9	67,617	16.67	0.056	831
		10	100,000	FIRQUEST	8.123	0.054	0.148	1.818	96.1	55,899	23.49	0.044	956
		1	1,000,000	FQUEST	8.128	0.053	0.159	1.954	97.0	62,403	19.56	0.052	654

Table 6.26: Experimental results for FIRQUEST with $R = 5, 10$ and FQUEST with regard to point and 95% CI estimation of y_p for the M/M/1/M/1 total waiting-time process in Section 6.4.6 for $p \in \{0.9, 0.95\}$ based on 1,000 independent replications.

p	y_p	R	Repl. Size	Method	Point Est.	Avg. |Bias|	Avg. 95% CI HL	Avg. 95% CI rel. prec. (%)	Avg. 95% CI cov. (%)	$\overline{m}$	$\overline{b}$	St. Dev. HL	Avg. Trunc. Point
0.9	13.931	5	10,000	FIRQUEST	13.918	0.488	1.784	12.750	94.4	4,089	12.81	1.320	400
		10	5,000	FIRQUEST	13.885	0.497	1.779	12.764	93.7	4,271	12.63	1.214	200
		1	50,000	FQUEST	13.929	0.468	1.900	13.577	95.9	4,308	12.61	1.305	645
		5	20,000	FIRQUEST	13.926	0.344	1.145	8.202	95.5	7,828	13.66	0.669	733
		10	10,000	FIRQUEST	13.916	0.346	1.175	8.429	94.4	8,101	14.06	0.771	400
		1	100,000	FQUEST	13.941	0.341	1.164	8.329	96.6	7,971	14.23	0.696	660
		5	40,000	FIRQUEST	13.935	0.241	0.758	5.436	96.6	14,737	14.93	0.382	854
		10	20,000	FIRQUEST	13.923	0.240	0.745	5.342	95.3	14,507	16.61	0.376	770
		1	200,000	FQUEST	13.939	0.236	0.780	5.586	96.6	15,031	15.55	0.382	661
		5	100,000	FIRQUEST	13.929	0.153	0.450	3.230	95.9	35,112	16.04	0.177	855
		10	50,000	FIRQUEST	13.929	0.156	0.440	3.160	94.4	31,831	20.33	0.182	966
		1	500,000	FQUEST	13.933	0.152	0.470	3.372	95.0	33,091	18.25	0.207	663
		5	200,000	FIRQUEST	13.933	0.105	0.319	2.287	96.3	68,473	16.48	0.131	854
		10	100,000	FIRQUEST	13.929	0.111	0.300	2.154	95.0	58,744	22.25	0.102	966
		1	1,000,000	FQUEST	13.931	0.111	0.322	2.314	96.6	63,294	19.12	0.125	664
0.95	17.349	5	10,000	FIRQUEST	17.320	0.719	2.812	16.116	92.9	4,278	12.00	2.222	400
		10	5,000	FIRQUEST	17.285	0.725	2.769	15.911	93.3	4,500	11.44	2.151	200
		1	50,000	FQUEST	17.344	0.681	2.966	16.990	95.1	4,541	11.58	2.164	632
		5	20,000	FIRQUEST	17.335	0.503	1.784	10.259	94.7	8,205	12.83	1.175	727
		10	10,000	FIRQUEST	17.325	0.500	1.785	10.272	93.4	8,529	12.73	1.253	400
		1	100,000	FQUEST	17.362	0.495	1.802	10.328	96.3	8,564	12.79	1.205	645
		5	40,000	FIRQUEST	17.352	0.354	1.148	6.609	95.6	15,627	13.96	0.655	835
		10	20,000	FIRQUEST	17.332	0.354	1.151	6.629	94.6	15,797	14.65	0.673	767
		1	200,000	FQUEST	17.351	0.351	1.188	6.833	96.1	16,023	14.31	0.690	646
		5	100,000	FIRQUEST	17.346	0.223	0.662	3.814	95.6	36,393	15.40	0.300	835
		10	50,000	FIRQUEST	17.343	0.227	0.656	3.778	94.3	35,338	17.82	0.310	949
		1	500,000	FQUEST	17.348	0.222	0.690	3.971	94.9	35,396	16.87	0.333	649
		5	200,000	FIRQUEST	17.350	0.150	0.467	2.687	96.5	69,678	16.20	0.209	835
		10	100,000	FIRQUEST	17.345	0.163	0.445	2.562	93.8	63,490	20.56	0.178	949
		1	1,000,000	FQUEST	17.346	0.164	0.478	2.756	96.9	66,141	18.37	0.206	650

Table 6.27: Experimental results for FIRQUEST with $R = 5, 10$ and FQUEST with regard to point and 95% CI estimation of y_p for the M/M/1/M/1 total waiting-time process in Section 6.4.6 for $p \in \{0.99, 0.995\}$ based on 1,000 independent replications.

p	y_p	R	Repl. Size	Method	Point Est.	Avg. |Bias|	Avg. 95% CI HL	Avg. 95% CI rel. prec. (%)	Avg. 95% CI cov. (%)	$\overline{m}$	$\overline{b}$	St. Dev. HL	Avg. Trunc. Point
0.99	24.928	5	10,000	FIRQUEST	24.793	1.548	5.318	21.072	90.5	4,677	10.44	3.596	400
		10	5,000	FIRQUEST	24.747	1.580	5.310	21.049	91.0	4,746	10.24	3.535	200
		1	50,000	FQUEST	24.903	1.536	5.555	21.919	91.9	4,834	10.37	3.696	623
		5	20,000	FIRQUEST	24.868	1.070	4.244	16.882	93.5	9,175	10.83	3.007	716
		10	10,000	FIRQUEST	24.839	1.090	4.108	16.365	92.4	9,443	10.36	2.849	400
		1	100,000	FQUEST	24.924	1.111	4.422	17.527	94.1	9,549	10.72	3.142	631
		5	40,000	FIRQUEST	24.923	0.755	3.223	12.866	95.2	17,888	11.58	2.351	806
		10	20,000	FIRQUEST	24.849	0.760	3.085	12.343	93.5	18,292	11.09	2.241	762
		1	200,000	FQUEST	24.920	0.810	3.183	12.670	94.2	18,214	11.74	2.453	632
		5	100,000	FIRQUEST	24.891	0.495	1.788	7.158	93.9	42,187	12.89	1.207	806
		10	50,000	FIRQUEST	24.897	0.499	1.739	6.963	94.7	44,144	12.45	1.124	926
		1	500,000	FQUEST	24.920	0.510	1.831	7.324	94.7	42,380	13.14	1.262	634
		5	200,000	FIRQUEST	24.908	0.331	1.148	4.602	96.0	79,860	13.87	0.679	806
		10	100,000	FIRQUEST	24.902	0.359	1.150	4.613	94.6	80,616	14.81	0.673	926
		1	1,000,000	FQUEST	24.918	0.366	1.167	4.676	95.6	78,415	14.79	0.654	636
0.995	28.096	5	10,000	FIRQUEST	27.878	2.097	6.348	22.110	87.8	4,734	10.22	4.201	400
		10	5,000	FIRQUEST	27.809	2.148	6.353	22.179	87.6	4,770	10.13	4.141	200
		1	50,000	FQUEST	27.966	2.124	6.814	23.574	87.9	4,858	10.31	4.858	621
		5	20,000	FIRQUEST	28.022	1.483	5.173	18.126	91.4	9,314	10.58	3.511	714
		10	10,000	FIRQUEST	27.958	1.519	5.134	18.066	90.9	9,512	10.19	3.303	400
		1	100,000	FQUEST	28.068	1.566	5.477	19.163	92.5	9,729	10.36	3.748	626
		5	40,000	FIRQUEST	28.080	1.058	4.306	15.219	94.5	18,527	10.98	2.954	803
		10	20,000	FIRQUEST	27.970	1.050	4.075	14.429	92.6	18,726	10.57	2.816	758
		1	200,000	FQUEST	28.071	1.145	4.291	15.131	92.0	19,038	10.83	3.053	627
		5	100,000	FIRQUEST	28.036	0.693	2.735	9.703	93.4	44,648	11.83	2.024	804
		10	50,000	FIRQUEST	28.048	0.688	2.700	9.581	93.7	46,271	11.34	1.941	907
		1	500,000	FQUEST	28.075	0.704	2.772	9.823	93.8	44,989	12.00	2.074	628
		5	200,000	FIRQUEST	28.055	0.472	1.719	6.109	96.1	84,151	12.93	1.173	804
		10	100,000	FIRQUEST	28.055	0.498	1.754	6.238	93.6	88,729	12.46	1.182	907
		1	1,000,000	FQUEST	28.081	0.503	1.813	6.441	95.9	84,986	13.23	1.222	629

Figure 6.10: Plots for the average 95% CI relative precision and estimated coverage probability for the M/M/1/M/1 total waiting-time process from Tables 6.25–6.27.

Table 6.28: Experimental results for FIRQUEST with $R = 5, 10$ and FQUEST with regard to point and 95% CI estimation of y_p for the response-time process in the Central Server Model 3 in Section 6.4.7 for $p \in \{0.3, 0.5, 0.7\}$ based on 1,000 independent replications.

p	y_p	R	Repl. Size	Method	Point Est.	Avg. |Bias|	Avg. 95% CI HL	Avg. 95% CI rel. prec. (%)	Avg. 95% CI cov. (%)	$\overline{m}$	$\overline{b}$	St. Dev. HL	Avg. Trunc. Point
0.3	7.078	5	10,000	FIRQUEST	7.091	0.187	0.540	7.622	96.4	3,317	16.47	0.170	400
		10	5,000	FIRQUEST	7.085	0.188	0.514	7.267	95.6	2,915	21.85	0.162	200
		1	50,000	FQUEST	7.090	0.190	0.533	7.531	95.2	3,168	18.84	0.174	662
		5	20,000	FIRQUEST	7.090	0.138	0.382	5.397	96.3	6,557	16.62	0.116	737
		10	10,000	FIRQUEST	7.091	0.134	0.368	5.188	96.3	5,666	22.61	0.110	400
		1	100,000	FQUEST	7.095	0.137	0.387	5.459	94.8	6,133	19.70	0.143	679
		5	40,000	FIRQUEST	7.092	0.097	0.271	3.821	95.4	13,007	16.99	0.087	870
		10	20,000	FIRQUEST	7.090	0.096	0.266	3.761	95.6	10,962	23.38	0.085	774
		1	200,000	FQUEST	7.092	0.095	0.276	3.898	95.7	12,779	19.10	0.094	678
		5	100,000	FIRQUEST	7.093	0.064	0.169	2.387	95.0	32,923	17.09	0.050	870
		10	50,000	FIRQUEST	7.091	0.061	0.167	2.350	95.1	27,672	23.75	0.056	987
		1	500,000	FQUEST	7.090	0.059	0.174	2.452	95.8	30,456	20.02	0.054	680
		5	200,000	FIRQUEST	7.088	0.045	0.121	1.704	96.1	65,279	17.31	0.039	870
		10	100,000	FIRQUEST	7.091	0.044	0.118	1.658	95.6	55,181	23.84	0.041	987
		1	1,000,000	FQUEST	7.087	0.043	0.123	1.732	96.0	61,169	19.87	0.040	679
0.5	10.771	5	10,000	FIRQUEST	10.783	0.211	0.577	5.360	95.7	3,216	16.98	0.165	400
		10	5,000	FIRQUEST	10.778	0.211	0.545	5.064	94.1	2,673	24.18	0.164	200
		1	50,000	FQUEST	10.783	0.211	0.567	5.265	94.0	2,990	20.09	0.178	660
		5	20,000	FIRQUEST	10.785	0.152	0.416	3.858	94.5	6,447	16.99	0.138	737
		10	10,000	FIRQUEST	10.784	0.149	0.400	3.708	95.0	5,246	24.12	0.116	400
		1	100,000	FQUEST	10.789	0.153	0.414	3.835	93.8	5,930	20.31	0.146	674
		5	40,000	FIRQUEST	10.788	0.107	0.295	2.736	95.9	12,924	17.16	0.089	864
		10	20,000	FIRQUEST	10.785	0.106	0.288	2.673	95.5	10,762	23.61	0.084	774
		1	200,000	FQUEST	10.786	0.106	0.302	2.802	94.9	12,273	19.83	0.109	674
		5	100,000	FIRQUEST	10.788	0.071	0.188	1.740	94.8	32,448	17.32	0.055	865
		10	50,000	FIRQUEST	10.786	0.067	0.184	1.703	94.6	26,649	24.52	0.064	986
		1	500,000	FQUEST	10.785	0.066	0.193	1.787	95.9	30,929	19.83	0.058	674
		5	200,000	FIRQUEST	10.783	0.049	0.133	1.238	95.0	65,102	17.28	0.045	865
		10	100,000	FIRQUEST	10.787	0.049	0.131	1.213	95.3	54,536	24.24	0.044	986
		1	1,000,000	FQUEST	10.782	0.047	0.136	1.265	95.7	61,396	19.92	0.043	674
0.7	15.364	5	10,000	FIRQUEST	15.375	0.205	0.584	3.804	95.6	3,348	16.29	0.220	400
		10	5,000	FIRQUEST	15.375	0.208	0.558	3.631	93.6	3,020	21.02	0.206	200
		1	50,000	FQUEST	15.375	0.204	0.584	3.798	95.1	3,321	18.00	0.220	645
		5	20,000	FIRQUEST	15.377	0.146	0.405	2.637	94.3	6,582	16.57	0.116	727
		10	10,000	FIRQUEST	15.377	0.146	0.399	2.599	94.1	5,686	22.33	0.132	400
		1	100,000	FQUEST	15.381	0.145	0.417	2.714	95.0	6,207	19.32	0.158	654
		5	40,000	FIRQUEST	15.380	0.104	0.289	1.879	95.7	13,070	17.00	0.089	839
		10	20,000	FIRQUEST	15.380	0.104	0.282	1.837	95.4	11,253	22.82	0.091	769
		1	200,000	FQUEST	15.379	0.102	0.297	1.933	96.1	12,423	19.59	0.113	654
		5	100,000	FIRQUEST	15.381	0.069	0.183	1.189	95.1	33,315	16.79	0.060	840
		10	50,000	FIRQUEST	15.381	0.066	0.176	1.141	95.1	27,451	23.83	0.053	958
		1	500,000	FQUEST	15.379	0.064	0.188	1.223	95.8	31,213	19.60	0.061	654
		5	200,000	FIRQUEST	15.377	0.046	0.129	0.838	95.3	65,817	17.14	0.045	840
		10	100,000	FIRQUEST	15.381	0.048	0.125	0.813	95.3	53,882	24.45	0.039	958
		1	1,000,000	FQUEST	15.376	0.046	0.131	0.851	95.9	61,158	19.98	0.039	654

Table 6.29: Experimental results for FIRQUEST with $R = 5, 10$ and FQUEST with regard to point and 95% CI estimation of y_p for the response-time process in the Central Server Model 3 in Section 6.4.7 for $p \in \{0.8, 0.85\}$ based on 1,000 independent replications.

p	y_p	R	Repl. Size	Method	Point Est.	Avg. |Bias|	Avg. 95% CI HL	Avg. 95% CI rel. prec. (%)	Avg. 95% CI cov. (%)	$\overline{m}$	$\overline{b}$	St. Dev. HL	Avg. Trunc. Point
0.8	18.868	5	10,000	FIRQUEST	18.876	0.191	0.558	2.957	95.1	3,395	16.05	0.203	400
		10	5,000	FIRQUEST	18.877	0.191	0.551	2.922	95.3	3,229	19.42	0.216	200
		1	50,000	FQUEST	18.879	0.192	0.570	3.021	96.0	3,516	16.73	0.237	619
		5	20,000	FIRQUEST	18.879	0.137	0.385	2.042	95.7	6,731	16.25	0.114	720
		10	10,000	FIRQUEST	18.877	0.138	0.383	2.029	94.4	6,174	20.40	0.133	400
		1	100,000	FQUEST	18.884	0.133	0.395	2.093	95.6	6,496	18.43	0.149	626
		5	40,000	FIRQUEST	18.880	0.097	0.269	1.425	95.2	13,071	17.07	0.086	815
		10	20,000	FIRQUEST	18.881	0.097	0.266	1.408	95.2	11,586	21.94	0.082	763
		1	200,000	FQUEST	18.881	0.094	0.283	1.498	96.3	12,909	18.80	0.114	626
		5	100,000	FIRQUEST	18.882	0.063	0.170	0.902	95.1	33,205	16.93	0.055	816
		10	50,000	FIRQUEST	18.882	0.063	0.163	0.861	94.7	28,029	23.31	0.047	927
		1	500,000	FQUEST	18.880	0.059	0.177	0.939	96.5	31,837	19.31	0.061	626
		5	200,000	FIRQUEST	18.878	0.043	0.119	0.633	95.3	67,015	16.89	0.039	816
		10	100,000	FIRQUEST	18.883	0.045	0.116	0.614	94.0	55,207	24.00	0.035	927
		1	1,000,000	FQUEST	18.878	0.042	0.123	0.650	96.6	62,613	19.42	0.043	626
0.85	21.631	5	10,000	FIRQUEST	21.642	0.181	0.542	2.506	95.9	3,422	15.92	0.189	400
		10	5,000	FIRQUEST	21.637	0.181	0.537	2.484	96.6	3,264	19.32	0.191	200
		1	50,000	FQUEST	21.642	0.180	0.548	2.532	96.9	3,502	16.87	0.204	585
		5	20,000	FIRQUEST	21.644	0.129	0.367	1.697	96.3	6,668	16.46	0.114	693
		10	10,000	FIRQUEST	21.637	0.131	0.365	1.685	95.3	6,202	20.59	0.119	400
		1	100,000	FQUEST	21.645	0.125	0.374	1.729	96.2	6,556	18.26	0.124	588
		5	40,000	FIRQUEST	21.642	0.092	0.253	1.169	95.7	13,199	16.84	0.075	762
		10	20,000	FIRQUEST	21.643	0.093	0.248	1.148	96.2	11,112	22.99	0.075	743
		1	200,000	FQUEST	21.643	0.087	0.259	1.199	96.7	12,283	19.76	0.089	588
		5	100,000	FIRQUEST	21.641	0.059	0.158	0.729	95.4	33,510	16.76	0.046	762
		10	50,000	FIRQUEST	21.642	0.060	0.154	0.709	93.6	27,646	23.62	0.042	866
		1	500,000	FQUEST	21.640	0.055	0.164	0.760	96.6	31,393	19.33	0.059	588
		5	200,000	FIRQUEST	21.638	0.040	0.111	0.511	96.1	66,386	17.00	0.033	761
		10	100,000	FIRQUEST	21.643	0.043	0.108	0.498	95.3	53,789	24.59	0.029	866
		1	1,000,000	FQUEST	21.638	0.039	0.116	0.536	96.1	62,836	19.35	0.043	588

Table 6.30: Experimental results for FIRQUEST with $R = 5, 10$ and FQUEST with regard to point and 95% CI estimation of y_p for the response-time process in the Central Server Model 3 in Section 6.4.7 for $p \in \{0.87, 0.89\}$ based on 1,000 independent replications.

p	y_p	R	Repl. Size	Method	Point Est.	Avg. |Bias|	Avg. 95% CI HL	Avg. 95% CI rel. prec. (%)	Avg. 95% CI cov. (%)	$\overline{m}$	$\overline{b}$	St. Dev. HL	Avg. Trunc. Point
0.87	23.236	5	10,000	FIRQUEST	23.248	0.182	0.594	2.554	97.9	3,471	15.67	0.224	400
		10	5,000	FIRQUEST	23.245	0.182	0.596	2.564	96.5	3,443	17.71	0.239	200
		1	50,000	FQUEST	23.246	0.176	0.604	2.598	97.6	3,566	16.60	0.215	560
		5	20,000	FIRQUEST	23.251	0.131	0.377	1.623	96.4	6,784	16.21	0.123	668
		10	10,000	FIRQUEST	23.240	0.132	0.385	1.655	96.3	6,111	20.83	0.131	400
		1	100,000	FQUEST	23.249	0.126	0.385	1.655	97.1	6,387	18.86	0.117	563
		5	40,000	FIRQUEST	23.244	0.093	0.255	1.095	95.1	13,236	16.85	0.072	715
		10	20,000	FIRQUEST	23.247	0.094	0.252	1.082	95.9	10,828	23.91	0.073	721
		1	200,000	FQUEST	23.245	0.087	0.264	1.136	97.0	12,375	19.61	0.095	562
		5	100,000	FIRQUEST	23.243	0.059	0.161	0.692	96.0	32,962	17.03	0.054	715
		10	50,000	FIRQUEST	23.243	0.059	0.158	0.680	94.4	27,081	24.29	0.054	809
		1	500,000	FQUEST	23.242	0.053	0.165	0.712	96.8	31,271	19.48	0.057	562
		5	200,000	FIRQUEST	23.240	0.039	0.112	0.480	97.1	66,259	17.05	0.035	715
		10	100,000	FIRQUEST	23.244	0.043	0.108	0.463	94.0	53,074	24.67	0.030	810
		1	1,000,000	FQUEST	23.240	0.039	0.115	0.495	96.1	63,539	19.18	0.042	563
0.89	25.514	5	10,000	FIRQUEST	25.528	0.211	0.976	3.821	98.5	4,188	12.31	0.543	400
		10	5,000	FIRQUEST	25.527	0.216	0.861	3.373	98.2	4,514	11.33	0.432	200
		1	50,000	FQUEST	25.529	0.207	1.009	3.951	98.7	4,453	11.95	0.574	561
		5	20,000	FIRQUEST	25.531	0.157	0.534	2.090	97.9	7,412	14.63	0.222	669
		10	10,000	FIRQUEST	25.516	0.151	0.525	2.058	98.4	7,889	14.53	0.216	400
		1	100,000	FQUEST	25.527	0.146	0.563	2.206	98.0	7,678	15.09	0.261	566
		5	40,000	FIRQUEST	25.520	0.109	0.326	1.277	96.4	13,730	16.19	0.109	721
		10	20,000	FIRQUEST	25.521	0.107	0.340	1.331	97.4	13,380	18.43	0.136	728
		1	200,000	FQUEST	25.520	0.103	0.346	1.355	97.2	13,429	18.01	0.136	567
		5	100,000	FIRQUEST	25.516	0.068	0.195	0.765	97.0	33,572	16.77	0.069	721
		10	50,000	FIRQUEST	25.516	0.068	0.192	0.753	95.8	28,601	22.97	0.066	824
		1	500,000	FQUEST	25.516	0.064	0.206	0.806	97.2	31,801	19.15	0.081	568
		5	200,000	FIRQUEST	25.514	0.047	0.134	0.525	96.0	67,214	16.79	0.045	721
		10	100,000	FIRQUEST	25.517	0.048	0.131	0.512	95.8	56,319	23.56	0.039	824
		1	1,000,000	FQUEST	25.515	0.046	0.141	0.553	96.9	62,827	19.45	0.054	569

Figure 6.11: Plots for the average 95% CI relative precision and estimated coverage probability for the response-time process in the Central Server Model 3 from Tables 6.28–6.30.

Table 6.31: Experimental results for FIRQUEST with $R = 5, 10$ and FQUEST with regard to point and 95% CI estimation of y_p for the response-time process in the Central Server Model 3 in Section 6.4.7 for $p \in \{0.9, 0.91, 0.93\}$ based on 1,000 independent replications.

p	y_p	R	Repl. Size	Method	Point Est.	Avg. |Bias|	Avg. 95% CI HL	Avg. 95% CI rel. prec. (%)	Avg. 95% CI cov. (%)	$\overline{m}$	$\overline{b}$	St. Dev. HL	Avg. Trunc. Point
0.9	27.181	5	10,000	FIRQUEST	27.197	0.274	1.789	6.568	99.0	4,620	10.63	1.163	400
		10	5,000	FIRQUEST	27.201	0.289	1.546	5.678	98.4	4,736	10.28	0.946	200
		1	50,000	FQUEST	27.199	0.280	1.890	6.939	98.8	4,768	10.63	1.234	575
		5	20,000	FIRQUEST	27.194	0.206	0.877	3.224	98.4	8,487	12.17	0.482	690
		10	10,000	FIRQUEST	27.177	0.199	0.818	3.009	98.8	9,125	11.08	0.420	400
		1	100,000	FQUEST	27.187	0.199	0.946	3.478	99.1	8,931	12.00	0.513	580
		5	40,000	FIRQUEST	27.180	0.143	0.511	1.880	97.2	15,670	13.90	0.242	752
		10	20,000	FIRQUEST	27.180	0.139	0.499	1.835	97.9	16,463	13.55	0.226	741
		1	200,000	FQUEST	27.179	0.141	0.533	1.960	97.8	16,179	14.07	0.241	582
		5	100,000	FIRQUEST	27.173	0.088	0.269	0.989	97.1	35,206	15.97	0.092	753
		10	50,000	FIRQUEST	27.174	0.088	0.276	1.015	96.7	33,907	18.73	0.105	851
		1	500,000	FQUEST	27.175	0.085	0.298	1.098	97.0	35,338	16.94	0.132	584
		5	200,000	FIRQUEST	27.173	0.064	0.183	0.673	95.1	68,169	16.56	0.068	752
		10	100,000	FIRQUEST	27.174	0.062	0.182	0.668	96.7	61,823	21.14	0.068	851
		1	1,000,000	FQUEST	27.175	0.062	0.192	0.708	96.8	65,556	18.53	0.069	586
0.91	29.648	5	10,000	FIRQUEST	29.686	0.478	4.173	14.011	99.4	4,734	10.22	2.469	400
		10	5,000	FIRQUEST	29.695	0.493	3.848	12.914	98.8	4,793	10.03	2.387	200
		1	50,000	FQUEST	29.690	0.500	4.411	14.798	99.4	4,899	10.14	2.754	593
		5	20,000	FIRQUEST	29.668	0.353	2.051	6.899	98.5	9,286	10.64	1.246	701
		10	10,000	FIRQUEST	29.647	0.342	1.919	6.461	99.0	9,509	10.19	1.204	400
		1	100,000	FQUEST	29.656	0.344	2.176	7.323	99.2	9,615	10.54	1.362	597
		5	40,000	FIRQUEST	29.639	0.246	1.093	3.686	98.1	17,735	11.69	0.638	778
		10	20,000	FIRQUEST	29.640	0.233	1.021	3.441	98.0	18,307	11.06	0.594	750
		1	200,000	FQUEST	29.639	0.241	1.181	3.979	98.4	18,229	11.65	0.653	598
		5	100,000	FIRQUEST	29.625	0.149	0.529	1.786	96.9	39,541	13.96	0.230	778
		10	50,000	FIRQUEST	29.628	0.145	0.516	1.741	96.8	41,646	13.82	0.223	882
		1	500,000	FQUEST	29.632	0.148	0.589	1.987	97.8	40,609	14.12	0.290	600
		5	200,000	FIRQUEST	29.627	0.110	0.340	1.147	96.2	73,255	15.35	0.149	778
		10	100,000	FIRQUEST	29.627	0.104	0.332	1.120	96.2	72,615	17.12	0.131	882
		1	1,000,000	FQUEST	29.633	0.108	0.366	1.234	97.6	72,436	16.31	0.152	603
0.93	44.766	5	10,000	FIRQUEST	44.811	2.690	8.840	19.899	95.7	4,351	11.63	4.468	400
		10	5,000	FIRQUEST	44.873	2.620	9.148	20.544	95.1	4,626	10.76	4.708	200
		1	50,000	FQUEST	44.883	2.778	8.988	20.170	94.4	4,480	11.70	4.757	615
		5	20,000	FIRQUEST	44.753	1.961	5.849	13.111	95.2	7,972	13.22	2.930	715
		10	10,000	FIRQUEST	44.714	1.863	6.018	13.469	95.9	8,625	12.25	3.126	400
		1	100,000	FQUEST	44.691	1.988	5.955	13.376	95.3	8,425	13.05	3.069	624
		5	40,000	FIRQUEST	44.665	1.393	4.047	9.079	95.1	14,936	14.62	1.931	809
		10	20,000	FIRQUEST	44.668	1.323	3.963	8.866	96.4	15,198	15.18	1.890	761
		1	200,000	FQUEST	44.640	1.381	4.139	9.276	94.3	15,441	14.88	1.849	626
		5	100,000	FIRQUEST	44.603	0.879	2.410	5.401	94.7	34,731	16.17	0.863	810
		10	50,000	FIRQUEST	44.624	0.845	2.373	5.317	94.8	33,198	19.16	0.904	931
		1	500,000	FQUEST	44.636	0.848	2.511	5.627	94.9	33,600	17.89	0.978	629
		5	200,000	FIRQUEST	44.642	0.626	1.719	3.851	94.6	68,187	16.56	0.625	810
		10	100,000	FIRQUEST	44.616	0.627	1.650	3.698	94.2	60,088	21.63	0.588	931
		1	1,000,000	FQUEST	44.658	0.598	1.783	3.993	96.4	66,094	18.27	0.676	629

Table 6.32: Experimental results for FIRQUEST with $R = 5, 10$ and FQUEST with regard to point and 95% CI estimation of y_p for the response-time process in the Central Server Model 3 in Section 6.4.7 for $p \in \{0.95, 0.99, 0.995\}$ based on 1,000 independent replications.

p	y_p	R	Repl. Size	Method	Point Est.	Avg. |Bias|	Avg. 95% CI HL	Avg. 95% CI rel. prec. (%)	Avg. 95% CI cov. (%)	$\overline{m}$	$\overline{b}$	St. Dev. HL	Avg. Trunc. Point
0.95	74.481	5	10,000	FIRQUEST	74.345	3.346	8.813	11.889	93.4	3,328	16.38	3.200	400
		10	5,000	FIRQUEST	74.446	3.277	8.478	11.420	93.4	3,038	20.45	3.305	200
		1	50,000	FQUEST	74.440	3.387	8.725	11.739	91.6	3,246	18.30	3.404	632
		5	20,000	FIRQUEST	74.343	2.462	6.413	8.636	94.0	6,428	17.02	2.068	722
		10	10,000	FIRQUEST	74.330	2.345	6.160	8.293	94.4	5,480	23.01	2.090	400
		1	100,000	FQUEST	74.305	2.411	6.444	8.684	93.1	6,213	19.56	2.467	638
		5	40,000	FIRQUEST	74.297	1.732	4.674	6.296	95.0	13,118	16.91	1.663	828
		10	20,000	FIRQUEST	74.314	1.652	4.448	5.985	94.4	10,545	24.16	1.413	767
		1	200,000	FQUEST	74.300	1.685	4.692	6.318	95.0	12,572	19.33	1.619	638
		5	100,000	FIRQUEST	74.289	1.113	2.930	3.945	94.2	33,166	17.00	0.832	829
		10	50,000	FIRQUEST	74.306	1.048	2.827	3.804	96.0	26,753	24.45	0.760	954
		1	500,000	FQUEST	74.340	1.054	3.018	4.061	95.6	30,440	20.18	0.957	639
		5	200,000	FIRQUEST	74.345	0.783	2.116	2.846	95.1	66,433	16.98	0.677	829
		10	100,000	FIRQUEST	74.324	0.750	2.034	2.737	95.0	55,253	24.01	0.696	954
		1	1,000,000	FQUEST	74.381	0.734	2.167	2.914	95.6	62,433	19.59	0.666	638
0.99	166.528	5	10,000	FIRQUEST	166.244	4.637	12.671	7.619	93.6	3,388	15.95	4.560	400
		10	5,000	FIRQUEST	166.396	4.671	12.616	7.583	94.2	3,312	18.92	4.739	200
		1	50,000	FQUEST	166.402	4.300	13.277	7.976	95.0	3,458	17.23	5.676	636
		5	20,000	FIRQUEST	166.312	3.288	9.143	5.499	95.1	6,726	16.28	3.298	719
		10	10,000	FIRQUEST	166.398	3.237	8.675	5.213	95.2	5,848	21.84	2.697	400
		1	100,000	FQUEST	166.218	3.101	9.220	5.547	96.0	6,519	18.67	3.643	642
		5	40,000	FIRQUEST	166.330	2.261	6.367	3.828	95.3	13,219	16.84	2.179	817
		10	20,000	FIRQUEST	166.348	2.270	6.231	3.745	95.6	11,305	22.86	2.175	764
		1	200,000	FQUEST	166.261	2.261	6.529	3.926	96.0	12,843	18.95	2.532	643
		5	100,000	FIRQUEST	166.281	1.454	4.028	2.422	95.7	33,467	16.93	1.161	817
		10	50,000	FIRQUEST	166.340	1.413	3.839	2.308	94.8	27,420	24.05	1.152	938
		1	500,000	FQUEST	166.374	1.369	4.088	2.457	96.3	31,644	19.16	1.414	644
		5	200,000	FIRQUEST	166.378	1.036	2.845	1.710	94.4	67,863	16.76	0.974	817
		10	100,000	FIRQUEST	166.348	1.005	2.737	1.645	95.0	54,333	24.04	0.922	938
		1	1,000,000	FQUEST	166.441	0.973	2.917	1.753	95.9	60,817	19.98	1.044	644
0.995	196.230	5	10,000	FIRQUEST	195.913	5.623	15.936	8.128	94.2	3,588	15.01	7.013	400
		10	5,000	FIRQUEST	196.074	5.517	16.100	8.202	94.1	3,826	15.34	7.076	200
		1	50,000	FQUEST	195.971	5.254	16.823	8.584	95.9	3,838	15.00	7.756	641
		5	20,000	FIRQUEST	195.961	3.910	10.838	5.531	94.5	6,885	15.94	3.763	728
		10	10,000	FIRQUEST	196.157	3.900	10.788	5.499	96.1	6,414	19.71	4.374	400
		1	100,000	FQUEST	195.898	3.709	11.282	5.761	95.6	7,043	16.99	4.841	651
		5	40,000	FIRQUEST	195.961	2.700	7.603	3.880	94.8	13,618	16.30	2.580	838
		10	20,000	FIRQUEST	196.044	2.761	7.571	3.861	94.6	12,170	21.10	2.873	765
		1	200,000	FQUEST	195.965	2.654	7.898	4.029	96.4	13,205	18.37	3.247	653
		5	100,000	FIRQUEST	195.959	1.719	4.760	2.429	95.3	33,796	16.70	1.555	839
		10	50,000	FIRQUEST	196.016	1.683	4.630	2.362	95.9	29,296	22.51	1.548	940
		1	500,000	FQUEST	196.062	1.667	4.864	2.481	95.5	31,418	19.38	1.656	654
		5	200,000	FIRQUEST	196.050	1.234	3.296	1.681	94.5	65,551	17.18	1.033	839
		10	100,000	FIRQUEST	196.041	1.188	3.293	1.680	96.1	59,495	22.51	1.139	940
		1	1,000,000	FQUEST	196.122	1.172	3.482	1.775	96.1	61,576	19.78	1.324	654

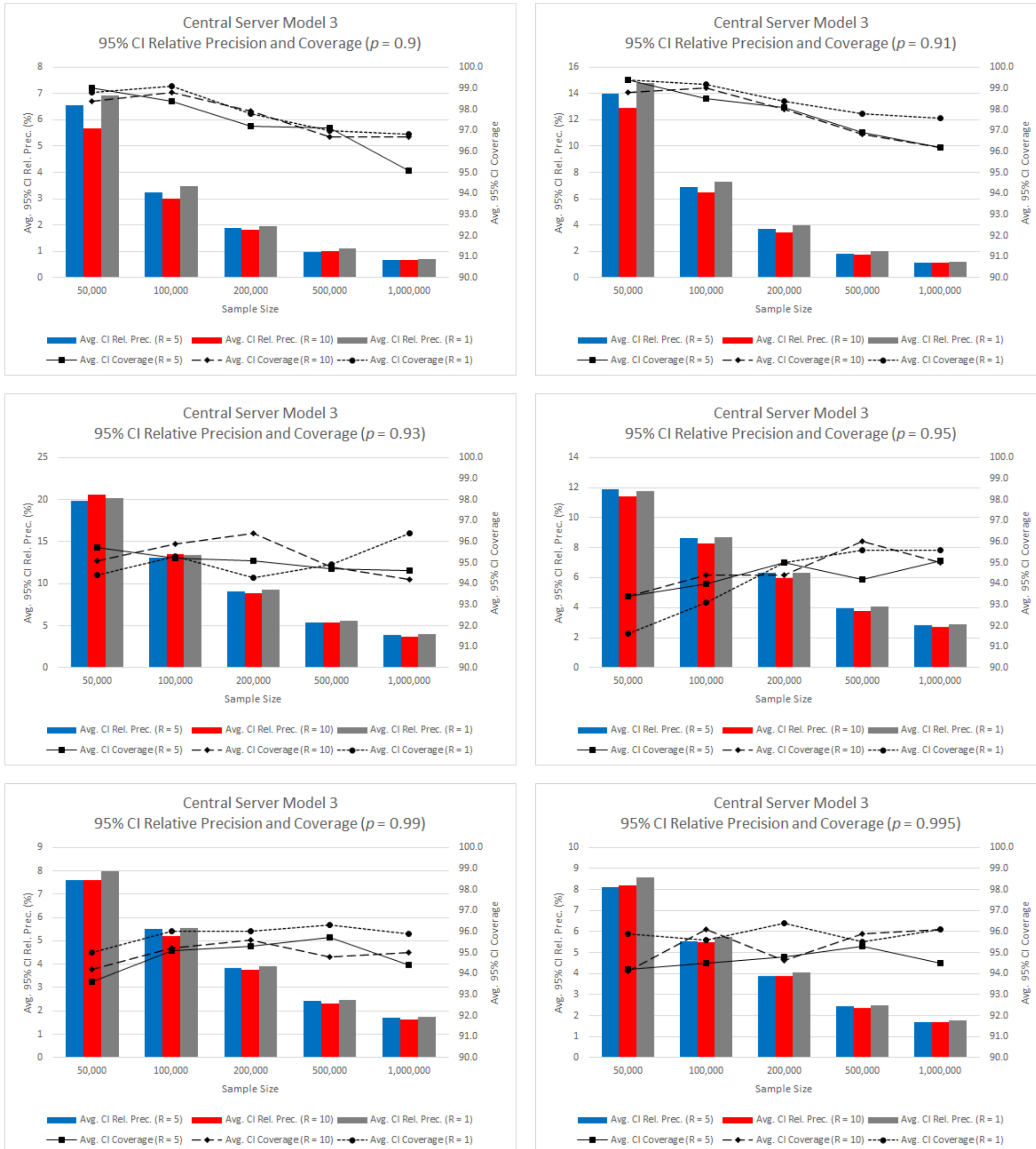

Figure 6.12: Plots for the average 95% CI relative precision and estimated coverage probability for the response-time process in the Central Server Model 3 from Tables 6.31–6.32.

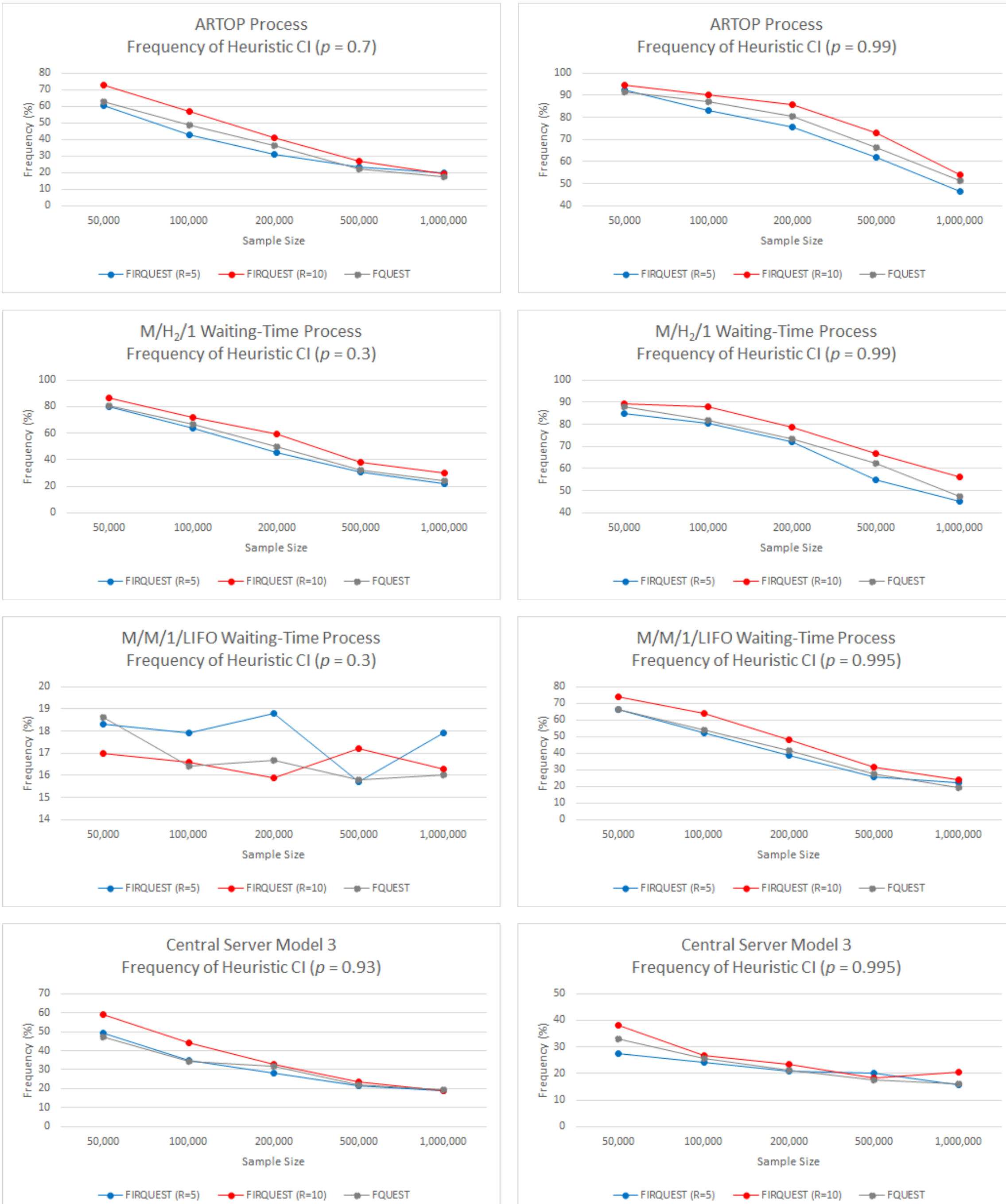

Figure 6.13: Frequency of Heuristic CI in Step **[10]** of FIRQUEST (for $R = 5, 10$) and FQUEST for selected examples. The results are based on 1,000 independent replications with total sample sizes {50,000, 100,000, 200,000, 500,000, 1,000,000}.

CHAPTER 7

CONCLUSIONS

This thesis had two main goals: (1) the formulation of the theoretical foundations for procedures based on STS for estimating steady-state quantiles with CIs having given coverage probability and, potentially precision; and (2) the development and experimental evaluation of three automated methods for effective estimation of marginal quantiles in steady-state simulations.

Chapter 1 provided an extended literature review on steady-state quantile estimation. Chapter 2 presented the theoretical results that constitute the basis of the proposed methods in Chapters 4–6 including the proof of a CLT for the vector of signed weighted areas of the STSs computed from nonoverlapping batches of the simulation output as the batch size increases while the batch count remains fixed. Further, Chapter 2 introduced a way to construct partial and stepwise weight functions for quantile estimation based on STS and provided results from the empirical evaluation of a variety of variance-parameter estimators. The experimental results in Chapter 2 did not provide a strong basis for using a weight function other than the constant $w_0(t) = \sqrt{12}$, for $t \in [0, 1]$, and revealed the benefits of the combined estimator $\widetilde{\mathscr{V}}_p(w; b, m)$ of the variance parameter associated with the empirical-quantile process. In Chapter 3 we provided exact (or nearly exact) calculations for the expected values of the variance-parameter estimators in Chapter 2 for the special case of i.i.d. data. These calculations verified that the STS area estimator has larger small-sample bias compared to the its competitors computed from batched empirical quantiles; this trend was already surfaced in Chapter 2.

Chapter 4 introduced SQSTS, the first fully automated sequential procedure for computing point estimators and CIs for steady-state quantiles of a stochastic process based on STSs. SQSTS estimates the variance parameter $\sigma_p^2 = \lim_{n\to\infty} n\mathrm{Var}\big[\widetilde{y}_p(n)\big]$ of the sample quantile process $\{\widetilde{y}_p(n) : n \geq 1\}$ by a linear combination of estimators computed from nonoverlapping batches: the first estimator is computed from the associated BQEs while the second estimator is obtained from STSs based on the batches. Extensive experimentation with a large test bed of output processes highlighted the potential benefits of SQSTS over Sequest (Alexopoulos *et al.* [7]) and Sequem (Alexopoulos *et al.* [23]): (i) under no CI precision requirement, SQSTS was frequently able to curtail excessive average sample sizes, often by an order of magnitude, despite its larger initial batch size—we believe that this dominance is partially due to the effectiveness of the von Neumann and Shapiro–Wilk tests for the signed areas; and (ii) under tight CI relative precision requirements, the lack of CI adjustments and lower standard deviation of the combined variance estimator allowed SQSTS to outperform its competitors with regard to average sample size in most cases. Moreover, SQSTS performed comparatively well against Sequest and Sequem with regard to average absolute bias of the point estimator and estimated CI coverage probability.

Chapter 5 presented FQUEST, a fully automated fixed-sample-size procedure for computing CIs for steady-state quantiles based on a single run. Although there are a few fixed-sample-size procedures for quantile estimation (e.g., Heidelberger and Lewis [30] and Bekki *et al.* [13]), to the best of our knowledge, FQUEST is the first such method that (i) uses the STS methodology; (ii) addresses the simulation initialization problem; and (iii) warns the user when the dataset is insufficient and, subject to user's approval, delivers a heuristic CI. The user provides the sample and specifies the probability of the quantile and the required coverage probability of the requested CI. FQUEST incorporates the analysis methods of batching, STS, and sectioning. If the sample size suffices to identify a set of signed weighted areas $\{A_p(w; j, m) : j = 1, \ldots, b\}$ and BQEs $\{\widehat{y}_p(j, m) : j = 1, \ldots, b\}$ computed from b batches of size m each that pass the von Neumman and Shapiro-Wilk tests for randomness and normality, respectively, FQUEST reports a CI for the quantile y_p under consideration centered at the empirical quantile from a truncated subset of the sample path and based on the combined estimator $\widetilde{\mathscr{V}}_p(w; b, m)$ of σ_p^2. Otherwise, the procedure issues a warning and, upon user's approval, formulates a wider CI from a set of CIs based on the quantile estimator computed from the entire truncated sample, the BQEs, and the batched area estimator $\mathscr{A}_p(w; b, m)$ obtained from the nonoverlapping batches. Experimentation with an extensive test bed of output processes showed that FQUEST delivered CIs with coverage probabilities close to the nominal level. This feat is quite remarkable, considering that the state-of-the-art sequential methods Sequest and SQSTS required substantial sample sizes for the same processes under no CI precision requirement.

Chapter 6 introduced FIRQUEST, the first fully automated procedure for computing point estimators and CIs for steady-state quantiles based on independent replications. The user provides a fixed number R of replicate sample paths, each with fixed length n, and specifies the probability of the quantile and the required coverage probability of the requested CI. FIRQUEST incorporates the analysis methods of batching, STS, and sectioning. If the total sample size and the replication length suffice to identify set of replicate signed weighted areas $\{A_p(w; j, m) : j = 1, \ldots, Rb\}$ and RBQEs $\left\{\widehat{y}_p(j, m) : j = 1, \ldots, Rb\right\}$ based on b batches of size m from each replication that pass both the von Neumman and Shapiro-Wilk tests, FIRQUEST reports a CI for the quantile y_p under consideration that is centered at the overall empirical quantile computed from all sample paths and based on the combined estimator $\widetilde{\mathscr{V}}_p(w; R, b, m)$ of σ_p^2. Otherwise, the procedure issues a warning and, upon user's approval, formulates a wider CI from a set of CIs based on the aforementioned overall quantile estimator, the RBQEs, and the replicate signed areas obtained from the nonoverlapping batches. Experimentation with an extensive test bed of output processes and 5 or 10 replications showed that for sufficiently large replicate paths FIRQUEST delivered CIs with coverage probabilities close to the nominal level. Our experimental analysis revealed that for relatively small sample sizes, it is preferable to use fewer independent replications with larger replication lengths (in these cases FQUEST outperformed FIRQUEST). However, in several experimental settings and with sufficiently large replication lengths, FIRQUEST outperformed FQUEST with regard to average CI relative precision.

We end with a list of topics worthy of future consideration:

- Identification of alternative weight functions for computing STS area estimators inducing lower small-sample bias than the constant weight $w_0(t) = \sqrt{12}$, $t \in [0, 1]$.
- Development of a sequential procedure for simultaneous estimation of multiple quantiles. In principle, the SQSTS, FQUEST, and FIRQUEST methods can be augmented to yield rectangular regions for a vector of percentiles via Bonferroni's inequality, but the CIs for individual quantiles will be conservative. Elliptical confidence regions for quantile vectors based on empirical quantiles computed from nonoveralpping and overlapping batches or generalized likehood ratios have been recently proposed by Lei *et al.* [90] and Pasupathy *et al.* [91], but the incorporation of the latter methodologies into automated procedures will be a significant challenge.
- Potential enhancements applied to SQSTS for estimation of extreme quantiles ($p \in (0, 0.05) \cup (0.95, 1)$).
- Development of automated fixed-sample-size methods for simultaneous estimation of multiple quantiles from a single run or multiple independent replications.
- Development of a hybrid sequential method with an upper threshold for the allowable sample size.
- Expansion of the experimental test bed for SQSTS, FQUEST, and FIRQUEST with additional processes.
- Incorporation of SQSTS, FQUEST, and FIRQUEST into the Sequest app.
- Prove that SQSTS or its descendants are asymptotically valid as the precision requirements tend to zero.

REFERENCES

[1] R. W. Conway, “Some Tactical Problems in Digital Simulation,” *Management Science*, vol. 10, no. 1, pp. 47–61, 1963.

[2] G. S. Fishman, *Principles of Discrete Event Simulation*. New York: John Wiley & Sons, 1978.

[3] W. J. Hopp and M. L. Spearman, *Factory Physics*, 3rd ed. New York: McGraw-Hill/Irwin, 2008.

[4] A. M. Law, *Simulation Modeling and Analysis*, 5th ed. New York: McGraw-Hill, 2015.

[5] B. L. Nelson, “The MORE Plot: Displaying Measures of Risk & Error from Simulation Output,” in *Proceedings of the 2008 Winter Simulation Conference*, S. J. Mason, R. R. Hill, L. Mönch, O. Rose, T. Jefferson, and J. W. Fowler, Eds., Institute of Electrical and Electronics Engineers, Piscataway, New Jersey, 2008, pp. 413–416.

[6] C. Alexopoulos, D. Goldsman, A. C. Mokashi, and J. R. Wilson, “Sequential Estimation of Steady-State Quantiles: Lessons Learned and Future Directions,” in *Proceedings of the 2018 Winter Simulation Conference*, M. Rabe, A. A. Juan, N. Mustafee, A. Skoogh, S. Jain, and B. Johansson, Eds., Piscataway, New Jersey: Institute of Electrical and Electronics Engineers, 2018, pp. 1814–1825.

[7] C. Alexopoulos, D. Goldsman, A. C. Mokashi, K.-W. Tien, and J. R. Wilson, “Sequest: A sequential procedure for estimating quantiles in steady-state simulations,” *Operations Research*, vol. 67, no. 4, pp. 1162–1183, 2019.

[8] W. B. Wu, “On the Bahadur representation of sample quantiles for dependent sequences,” *The Annals of Statistics*, vol. 33, no. 4, pp. 1934–1963, 2005.

[9] D. L. Iglehart, “Simulating Stable Stochastic Systems, VI: Quantile Estimation,” *Journal of the Association for Computing Machinery*, vol. 23, no. 2, pp. 347–360, 1976.

[10] L. W. Moore, “Quantile estimation methods in regenerative processes,” Ph.D. dissertation, Department of Statistics, University of North Carolina, Chapel Hill, NC, 1980.

[11] A. F. Seila, “A Batching Approach to Quantile Estimation in Regenerative Simulations,” *Management Science*, vol. 28, no. 5, pp. 573–581, 1982.

[12] A. F. Seila, "Estimation of Percentiles in Discrete Event Simulation," *Simulation*, vol. 39, no. 6, pp. 193–200, 1982.

[13] J. M. Bekki, J. W. Fowler, G. T. Mackulak, and B. L. Nelson, "Indirect Cycle Time Quantile Estimation Using the Cornish–Fisher Expansion," *IIE Transactions*, vol. 42, no. 1, pp. 31–44, 2010.

[14] R. A. Fisher and E. A. Cornish, "The percentile points of distributions having known cumulants," *Technometrics*, vol. 2, no. 2, pp. 209–225, 1960.

[15] J. M. Bekki, J. W. Fowler, G. T. Mackulak, and M. Kulahci, "Simulation-Based Cycle-Time Quantile Estimation in Manufacturing Settings Employing Non-FIFO Dispatching Policies," *Journal of Simulation*, vol. 3, pp. 69–83, 2009.

[16] K. E. E. Raatikainen, "Simultaneous Estimation of Several Percentiles," *Journal of Statistical Modeling and Analytics*, vol. 2, pp. 159–163, 1987.

[17] K. E. E. Raatikainen, "Sequential procedure for simultaneous estimation of several percentiles," *Transactions of the Society for Computer Simulation*, vol. 7, no. 1, pp. 21–44, 1990.

[18] R. Jain and I. Chlamtac, "The P^2 Algorithm for Dynamic Calculation of Quantiles and Histograms without Storing Observations," *Communications of the ACM*, vol. 28, no. 10, pp. 1076–1085, 1985.

[19] P. Billingsley, *Convergence of Probability Measures*, 2nd ed. New York: John Wiley & Sons, 1999.

[20] A. J. McNeil and R. Frey, "Estimation of Tail-Related Risk Measures for Heteroscedastic Financial Time Series: An Extreme Value Approach," *Journal of Empirical Finance*, vol. 7, pp. 271–300, 2000.

[21] T. Bollerslev, R. Chou, and K. Kroner, "ARCH modeling in finance," *Journal of Econometrics*, vol. 52, pp. 5–59, 1992.

[22] H. Drees, "Extreme Quantile Estimation for Dependent Data, with Applications to Finance," *Bernoulli*, vol. 9, no. 1, pp. 617–657, 2003.

[23] C. Alexopoulos, D. Goldsman, A. C. Mokashi, and J. R. Wilson, "Automated estimation of extreme steady-state quantiles via the maximum transformation," *ACM Transactions on Modeling and Computer Simulation*, vol. 27, no. 4, 22:1–22:29, 2017.

[24] E. J. Chen and W. D. Kelton, "Quantile and tolerance-interval estimation in simulation," *European Journal of Operational Research*, vol. 168, pp. 520–540, 2006.

[25] E. J. Chen and W. D. Kelton, "Estimating steady-state distributions via simulation-generated histograms," *Computers & Operations Research*, vol. 35, no. 4, pp. 1003–1016, 2008.

[26] H. Dong and M. K. Nakayama, "Quantile estimation with Latin hypercube sampling," *Operations Research*, vol. 65, no. 6, pp. 1678–1695, 2017.

[27] X. Jin, M. C. Fu, and X. Xiong, "Probabilistic error bounds for simulation quantile estimators," *Management Science*, vol. 49, no. 2, pp. 230–246, 2003.

[28] A. Tafazzoli and J. R. Wilson, "Skart: A Skewness- and Autoregression-Adjusted Batch-Means Procedure for Simulation Analysis," *IIE Transactions*, vol. 43, no. 2, pp. 110–128, 2011.

[29] S. Asmussen and P. W. Glynn, *Stochastic Simulation: Algorithms and Analysis*. New York: Springer Science+Business Media, 2007.

[30] P. Heidelberger and P. A. W. Lewis, "Quantile estimation in dependent sequences," *Operations Research*, vol. 32, no. 1, pp. 185–209, 1984.

[31] L. W. Schruben, "Confidence interval estimation using standardized time series," *Operations Research*, vol. 31, pp. 1090–1108, 1983.

[32] D. Goldsman and L. W. Schruben, "New confidence interval estimators using standardized time series," *Management Science*, vol. 36, pp. 393–397, 1990.

[33] D. Goldsman, M. S. Meketon, and L. W. Schruben, "Properties of standardized time series weighted area variance estimators," *Management Science*, vol. 36, pp. 602–612, 1990.

[34] C. Alexopoulos, N. T. Argon, D. Goldsman, G. Tokol, and J. R. Wilson, "Overlapping variance estimators for simulation," *Operations Research*, vol. 55, no. 6, pp. 1090–1103, 2007.

[35] J. Dong and P. W. Glynn, "The asymptotic validity of sequential stopping rules for confidence interval construction using standardized time series," in *Proceedings of the 2019 Winter Simulation Conference*, N. Mustafee *et al.*, Eds., Piscataway, New Jersey: Institute of Electrical and Electronic Engineers, 2019, pp. 332–343.

[36] H. Damerdji, "Strong consistency of the variance estimator in steady-state simulation output analysis," *Mathematics of Operations Research*, vol. 19, no. 2, pp. 494–512, 1994.

[37] J. M. Calvin and M. K. Nakayama, "Confidence intervals for quantiles with standardized time series," in *Proceedings of the 2013 Winter Simlation Conference*, R.

Pasupathy, S.-H. Kim, R. H. A. Tolk, and M. E. Kuhl, Eds., Piscataway, New Jersey: Institute of Electrical and Electronics Engineers, 2013, pp. 601–612.

[38] C. Alexopoulos, J. H. Boone, D. Goldsman, A. Lolos, K. D. Dingeç, and J. R. Wilson, "Steady-state quantile estimation using standardized time series," in *Proceedings of the 2020 Winter Simulation Conference*, K.-H. Bae *et al.*, Eds., Orlando, Florida: Institute of Electrical and Electronics Engineers, 2020, pp. 289–300.

[39] C. Alexopoulos, D. Goldsman, A. Lolos, K. D. Dingeç, and J. R. Wilson, "Steady-state quantile estimation using standardized time series," Gebze Technical University, Georgia Institute of Technology, and North Carolina State University, Tech. Rep., 2023, accessed 8$^{\text{th}}$ November 2022.

[40] C. Alexopoulos, D. Goldsman, P. Tang, and J. R. Wilson, "SPSTS: A sequential procedure for estimating the steady-state mean using standardized time series," *IIE Transactions*, vol. 48, no. 9, pp. 864–880, 2016.

[41] C. Alexopoulos, D. Goldsman, A. C. Mokashi, K.-W. Tien, and J. R. Wilson, "Online availability of the Sequest software for Linux, MacOS, and Windows.," 2019, Accessed April 30, 2021.

[42] A. Tafazzoli, N. M. Steiger, and J. R. Wilson, "N-Skart: A nonsequential skewness- and autoregression-adjusted batch means procedure for simulation analysis," *IEEE Transactions on Automatic Control*, vol. 56, no. 2, pp. 254–264, 2011.

[43] J. von Neumann, "Distribution of the ratio of the mean square successive difference to the variance," *Annals of Mathematical Statistics*, vol. 12, no. 4, pp. 367–395, 1941.

[44] W. D. Kelton, N. Zupick, and N. Ivey, *Simulation with Arena*, 7th ed. McGraw Hill, 2023.

[45] J. S. Smith and D. T. Sturrock, *Simio and Simulation: Modeling, Analysis, Applications*, 6th ed. Simio LLC, 2023.

[46] W. J. Conover, *Practical Nonparametric Statistics*, 3rd ed. New York: John Wiley & Sons, 1999.

[47] C. Alexopoulos and D. Goldsman, "To batch or not to batch?" *ACM Transactions on Modeling and Computer Simulation*, vol. 14, no. 1, pp. 76–114, 2004.

[48] G. S. Fishman, *Discrete-Event Simulation: Modeling, Programming, and Analysis*. New York: Springer-Verlag, 2001.

[49] A. N. Kolmogorov and S. V. Fomin, *Introductory Real Analysis*. New York: Dover Publications Inc., 1975.

[50] W. Whitt, *Stochastic-Process Limits: An Introduction to Stochastic-Process Limits and Their Application to Queues*. New York: Springer, 2002.

[51] X. Shao and W. B. Wu, "Asymptotic spectral theory for nonlinear time series," *The Annals of Statistics*, vol. 35, no. 4, pp. 1773–1801, 2007.

[52] K. D. Dingeç, C. Alexopoulos, D. Goldsman, A. Lolos, and J. R. Wilson, "Geometric moment-contraction of G/G/1 waiting times," in *Advances in Modeling and Simulation: Festschrift for Pierre L' Ecuyer*, Z. Botev, A. Keller, C. Lemieux, and B. Tuffin, Eds., New York: Springer, 2022, pp. 111–130.

[53] K. D. Dingeç, C. Alexopoulos, D. Goldsman, A. Lolos, and J. R. Wilson, "Geometric-moment contraction, stationary processes, and their indicator processes, I: Theory," Gebze Technical University, Tech. Rep., 2022.

[54] R. D. Foley and D. Goldsman, "Confidence intervals using orthonormally weighted standardized time series," *ACM Transactions on Modeling and Simulation*, vol. 9, pp. 297–325, 1999.

[55] W. Rudin, *Principles of Mathematical Analysis*, 3rd ed. New York: McGraw-Hill, 1976.

[56] P. J. Bickel and K. A. Doksum, *Mathematical Statistics: Basic Ideas and Selected Topics*, 2nd. Upper Saddle River, NJ: Pearson Prentice Hall, 2007.

[57] T. Aktaran-Kalaycı, C. Alexopoulos, N. T. Argon, D. Goldsman, and J. R. Wilson, "Exact expected values of variance estimators in steady-state simulation," *Naval Research Logistics*, vol. 54, no. 4, pp. 397–410, 2007.

[58] K. D. Dingeç, C. Alexopoulos, D. Goldsman, A. Lolos, and J. R. Wilson, "Variance parameter estimation for the quantile indicator process," Gebze Technical University, Tech. Rep., 2022.

[59] P. McIlroy, "Optimistic sorting and information theoretic complexity," in *Proceedings of the Fourth Annual ACM-SIAM Symposium on Discrete Algorithms*, 1993, pp. 467–474.

[60] T. H. Cormen, C. E. Leiserson, R. L. Rivest, and C. Stein, *Introduction to Algorithms*, 3rd. Cambridge, Massachusetts: MIT Press, 2009.

[61] E. K. Lada, J. R. Wilson, N. M. Steiger, and J. A. Joines, "Performance of a wavelet-based spectral procedure for steady-state simulation analysis," *INFORMS Journal on Computing*, vol. 19, no. 2, pp. 150–160, 2007.

[62] L. Kleinrock, *Queueing Systems, Volume I: Theory*. New York: John Wiley & Sons, 1975.

[63] E. K. Lada, N. M. Steiger, and J. R. Wilson, "Performance evaluation of recent procedures for steady-state simulation analysis," *IIE Transactions*, vol. 38, no. 9, pp. 711–727, 2006.

[64] J. Abate and W. Whitt, "A unified framework for numerically inverting Laplace transforms," *INFORMS Journal on Computing*, vol. 18, no. 4, pp. 408–421, 2006.

[65] A. Tafazzoli, J. R. Wilson, E. K. Lada, and N. M. Steiger, "Performance of Skart: A skewness- and autoregression-adjusted batch-means procedure for simulation analysis," *INFORMS Journal on Computing*, vol. 23, no. 2, pp. 297–314, 2011.

[66] A. M. Law and J. S. Carson, "A sequential procedure for determining the length of a steady-state simulation," *Operations Research*, vol. 27, no. 5, pp. 1011–1025, 1979.

[67] P. L'Ecuyer, R. Simard, E. J. Chen, and W. D. Kelton, "An object-oriented random number package with many long streams and substeams," *Operations Research*, vol. 90, no. 6, pp. 1073–1075, 2002.

[68] K. D. Dingeç, C. Alexopoulos, D. Goldsman, A. Lolos, and J. R. Wilson, "Geometric-moment contraction, stationary processes, and their indicator processes, II: Examples," Gebze Technical University, Tech. Rep., 2022.

[69] C. Meyer, "The bivariate normal copula," *Communications in Statistics-Theory and Methods*, vol. 42, no. 13, pp. 2402–2422, 2013.

[70] A. Azzalini, *The R package 'sn': The skew-normal and related distributions such as the skew-t (version 1.6–2).* Accessed April 30, 2021., University of Padua, Padua, Italy, 2020.

[71] N. Blomqvist, "The covariance function of the M/G/1 queuing system," *Skandinavisk Aktuarietidskrift*, vol. 50, pp. 157–174, 1967.

[72] N. Henze and Y. Y. Nikitin, "A new approach to goodness-of-fit testing based on the integrated empirical process," *International Journal of Computer Mathematics*, vol. 12, no. 3, pp. 391–416, 2000.

[73] A. Dołęgowski and J. Wesołowski, "Linearity of regression for overlapping order statistics," *Metrika*, vol. 78, no. 2, pp. 205–218, 2015.

[74] M. Ahsanullah, V. B. Nevzorov, and M. Shakil, *An Introduction to Order Statistics*. Paris: Atlantis Press, 2013, vol. 8.

[75] Wolfram Research, Inc., "Mathematica 10.0," Champaign, Illinois, 2014.

[76] J. Huang, "A note on order statistics from Pareto distribution," *Scandinavian Actuarial Journal*, vol. 1975, no. 3, pp. 187–190, 1975.

[77] H. J. Malik, "Exact moments of order statistics from the Pareto distribution," *Scandinavian Actuarial Journal*, vol. 1966, no. 3-4, pp. 144–157, 1966.

[78] Z. Govindarajulu, "Relationships among moments of order statistics in samples from two related populations," *Technometrics*, vol. 5, no. 4, pp. 514–518, 1963.

[79] J. E. Gentle, *Computational Statistics*. New York: Springer, 2009.

[80] M. Ahsanullah and V. B. Nevzorov, "Generalized spacings of order statistics from extended sample," *Journal of Statistical Planning and Inference*, vol. 85, no. 1–2, pp. 75–83, 2000.

[81] S. S. Shapiro and M. B. Wilk, "An analysis of variance test for normality," *Biometrika*, vol. 52, pp. 591–611, 1965.

[82] M. S. Meketon and B. W. Schmeiser, "Overlapping batch means: Something for nothing?" In *Proceedings of the 1984 Winter Simulation Conference*, S. Sheppard, U. W. Pooch, and C. D. Pegden, Eds., Piscataway, NJ: Institute of Electrical and Electronics Engineers, 1984, pp. 227–230.

[83] L. C. Young, "Randomness in ordered sequences," *Annals of Mathematical Statistics*, vol. 12, pp. 293–300, 1941.

[84] R. Bartels, "The rank version of von Neumann's ratio test for randomness," *Journal of the American Statistical Association*, vol. 77, pp. 40–46, 1982.

[85] P. Royston, "Remark AS R94," *Applied Statistics*, vol. 44, no. 4, pp. 547–551, 1995.

[86] G. S. Fishman, "Bias considerations in simulation experiments," *Operations Research*, vol. 20, pp. 785–790, 1972.

[87] B. Mandelbrot, "The variation of certain speculative prices," *The Journal of Business*, vol. 36, no. 4, pp. 394–419, 1963.

[88] R. Willink, "A confidence interval and test for the mean of an asymmetric distribution," *Communications in Statistics—Theory and Methods*, vol. 34, pp. 753–766, 2005.

[89] N. T. Argon and S. Andradóttir, "Replicated batch means for steady-state simulations," *Naval Research Logistics*, vol. 53, pp. 508–524, 2006.

[90] L. Lei, C. Alexopoulos, Y. Peng, and J. R. Wilson, "Confidence intervals and regions for quantiles using conditional monte carlo and generalized likelihood ratios," in *Proceedings of the 2020 Winter Simulation Conference*, K.-H. Bae *et al.*, Eds., Orlando, FL: Institute of Electrical and Electronics Engineers, 2020, pp. 2071–2082.

[91] R. Pasupathy, D. I. Singham, and Y. Yeh, "Overlapping batch confidence regions on the steady-state quantile vector," in *Proceedings of the 2022 Winter Simulation Conference*, B. Feng *et al.*, Eds., Singapore: Institute of Electrical and Electronics Engineers, 2022, pp. 25–36.

VITA

Athanasios (Thanos) Lolos was born on October 2, 1994, in Greece. He received his Diploma in Naval Architecture and Marine Engineering from the National Technical University of Athens in 2017. After completing his compulsory military service in 2018, he started his Ph.D. in Operations Research at the School of Industrial and Systems Engineering at Georgia Institute of Technology (Atlanta, United States), under the supervision of Professor Christos Alexopoulos. During the fourth year of his studies, he also joined the MBA program at Scheller College of Business at Georgia Institute of Technology. After graduating in May 2023 with an M.S. and a Ph.D. in Operations Research and an MBA, he will join Navy Federal Credit Union, in Vienna, Virginia, as a Predictive Modeler II.